VOLUME I

INTERPLANETARY MIDCOURSE GUIDANCE ANALYSIS

by

ROBERT GOTTLIEB STERN

B.S., Lehigh University, 1941
M.S., Stevens Institute of Technology, 1950

SUBMITTED IN PARTIAL FULFILLMENT
OF THE REQUIREMENTS FOR THE
DEGREE OF DOCTOR OF SCIENCE

at the

MASSACHUSETTS INSTITUTE OF TECHNOLOGY

Signature of Author_____
Department of Aeronautics and Astronautics,
May 10, 1963

Certified by_____
Thesis Supervisor

Certified by_____
Thesis Supervisor

Certified by_____
Thesis Supervisor

Accepted by_____
Chairman, Departmental Committee
on Graduate Students

INTERPLANETARY MIDCOURSE GUIDANCE ANALYSIS

by

Robert G. Stern

Submitted to the Department of Aeronautics and Astronautics on May 10, 1963 in partial fulfillment of the requirements for the degree of Doctor of Science.

ABSTRACT

The problem studied in this thesis is the midcourse correction of the path of an interplanetary vehicle by means of several intermittent thrust impulses. The analysis is linearized by assuming that the vehicle's actual path differs only slightly from a known pre-computed reference path. The difference between the actual path and the reference path is known as the variant path. The linearized equations of motion are those in which the dependent variables are the position and velocity components of the variant path.

The emphasis in the thesis is placed on the analytic solution of the linearized equations of motion. Two distinct methods are developed for obtaining an analytic solution when the reference trajectory is an ellipse. The first method involves the separation of the sixth-order system into two independent systems, one of fourth order and the other of second order. Although the two independent systems have variable coefficients, both are integrated directly in closed form. The second method of solution utilizes variational techniques to determine the effect on the path of small variations in a set of six orbital elements. The two solutions are shown to be mathematically equivalent.

The analytic solution is used to obtain closed-form expressions for the elements of all the matrices appearing in the guidance equations.

Both fixed-time-of-arrival and variable-time-of-arrival guidance schemes are discussed. In fixed-time-of-arrival guidance the three-dimensional velocity correction vector is expressed as a linear function of the three-dimensional predicted position variation at the destination. In variable-time-of-arrival guidance both the correction vector and the position variation vector to be corrected are expressed as two-dimensional vectors in a special coordinate system known as the critical-plane coordinate system.

In the case of variable-time-of-arrival guidance an empirical technique is developed for determining the optimum time to apply a midcourse correction. The optimum correction time is a function of a single characteristic of the vehicle's variant path.

There are three types of singularities that appear in the fixed-time-of-arrival guidance equations for elliptical reference trajectories. Two of the types are readily explained physically. The third type, no previous mention of which has been found in the literature, is shown to be related to the minima of the time-of-flight curves obtained from Lambert's theorem. No finite fixed-time-of-arrival correction can be computed at a correction time corresponding to any one of the three types of singularity. If variable-time-of-arrival guidance is used, two of the singularity types are effectively cancelled out, but the third type still remains.

Both Earth-based and self-contained navigation systems are described. The function of the navigation system is to determine the vehicle's variant path from measurements made during the flight. The six parameters selected to define the variant path are the components of position variation and velocity variation at the nominal time of arrival at the destination.

In the self-contained navigation system vehicle position is determined from the optical sighting of the angles between pairs of celestial bodies, and the variant path is computed after several position determinations have been made. A survey is made of all first-magnitude stars to determine which are most useful for position determination. A graphical technique is evolved for selecting the angular sightings which result in the greatest accuracy of position determination.

The guidance theory is illustrated by a numerical example of a long-duration Earth-Mars trajectory.

A midcourse guidance system is outlined which utilizes the analytic results of the theoretical investigation.

Thesis Supervisors:

Professor Walter Wrigley

Title: Professor of Instrumentation and Astronautics

Professor Walter McKay

Title: Associate Professor of Aeronautics and Astronautics

Dr. Richard H. Battin

Title: Assistant Director, M. I. T. Instrumentation Laboratory

In the case of variable-time-of-arrival guidance an empirical technique is developed for determining the optimum time to apply a midcourse correction. The optimum correction time is a function of a single characteristic of the vehicle's variant path.

There are three types of singularities that appear in the fixed-time-of-arrival guidance equations for elliptical reference trajectories. Two of the types are readily explained physically. The third type, no previous mention of which has been found in the literature, is shown to be related to the minima of the time-of-flight curves obtained from Lambert's theorem. No finite fixed-time-of-arrival correction can be computed at a correction time corresponding to any one of the three types of singularity. If variable-time-of-arrival guidance is used, two of the singularity types are effectively cancelled out, but the third type still remains.

Both Earth-based and self-contained navigation systems are described. The function of the navigation system is to determine the vehicle's variant path from measurements made during the flight. The six parameters selected to define the variant path are the components of position variation and velocity variation at the nominal time of arrival at the destination.

In the self-contained navigation system vehicle position is determined from the optical sighting of the angles between pairs of celestial bodies, and the variant path is computed after several position determinations have been made. A survey is made of all first-magnitude stars to determine which are most useful for position determination. A graphical technique is evolved for selecting the angular sightings which result in the greatest accuracy of position determination.

The guidance theory is illustrated by a numerical example of a long-duration Earth-Mars trajectory.

A midcourse guidance system is outlined which utilizes the analytic results of the theoretical investigation.

Thesis Supervisors:

Professor Walter Wrigley

Title: Professor of Instrumentation and Astronautics

Professor Walter McKay

Title: Associate Professor of Aeronautics and Astronautics

Dr. Richard H. Battin

Title: Assistant Director, M.I.T. Instrumentation Laboratory

ACKNOWLEDGMENTS

The author wishes to thank Professor Walter Wrigley and Professor Walter McKay, faculty supervisors of this thesis. Their sympathetic understanding and encouragement are deeply appreciated.

He also wishes to acknowledge the helpful suggestions of Dr. Richard H. Battin, research supervisor, whose work provided the original motivation for this investigation.

He is indebted to the M.I.T. Instrumentation Laboratory, under the directorship of Dr. C. Stark Draper, for supplying facilities and financial support during the course of the study.

Thanks are due to Captain Mack Mauldin, Jr. and Captain Robert G. Millard, of the United States Air Force, who programmed the computations and supervised the plotting of the curves contained in Chapter 4.

There are many members of the M.I.T. community, both students at the Institute and colleagues at the Instrumentation Laboratory, with whom the author has engaged in stimulating critical discussion that has led to a clearer understanding of the physical phenomena that are treated. The author takes this opportunity to express his gratitude to all these people.

Finally, he wishes to thank Miss Kelly Brouillette, Miss Theo Coughlin, and Miss Mimi Ganem, who typed early drafts of this thesis; Mr. Ray Parks, who made some of the sketches; and the staff of Jackson & Moreland, Inc., under the supervision of Messrs. Gardner Pope, Chester Brimblecom, and Frank Cross, who prepared the final draft for publication.

This research was sponsored in part by DSR Project 52-156 through USAF Contract AF 04(647)-303 and in part by DSR Project 55-191 through NASA Contract NAS 9-153. The costs of preparing the final draft for publication were underwritten by DSR Project 9406 through NASA Contract NsG 254-62.

TABLE OF CONTENTS
VOLUME I

TABLE OF CONTENTS (Cont.)
VOLUME I

TABLE OF CONTENTS (Cont.)
VOLUME I

TABLE OF CONTENTS (Cont.)
VOLUME I

LIST OF ILLUSTRATIONS
VOLUME I

LIST OF ILLUSTRATIONS (Cont.)

VOLUME I

LIST OF TABLES
VOLUME I

TABLE OF CONTENTS
VOLUME II

TABLE OF CONTENTS (Cont.)

VOLUME II

TABLE OF CONTENTS (Cont.
VOLUME II

TABLE OF CONTENTS (Cont.)
VOLUME II

Appendix

TABLE OF CONTENTS (Cont.)
VOLUME II

Appendix

TABLE OF CONTENTS (Cont.)
VOLUME II

Appendix

LIST OF ILLUSTRATIONS
VOLUME II

LIST OF ILLUSTRATIONS (Cont.)

VOLUME II

LIST OF TABLES
VOLUME II

LIST OF SYMBOLS

General Notation Rules

An asterisk over a capital letter indicates a matrix.

An underlined lower-case letter indicates a vector, which is equivalent to a one-column matrix. A vector symbol without the underlining indicates the magnitude of the vector.

A bar over a symbol signifies the average value of the quantity represented by the symbol. A bar over a group of symbols signifies the average value of the product of the quantities represented by the symbols.

A single dot over a symbol indicates the first derivative with respect to time of the quantity represented by the symbol. Two dots indicate the second derivative with respect to time. Time derivatives of vectors are taken with respect to an inertial coordinate system unless noted otherwise.

English Symbols

a	semi-major axis of reference trajectory
a_i	i-component of acceleration vector
$\underline{a}$	acceleration vector on reference trajectory
a. u.	astronomical unit
A	area of equi-probability ellipse (See Section P. 8.)
A	parameter used in development of expression for $\overset{*}{Y}$ (See Section N.8.)
δA_{SR}	variation of R-th angular measurement made at time t_S (See Section 5.7.)
$\overset{*}{A}$	typical square matrix (See Section F.9.)
$\overset{*}{A}_1, \ldots, \overset{*}{A}_4$	2-by-2 sub-matrices of the 4-by-4 matrix relating in-plane variations in position and velocity to variations in the orbital elements (See Section K.5.)
$\overset{*}{A}_{ij}$	6-by-6 matrix relating $\delta \underline{r}_i$ and $\delta \underline{r}_j$ to $\delta \underline{e}$ (See Section O.3.)

b	semi-minor axis of reference trajectory
B	parameter used in development of expression for $\overset{*}{Y}$ (See Section O.13.)
$\overset{*}{B}_S$	covariance matrix of components of uncertainty in position at time t_S (See Section 5.7.)
$\lvert\overset{*}{B}_S\rvert$	determinant of $\overset{*}{B}_S$ (See Section 5.11.)
c	linear eccentricity of reference trajectory
$\underline{c}$	midcourse velocity correction vector
$\underline{c}_F$	midcourse velocity correction vector for FTA guidance
$\underline{c}_V$	midcourse velocity correction vector for VTA guidance
$\underline{c}_W$	two-dimensional midcourse velocity correction vector for VTA guidance (See Section N.6.)
C	constant of integration (See Section G.4.)
C	parameter used in development of expression for $\overset{*}{Y}$ (See Section O.13.)
$\overset{*}{C}_{ji}$	transition matrix; 6-by-6 matrix relating components of $\delta\underline{x}_j$ to components of $\delta\underline{x}_i$
CPE	circular probable error (See Section P.8.)
d	distance between initial position and final position (See Section O.10 and Figure O.6.)
d	distance between near bodies P and Q (See Section 5.10.)
det	determinant of a square matrix
$(\det)_{pq}$	determinant of 4-by-4 matrix of Equation (K-13)
$(\det)_z$	determinant of 2-by-2 matrix of Equation (K-24)
$\underline{d}_i$	position vector of space vehicle relative to i-th disturbing body (See Section B.2)
D	operator representing first derivative with respect to time (See Section G.3.)

D	parameter used in development of expression for $\overset{*}{Y}$ (See Section O.13.)
$\overset{*}{D}_{ji}$	6-by-6 vector relating $\underline{\lambda}_j$ to $\underline{\lambda}_i$ (See Section F.8.)
e	eccentricity of reference trajectory
$\delta\underline{e}$	variation in grouping of six orbital elements
E	eccentric anomaly on reference trajectory
E_M	one half the difference between E_j and E_i (See Section K.6.)
E_P	one half the sum of E_j and E_i (See Section K.6.)
δE	variation in eccentric anomaly
$\overset{*}{E}$	covariance matrix of the uncertainty vector $\underline{\epsilon}$ (See Section P.6.)
$\lvert\overset{*}{E}\rvert$	determinant of $\overset{*}{E}$ (See Section P.7.)
$\overset{*}{E}_\rho$	covariance matrix of the uncertainty in $\delta\hat{\underline{\rho}}$ (See Section 6.8.)
f	true anomaly on reference trajectory (See Figure A.2.)
f'	true anomaly on actual trajectory (See Figure H.1.)
$\dot{f}$	rate of change of true anomaly; angular velocity of r s z coordinate system
δf	variation in true anomaly
F	operator representing first derivative with respect to true anomaly (See Section G.3.)
$\overset{*}{F}_m$	3-by-6 matrix relating components of $\delta\underline{r}_m$ to components of $\delta\underline{e}$ (See Section F.3.)
FTA	fixed-time-of-arrival
g	angle between velocity vector on reference trajectory and y-axis (See Figure A.2.)
$\dot{g}$	angular velocity of p q z coordinate system

$\underline{g}_{SR}^{T}$	four-component row vector relating δA_{SR} to $\delta \underline{s}_S$ (See Section 5.7.)
G	constant of gravitation
$\overset{*}{G}$	3-by-3 matrix relating components of $\delta \ddot{\underline{r}}$ to elements of $\delta \underline{r}$ (See Section E.3.)
$\overset{*}{G}_S^T$	(K+1) - by - 4 matrix relating $\delta \underline{m}_S$ to $\delta \underline{s}_S$ (See Section 5.7.)
h	orbital angular momentum per unit mass of space vehicle
H	total energy per unit mass of space vehicle
$\overset{*}{H}_{ij}$	6-by-3 matrix relating components of $\delta \underline{e}$ to components of $\delta \underline{r}_i$ when $\delta \underline{r}_j$ is constant (See Section F.2.)
i	inclination angle of reference trajectory plane
i_C	angle between positive z-axis and positive ζ_C-axis (See Section N.3.)
i_E	inclination angle of reference trajectory plane relative to axes of heliocentric ecliptic coordinate system (See Section A.3.)
δi	angle between z' - axis and z-axis (See Figure H,1.)
$\overset{*}{I}_N$	N-by-N identity matrix
j	clock drift rate (See Section 5.6.)
J	operator representing first derivative with respect to eccentric anomaly (See Section G.5.)
$\overset{*}{J}_{ij}$	3-by-3 matrix relating components of $\delta \underline{v}_i$ to components $\delta \underline{r}_i$ when $\delta \underline{r}_j$ is constant (See Section F.4.)
k	arbitrary constant (See Section D.2.)
k	constant in definition of equi-probability ellipsoid (See Section P.7.)
$k_1, \ldots, k_6$	constants of integration (See Section G.6.)

$k_{i\xi}$, $k_{i\eta}$, $k_{i\zeta}$	components of $\underline{k}_i$ along ξ_D, η_D, and ζ_D axes, respectively (See Section N.5.)
k_{rs}	element in r-th row and s-th column of $\overset{*}{K}_{ij}$ (See Section K.9.)
$\underline{k}_i$	three-dimensional vector composed of elements in i-th row of $\overset{*}{K}_{CD}$ (See Section N.5.)
K	number of measurements made at t_S (See Section 5.4.)
K_1, K_2	constants of integration (See Section 3.5.)
K_{mn}	adjusted element in m-th row and n-th column of $\overset{*}{K}_{CD}$ (See Section O.13.)
$\overset{*}{K}_{CD}$	3-by-3 correction matrix
$\overset{*}{K}_{ij}$	3-by-3 matrix relating components of $\delta\underline{v}_i$ to components $\delta\underline{r}_j$ when $\delta\underline{r}_i$ is constant (See Section F.4.)
ℓ	semi-latus rectum of reference trajectory
log	Napierian logarithm (to base e = 2.71828)
$L(\delta\underline{x})$	likelihood function of $\delta\underline{x}$ (See Section P.4.)
$\overset{*}{L}_m$	3-by-6 matrix relating components of $\delta\underline{v}_m$ to components of $\delta\underline{e}$ (See Section F.4.)
m	mass of space vehicle
m_o	mass of sun
m_i	mass of i-th disturbing body (See Section B.2)
m_i	i-th measurement (See Section P.3.)
δm_i	variation in i-th measurement (See Section P.3.)
$\underline{m}$	measurement vector (See Section P.3.)
$\underline{m}_P$, $\underline{m}_Q$	line-of-sight unit vectors (See Section 5.10.)
δm_{SR}	variation in R-th measurement at time t_S (See Section 5.4.)

$\delta \underline{m}$	variation in measurement vector (See Section P.3.)
$\delta \underline{m}_S$	measurement variation vector for measurements made at time t_S (See Section 5.4.)
M	mean anomaly on reference trajectory
M	total number of measurements (See Section P.3.)
M_o	value of mean anomaly at $t = 0$
$\tilde{M}$	graphical approximation of mean anomaly (See Section C.2.)
δM	variation in mean anomaly
δM_o	variation in mean anomaly at epoch
ΔM	error in graphical approximation of mean anomaly (See Section C.2.)
$\overset{*}{M}_{ji}'$	two-dimensional version of $\overset{*}{M}_{ji}$ (See Section K.5.)
$\overset{*}{M}_{mk}$	3-by-3 matrix relating components of $\delta \underline{r}_m$ to components of $\delta \underline{r}_k$ when $\delta \underline{v}_k$ is constant (See Section F.3.)
ML	maximum likelihood
n	number of disturbing bodies (See Section B.2.)
n	mean angular motion (See Section B.8.)
$\underline{n}_P$	unit vector normal to $\underline{m}_P$ and in the plane containing $\underline{m}_P$ and $\underline{m}_Q$ (See Section 5.10.)
N	positive integer
N	number of complete circuits of the attractive focus (See Section O.10.)
N	number of components of generalized vector $\delta \underline{x}$ (See Section P.3.)
$\overset{*}{N}_{ji}'$	two-dimensional version of $\overset{*}{N}_{ji}$ (See Section K.5.)
$\overset{*}{N}_{mk}$	3-by-3 matrix relating components of $\delta \underline{r}_m$ to components of $\delta \underline{v}_k$ when $\delta \underline{r}_k$ is constant (See Section F.3.)

$\overset{*}{O}_N$	N-by-N zero matrix
p	distance along first axis of reference trajectory flight path coordinate system (See Section A.5.)
$p(\underline{u})$	joint probability density of the components of the vector $\underline{u}$ (See Section P.5.)
$p(\delta\underline{x}\|\delta\underline{\tilde{m}})$	conditional probability density of $\delta\underline{x}$, given $\delta\underline{\tilde{m}}$ (See Section P.4.)
$p(\delta\underline{\tilde{m}}\|\delta\underline{x})$	likelihood function of $\delta\underline{x}$; conditional probability density of $\delta\underline{\tilde{m}}$, given $\delta\underline{x}$ (See Section P.4.)
δp	variation in distance parallel to p-axis
$\underline{p}_{SR}{}^T$	six-component row vector relating δm_{SR} to $\delta\underline{x}_S$ (See Section 5.4.)
P	period of reference trajectory
δP	variation in reference period
$\overset{*}{P}$	6-by-6 matrix relating $\underline{\lambda}'$ to $\underline{\lambda}$ (See Section F.8.)
q	distance along second axis of reference trajectory flight path coordinate system (See Section A.5.)
δq	variation in distance parallel to q-axis
$\underline{q}_i$	vector relating δm_i to $\delta\underline{x}$ (See Section P.3.)
$\underline{q}_{SR}{}^T$	six-component row vector relating δm_{SR} to $\delta\underline{x}_D$ (See Section 5.4.)
$\overset{*}{Q}$	N-by-M matrix whose transpose relates $\delta\underline{m}$ to $\delta\underline{x}$ (See Section P.3.)
$\overset{*}{Q}_S{}^T$	K-by-N matrix relating $\delta\underline{m}_S$ to $\delta\underline{x}_D$ (See Section 5.4.)
r	distance along first axis of reference trajectory local vertical coordinate system (See Section A.4.)
δr	variation in radial distance (See Section H.3.)
$\underline{r}$	position vector on reference trajectory

$\underline{r}'$	position vector on actual trajectory
$\delta\underline{r}$	variation in position vector
$\delta\tilde{\underline{r}}_S$	position variation at time t_S inferred from measurements made at time t_S (See Section 5.5.)
$(\delta\underline{r}_D)_R$	vehicle's position variation relative to destination point at time t_D (See Section 5.6.)
R	disturbing function (See Section 2.5.)
$\overset{*}{R}_k$	6-by-3 matrix relating components of $\delta\underline{e}$ to components of $\delta\underline{r}_k$ when $\delta\underline{v}_k$ is constant (See Section F.2.)
s	distance along second axis of reference trajectory local vertical coordinate system (See Section A.4.)
δs	variation in transverse distance (See Section H.3.)
$\delta\underline{s}_S$	four-component vector composed of δt_S and $\delta\underline{r}_S$ (See Section 5.7.)
S	sensitivity factor (See Section 5.10.)
$\overset{*}{S}_{ji}'$	two-dimensional version of $\overset{*}{S}_{ji}$ (See Section K.5.)
$\overset{*}{S}_{mk}$	3-by-3 matrix relating components of $\delta\underline{v}_m$ to components of $\delta\underline{r}_k$ when $\delta\underline{v}_k$ is constant (See Section F.4.)
sgn	signum (See Equation (O-51))
SPE	spherical probable error (See Section P.8.)
t	time
t_o	time of perihelion passage for reference trajectory (See Section B.6.)
δt_o	variation in time of perihelion passage
$t_{C_{opt}}$	optimum time of midcourse correction in VTA guidance (See Section N.7.)
Δt_D	change in time of arrival due to VTA guidance (See Section M.3.)
t_F	time of flight (See Section O.10.)

$\tilde{t}_F$	alternate time of flight (See Section O.10.)
t_L	time of last measurement (See Section 5.4.)
$\tilde{\delta t}_S$	clock error at time t_S inferred from measurements made at time t_S (See Section 5.5.)
δt_{SR}	time interval between nominal measurement time t_S and actual time of R-th measurement (See Section 5.7.)
T	kinetic energy per unit mass of space vehicle
T_{ji}'	two-dimensional version of $\overset{*}{T}_{ji}$ (See Section K.5.)
$\overset{*}{T}_{mk}$	3-by-3 matrix relating components of $\delta\underline{v}_m$ to components of $\delta\underline{v}_k$ when $\delta\underline{r}_k$ is constant (See Section F.4.)
u	reciprocal of radial distance r (See Section B.5.)
u	integration variable (See Section G.4.)
u	difference between observed value and true value of measured quantity (See Section 5.4.)
$\underline{u}$	measurement uncertainty vector (See Section P.3.)
$\underline{u}_i$	unit vector in direction of i-axis
U	potential energy per unit mass of space vehicle
$\overset{*}{U}$	covariance matrix of measurement uncertainties (See Section P.3.)
$\lvert\overset{*}{U}\rvert$	determinant of $\overset{*}{U}$ (See Section P.5.)
v	integration variable (See Section G.4.)
v_i	i-component of velocity vector
$\underline{v}$	velocity vector on reference trajectory
$\underline{v}_P$	velocity of destination planet at nominal time of arrival (See Section M.2.)
$\underline{v}_R$	velocity of space vehicle relative to destination planet at nominal time of arrival (See Section M.2.)
$\underline{v}_S$	velocity of space vehicle on its reference trajectory at nominal time of arrival (See Section M.2.)

$\delta\underline{v}$	variation in velocity vector
V	volume of equi-probability ellipsoid (See Section P.8.)
$\overset{*}{V}_k$	6-by-3 matrix relating components of $\delta\underline{e}$ to components of $\delta\underline{v}_k$ when $\delta\underline{r}_k$ is constant (See Section F.2.)
VTA	variable-time-of-arrival
$\underline{w}$	vector in noncritical direction (See Section M.3. and Figure M.3.)
$\underline{w}_i$	tangent vector in direction of i-axis (See Section D.3.)
$\overset{*}{W}$	angular velocity matrix (See Section F.5.)
x	distance along first axis of reference trajectory stationary coordinate system (See Section A.3.)
x	integration variable (See Section G.4.)
x'	distance along first axis of actual trajectory stationary coordinate system (See Section H.3.)
x_o	distance from center of ellipse, measured parallel to x-axis (See Section D.2.)
x_E	distance along first axis of heliocentric ecliptic coordinate system (See Section Q.2.)
δx	variation in distance parallel to x-axis
$(\delta x_m)_u$	u-th component of $\delta\underline{x}_m$ (See Section 2.18.)
$\underline{x}$	six-component vector consisting of $\underline{r}$ and $\underline{v}$
$\underline{x}$	generalized parameter vector (See Section P.3.)
$\delta\underline{x}$	six-component vector consisting of $\delta\underline{r}$ and $\delta\underline{v}$
$\delta\underline{x}$	variation in generalized parameter vector (See Section P.3.)
X	singularity factor (See Section K.6.)
$\overset{*}{X}$	transformation matrix for transforming a three-dimensional vector from one of the reference trajectory coordinate systems to the critical-plane coordinate system (See Section N.5.)

y	distance along second axis of reference trajectory stationary coordinate system (See Section A.3.)
y'	distance along second axis of actual trajectory stationary coordinate system (See Section H.3.)
y_E	distance along second axis of heliocentric ecliptic coordinate system (See Section A.2.)
y_{ij}	element in i-th row and j-th column of $\overset{*}{Y}$ (See Section N.8.)
δy	variation in distance parallel to y-axis
$\overset{*}{Y}$	2-by-2 matrix relating $\underline{c}_W$ to $(\delta\underline{\rho}^-)_W$ (See Section N.6.)
$\overset{*}{Y}_D$	transformation matrix for transforming the state vector $\delta\underline{x}_D$ from one of the reference trajectory coordinate systems to the critical-plane coordinate system (See Section 6.8.)
z	distance normal to reference trajectory plane
z'	distance normal to actual trajectory plane
z_E	distance normal to ecliptic plane
δz	variation in distance normal to reference trajectory plane (See Section H.3.)
z_P	distance of space vehicle from near body P (See Section 5.10)
$\overset{*}{Z}$	6-by-6 matrix relating $\delta\dot{\underline{x}}$ to $\delta\underline{x}$ (See Section F.8.)

Greek Symbols

α	coordinate in elliptical cylindrical coordinate system (See Section D.2.)
α	variable in development of simplified expression for $\overset{*}{Y}$ (See Section N.6.)
α	angle used in development of Lambert's theorem (See Section O.10.)
α	right ascension (See Section 5.12.)

(α,x)	angle between $\underline{u}_\alpha$ and $\underline{u}_x$ (See Section D.3.)
(α,y)	angle between $\underline{u}_\alpha$ and $\underline{u}_y$ (See Section D.3.)
β	coordinate in elliptical cylindrical coordinate system (See Section D.2.)
β	variable in development of simplified expression for $\overset{*}{Y}$ (See Section N.6.)
β	angle used in development of Lambert's theorem (See Section O.10.)
β	celestial latitude
$\underline{\beta}_S$	difference between inferred position variation vector and true position variation vector (See Section 5.7.)
γ	flight path angle of reference trajectory (See Figure A.2.)
γ	first point of Aries (See Figure 5.3.)
$\Gamma(\ )$	gamma function of the argument (See Section P.8.)
δ	operator signifying first variation
δ	declination (See Section 5.12.)
δ_{ij}	Kronecker delta (See Section 5.4.)
∇	gradient of a scalar quantity
ϵ	infinitesimal quantity (See Section O.14.)
ϵ	obliquity of the ecliptic (See Section 5.12.)
$\underline{\epsilon}$	uncertainty vector associated with the maximum likelihood estimate $\delta\hat{\underline{x}}$ (See Section P.6.)
ζ	distance normal to the critical plane (See Section N.3.)
η	distance along second axis of critical-plane coordinate system (See Section N.3.)
η	angle used in development of Lambert's theorem (See Section O.10.)
$\underline{\eta}$	difference between desired midcourse correction vector and midcourse correction vector actually applied (See Section 5.9.)

θ	angle subtended at attractive focus by initial position and final position on elliptical trajectory (See Section O.10.)
λ	celestial longitude
$\underline{\lambda}$	adjoint vector to $\delta\underline{x}$ (See Section F.8.)
$\underline{\lambda}'$	modified adjoint vector (See Section F.8.)
μ	gravitational invariant in sun's gravitational field
μ_C, μ_D	angles used in analysis of X = 0 singularity (See Section O.9.)
μ_i	angle between $\delta\underline{r}_i$ and p_i - axis (See curves of Chapter 4.)
$\underline{\mu}$	three-component vector constituting upper half of adjoint vector $\underline{\lambda}$ (See Section F.8.)
ν_S	difference between inferred time variation and true time variation (See Section 5.7.)
ν_1	angle between $\delta\underline{v}_1$ and p_1 - axis (See Figures 4.16 and 4.17.)
$\underline{\nu}$	three-component vector constituting lower half of adjoint vector $\underline{\lambda}$ (See Section F.8.)
ξ	distance along first axis of critical-plane coordinate system (See Section N.3.)
$\underline{\xi}_S$	difference between $\delta\underline{\tilde{s}}_S$ and $\delta\underline{s}_S$ (See Section 5.7.)
ρ	projection of $\underline{r}$ in reference trajectory plane (See Section B.3.)
$\delta\underline{\rho}$	miss distance vector (See Section M.2.)
σ	standard deviation of angular measurement (See Section 5.11.)
σ_c^2	variance in clock drift rate (See Section 5.7.)
σ_i^2	variance of u_i (See Section 5.4.)
Σ	summation symbol

ϕ	longitude of perihelion of reference trajectory
ϕ	angle subtended at vacant focus by initial position and final position on elliptical trajectory (See Section O.10.)
ϕ_E	longitude of perihelion of reference trajectory relative to axes of heliocentric ecliptic coordinate system (See Section A.3.)
$\delta\phi$	longitude of perihelion of actual trajectory relative to perihelion of reference trajectory (See Section H.3.)
ψ	phase angle of miss distance vector in critical-plane coordinate system (See Section N.7.)
ω	latitude of perihelion of reference trajectory
ω_E	latitude of perihelion of reference trajectory relative to axes of heliocentric ecliptic coordinate system (See Section A.3.)
$\delta\omega$	angle, in actual trajectory plane, between positive half of line of nodes and x' - axis (See Figure H.1.)
$\underline{\omega}$	angular velocity vector of rotating coordinate system (See Section F.5.)
Ω	longitude of ascending node of reference trajectory
Ω_C	angle between positive r_1 - axis and positive ξ_C - axis (See Section N.3.)
Ω_E	longitude of ascending node of reference trajectory relative to axes of heliocentric ecliptic coordinate system (See Section A.3.)
$\delta\Omega$	angle, in reference trajectory plane, between x-axis and positive half of line of nodes (See Figure H.1.)

Superscripts

T	transpose of a vector or matrix
-1	inverse of a square matrix
'	pertaining to actual trajectory as opposed to reference trajectory (See Section H.3.)

-	pertaining to variant path before application of midcourse correction
+	pertaining to variant path after application of midcourse correction
~	observed value of measurement, as distinguished from true value (See Section P.3.)
^	maximum likelihood estimate (See Section P.4.)

Subscripts

C	corresponding to time of midcourse velocity correction
D	corresponding to nominal time of arrival at destination
i	general index; i = 1, ..., n (See Section B.2.)
i	corresponding to time t_i
I	corresponding to time of injection into heliocentric orbit
j	corresponding to time t_j
k	corresponding to time t_k
min	minimum
NR	relative to non-rotating coordinate system
o	pertaining to low-eccentricity reference trajectories (See Section J.3.)
opt	corresponding to optimum time of midcourse correction
p	component along p-axis
q	component along q-axis
r	component along r-axis
R	relative to rotating coordinate system
s	component along s-axis
S	corresponding to time t_S
SR	corresponding to R-th measurement at t_S (See Section 5.4.)
W	vector expressed in critical-plane coordinate system (See Section N.5.)

x	component along x-axis
x_E	component along x_E-axis
y	component along y-axis
y_E	component along y_E-axis
z	component along z-axis
z_E	component along z_E-axis
1	corresponding to an intermediate point of the trajectory, usually the point at which a midcourse correction is applied (See Section 4.4.)
2	corresponding to nominal time of arrival at destination (See Section 4.4.)
1 2 3	components along axes of an arbitrary reference trajectory coordinate system (See Section F.5 and N.3.)
1 2	corresponding to initial point and final point, respectively, in development of Lambert's theorem (See Section O.10.)
ζ	component along ζ-axis
η	component along η-axis
ξ	component along ξ-axis

CHAPTER 1

INTRODUCTION

1.1 Object

The object of this thesis is to utilize the techniques of linear perturbation theory and the characteristics of elliptical motion in making an intensive analytical study of interplanetary midcourse guidance. Possible applications of the results of the academic study in the design of a guidance system are to be considered.

1.2 Summary of Chapter 1

This introductory chapter contains a general discussion of the midcourse guidance problem and indicates the relationship between the present study and previous work in the field. There is also a synopsis of the material in succeeding chapters and in the appendices.

1.3 Phases of an Interplanetary Mission

A one-way interplanetary journey from one planet to the vicinity of a second planet may be divided into three phases – the launch phase, the midcourse phase, and the terminal phase. In the launch phase sufficient thrust is imparted to the vehicle so that it escapes the gravitational field of the launch planet and is injected into a heliocentric ballistic trajectory which carries it toward the desired destination. The midcourse phase is the phase in which the vehicle is traversing the heliocentric ballistic trajectory. The terminal phase involves any final maneuvering required to achieve the specific objectives of the mission.

The purpose of guidance during the launch phase is to inject the vehicle into the proper heliocentric trajectory. Because the launch guidance system is not ideal, the velocity of the vehicle at injection is subject to uncertainties which cause the actual heliocentric trajectory to differ from the desired trajectory. The function of the midcourse guidance system is to make measurements from which the differences between the two trajectories can be ascertained and then to compute a correction which can be applied to the vehicle so that it will reach its destination.

1.4 The Reference Trajectory

The desired heliocentric ballistic trajectory is known as the reference trajectory. The determination of a suitable reference trajectory for a given mission is a separate field in itself which falls beyond the scope of the present paper. Battin[1]* presents a technique for generating three-dimensional reference trajectories.

For the purposes of this study it is assumed that a reference trajectory has been pre-computed and that its characteristics are known to the designer of the midcourse guidance system.

1.5 Sequence of Operations

In a typical midcourse guidance system the sequence of operations is as follows:

1. A series of measurements is made. The measured values are compared with the computed values, i.e., those values that would be measured if the vehicle were on the reference trajectory and if there were no errors in making the measurements themselves.

2. The differences between the measured values and the ideal values are processed by a computer, usually a digital computer, to determine the difference between the vehicle's actual ballistic trajectory and the reference trajectory.

3. The required midcourse correction is computed as a function of the difference between actual and reference trajectories and of the time at which the correction is to be applied.

The signals representing the midcourse correction constitute the output of the guidance system and the input to the control system. The operation of the control system in actually applying the computed correction is not considered in this analysis.

1.6 Midcourse Guidance Development at the M.I.T. Instrumentation Laboratory

Of the various midcourse guidance systems that have been suggested during recent years, three, all apparently developed independently, are

*When not otherwise identified, single-digit or two-digit numbers indicate correspondingly numbered items listed in the References.

considered by the author to be representative of current thinking in the midcourse guidance field in this country. The first of the three is the work of the M.I.T. Instrumentation Laboratory, the second is the system proposed by the Jet Propulsion Laboratory of the California Institute of Technology, and the third comes from the Ames Research Center of NASA.

Reference (2), the first report in the M.I.T. series, discusses the technical feasibility of an unmanned round-trip reconnaissance of Mars. It is estimated that, if no midcourse corrections are made, the position error of the vehicle at its nominal time of arrival at Mars will be of the order of several hundred thousand miles. The weight break-down of a vehicle whose total weight is 300 lb. allots 80 lb. for the midcourse propulsion device and propellant and 60 lb. for guidance and control equipment, including the central computer.

An analysis of the proposed midcourse guidance system is presented in Reference (3). Unlike most studies that preceded it, this report uses a three-dimensional mathematical model. The system is completely self-contained within the space vehicle. The measurements consist of the angles subtended at the vehicle between the lines of sight to pairs of celestial bodies. A group of four or more angular measurements made within a relatively short time interval is used to estimate the difference between the vehicle's position on the actual trajectory at the nominal time of the measurements and the corresponding position on the reference trajectory; an estimate of the error in the vehicle's clock is also obtained. The groups of angular measurements are made at several pre-determined times during the journey.

Position estimates at two distinct times are sufficient to compute a midcourse correction. After each set of measurements has been completed, a correction is made, based on the position estimate just determined and the position estimate at the immediately preceding time of measurement.

Each correction is treated as a thrust impulse, which causes a step change in the vehicle's velocity vector. The computation of the correction is in terms of the required velocity step. Linear perturbation theory, based on the known reference trajectory, is used in all computations.

The report also contains an error analysis, including the effects of uncertainties in launch velocity, uncertainties in angular measurements, uncertainty in the measurement of elapsed time, and uncertainties in the application of the computed midcourse corrections.

In Reference (3) the midcourse correction is computed under the assumption that the destination is a point that is fixed both in heliocentric space and in time. Computation of the correction on this basis is known as fixed-time-of-arrival (FTA) guidance. For many space missions small variations in the time of arrival at the destination can be tolerated. In Reference (4) Battin developes the theory for a navigation concept in which the time of arrival is permitted to vary slightly, so that the magnitude of the required step change in velocity can be minimized. This type of computation is called variable-time-of-arrival (VTA) guidance.

A digital computer study in Reference (4) indicates that a saving of as much as 50% in weight of propellant can be realized by the use of VTA guidance. In a typical one-way trip to Mars in which four VTA midcourse corrections are applied, the first correction, made soon after launch, is by far the largest; the magnitude of the velocity step is 126 ft./sec. The sum of the magnitudes of the four corrections, which is directly proportional to the weight of propellant consumed, is 179 ft./sec. The rms value of the predicted position error at the destination is 26 miles.

The analysis in (3) and (4), as well as that in (1), is contained in the appendices of a four-volume proposal[5] for a recoverable interplanetary space probe. Chapter 5 of the proposal contains the results of an extensive computer study of the guidance system. There are also chapters describing the on-board digital computer, the communications system, and the propulsion system for supplying the corrective thrust impulses.

References (6), (7), and (8) are additional contributions by Battin. All three are concerned with the problem of optimizing particular phases of the guidance system. In (6) the problem of selecting angular sightings to be used in determining position is considered. Optimum combinations of three sightings are found for the case when there is

no clock error. When errors in both the clock and the sightings are taken into consideration, the maximum likelihood method is applied to estimate position from a redundant set of measurements.

The first part of (7) uses the filter theory approach to determine the best estimate of the actual path of the vehicle when more than two position fixes have been made. In the second part of (7) clock errors are neglected; individual angular measurements are used directly to estimate the actual path without the intermediate step of computing a position fix. An optimizing procedure is developed for selecting the particular angular measurement which provides the maximum reduction in the uncertainty of the estimate of the actual path.

Reference (8) is a continuation of the development of a method for selecting the best angular measurement. It also describes a decision-making procedure for determining when a measurement should be made and when a correction should be applied. There are tables of numerical results obtained from a computer study in which the recommended decision-making procedure is used in the midcourse guidance system of a lunar probe.

1.7 Midcourse Guidance Development at the C. I. T. Jet Propulsion Laboratory

The Jet Propulsion Laboratory's approach to midcourse guidance is described in References (9), (10), and (11).

In (9) Noton discusses "post-injection" guidance, which includes both midcourse guidance and terminal guidance. The mission is a one-way journey from Earth to either Venus or Mars. The analysis is three-dimensional, and it makes use of perturbation theory based on the pre-computed reference trajectory.

Noton considers the possibility of using either a radio-command system or a self-contained system for midcourse guidance. He makes a strong case for the use of the radio-command system for relatively simple missions, and he recommends the development of self-contained systems to be used in conjunction with the radio-command system for more sophisticated missions.

In the radio-command system several tracking stations on the surface of the earth make measurements of the angular orientation of the line of sight to the vehicle, of the vehicle's radial velocity (range rate), and possibly of range. The observed data are read into ground-based digital computers to determine the vehicle's actual trajectory. The maximum likelihood technique is used in the data processing. The required midcourse velocity correction is then computed and is transmitted to the vehicle as a radio-command signal from one of the tracking stations.

For a one-way interplanetary journey, one midcourse correction, made within ten days after launch, is deemed to be adequate to achieve the mission objective.

Both fixed-time-of-arrival and variable-time-of-arrival guidance concepts are described. It is pointed out that the fixed-time-of-arrival midcourse correction can be expressed as a linear function of the three components of the estimated position error at the nominal time of arrival at the destination. The variable-time-of-arrival correction can be expressed as a linear function of only two components of the estimated position error at the destination, these two components comprising the estimated miss distance vector.

Several types of variable-time-of-arrival guidance systems are listed. The "optimum" type is that which minimizes the magnitude of the velocity correction. The "nonoptimum" types are all intended to simplify the control system. In one such system the total impulse of the propulsion system supplying the correction is assumed to be fixed; in another the magnitude of the thrust impulse is variable, but its direction is constrained to a particular plane (either the plane perpendicular to the vehicle-sun line or the plane perpendicular to the vehicle-earth line).

Reference (10) is an extension of the work in (9). An iterative process is developed for improving the accuracy of the computation of the midcourse correction beyond that which is obtained from the initial value given by linear perturbation theory. A statistical estimate is made of the magnitude of the velocity correction and hence of the weight of propellant required. Statistical theory is also used to estimate errors at the destination.

There is a detailed discussion of the method of determining the vehicle's actual trajectory from radio measurements. During the interval that the vehicle is visible to a particular tracking station, samples of each type of measurement are taken once every ten seconds. Range rate information, obtained from doppler data, is shown to be the most effective type of measurement for reducing the uncertainty in the estimate of miss distance at the destination.

It is pointed out that all the guidance systems under consideration are characterized by the fact that the two components of miss distance are controlled. Thus, fixed-time-of-arrival guidance may be regarded as a special case of nonoptimum variable-time-of-arrival guidance in which time of arrival is the third controlled quantity. The magnitude of the velocity vector at arrival is also suggested as a possible third controlled quantity for a nonoptimum system.

Gates, Scull, and Watkins[11] present a general survey of the space guidance problem, based on the work done at the Jet Propulsion Laboratory. The guidance phase defined as midcourse guidance in Section 1.3 is sub-divided by these authors into Earth-based midcourse guidance and planetary-approach guidance. The former is the radio-command system already described; the latter, which is used only during the last one or two million miles of the interplanetary voyage, utilizes optical measurements involving the line of sight to the destination planet. It is stated that a single velocity correction derived from the earth-based midcourse system reduces the probable position error at the destination from several hundred thousand miles to several thousand miles, and the planetary-approach system causes a further reduction to a few tens or hundreds of miles.

1.8 Midcourse Guidance Development at Ames Research Center

The Ames contribution to midcourse guidance is contained in References (12) and (13). Both are concerned with guidance on a circumlunar mission, but the techniques developed are applicable to interplanetary missions as well.

Smith, Schmidt, and McGee[12] obtain an optimal estimate of a space vehicle's actual position and velocity relative to the reference trajectory by means of statistical filter theory. Whenever a set of measurements is made, the old optimal estimate is up-dated by including the effect of the new data in formulating a new optimal estimate. The key to applying the method is the determination of the weighting matrix to be applied to each new set of data; it is in the derivation of the equation for the weighting matrix that linear filter theory is utilized.

McLean, Schmidt, and McGee[13] describe a fixed-time-of-arrival guidance system. The adjoint method is used in deriving the guidance equations. The analysis is three-dimensional and is based on linear perturbation theory. The effect of neglecting nonlinear terms is discussed.

A computer study of the effects of uncertainties in the input variables shows that the total weight of propellant required for midcourse corrections is primarily a function of the accuracy of the launch guidance system. Increasing the uncertainties in the measurements made during the journey or increasing the uncertainties in the application of midcourse corrections has little effect on propellant weight but materially increases the magnitude of the predicted position and velocity errors at the destination.

1.9 Additional Literature Related to Midcourse Guidance

In this section additional papers pertinent to the study of midcourse guidance are briefly summarized.

Porter[14] is one of the first to point out the necessity for midcourse guidance on interplanetary flights because of the extreme sensitivity of position at the destination to errors in launch velocity. He also states that the determination of realistic three-dimensional reference trajectories for interplanetary journeys is considerably more complex than is indicated by a two-dimensional approach based on the assumption of coplanar planetary orbits.

Lawden[15] presents one of the first analytic treatments of midcourse guidance. He develops analytic expressions for the required midcourse velocity correction for a two-dimensional two-body model.

Baker[16] points out that the fundamental problem in interplanetary guidance is how to get the vehicle to the proper destination; a knowledge of the vehicle's position and velocity in transit may not be necessary to solve the fundamental problem. He also indicates the computational advantages of working with the differences between observed measurements and precomputed ideal values of the measurements in determining the corrections to be applied.

Wheelon[17] makes a survey of the problems of midcourse and terminal guidance. This paper was prepared as one of a group of papers which constitute a lecture course with the title Space Technology. The emphasis is on physical reasoning, with some analytic expressions being derived to illustrate the techniques involved.

The work of Magness, McGuire, and Smith[18] is not directly related to midcourse guidance, but its conclusions are relevant to a midcourse guidance study. A two-dimensional two-body analysis is made of the sensitivity of miss distance at the destination to errors in launch velocity. It is shown that this sensitivity varies widely for different reference trajectories, and certain desirable trajectories, called "guidance minimum" trajectories, are defined.

Gunkel, Lascody, and Merrilees[19] determine permissible errors in launch guidance if a Martian impact is to be achieved without the use of midcourse corrections. They devise "preferred" reference trajectories which are similar to the "guidance minimum" trajectories described in (18). Launch accuracy requirements obtained from a two-dimensional analysis are shown to be less stringent but generally of the same order of magnitude as those obtained from a more elaborate three-dimensional analysis. In order to relax the launch requirements, a single midcourse correction is recommended.

Kierstead[20], [21] extends the sensitivity analysis of (18) to three dimensions. He points out that the component of the vehicle's actual motion in the ecliptic plane, which in his simplified model is also the plane of the reference trajectory, is only loosely coupled with the component of actual motion normal to the ecliptic plane. Thus, as a first approximation for guidance studies, a considerable saving in computation is effected by studying the two types of motion independently. A

simple analytic expression is obtained for the out-of-plane motion; the in-plane motion is handled numerically. The effect of midcourse corrections on guidance requirements is treated for both Earth-based and self-contained guidance systems.

Breakwell[22] attacks the problem of determining the times at which midcourse corrections should be made in order to satisfy the criterion that the total fuel expenditure be minimized. The analysis is statistical, based on a priori knowledge of the variances in the launch velocity, the measurements, and the applied corrections. The basic mathematical model is two-dimensional, with the reference trajectory being a Hohmann-type ellipse. With these assumptions Breakwell's analysis leads to the following simple rule: After a correction has been made, wait until two thirds of the remaining transit time has elapsed before applying the next correction.

In a more recent paper[23] by Breakwell the analysis is extended to several special cases which include the effect of position error in the direction normal to the reference trajectory plane. This paper points out that a considerable saving in fuel can be achieved if a procedure is developed for utilizing all measurements made since launch in computing the next correction to be applied, rather than using only those measurements made subsequent to the immediately preceding correction.

Bock and Mundo,[24] in a survey of interplanetary guidance problems, discuss the choice of a reference trajectory and the various types of measurement systems that may be used. Measurement systems are classified as active electromagnetic, passive electromagnetic, or inertial. The physical equipment associated with each system is described, and some indication is given of performance characteristics and limitations.

Safren[25] introduces the concept of a six-component vector, consisting of three components of position variation and three components of velocity variation between actual trajectory and reference trajectory at a specified time, to define the space vehicle's actual path. It is shown that the matrix equation for the midcourse velocity correction is simplified if the specified time for which the elements of the six-component vector are evaluated is the time of arrival at the destination.

Haake and Welch[26] discuss several types of self-contained space guidance systems. The discussion includes a summary of the linearized guidance equations and a description of the required physical equipment. The problem of position determination from optical sightings of celestial angles is analyzed, and a qualitative method is proposed for the selection of angles to be measured. The advantages and disadvantages of large-angle optical trackers and small-field optical trackers are weighed; performance specifications are proposed for the design of a small-field tracker.

The method of adjoints has already been mentioned in connection with the work at Ames Research Center.[13] The application of this method to the midcourse guidance problem was suggested earlier by Dunn and Giannetto,[27] who point out that a considerable saving in computation time can be achieved by its use in generating the matrix coefficients of the linearized guidance equations.

1.10 Relation of Present Study to Previous Work in the Field

The development of midcourse guidance theory has involved the linearization of a fundamentally nonlinear set of differential equations by means of small perturbation theory. The solution of the linearized equations is manipulated to yield a matrix equation expressing the components of the midcourse velocity correction vector as a time-varying function of a set of constants which define the difference between the vehicle's actual trajectory and its reference trajectory.

Even after the differential equations are linearized, they cannot in general be solved analytically in closed form because the coefficients are time-varying. The usual procedure is to perform the necessary integrations numerically on digital computers.

The problem of determining when to apply a correction has received only cursory treatment in the literature, most investigators contenting themselves by drawing inferences from the numerical results of their computer programs. The single exception to this generalization is the work of Breakwell,[22], [23] who has performed a statistical optimization of the time of correction for several special types of reference trajectories.

The present paper extends the linear theory and develops a simple deterministic method of computing the optimum correction time as a function of one of the parameters which characterize the difference between actual and reference trajectories. The method is applicable to all types of reference trajectories.

In order to provide a deeper insight into the physics of the problem, this paper presents a complete analytic solution of the guidance equations for a mathematical model in which the reference trajectory is an ellipse. This solution materially reduces computation time required for preliminary guidance studies, and it may be applicable in the final guidance mechanization for some missions.

The determination of the six independent parameters needed to specify completely the vehicle's actual trajectory relative to the reference trajectory is the navigation problem. The parameters are evaluated from measurements made during the journey. Usually a redundant number of measurements is made, and statistical theory is used in obtaining an estimate of the parameters.

Estimation techniques for this application are discussed in References (10) and (12). Each individual measurement, when properly weighted, reduces the uncertainty in the computed values of the six parameters. Implicit in the development of the procedures in these references is the assumption that errors in the clock, if they exist at all, are so small that their effect on the numerical values of the parameters is insignificant. This assumption is undoubtedly justified when the measurements are made from Earth, as in (10), or when the duration of the voyage is relatively short, as in the case of the circumlunar trajectories considered in (12). However, for interplanetary trajectories, extending over an interval of months or possibly years, neglect of clock errors may have a significant effect.

The clock error is taken into account in Reference (3), in which the measurements are processed not singly but in groups, each group being related to a single nominal time of measurement. From each group an estimate is obtained of clock error and position variation at the nominal measurement time.

This paper extends the procedure of (3). The maximum likelihood method of estimation is used to compute position variation at the nominal measurement time and also to compute the six orbital parameters from several position variations. A simple practical technique is developed for selecting the optical measurements to be made in a self-contained guidance system.

The choice of the set of six parameters which define the actual trajectory can have a material effect on the amount of computation required. This paper exploits the suggestion of Safren[25] by selecting the six-component vector consisting of the three components of position variation and the three components of velocity variation at the nominal time of arrival at the destination.

1.11 Synopsis

An attempt has been made in the format of this thesis to emphasize in the main text the physical principles underlying guidance theory. Detailed mathematical derivations and some background material are relegated to the appendices. Each chapter and each appendix opens with a brief summary of its salient features.

The remainder of this section describes the inter-relationships among the various chapters and appendices.

Appendix A and Appendix B provide background material. They provide some of the mathematical tools that are useful in succeeding appendices.

Appendix C is parenthetical; it does not contribute to the development of guidance theory. It presents two simple and illuminating graphical constructions, not previously known to the author, which were suggested by the formulation of the equations of elliptical motion in Appendix B.

Appendix D is also parenthetical. It investigates the possibility of using elliptical cylindrical coordinates for developing the guidance theory for elliptical reference trajectories and concludes that there is no significant advantage in using this system.

Appendix E develops the variant equations of motion of the space vehicle in several coordinate systems.

Appendix F expresses the variant equations of motion and their solution in matrix form. Some special symmetry properties of the matrices are derived.

Appendices G and H present two distinct methods of solving the variant equations of motion of Appendix E for the special case when the reference trajectory is an ellipse.

Appendix I and Appendix J express the analytic solution of Appendix H as a matrix equation in several coordinate systems, the difference between the two appendices being that Appendix I treats reference trajectories for which the eccentricity is significantly greater than zero but less than unity, while Appendix J is concerned only with low-eccentricity reference trajectories.

Appendix K utilizes the results of Appendix I to obtain analytic expressions for the terms in the matrices of Appendix F.

Appendices L and M formulate the basic matrix equations of midcourse guidance, the former for FTA guidance and the latter for VTA guidance.

Appendix N develops the method of selecting the optimum time at which to apply a midcourse VTA velocity correction.

Appendix O analyzes the singularities occurring in some of the matrices of Appendix K.

Chapter 2 describes the linear approach to midcourse guidance of a vehicle in an n-body gravitational field. It makes use of the mathematical developments in Appendices E, F, L, M, and N.

Chapter 3 applies the results of Chapter 2 to missions for which the reference trajectory is an ellipse. It utilizes the material in Appendices E, G, H, I, K, L, M, N, and O.

Chapter 4 contains a numerical example which illustrates the theory developed in Chapters 2 and 3.

Appendix P is a mathematical development of the equations for the maximum likelihood estimate of a multi-dimensional random variable.

Chapter 5 discusses linear navigation theory for both Earth-based radio-command systems and self-contained optical systems. It utilizes the results of the statistical theory in Appendix P.

Chapter 6 represents an attempt to utilize the novel features of this analysis in conjunction with the best features of previous proposals in the synthesis of a simple and effective midcourse guidance system.

Chapter 7 summarizes the salient points of the study and suggests the areas in which additional work may be desirable.

CHAPTER 2

LINEAR GUIDANCE THEORY FOR AN N-BODY GRAVITATIONAL FIELD

2.1 Summary

The guidance equations for both fixed-time-of-arrival guidance and variable-time-of-arrival guidance are developed from the solution of the linearized equations of motion of a space vehicle in an n-body gravitational field. A method is outlined for determining the optimum time at which to apply a midcourse correction.

2.2 Introduction

The literature reviewed in Chapter 1 contains several papers which develop methods of computing the midcourse velocity correction as a function of the time of correction and the parameters which define the difference between the space vehicle's actual trajectory and its reference trajectory. The first part of the present chapter collates much of this material, the primary sources being References (5), (9), (13), (22), and (25).

The latter portion of the chapter extends the previously known theory by developing a relatively simple deterministic method of specifying the optimum time to apply a VTA velocity correction as a function of a single parameter of the vehicle's variant path.

2.3 Clarification of the Term "Perturbation"

In the study of guidance theory a certain amount of confusion is caused by the fact that investigators with different backgrounds sometimes use the same technical term to describe similar but not identical situations. In particular, this problem in semantics arises in the use of the word perturbation.

In the development of planetary theory astronomers start with a two-body orbit of the planet about the focus at the sun, then refine the

computation by taking into account the gravitational effects of the other planets. Smart* refers to these planets as "disturbing" planets, and the relatively small changes they cause in the two-body orbit are known as "perturbations."

A similar approach is currently used to develop desirable reference trajectories for space vehicles on interplanetary missions. The differences between the numerically computed trajectories, which include such effects as earth oblateness and gravitation due to the planets, and the corresponding two-body heliocentric trajectories are again called "perturbations." This usage is consistent with the older use of the term by astronomers.

The primary concern of the guidance analyst is the difference between the actual trajectory traversed by a space vehicle and the pre-computed reference trajectory. This difference, due to imperfect instrumentation and inexact guidance equations, is also referred to in some of the literature as a "perturbation." The mathematical technique of expressing the actual trajectory as a series expansion of certain measured or inferred deviations between the two trajectories is an application of "perturbation theory." If no terms higher than first-order are retained in the series expansion, the process is "linear perturbation theory."

Thus, the term perturbation describes two similar, but nevertheless distinct, phenomena. The older astronomical usage indicates the small deviations from a two-body orbit due to the effect of forces that have not previously been considered; the more recent space guidance usage refers to deviations from a pre-computed reference trajectory caused primarily by a change in initial conditions and to a lesser extent by a lack of precise knowledge of the required astronomical constants.

To resolve this dilemma, "perturbation" in this analysis will be used only in the sense that it is used by astronomers. The differences between the vehicle's actual trajectory and the reference trajectory will be referred to as "variations" or "deviations." The differential equations describing the motion of the vehicle relative to the reference trajectory will be called the "variant" equations of motion.

---

*Page 9 of (28).

2.4 Mathematical Model

For the purposes of this analysis the space vehicle is regarded as a small mass point moving in a three-dimensional gravitational field dominated by the sun. The masses of the planets cause disturbances which produce perturbations of the two-body motion of the vehicle in the sun's field.

All motions are referred to an origin at the center of mass of the sun. The positions of the planets as a function of time are obtained from an ephemeris; no simplifying assumptions are necessary, such as the assumption that the planetary orbits are exact conic sections or that they are exactly planar.

During the midcourse phase the vehicle's distance from any of the planets is large enough so that the effect of planetary oblateness can be neglected; therefore, the planets are treated as mass points.

Non-gravitational forces, such as those due to aerodynamic, electromagnetic, or solar radiation effects, are not considered.

Although oblateness is neglected in the variational analysis to be presented, the effect of earth oblateness should certainly be included in the computation of the reference trajectory for a trip from the earth to another planet. The reference trajectory is obtained by numerical integration of all significant gravitational forces.

The departure of the vehicle's actual trajectory from the reference trajectory is assumed to be small enough so that a linear variational analysis is acceptable.

Midcourse corrections take the form of small thrust impulses applied at several distinct times during the midcourse phase of the journey.

2.5 Equations of Motion

In vector form, the motion of the space vehicle in the gravitational field can be expressed by one compact equation.

$$\ddot{\underline{r}} + \frac{\mu}{r^3}\,\underline{r} = \nabla R \qquad (2\text{-}1)$$

where

$$R = G \sum_{i=1}^{n} m_i \left(\frac{1}{d_i} - \frac{\underline{r} \cdot \underline{r}_i}{r_i^3} \right) \qquad (2\text{-}2)$$

These equations are adapted from Page 9 of Smart.[28] They are equivalent to Equation (B-3) of Appendix B.

The function R is known as the disturbing function. It represents the effect of the n disturbing planets on the vehicle's motion.

The notation used in this thesis includes the following: Underlining a lower-case letter indicates that the letter represents a vector. The same symbol used without underlining signifies the magnitude of the vector quantity. A single dot over a symbol indicates the first derivative with respect to time of the variable represented by the symbol; similarly, two dots indicate the second time derivative, etc. Time derivatives of vectors are taken with respect to inertial space unless specified otherwise.

In Equation (2-1), $\underline{r}$ is the position vector of the vehicle on the reference trajectory with respect to the origin at the center of the sun, and $\ddot{\underline{r}}$ is the acceleration of the vehicle on the reference trajectory relative to the origin. ∇R is the gradient of the scalar function R.

The gravitational symbols G and μ are defined in Section B. 2 of Appendix B. d_i is the distance of the i-th disturbing planet, whose mass is m_i, from the space vehicle. $\underline{r}_i$ is the position vector of the i-th disturbing planet. Vectors $\underline{r}$, $\underline{r}_i$, and $\underline{d}_i$ are illustrated in Figure B. 1 of Appendix B for the case i = 1.

The component equations represented by (2-1), modified to include the effect of earth oblateness, are the equations that are integrated numerically (with the proper initial conditions) to obtain the vehicle's reference trajectory.

The variant equations of motion are obtained from the variations in the terms of (2-1) due to variations in the components of $\underline{r}$ at some arbitrary time t. In matrix form the variant equations can be written as follows:

$$\delta \ddot{\underline{r}} = \overset{*}{G}\, \delta \underline{r} \tag{2-3}$$

where

$$\overset{*}{G} = \frac{\mu}{r^5} (3\, \underline{r}\, \underline{r}^T - \underline{r}^T\, \underline{r}\, \overset{*}{I}_3) + G \sum_{i=1}^{n} \frac{m_i}{d_i^5} (3\, \underline{d}_i\, \underline{d}_i^T - \underline{d}_i^T \underline{d}_i\, \overset{*}{I}_3) \tag{2-4}$$

An asterisk over a capital letter indicates a matrix. $\overset{*}{I}_3$ is a 3-by-3 identity matrix. The superscript T signifies the transpose of a vector or matrix. The symbol δ denotes the first variation of the quantity immediately following it. The product $\underline{r}\, \underline{r}^T$, unlike the conventional dot product or cross product of vector analysis, is a 3-by-3 symmetric matrix.

It is evident from (2-4) that $\overset{*}{G}$ is a symmetric 3-by-3 matrix. It is shown in Section E. 4 that $\overset{*}{G}$ remains symmetric even when oblateness effects are taken into consideration.

The elements of $\overset{*}{G}$ are time-varying because $\underline{r}$ and $\underline{d}_i$ are time-varying. It may be noted that these elements are functions of vehicle position on the reference trajectory and do not depend on vehicle velocity. Once the reference trajectory has been determined, the elements of $\overset{*}{G}$ can be computed directly.

The derivation of (2-3) and (2-4) is given in Appendix E.

2.6 State Vector

Equation (2-3) represents three coupled second-order linear differential equations. The solution of these equations for the components of $\delta \underline{r}$ as a function of time contains six arbitrary constants, which can be regarded as the elements of a six-component column vector; such a vector is designated a path deviation vector.

In Section F. 2 several types of path deviation vectors are defined, and linear relations among the types are presented. The most useful type is that which consists of the three components of position variation and the three components of velocity variation at some specified time t_k. This particular path deviation vector is known as the state vector and is symbolized by $\delta \underline{x}_k$. The subscript k indicates that the vector refers to conditions existing at time t_k. In matrix notation,

$$\delta \underline{x}_k = \left\{ \begin{array}{c} \delta \underline{r}_k \\ \delta \underline{v}_k \end{array} \right\} \tag{2-5}$$

The state vector defines the difference between the vehicle's actual trajectory and the reference trajectory in terms of its position and velocity variations (i.e., its "state") at time t_k. For an initial condition problem, t_k becomes t_I, the time of injection into the heliocentric orbit; for a final condition problem, t_k becomes t_D, the time of arrival at the destination.

2.7 Transition Matrix

The solution of (2-3) has the form

$$\begin{aligned} \delta \underline{r}_m &= \overset{*}{M}_{mk}\, \delta \underline{r}_k + \overset{*}{N}_{mk}\, \delta \underline{v}_k \\ &= \left\{ \overset{*}{M}_{mk} \qquad \overset{*}{N}_{mk} \right\} \delta \underline{x}_k \end{aligned} \tag{2-6}$$

$\delta \underline{r}_m$ is the position variation at any arbitrary time t_m. The elements of the 3-by-3 matrices $\overset{*}{M}_{mk}$ and $\overset{*}{N}_{mk}$ depend on t_m and t_k and also on the characteristics of the reference trajectory.

By differentiating (2-6) with respect to the variable time t_m, an expression is obtained for the velocity variation $\delta \underline{v}_m$.

$$\delta \underline{v}_m = \left\{ \overset{*}{S}_{mk} \qquad \overset{*}{T}_{mk} \right\} \delta \underline{x}_k \tag{2-7}$$

$\overset{*}{S}_{mk}$ and $\overset{*}{T}_{mk}$ are 3-by-3 time-varying matrices.

Equations (2-6) and (2-7) can be combined into a single equation.

$$\delta \underline{x}_m = \overset{*}{C}_{mk}\, \delta \underline{x}_k \tag{2-8}$$

where

$$\overset{*}{C}_{mk} = \left\{ \begin{array}{cc} \overset{*}{M}_{mk} & \overset{*}{N}_{mk} \\ \overset{*}{S}_{mk} & \overset{*}{T}_{mk} \end{array} \right\} \tag{2-9}$$

The 6-by-6 matrix $\overset{*}{C}_{mk}$ is known as the transition matrix; it is the means by which the state at time t_m is determined from a specified

state at time t_k. The transition matrix has some interesting mathematical properties which are discussed in detail in Appendix F and are summarized here. First, when $t_m = t_k$, it is obvious that the transition matrix must reduce to the 6-by-6 identity matrix.

$$\overset{*}{C}_{kk} = \overset{*}{I}_6 \tag{2-10}$$

Secondly, the transition matrix relating $\delta \underline{x}_k$ to $\delta \underline{x}_m$ is the inverse of the transition matrix relating $\delta \underline{x}_m$ to $\delta \underline{x}_k$.

$$\overset{*}{C}_{km} = \overset{*}{C}_{mk}^{-1} \tag{2-11}$$

The third property also is concerned with the inverse of the transition matrix. It is shown in Appendix F that the elements of $\overset{*}{C}_{mk}^{-1}$ are the elements of $\overset{*}{C}_{mk}$ arranged in different order.

$$\overset{*}{C}_{mk}^{-1} = \begin{Bmatrix} \overset{*}{T}_{mk}^{T} & -\overset{*}{N}_{mk}^{T} \\ -\overset{*}{S}_{mk}^{T} & \overset{*}{M}_{mk}^{T} \end{Bmatrix} \tag{2-12}$$

Thus, if the elements of $\overset{*}{C}_{mk}$ have been determined, the elements of its inverse are available without need for the tedious numerical computations normally associated with inverting a 6-by-6 matrix.

Finally, despite the fact that the elements of $\overset{*}{C}_{mk}$ are time-varying, its determinant is always equal to +1.

$$\det \overset{*}{C}_{mk} = +1 \tag{2-13}$$

2.8 Numerical Solution of Variant Equations of Motion

The numerical integration of (2-3) to yield a solution of the form (2-8) is facilitated if the three second-order equations comprising (2-3) are re-arranged as six first-order equations.

$$\delta \dot{\underline{r}} = \delta \underline{v} \tag{2-14}$$

$$\delta \dot{\underline{v}} = \overset{*}{G}\, \delta \underline{r} \tag{2-15}$$

In terms of the state vector,

$$\delta \dot{\underline{x}} = \overset{*}{Z}\, \delta \underline{x} \tag{2-16}$$

where

$$\overset{*}{Z} = \begin{Bmatrix} \overset{*}{0}_3 & \overset{*}{I}_3 \\ \overset{*}{G} & \overset{*}{0}_3 \end{Bmatrix} \tag{2-17}$$

The subscript 3 on the zero and identity sub-matrices of (2-17) indicates the order of these matrices.

Since (2-8) is the solution of (2-16), it follows that

$$\frac{\partial \overset{*}{C}_{mk}}{\partial t_m} \delta \underline{x}_k = \overset{*}{Z}_m \overset{*}{C}_{mk} \delta \underline{x}_k \tag{2-18}$$

For an arbitrary $\delta \underline{x}_k$,

$$\frac{\partial \overset{*}{C}_{mk}}{\partial t_m} = \overset{*}{Z}_m \overset{*}{C}_{mk} \tag{2-19}$$

(2-19) represents thirty-six first-order equations which can be integrated numerically from $t_m = t_k$ to any other value of t_m. The initial conditions are given by the fact that $\overset{*}{C}_{kk}$ is the identity matrix. As a result of the integration the terms of $\overset{*}{C}_{mk}$ are obtained as a function of t_m for the specified value of t_k, and consequently $\delta \underline{x}_m$ is determined as a function of $\delta \underline{x}_k$.

2.9 Choice of Coordinate System

In choosing a coordinate system in which to carry out the numerical integration, there are two important considerations. First, it is desirable to use an inertially non-rotating system so that Coriolis effects do not complicate the problem. Secondly, it is advisable to choose the fixed axes such that two of them lie in the plane of the two-body motion that would occur ideally if there were no disturbing forces, and the third axis is perpendicular to that plane. With these axes the only coupling between the variant motion in the plane and the variant motion normal to the plane is due to the effect of the disturbing forces, and this effect is usually quite small. Thus, the sixth-order system can be sub-divided into two systems, one of fourth order and the other of second order, with weak coupling between the two.

Then in each of the four 3-by-3 matrices $\overset{*}{M}_{mk}$, $\overset{*}{N}_{mk}$, $\overset{*}{S}_{mk}$, and $\overset{*}{T}_{mk}$, the first two terms of the third row and the first two terms of the third column will, in general, be numerically small compared to the other five terms of the matrix, and round-off errors in the integration procedure will be materially reduced.

The two orthogonal in-plane axes may have any desired orientation; a convenient choice is that in which the positive x-axis is in the direction of perihelion from the origin at the center of the sun; then the positive y-axis is in the direction of the positive semi-latus rectum; this axis system is described in Appendix A as the "reference trajectory stationary coordinate system."

In the non-rotating coordinate system the thirty-six equations of (2-19) may be re-written as follows:

$$\frac{\partial \overset{*}{M}_{mk}}{\partial t_m} = \overset{*}{S}_{mk} \tag{2-20}$$

$$\frac{\partial \overset{*}{N}_{mk}}{\partial t_m} = \overset{*}{T}_{mk} \tag{2-21}$$

$$\frac{\partial \overset{*}{S}_{mk}}{\partial t_m} = \overset{*}{G}_m \overset{*}{M}_{mk} \tag{2-22}$$

$$\frac{\partial \overset{*}{T}_{mk}}{\partial t_m} = \overset{*}{G}_m \overset{*}{N}_{mk} \tag{2-23}$$

It is evident from these equations that $\overset{*}{M}_{mk}$ and $\overset{*}{S}_{mk}$ are inter-related, and $\overset{*}{N}_{mk}$ and $\overset{*}{T}_{mk}$ are inter-related, but there is no coupling between $\overset{*}{M}_{mk}$ and $\overset{*}{S}_{mk}$ on one hand and $\overset{*}{N}_{mk}$ and $\overset{*}{T}_{mk}$ on the other. Therefore, the thirty-six equations consist of two independent sets, each containing eighteen coupled equations.

2.10 State Vector at Destination

The most important state vector to the guidance analyst is $\delta \underline{x}_D$, the state vector at the nominal time of arrival at the destination. It is useful to be able to ascertain the effect of small variations in position and velocity at time t_C, the time of a midcourse correction, on the corresponding variations at t_D. From Equation (2-8) the effect is determined from the equation

$$\delta \underline{x}_D = \overset{*}{C}_{DC} \, \delta \underline{x}_C \tag{2-24}$$

Although t_D is a fixed time for a specified reference trajectory, t_C can take on any value between t_I and t_D. It is of interest to find the effect of varying t_C on the transition matrix $\overset{*}{C}_{DC}$. If normal forward integration is used, the thirty-six equations comprising (2-19) must be integrated from the initial values at $t = t_C$ to the end point at $t = t_D$ for each separate value of t_C. If many values of t_C are to be investigated, the amount of computing required quickly becomes prohibitive.

By making use of (2-12) and integrating backward in time from an "initial" condition at $t = t_D$, the integration process need be carried out only once. The result of the integration is a relation between $\overset{*}{C}_{CD}$ and t_C for the known fixed value of t_D. Then $\overset{*}{C}_{DC}$, the desired matrix, is obtained from $\overset{*}{C}_{CD}$ for any t_C by a simple re-arrangement of terms.

$$\overset{*}{C}_{DC} = \overset{*}{C}_{CD}^{-1} = \begin{Bmatrix} \overset{*}{M}_{DC} & \overset{*}{N}_{DC} \\ \overset{*}{S}_{DC} & \overset{*}{T}_{DC} \end{Bmatrix} = \begin{Bmatrix} \overset{*}{T}_{CD}^{T} & -\overset{*}{N}_{CD}^{T} \\ -\overset{*}{S}_{CD}^{T} & \overset{*}{M}_{CD}^{T} \end{Bmatrix} \tag{2-25}$$

2.11 Two-Position Path Deviation Vector

The only type of path deviation vector that has been discussed thus far is the state vector $\delta\underline{x}$. Another type of path deviation vector that is useful in the analysis of midcourse guidance is the two-position vector, which consists of the position variation vectors at two different times. If the two times are t_i and t_j, the two-position vector is

$$\begin{Bmatrix} \delta\underline{r}_i \\ \delta\underline{r}_j \end{Bmatrix}$$

The velocity variation at time t_i can be written in terms of the two-position vector.

$$\delta\underline{v}_i = \overset{*}{J}_{ij}\, \delta\underline{r}_i + \overset{*}{K}_{ij}\, \delta\underline{r}_j \tag{2-26}$$

where $\overset{*}{J}_{ij}$ and $\overset{*}{K}_{ij}$ are 3-by-3 matrices. From the results obtained in Appendix F, $\overset{*}{J}_{ij}$ and $\overset{*}{K}_{ij}$ can be related to the 3-by-3 sub-matrices of $\overset{*}{C}_{ji}$ and $\overset{*}{C}_{ij}$.

$$\overset{*}{J}_{ij} = - \overset{*}{N}_{ji}^{-1} M_{ji} = (\overset{*}{N}_{ij}^{T})^{-1} \overset{*}{T}_{ij}^{T} \qquad (2\text{-}27)$$

$$\overset{*}{K}_{ij} = \overset{*}{N}_{ji}^{-1} = - (\overset{*}{N}_{ij}^{T})^{-1} \qquad (2\text{-}28)$$

It is also shown in Appendix F that $\overset{*}{J}_{ij}$ is a symmetric matrix.

Equations (2-27) and (2-28) will be used in the analysis of the midcourse correction.

2.12 Midcourse Velocity Correction

The preceding sections describe the variant motion of a space vehicle in a gravitational field. Once the variant motion is known, the problem is to alter this motion by means of a midcourse correction so that the objective of the mission can be achieved.

The means of altering the motion is a short application of thrust from a reaction-type engine. Because the thrust application is so short in duration relative to the time required for the space voyage, it is treated mathematically as a thrust impulse. At the time of the correction, t_C, there is a step change in vehicle velocity but no instantaneous change in vehicle position.

Obviously, the correction causes a change in the state vector $\delta \underline{x}_k$ which characterizes the variant motion. The superscripts - and + will be used to distinguish conditions applicable before the correction from those applicable after the correction. The change in the state vector $\delta \underline{x}_C$ is given by

$$\delta \underline{x}_C^{+} - \delta \underline{x}_C^{-} = \begin{Bmatrix} \underline{0}_3 \\ \underline{c} \end{Bmatrix} \qquad (2\text{-}29)$$

where $\underline{0}_3$ is the three-dimensional zero vector and $\underline{c}$ is the velocity correction vector. The three components of $\underline{c}$ are to be computed in such a manner that three specified design conditions are satisfied.

It is apparent that a single correction cannot cause the vehicle to return immediately to its reference trajectory, because accomplishing this would require that six conditions be met (i.e., $\delta \underline{r} = \underline{0}_3$, $\delta \underline{v} = \underline{0}_3$). The three design conditions that are to be satisfied are generally associated with the vehicle's state vector when it arrives at the destination.

Thus, the correction is intended to establish a new variant path which modifies $\delta \underline{x}_D$ in some desired fashion. The difference between the corrected and the original state vectors at time t_D is related to the corresponding difference in state vectors at t_C by the equation

$$\delta \underline{x}_D^+ - \delta \underline{x}_D^- = \overset{*}{C}_{DC} (\delta \underline{x}_C^+ - \delta \underline{x}_C^-)$$

$$= \overset{*}{C}_{DC} \begin{Bmatrix} \underline{0}_3 \\ \underline{c} \end{Bmatrix} = \begin{Bmatrix} \overset{*}{N}_{DC} \\ \overset{*}{T}_{DC} \end{Bmatrix} \underline{c} \qquad (2\text{-}30)$$

In the two types of guidance system to be analyzed, all three design conditions are related to the desired position variation at the destination, $\delta \underline{r}_D^+$. Then the velocity correction can be found in terms of $(\delta \underline{r}_D^+ - \delta \underline{r}_D^-)$.

$$\underline{c} = \overset{*}{N}_{DC}^{-1} (\delta \underline{r}_D^+ - \delta \underline{r}_D^-)$$

$$= \overset{*}{K}_{CD} (\delta \underline{r}_D^+ - \delta \underline{r}_D^-) \qquad (2\text{-}31)$$

When the elements of $\overset{*}{C}_{CD}$ have been computed by backward integration, the elements of $\overset{*}{K}_{CD}$ are obtained from the sub-matrix $\overset{*}{N}_{CD}$ by means of (2-28). It may be noted that evaluation of $\overset{*}{K}_{CD}$ requires the integration of only eighteen of the thirty-six first-order equations comprising (2-19).

2.13 Fixed-Time-of-Arrival Guidance

In fixed-time-of-arrival guidance it is stipulated that the space vehicle arrive at the destination at the exact time specified by the reference trajectory. Thus, the three mathematical conditions to be satisfied by the midcourse correction are contained in the simple equation

$$\delta \underline{r}_D^+ = \underline{0}_3 \qquad (2\text{-}32)$$

With the subscript F used to denote fixed-time-of-arrival guidance, the equation for the correction is

$$\underline{c}_F = - \overset{*}{K}_{CD} \delta \underline{r}_D^- \qquad (2\text{-}33)$$

The resulting velocity variation $\delta \underline{v}_D^+$ can be determined from (2-30), with the aid of the relations given by (2-27) and (2-28).

$$\begin{aligned} \delta \underline{v}_D^+ &= \delta \underline{v}_D^- + \overset{*}{T}_{DC}\, \underline{c}_F \\ &= \delta \underline{v}_D^- - \overset{*}{T}_{DC}\, \overset{*}{K}_{CD}\, \delta \underline{r}_D^- \\ &= \left\{ -\overset{*}{J}_{DC} \qquad \overset{*}{I}_3 \right\} \delta \underline{x}_D^- \end{aligned} \tag{2-34}$$

From (2-32) and (2-34), the new and the old state vectors at t_D are related by the equation

$$\delta \underline{x}_D^+ = \begin{Bmatrix} \overset{*}{0}_3 & \overset{*}{0}_3 \\ -\overset{*}{J}_{DC} & \overset{*}{I}_3 \end{Bmatrix} \delta \underline{x}_D^- \tag{2-35}$$

A more detailed analysis of fixed-time-of-arrival guidance is presented in Appendix L.

2.14 Variable-Time-of-Arrival Guidance

In variable-time-of-arrival guidance it is required that the vehicle reach its proper destination point relative to the destination planet, but it is not required that the actual time of arrival coincide with the nominal arrival time indicated by the reference trajectory. The problem then is analogous to a simple fire-control problem, in which the motion of the "target" (i.e., the destination planet) is completely predictable.

Instead of arriving at $t = t_D$, the vehicle actually arrives at $t = t_D + \Delta t_D$, the increment Δt_D being small relative to the period of the orbital motion. At $t = t_D$ the deviation of the vehicle's actual position from the destination point on the reference trajectory is

$$\delta \underline{r}_D^+ = -\underline{v}_R\, \Delta t_D \tag{2-36}$$

where $\underline{v}_R$ is the velocity of the vehicle relative to the destination planet at $t = t_D$. It is assumed in the linear theory that $\underline{v}_R$ remains constant in the time interval between t_D and $(t_D + \Delta t_D)$. Clearly, at $t = t_D$ the vehicle's position must lie on the line through the nominal destination point and parallel to $\underline{v}_R$; this is illustrated by Figure M. 2 of Appendix M.

The variable-time-of-arrival guidance concept requires that the component of $\delta \underline{r}_D^-$ lying in the plane normal to $\underline{v}_R$ be reduced to zero by the midcourse correction. This component is designated $\delta \underline{\rho}^-$, the miss distance vector. Since $\delta \underline{\rho}$ can be considered a two-dimensional vector, only two of the three conditions that can be satisfied by the correction are contained in the equation

$$\delta \underline{\rho}^+ = \underline{0} \tag{2-37}$$

The third condition, which uniquely determines $\delta \underline{r}_D^+$ and Δt_D, is that the magnitude of the correction be a minimum.

From Eq. (2-31), the VTA correction, designated $\underline{c}_v$, is

$$\underline{c}_v = \overset{*}{K}_{CD} (-\underline{v}_R \Delta t_D - \delta \underline{r}_D^-)$$

$$= \underline{c}_F - \underline{w} \Delta t_D \tag{2-38}$$

where the vector $\underline{w}$ is defined by

$$\underline{w} = \overset{*}{K}_{CD} \underline{v}_R \tag{2-39}$$

In Section M. 4 it is shown that the magnitude of $\underline{c}_v$ is a minimum when

$$\Delta t_D = \frac{\underline{w}^T \underline{c}_F}{\underline{w}^T \underline{w}} \tag{2-40}$$

When (2-40) is substituted into (2-38), the correction becomes

$$\underline{c}_v = \left(\overset{*}{I}_3 - \frac{\underline{w}\,\underline{w}^T}{\underline{w}^T \underline{w}} \right) \underline{c}_F = -\left(\overset{*}{I}_3 - \frac{\underline{w}\,\underline{w}^T}{\underline{w}^T \underline{w}} \right) \overset{*}{K}_{CD} \delta \underline{r}_D^- \tag{2-41}$$

In Section M. 5 $\underline{c}_v$ is proved to be perpendicular to $\underline{w}$. Thus, Eq. (2-38) represents a vector right triangle whose hypotenuse is $\underline{c}_F$. The direction of $\underline{w}$ is known as the "noncritical direction," and the plane perpendicular to $\underline{w}$ is the "critical plane." $\underline{c}_v$ is the component of $\underline{c}_F$ in the critical plane.

The expected position and velocity variations at $t = t_D$ after the VTA correction is applied may be written as

$$\delta \underline{r}_D^{+} = - v_R \, \Delta t_D = \frac{\underline{v}_R \, \underline{w}^T}{\underline{w}^T \, \underline{w}} \overset{*}{K}_{CD} \, \delta \underline{r}_D^{-} \tag{2-42}$$

$$\begin{aligned} \delta \underline{v}_D^{+} &= \delta \underline{v}_D^{-} + \overset{*}{T}_{DC} \, \underline{c}_v \\ &= \delta \underline{v}_D^{-} - \overset{*}{T}_{DC} \left(\overset{*}{I}_3 - \frac{\underline{w} \, \underline{w}^T}{\underline{w}^T \, \underline{w}} \right) \overset{*}{K}_{CD} \, \delta \underline{r}_D^{-} \\ &= \delta \underline{v}_D^{-} - \overset{*}{J}_{DC} \left(\overset{*}{I}_3 - \frac{\underline{v}_R \, \underline{w}^T}{\underline{w}^T \, \underline{w}} \overset{*}{K}_{CD} \right) \delta \underline{r}_D^{-} \end{aligned} \tag{2-43}$$

The matrix relationship between $\delta \underline{x}_D^{+}$ and $\delta \underline{x}_D^{-}$ is

$$\delta \underline{x}_D^{+} = \begin{Bmatrix} \dfrac{\underline{v}_R \, \underline{w}^T}{\underline{w}^T \, \underline{w}} \overset{*}{K}_{CD} & \overset{*}{0}_3 \\ -\overset{*}{J}_{DC} \left(\overset{*}{I}_3 - \dfrac{\underline{v}_R \, \underline{w}^T}{\underline{w}^T \, \underline{w}} \overset{*}{K}_{CD} \right) & \overset{*}{I}_3 \end{Bmatrix} \delta \underline{x}_D^{-} \tag{2-44}$$

A more detailed discussion of the material in this section will be found in Appendix M.

2.15 Critical-Plane Coordinate System

The fact that the VTA correction lies in a plane perpendicular to $\underline{w}$ and the miss distance lies in a plane perpendicular to $\underline{v}_R$ suggests the possibility of simplifying the guidance equations by the use of a rotating coordinate system in which one axis, the noncritical axis, is parallel to $\underline{w}$ for any given t_C, and the other two axes lie in the critical plane. At $t = t_D$ the noncritical axis is parallel to $\underline{v}_R$, and the other two axes lie in the plane containing $\delta \underline{\rho}^{-}$.

The axis system incorporating these characteristics is designated the critical-plane coordinate system, with axes ξ, η, and ζ. The ξ-η

plane is the critical plane, and the ζ-axis is the noncritical axis. The ξ-axis lies along the line of nodes between the critical plane and the reference trajectory plane.

As t_C varies, the coordinate system rotates about the z-axis. The ξ-axis is always in the reference trajectory plane; the z-axis is always in the η-ζ plane.

In the new coordinate system the miss distance vector is

$$(\delta\underline{\rho}^-)_W = \begin{Bmatrix} \delta\xi_D^- \\ \delta\eta_D^- \end{Bmatrix} = (\delta\underline{\rho}^-) \begin{Bmatrix} \cos\ \psi \\ \sin\ \psi \end{Bmatrix} \tag{2-45}$$

where the subscript W indicates that the miss distance vector is expressed in terms of its two components in the ξ_D - η_D plane. ψ is the angle between $\delta\underline{\rho}^-$ and the positive ξ_D-axis.

The VTA correction vector, designated $\underline{c}_W$ in the critical-plane system, is given by

$$\underline{c}_W = \overset{*}{Y}\,(\delta\underline{\rho}^-)_W \tag{2-46}$$

Equation (N-30) expresses the elements of the 2-by-2 matrix $\overset{*}{Y}$ as functions of the elements of $\overset{*}{K}_{CD}$ and the orientation of $\underline{v}_R$.

Comparison of (2-46) with (2-41) indicates the conceptual simplicity achieved by use of the new coordinate system.

2.16 Optimum Time of Correction

Either (2-41) or (2-46) defines the VTA velocity correction as a function of $\delta\underline{\rho}^-$ and t_C. On an actual space mission the value of $\delta\underline{\rho}^-$ is estimated from measurements made during the voyage. The value of t_C can be chosen as any time after the last measurement and prior to t_D, the nominal time of arrival. The problem to be considered in this section is the determination of the value of t_C which, for the given $\delta\underline{\rho}^-$, minimizes the magnitude of $\underline{c}_V$.

From (2-45) and (2-46),

$$\underline{c}_W = \overset{*}{Y} \begin{Bmatrix} \delta\xi_D^- \\ \\ \delta\eta_D^- \end{Bmatrix} = (\delta\rho^-) \overset{*}{Y} \begin{Bmatrix} \cos\ \psi \\ \\ \sin\ \psi \end{Bmatrix} \qquad (2\text{-}47)$$

The magnitude of $\underline{c}_W$ varies linearly with $\delta\rho^-$ but in a nonlinear fashion with ψ and, through $\overset{*}{Y}$, with t_C. The procedure to be followed now is to find that value of t_C which minimizes $c_W^2 = c_V^2$ for the known estimate of ψ.

$$c_V^2 = \underline{c}_W^T \underline{c}_W = (\delta\rho^-)^2 \begin{Bmatrix} \cos\psi & \sin\psi \end{Bmatrix} \overset{*T}{Y} \overset{*}{Y} \begin{Bmatrix} \cos\psi \\ \\ \sin\psi \end{Bmatrix} \qquad (2\text{-}48)$$

For each of several values of ψ, Equation (2-48) is used to compute and plot $c_V/\delta\rho^-$ as a function of t_C. The minimum value of $c_V/\delta\rho^-$ for each curve occurs at the optimum correction time, $t_{C_{opt}}$, for the ψ corresponding to that curve. A cross-plot can then be made of $t_{C_{opt}}$ versus ψ. This single design curve serves to define the optimum correction time as a function of the angular orientation of the predicted miss distance vector.

A second cross-plot, $(c_V/\delta\rho^-)_{min}$ versus ψ, can be drawn if desired, to indicate the magnitude of the minimum correction for a given $\delta\rho^-$.

Although ψ, as defined, can vary from 0° to 360°, only angles between 0° and 180° need be used in the plots and the cross-plots, since an increase of 180° in ψ reverses the direction of $\underline{c}_V$ but has no effect on its magnitude.

2.17 Multiple Corrections

The analysis of the past few sections relates to the determination of a single velocity correction, applied at $t = t_C$, which under ideal conditions enables the space vehicle to achieve the desired objective at

$t = t_D$ without the need for any further corrections. In any practical situation conditions are not ideal. The estimated position variation at the destination, $\delta \underline{r}_D^-$, is inaccurate due to inaccuracies in the measurements made during the voyage, and also there are inaccuracies in the application of the computed velocity correction.

The consequence of these inaccuracies is that, after a midcourse correction has been applied, additional measurements indicate a new non-zero value of the vector that is to be nulled ($\delta \underline{r}_D$ in FTA navigation, $\delta \underline{\rho}$ in VTA navigation), and a new correction vector can be computed. The guidance theory that has been presented is applicable to each individual correction in turn, irrespective of the number of corrections that have preceded.

For VTA corrections made late in the flight, it is likely that the optimum t_C will have occurred before the time of the last measurement; in that case the determination of $t_{C_{opt}}$ has no practical significance.

2.18 Applicability of Linear Theory

The basic vector equation of motion of a space vehicle in a gravitational field is (2-1), which is nonlinear. Once a reference trajectory has been established, the general solution for the actual motion can be expressed as an equation relating the state vector $\delta \underline{x}_m$ at any arbitrary time t_m to the characteristics of the reference trajectory and the components of the state vector $\delta \underline{x}_k$ at some specified time t_k.

$$\delta \underline{x}_m = \delta \underline{x}_m (\underline{x}_k, \delta \underline{x}_k, t_k, t_m) \qquad (2\text{-}49)$$

In this equation the characteristics of the reference trajectory are contained in $\underline{x}_k$, which represents the components of position and velocity on the reference trajectory at t_k.

The components of $\delta \underline{x}_m$ can be written as a Taylor series expansion in the components of $\delta \underline{x}_k$. Let $(\delta x_m)_u$ represent the u-th component of $\delta \underline{x}_m$. Also let $(\delta x_k)_i$ and $(\delta x_k)_j$ represent the i-th and j-th components of $\delta \underline{x}_k$. The series expansion for $(\delta x_m)_u$ is

$$(\delta x_m)_u = \sum_{i=1}^{6} \frac{\partial (x_m)_u}{\partial (x_k)_i} (\delta x_k)_i$$

$$+ \frac{1}{2} \sum_{i=1}^{6} \sum_{j=1}^{6} \frac{\partial^2 (x_m)_u}{\partial (x_k)_i \, \partial (x_k)_j} (\delta x_k)_i (\delta x_k)_j + \cdots \qquad (2\text{-}50)$$

The six partial derivatives in the first term on the right-hand side of (2-50) are the elements of the u-th row of the transition matrix $\overset{*}{C}_{mk}$.

In the linear theory $(\delta x_m)_u$ is equated to the first term on the right-hand side; the remaining terms on the right-hand side constitute the truncation error, the lead term of which appears on the second line of (2-50). The magnitude of the truncation error is a function of the magnitudes of the higher-order partial derivatives in (2-50) and also of the magnitudes of the components of $\delta \underline{x}_k$. The applicability of linear theory is determined by the magnitude of the truncation error in relation to the permissible error in the components of $\delta \underline{x}_D$, the state vector at the destination.

The magnitudes of the components of $\delta \underline{x}_k$ are determined primarily by the accuracy with which the vehicle is injected into its heliocentric orbit. The more accurate the injection guidance system, the greater is the likelihood that linear theory is acceptable for midcourse guidance.

The magnitudes of the higher-order partial derivatives depend on the reference trajectory and on the times t_k and t_m. For interplanetary missions the magnitudes are relatively high in regions close to a planet, where the nonlinear gravitational force field is strong. If times t_k and t_m are such that at neither time is the vehicle close to a planet, the truncation error is materially reduced.

The fundamental state vector in midcourse guidance is $\delta \underline{x}_D$. Equation (2-50) is used to determine the components of $\delta \underline{x}_D$. For missions in which the vehicle at its point of closest approach to the destination planet is within several planet radii of the surface of the planet, the truncation error in computing $\delta \underline{x}_D$ by linear analysis may be reduced by selecting as the

destination point for the midcourse guidance system an earlier point on the reference trajectory, such as the point at which the reference trajectory intersects the planet's sphere of influence, and then using a separate terminal guidance scheme for final maneuvering. (The sphere of influence is that region surrounding the surface of a planet in which the planet itself, rather than the sun, should be used as the main body in Equation (2-1). A mathematical derivation of the expression for the radius of the sphere appears on Pages 234 and 235 of Plummer[29] and also on Pages 478 and 479 of Ehricke, Vol. I.[30] Ehricke refers to the sphere as the "activity sphere" rather than the "sphere of influence".)

A quantitative study of the truncation error has been reported by McLean, Schmidt, and McGee.[13] In this work the FTA correction was computed at several points on both the outbound and the inbound legs of a circumlunar trajectory. For the outbound leg the destination point is the perilune, at a lunar altitude of 2960 miles; the inbound destination point is at vacuum perigee. It is shown that the truncation error in position at the destination due to the neglect of second-order variational terms in computing the midcourse velocity correction is proportional to the square of the magnitude of the position variation $\delta \underline{r}_C$ at the time of the correction, the proportionality factor being a function of the range $\underline{r}_C$ (in a geocentric coordinate system). The proportionality factor is of the order of 10^{-4} mi./mi.^{2} near the two ends of either leg of the reference trajectory and is smaller in the middle, the minimum value of 10^{-6} mi./mi.^{2} occurring about two-thirds of the way out on the outbound leg. Thus, if at two-thirds of the way out, the position variation is 10,000 miles and a velocity correction is applied in accordance with linear theory, the position variation at perilune due to truncation error is approximately 100 miles. The author is not aware of any similar quantitative study of truncation error for interplanetary trajectories.

CHAPTER 3

LINEAR GUIDANCE THEORY FOR ELLIPTICAL REFERENCE TRAJECTORIES

3.1 Summary

For the special case of two-body motion the variant motion in the plane of the reference trajectory is uncoupled from the variant motion normal to that plane. Therefore, with the proper choice of a coordinate system, each of the 3-by-3 matrices defined in the linear theory of Chapter 2 contains four elements which are identically zero for all values of time.

Two different methods are presented for solving analytically the variant equations of motion when the reference trajectory is an ellipse. The solution is used to obtain analytic expressions for the five non-zero elements of each of the 3-by-3 matrices of Chapter 2. Singularities occurring in some of the matrix elements are discussed.

3.2 Introduction

The linear theory of Chapter 2 enables the solution of the variant equations of motion to be expressed by the simple matrix equation (2-8). However, the time-varying elements of the transition matrix $\overset{*}{C}_{mk}$ cannot be found analytically; numerical integration is required to evaluate the elements. In this chapter an analytic solution is obtained by imposing a limitation on the mathematical model of Chapter 2. The new limitation is the assumption that the perturbations due to the disturbing planets are neglibible and therefore the resulting motion of the vehicle is two-body motion in the sun's gravitational field. This two-body approximation is deemed to be reasonably realistic for the midcourse phase of an interplanetary flight, when the vehicle's distance from the nearest planet is relatively large.

Utilization of the two-body assumption in the guidance analysis does not require that the same assumption be used in obtaining the reference trajectory. The reference trajectory is still to be obtained accurately by the numerical integration of the basic vector equation (2-1). The midcourse phase of the trajectory is then approximated by a conic section with one focus at the center of the sun, and the orbital elements

of this conic section are computed for use in the guidance analysis. However, variations measured or inferred from the analysis are variations of the actual trajectory from the numerically computed reference trajectory, not variations from the conic approximation. Thus, the primary effects of the disturbing forces are included in the analysis, but the changes in the disturbing forces due to the fact that the vehicle is not on the reference trajectory are ignored.

The assumption of two-body motion gives rise to two interesting conditions, each of which can be used to obtain an analytic solution of the variant equations of motion. The first condition is that the variant motion in the plane of the reference trajectory is independent of the variant motion normal to that plane. Because of this condition, the sixth-order system represented by Equation (2-3) can be replaced by two uncoupled systems, one of fourth order and one of second order, and both systems can be integrated analytically. The second condition is that, inasmuch as the reference trajectory is approximated by a conic section, the actual trajectory, which differs from the reference trajectory only due to a change in initial conditions, can also be approximated by a conic section, and the relation between the two trajectories can be expressed in terms of the variations of six orbital elements.

The first condition was recognized by Kierstead, [20], [21] who solved the second-order system describing the out-of-plane motion but apparently made no attempt to obtain a similar solution for the fourth-order system describing in-plane motion. The second condition was utilized by Battin in Appendix G of (5) in developing analytic expressions for an elaborate set of matrices which can be combined to yield a solution for the variant motion without the use of integration. However, the author is not aware of any previously published literature which carries out the two-body analysis, as in the succeeding sections of this chapter, to derive relatively straightforward analytic expressions for all the elements in the basic matrices of Chapter 2.

In performing the detailed analysis, only elliptical reference trajectories are considered, since these are deemed to be the only conic sections of practical importance in the midcourse phase of interplanetary transfers.

3.3 Coordinate Systems

The problem of selecting a coordinate system has already been discussed in Section 2.9 in connection with the numerical integration of the equations of the many-body problem. It was pointed out in that section that there is an advantage to selecting a system in which two of the three axes lie in the reference trajectory plane. This advantage is even more pronounced in the analysis of two-body motion, for now the uncoupling between in-plane and out-of-plane motion is complete, and consequently the two types of motion may be treated independently.

Appendix A describes three reference trajectory coordinate systems, each of which has been found to be useful in one phase of the development. The three are the stationary system with axes x y z, the local vertical system with axes r s z, and the flight path system with axes p q z. In all three the origin is at the center of the sun, and all have the same z-axis. In the x y z system the x-axis is in the direction of perihelion of the reference trajectory; the axes are non-rotating. In the r s z system the r-axis is in the direction of the vehicle's position vector on the reference trajectory; the r and s axes are rotating in the reference trajectory plane with angular velocity f, where f is the true anomaly (the angle between the position vector on the reference trajectory and the x-axis). In the p q z system the q-axis is parallel to the instantaneous velocity vector of the vehicle in its motion on the reference trajectory; the p and q axes rotate with angular velocity $\dot{g}$, where g is the angle between the velocity vector and the y-axis. It may be noted that when the vehicle is at perihelion of its reference trajectory all three coordinate systems instantaneously coincide.

The x y z system is most appropriate when the problem is to be solved numerically, as in Chapter 2. The r s z system is used to obtain an analytic solution of the variant equations of motion of the two-body problem. The p q z system yields the simplest form for the analytic expressions for the elements of the basic matrices of Chapter 2.

A fourth coordinate system that might at first glance appear useful is the elliptical cylindrical coordinate system. There are some striking similarities between this system and the p q z system. Appendix D is an analysis of the elliptical system and its applicability to the guidance problem. It is concluded that this curvilinear coordinate system offers no significant advantages over the three rectilinear systems that have already been discussed.

3.4 Equations of Motion

For the two-body problem, the vector equation of motion, (2-1), simplifies to

$$\ddot{\underline{r}} + \frac{\mu}{r^3}\,\underline{r} = \underline{0}_3 \tag{3-1}$$

where $\underline{0}_3$ is the three-dimensional zero vector. If (3-1) is regarded as describing motion along the reference trajectory, the component equations in the x y z coordinate system are

$$\begin{pmatrix} \ddot{x} \\ \ddot{y} \end{pmatrix} + \frac{\mu}{r^3}\begin{pmatrix} x \\ y \end{pmatrix} = \begin{pmatrix} 0 \\ 0 \end{pmatrix} \tag{3-2}$$

where

$$x^2 + y^2 = (r^2 \cos^2 f + r^2 \sin^2 f) = r^2 \tag{3-3}$$

In the r s z coordinate system the component equations are

$$\begin{pmatrix} \ddot{r} - r\dot{f}^2 \\ r\ddot{f} + 2\dot{r}\dot{f} \end{pmatrix} + \frac{\mu}{r^3}\begin{pmatrix} r \\ 0 \end{pmatrix} = \begin{pmatrix} 0 \\ 0 \end{pmatrix} \tag{3-4}$$

No z-axis equation is required because the coordinate systems have been defined in such a manner that the motion is confined to the plane perpendicular to the z-axis; i.e., z is identically zero for all values of t.

Equations (3-4) can be integrated directly. A single integration of the lower equation yields

$$r^2 \dot{f} = h \tag{3-5}$$

The constant h is the orbital angular momentum of the space vehicle per unit mass. (3-5) is used in integrating the upper equation of (3-4). The result is

$$r = \frac{h^2/\mu}{1 + e \cos f} \tag{3-6}$$

(3-5) and (3-6) constitute the familiar solution of two-body motion. (3-6) is the general equation of a conic section with the origin at one focus and the line f = 0 coinciding with the major axis of the conic.

These relations, as well as many more that are useful in celestial mechanics, are discussed in Appendix B. Appendix C, which has no direct bearing on the main subject matter of this thesis, describes two interesting graphical constructions which evolved from the formulations for elliptical motion in Appendix B.

The vector form of the variant equations of motion for the two-body problem, corresponding to (2-3) and (2-4) for the n-body problem, is

$$\delta \ddot{\underline{r}} = \overset{*}{G}\, \delta \underline{r} \tag{3-7}$$

with

$$\overset{*}{G} = \frac{\mu}{r^5} (3 \underline{r}\, \underline{r}^T - \underline{r}^T\, \underline{r}\, \overset{*}{I}_3) \tag{3-8}$$

Equation (3-7), like (3-1), is most easily integrated when the component equations are expressed in the r s z coordinate system. In this system $\overset{*}{G}$ is a diagonal matrix.

$$\overset{*}{G} = \frac{\mu}{r^3}\begin{pmatrix} 2 & 0 & 0 \\ 0 & -1 & 0 \\ 0 & 0 & -1 \end{pmatrix} \tag{3-9}$$

The component equations are simplified if δf is used in place of δs.

$$\delta s = r\,\delta f \tag{3-10}$$

Then the three equations to be integrated are

$$\begin{pmatrix} \delta\ddot{r} - \dot{f}^2\,\delta r - 2r\dot{f}\,\delta\dot{f} \\ 2\dot{f}\delta\dot{r} + \ddot{f}\delta r + r\delta\ddot{f} + 2\dot{r}\delta\dot{f} \\ \delta\ddot{z} \end{pmatrix} = \frac{\mu}{r^3}\begin{pmatrix} 2\delta r \\ 0 \\ -\delta z \end{pmatrix} \tag{3-11}$$

The detailed derivation of (3-11) is presented in Appendix E and Section G.2 of Appendix G.

The uncoupling effect mentioned previously is brought out by (3-11). The first two equations, involving the dependent variables δr and δf, are not coupled to the third equation, in which δz is the only dependent variable.

3.5 Variant Motion Normal to the Reference Trajectory Plane

The z-axis equation of (3-11) may be written as

$$\delta\ddot{z} + \frac{\mu}{r^3}\delta z = 0 \tag{3-12}$$

Comparison of (3-12) with (3-2) indicates that x and y are independent solutions for δz.

$$\delta z = K_1 x + K_2 y \tag{3-13}$$

$$= r (K_1 \cos f + K_2 \sin f) \tag{3-14}$$

$$= (K_1^2 + K_2^2)^{1/2} r \sin \left(f + \tan^{-1} \frac{K_1}{K_2} \right) \tag{3-15}$$

where K_1 and K_2 are arbitrary constants.

This simple solution for the variant motion normal to the reference trajectory plane is independent of the nature of the two-body reference trajectory; the reference trajectory may be elliptical, parabolic, or hyperbolic.

3.6 Integration of the Variant Equations for Elliptical Reference Trajectories

The integration of the first two equations of (3-11) is carried out in Sections G.3 and G.4. The two equations constitute a fourth-order system in δr and δf. The first of the four independent solutions can be obtained directly by virtue of the fact that δf does not appear explicitly in either equation. It is apparent that both equations are satisfied if δf is a constant and δr is identically zero. Thus, the first solution is

$$\delta r = 0 \qquad \delta f = k_1 \tag{3-16}$$

where k_1 is an arbitrary constant.

If the independent variable in the two equations is changed from the time t to the true anomaly f and the two equations are combined, the following third-order equation is obtained:

$$[(1 + e \cos f) F - (3 e \sin f)] (F^2 + 1) \delta r = 0 \tag{3-17}$$

where F represents the operator d/df and e is the eccentricity of the reference trajectory. Two more solutions for δr follow immediately from

$$(F^2 + 1)\,\delta r = 0 \tag{3-18}$$

These are

$$\delta r = k_2 \cos f \tag{3-19}$$

$$\delta r = k_3 \sin f \tag{3-20}$$

The corresponding solutions for δf are

$$\delta f = -\frac{k_2}{a\,(1 - e^2)}\,(2 + e \cos f) \sin f \tag{3-21}$$

$$\delta f = \frac{k_3}{a\,(1 - e^2)}\,(2 + e \cos f) \cos f \tag{3-22}$$

To obtain the fourth solution, the new variable x is introduced, where

$$x = (F^2 + 1)\,\delta r \tag{3-23}$$

Then, Equation (3-17) becomes

$$(1 + e \cos f)\,\frac{dx}{df} - (3\,e \sin f)\,x = 0 \tag{3-24}$$

After the variables x and f are separated, the equation is integrated, with the result

$$x = \frac{C}{(1 + e \cos f)^3} \tag{3-25}$$

C is another integration constant. The method of variation of parameters is used to solve (3-25) for the fourth solution of δr. After considerable mathematical manipulation, all of which is explained in

Section G.4, the solution is

$$\delta r = k_4 \left[- \frac{3 e M \sin f}{2 (1 - e^2)^{3/2}} + \frac{1}{1 + e \cos f} \right] \qquad (3\text{-}26)$$

where M is the mean anomaly. For this value of δr, δf is

$$\delta f = - \frac{3 k_4}{2 a (1 - e^2)^{5/2}} M (1 + e \cos f)^2 \qquad (3\text{-}27)$$

Section G.5 presents a method of solution of the z-axis equation of (3-11) which is less direct than that given in Section 3.5. The solution in G.5 involves the substitution of the eccentric anomaly E for the time t as the independent variable. The differential equation becomes

$$[(1 - e \cos E) J^2 - (e \sin E) J + 1] \delta z = 0 \qquad (3\text{-}28)$$

where J signifies the operator d/dE. The two independent solutions for δz are

$$\delta z = \frac{k_5}{(1 - e^2)^{1/2}} \sin E = k_5 \frac{\sin f}{1 + e \cos f} \qquad (3\text{-}29)$$

$$\delta z = \frac{k_6}{(1 - e^2)} (\cos E - e) = k_6 \frac{\cos f}{1 + e \cos f} \qquad (3\text{-}30)$$

Since the radius r is proportional to $1/(1 + e \cos f)$, it is apparent that the second forms of (3-29) and (3-30) are consistent with the solution of (3-14).

The results of this section may be combined to give the complete homogeneous solution of the equations of (3-11), the dependent variables δr, δs, and δz being expressed in terms of the anomalies f and M.

$$\delta r = k_2 \cos f + k_3 \sin f + k_4 \left[- \frac{3 e M \sin f}{2 (1 - e^2)^{3/2}} + \frac{1}{1 + e \cos f} \right] \qquad (3\text{-}31)$$

$$\delta s = \frac{k_1 a (1 - e^2)}{1 + e \cos f} - \frac{k_2 (2 + e \cos f) \sin f}{1 + e \cos f}$$

$$+ \frac{k_3 (2 + e \cos f) \cos f}{1 + e \cos f} - \frac{3 k_4 M (1 + e \cos f)}{2 (1 - e^2)^{3/2}} \qquad (3\text{-}32)$$

$$\delta z = \frac{k_5 \sin f}{1 + e \cos f} + \frac{k_6 \cos f}{1 + e \cos f} \qquad (3\text{-}33)$$

3.7 Solution by Variation of the Orbital Elements of the Elliptical Reference Trajectory

The past few sections have presented a method of determining position along the actual trajectory by formulating and then integrating the differential equations of the variant motion. A second method, to be presented in this section, follows a different procedure. The basic vector equation of two-body motion, (3-1), is integrated, the result being the familiar conic section. The solution for position on the actual trajectory is obtained by finding the effect on position at any given time of small variations in each of the six orbital elements characterizing the basic conic section. Whereas the first method involves taking variations and then integrating, the second method involves integrating and then taking variations. A detailed analysis of the second method appears in Appendix H.

The fundamental premise of the second method is that the actual trajectory, like the reference trajectory, is an ellipse and that the two ellipses lie close to each other in space. To distinguish quantities on the actual trajectory from the corresponding quantities on the reference trajectory, a prime will be added to each symbol referring to the actual trajectory. Thus, the position variation $\delta \underline{r}$ is

$$\delta \underline{r} = \underline{r}' - \underline{r} \qquad (3\text{-}34)$$

The six orbital elements whose variations are to be investigated are the semi-major axis length a, the eccentricity e, the longitude of the ascending node Ω, the inclination i, the latitude of perihelion ω, and the time of perihelion passage t_o. These elements are discussed in Section B.6. Later the longitude of perihelion ϕ is substituted for ω, and the mean anomaly M_o at epoch is substituted for t_o.

$$\phi = \Omega + \omega \tag{3-35}$$

$$M_o = - n t_o \tag{3-36}$$

where n is the mean angular motion, i.e., the mean angular velocity of the space vehicle in its elliptical orbit about the sun.

The basic analysis is applicable to all elliptical reference trajectories for which the eccentricity is not very close to either zero or one.

As shown in Figure H.1, the orientation of the actual trajectory with respect to the reference trajectory is defined by the three angles $\delta\Omega$, δi, and $\delta\omega$. The angles $\delta\Omega$ and $\delta\omega$ need not be small, but their sum, which is equal to $\delta\phi$, is a small angle. The angle δi is always small. The variation in true anomaly, δf, although time-varying, is also small.

The components of $\underline{r}'$ along the r, s, and z axes are designated r'_r, r'_s, and r'_z, respectively. The components of $\underline{r}$ along these axes are, by definition, r, 0, and 0. From Figure H.1, the effect of variations in the orientation angles on the components of $\delta\underline{r}$ are

$$\begin{aligned}
\delta r &= r'_r - r \\
&= r' \left[\cos (f' + \delta\omega) \cos (f - \delta\Omega) \right. \\
&\quad \left. + \sin (f' + \delta\omega) \cos \delta i \sin (f - \delta\Omega) \right] - r \\
&= r' \cos (\delta f + \delta\phi) - r \\
&= r' - r
\end{aligned} \tag{3-37}$$

$$\delta s = r'_s - 0$$

$$= r' [- \cos (f' + \delta \omega) \sin (f - \delta \Omega)$$

$$+ \sin (f' + \delta \omega) \cos \delta i \cos (f - \delta \Omega)]$$

$$= r' \sin (\delta f + \delta \phi)$$

$$= r (\delta f + \delta \phi) \qquad (3\text{-}38)$$

$$\delta z = r'_z - 0$$

$$= r' \sin (f' + \delta \omega) \sin \delta i$$

$$= r \delta i \sin (f - \delta \Omega) \qquad (3\text{-}39)$$

In these relations the usual small-angle approximations have been applied to $\delta \phi$, δi, and δf. Also, second-order terms in the small variational quantities have been neglected, the small quantities consisting of $(\delta r/r)$ in addition to the angles just cited.

Comparison of (3-39) with (3-15) indicates that

$$(K_1^2 + K_2^2)^{1/2} = \delta i \qquad (3\text{-}40)$$

$$\tan^{-1} \frac{K_1}{K_2} = - \delta \Omega \qquad (3\text{-}41)$$

The analysis presented below for determining the effects of δa, δe, and δt_o on $\delta \underline{r}$ differs from the basic presentation in Appendix H in that the former is applicable only to ellipses of "moderate" eccentricity (the only practical ones for interplanetary transfers to neighboring planets), while the latter can be used in the circular or nearly circular case as well as in the case of moderate eccentricity. The restriction to moderate eccentricity simplifies the analysis considerably.

For ellipses of moderate eccentricity, linear theory requires that the angular variations δE, δM, and δM_o, like δf, be small angles.

The analysis proceeds as follows:

1. δr is expressed as a function of δa, δe, and δf.

2. δr is expressed as a function of δa, δe, and δE.

3. By equating the two expressions for δr, a relation is found between δf and δE.

4. Kepler's equation and Kepler's third law are used to find δE as a function of δa, δe, and δt_o.

5. The expression for δE is substituted into the expressions for δr and δf to obtain final relations for δr and δs in terms of variations in the orbital elements.

From the basic equation

$$r = \frac{a(1-e^2)}{1+e\cos f} \tag{3-42}$$

δr becomes

$$\delta r = r' - r$$

$$= \frac{(a+\delta a)\left[1-(e+\delta e)^2\right]}{1+(e+\delta e)\cos(f+\delta f)} - \frac{a(1-e^2)}{1+e\cos f}$$

$$= a\left[\frac{(1-e^2-2e\,\delta e)+(1-e^2)\frac{\delta a}{a}}{1+e\cos f - e\sin f\,\delta f+\cos f\,\delta e} - \frac{1-e^2}{1+e\cos f}\right]$$

(equation continued on next page)

$$= \frac{a}{1 + e \cos f} \left\{ \left[(1 - e^2 - 2 e \delta e) + (1 - e^2) \frac{\delta a}{a} \right] \right.$$

$$\left. \cdot \left[1 + \frac{e \sin f \delta f - \cos f \delta e}{1 + e \cos f} \right] - (1 - e^2) \right\}$$

$$= \frac{a}{1 + e \cos f} \left[(1 - e^2) \frac{\delta a}{a} - \left(e + \frac{\cos f + e}{1 + e \cos f} \right) \delta e \right.$$

$$\left. + \frac{(1 - e^2) e \sin f}{1 + e \cos f} \delta f \right] \qquad (3\text{-}43)$$

The expression for r in terms of E is

$$r = a (1 - e \cos E) \qquad (3\text{-}44)$$

Then δr is

$$\delta r = (a + \delta a) [1 - (e + \delta e) \cos (E + \delta E)]$$

$$- a (1 - e \cos E)$$

$$= (a + \delta a) (1 - e \cos E + e \sin E \delta E - \cos E \delta e)$$

$$- a (1 - e \cos E)$$

$$= a [(1 - e \cos E) \frac{\delta a}{a} - \cos E \delta e + e \sin E \delta E]$$

$$= \frac{a}{1 + e \cos f} \left[(1 - e^2) \frac{\delta a}{a} - (\cos f + e) \delta e \right.$$

$$\left. + (1 - e^2)^{1/2} e \sin f \delta E \right] \qquad (3\text{-}45)$$

When (3-43) is equated to (3-45),

$$\delta f = \frac{1 + e \cos f}{(1 - e^2) e \sin f} \left[\left(e + \frac{\cos f + e}{1 + e \cos f} - \cos f - e \right) \delta e \right.$$

$$\left. + (1 - e^2)^{1/2} e \sin f \delta E \right]$$

$$= \frac{\sin f}{1 - e^2} \delta e + \frac{1 + e \cos f}{(1 - e^2)^{1/2}} \delta E \qquad (3\text{-}46)$$

Two expressions for the mean anomaly can be obtained from the definition of mean anomaly and from Kepler's equation.

$$M = n\,(t - t_o) = E - e \sin E \tag{3-47}$$

The variation in M is

$$\begin{aligned} \delta M &= (n + \delta n)\,(t - t_o - \delta t_o) - n\,(t - t_o) \\ &= (E + \delta E) - (e + \delta e) \sin (E + \delta E) \\ &\quad - E + e \sin E \end{aligned} \tag{3-48}$$

(3-48) is solved for δE.

$$\delta E = \frac{1}{1 - e \cos E}\,\left[(t - t_o)\,\delta n - n\,\delta t_o + \sin E\,\delta e\right] \tag{3-49}$$

δn can be expressed in terms of δa by means of Kepler's third law of planetary motion.

$$\mu = n^2 a^3 \tag{3-50}$$

Since μ is invariant,

$$\delta \mu = 0 = 2 n a^3\,\delta n + 3 n^2 a^2\,\delta a \tag{3-51}$$

$$\delta n = -\frac{3}{2}\,n\,\frac{\delta a}{a} \tag{3-52}$$

Then δE becomes

$$\delta E = \frac{1 + e \cos f}{1 - e^2}\left(-\frac{3}{2}\,M\,\frac{\delta a}{a} - n\,\delta t_o\right) + \frac{\sin f}{(1 - e^2)^{1/2}}\,\delta e \tag{3-53}$$

This expression is substituted into (3-45) and (3-46) to yield equations for δr and δs in terms of $(\delta a/a)$, $n\,\delta t_o$, δe, and $\delta \phi$, with the time-varying quantities being f and M. The parameters representing the variations of the orbital elements have been arranged such that they are all non-dimensional. The final equations for the components of $\delta \underline{r}$ are

$$\delta r = a\left[\left(\frac{1-e^2}{1+e\cos f} - \frac{3\,M\,e\sin f}{2\,(1-e^2)^{1/2}}\right)\frac{\delta a}{a} - \frac{e\sin f}{(1-e^2)^{1/2}}\,n\,\delta t_o - \cos f\,\delta e\right] \tag{3-54}$$

$$\delta s = a\left[-\frac{3M\,(1+e\cos f)}{2\,(1-e^2)^{1/2}}\,\frac{\delta a}{a} - \frac{(1+e\cos f)}{(1-e^2)^{1/2}}\,n\,\delta t_o + \left(\frac{2+e\cos f}{1+e\cos f}\right)\sin f\,\delta e + \frac{(1-e^2)}{(1+e\cos f)}\,\delta\phi\right] \tag{3-55}$$

$$\delta z = \frac{a\,(1-e^2)}{1+e\cos f}\,(\sin f\,\delta i\cos\delta\Omega - \cos f\,\delta i\sin\delta\Omega) \tag{3-56}$$

It is shown in Section H.7 that the six constants of integration in (3-31), (3-32), and (3-33) can be written in terms of the variations in the orbital elements, and therefore the two methods of solution of the problem of the variant motion of the space vehicle are mathematically equivalent. The conclusion that can be drawn is that, in the solution for the deviation of the actual trajectory from the reference trajectory caused by small variations in initial conditions, the processes of integration and taking of first variations are commutative.

3.8 Variation in Position, Velocity, and Acceleration

The time-varying elements of Equations (3-54), (3-55), and (3-56) can be expressed in terms of the components of position and velocity along the reference trajectory by the use of the standard relations developed in Appendix B. The components of velocity variation $\delta \underline{v}$ are obtained by differentiating $\delta \underline{r}$, and the components of variation in acceleration $\delta \underline{a}$ are obtained by differentiating $\delta \underline{v}$. All of these results are contained in the following three vector equations, the details of which are developed in Appendix I.

$$\delta \underline{r} = \left(r \underline{u}_r - \frac{3}{2} v t \underline{u}_q\right)\frac{\delta a}{a} + \frac{v}{n} \underline{u}_q \delta M_o + \left(\frac{y}{1 - e^2} \underline{u}_s - a \underline{u}_x\right) \delta e + r \underline{u}_s \delta \phi + r \sin (f - \delta \Omega) \delta i \underline{u}_z \tag{3-57}$$

$$\delta \underline{v} = \left(-\frac{v}{2} \underline{u}_q - \frac{3}{2} a_r t \underline{u}_r\right) \frac{\delta a}{a} + \frac{a_r}{n} \underline{u}_r \delta M_o + \left(\frac{-v \sin f \underline{u}_p + v_s \cos f \underline{u}_s}{1 - e^2}\right) \delta e - v \underline{u}_p \delta \phi + v \cos (g - \delta \Omega) \delta i \underline{u}_z \tag{3-58}$$

$$\delta \underline{a} = \frac{\mu}{r^3}\left\{\left[(2 r - 3 v_r t) \underline{u}_r + \frac{3}{2} v_s t \underline{u}_s\right] \frac{\delta a}{a} + \frac{1}{n} (2 v_r \underline{u}_r - v_s \underline{u}_s) \delta M_o - \left[2 a \cos f \underline{u}_r + \left(\frac{y}{1 - e^2} + a \sin f\right) \underline{u}_s\right] \delta e - r \underline{u}_s \delta \phi - r \sin (f - \delta \Omega) \delta i \underline{u}_z\right\} \tag{3-59}$$

$$
\begin{pmatrix} \delta r \\ \delta s \\ \delta z \\ \delta v_r \\ \delta v_s \\ \delta v_z \\ \delta a_r \\ \delta a_s \\ \delta a_z \end{pmatrix} =
\left[\begin{array}{cccccc}
r - \frac{3}{2} v_r t & \frac{v_r}{n} & -a\cos f & 0 & 0 & 0 \\
-\frac{3}{2} v_s t & \frac{v_s}{n} & \frac{y}{1-e^2} + a\sin f & r & 0 & 0 \\
0 & 0 & 0 & 0 & y & -x \\
-\frac{v_r}{2} - \frac{3}{2} a_r t & \frac{a_r}{n} & -\frac{v_s \sin f}{1-e^2} & -v_s & 0 & 0 \\
-\frac{v_s}{2} & 0 & \frac{v_y}{1-e^2} & v_r & 0 & 0 \\
\hline
\frac{\mu}{r^3}\begin{pmatrix} 0 & 0 & 0 & 0 & v_y & -v_x \\ 2r - 3v_r t & \frac{2v_r}{n} & -2a\cos f & 0 & 0 & 0 \\ \frac{3}{2} v_s t & -\frac{v_s}{n} & -\frac{y}{1-e^2} - a\sin f & -r & 0 & 0 \\ 0 & 0 & 0 & 0 & -y & x \end{pmatrix}
\end{array}\right]
\begin{pmatrix} \frac{\delta a}{a} \\ \delta M_o \\ \delta e \\ \delta\phi \\ \delta i \cos\delta\Omega \\ \delta i \sin\delta\Omega \end{pmatrix}
\tag{3-61}
$$

In these equations $\underline{u}$ represents a unit vector, with the appended subscript indicating its direction. v_r and v_s are the r-direction and s-direction components of the orbital velocity vector $\underline{v}$. a_r is the radial component of acceleration; it is equal to the magnitude of the acceleration vector $\ddot{\underline{r}}$.

$$a_r = -\frac{\mu}{r^2} \tag{3-60}$$

Equation (3-61) is a composite matrix equation presenting the components of $\delta \underline{r}$, $\delta \underline{v}$, and $\delta \underline{a}$ in the r s z coordinate system. The symbols v_x and v_y, introduced in this equation, are the components of $\underline{v}$ in the x and y directions, respectively.

A comparison of the last three rows of (3-61) with the first three rows indicates that (3-7), in conjunction with (3-9), is satisfied by the solution obtained for $\delta \underline{r}$.

It may be noted that, of the fifty-four terms in the 9-by-6 matrix of (3-61), twenty-seven, half of the total number, are equal to zero.

3.9 Discussion of Effects of Variations in Orbital Elements

Some insight into the geometric and dynamic effects of variations of the orbital elements on the position and velocity of the space vehicle may be gained from Equations (3-57), (3-58), and (3-61), and Figures 3.1 to 3.5. The lack of coupling between the variant motion in the reference trajectory plane and the variant motion normal to that plane is indicated by the equations; position and velocity in the plane are affected only by variations in the elements a, M_o, e, and ϕ, while position and velocity in the z direction are affected only by variations of the other two elements, Ω and i.

In the following paragraphs the effect of a positive variation in each of the orbital elements will be investigated. Because of the linearity assumption, negative variations of the elements produce effects that are exactly opposite to their positive counterparts. (In this context, the out-of-plane "elements" are $\delta i \cos \delta\Omega$ and $\delta i \sin \delta\Omega$.)

The effect of a positive ($\delta a/a$) is illustrated in Figure 3.1. There are two distinct components, one geometric and the other dynamic in origin. The geometric effect is manifested by a change in size, but not in shape, of the elliptical trajectory. All linear dimensions on the actual trajectory are in the ratio $1 + (\delta a/a)$ to the corresponding dimensions on the reference trajectory. The two trajectories are confocal rather than concentric, since the attractive focus (i.e., the center of the sun) is the only point directly related to the reference orbit that cannot be affected by any variations.

The geometric effect on position can be derived very simply from Equation (3-44). Since e and E are independent of δa,

$$\frac{\delta r}{r} = \frac{\delta a}{a} \tag{3-62}$$

Then the ratio of the magnitude of r' to the magnitude of r is

$$\frac{r'}{r} = \frac{r + \delta r}{r} = 1 + \frac{\delta r}{r} = 1 + \frac{\delta a}{a} \tag{3-63}$$

The increased size of the elliptical trajectory reduces the magnitude of the velocity vector. This is readily seen from the vis viva integral.

$$v^2 = \mu \left(\frac{2}{r} - \frac{1}{a} \right) \tag{3-64}$$

$$= \frac{\mu}{a} \left(\frac{1 + e \cos E}{1 - e \cos E} \right) \tag{3-65}$$

Since μ is invariant and e and E are independent of δa,

$$\left(\frac{v'}{v} \right)^2 = \left(\frac{v + \delta v}{v} \right)^2 = \frac{a}{a'} = \frac{a}{a + \delta a} \tag{3-66}$$

$$1 + 2 \frac{\delta v}{v} = \frac{1}{1 + \frac{\delta a}{a}} = 1 - \frac{\delta a}{a} \tag{3-67}$$

$$\frac{\delta v}{v} = -\frac{1}{2} \frac{\delta a}{a} \tag{3-68}$$

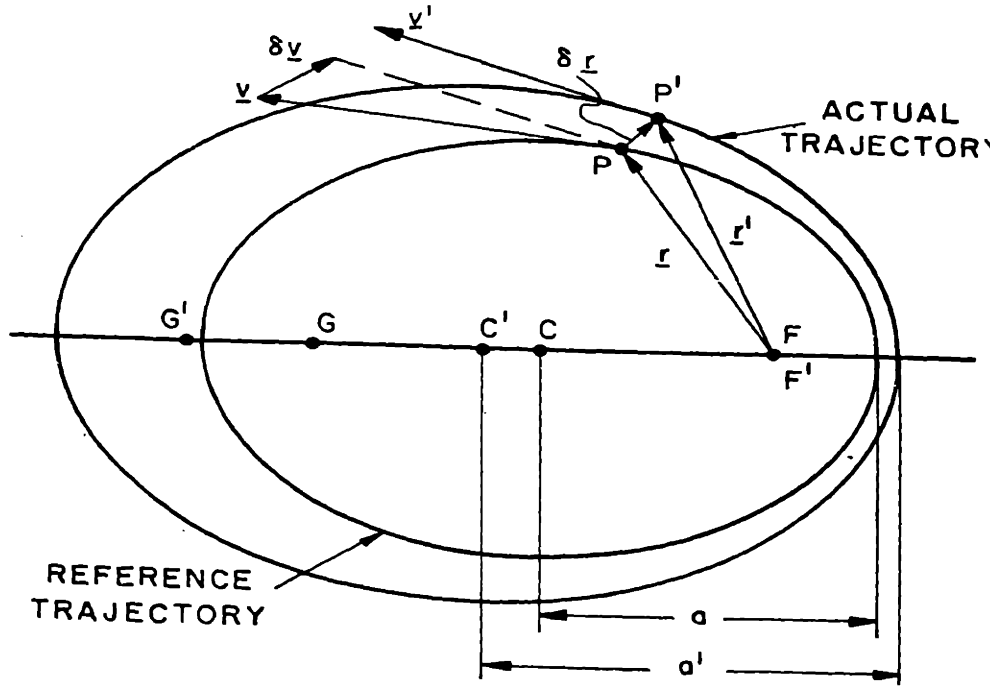

Unprimed capital letters apply to reference trajectory.
Primed capital letters apply to actual trajectory.

F,F' – common attractive focus of two trajectories

C,C' – centers of two trajectories

G,G' – vacant foci of two trajectories

P,P' – position on two trajectories at time t

$\delta a = a' - a$ = variation in length of semi-major axis

$\delta \underline{r} = \underline{r}' - \underline{r}$ = variation in position

$\delta \underline{v} = \underline{v}' - \underline{v}$ = variation in velocity

Figure 3.1 Effect of δa, Variation in Length of Semi-Major Axis

The dynamic effect of ($\delta a/a$) is a consequence of Kepler's third law of planetary motion, which states that the squares of the periods of the planetary orbits are proportional to the cubes of their mean distances from the sun. Since the period P is inversely proportional to the mean angular motion n, the following expression for δP is obtained from (3-52):

$$\frac{\delta P}{P} = -\frac{\delta n}{n} = \frac{3}{2}\frac{\delta a}{a} \tag{3-69}$$

Thus, increasing the length of the semi-major axis increases the period of the elliptical motion and consequently causes a retardation in position. From (3-57), the position change is

$$-\frac{3}{2} v t \frac{\delta a}{a} \underline{u}_q = -v t \frac{\delta P}{P} \underline{u}_q \tag{3-70}$$

Unlike all the other variational effects, which are either periodic in time or constant, the dynamic effect of ($\delta a/a$) increases in magnitude continuously with elapsed time. If the space vehicle makes several circuits of the sun, the total change in position between two times that are exactly one period of the reference trajectory apart is

$$\begin{aligned} \delta \underline{r}\,(t+P) - \delta \underline{r}\,(t) &= -v\,\delta P\,\underline{u}_q \\ &= -3\pi \frac{v}{n}\frac{\delta a}{a}\underline{u}_q \end{aligned} \tag{3-71}$$

This position retardation is parallel to the local reference velocity vector $\underline{v}$.

The velocity change due to the dynamic effect is

$$-\frac{3}{2} a_r t \frac{\delta a}{a} \underline{u}_r = -a_r t \frac{\delta P}{P} \underline{u}_r \tag{3-72}$$

Since a_r is a negative quantity, a positive ($\delta a/a$) causes a change in $\underline{v}$ in the positive r direction. This effect can be seen qualitatively in Figure 3.1. The position retardation due to ($\delta a/a$) causes $\underline{v}'$ to be rotated clockwise relative to $\underline{v}$, thereby producing a positive component of $\delta \underline{v}$ in the r direction. The velocity equation corresponding to (3-71) is

$$\delta \underline{v}\,(t + P) - \delta \underline{v}\,(t) = - a_r\, \delta P\, \underline{u}_r$$

$$= - 3\pi \frac{a_r}{n} \frac{\delta a}{a} \underline{u}_r = \frac{3\pi\mu}{n\, r^2} \frac{\delta a}{a} \underline{u}_r \qquad (3\text{-}73)$$

It may be noted that the geometric component of (δ a/a) changes the magnitude of $\underline{r}$ and $\underline{v}$ but has no effect on their directions, while the dynamic component causes a position change in the direction of the reference velocity vector and a velocity change in the direction of the reference acceleration vector, which is also the direction of the reference position vector.

Figure 3.2 indicates the effect of a positive variation of mean anomaly at epoch. The actual trajectory coincides with the reference trajectory. The position and velocity of the vehicle on the actual trajectory at time t are those that it would have at a slightly later time if it were on the reference trajectory.

The mathematical explanation of this effect is straightforward. From (3-36), since n is independent of δM_o,

$$\frac{\partial t_o}{\partial M_o} = - \frac{1}{n} \qquad (3\text{-}74)$$

Thus, when M_o is the only orbital element of those appearing in (3-57) and (3-58) to experience a variation, the variations in position and velocity are

$$\frac{\partial \underline{r}}{\partial M_o}\, \delta M_o = \frac{v}{n}\, \delta M_o\, \underline{u}_q = - v\, \delta t_o\, \underline{u}_q \qquad (3\text{-}75)$$

$$\frac{\partial \underline{v}}{\partial M_o}\, \delta M_o = \frac{a_r}{n}\, \delta M_o\, \underline{u}_q = - a_r\, \delta t_o\, \underline{u}_q \qquad (3\text{-}76)$$

The positive δM_o signifies that at epoch (i.e., at t = 0) the actual mean anomaly is slightly more positive than the reference mean anomaly. Correspondingly, the vehicle actually passes perihelion (M = 0) at a time slightly earlier than the time t_o at which it would have passed

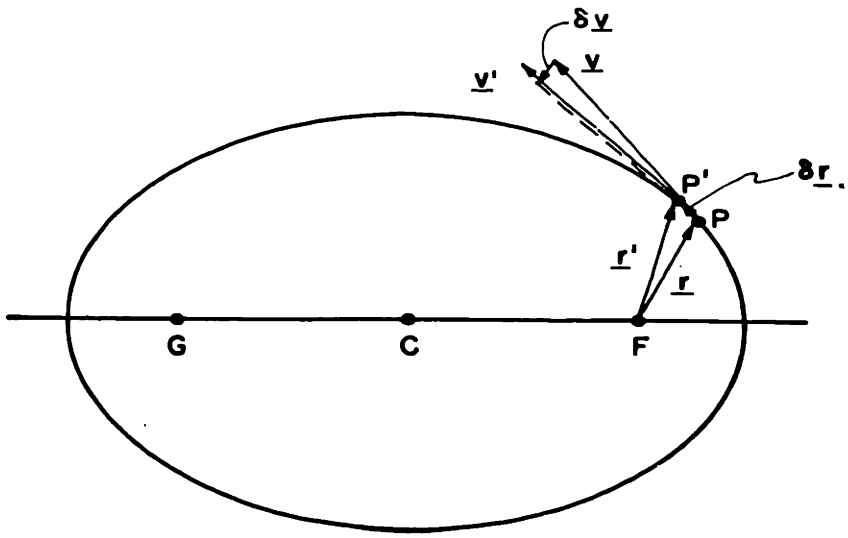

Reference trajectory and actual trajectory coincide.

F – attractive focus

C – center

G – vacant focus

P – reference position at time t

P' – actual position at time t

δM_o = variation in mean anomaly at epoch

$\delta \underline{r} = \underline{r}' - \underline{r}$ = variation in position

$\delta \underline{v} = \underline{v}' - \underline{v}$ = variation in velocity

Figure 3.2 Effect of δM_o, Variation in Mean Anomaly at Epoch

if it were on the reference trajectory. Therefore t_o', the actual time of perihelion passage, is less positive than t_o, and δt_o, which is equal to $(t_o' - t_o)$, is negative, as indicated in (3-74). Since the time interval between the vehicle's actual state and its reference state is shown by (3-75) and (3-76) to remain fixed at δt_o for all values of elapsed time, the actual position and velocity vectors may be related to the reference vectors as follows:

$$\underline{r}'(t) = \underline{r}(t - \delta t_o) \tag{3-77}$$

$$\underline{v}'(t) = \underline{v}(t - \delta t_o) \tag{3-78}$$

The effect of an increase in eccentricity, shown in Figure 3.3, is somewhat more complex than the effect of variations of any of the other elements. The elliptical trajectory undergoes both a translation and a distortion. The translation is a shift parallel to the major axis in the direction of aphelion, with the attractive focus remaining fixed. This is indicated by the term $-a\,\delta e\,\underline{u}_x$ in (3-57). Geometrically, it can be explained by the fact that the perihelion distance is changed from $a(1 - e)$ to $a(1 - e - \delta e)$ and the aphelion distance is changed from $a(1 + e)$ to $a(1 + e + \delta e)$; thus, both perihelion and aphelion are shifted an amount $a\,\delta e$ in the negative x direction.

The distortion effect produces the reduction in the length of the ordinates of the ellipse that is required by the increase in eccentricity. The first term in the coefficient of δe in (3-57) is the mathematical expression for the distortion. Its physical meaning is clarified if it is expanded as follows:

$$\frac{y}{1 - e^2}\,\underline{u}_s\,\delta e = \left(-\frac{y \sin f}{1 - e^2}\,\underline{u}_x + \frac{y \cos f}{1 - e^2}\,\underline{u}_y\right)\delta e \tag{3-79}$$

Since $y = 0$ at both perihelion and aphelion, neither point is affected by the distortion. Because $y \sin f$ is non-negative, all other points on the reference trajectory are displaced in the negative x direction; this displacement is in addition to the fixed shift that has already been noted. The y coordinate is increased in magnitude on the perihelion side of the attractive focus and decreased in magnitude on the aphelion side.

The computation of the change in the length of the semi-minor axis b can be used to illustrate the way in which (3-79) provides the required distortion. The eccentric anomaly E corresponding to the positive semi-minor axis is 90°. The length of the semi-minor axis is

$$b = a\,(1 - e^2)^{1/2} \tag{3-80}$$

The variation of b due to a variation in e can be obtained quite simply from (3-80) without recourse to (3-79).

$$\frac{\partial b}{\partial e}\,\delta e = -\frac{a\,e}{(1 - e^2)^{1/2}}\,\delta e \tag{3-81}$$

The same result can be derived from (3-79) by first determining the variation of any value of y due to δe and making use of the relations in Section B.8.

$$\frac{\partial y}{\partial e}\,\delta e = \frac{y \cos f}{1 - e^2}\,\delta e = \frac{a \sin E\,(\cos E - e)}{(1 - e^2)^{1/2}\,(1 - e \cos E)}\,\delta e \tag{3-82}$$

The variation in b is then obtained by substituting E = 90° into (3-82).

$$\frac{\partial b}{\partial e}\,\delta e = -\frac{a\,e}{(1 - e^2)^{1/2}}\,\delta e \tag{3-83}$$

As a final note on the effect of δe on $\delta \underline{r}$, the coefficient of δe in (3-57) will be derived directly from the relations for x and y in terms of E given in Section B.8. On the reference trajectory,

$$\begin{aligned} \underline{r} &= x\,\underline{u}_x + y\,\underline{u}_y \\ &= a\,(\cos E - e)\,\underline{u}_x + a\,(1 - e^2)^{1/2} \sin E\,\underline{u}_y \end{aligned} \tag{3-84}$$

The variation in $\underline{r}$ due to δe is

$$\frac{\partial \underline{r}}{\partial e} \delta e = a (- \sin E \, \delta E - \delta e) \, \underline{u}_x + a \left[(1 - e^2)^{1/2} \cos E \, \delta E - \frac{e \sin E}{(1 - e^2)^{1/2}} \delta e \right] \underline{u}_y \tag{3-85}$$

Equation (3-47) is used to relate δE to δe. Since t is the independent variable and n and t_o are unaffected by δe, the variation in M is zero.

$$\delta M = 0 = (1 - e \cos E) \, \delta E - \sin E \, \delta e \tag{3-86}$$

$$\delta E = \frac{\sin E}{1 - e \cos E} \delta e \tag{3-87}$$

(3-87) is substituted into (3-85). After simplification the result is

$$\frac{\partial \underline{r}}{\partial e} \delta e = \left[- \left(a + \frac{y \sin f}{1 - e^2} \right) \underline{u}_x + \frac{y \cos f}{1 - e^2} \underline{u}_y \right] \delta e$$

$$= \left(\frac{y}{1 - e^2} \underline{u}_s - a \, \underline{u}_x \right) \delta e \tag{3-88}$$

The coefficient of δe in (3-88) is identical with the coefficient of δe in (3-57).

Equation (3-58) indicates that the velocity change due to δe can be written as the vector sum of two components, one in the s direction and the other in the p direction. The s, or transverse, component can be explained in terms of Kepler's second and third laws of planetary motion. Since both the reference trajectory and the actual trajectory have the same major axis length, according to the third law both have the same period. From the second law, the "swept area" law, which can be deduced from (3-5), the rate at which the position vector sweeps through the area of an elliptical trajectory is constant. The constant is not the same for

the reference and actual trajectories because, although they have the same period, the area of the former is larger than the area of the latter.

Figure 3.3 indicates that the percentage of the total area of the actual trajectory that is on the perihelion side of the attractive focus is smaller than the percentage of the total area of the reference trajectory on the perihelion side. Therefore, $\underline{r}'$ must rotate more rapidly than $\underline{r}$ on the perihelion side, and, since the periods are equal, $\underline{r}'$ must rotate less rapidly than $\underline{r}$ on the aphelion side. This line of reasoning is borne out by the fact that the time-varying part of the coefficient of $\underline{u}_s \, \delta e$ in (3-58) is $v_s \cos f$. The direction of the rotation of $\underline{r}$ is by definition the s direction. Since v_s is always positive, the sign of the coefficient of $\underline{u}_s \, \delta e$ is the sign of cos f; consequently, $\delta \underline{v}$ has a component in the s direction that is positive when cos f is positive (i.e., on the perihelion side of the attractive focus) and negative when cos f is negative (i.e., on the aphelion side of the attractive focus).

Since the y component of $\delta \underline{r}$ is zero when sin f is zero, vehicles on the actual and reference trajectories pass through their respective perihelions at the same time, and they also pass through their respective aphelions at the same time. In the journey from perihelion to aphelion the actual position vector leads the reference position vector (that is, $f' > f$), while in the journey from aphelion to perihelion the actual position vector lags the reference position vector ($f' < f$). The lead of $\underline{r}'$ relative to $\underline{r}$ in motion from perihelion toward aphelion causes $\underline{v}'$ to be rotated toward the attractive focus (i.e., in the negative p direction) relative to $\underline{v}$. Conversely, the lag of $\underline{r}'$ relative to $\underline{r}$ in motion from aphelion toward perihelion causes a rotation of the velocity vector in the positive p direction. The rotation of the $\underline{v}$ vector is one of the two sources of the p component of velocity variation due to δe.

The other source of the p component of velocity variation due to δe is the variation in the rate of change of the magnitude of $\underline{r}$. In flight from perihelion to aphelion, for which the time duration is one half the period on both trajectories, the magnitude of $\underline{r}$ increases from $a(1 - e)$ to $a(1 + e)$, the net change being $2ae$; in a similar flight the net change in the magnitude of $\underline{r}'$ is $2a(e + \delta e)$. Since the change in the magnitude

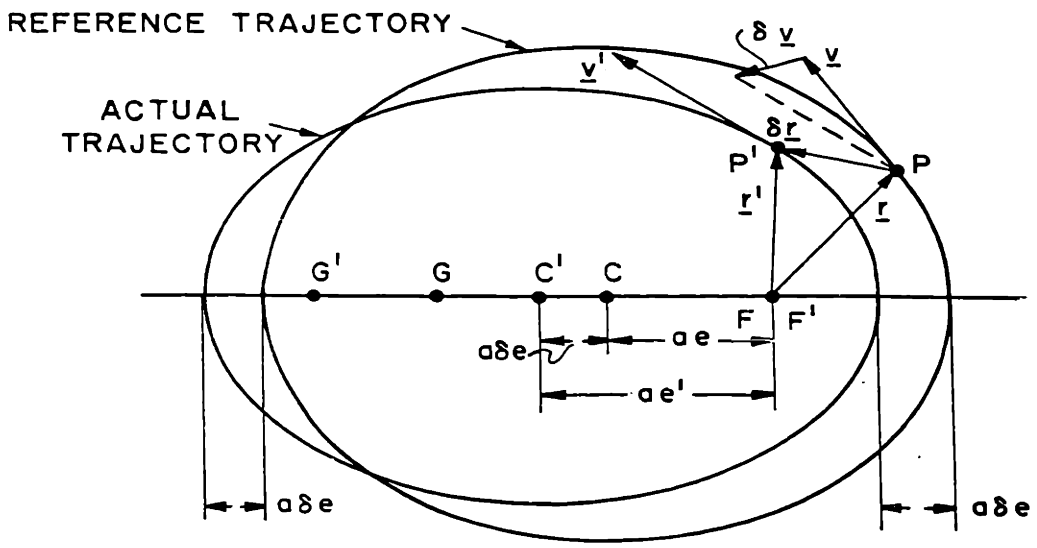

Unprimed capital letters apply to reference trajectory.
Primed capital letters apply to actual trajectory.

F,F' — common attractive focus of two trajectories

C,C' — centers of two trajectories

G,G' — vacant foci of two trajectories

P,P' — position on two trajectories at time t

$\delta e = e' - e$ = variation in eccentricity

$\delta \underline{r} = \underline{r}' - \underline{r}$ = variation in position

$\delta \underline{v} = \underline{v}' - \underline{v}$ = variation in velocity

Figure 3.3 Effect of δe, Variation in Eccentricity

of $\underline{r}'$ is more positive than the change in the magnitude of $\underline{r}$ and the same time is required for both journeys, the average value of $\dot{r}'$ is more positive than the average value of $\dot{r}$. On the trip from aphelion to perihelion the reverse is true; the average value of $\dot{r}'$ is more negative than the average value of $\dot{r}$.

The effect of the rotation of $\underline{v}$ and the effect of the variation in $\dot{r}$ tend to balance each other. On the basis of the qualitative discussion that has been presented, it is not possible to assign any relative weighting to the two factors. A mathematical analysis will now be made in order to relate the two quantitatively. The effect of both factors on δv_r, the component of $\delta \underline{v}$ in the radial direction, will be determined.

From Figure 3.3 the effect of the rotation of $\underline{v}$ on δv_r is

$$\delta v_r = - v \cos \gamma \sin \delta f = - v_s \delta f \tag{3-89}$$

The effect of the variation in $\dot{r}$ is

$$\delta v_r = \dot{r}' \cos \delta f - \dot{r} = \dot{r}' - \dot{r} = \delta \dot{r} \tag{3-90}$$

From Equation (B-65),

$$\dot{r} = \frac{n a e \sin f}{(1 - e^2)^{1/2}} \tag{3-91}$$

The variation of $\dot{r}$ is

$$\delta \dot{r} = \frac{n a}{(1 - e^2)^{3/2}} [\sin f \, \delta e + (1 - e^2) e \cos f \, \delta f] \tag{3-92}$$

The variation of the true anomaly can be obtained from the relation for sin f in terms of e and E.

$$\sin f = \frac{(1 - e^2)^{1/2} \sin E}{1 - e \cos E} \tag{3-93}$$

The variation of sin f is

$$\cos f \, \delta f = \frac{(\cos E - e)[\sin E \, \delta e + (1 - e^2) \, \delta E]}{(1 - e^2)^{1/2} (1 - e \cos E)^2} \tag{3-94}$$

But cos f is given by

$$\cos f = \frac{\cos E - e}{1 - e \cos E} \tag{3-95}$$

so that

$$\delta f = \frac{\sin E \, \delta e + (1 - e^2) \, \delta E}{(1 - e^2)^{1/2} \quad (1 - e \cos E)} \tag{3-96}$$

(3-87) is substituted into (3-96) in order to express δf in terms of the single variation δe.

$$\delta f = \frac{[(1 - e \cos E) + (1 - e^2)] \sin E}{(1 - e^2)^{1/2} \quad (1 - e \cos E)^2} \, \delta e$$

$$= \frac{(2 + e \cos f) \sin f}{1 - e^2} \, \delta e \tag{3-97}$$

(3-97) is substituted into (3-92), and the expression for v_s given by (B-66) is utilized.

$$\delta \dot{r} = \frac{n a}{(1 - e^2)^{3/2}} \, (1 + e \cos f)^2 \sin f \, \delta e$$

$$= \frac{(1 + e \cos f) \, v_s \sin f}{1 - e^2} \, \delta e \tag{3-98}$$

From (3-89) and (3-97) the effect of the rotation of $\underline{v}$ is

$$- v_s \, \delta f = - \frac{(2 + e \cos f) \, v_s \sin f}{1 - e^2} \, \delta e \tag{3-99}$$

The total effect of δe on δv_r is

$$\frac{\partial v_r}{\partial e}\,\delta e = -\,v_s\,\delta f + \delta \dot{r}$$

$$= \left[-\,(2 + e\cos f) + (1 + e\cos f)\right]\frac{v_s \sin f}{1 - e^2}\,\delta e$$

$$= -\frac{v_s \sin f}{1 - e^2}\,\delta e \qquad (3\text{-}100)$$

This equation is in agreement with the term in the fourth row, third column of the matrix in (3-61).

From (3-100) it is apparent that the rotation of $\underline{v}$ is the dominant factor in determining the direction of the effect of δe on δv_r (and also on δv_p).

Equation (3-100) points up the analogy between the variational operator δ and the derivative operator (d/dt) in the rotating r s z coordinate system. The radial component of the acceleration $\underline{a}$ on the reference trajectory is

$$a_r = \frac{d}{dt}(\underline{v}) \cdot \underline{u}_r = \frac{d}{dt}(\dot{r}) - v_s \frac{d}{dt}(f) \qquad (3\text{-}101)$$

The radial component of the velocity variation $\delta \underline{v}$ relative to the reference trajectory is

$$\delta v_r = \delta \underline{v} \cdot \underline{u}_r = \delta \dot{r} - v_s\,\delta f \qquad (3\text{-}102)$$

Variation in ϕ, the longitude of perihelion, causes a simple rotation, in the reference trajectory plane, of the actual trajectory relative to the reference trajectory. The angle of rotation is the fixed angle $\delta\phi$. The effect is to rotate both the position vector and the velocity vector through $\delta\phi$ without affecting the magnitude of either.

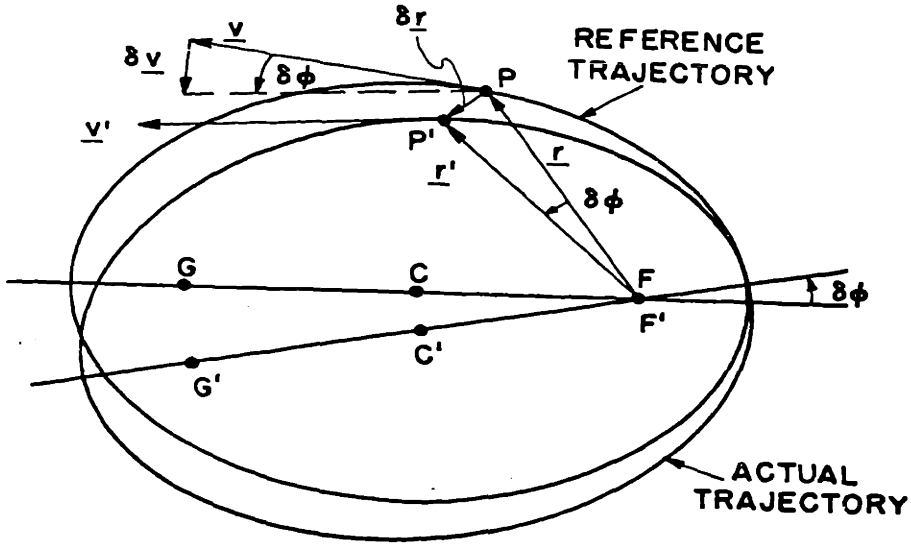

Unprimed capital letters apply to reference trajectory.
Primed capital letters apply to actual trajectory.

F,F' – common attractive focus of two trajectories

C,C' – centers of two trajectories

G,G' – vacant foci of two trajectories

P,P' – position on two trajectories at time t

$\delta\phi$ = variation in longitude of perihelion

$\delta\underline{r} = \underline{r}' - \underline{r}$ = variation in position

$\delta\underline{v} = \underline{v}' - \underline{v}$ = variation in velocity

Figure 3.4 Effect of $\delta\phi$, Variation in Longitude of Perihelion

$$\frac{\partial \underline{r}}{\partial \phi}\,\delta\phi = r\,\delta\phi\,\underline{u}_s \qquad (3-$$

$$\frac{\partial \underline{v}}{\partial \phi}\,\delta\phi = -\,v\,\delta\phi\,\underline{u}_p \qquad (3-$$

These relations are illustrated by Figure 3.4.

Because z and v_z are identically zero on the reference trajecto for all values of time, δz and δv_z are simply the projections on the z-axis of $\underline{r}'$ and $\underline{v}'$, respectively, as shown in Figure 3.5. In the lin approximation, the magnitudes of $\underline{r}$ and $\underline{v}$ are not affected by the var tions δz and δv_z. Also, the actual true anomaly f' is equal to the r erence true anomaly f. Then,

$$\delta z = \underline{r}' \cdot \underline{u}_z = r\,\delta i \sin (f - \delta\Omega) \qquad (3$$

$$\delta v_z = \underline{v}' \cdot \underline{u}_z = v\,\delta i \cos (g - \delta\Omega) \qquad (3$$

Angles $\delta\Omega$ and δi define the orientation of the actual trajectory plane relative to the reference trajectory plane. If δi is zero, $\delta\Omega$ undefined, and there are no variations in the z direction. Since $\delta\Omega$ defined as the variation (from zero) of the longitude of the ascendi node, δi is always positive. $\delta\Omega$ may have any value from 0° to 360 The out-of-plane "elements" appearing in the six-component vecto the right-hand side of (3-61) are $\delta i \cos \delta\Omega$ and $\delta i \sin \delta\Omega$, each of which is small and can take on either positive or negative values.

Because the force field is conservative, the variation in accel tion, $\delta \underline{a}$, depends only on $\delta \underline{r}$ and is independent of $\delta \underline{v}$. The variat in the magnitude of $\underline{a}$ comes directly from (3-60).

$$\delta a_r = \frac{2\mu}{r^3}\,\delta r \qquad (3$$

On the reference trajectory $\underline{a}$ is collinear with $\underline{r}$; on the actu trajectory $\underline{a}'$ is collinear with $\underline{r}'$. Therefore, the small angle bet

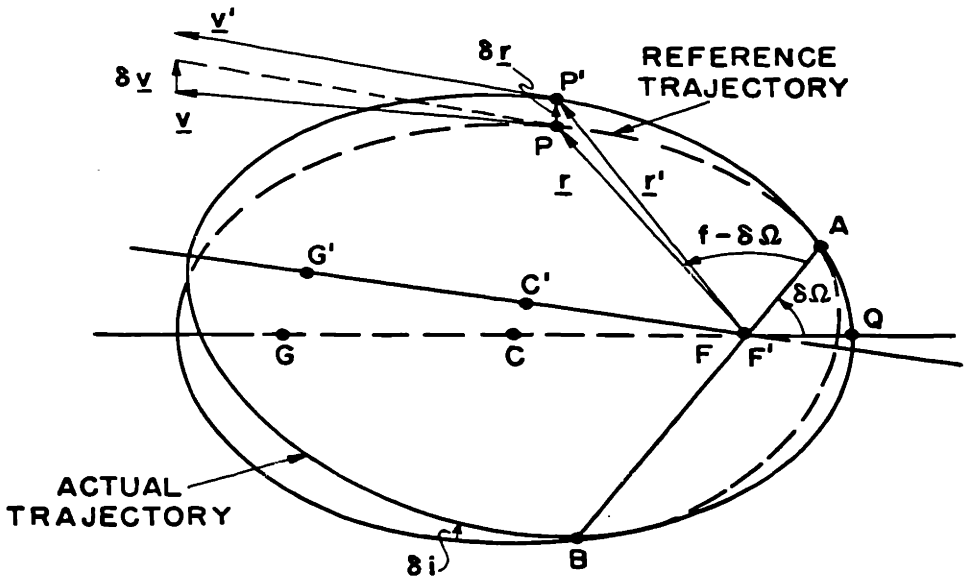

Unprimed capital letters apply to reference trajectory.
Primed capital letters apply to actual trajectory.

F,F' — common attractive focus of two trajectories

C,C' — centers of two trajectories

G,G' — vacant foci of two trajectories

P,P' — position on two trajectories at time t

AB — line of nodes

$f = \sphericalangle QFP$ = true anomaly of P

$\delta\Omega$ = variation in longitude of ascending node

δi = variation in inclination

$\delta\underline{r} = \underline{r}' - \underline{r}$ = variation in position

$\delta\underline{v} = \underline{v}' - \underline{v}$ = variation in velocity

Figure 3.5 Effect of $\delta\Omega$, Variation in Longitude of Ascending Node, and δi, Variation in Inclination

$\underline{a}$ and $\underline{a}'$ is equal to the angle between $\underline{r}$ and $\underline{r}'$. Then, since a_s and s are both zero on the reference trajectory, the acceleration variation component δa_s is

$$\delta a_s = a_s' = \underline{a}' \cdot \underline{u}_s = \frac{\underline{a}'}{r'} \underline{r}' \cdot \underline{u}_s$$

$$= \frac{a_r \delta s}{r} = -\frac{\mu}{r^3} \delta s \qquad (3\text{-}108)$$

In similar fashion,

$$\delta a_z = a_z' = -\frac{\mu}{r^3} \delta z \qquad (3\text{-}109)$$

Equations (3-107), (3-108), and (3-109) are the component equations of the matrix formulation given by (3-7) and (3-9).

3.10 Transition Matrix

Equation (3-61) can be used to find analytic expressions for the terms of the transition matrix $\overset{*}{C}_{ji}$, defined by Equations (2-8) and (2-9). The first six rows of (3-61) define a 6-by-6 matrix which relates the state vector $\delta \underline{x}$ to the variations in the orbital elements. The inverse of this matrix provides an expression for the variations of the elements in terms of the components of $\delta \underline{x}$. If the subscript j is added to all the time-varying quantities in the first matrix, the state vector is $\delta \underline{x}_j$, corresponding to time t_j. If the subscript i is added to the time-varying quantities in the inverse matrix, the variations in the elements are expressed in terms of the components of $\delta \underline{x}_i$. The product of these two matrices is the transition matrix $\overset{*}{C}_{ji}$, relating $\delta \underline{x}_j$ to $\delta \underline{x}_i$.

The algebraic manipulations required to perform the matrix inversion and the matrix multiplication are quite laborious. It is therefore worthwhile, before performing the indicated operations, to give careful consideration to the choice of a single time-varying parameter, the choice of a coordinate system, and the choice of a combination of variations in the six orbital elements. A discussion of these choices appears in the early sections of Appendix K. The amount of algebra is reduced (but is still by no means trivial) if the time-varying quantity is

the eccentric anomaly E, the coordinate system is the reference trajectory flight path (p q z) system, and the variations in the orbital elements are grouped as shown below in the path deviation vector $\delta \underline{e}$.

$$\delta \underline{e} = \begin{Bmatrix} (1 - e^2)^{1/2} \, \delta\phi - n \, \delta t_o \\ \dfrac{\delta e}{(1 - e^2)^{1/2}} \\ \dfrac{1}{2} \dfrac{\delta a}{a} \\ e \, \delta\phi \\ (1 - e^2)^{1/2} \, \delta i \cos \delta\Omega \\ \delta i \sin \delta\Omega \end{Bmatrix} \tag{3-110}$$

With these selections, the first six equations of (3-61) are transformed into the following:

$$\delta \underline{x}_j = \begin{Bmatrix} \delta p_j \\ \delta q_j \\ \delta z_j \\ \delta v_{p_j} \\ \delta v_{q_j} \\ \delta v_{z_j} \end{Bmatrix} = \begin{Bmatrix} \overset{*}{F}_j \\ \overset{*}{L}_j \end{Bmatrix} = \begin{Bmatrix} (1 - e^2)^{1/2} \, \delta\phi - n \, \delta t_o \\ \dfrac{\delta e}{(1 - e^2)^{1/2}} \\ \dfrac{1}{2} \dfrac{\delta a}{a} \\ e \, \delta\phi \\ (1 - e^2)^{1/2} \, \delta i \cos \delta\Omega \\ \delta i \sin \delta\Omega \end{Bmatrix} \tag{3-111}$$

This equation is the same as Equation (K-30) of Appendix K. The 3-by-6 matrix $\overset{*}{F}_j$ relates $\delta \underline{r}_j$ to $\delta \underline{e}$; the 3-by-6 matrix $\overset{*}{L}_j$ relates $\delta \underline{v}_j$ to $\delta \underline{e}$. Equations (K-31) and (K-32) express the elements of $\overset{*}{F}_j$ and $\overset{*}{L}_j$ in terms of a, e, n, and E_j.

The inverse of the 6-by-6 matrix $\begin{Bmatrix} \overset{*}{F} \\ \overset{*}{L} \end{Bmatrix}$ is designated $\begin{Bmatrix} \overset{*}{R} & \overset{*}{V} \end{Bmatrix}$. The equation relating the orbital element variations to state vector $\delta \underline{x}_i$ is

$$\delta \underline{e} = \begin{Bmatrix} (1 - e^2)^{1/2} \, \delta\phi - n \, \delta t_o \\ \dfrac{\delta e}{(1 - e^2)^{1/2}} \\ \dfrac{1}{2} \dfrac{\delta a}{a} \\ e \, \delta\phi \\ (1 - e^2)^{1/2} \, \delta i \cos \delta\Omega \\ \delta i \sin \delta\Omega \end{Bmatrix} = \begin{Bmatrix} \overset{*}{R}_i & \overset{*}{V}_i \end{Bmatrix} \begin{Bmatrix} \delta p_i \\ \delta q_i \\ \delta z_i \\ \delta v_{p_i} \\ \delta v_{q_i} \\ \delta v_{z_i} \end{Bmatrix} \qquad (3\text{-}112)$$

$\overset{*}{R}_i$ is a 6-by-3 matrix which gives the effect of $\delta \underline{r}_i$ on $\delta \underline{e}$. $\overset{*}{V}_i$ is a 6-by-3 matrix giving the effect of $\delta \underline{v}_i$ on $\delta \underline{e}$. Equations (K-34) and (K-35) in Appendix K contain analytic expressions for the elements of $\overset{*}{R}_i$ and $\overset{*}{V}_i$.

The transition matrix is obtained by substituting (3-112) into (3-111).

$$\delta \underline{x}_j = \begin{Bmatrix} \overset{*}{F}_j \\ \overset{*}{L}_j \end{Bmatrix} \begin{Bmatrix} \overset{*}{R}_i & \overset{*}{V}_i \end{Bmatrix} \delta \underline{x}_i$$

$$= \overset{*}{C}_{ji} \, \delta \underline{x}_i \qquad (3\text{-}113)$$

$$
\begin{bmatrix}
\left[\frac{(1 - e\cos E_1)(1 - e\cos E_2)}{(1 - e\cos E_1)(1 + e\cos E_2)}\right]^{1/2} & 0 & 0 & 0 & 0 & 0 \\
0 & \left[\frac{(1 - e\cos E_1)(1 - e\cos E_2)}{(1 - e\cos E_1)(1 - e\cos E_2)}\right]^{1/2} & 0 & 0 & 0 & 0 \\
0 & 0 & 1 & 0 & 0 & 0 \\
0 & 0 & 0 & \left[\frac{(1 - e\cos E_1)(1 - e\cos E_2)}{(1 + e\cos E_1)(1 - e\cos E_2)}\right]^{1/2} & 0 & 0 \\
0 & 0 & 0 & 0 & \left[\frac{(1 - e\cos E_1)(1 - e\cos E_2)}{(1 - e\cos E_1)(1 - e\cos E_2)}\right]^{1/2} & 0 \\
0 & 0 & 0 & 0 & 0 & 1
\end{bmatrix}
\begin{bmatrix}
\\ \\ \\ \\ \\ \\
\end{bmatrix}
$$

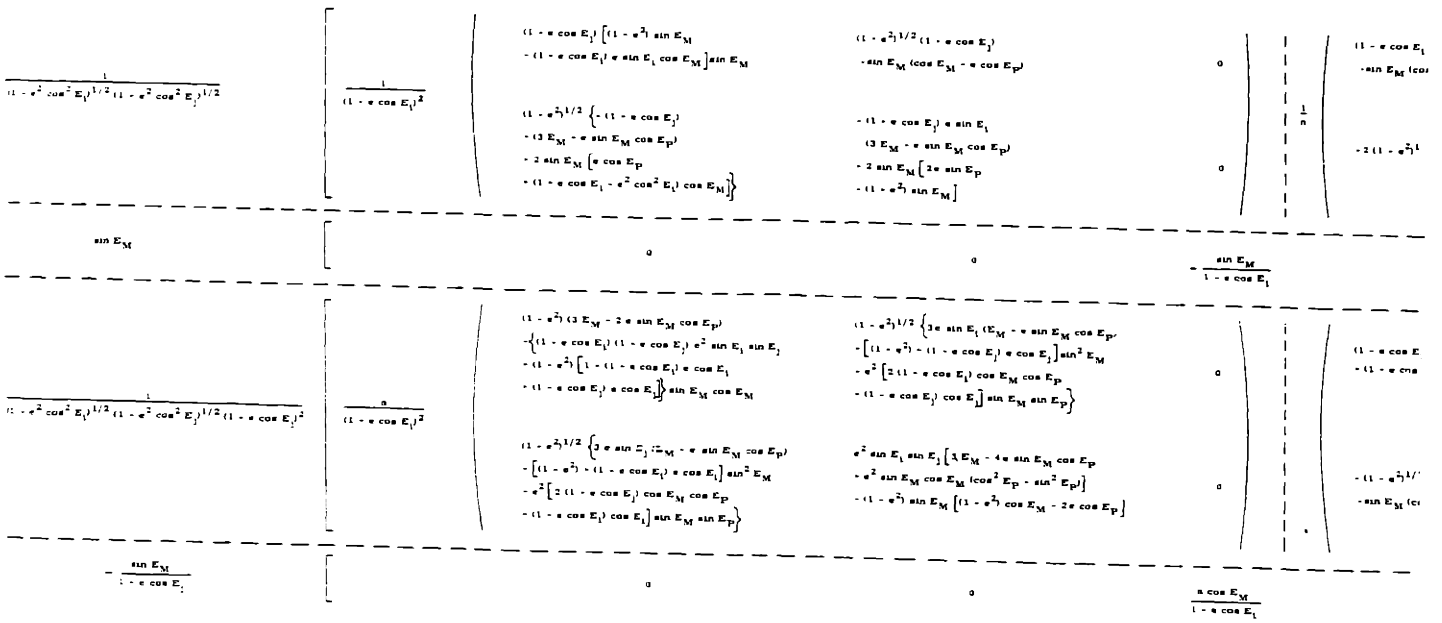

where
$$\overset{*}{C}_{ji} = \begin{Bmatrix} \overset{*}{M}_{ji} & \overset{*}{N}_{ji} \\ \overset{*}{S}_{ji} & \overset{*}{T}_{ji} \end{Bmatrix} \tag{3-114}$$

and

$$\overset{*}{M}_{ji} = \overset{*}{F}_j \; \overset{*}{R}_i \tag{3-115}$$

$$\overset{*}{N}_{ji} = \overset{*}{F}_j \; \overset{*}{V}_i \tag{3-116}$$

$$\overset{*}{S}_{ji} = \overset{*}{L}_j \; \overset{*}{R}_i \tag{3-117}$$

$$\overset{*}{T}_{ji} = \overset{*}{L}_j \; \overset{*}{V}_i \tag{3-118}$$

The matrix multiplications indicated by Equations (3-115) to (3-118) have been performed, and the analytic results are contained in Equations (K-39) to (K-42). The complete expression for $\overset{*}{C}_{ji}$ is Equation (3-119). The angles E_M and E_P, introduced in these equations for the purpose of simplification, are defined as follows:

$$E_M = \frac{1}{2} (E_j - E_i) \tag{3-120}$$

$$E_P = \frac{1}{2} (E_j + E_i) \tag{3-121}$$

Equation (3-119) expresses all the elements of $\overset{*}{C}_{ji}$ in terms of only four parameters, namely, the eccentricity e and the mean angular motion n of the reference trajectory, and the eccentric anomalies E_i and E_j. $\overset{*}{C}_{ji}$ is presented as the sum of two matrices. The first of the two is a diagonal matrix whose diagonal elements, reading from top to bottom, are equal, respectively, to

$$\frac{v_i}{v_j} \quad , \quad \frac{v_j}{v_i} \quad , \quad 1 \quad , \quad \frac{v_j}{v_i} \quad , \quad \frac{v_i}{v_j} \quad , \quad 1 \quad .$$

Every term in every element of the second of the two matrices contains either E_M or sin E_M. From this information it is clear that when

$t_j = t_i$, the first matrix becomes the identity matrix and the second matrix becomes the zero matrix. Thus, $\overset{*}{C}_{ii}$ is the sixth-order identity matrix, as indicated in Chapter 2 by Equation (2-10).

For this special case in which the reference trajectory is an ellipse, a stronger statement can be made about the determinant of $\overset{*}{C}_{ji}$ than that of Equation (2-13). Not only is the determinant of $\overset{*}{C}_{ji}$ equal to unity, but there are two sub-matrices that can be formed, the determinant of each of which is equal to unity. The first sub-matrix consists of the sixteen in-plane elements of $\overset{*}{C}_{ji}$; the second consists of the four out-of-plane elements of $\overset{*}{C}_{ji}$.

A visual check of the terms in (3-119) can be made by comparing $\overset{*}{C}_{ji}$ with its inverse $\overset{*}{C}_{ij}$ and noting that the inverse satisfies the relationship given by Equation (2-12).

If (3-119) is to be used for numerical computations performed on a digital computer, the accuracy with which the terms have been entered into the program can be effectively checked by the matrix multiplication of $\overset{*}{C}_{ji}$ by $\overset{*}{C}_{ij}$ for arbitrary values of E_i and E_j. If all terms have been entered correctly, the product matrix is the identity matrix. If the term in the m-th row and the n-th column is entered incorrectly, all the terms in the m-th row and all the terms in the n-th column of the product matrix will, in general, differ from the corresponding terms of the identity matrix.

3.11 Fixed-Time-of-Arrival Guidance

The two basic equations in FTA guidance are (2-33) and (2-35); the former relates the velocity correction $\underline{c}_F$ to the predicted position variation at the target, the latter relates the state vector after the correction is applied to the state vector before it is applied. The two equations are repeated below for convenience.

$$\underline{c}_F = - K_{CD} \, \delta \, \underline{r}_D \qquad (3\text{-}122)$$

$$\delta \underline{x}_D^{+} = \begin{Bmatrix} \overset{*}{0}_3 & \overset{*}{0}_3 \\ -\overset{*}{J}_{DC} & \overset{*}{I}_3 \end{Bmatrix} \delta \underline{x}_D^{-} \qquad (3\text{-}123)$$

Analytic expressions for $\overset{*}{J}_{DC}$ and $\overset{*}{K}_{CD}$ can be determined directly from the sub-matrices of $\overset{*}{C}_{DC}$ by the use of (2-27) and (2-28).

An alternate method of developing the terms of $\overset{*}{J}_{DC}$ and $\overset{*}{K}_{CD}$ is presented in Appendix K. This method involves the formulation of a path deviation vector consisting of the position variations at two times, t_i and t_j. First, $\delta \underline{r}_i$ and $\delta \underline{r}_j$ are expressed in terms of $\delta \underline{e}$.

$$\begin{Bmatrix} \delta \underline{r}_i \\ \delta \underline{r}_j \end{Bmatrix} = \begin{Bmatrix} \overset{*}{F}_i \\ \overset{*}{F}_j \end{Bmatrix} \delta \underline{e} = \overset{*}{A}_{ij}\, \delta \underline{e} \qquad (3\text{-}124)$$

where $\overset{*}{A}_{ij}$ is a 6-by-6 matrix whose first three rows depend only on t_i and whose last three rows depend only on t_j. The inverse of (3-124) is

$$\delta \underline{e} = \overset{*}{A}_{ij}^{-1} \begin{Bmatrix} \delta \underline{r}_i \\ \delta \underline{r}_j \end{Bmatrix} = \begin{Bmatrix} \overset{*}{H}_{ij} & \overset{*}{H}_{ji} \end{Bmatrix} \begin{Bmatrix} \delta \underline{r}_i \\ \delta \underline{r}_j \end{Bmatrix} \qquad (3\text{-}125)$$

$\overset{*}{H}_{ij}$ is the 6-by-3 matrix relating $\delta \underline{e}$ to $\delta \underline{r}_i$ when $\delta \underline{r}_j$ is held constant, and $\overset{*}{H}_{ji}$ is the 6-by-3 matrix relating $\delta \underline{e}$ to $\delta \underline{r}_j$ when $\delta \underline{r}_i$ is held constant. Equation (K-44) of Appendix K is an analytic expression for the elements of $\overset{*}{H}_{ij}$. The elements of $\overset{*}{H}_{ji}$ are obtained by interchanging subscripts i and j in (K-44).

The state vector at any given time can now be related to the path deviation vector consisting of $\delta \underline{r}_i$ and $\delta \underline{r}_j$. In particular, the state vector at t_i is

$$\delta \underline{x}_i = \begin{Bmatrix} \overset{*}{F}_i \\ \overset{*}{L}_i \end{Bmatrix} \delta \underline{e} = \begin{Bmatrix} \overset{*}{F}_i \\ \overset{*}{L}_i \end{Bmatrix} \begin{Bmatrix} \overset{*}{H}_{ij} & \overset{*}{H}_{ji} \end{Bmatrix} \begin{Bmatrix} \delta \underline{r}_i \\ \delta \underline{r}_j \end{Bmatrix} \qquad (3\text{-}126)$$

Equation (3-126) can be sub-divided into two equations, one for position variation and the other for velocity variation.

$$\delta \underline{r}_i = \overset{*}{F}_i \left(\overset{*}{H}_{ij} \, \delta \underline{r}_i + \overset{*}{H}_{ji} \, \delta \underline{r}_j \right) \tag{3-127}$$

$$\delta \underline{v}_i = \overset{*}{L}_i \left(\overset{*}{H}_{ij} \, \delta \underline{r}_i + \overset{*}{H}_{ji} \, \delta \underline{r}_j \right) \tag{3-128}$$

The former equation indicates that

$$\overset{*}{F}_i \overset{*}{H}_{ij} = \overset{*}{I}_3 \qquad \overset{*}{F}_i \overset{*}{H}_{ji} = \overset{*}{0}_3 \tag{3-129}$$

The equation for velocity variation is simplified as follows:

$$\delta \underline{v}_i = \overset{*}{J}_{ij} \, \delta \underline{r}_i + \overset{*}{K}_{ij} \, \delta \underline{r}_j \tag{3-130}$$

where

$$\overset{*}{J}_{ij} = \overset{*}{L}_i \overset{*}{H}_{ij} \qquad \overset{*}{K}_{ij} = \overset{*}{L}_i \overset{*}{H}_{ji} \tag{3-131}$$

(3-130) is the same equation as (2-26). Equations (3-131) are the defining relations for the 3-by-3 matrices $\overset{*}{J}_{ij}$ and $\overset{*}{K}_{ij}$, which are the fundamental matrices of linear guidance theory. With the proper substitution of subscripts they are the matrices appearing in (3-122) and (3-123). Analytic expressions for the elements of $\overset{*}{J}_{DC}$ are obtained by substituting D for i, C for j in Equation (K-47) of Appendix K. Since the subscript D precedes the subscript C in $\overset{*}{J}_{DC}$, the angle E_M is given by

$$E_M = \frac{1}{2} \left(E_C - E_D \right) \tag{3-132}$$

The correction matrix $\overset{*}{K}_{CD}$ is obtained from (K-48) and because of its importance is reproduced here as Equation (3-133). In this equation, since the subscript C precedes the subscript D,

$$E_M = \frac{1}{2} \left(E_D - E_C \right) \tag{3-134}$$

$$
\dot{K}_{CD} = \frac{n}{2} \left\{ \frac{1}{(1 - e^2 \cos^2 E_C)^{1/2} (1 - e^2 \cos^2 E_D)^{1/2}} \times \begin{pmatrix} (1 + e \cos E_C)(1 + e \cos E_D) \cdot \left(\frac{3 E_M}{\sin E_M} - e \cos E_P \right) & 2 (1 - e^2)^{1/2} (1 - e \cos E_D) \sin E_M & 0 \\ - 4(\cos E_M + e \cos E_P) & & \\ - 2(1 - e^2)^{1/2} (1 - e \cos E_C) \sin E_M & - (1 - e \cos E_C)(1 - e \cos E_D) \cdot (\cos E_M + e \cos E_P) & 0 \\ 0 & 0 & \frac{1}{\sin E_M (\cos E_M - e \cos E_P)} \end{pmatrix} \right\} \tag{3-133}
$$

The denominator factor X in the expressions for $\overset{*}{J}_{DC}$ and $\overset{*}{K}_{CD}$ is defined by

$$X = (3\,E_M - e \sin E_M \cos E_P)\ (\cos E_M + e \cos E_P) - 4 \sin E_M \tag{3-135}$$

It is interesting and perhaps somewhat surprising to note that, of all the matrices considered in the last two sections, $\overset{*}{K}_{CD}$, the only one needed to compute the velocity correction, is one of the simplest.

3.12 Variable-Time-of-Arrival Guidance

The VTA velocity correction and the corresponding relation between $\delta \underline{x}_D^+$ and $\delta \underline{x}_D^-$ are determined from Equations (2-41) and (2-44), respectively. Aside from utilizing the analytic expressions for $\overset{*}{K}_{CD}$ and $\overset{*}{J}_{DC}$, no further simplification of these two equations is afforded by the assumption of an elliptical reference trajectory.

When the expression for the VTA correction is formulated in the critical-plane coordinate system, there is an additional simplification for any two-body reference trajectory, whether it be elliptical, parabolic, or hyperbolic. From Equation (2-47) the correction may be written as

$$\underline{c}_W = \begin{Bmatrix} c_\xi \\ c_\eta \end{Bmatrix} = \overset{*}{Y} \begin{Bmatrix} \delta \xi_D^- \\ \delta \eta_D^- \end{Bmatrix} \tag{3-136}$$

It is shown in Section N.8 of Appendix N that the upper right-hand term of the 2-by-2 matrix $\overset{*}{Y}$ is equal to zero for two-body reference trajectories. Thus, only three quantities need be evaluated in order to compute the correction vector required at some time t_C for a given miss distance vector.

In Section O. 13 the following expression is derived for $\overset{*}{Y}$:

$$\overset{*}{Y} = n \left\{ \begin{bmatrix} \frac{1}{4B} & 0 \\ \frac{K_{33}}{C}\left(\frac{D \cos i_D}{B}\right) & -B \end{bmatrix} \right\} \tag{3-137}$$

where

$$B = [(K_{11} \sin \Omega_D - K_{12} \cos \Omega_D)^2 + (K_{21} \sin \Omega_D - K_{22} \cos \Omega_D)^2]^{1/2}$$

$$C = [B^2 \sin^2 (f_D - f_C) \sin^2 i_D + K_{33}{}^2 X^2 \sin^2 E_M \cos^2 i_D]^{1/2} \tag{3-139}$$

$$D = (K_{11}{}^2 - K_{12}{}^2 + K_{21}{}^2 - K_{22}{}^2) \sin \Omega_D \cos \Omega_D$$

$$+ (K_{11} K_{12} + K_{21} K_{22}) (\sin^2 \Omega_D - \cos^2 \Omega_D) \tag{3-140}$$

The K factors are functions of the eccentricity e and the two eccentric anomalies E_C and E_D; they are defined in Equations (O-77) to (O-81). Ω_D and i_D are the orientation angles of the relative velocity vector $\underline{v}_R$ with respect to the p_D, q_D, z axes.

Equation (3-137) indicates that reducing the magnitude of K_{33} and D and increasing the magnitude of C all have the desirable effect of reducing the magnitude of $\underline{c}_V$. The role of the magnitude of B is more equivocal. If $\delta \bar{\xi}_D$ is much larger than $\delta \bar{\eta}_D$, B should be as large as possible; if $\delta \bar{\eta}_D$ is much larger than $\delta \bar{\xi}_D$, the magnitude of B should be kept small. All of these factors are properly weighted in the determination of the optimum correction time in the manner indicated in Section 2. 16.

The physical significance of the zero element in $\overset{*}{Y}$ is that the component of the correction vector along the line of nodes between the critical plane at $t = t_C$ and the reference trajectory plane is affected by only that component of the miss distance vector that lies along the line of nodes between the critical plane at $t = t_D$ and the reference trajectory plane.

The nodal component of $\underline{c}_W$ is completely independent of the variant motion along the z-axis; it depends only on $\delta \bar{\xi}_D$, which by definition lies in the reference trajectory plane, on the in-plane elements of $\overset{*}{K}_{CD}$, and on Ω_D, the angle in the reference trajectory plane between the p_D-axis and the line of nodes. Therefore, the correction required for the out-of-plane component of the predicted position variation (i.e., for $\delta \bar{z}_D$) is contained entirely in the η_C-component of the correction.

3.13 General Discussion of Singularities in the Matrix Solution

The solution for the state vector at time t_j as a function of the state vector at time t_i has no singularities. Irrespective of the time selected for t_i, the six components of $\delta \underline{x}_i$ are independent and therefore can be used to determine the components of the state vector $\delta \underline{x}_j$ for any t_j. The mathematical validity of this statement is manifest from the fact that the determinant of $\overset{*}{C}_{ji}$ can never vanish; it is always equal to one.

However, if the path deviation vector $\delta \underline{e}$ is expressed as a function of the path deviation vector consisting of two position variation vectors $\delta \underline{r}_i$ and $\delta \underline{r}_j$, as in Equation (3-124), there may be singularities in the solution. There are certain combinations of t_i and t_j for which the components of $\delta \underline{r}_j$ are not independent of the components of $\delta \underline{r}_i$. For these combinations the determinant of $\overset{*}{A}_{ij}$ vanishes, and hence matrices $\overset{*}{H}_{ij}$, $\overset{*}{H}_{ji}$, $\overset{*}{J}_{ij}$, and $\overset{*}{K}_{ij}$ cannot be determined.

There are three different types of combinations of t_i and t_j for which $\overset{*}{A}_{ij}$ becomes singular. The first type occurs when the difference between t_i and t_j is an integer multiple of the reference period P; the second type occurs when the difference in true anomaly $(f_j - f_i)$ is equal to $(2N-1)\pi$ radians; the third type occurs when the factor X, defined by Equation (3-135), is equal to zero. These three types are discussed individually in the following three sections. A more comprehensive analysis appears in Appendix O.

A study of these singularities can be justified on academic grounds simply because they do exist, and an understanding of why they exist leads to a more thorough comprehension of the characteristics of elliptical motion. In addition, the study has practical significance if space

journeys are contemplated in which the total difference in true anomaly (between injection and arrival at the destination) is greater than π radians.

In order of increasing value of $(f_j - f_i)$, the first three singularities occur at $(f_j - f_i) = 0, \pi$, and 2π radians. The first is a trivial case; if $t_i = t_j$, it is obvious that $\delta \underline{r}_i = \delta \underline{r}_j$, and hence the components of the six-vector composed of $\delta \underline{r}_i$ and $\delta \underline{r}_j$ are not independent. The singularities at π and 2π radians are examples, respectively, of the second type and the first type. The first non-trivial case of a singularity at $X = 0$ occurs at a value of $(f_j - f_i)$ between 2π and 4π radians.

For manned interplanetary reconnaissance missions, minimization of total flight time is of prime importance because of logistic considerations. Such missions will normally involve a total change in true anomaly of approximately π radians for each of the two legs, outbound and return. The only singularity that need be considered on such missions is the one of the second type that occurs at $(f_j - f_i) = \pi$ radians.

There are two types of space missions which involve considerably larger changes in true anomaly. The first is an unmanned nonstop round-trip reconnaissance of either Mars or Venus as described in Reference (2). The mission can be accomplished with relatively low expenditure of energy if the vehicle makes two circuits of the sun during the time that the earth makes three circuits, i.e., in three years. In one of the legs of such a journey, either outbound or return, the true anomaly difference must be greater than 2π radians.

The second type of mission with large difference in true anomaly is that of a space vehicle in a temporary parking orbit about another planet. Such a trajectory may entail an appreciable number of complete circuits before the vehicle reaches its "destination", which is the point at which thrust is to be applied for the return trip to earth.

In both of these types of extended missions singularities of all three types can be encountered.

It is shown in the following sections that, in general, it is not possible to compute a finite FTA velocity correction when t_C and t_D are such that the conditions for any one of the three types of singularities are

satisfied. If VTA guidance is used, a finite correction can be computed under the conditions for the second and third types of singularities, but no finite VTA correction can be computed if the singularity is of the first type.

3.14 Singularities at $(t_j - t_i) = NP$

When t_i and t_j are an exact number of reference periods apart, the position variations $\delta \underline{r}_i$ and $\delta \underline{r}_j$ can differ from each other only due to the fact that the period P' of the actual trajectory differs slightly from P, the period of the reference trajectory.

$$\begin{Bmatrix} \delta p_j \\ \delta q_j \\ \delta z_j \end{Bmatrix} = \begin{Bmatrix} \delta p_i \\ \delta q_i \\ \delta z_i \end{Bmatrix} - \begin{Bmatrix} 0 \\ N v_i \delta P \\ 0 \end{Bmatrix} \qquad (3\text{-}141)$$

In the path deviation vector consisting of $\delta \underline{r}_i$ and $\delta \underline{r}_j$, only four of the six components are independent. Hence the rank of matrix $\overset{*}{A}_{ij}$ is reduced from six to four. Despite the fact that $\overset{*}{A}_{ij}$ is singular, (3-141) can be used to solve for δP, and by the use of Kepler's third law $\frac{1}{2}\frac{\delta a}{a}$, the third element of $\delta \underline{e}$, can be computed.

$$\frac{1}{2}\frac{\delta a}{a} = \frac{1}{3}\frac{\delta P}{P} = -\frac{(\delta q_j - \delta q_i)}{3 N P v_i} \qquad (3\text{-}142)$$

The other five elements of $\delta \underline{e}$ cannot be determined.

If correction time t_C and arrival time t_D are an exact number of reference periods apart, it is not possible to compute a small finite FTA velocity correction which will affect the predicted values of δp_D^- and δz_D^-. If either of these components of $\delta \underline{r}_D^-$ is non-zero, $\delta \underline{r}_D^+$ must be non-zero. The only condition under which it is possible to compute a finite $\underline{c}_F$ that nulls $\delta \underline{r}_D^-$ is when $\delta \underline{r}_D^-$ is parallel to the velocity vector $\underline{v}_D$. Then the required correction changes the period of the motion in such a manner that δq_D is reduced to zero. The equation for the correction in this special case, developed as (O-13) in Appendix O, is

$$\underline{c}_F = \frac{\mu}{3 N P a v_D^2} (\delta q_D^-) \underline{u}_{q_D} \qquad (3\text{-}143)$$

Equation (3-143) has little practical value inasmuch as it applies to a condition whose likelihood of occurrence is essentially zero. However, it does serve to illustrate a paradoxical characteristic of elliptical motion. A positive δq_D^- indicates that the predicted vehicle position at t_D is slightly ahead of the desired position. The correction therefore must slow the vehicle down somewhat in order to reduce δq_D to zero. But (3-143) indicates that for a positive δq_D^- the required velocity increment along the q_D-axis, which is also the q_C-axis, is positive, so that the vehicle experiences an instantaneous increase in orbital velocity. The question that arises is this: How can an initial increase in velocity cause an eventual retardation of the vehicle motion so that a positive δq_D is reduced to zero? The seeming contradiction is clarified by Kepler's third law. The initial increase in velocity increases the total energy of the path. An increase in total energy signifies an increase in the length of the semi-major axis a, which, from Kepler's third law, is accompanied by an increase in the period P. The increased period is so determined that after N circuits of the focus the vehicle arrives at the desired destination point at time t_D. Thus, the vehicle's position variation is initially increased by the correction but is eventually reduced to zero at t_D.

If VTA guidance rather than FTA guidance is used, it is still not possible in the general case to compute a finite velocity correction when $(t_D - t_C) = N P$. There are three special situations, however, in which a finite correction can be determined. The first is the trivial case when $\delta \underline{r}_D^-$ is parallel to $\underline{v}_R$ and no correction is required. The second is the same as the special case for FTA guidance; i.e., $\delta \underline{r}_D^-$ is parallel to $\underline{v}_D$; in this case the VTA correction is the same as the FTA correction given by Equation (3-143). The third special case is the two-dimensional case, in which both $\delta \underline{r}_D^-$ and $\underline{v}_R$ lie in the reference trajectory plane; under these circumstances, the VTA correction is again given by the right-hand side of Equation (3-143).

A physical explanation of the inability to compute a finite FTA correction is based on the fact that the new path resulting from any correction must contain both the vehicle's actual position C' at the time of the correction and the desired destination point D. When C'

and D are spatially close to each other but not coincident and the line C' D is not tangent to the reference trajectory, the difference between the required new trajectory and the reference trajectory is generally so great that it precludes the use of linear theory in computing the velocity correction. Even when the requirements on the correction are relaxed by the use of VTA navigation, it is not possible in the general case to compute a finite correction, because there is no path lying close to the reference path that passes through C' and some point on the line through D parallel to $\underline{v}_R$.

A more detailed analysis of the singularities at $(t_D - t_C) = N\,P$ appears in Sections O.4, O.5, O.14, and O.17.

3.15 Singularities at $(f_j - f_i) = (2N-1)\pi$

If the difference in true anomaly $(f_j - f_i)$ is an odd multiple of π radians, the in-plane components of $\delta \underline{r}_i$ and $\delta \underline{r}_j$ are independent of each other, but δz_i and δz_j are not independent. The relationship between the latter two can be derived from the z-component of (3-57), the vector equation for $\delta \underline{r}$.

$$\delta z_i = r_i \sin (f_i - \delta\Omega)\, \delta i \tag{3-144}$$

$$\begin{aligned} \delta z_j &= r_j \sin (f_j - \delta\Omega)\, \delta i \\ &= r_j \sin [f_i + (2N-1)\pi - \delta\Omega]\, \delta i \\ &= - r_j \sin (f_i - \delta\Omega)\, \delta i \\ &= - \frac{r_j}{r_i}\, \delta z_i \end{aligned} \tag{3-145}$$

Only five of the six elements of the two-position path deviation vector are independent, and the rank of $\overset{*}{A}_{ij}$ is reduced from six to five. The four in-plane components of $\delta \underline{e}$ can be determined uniquely from measurements of $\delta \underline{r}_i$ and $\delta \underline{r}_j$; the two out-of-plane elements cannot.

If the correction time is such that $(f_D - f_C) = (2N-1)\pi$, no finite FTA velocity correction can in general be computed. If VTA guidance is used, a finite correction can be applied as long as $\underline{v}_R$ has a non-zero component in the z direction. The computed VTA correction vector lies in the reference trajectory plane.

As in the case of the singularities at $(t_D - t_C) = NP$, the singularities at $(f_D - f_C) = (2N-1)\pi$ can be interpreted physically by a consideration of the requirements imposed on the corrected path. If the actual correction point C' has a small position variation δz_C normal to the reference trajectory plane and if the difference in true anomaly between C' and D is an odd multiple of 180°, then the plane containing position vectors $\underline{r}_{C'}$ and $\underline{r}_D$ is perpendicular to the reference trajectory plane. But the plane containing $\underline{r}_{C'}$ and $\underline{r}_D$ is also the plane of the corrected trajectory computed by means of FTA guidance. Because the planes of the reference trajectory and the corrected trajectory are perpendicular to each other, a finite FTA velocity correction cannot be determined.

If VTA guidance is used, the destination point is changed from D to the point at which the line through D parallel to $\underline{v}_R$ intersects the plane of the uncorrected trajectory. Thus the VTA correction does not alter the plane of the vehicle's motion; rather, it adjusts the trajectory so that the vehicle arrives at the destination planet at precisely that time when the planet is passing through the plane of the vehicle's actual trajectory.

This type of singularity is discussed further in Sections O.6, O.7, O.15, and O.17.

3.16 Singularities at X = 0

If t_i and t_j are such that X = 0, δz_i and δz_j are independent of each other, but a linear relation exists among the components δp_i, δq_i, δp_j, and δq_j. This relation, as presented in Equation (O-30), is

$$p_j \, \delta q_j - p_i \, \delta q_i = -\frac{b}{2} (3E_M - e \sin E_M \cos E_P) \cdot (\cos \gamma_j \, \delta p_j + \cos \gamma_i \, \delta p_i) \qquad (3\text{-}146)$$

where b is the length of the semi-minor axis of the reference ellipse. Only five of the six components of the two-position path deviation vector are independent; the rank of matrix $\overset{*}{A}_{ij}$ is five. Observations of $\delta \underline{r}_i$ and $\delta \underline{r}_j$ can be used to determine the two out-of-plane elements of $\delta \underline{e}$, but the four in-plane elements are indeterminate.

The X = 0 singularities differ from the other two types in that the singularity points depend on e, an orbital element of the reference ellipse. In the first two types the singularities occur at known values of the difference in true anomaly, irrespective of the characteristics of the reference trajectory.

Figure O.3 of Appendix O is a plot of X as a function of $(E_j - E_i)$ for e = 0.25 and E_j = 210°; these values are typical for outbound journeys from Earth to Mars or return trips from Venus to Earth. The singularity points in the plot are the points at which the curve crosses the abscissa axis. The graph indicates an X = 0 point at $(E_j - E_i) = 0°$ and one additional X = 0 point in the range $2N\pi < (E_j - E_i) < 2(N + 1)\pi$ for each positive value of N. It is shown in Section O.8 that as N gets very large, the singularity point associated with a given end point P_j is the point at which the line joining P_j and the vacant focus intersects the ellipse when extended through the vacant focus; this is illustrated in Figure O.4.

In the general case, when t_C and t_D are such that X = 0 it is not possible to compute a finite FTA correction. A finite VTA correction can be computed as long as $\underline{v}_R$ has a non-zero component in the reference trajectory plane.

A physical interpretation of the X = 0 singularities can be obtained from an examination of a set of curves in which the time of flight t_F for a journey from a planet at distance r_1 from the sun to a planet at distance r_2 from the sun is plotted as a function of the length a of the semi-major axis of the elliptical path. Figure O.8 is such a plot for a journey from Earth to Mars. Each curve in the figure corresponds to a particular value of the transfer angle, which is defined as the total change in true anomaly.

The curves indicate that when N = 0, corresponding to a transfer angle smaller than 360°, there is no minimum value of t_F for a given transfer angle at any finite value of a. However, for N = 1, corresponding to a transfer angle between 360° and 720°, each curve has a distinct minimum value of t_F. The type of behavior indicated by the N = 1 curves would also be present in curves for higher values of N if they were plotted.

In Section O. 11 it is proved that the slope of each time-of-flight curve in Figure O. 8 is proportional to the factor X, and thus the X = 0 singularities occur at the points corresponding to the minimum time of flight on the various curves.

The physical meaning of the zero-slope points on the curves is that at such points if r_1, r_2, and the transfer angle are held fixed, the time of flight is insensitive to small changes in a. It follows that if r_1, r_2, t_F, and the transfer angle are known at a zero-slope point, it is still not possible to solve for a unique value of a. This conclusion corroborates the earlier statement, at the beginning of this section, that the in-plane components of $\delta \underline{e}$ cannot be found from $\delta \underline{r}_i$ and $\delta \underline{r}_j$ if X = 0.

In Section O. 12 the partial derivatives are manipulated to derive a relation that indicates that if $\underline{r}_1$, t_F, and N are specified and if $\underline{r}_2$ is such that X = 0, then $\underline{r}_2$ is insensitive to small changes in the in-plane orbital elements. Therefore, it is not possible to compute a small FTA velocity correction which, if applied at t_1, can correct a predicted position variation at t_2.

The factor X is a function of the eccentricity e and the two eccentric anomalies E_C and E_D. When t_C and t_D are such that X = 0 for a specified reference trajectory, any small finite change made in the time of arrival alters the effective value of E_D, so that X is no longer equal to zero and the singularity condition no longer exists. This, in essence, is what occurs when VTA guidance is utilized at a correction time for which X would be equal to zero if the arrival time were fixed. The VTA scheme changes the arrival time and computes the finite velocity correction required by the new arrival time.

The ramifications of the X = 0 singularity, including a development of Lambert's theorem for the time of flight, are taken up in considerably greater detail in Sections O.8, O.9, O.10, O.11, O.12, O.16, and O.17.

3.17 The Noncritical Vector

The key to a more fundamental understanding of the physics of VTA guidance may lie in an intensive investigation of the rotation of the noncritical vector $\underline{w}$ as a function of the time of correction t_C. Such an investigation has not been undertaken in the present study, but certain characteristics of the orientation of $\underline{w}$ have been determined as a consequence of the analysis of singularities in Appendix O. These characteristics may be summarized as follows:

(1) At $t_C = t_D$ the $\underline{w}$ vector is parallel to $\underline{v}_R$.

(2) When $(t_D - t_C) = NP$, $\underline{w}$ lies in the plane perpendicular to $\underline{v}_D$; i.e., the component of $\underline{w}$ in the q_C direction is zero. The z-component of $\underline{w}$ remains the same for all values of N; the p_C-component alternates in sign for successive values of N. This behavior is indicated by Equation (O-107).

(3) When $(f_D - f_C) = (2N-1)\pi$, $\underline{w}$ is parallel to the z-axis.

(4) When X = 0, $\underline{w}$ lies in the reference trajectory plane, its direction in the plane being a function of the number of complete circuits between t_C and t_D. This is deduced from Equation (O-117).

3.18 Low-Eccentricity Reference Trajectories

It has already been pointed out in Section 3.7 that the analysis presented in that section is applicable to ellipses of "moderate" eccentricity and is not directly applicable when the reference trajectory is circular or nearly circular. In this section the effects of small variations of the elements of reference trajectories of low eccentricity are considered. It is shown that the relations already formulated for the transition matrix $\overset{*}{C}_{ji}$ and the correction matrix $\overset{*}{K}_{CD}$ are applicable to low-eccentricity two-body orbits.

The term "low eccentricity," as used here, indicates that the eccentricity of the reference trajectory is of the same order of magnitude as the non-dimensional orbital variations ($\delta a/a$), δe, etc. Thus, a term involving the product of e and one of the small orbital variations is a second-order term in the "small" quantities.

The troublesome characteristic of low-eccentricity trajectories is the fact that large variations in the position of perhelion produce only small variations of the actual trajectory from the reference trajectory. Consequently $\delta\phi$, the variation in the longitude of perhelion, which is assumed to be small when e is appreciably greater than zero, need not be small when e is close to zero. Likewise, the variations in the anomalies, δf, δE, and δM, need not be small when e is close to zero. However, the angles $(\delta f + \delta\phi)$, $(\delta E + \delta\phi)$, and $(\delta M + \delta\phi)$, which define angular position on the actual trajectory relative to the well-defined and fixed x-axis of the reference trajectory, are small regardless of whether or not e is small.

With these factors taken into consideration, general relations (i.e., relations applicable for low e as well as moderate e) for $(\delta E + \delta\phi)$, δr, and δs are developed in Appendix H as Equations (H-25), (H-28), and (H-32), respectively. δz is unaffected by the fact that the eccentricity is low. In Appendix J equations specifically applicable when e is small are derived for $\delta \underline{r}$, $\delta \underline{v}$, and $\delta \underline{a}$. The expressions for the components of $\delta \underline{r}$ and $\delta \underline{v}$ are contained in the matrix equation (J-20); the components of $\delta \underline{a}$ are presented in (J-21). These equations can be compared with (3-61), which gives the corresponding relations for ellipses of moderate eccentricity.

In Section J.5 it is shown that the constants comprising the vector on the right-hand sides of (J-20) and (J-21) are linearly related to the constants of integration k_1 through k_6 developed in the integration procedure of Appendix G and described in Section 3.6. Therefore, the equations resulting from the integration, (3-31), (3-32), and (3-33), are applicable when the eccentricity is low. From this it can be deduced that the formulation for the transition matrix given by (3-119) and the formulations for $\overset{*}{J}_{DC}$ and $\overset{*}{K}_{CD}$ described in Section 3.11 are also applicable when e is small.

The equations for $\overset{*}{C}_{ji}$, $\overset{*}{J}_{DC}$, and $\overset{*}{K}_{CD}$ are not applicable when the eccentricity is so close to unity that a small variation may cause e to equal or even exceed unity.

3.19 The Destination Point

In Section 2.18 it was pointed out that the magnitude of the truncation error due to linearization can be reduced by choosing as the nominal "destination" of the midcourse guidance system a point on the reference trajectory which the vehicle is scheduled to reach at some time earlier than the time of its closest approach to the destination planet. When the assumption of a two-body heliocentric reference trajectory is superimposed on the linearity assumption, there is an even more cogent reason for selecting an early nominal destination point. The two-body approximation neglects, in addition to all second-order and higher-order terms in the Taylor series expansion, the first-order terms associated with the gravitational forces due to the disturbing planets. Thus, the approximation deteriorates markedly as the vehicle approaches the vicinity of a planet.

It is now necessary to establish a criterion for selecting the early destination point. The point at which the reference trajectory intersects the sphere of influence of the destination planet is a reasonable destination point for the linear n-body analysis of Chapter 2. For the linear two-body analysis this point is too close to the planet; a more conservative selection is the point at which the reference trajectory intersects the sphere of perturbative relevance of the destination planet. This sphere is defined as the boundary along which the gravitational attraction due to the planet is equal to 1/100 of the gravitational attraction due to the sun.

Table 3-1 lists the radii of the spheres of influence and the spheres of perturbative relevance for all the planets. The data are derived from Table 9-1a of Ehricke, Vol. II[31].

Table 3-1
Planetary Data

Planet	Semi-major Axis (a.u.)	Planet Radius (mi.)	Radius of Sphere of Influence (mi.)	Radius of Sphere of Perturbative Relevance (mi.)
Mercury	0.387	1560	0.694×10^5	0.147×10^6
Venus	0.723	3860	0.383×10^6	1.055×10^6
Earth	1.0	3960	0.575×10^6	1.86×10^6
Mars	1.524	2060	0.358×10^6	0.824×10^6
Jupiter	5.203	43,500	27.8×10^6	154×10^6
Saturn	9.539	35,800	26.6×10^6	160×10^6
Uranus	19.182	15,900	32.2×10^6	122.5×10^6
Neptune	30.058	15,600	54.0×10^6	207×10^6
Pluto	39.518	(2080)	21.1×10^6	(21.5×10^6)

CHAPTER 4

ILLUSTRATIVE CALCULATIONS

4.1 Summary

Calculations are performed on an Earth-Mars reference trajectory to illustrate the method of determining the optimum time to apply a VTA velocity correction. Curves are obtained for FTA as well as VTA guidance. Additional computations show the effect of position variation and velocity variation at any intermediate time on position variation and velocity variation at the nominal time of arrival at the destination. The analytic formulations of the required matrices, as developed in Chapter 3, are used in the calculations. The physical significance of the curves is discussed.

4.2 Introduction

The method of utilization of the guidance theory developed in Chapters 2 and 3 can best be demonstrated by numerical computations based on a specified interplanetary reference trajectory. In order to show the effects of all three types of singularities discussed in Chapter 3, a reference trajectory has been chosen in which the total transfer angle is greater than 360°. Such a trajectory is the outbound leg of Mars Trajectory No. 1034, described on Pages 102 and 103 of Reference (5). This trajectory is one of those generated by the staff of the M.I.T. Instrumentation Laboratory in connection with its study of the feasibility of an unmanned recoverable interplanetary space probe.

Figure 4-1, which illustrates the trajectory, is a reprint of a portion of Figure 4-8 of Reference (5). The orbits of Earth, Mars, and the space vehicle are shown, and their respective positions at three different times during the voyage are indicated. In the cases of Mars and the space vehicle, that part of the orbit which is represented by a solid line is the part for which the orbital plane is "above" the ecliptic (i.e., z_E is positive), while the dashed lines indicate the parts of the orbital planes "below" the ecliptic. The last frame of the figure shows the vehicle's trajectory relative to Mars as it passes by the planet.

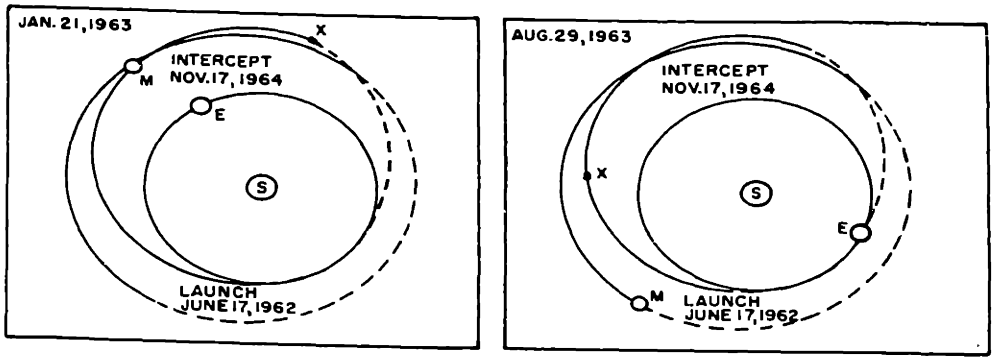

S – Sun

E – Earth

M – Mars

X – Space vehicle

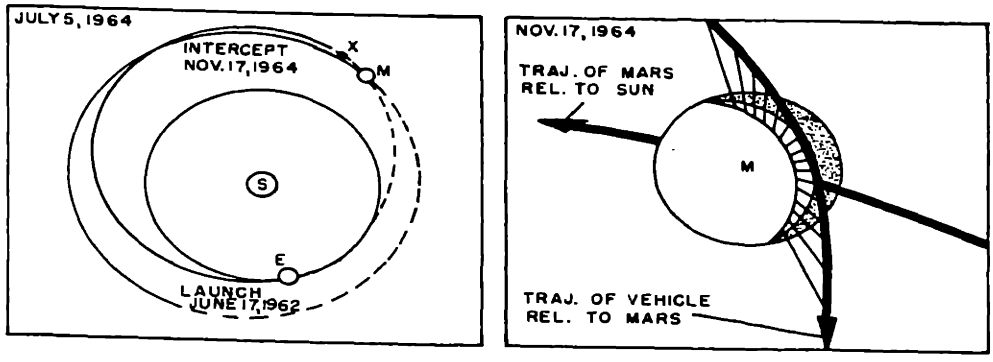

Figure 4.1 Outbound Leg of Trajectory No. 1034

For these illustrative calculations the destination point has been taken as the point of closest approach to Mars, and an elliptical reference trajectory between injection and arrival at the destination has been formulated. The perturbative effect of Mars on the vehicle has been ignored. Although this combination of conditions is not realistic for an accurate guidance analysis (as indicated in Section 3.19), it has the advantage of being more easily adapted to the data that were initially available, and it is adequate to demonstrate the techniques that have been formulated.

The programming of the computations and the plotting of the graphs in this chapter have been carried out by Captain Mack Mauldin, Jr. and Captain Robert G. Millard, both of the United States Air Force, and are described in detail in their Master of Science thesis.[32]

4.3 Characteristics of the Reference Trajectory

The following data apply to Trajectory No. 1034:

Departure date from Earth	June 17, 1962
Arrival date in vicinity of Mars	November 17, 1964
Time of flight	2.422 years
Minimum distance of space vehicle from surface of Mars	4,693 miles

The orbital elements of the heliocentric elliptical trajectory are

$a = 1.3242$ a.u.

$e = 0.2432$

$t_o = 0.0545$ years after epoch at injection into heliocentric orbit

$\Omega_E = 85.80°$

$i_E = 3.130°$

$\omega_E = -158.41°$

The alternate orbital elements are

$$M_o = -12.86° = M_I$$

$$\phi_E = -72.61°$$

The period and mean angular motion are

$$P = 1.524 \text{ years}$$

$$n = 4.123 \text{ radians/year}$$

At the time of injection,

$$t_I = 0$$

$$f_I = -21.59°$$

$$E_I = -16.92°$$

At the time of arrival at Mars,

$$t_D = 2.422 \text{ years}$$

$$f_D = 552.24°$$

$$E_D = 555.66°$$

$$M_D = 559.42°$$

The total differences in the anomalies are

$$f_D - f_I = 573.83°$$

$$E_D - E_I = 572.58°$$

$$M_D - M_I = 572.28°$$

The magnitude and orientation angles of the relative velocity $\underline{v}_R$ are

$$v_R = 11,390 \text{ ft/sec}$$

$$\Omega_D = 123.25°$$

$$i_D = 77.12°$$

4.4 Description of Data and Graphs

Figures 4.2 through 4.17 are graphs representing the guidance parameters that have been computed for Trajectory No. 1034. In this section the individual figures are described, and the methods of obtaining the plotted data are indicated. In some cases the equations used by Mauldin and Millard to obtain the data differ in form, but not in substance, from those that are suggested here. The difference is due to the fact that the final forms of some of the equations developed in this thesis were evolved subsequent to the time that the computations were made.

The unit of length used in the computations is the astronomical unit (a.u.), and the unit of time is the year.

In most of the plots the abscissa is $(f_2 - f_1)$. f_2 is the same as f_D, the true anomaly at the destination point; it is equal to 552.24°. The variable part of the abscissa is f_1, the true anomaly at any earlier point of the trajectory. f_1 is usually associated with the time of a midcourse correction. The value of f_1 (and of time t_1) increases from left to right in the graphs; the plotted value of $(f_2 - f_1)$ increases from right to left. The choice of $(f_2 - f_1)$ as the abscissa is motivated by the fact that two of the three types of singularities in FTA guidance occur when $(f_2 - f_1)$ is an integer multiple of 180°.

The reciprocal of the velocity correction is plotted instead of the correction itself, in order to circumvent the scaling difficulty at the singular points, where the FTA correction becomes infinite.

Figure 4.2 is the basic plot for the determination of the optimum time of correction. $1/c_V$ is plotted as a function of $(f_2 - f_1)$ for several fixed values of ψ. The computation is normalized by computing c_V and $1/c_V$ for a miss distance magnitude, $\delta\rho^-$, of one astronomical unit. The ordinate $1/c_V$ in the graph has the dimensions of years/a.u. To give the ordinate more physical significance, it may be noted that a velocity of 1 a.u./year is equivalent to 2.94 mi/sec or 15,540 ft/sec. Thus, if the value of $1/c_V$ read from the graph is 1 year/a.u. and the miss distance is 9270 miles (10^{-4} a.u.), the magnitude of the correction is approximately $1\frac{1}{2}$ ft/sec.

Figures 4.3 and 4.4 are cross-plots of the data in Figure 4.2. In 4.3 the values of $(f_2 - f_1)_{opt}$, corresponding to the maxima of $1/c_V$, are plotted as a function of ψ; in 4.4 the maxima of $1/c_V$ are plotted as a function of ψ. The dotted portions of the curves, occurring at ψ's between 170° and 180°, are caused by the fact that the constant-ψ curves in this region (which are not shown in Figure 4.2) exhibit a high zero-slope plateau, with no definitive values of $(f_2 - f_1)_{opt}$.

Figures 4.5 and 4.6 are the FTA correction curves corresponding to the VTA curves of Figure 4.2. These curves are drawn for $\delta\rho^- = 1$ a.u. and $\delta\zeta_D^- = 0$. It is necessary in the FTA case to assume a value of $\delta\zeta_D^-$, because this component of the position variation does affect the FTA correction, although it has no effect on the VTA correction.

The data for Figures 4.2, 4.5, and 4.6 are obtained by use of the equations of Appendix N.

$$(\underline{c}_F)_W = \overset{*}{X}_C \, \underline{c}_F = - \overset{*}{X}_C \, \overset{*}{K}_{CD} \, \overset{*}{X}_D{}^T \, (\delta \underline{r}_D{}^-)_W \qquad (4\text{-}1)$$

Since $\delta\zeta_D^-$ has been arbitrarily set at zero and $\delta\rho^-$ has been arbitrarily set at 1 a.u.,

$$(\delta \underline{r}_D{}^-)_W = (\delta\rho^-) \begin{Bmatrix} \cos\psi \\ \sin\psi \\ 0 \end{Bmatrix} = \begin{Bmatrix} \cos\psi \\ \sin\psi \\ 0 \end{Bmatrix} \qquad (4\text{-}2)$$

(4-2) is substituted into (4-1).

$$(\underline{c}_F)_W = - \overset{*}{X}_C \, \overset{*}{K}_{CD} \, \overset{*}{X}_D{}^T \begin{bmatrix} 1 & 0 & 0 \\ 0 & 1 & 0 \\ 0 & 0 & 0 \end{bmatrix} \begin{Bmatrix} \cos\psi \\ \sin\psi \end{Bmatrix} \qquad (4\text{-}3)$$

The elements of $\overset{*}{X}_C \overset{*}{K}_{CD} \overset{*}{X}_D{}^T$ are given by Equation (N-25). The non-zero element in the third row and third column is not used. The first two components of the solution for $(\underline{c}_F)_W$ constitute the two-dimensional vector $\underline{c}_W$.

The computation is carried out by fixing E_1, determining the corresponding value of $(f_2 - f_1)$, then computing the components of $(c_F)_W$ for ten-degree increments in ψ between 0° and 170°. The process is repeated for a range of E_1's between E_I (- 16.92°) and E_D (555.66°).

Figures 4.2, 4.5 and 4.6 show the effect on the velocity correction of a position variation at the destination which lies in the critical plane. Figures 4.7 through 4.11 are the results of a similar study, the difference being that in these plots the position variation at the destination lies either normal to or in the reference trajectory plane. In the figures $1/c_V$ and $1/c_F$ are plotted as a function of $(f_2 - f_1)$ for various orientations of a $\delta \underline{r}_D$ vector whose magnitude is 10^{-4} a.u. The basic equations used in the computations are

$$\underline{c}_F = - \overset{*}{K}_{CD} \, \delta \underline{r}_D \tag{4-4}$$

$$\underline{c}_V = \left(\overset{*}{I}_3 - \frac{\underline{w} \, \underline{w}^T}{\underline{w}^T \, \underline{w}} \right) \underline{c}_F \tag{4-5}$$

where

$$\underline{w} = \overset{*}{K}_{CD} \, \underline{v}_R \tag{4-6}$$

and Equation (3-133) contains analytic expressions for the elements of $\overset{*}{K}_{CD}$.

Figures 4.12 through 4.17 indicate the effect of a position variation or a velocity variation at time t_1 on the magnitude of the position and velocity variations at time t_2. The data are obtained by use of the transition matrix, the elements of which are given in Equation (3-119).

$$\delta \underline{x}_2 = \begin{Bmatrix} \delta \underline{r}_2 \\ \delta \underline{v}_2 \end{Bmatrix} = \overset{*}{C}_{21} \begin{Bmatrix} \delta \underline{r}_1 \\ \delta \underline{v}_1 \end{Bmatrix} \tag{4-7}$$

4.5 Analysis of Graphical Results

Figure 4.2 indicates that for the given reference trajectory there is a minimum value of c_V between 0° and 180° of true anomaly difference, another minimum between 180° and 360°, and a third between 360° and 540°. Except for the unusual behavior of the curves in the range of ψ close to 175°, the three minima of c_V for a given ψ are roughly equal; this is indicated by the cross-plot of Figure 4.4. The actual value of $c_{V_{min}}$ is strongly affected by the predicted ψ. When ψ is equal to 90°, the required correction is approximately an order of magnitude greater than it is when ψ is in the vicinity of 0° (or 180°).

The optimum time of correction, $t_{C_{opt}}$, can be determined directly from the value of $(f_2 - f_1)$ corresponding to $c_{V_{min}}$. Figure 4.3 indicates that in the range of ψ between 45° and 135° there is little variation of $t_{C_{opt}}$ with ψ, but in the ψ ranges 0° to 45° and 135° to 180° (particularly in the vicinity of ψ = 175°) the variation of $t_{C_{opt}}$ with ψ is noticeable.

Curves similar to those of Figure 4.3, but with $t_{C_{opt}}$ replacing $(f_2 - f_1)_{opt}$ as the ordinate, can be built into the on-board computer of a space vehicle and used to determine the time of the next VTA velocity correction. The fact that there are three values of $t_{C_{opt}}$ for each ψ requires that some type of simple strategy be designed to determine which of the three to choose if all three are subsequent to the time at which a reliable value of ψ has been computed. If the space mission is such that three or more midcourse corrections are to be made, an effective strategy is to apply the correction at the earliest $t_{C_{opt}}$ following the time of determination of ψ. It is then possible to apply three corrections, each at the $t_{C_{opt}}$ corresponding to the ψ computed for a particular segment of the actual trajectory. If only one midcourse correction is to be applied during the voyage, it is generally advantageous to select the last of the three values of $t_{C_{opt}}$ in order to reduce the uncertainty in position at the time of arrival at the destination. Selection of the last $t_{C_{opt}}$ tends to reduce position uncertainty in two ways: first, it allows more time for gathering data

from which $\delta \underline{x}_D^-$ is estimated, and consequently the accuracy of the computation of $\underline{c}_V$ is improved; secondly, uncertainty in the application of corrective thrust generally causes a smaller uncertainty in final position if the time of the correction is closer to the time of arrival.

The problem of which $t_{C_{opt}}$ to select for a given ψ has no relevance for manned space missions. The primary consideration for such missions is minimization of the time of flight. The total transfer angle $(f_D - f_I)$ for one leg of a manned flight is normally less than 180°; consequently there is only one value of $t_{C_{opt}}$ for each ψ. The portion of Figure 4.2 for the range of $(f_2 - f_1)$ between 0° and 180° is typical of the curves that may be expected on an outbound manned trip to Mars.

Figure 4.3 indicates that the minimum value of $(f_2 - f_1)_{opt}$ is 80°. If the vehicle is less than 80° away from its destination, there is no need to determine $(f_2 - f_1)_{opt}$, for it will have occurred at a point on the trajectory that the vehicle has already passed. The most economical time to correct is then the earliest feasible time (i.e., the earliest time at which a reliable estimate of $\delta \underline{\rho}^-$ is available).

Figures 4.5 and 4.6 contain FTA curves corresponding to the VTA curves of Figure 4.2. It is difficult to make a direct comparison of the VTA and FTA velocity corrections, because the latter are dependent on the additional variable $\delta \zeta_D^-$; the curves of Figures 4.5 and 4.6 are drawn for $\delta \zeta_D^-$ equal to zero. For the non-singular points in the two figures, the effect of varying $\delta \zeta_D^-$ at a given $(f_2 - f_1)$ and a given ψ is to produce a variation in c_F from a minimum value which is equal to c_V under the given conditions to a maximum value which is at least as much greater than the plotted value of c_F as the plotted value is greater than c_V. At the singular points c_F is infinite regardless of the value of $\delta \zeta_D^-$.

The most immediately noticeable difference between the VTA and FTA curves is the difference in the number of singularities. Whereas the only singularities in c_V occur at $(f_2 - f_1) = 0°$ and 360°, there are singularities in c_F at $(f_2 - f_1) = 0°$, 180°, 360°, 470°, and 540°. The singularity at 470° is the X = 0 singularity. These results are in agreement with the analysis of Appendix O. Although there is no singularity in the c_V curves

at true anomaly differences of 180° and 540°, the curves do exhibit minima of $1/c_V$ (or maxima of c_V) at these points; however, the effect of the X = 0 singularity is completely obliterated by VTA guidance. This behavior is due in part to the fact that $i_D = 77°$, and consequently $\underline{v}_R$ is inclined only slightly to the reference trajectory plane. This orientation of $\underline{v}_R$ tends to make the VTA system relatively more effective in counteracting the in-plane singularity at 470° and relatively less effective in counteracting the out-of-plane singularities at 180° and 540°.

When the vehicle is fairly close to its destination, i.e., for values of $(f_2 - f_1)$ of 20° or less, the velocity correction is essentially independent of ψ and is the same for VTA as it is for FTA. The variation of 1/c with $(f_2 - f_1)$ is fairly linear in this range; the slope is approximately 0.0067 yr./a.u. per degree of true anomaly for a predicted miss distance of 1 a.u.

When $(f_2 - f_1)$ increases from 20° toward 45°, the curves for the various values of ψ start to diverge from the common curve characterizing the region below 20°, but for a given ψ and a given $(f_2 - f_1)$ the ordinate is still about the same in the FTA case as it is in the VTA case. Consequently, if a final vernier correction is to be made at a value of $(f_2 - f_1)$ less than 45° and if δr_D^- is equal to $\delta \rho^-$ (i.e., if the noncritical component $\delta \zeta_D^-$ is small enough so that it does not appreciably affect the magnitude of $\delta \underline{r}_D^-$), there is no fuel saving effected by the use of VTA for this correction. The really important consideration in making the vernier correction is to make it as early as possible.

The general shapes of the curves for VTA and FTA guidance are quite similar through the range 0° to 180° in $(f_2 - f_1)$, and there is still some similarity in the range 180° to 360°. The similarity is greatest for ψ's near 90°. In the range of $(f_2 - f_1)$ between 360° and 540° the VTA and FTA curves are decidedly different due to the effect of the X = 0 singularity at $(f_2 - f_1) = 470°$.

With the exception of the special case $\psi = 0°$, each of the constant-ψ curves for FTA guidance has four minimum values of c_F in the plotted range of $(f_2 - f_1)$. The minima occur at intermediate points between the singularities at $(f_2 - f_1) = 540°$, 470°, 360°, 180°, and 0°. For ψ's near 0° (or 180°) the minima tend to decrease in magnitude as the vehicle gets closer to the

destination. For ψ's near 90°, the minima in the ranges 470° to 360°, 360° to 180°, and 180° to 0° are roughly equal, and the minimum in the range 540° to 470° is somewhat higher than the other three. If FTA guidance is to be used and if the predicted ψ is near 0° or 180°, an appreciable amount of fuel can usually be saved by delaying the correction until the point corresponding to the last minimum of c_F has been reached.

When ψ = 0°, there is no singularity in c_F at $(f_2 - f_1)$ = 180° or 540°. This is due to the fact that in this special case, with $\delta\zeta_D$ stipulated to be zero, $\delta\underline{r}_D$ lies in the reference trajectory plane; consequently, δz_D is equal to zero, and the out-of-plane singularities have no effect. Instead of there being singularities at $(f_2 - f_1)$ = 180° and 540°, a comparison of Figure 4.5 with Figure 4.2 indicates that at each of these points c_F is equal to c_V. The two are equal because at these points the noncritical vector $\underline{w}$ is parallel to the z-axis; therefore, $\underline{c}_V$ is the component of $\underline{c}_F$ in the reference trajectory plane. But since δz_D is zero, $\underline{c}_F$ itself lies in the reference trajectory plane, and consequently $\underline{c}_F$ and $\underline{c}_V$ are identical.

When ψ = 0°, the miss distance vector $\delta\underline{\rho}$ lies in the reference trajectory plane. If the position variation vector $\delta\underline{r}_D$ lies along the z-axis, the miss distance vector is parallel to the η_D-axis, and ψ = 90°. Thus, ψ's in the vicinity of 0° or 180° are associated primarily with position variations in the reference trajectory plane, while ψ's close to 90° are associated with position variations normal to the reference trajectory plane. Additional insight into the guidance problem can be obtained by studying the way in which a position variation either in or normal to the reference trajectory plane affects the magnitude of $\underline{c}_V$ and $\underline{c}_F$. Figures 4.7 through 4.11 present the results of such a study; $1/c_V$ and $1/c_F$ are plotted for various orientations of a position variation $\delta\underline{r}_D$ whose magnitude is 10^{-4} a.u. or 9270 miles.

A link may be established between the curves that have already been analyzed and the curves of Figures 4.7 through 4.11. The ψ = 90° curve of Figure 4.2 is the same, except for a difference in the scale and the dimensions of the ordinate, as the VTA curve of Figure 4.7. The ψ = 0° curve of Figure 4.2 would be the same as a curve for $\mu_2 = \Omega_D$ = 123° in Figure 4.9 if such a curve were drawn; the μ_2 = 120° curve of 4.9 closely

resembles the $\psi = 0°$ curve in 4.2. μ_2 is the angle between $\delta \underline{r}_2$ and the p_2-axis. The FTA curve for $\psi = 90°$ in Figure 4.5 bears a close similarity to the FTA curve of Figure 4.7 for values of $(f_2 - f_1)$ between 0° and 360°; at higher values of $(f_2 - f_1)$ the curves are no longer similar. The reason that these two curves are not completely equivalent, as is the case for their VTA counterparts, is that in the curve of 4.5 the position variation to be corrected is parallel to the η_D-axis, while in the curve of 4.7 the variation is parallel to the z_D-axis; the two axes are 13° apart. The in-plane singularity at $(f_2 - f_1) = 470°$ affects the curve of Figure 4.5 but has no effect on the curve of Figure 4.7. Finally, the FTA curve for $\psi = 0°$ in Figure 4.5 is quite similar to the $\mu_2 = 120°$ curve in Figure 4.11.

The curves of Figure 4.7 show that the maxima and minima of c_V occur at the same values of $(f_2 - f_1)$ as the maxima and minima of c_F when $\delta \underline{r}_D$ is parallel to the z-axis. At each of its maxima c_F goes to infinity, while c_V goes to infinity at $(f_2 - f_1) = 0°$ and 360° but reaches finite maxima at $(f_2 - f_1) = 180°$ and 540°. The minima of c_V are not materially lower than the corresponding minima of c_F. The variation of $1/c_F$ with $(f_2 - f_1)$ is periodic, repeating itself every 360° of $(f_2 - f_1)$. The periodicity becomes apparent if k_{33}, the only element in the correction matrix $\overset{*}{K}_{CD}$ that affects z-axis motion, is written as follows:

$$k_{33} = \frac{h}{r_C \, r_D \sin(f_D - f_C)} \tag{4-8}$$

The variation of $1/c_V$ with $(f_2 - f_1)$ does not repeat itself exactly every 360° of $(f_2 - f_1)$ due to the presence of the secular term in k_{11}, which affects $\underline{w}$, which in turn affects $\underline{c}_V$. The fact that the FTA and VTA curves are so close to each other is a manifestation of a point that has already been made, namely that for this particular reference trajectory, with $\underline{v}_R$ being situated close to the reference trajectory plane, VTA guidance is relatively ineffective in reducing the magnitude of the velocity correction if $\delta \underline{r}_D$ is parallel to the z-axis.

Comparison of the VTA curves of Figures 4.8 and 4.9 with the FTA curves of Figures 4.10 and 4.11 indicates that VTA usually reduces the magnitude of the required correction by an appreciable percentage if $\delta \underline{r}_2$ is in the reference trajectory plane. For any value of μ_2, the VTA and

FTA curves are tangent to each other at $(f_2 - f_1) = 180°$ and 540°; this is due to the fact that the noncritical vector $\underline{w}$ is parallel to the z-axis at these two values of $(f_2 - f_1)$. Both c_V and c_F go to infinity at $(f_2 - f_1) = 360°$ for all values of μ_2 except $\mu_2 = 90°$. For the special case $(f_2 - f_1) = 360°$ and $\mu_2 = 90°$, the VTA and FTA curves are tangent to each other at a finite value of 1/c. Sections O.4, O.5, and O.14 indicate the reason for the absence of the singularity at $(f_2 - f_1) = 360°$ when $\mu_2 = 90°$, i.e., when $\delta\underline{r}_2^-$ is parallel to $\underline{v}_2$.

The really striking feature of the curves of Figures 4.7 to 4.11 is the large difference in magnitude between an optimum VTA correction of a z-axis position variation and an optimum VTA correction of a position variation in the plane of the reference trajectory. To emphasize this point, the VTA curve of Figure 4.7 has been added to Figures 4.8 and 4.9, and the FTA curve of Figure 4.7 has been added to Figures 4.10 and 4.11. If only the range of $(f_2 - f_1)$ between 0° and 180° is considered, $c_{V_{opt}}$ for a z-axis position variation is at least three to four times as large as $c_{V_{opt}}$ for a position variation of the same magnitude that lies in the reference trajectory plane. For the optimum points at larger values of $(f_2 - f_1)$, the ratio of out-of-plane $c_{V_{opt}}$ to in-plane $c_{V_{opt}}$ is at least as large and may be considerably larger, depending on the orientation of $\delta\underline{r}_2^-$ in the reference trajectory plane; when $\delta\underline{r}_2^-$ lies close to the q_2-axis, $c_{V_{opt}}$ is much smaller than it is when $\delta\underline{r}_2^-$ is close to the p_2-axis.

When FTA guidance is used, the disparity between out-of-plane $c_{F_{opt}}$ and in-plane $c_{F_{opt}}$ is significant but not nearly so great as in the VTA case. This is shown in Figures 4.10 and 4.11.

Figures 4.12 through 4.17 illustrate the contrast between in-plane motion and out-of-plane motion in a different way. The effect on δr_2 and δv_2 is shown for either a position variation of 927 miles = 10^{-5} a.u. at t_1 or a velocity variation of one foot per second at t_1. The most significant curves from the guidance standpoint are the curves relating δr_2 to $\delta\underline{v}_1$ in Figures 4.13 and 4.16. When $\delta\underline{v}_1$ is parallel to the q_1-axis,

δr_2 is usually several times as large as it is when $\delta \underline{v}_1$ is parallel to the p_1-axis; in turn, when $\delta \underline{v}_1$ is parallel to the p_1-axis, δr_2 is usually several times as large as it is when $\delta \underline{v}_1$ is parallel to the z-axis. If the concept of "sensitivity" is introduced, it may be stated that the magnitude of the position variation at the destination is most sensitive to a velocity variation in the q_1 direction at time t_1, is less sensitive to a velocity variation in the p_1 direction, and is least sensitive to a velocity variation in the z direction. Thus, for a given magnitude of $\delta \underline{r}_2$, the magnitude of the optimum FTA correction is generally smallest if the direction of the required correction is close to the q_C-axis, larger if its direction is close to the p_C-axis, and largest of all if its direction is close to the z-axis.

Figures 4.13 and 4.16 also show the effect of an error in injection velocity on position variation at the destination. For an injection velocity error of 1 ft/sec, δr_2 is equal to almost 50,000 miles if the velocity error is in the q_I direction, about 5,000 miles if the velocity error is in the p_I direction, and slightly less than 1,000 miles if the velocity error is in the z direction. If the uncertainty in injection velocity is isotropic, it is probable that the vector $\delta \underline{r}_2$, before the first midcourse correction, will lie close to the reference trajectory plane.

It may be noted from Figure 4.16 that in this particular example the time of actual injection is worse than any later time from the standpoint of sensitivity of position variation at the destination to initial velocity error. For a Hohmann-type transfer, in which $(f_D - f_I)$ is 180°, the sensitivity to an injection velocity error in the q_I direction would be less than half of the value shown for $(f_D - f_I) = 574°$.

The effect of a position variation at t_1 on position variation at t_2 is indicated in Figures 4.12 and 4.14. Again the sensitivity in the z direction is very much less than the sensitivity in the p-q plane. This time, however, the p_1-axis is the most sensitive axis. A position error of one mile in the p_I direction at injection causes a position variation of forty miles at the destination. For the q_I and z directions the sensitivity factor is approximately one mile of position variation at t_D per mile of position variation at t_I. The actual launch point at $(f_D - f_I) = 574°$ has a sensitivity factor in the critical p_1 direction that is twice as large as the factor for a Hohmann transfer.

An isotropic distribution of the uncertainties in position and velocity at injection is not the most desirable distribution. It is preferable to design the injection guidance system in such a manner that the velocity uncertainty in the direction of the velocity vector is minimized even if this results in an increased velocity uncertainty along the other two axes of the p q z coordinate system. In the case of position variation, the uncertainty in the p_I direction should be reduced as much as possible.

A position variation δr_1 of 10^{-5} a.u. produces an effect on δr_2 that is of the same order of magnitude as a velocity variation δv_1 of 1 ft/sec. In the design of the injection guidance system it is relatively easy to keep the uncertainty in heliocentric position at injection below 10^{-5} a.u., but it is virtually impossible to design a system in which the uncertainty in injection velocity is as low as 1 ft/sec. Therefore, the curves relating δr_2 to $\delta \underline{v}_1$ are of considerably greater importance to the guidance system analyst than the curves relating δr_2 to $\delta \underline{r}_1$.

In the guidance concepts considered in this study, $\delta \underline{r}_D$ is the controlled vector and hence is of paramount importance. The vector $\delta \underline{v}_D$, although not controlled, is monitored. It is of some interest, therefore, to examine the effects of $\delta \underline{r}_1$ and $\delta \underline{v}_1$ on the magnitude of $\delta \underline{v}_2$. These effects are shown in Figures 4.12, 4.13, 4.15, and 4.17. For $\delta z_1 = 10^{-5}$ a.u., the maximum magnitude of δv_{z_2} is 0.57 ft/sec; for $\delta v_{z_1} = 1$ ft/sec, the maximum magnitude of δv_{z_2} is 1 ft/sec. When $\delta \underline{r}_1$ lies in the reference trajectory plane, its effect on δv_2 is greatest if $\delta \underline{r}_1$ is close to the p_1-axis, much smaller if $\delta \underline{r}_1$ is close to the q_1-axis (but still considerably larger than the effect of δv_{z_1}). The in-plane relationship between $\delta \underline{v}_1$ and δv_2 is such that δv_2 is most sensitive to a $\delta \underline{v}_1$ in the q_1 direction and much less sensitive to a $\delta \underline{v}_1$ in the p_1 direction.

The shapes of the curves in Figure 4.14 are quite similar to the shapes of the curves in Figure 4.15 for like orientations of $\delta \underline{r}_1$; also, the shapes of the curves in Figure 4.16 are similar to the shapes in Figure 4.17 for like orientations of $\delta \underline{v}_1$. Thus, in relating $\delta \underline{r}_1$ to either δr_2 or δv_2, the p_1 direction is the critical direction; in relating $\delta \underline{v}_1$ to either δr_2 or δv_2, the q_1 direction is the critical direction.

As in the case of the effects on δr_2, the effect on δv_2 of a small error in injection position in the critical p_I direction or a small error in injection velocity in the critical q_I direction is greater at the actual injection point than at any subsequent point of the trajectory. For a Hohmann transfer the sensitivity of δv_2 to injection errors in the critical directions would be halved.

To conclude this section, the effect on the magnitude of the required VTA velocity correction of using a pre-programmed correction time rather than one determined from the phase angle ψ will be investigated. The analysis is based on consideration of a manned flight; therefore, only the range of $(f_2 - f_1)$ between 0° and 180° is studied.

The pre-programmed t_C can be chosen after an analysis of the curves of Figure 4.2. The fact that $\delta \underline{r}_D$ is likely to be oriented close to the reference trajectory plane and the critical plane is inclined at an angle of 77° to the reference trajectory plane indicates that values of ψ close to 0° or 180° are more likely to occur than values in the vicinity of 90°; this suggests that the curves for ψ = 0°, 10°, and 170° be favored in selecting a fixed value of t_C. On the other hand, if the unlikely does occur and ψ on a particular flight is computed to be close to 90°, the minimum correction for a given $\delta \rho$ is much larger than it would be if ψ were 0°; the preselected t_C should not have too adverse an effect on the magnitude of the correction when ψ = 90°. Based on these considerations, a reasonable compromise is to apply the midcourse correction at a t_C corresponding to $(f_2 - f_1) = 100°$.

The effect of the fixed correction time on the magnitude of the VTA correction is shown in Table 4-1 for four different ψ's. The effect is most pronounced for ψ = 0°, where the ratio of the correction at $(f_2 - f_1) = 100°$ to $c_{V_{min}}$ is 1.82; for the other values of ψ in the table the ratio is less than 1.1. At ψ = 90° $c_{V_{min}}$ is seven times the value at ψ = 0°; therefore, even though the ratio is only 1.08 at ψ = 90°, the numerical increase in c_V is sizeable.

TABLE 4-1

Effect of Fixed Correction Time on Magnitude of VTA Correction

ψ	$c_{V_{min}}$	$c_{V_{(f_2 - f_1) = 100°}}$	$\left[c_{V_{(f_2 - f_1) = 100°}} - c_{V_{min}}\right]$	$\frac{c_{V_{(f_2 - f_1) = 100°}}}{c_{V_{min}}}$
	(a.u./yr.)	(a.u./yr.)	(a.u./yr.)	
0°	0.44	0.80	0.36	1.82
10°	0.88	0.91	0.03	1.03
170°	0.96	1.05	0.09	1.09
90°	3.08	3.33	0.25	1.08

4.6 Concluding Remarks

The salient points of the analysis in the last section may be summarized as follows:

1. The method presented for determining the optimum time of application of a VTA correction as a function of the phase angle of the miss distance vector is practical.

2. The same set of curves (Figure 4.2) used to determine the optimum correction time *a posteriori* can also be used alternatively for the determination of a pre-programmed correction time.

3. The variant motion along the z-axis is quantitatively quite different from the variant motion in the reference trajectory plane. The state of the vehicle at the time of arrival at the destination is relatively insensitive to changes in state along the z-axis at the initial or midcourse points. Conversely, the midcourse velocity correction required to produce a specified change in state along the z-axis at the time of arrival is relatively large.

4. The sensitivity of a Venus or Mars trajectory to a 1 ft/sec variation in velocity at a given time is roughly equivalent to the sensitivity of the trajectory to a 1,000 mile variation in position at the same time.

5. The sensitivity of the trajectory is greatest to that component of velocity variation which is parallel to the reference velocity vector and to that component of position variation which is perpendicular to the reference velocity vector and in the reference trajectory plane.

6. It is desirable to design the injection guidance system so that the uncertainty in the magnitude of the injection velocity vector is reduced to a minimum, even at the expense of some increase in the uncertainty of the direction of the injection velocity vector.

7. Although position uncertainty at injection is far less critical than velocity uncertainty, the injection guidance scheme is improved if the position variation component in the direction normal to the injection velocity vector and in the reference trajectory plane is minimized.

8. For "wrap-around" trajectories, in which the total transfer angle is greater than 360°, the sensitivity to injection errors is considerably greater than it is for Hohmann-type trajectories, in which the total transfer angle is 180°.

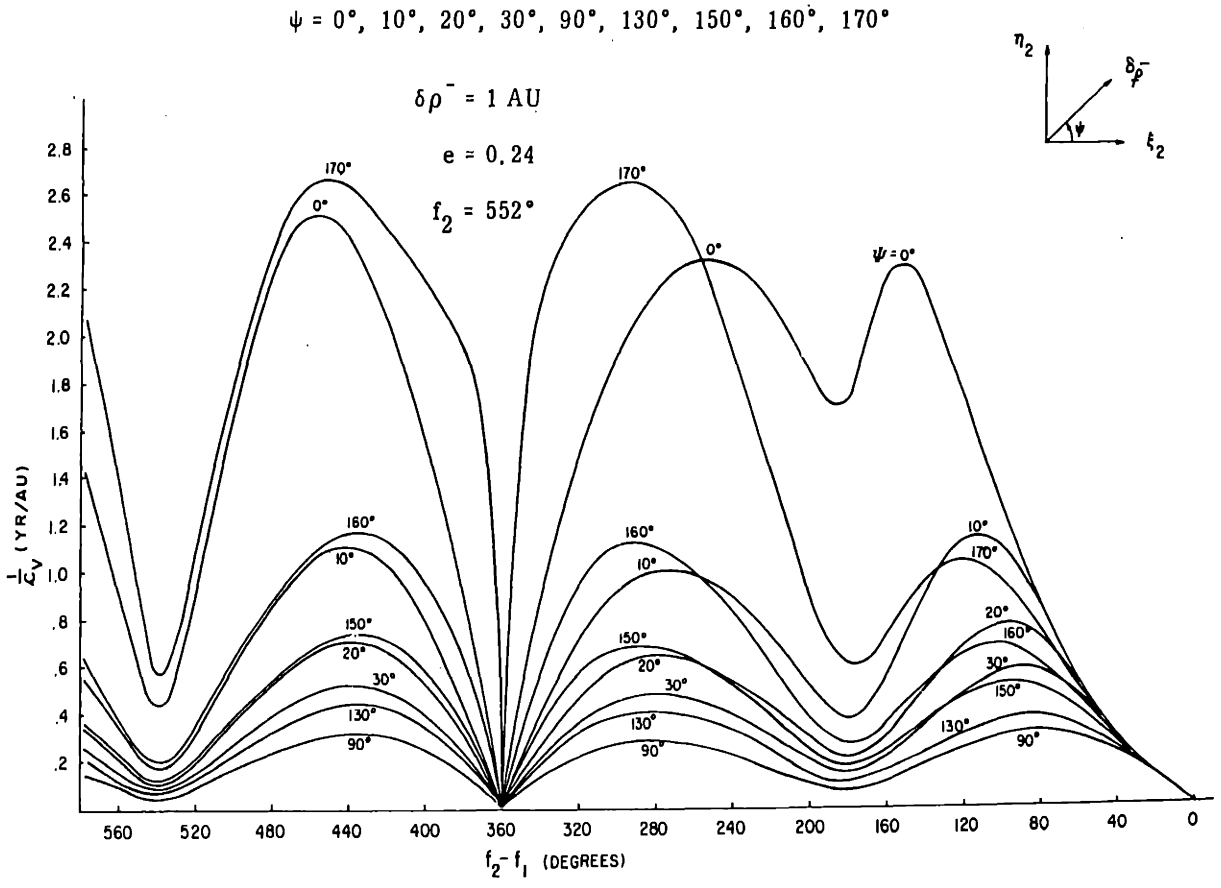

Figure 4.2 Reciprocal of Magnitude of VTA Velocity Correction, $1/c_V$, vs. Difference in True Anomaly, $(f_2 - f_1)$, for Constant Values of Phase Angle ψ.

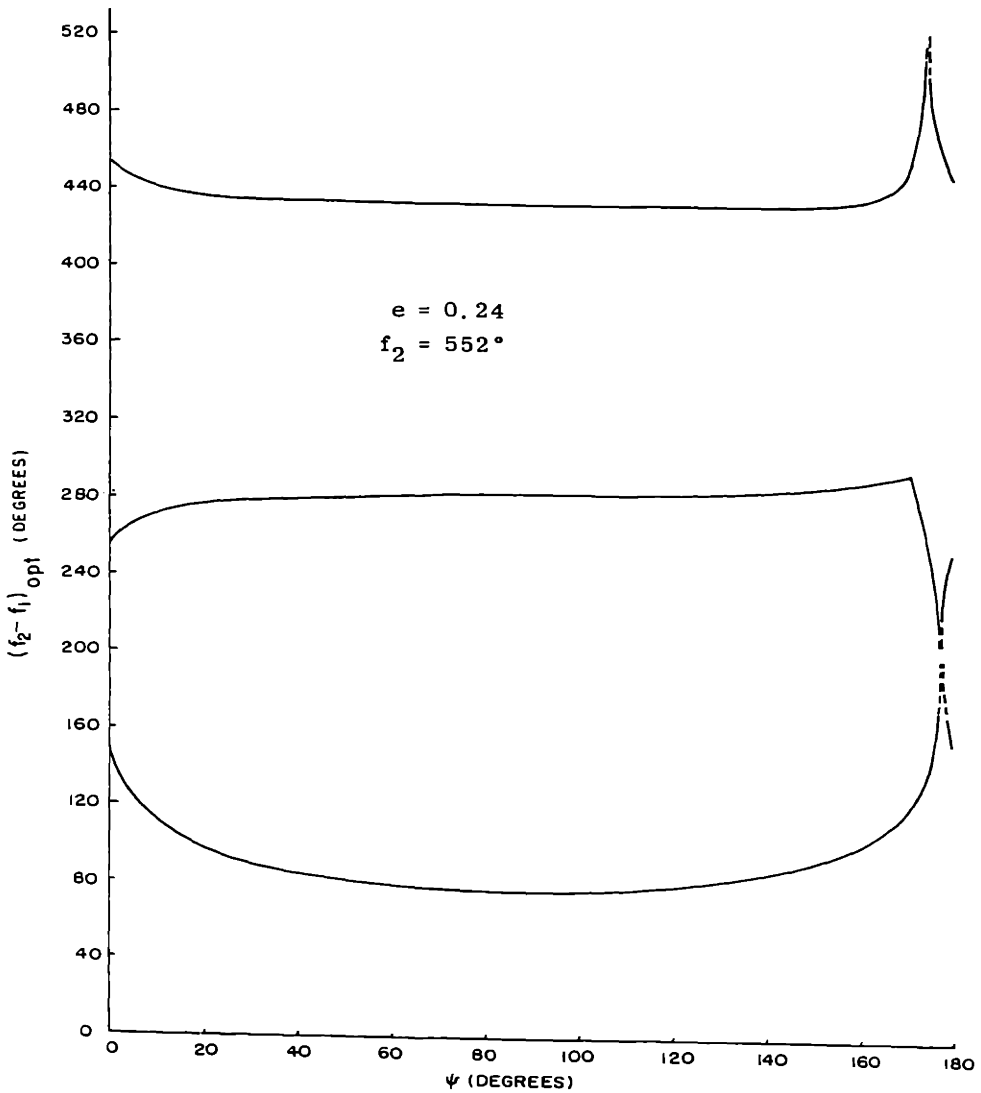

Figure 4.3 Optimum Value of True Anomaly Difference for Application of VTA Velocity Correction

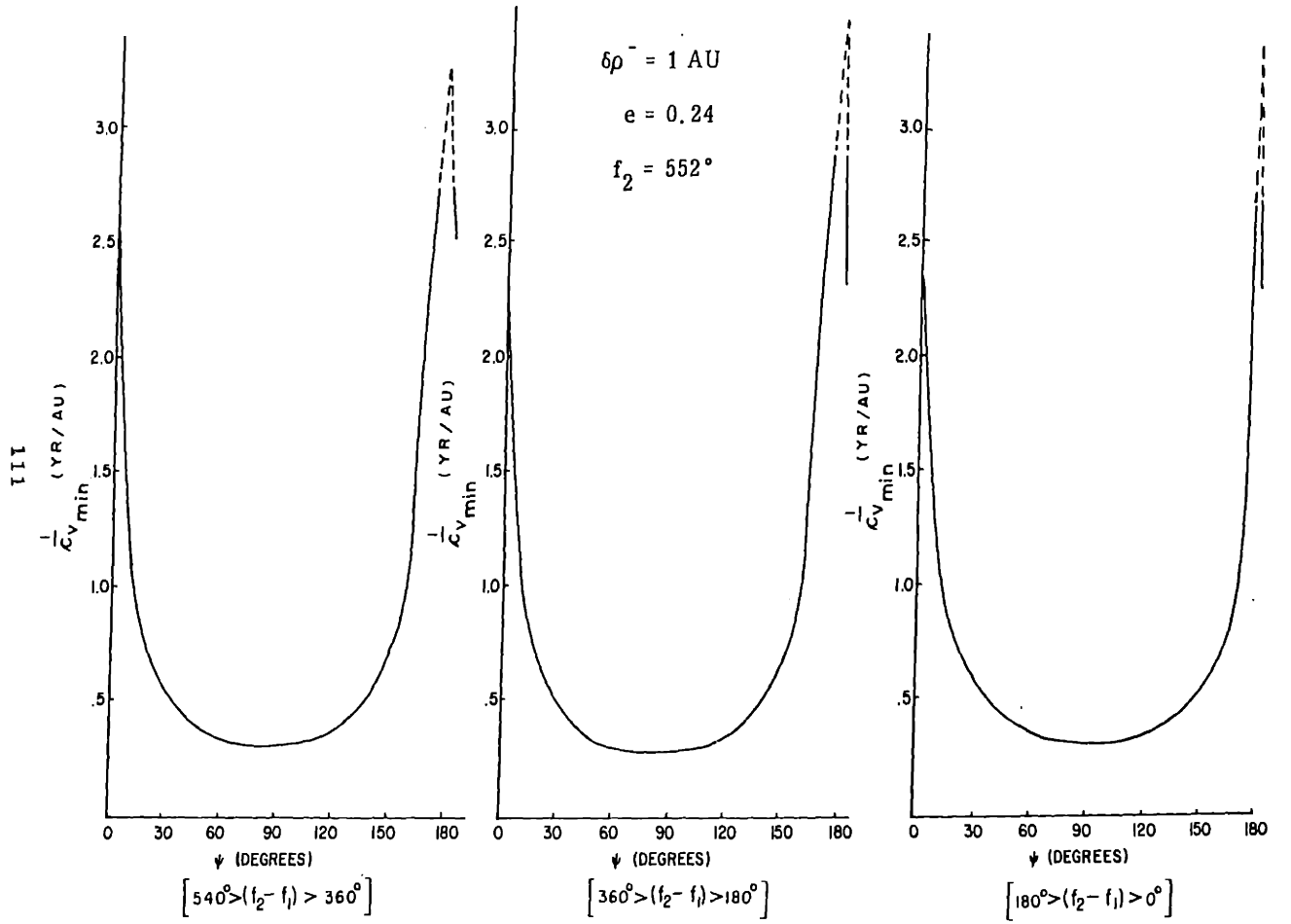

Figure 4.4 Reciprocal of Minimum Value of Magnitude of VTA Velocity Correction, $1/c_{V\ min}$, as a Function of Phase Angle ψ.

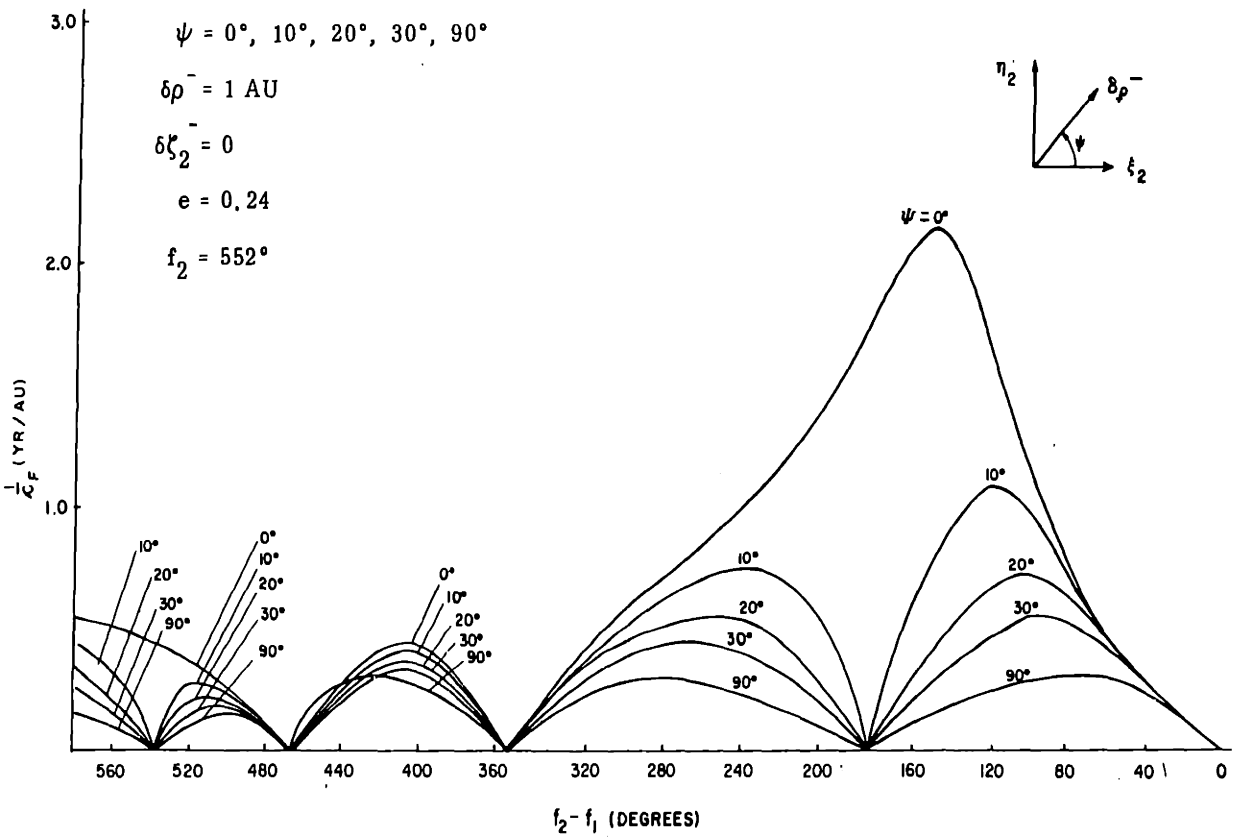

Figure 4.5 Reciprocal of Magnitude of FTA Velocity Correction, $1/c_F$, vs. Difference in True Anomaly, $(f_2 - f_1)$, for Constant Values of Phase Angle ψ between 0° and 90°

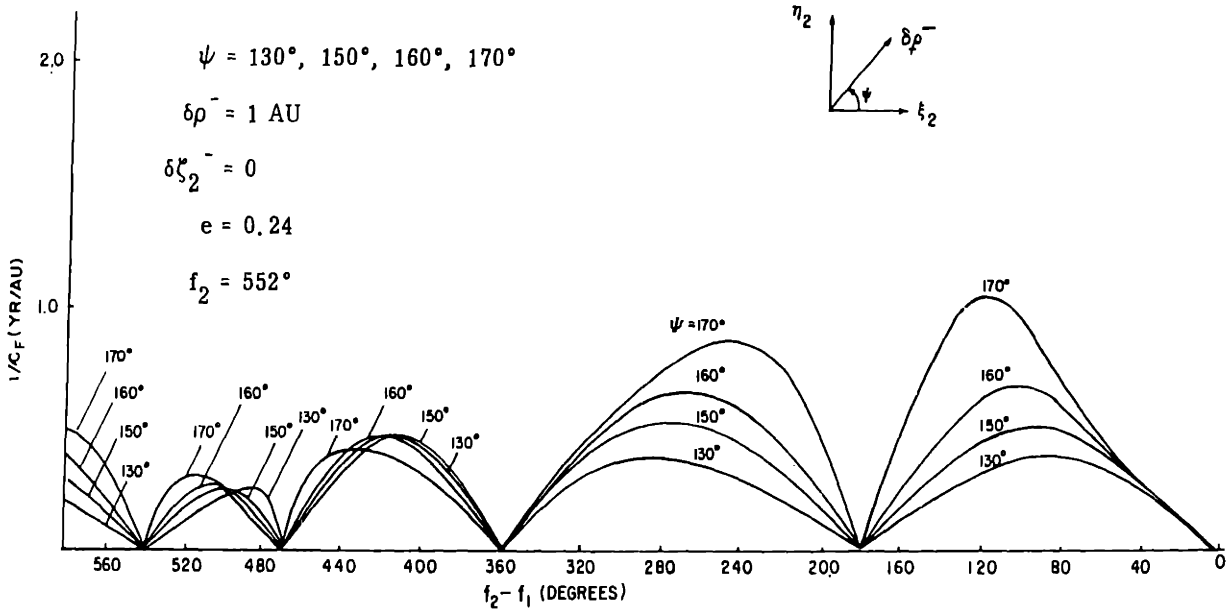

Figure 4.6 Reciprocal of Magnitude of FTA Velocity Correction, $1/c_F$, vs. Difference in True Anomaly, $(f_2 - f_1)$, for Constant Values of Phase Angle ψ between 130° and 170°

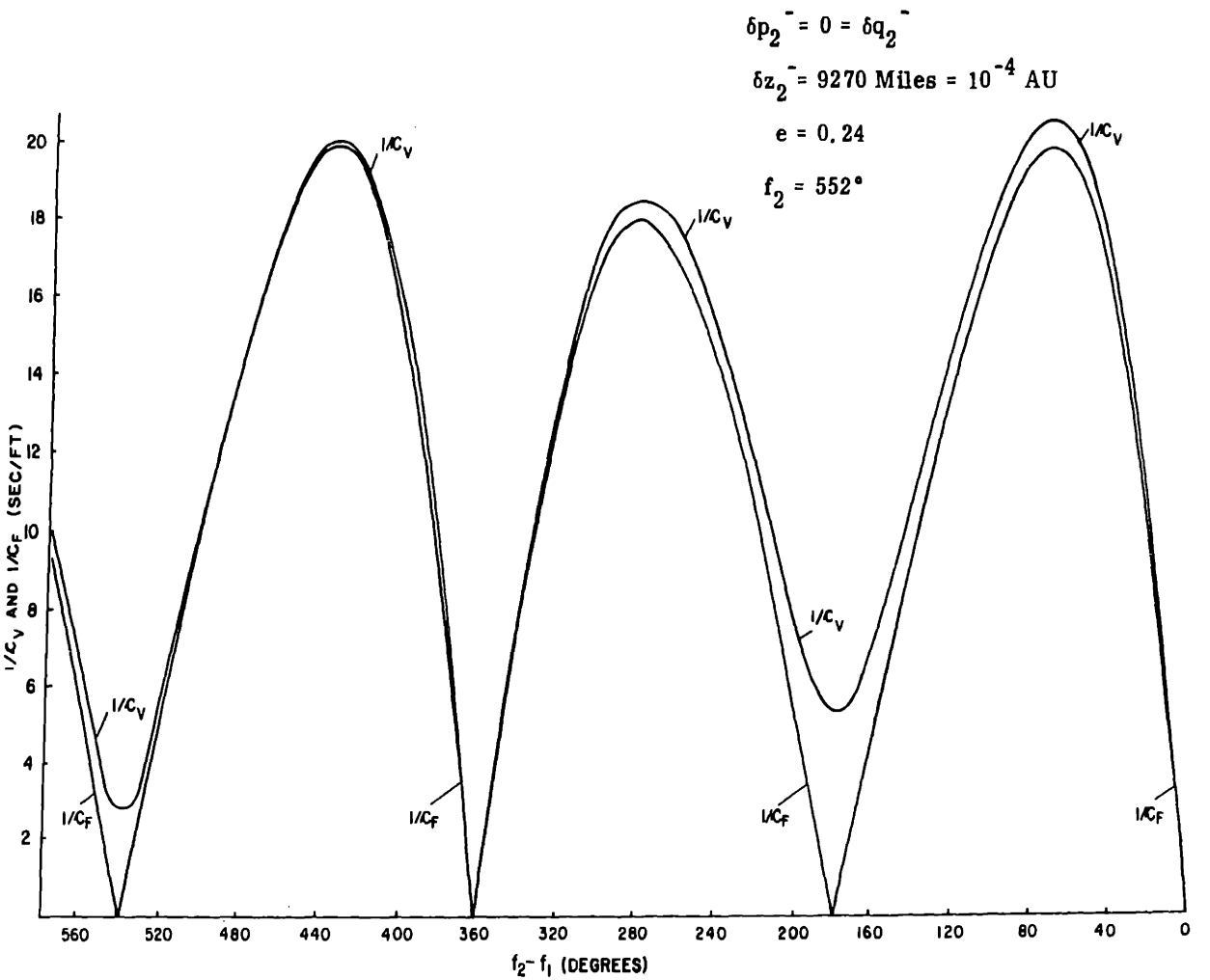

Figure 4.7 Comparison of FTA and VTA Velocity Corrections When Position Variation at Destination is Normal to Reference Trajectory Plane

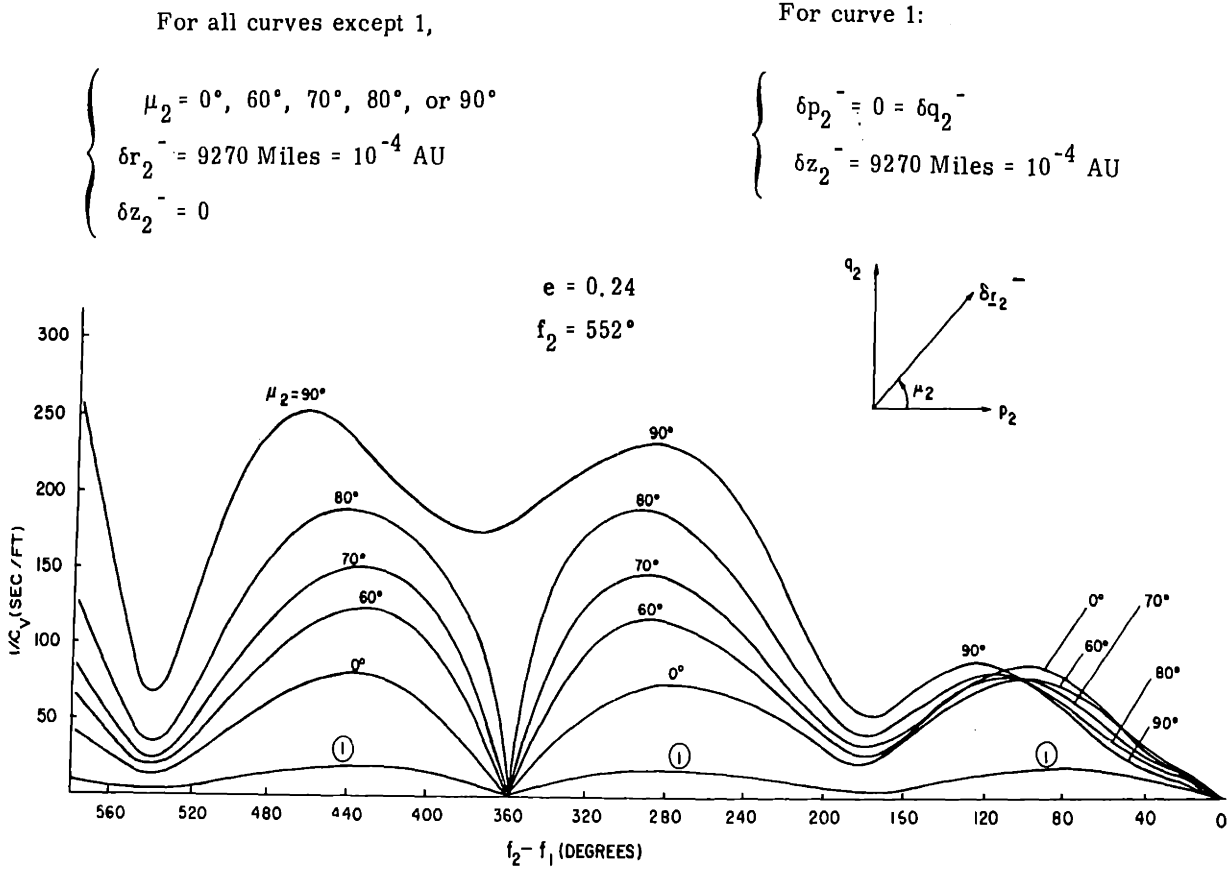

Figure 4.8 Reciprocal of Magnitude of VTA Velocity Correction, $1/c_V$, vs. Difference in True Anomaly, $(f_2 - f_1)$, for Constant Values of Phase Angle μ_2 between 0° and 90°

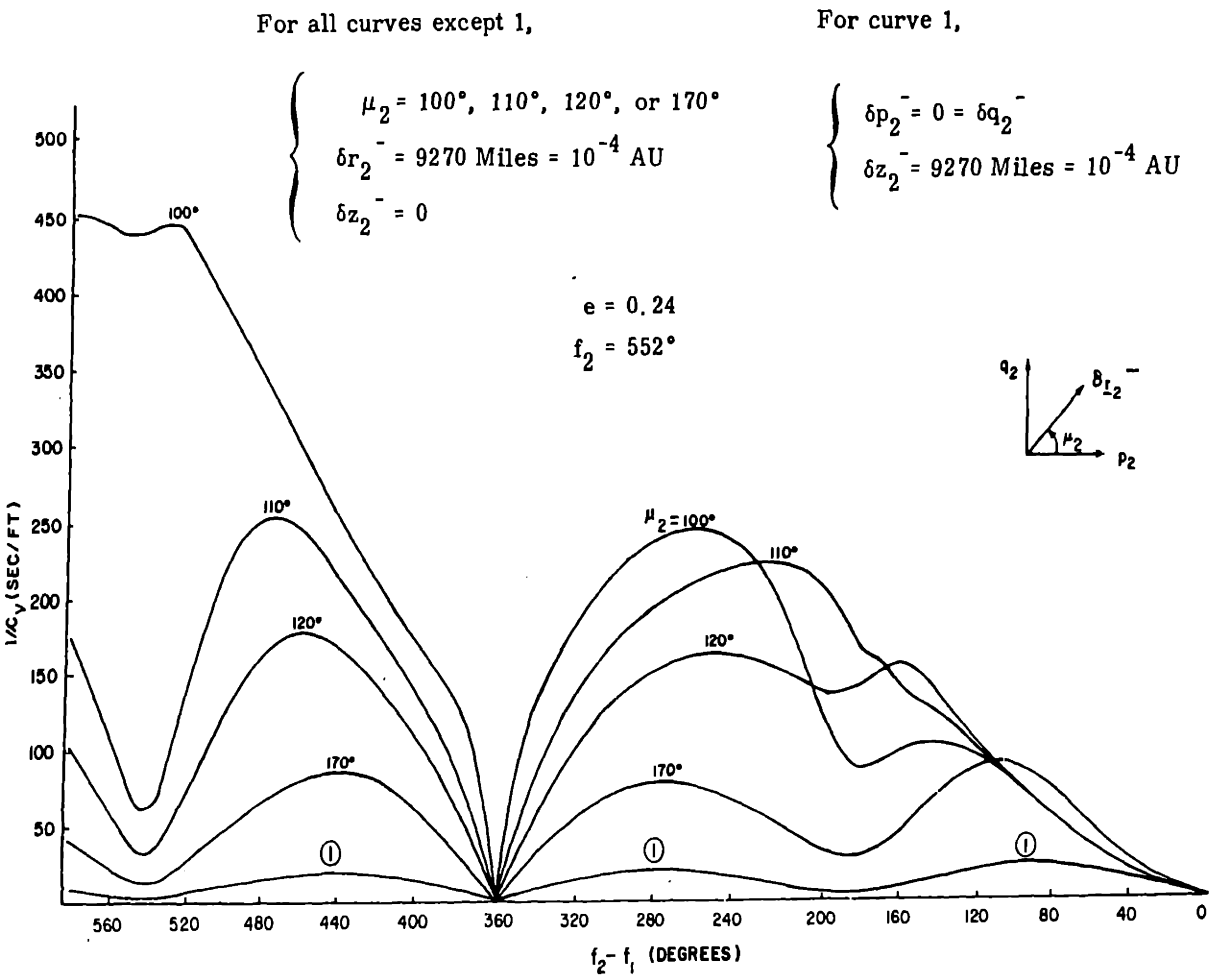

Figure 4.9 Reciprocal of Magnitude of VTA Velocity Correction, $1/c_V$, vs. Difference in True Anomaly, $(f_2 - f_1)$, for Constant Values of Phase Angle μ_2 between 100° and 170°

For all curves except 1,

$$\begin{cases} \mu_2 = 0°,\ 60°,\ 70°,\ 80°,\ \text{or } 90° \\ \delta r_2^- = 9270 \text{ Miles} = 10^{-4} \text{ AU} \\ \delta z_2^- = 0 \end{cases}$$

For curve 1,

$$\begin{cases} \delta p_2^- = 0 = \delta q_2^- \\ \delta z_2^- = 9270 \text{ Miles} = 10^{-4} \text{ AU} \end{cases}$$

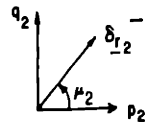

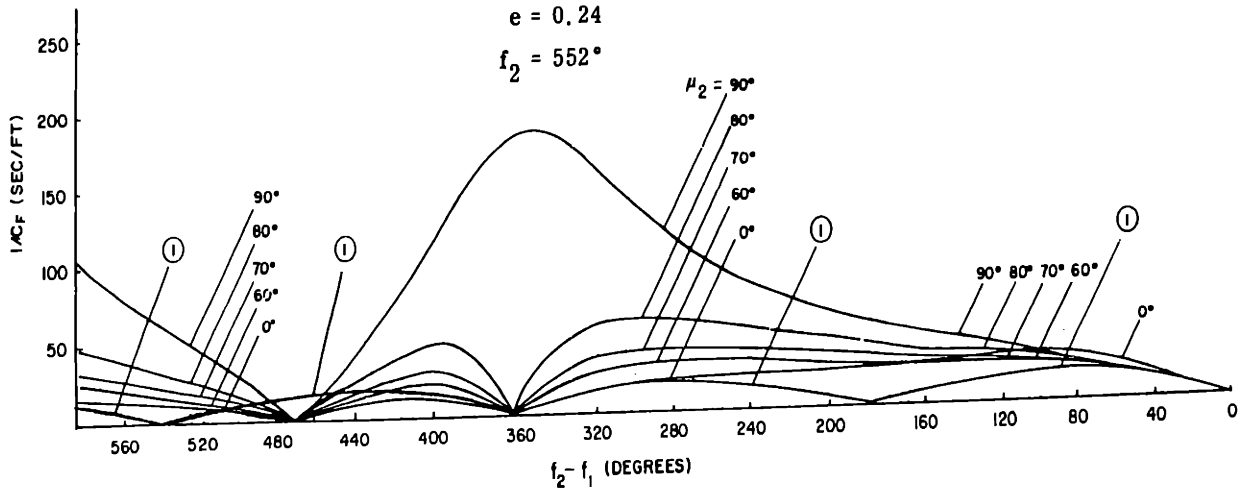

Figure 4.10 Reciprocal of Magnitude of FTA Velocity Correction, $1/c_F$, vs. Difference in True Anomaly, $(f_2 - f_1)$, for Constant Values of Phase Angle μ_2 between 0° and 90°

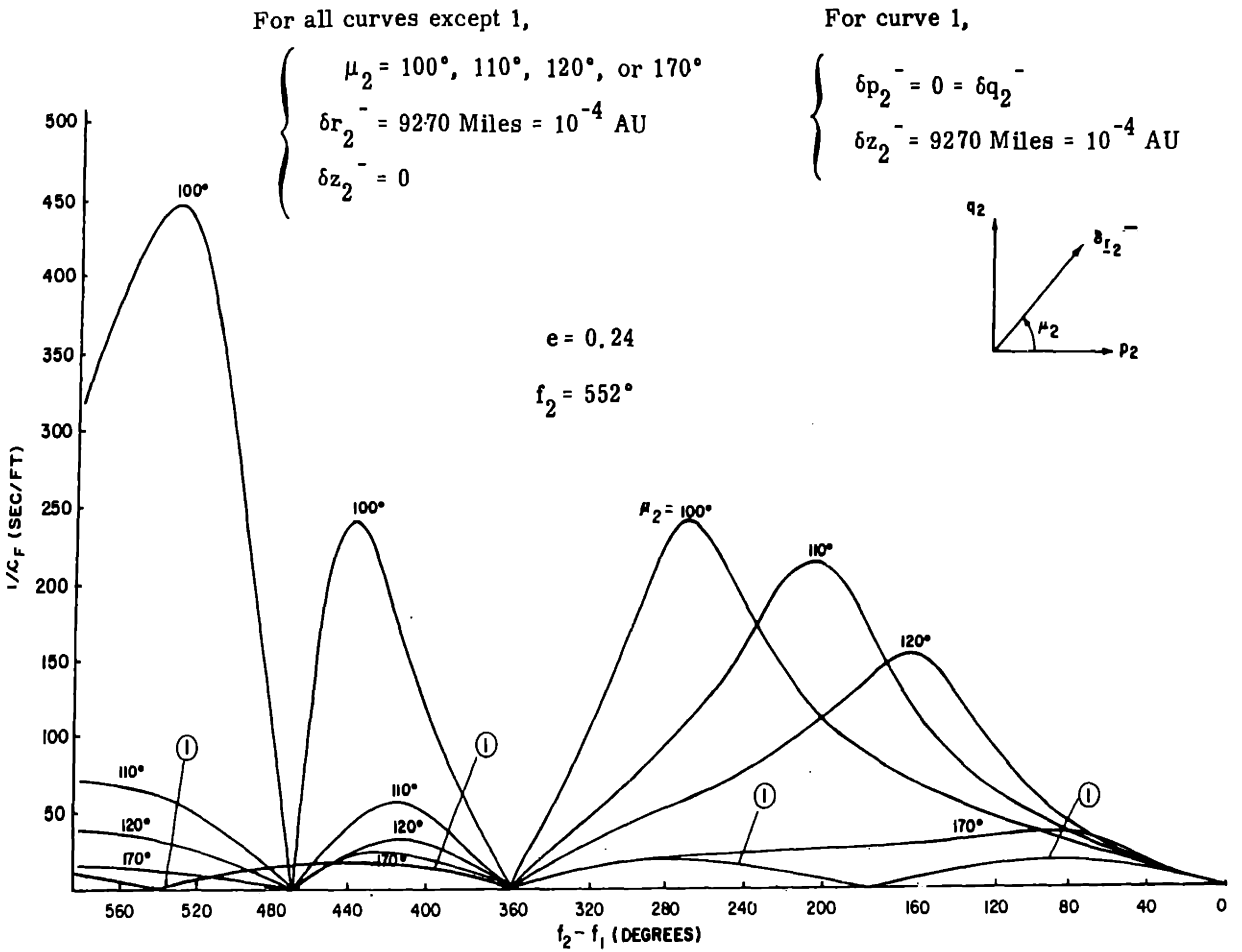

Figure 4.11 Reciprocal of Magnitude of FTA Velocity Correction, $1/c_F$, vs. Difference in True Anomaly, $(f_2 - f_1)$, for Constant Values of Phase Angle μ_2 between 100° and 170°

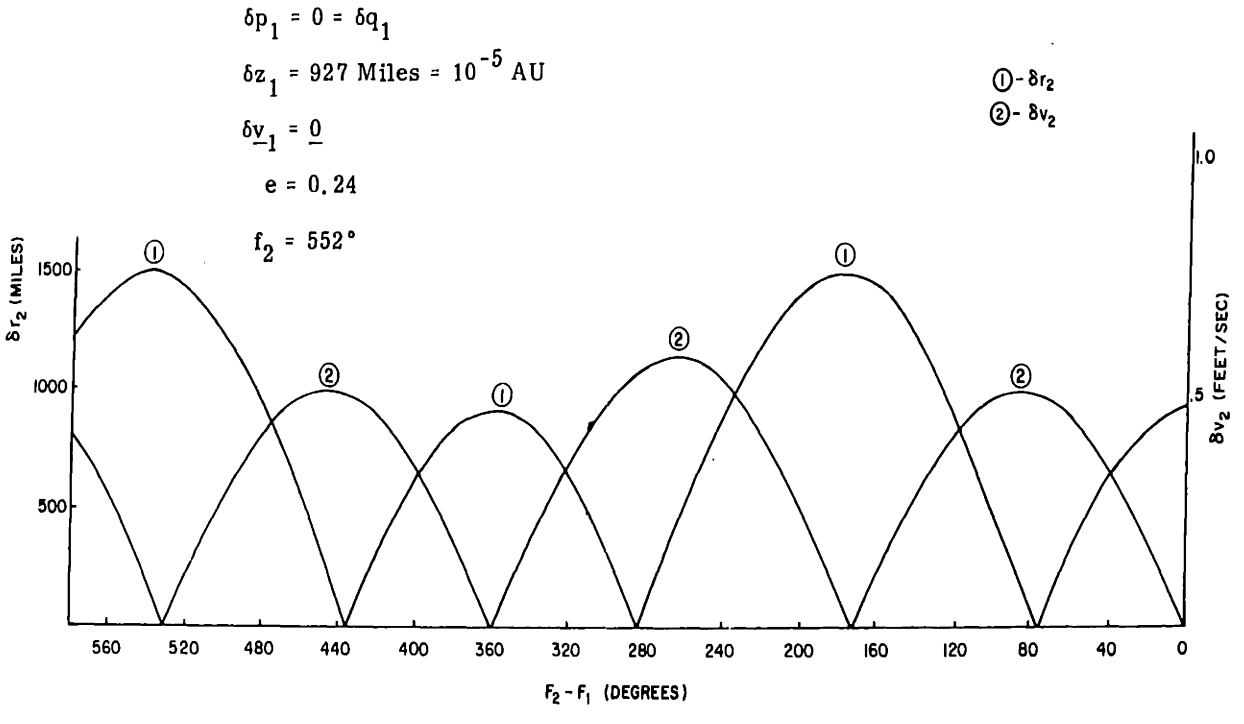

Figure 4.12 Effect of Position Variation Normal to Reference Trajectory Plane at Time t_1 on Position Variation and Velocity Variation at Time t_2

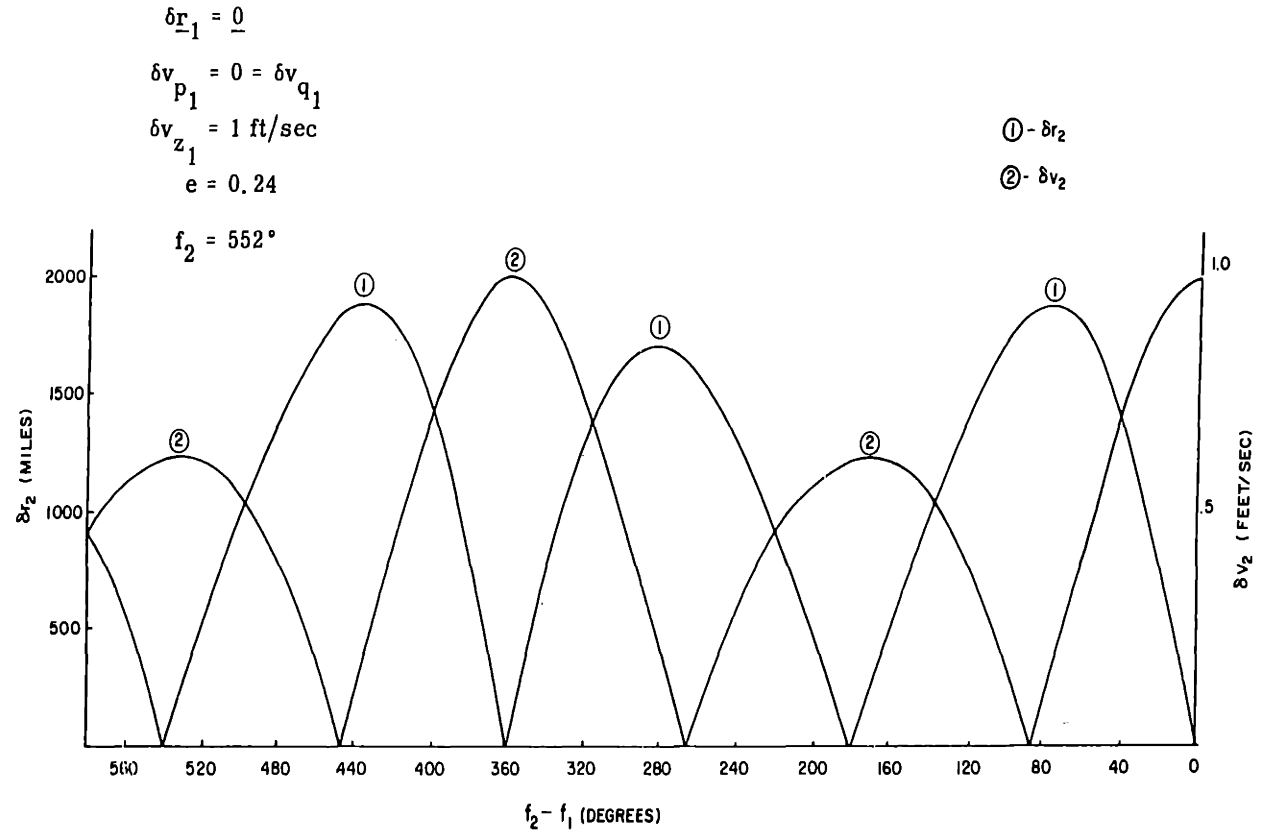

Figure 4.13 Effect of Velocity Variation Normal to Reference Trajectory Plane at Time t_1 on Position Variation and Velocity Variation at Time t_2

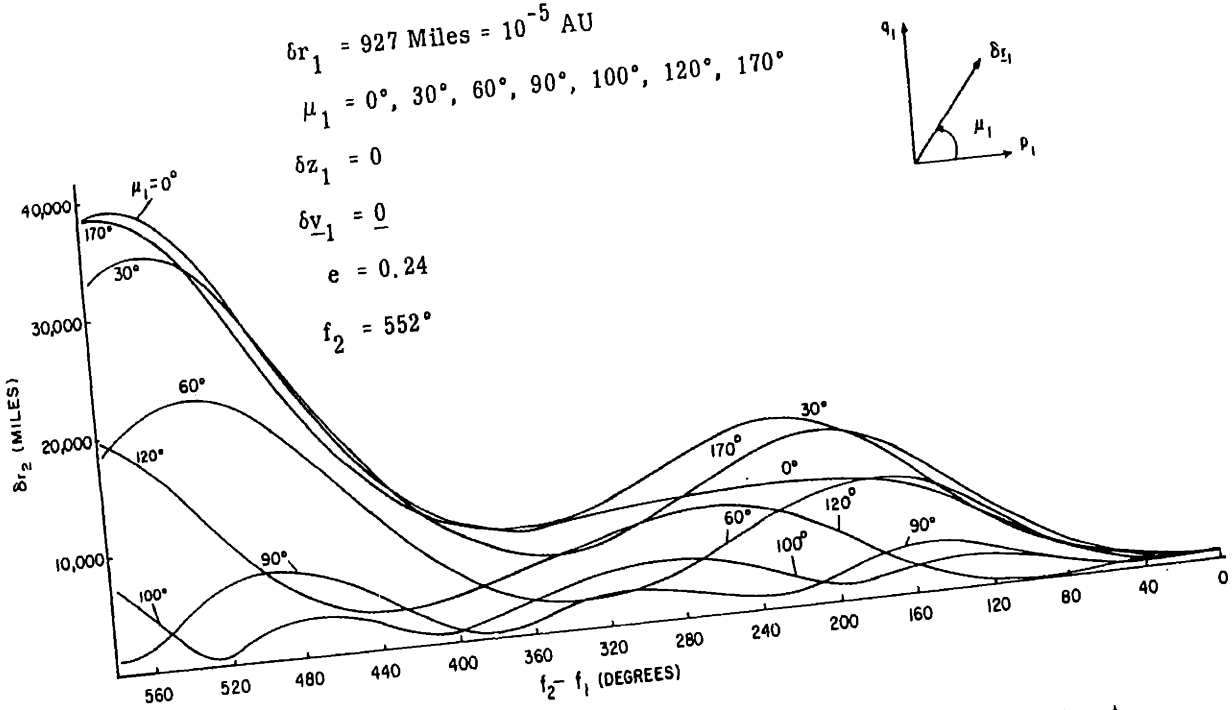

Figure 4.14 Effect of Position Variation in Reference Trajectory Plane at Time t_1 on Position Variation at Time t_2

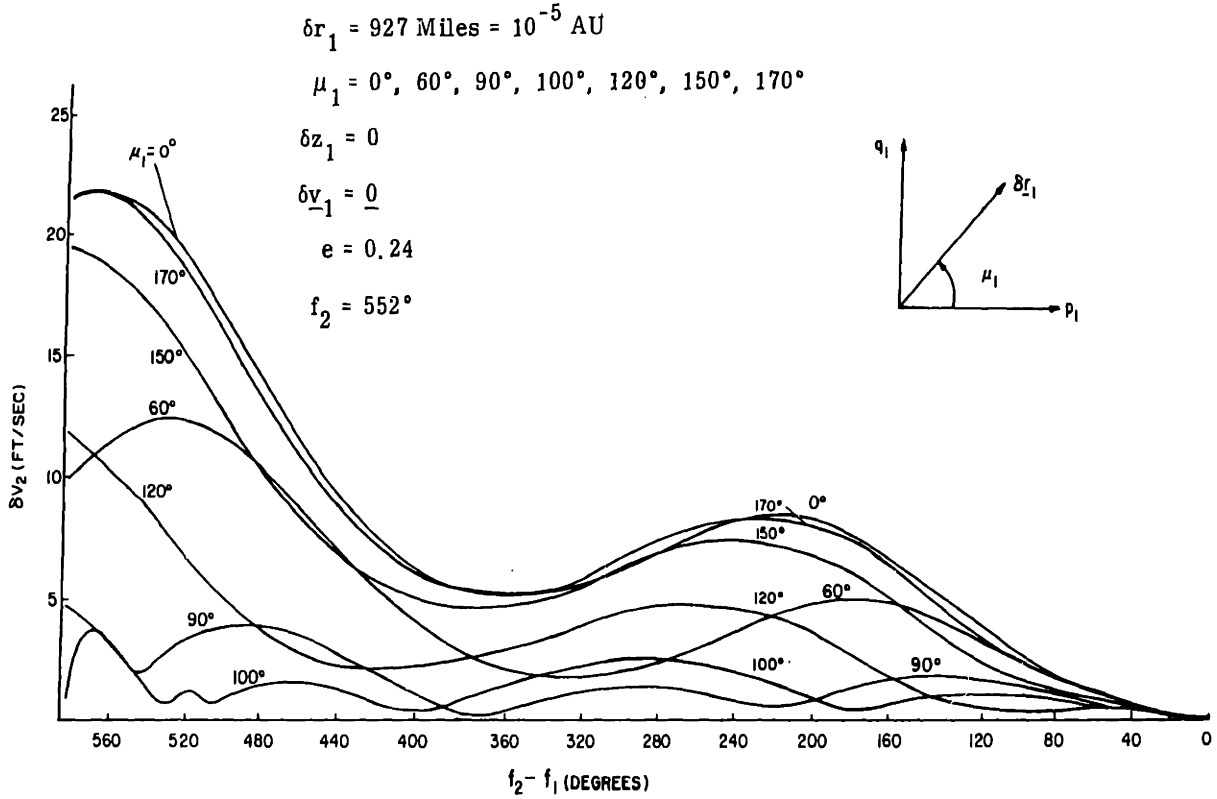

Figure 4.15 Effect of Position Variation in Reference Trajectory Plane at Time t_1 on Velocity Variation at Time t_2

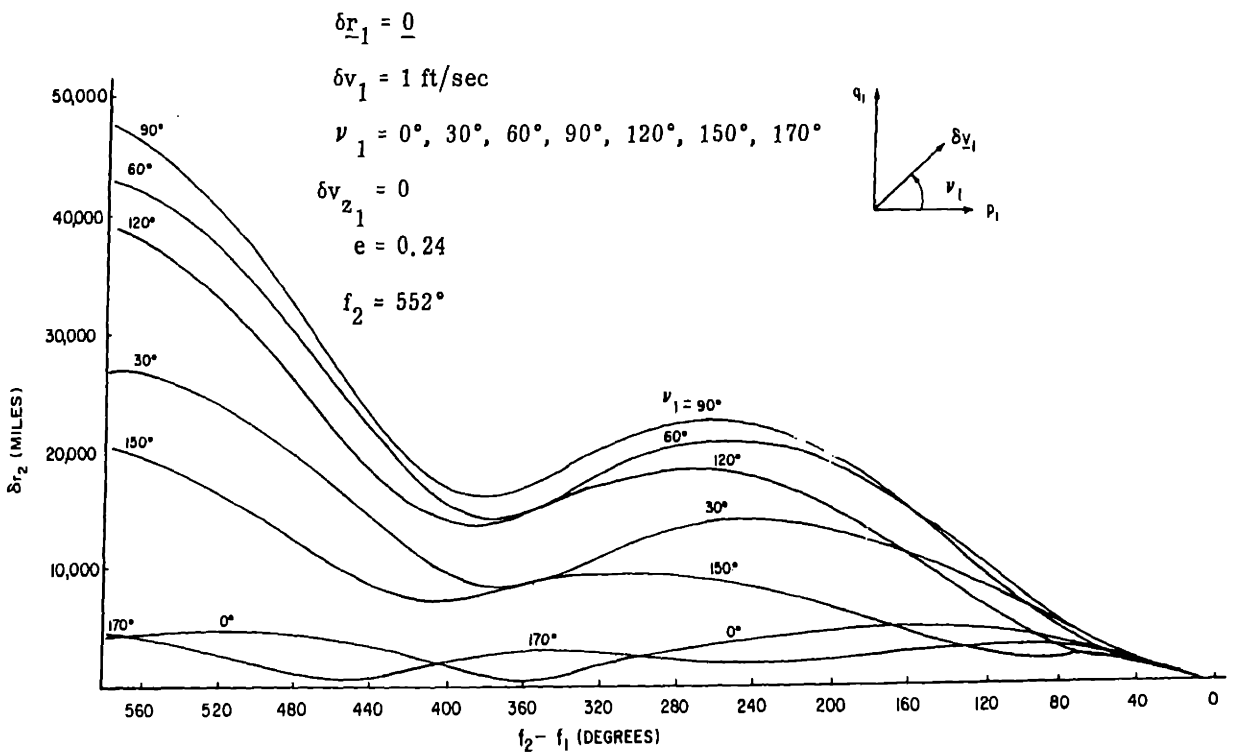

Figure 4.16 Effect of Velocity Variation in Reference Trajectory Plane at Time t_1 on Position Variation at Time t_2

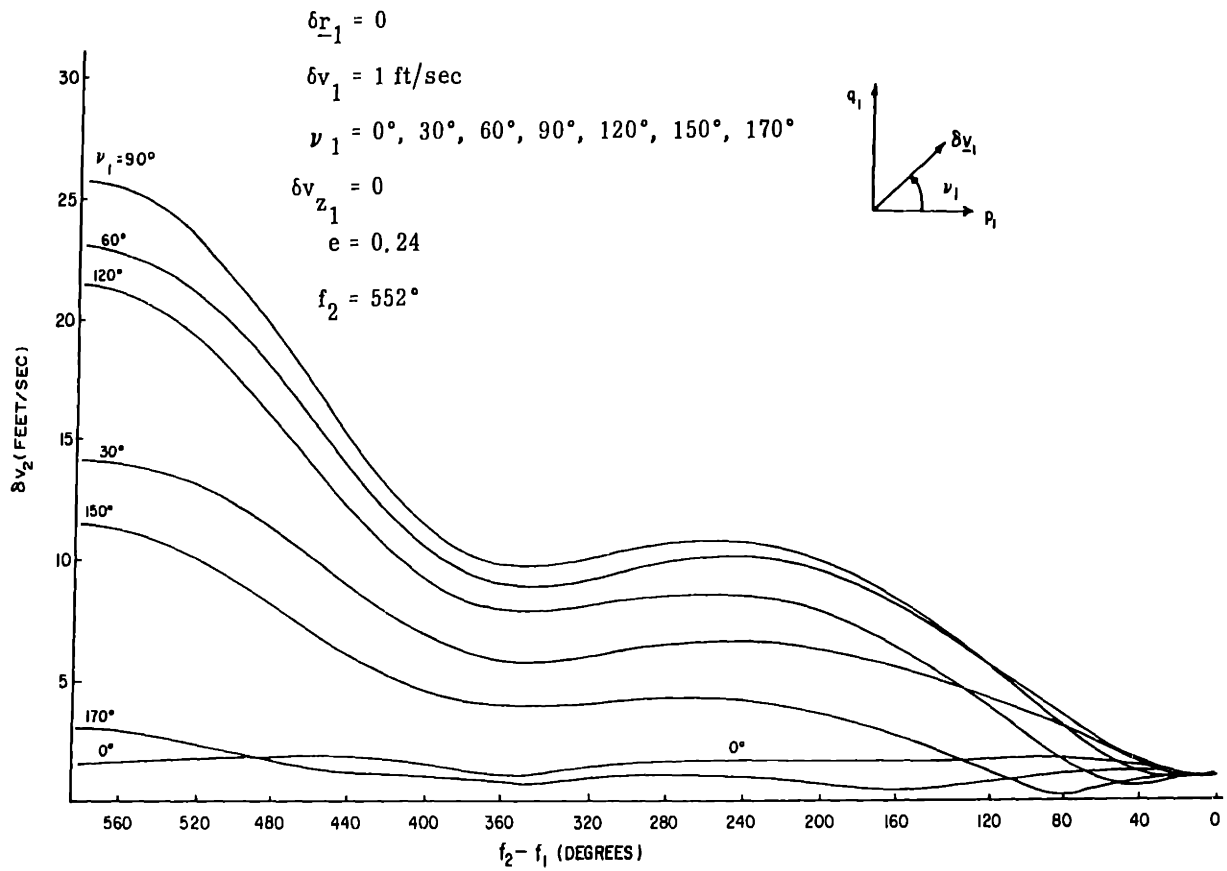

Figure 4.17 Effect of Velocity Variation in Reference Trajectory Plane at Time t_1 on Velocity Variation at Time t_2

CHAPTER 5

NAVIGATION THEORY

5.1 Summary

The method of determining the space vehicle's variant path from measurements made during the voyage is developed. Earth-based radio-command and on-board self-contained measurement techniques are discussed. In both techniques there are redundant data which are processed statistically to obtain an estimate of the variant path.

In the radio-command system the variant path is estimated directly from the observed data. In the self-contained system there is an intermediate step; the vehicle's position is estimated from a set of simultaneous measurements, and the variant path is estimated after several position determinations, made at different times, have been obtained.

For the specific self-contained system in which the measured quantities are the angles between the lines of sight to pairs of celestial bodies, a simple method is proposed for selecting the stars to be used in the sightings.

5.2 Introduction

In the guidance theory of Chapters 2 and 3 it is assumed that the vehicle's variant path is already known. The present chapter describes methods of determining the variant path from observed data; this determination is the objective of navigation theory. The chapter is primarily a review of previously proposed techniques for obtaining and processing measurements, with the addition of several suggested new features. It rounds out the analytic study of the midcourse guidance problem.

The number of indpendent measurements usually exceeds six, the number of parameters required to define the variant path. All measurements are subject to uncertainties and possibly to fixed biases as well. To estimate the parameters of the variant path from redundant measurements containing uncertainties, the method of maximum likelihood is used. The mathematical development of the method appears in Appendix P.

It is assumed that the distribution of the uncertainty in each measurement is normal with zero mean. The variance of each measurement is assumed to be known a priori.

Computations are based not on the observed value of each measured quantity but rather on the difference between the observed value and a pre-computed reference value. Since the difference is assumed to be small, linear theory is applicable.

The two types of navigation systems to be discussed are the Earth-based radio-command system developed by the Jet Propulsion Laboratory (JPL) at California Institute of Technology and the self-contained optical system of the M.I.T. Instrumentation Laboratory.

5.3 Earth-Based Radio-Command System

A general description of the Earth-based navigation system is presented in Reference (11). A detailed explanation of the method of computing the variant path appears in Reference (33).

Radio signals transmitted from the vehicle are received by a tracking station on Earth. To provide line-of-sight tracking of the vehicle at all times, three such stations are required. The observed quantities are the azimuth and elevation of the line of sight relative to the tracking station, range rate, and possibly range. Repeated measurements of any combination of these quantities are processed on a centrally located Earth-based computer by use of the method of maximum likelihood.

Many measurements can be made relatively easily during the early phase of an outbound interplanetary voyage. For this phase the two-body mathematical model does not accurately represent the physical situation; therefore, the more elaborate n-body model of Chapter 2, with the effect of earth oblateness included, is used.

In Reference (33) the solution for the variant path is obtained in terms of the six components of $\delta \underline{x}_I$, the state vector at the time of injection. The selection of $\delta \underline{x}_I$ to define the variant path is motivated physically by the fact that, before any midcourse corrections are applied, the variations of the observed quantities from their reference values are due primarily to the variations in position and velocity at injection. However, it has been

shown in Chapter 2 that the really significant state vector for guidance analysis is not $\delta \underline{x}_I$ but rather $\delta \underline{x}_D$, the state vector at the nominal time of arrival at the destination. With a caret superscript used to designate the maximum likelihood (ML) estimate of a quantity, the estimate of $\delta \underline{x}_D$ is related to the estimate of $\delta \underline{x}_I$ by the equation

$$\delta \hat{\underline{x}}_D = \overset{*}{C}_{DI} \, \delta \hat{\underline{x}}_I \tag{5-1}$$

The tracking and orbit determination functions are sub-divisions of the larger problem of vehicle guidance. It would therefcre be appropriate to solve the likelihood equations directly for an estimate of $\delta \underline{x}_D$, without going through the intermediate step of estimating $\delta \underline{x}_I$. An outline of the mathematical development of the modification of the JPL system being suggested here is presented in the next section of this chapter.

In addition to the components of the state vector $\delta \underline{x}_I$, the JPL computation yields estimates of the fixed bias of each type of measurement made at each tracking station. An iterative procedure is used to refine the estimates of the state vector and the biases beyond the results that are obtained from a single solution of the linearized equations.

The Earth-based navigation system makes use of virtually continuous computation throughout the period during which the vehicle is being tracked. According to Reference (10), measurements are made every ten seconds, so that in a tracking period of ten hours 3600 sets of input data are fed into the computer. The computer facility required is large, far beyond that which could be carried in any space vehicle. The fundamental advantage of this system is that it utilizes such a large volume of input data that, even if the individual measurements have fairly high uncertainties, the uncertainty in the estimated state vector, from which the velocity correction is computed, is quite low.

The system shows to best advantage when the vehicle is close to Earth. As the distance from Earth increases, the signal-to-noise ratio of the radio signals transmitted from vehicle to tracking station is reduced, with a consequent increase in the uncertainty of the measurements. In addition, the sensitivity of the predicted state vector to errors in angular measurements increases linearly with distance of vehicle from station.

The radio-command system is most useful in accurately determining when and how to apply the first midcourse correction on an outbound journey from Earth to another planet.

5.4 Estimate of the State Vector from Earth-Based Measurements

In this simplified analysis it will be assumed that the measurements are unbiased, and consequently the likelihood equations are to be solved only for the components of $\delta \hat{\underline{x}}_D$.

At time t_S a set of measurements is obtained. The R-th type of measurement made at t_S is designated m_{SR}. The variation of the actual measurement from its reference value is δm_{SR}. This variation is a linear function of the components of the state vector $\delta \underline{x}_S$.

$$\delta m_{SR} = \underline{p}_{SR}^T \delta \underline{x}_S \tag{5-2}$$

$\underline{p}_{SR}$ is a six-component vector whose elements are the partial derivatives of m_{SR} with respect to the components of $\underline{x}_S$. Analytic expressions for the partial derivatives used by JPL are listed in Appendix A of Reference (33).

δm_{SR} can be related to $\delta \underline{x}_D$ by means of the transition matrix.

$$\delta m_{SR} = \underline{p}_{SR}^T \overset{*}{C}_{SD} \delta \underline{x}_D = \underline{q}_{SR}^T \delta \underline{x}_D \tag{5-3}$$

where

$$\underline{q}_{SR}^T = \underline{p}_{SR}^T \overset{*}{C}_{SD} \tag{5-4}$$

The method of computing the elements of $\overset{*}{C}_{SD}$ by numerical integration is described in Section 2.10.

If K different types of measurement are made at t_S, the K measurement variations can be combined in a vector designated $\delta \underline{m}_S$.

$$\delta \underline{m}_S = \begin{Bmatrix} \delta m_{S1} \\ \vdots \\ \delta m_{SK} \end{Bmatrix} = \begin{bmatrix} q_{S1}^T \\ \vdots \\ q_{SK}^T \end{bmatrix} \delta \underline{x}_D = \overset{*}{Q}_S^T \, \delta \underline{x}_D \qquad (5\text{-}5)$$

where

$$\overset{*}{Q}_S^T = \begin{bmatrix} q_{S1}^T \\ \vdots \\ q_{SK}^T \end{bmatrix} \qquad (5\text{-}6)$$

Finally, if measurements have been made at times extending from t_1 to t_L, the total measurement variation vector $\delta \underline{m}$ is defined as follows:

$$\delta \underline{m} = \begin{Bmatrix} \delta \underline{m}_1 \\ \vdots \\ \delta \underline{m}_L \end{Bmatrix} = \begin{bmatrix} \overset{*}{Q}_1^T \\ \vdots \\ \overset{*}{Q}_L^T \end{bmatrix} \delta \underline{x}_D = \overset{*}{Q}^T \delta \underline{x}_D \qquad (5\text{-}7)$$

where

$$\overset{*}{Q}^T = \begin{bmatrix} \overset{*}{Q}_1^T \\ \vdots \\ \overset{*}{Q}_L^T \end{bmatrix} \qquad (5\text{-}8)$$

$\overset{*}{Q}^T$ is an M-by-6 matrix, where M is the total number of individual measurements being processed.

A superscript tilde will be used to indicate the observed measurement, as distinguished from the true value of the observed quantity. The difference between the two is the random measurement error u, which is normally distributed with zero mean and known standard deviation. For all M measurements,

$$\delta \tilde{\underline{m}} = \delta \underline{m} + \underline{u} \qquad (5\text{-}9)$$

The covariance matrix of the uncertainty vector $\underline{u}$ is defined as

$$\overset{*}{U} = \overline{\underline{u}\ \underline{u}^T} \tag{5-10}$$

A bar over a quantity signifies the average value of the quantity. $\overset{*}{U}$ is a symmetrical M-by-M matrix.

The estimated state vector $\delta\underline{\hat{x}}_D$ is computed from $\overset{*}{Q}$, $\overset{*}{U}$, and $\delta\underline{\tilde{m}}$ by the use of Equation (P-20).

$$\delta\underline{\hat{x}}_D = (\overset{*}{Q}\ \overset{*}{U}^{-1}\ \overset{*}{Q}^T)^{-1}\ \overset{*}{Q}\ \overset{*}{U}^{-1}\ \delta\underline{\tilde{m}} \tag{5-11}$$

If the error $\underline{\epsilon}_D$ in the estimate is defined by

$$\underline{\epsilon}_D = \delta\underline{\hat{x}}_D - \delta\underline{x}_D \tag{5-12}$$

the covariance matrix $\overset{*}{E}_D$ of $\underline{\epsilon}_D$ is obtained from Equation (P-25).

$$\overset{*}{E}_D = \overline{\underline{\epsilon}_D\ \underline{\epsilon}_D^T} = (\overset{*}{Q}\ \overset{*}{U}^{-1}\ \overset{*}{Q}^T)^{-1} \tag{5-13}$$

The uncertainties in the individual measurements are assumed to be uncorrelated. Therefore, for measurements m_i and m_j,

$$\overline{u_i\ u_j} = \delta_{ij}\ \sigma_i^2 \tag{5-14}$$

where δ_{ij} is the Kronecker delta and σ_i^2 is the variance of u_i. Then $\overset{*}{U}$ is a diagonal matrix, the non-zero element in the k-th row being σ_k^2, and $\overset{*}{U}^{-1}$ is also a diagonal matrix with $\frac{1}{\sigma_k^2}$ being the non-zero element in its k-th row. When all uncertainties are uncorrelated, the maximum likelihood estimate is the same as the least squares estimate.

The matrix $\overset{*}{Q}\ \overset{*}{U}^{-1}\ \overset{*}{Q}^T$, which must be inverted in order to solve for $\delta\underline{\hat{x}}_D$, is a symmetrical 6-by-6 matrix. This inversion is the most time-consuming operation in the computation process; it must be performed every time a new estimate is calculated from (5-11).

5.5 Self-Contained Optical System

The self-contained optical system for space navigation that is discussed in this section is the one that is described in Reference (5). The

mathematical development is given in Appendix B of that reference and also in Reference (3).

The first step in the procedure is the estimation of vehicle position relative to the reference trajectory at some specified time t_S. Position is estimated by making a set of measurements of the angles between the lines of sight to pairs of celestial bodies; all measurements are made within a short time interval centered at t_S. When more than three such measurements are made in the interval, the maximum likelihood technique is used to compute the estimated position variation $\delta\tilde{\underline{r}}_S$ and the estimated clock error $\delta\tilde{t}_S$.

For each angular measurement at least one of the two celestial bodies involved must be a "near" body, i.e., one whose motion relative to the space vehicle is significant. The near bodies are confined to the solar system; either the sun or one of the planets is usually used. The second body involved in the measurement may be a "far" body (i.e., a star other than the sun), or it may be another near body.

The position estimation procedure is repeated for a number of different values of t_S during the flight. The final phase of the computation is the determination by means of maximum likelihood of $\delta\hat{\underline{x}}_D$ from the estimates of $\delta\underline{r}$ that have already been obtained.

The assumption is made that all angular measurements have zero bias. The uncertainty in each measurement is normally distributed with zero mean and known standard deviation.

When the self-contained system is compared with the Earth-based system, the following differences are noted:

1. All measurements in the self-contained system are of the same type; they are optical measurements of celestial angles. Measurements in the Earth-based system are of several types, including angular measurements, doppler measurement of range rate, and measurement of range.

2. Each on-board angular measurement requires an appreciable amount of time for adjustment of the two telescopes involved. The Earth-based tracking system allows measurements to be made very quickly.

3. The frequency of measurements is very much smaller for the self-contained system; the number of position determinations is limited by the capacity of the on-board computer. Since the Earth-based measurements are linked to a computer of large capacity, large numbers of measurements can be effectively processed.

4. The error in the measurement of time, if uncorrected, can be significant in the self-contained system; it is negligible in the Earth-based system.

5. The self-contained navigation system uses a two-step computation: first, position variation and clock error are determined; then $\delta\hat{\underline{x}}_D$ is determined. The Earth-based system computes $\delta\hat{\underline{x}}_D$ directly.

6. The accuracy obtainable from the self-contained system is improved when the vehicle is close to any planet. The accuracy of the Earth-based measurements depends on the vehicle's distance from Earth.

7. In the self-contained system the designer has the problem of selecting the angles to be measured at each measurement time. There are usually several near bodies that can be used, and there are always many bright stars from which a selection can be made. By contrast, there is no problem of selection in the Earth-based system. The types of measurement are limited, the number of tracking stations from which the vehicle is visible is limited, and the space vehicle is the only object being tracked.

5.6 The Effect of Clock Error

Some justification is required for the two-step computation procedure called for in the self-contained system, as opposed to the single-step procedure in the Earth-based system. If the angular measurements were all made at times that were known accurately, all the data could be processed together to determine $\delta\hat{\underline{x}}_D$ directly. Unfortunately the times of the measurements are not known accurately in the self-contained system, because the space vehicle's clock is itself subject to error. The maximum likelihood method is incapable of distinguishing a clock error from a variation in the trajectory parameters if the single-step computation is used. This problem is not present in the Earth-based system, because in that system the clock error is negligibly small.

3. The frequency of measurements is very much smaller for the self-contained system; the number of position determinations is limited by the capacity of the on-board computer. Since the Earth-based measurements are linked to a computer of large capacity, large numbers of measurements can be effectively processed.

4. The error in the measurement of time, if uncorrected, can be significant in the self-contained system; it is negligible in the Earth-based system.

5. The self-contained navigation system uses a two-step computation: first, position variation and clock error are determined; then $\delta\hat{\underline{x}}_D$ is determined. The Earth-based system computes $\delta\hat{\underline{x}}_D$ directly.

6. The accuracy obtainable from the self-contained system is improved when the vehicle is close to any planet. The accuracy of the Earth-based measurements depends on the vehicle's distance from Earth.

7. In the self-contained system the designer has the problem of selecting the angles to be measured at each measurement time. There are usually several near bodies that can be used, and there are always many bright stars from which a selection can be made. By contrast, there is no problem of selection in the Earth-based system. The types of measurement are limited, the number of tracking stations from which the vehicle is visible is limited, and the space vehicle is the only object being tracked.

5.6 The Effect of Clock Error

Some justification is required for the two-step computation procedure called for in the self-contained system, as opposed to the single-step procedure in the Earth-based system. If the angular measurements were all made at times that were known accurately, all the data could be processed together to determine $\delta\hat{\underline{x}}_D$ directly. Unfortunately the times of the measurements are not known accurately in the self-contained system, because the space vehicle's clock is itself subject to error. The maximum likelihood method is incapable of distinguishing a clock error from a variation in the trajectory parameters if the single-step computation is used. This problem is not present in the Earth-based system, because in that system the clock error is negligibly small.

When four or more angular measurements are made at the nominal time t_S, the solution of the resulting likelihood equations yields an estimate of the clock error $\delta\tilde{t}_S$ as well as an estimate of the position variation $\delta\tilde{\underline{r}}_S$. Thus, the celestial bodies are used to determine the correct time. After every set of angular measurements has been completed and processed, a correction of $\delta\tilde{t}_S$ seconds is applied to the vehicle's clock.

Two simple examples serve to illustrate the inability of the computer to detect a clock error when all the angular measurements are processed together. The first is the case in which the clock has a fixed bias; assume that it is δt_S seconds slow. Then every measurement is made at a later time than it is supposed to be, and the vehicle appears to be farther along the path than it should be. The computer interprets this situation as a variation in t_0, the time of perihelion passage. δt_0 is computed to be the negative of δt_S; that is, the trajectory appears to be such that the vehicle passed through perihelion δt_S seconds early. The computed FTA correction retards the motion so that the vehicle arrives at the destination at the correct time according to its clock, but actually δt_S seconds late.

The second example is that in which the vehicle's clock has a constant drift rate; assume that the clock reads correctly at injection and loses j days per day thereafter. The interval between the actual time of an angular measurement and the apparent time of the measurement gets progressively longer; a measurement apparently made t_S days after injection is actually made $[(1 + j)t_S]$ days after injection. The computer interprets the data as indicating that the period of the actual trajectory is smaller than the reference period. The computed FTA correction increases the period so that the vehicle arrives at its destination at the correct time according to its clock, but actually $[j\,(t_D - t_I)]$ seconds late, where $(t_D - t_I)$ is expressed in seconds.

In general, a consistent clock error for which the clock reading will be t_D when the correct time is $(t_D + \delta t_D)$ results in a computation that causes the vehicle to reach the destination at $(t_D + \delta t_D)$ if FTA guidance is used. At time t_D the vehicle's position variation relative to the moving destination point is

$$(\delta\underline{r}_D)_R = -\underline{v}_R\,\delta t_D \qquad (5\text{-}15)$$

where $\underline{v}_R$ is the velocity of the vehicle relative to the destination planet.

When VTA guidance is used, a consistent clock error (either a fixed bias or a constant drift rate) requires no velocity correction. The vehicle achieves the objective of reaching the destination even though the time of arrival is not known accurately. If the clock is subject to random fluctuations, a velocity correction is computed even by the VTA system.

As a numerical illustration, consider a mission whose duration is 200 days, a clock whose drift rate is one second per day (roughly 10^{-5}), and a relative velocity vector whose magnitude is 3 mi/sec. When t is actually equal to t_D, the clock error is 200 seconds. With FTA guidance the magnitude of $(\delta \underline{r}_D)_R$ is $200 \times 3 = 600$ miles; with VTA guidance no corrections are applied, and the magnitude of the miss distance is zero.

It is apparent that the effect of an unknown clock error is reduced considerably by the VTA system. However, the two-step computation procedure is still felt to be justified for two reasons. First, even when it is permissible to vary the time of arrival, it is desirable on most missions to be able to predict accurately what that time will be; secondly, in the usual case the clock fluctuation is random, and some fuel will be expended unnecessarily for VTA corrections if the one-step procedure is used.

There is one final reason for the development of the two-step computation. In the event of a partial computer failure on a manned mission, despite the fact that the elaborate timing mechanism associated with the computer is inoperative, it may still be possible to navigate adequately with more conventional and simpler timepieces if the two-step procedure is utilized.

5.7 Estimate of the State Vector from Optical Measurements

The first step in the two-step computation is the determination of the position variation $\delta \underline{r}_S$ at nominal time t_S from angular measurements made in a short time interval centered at t_S. The variation δA_{SR} of the R-th angle measurement made at t_S from its reference value is assumed to be a linear function of the position variation $\delta \underline{r}_S$ and the clock error δt_S.

$$\delta A_{SR} = \underline{g}_{SR}^{T}\, \delta \underline{s}_S \tag{5-16}$$

where

$$\delta \underline{s}_S = \begin{Bmatrix} \delta t_S \\ \delta \underline{r}_S \end{Bmatrix} \tag{5-17}$$

and $\underline{g}_{SR}$ is a four-component vector composed of the partial derivatives of A_{SR} with respect to δt_S and the components of $\delta \underline{r}_S$. Analytic expressions for the partial derivatives are developed in Reference (3).

The number of angles measured at t_S is K. Obviously, all these measurements cannot be made simultaneously, so that the angle A_{SR} is actually measured at time $(t_S + \delta t_{SR})$. The time increment δt_{SR} is small and can be accurately recorded. The observed value $\delta \tilde{A}_{SR}$ used in the computation is compensated for the effect of δt_{SR}; therefore, $\delta \tilde{A}_{SR}$ is the "effective" angle variation that would have been observed if the measurement had taken place when the space vehicle's clock read t_S.

The measurement variation vector $\delta \underline{m}_S$ consists of the variation in the clock reading in addition to the variations in the K angular measurements.

$$\delta \underline{m}_S = \begin{Bmatrix} \delta t_S \\ \delta A_{S1} \\ \vdots \\ \delta A_{SK} \end{Bmatrix} = \overset{*}{G}_S^{T}\, \delta \underline{s}_S \tag{5-18}$$

where

$$\overset{*}{G}_S^{T} = \begin{Bmatrix} \underline{g}_{S0}^{T} \\ \underline{g}_{S1}^{T} \\ \vdots \\ \underline{g}_{SK}^{T} \end{Bmatrix} \tag{5-19}$$

and

$$\underline{g}_{S0} = \begin{Bmatrix} 1 \\ 0 \\ 0 \\ 0 \end{Bmatrix} \tag{5-20}$$

The observed measurement vector $\delta\underline{\tilde{m}}_S$, the true measurement vector $\delta\underline{m}$, and the uncertainty vector $\underline{u}_S$ are related by the equation

$$\delta\underline{\tilde{m}}_S = \delta\underline{m}_S + \underline{u}_S \tag{5-21}$$

In component form,

$$\begin{Bmatrix} 0 \\ \delta\tilde{A}_{S1} \\ \vdots \\ \delta\tilde{A}_{SK} \end{Bmatrix} = \begin{Bmatrix} \delta t_S \\ \delta A_{S1} \\ \vdots \\ \delta A_{SK} \end{Bmatrix} + \begin{Bmatrix} u_{S0} \\ u_{S1} \\ \vdots \\ u_{SK} \end{Bmatrix} \tag{5-22}$$

The "observed" value of δt_S is zero. The uncertainty in the time measurement is designated u_{S0}.

The covariance matrix of the uncertainty vector is

$$\overset{*}{U}_S = \overline{\underline{u}_S \quad \underline{u}_S^T} \tag{5-23}$$

Since the uncertainties in all the measurements are assumed to be independent with zero mean, $\overset{*}{U}_S$ is a diagonal matrix, and so is $\overset{*}{U}_S^{-1}$.

Then the ML estimate of the vector $\delta\underline{s}_S$ is

$$\delta\underline{\tilde{s}}_S = \begin{Bmatrix} \delta\tilde{t}_S \\ \delta\underline{\tilde{r}}_S \end{Bmatrix} = (\overset{*}{G}_S \overset{*}{U}_S^{-1} \overset{*}{G}_S^T)^{-1} \overset{*}{G}_S \overset{*}{U}_S^{-1} \delta\underline{\tilde{m}}_S \tag{5-24}$$

Vector $\delta\tilde{\underline{s}}_S$ is an "inferred measurement" vector. Note that the inferred measurement of δt_S is not zero, even though the observed measurement is. The correction $\delta\tilde{t}_S$ is applied to the clock.

The error vector $\underline{\xi}_S$ is the difference between the inferred measured vector and the true measurement vector.

$$\underline{\xi}_S = \delta\tilde{\underline{s}}_S - \delta\underline{s}_S \tag{5-25}$$

or

$$\begin{Bmatrix} \nu_S \\ \underline{\beta}_S \end{Bmatrix} = \begin{Bmatrix} \delta\tilde{t}_S \\ \delta\tilde{\underline{r}}_S \end{Bmatrix} - \begin{Bmatrix} \delta t_S \\ \delta\underline{r}_S \end{Bmatrix} \tag{5-26}$$

The covariance matrix of $\underline{\xi}_S$ is

$$\overline{\underline{\xi}_S \ \underline{\xi}_S^T} = (\overset{*}{G}_S \overset{*}{U}_S^{-1} \overset{*}{G}_S^T)^{-1} \tag{5-27}$$

The variance in the inferred estimate of clock error is $\overline{\nu_S^2}$, the upper left-hand element of $\overline{\underline{\xi}_S \ \underline{\xi}_S^T}$.

In order to solve (5-24) for $\delta\tilde{\underline{s}}_S$, it is necessary to know the variances in the uncertainties of all measurements comprising $\delta\tilde{\underline{m}}_S$. For the angular measurements these variances are known a priori. For the clock measurement Reference (3) suggests a simple yet effective model that can be used to determine $\overline{u_{S0}^2}$.

Clock errors are important only during those short time intervals when measurements are being made or a velocity correction is being applied. It is therefore reasonable to assume that the clock has a constant drift rate between measurement time t_{S-1} and measurement time t_S. The variance

of this drift rate is σ_c^2, which is known a priori. Then $\overline{u_{S0}^2}$ is given by

$$\overline{u_{S0}^2} = \sigma_c^2 (t_S - t_{S-1})^2 + \overline{\nu_{S-1}^2} \tag{5-28}$$

The recursive operation is started by stating that at injection $\overline{u_{I0}^2}$ is known a priori.

The inferred measurements to be used in the determination of $\delta\hat{\underline{x}}_D$ are the components of $\delta\tilde{\underline{r}}_S$. The covariance matrix of the uncertainties in $\delta\tilde{\underline{r}}_S$ is

$$\overset{*}{B}_S = \overline{\underline{\beta}_S \ \underline{\beta}_S^T} = \begin{Bmatrix} 0 & 1 & 0 & 0 \\ 0 & 0 & 1 & 0 \\ 0 & 0 & 0 & 1 \end{Bmatrix} (\overset{*}{G}_S \overset{*}{U}_S^{-1} \overset{*}{G}_S^T)^{-1} \begin{Bmatrix} 0 & 0 & 0 \\ 1 & 0 & 0 \\ 0 & 1 & 0 \\ 0 & 0 & 1 \end{Bmatrix} \tag{5-29}$$

The second major step in the two-step method can now be carried out. At each of L measurement times an inferred position variation vector is obtained, and for each of these vectors the corresponding moment matrix is computed. The equation

$$\delta\tilde{\underline{m}} = \delta\underline{m} + \underline{u} \tag{5-30}$$

now takes the form

$$\begin{Bmatrix} \delta\tilde{\underline{r}}_1 \\ \vdots \\ \delta\tilde{\underline{r}}_L \end{Bmatrix} = \begin{Bmatrix} \delta\underline{r}_1 \\ \vdots \\ \delta\underline{r}_L \end{Bmatrix} + \begin{Bmatrix} \underline{\beta}_1 \\ \vdots \\ \underline{\beta}_L \end{Bmatrix} \tag{5-31}$$

The uncertainty in the inferred measurement vector $\delta\tilde{\underline{r}}_S$ is assumed to be uncorrelated with the uncertainties in the other inferred measurement vectors. The covariance matrix $\overset{*}{U}$, which is again defined as $\overline{\underline{u} \ \underline{u}^T}$, is a

diagonal matrix of 3-by-3 sub-matrices. This is illustrated by the equations shown below for $\overset{*}{U}$ and $\overset{*}{U}^{-1}$ when L = 3. The extension to higher values of L is obvious.

$$\overset{*}{U} = \begin{Bmatrix} \overset{*}{B}_1 & \overset{*}{O}_3 & \overset{*}{O}_3 \\ \overset{*}{O}_3 & \overset{*}{B}_2 & \overset{*}{O}_3 \\ \overset{*}{O}_3 & \overset{*}{O}_3 & \overset{*}{B}_3 \end{Bmatrix} \tag{5-32}$$

$$\overset{*}{U}^{-1} = \begin{Bmatrix} \overset{*}{B}_1^{-1} & \overset{*}{O}_3 & \overset{*}{O}_3 \\ \overset{*}{O}_3 & \overset{*}{B}_2^{-1} & \overset{*}{O}_3 \\ \overset{*}{O}_3 & \overset{*}{O}_3 & \overset{*}{B}_3^{-1} \end{Bmatrix} \tag{5-33}$$

$\delta \underline{r}_S$ is related to $\delta \underline{x}_D$ by the equation

$$\delta \underline{r}_S = \begin{Bmatrix} \overset{*}{M}_{SD} & \overset{*}{N}_{SD} \end{Bmatrix} \delta \underline{x}_D \tag{5-34}$$

The 3-by-3 matrices $\overset{*}{M}_{SD}$ and $\overset{*}{N}_{SD}$ are sub-matrices of the transition matrix $\overset{*}{C}_{SD}$; they are explained in Section 2.7. Then

$$\delta \underline{m} = \overset{*}{Q}^T \delta \underline{x}_D \tag{5-35}$$

where

$$\overset{*}{Q}^T = \begin{Bmatrix} \overset{*}{M}_{1D} & \overset{*}{N}_{1D} \\ \vdots & \vdots \\ \overset{*}{M}_{LD} & \overset{*}{N}_{LD} \end{Bmatrix} \tag{5-36}$$

With these definitions of $\overset{*}{Q}$, $\overset{*}{U}$, and $\delta \underline{\tilde{m}}$, the ML estimate of $\delta \underline{x}_D$ has the same form as (5-11).

$$\delta \hat{\underline{x}}_D = (\overset{*}{Q}\, \overset{*}{U}^{-1}\, \overset{*}{Q}^T)^{-1}\, \overset{*}{Q}\, \overset{*}{U}^{-1}\, \delta \underline{\tilde{m}} \tag{5-37}$$

The error $\underline{\epsilon}_D$ in the estimate and the covariance matrix $\overset{*}{E}_D$ are given by Equations (5-12) and (5-13), respectively.

5.8 The Initial Estimate

An improvement in the estimate of the variant path of the vehicle can be achieved by regarding as additional measurements the design value of the state vector at injection. This suggestion has been made in References (12) and (33).

The "pseudo-measurement" of the injection state vector is

$$\delta\underline{\tilde{x}}_I = \underline{0}_6 \tag{5-38}$$

This is the vector that would be achieved if there were no errors in the injection guidance system. Because such errors do exist, the actual vector $\delta\underline{x}_I$ is not the zero vector. The injection error vector $\underline{\epsilon}_I$ is defined as

$$\underline{\epsilon}_I = \delta\underline{\tilde{x}}_I - \delta\underline{x}_I \tag{5-39}$$

The corresponding covariance matrix is

$$\overset{*}{U}_I = \overline{\underline{\epsilon}_I \quad \underline{\epsilon}_I^T} \tag{5-40}$$

The elements of $\overset{*}{U}_I$ are assumed to be known a priori from the characteristics of the injection guidance system.

$\delta\underline{x}_I$ is related to $\delta\underline{x}_D$ by the transition matrix $\overset{*}{C}_{ID}$.

$$\delta\underline{x}_I = \overset{*}{C}_{ID}\,\delta\underline{x}_D \tag{5-41}$$

To incorporate $\delta\underline{\tilde{x}}_I$ into the computation for the ML estimate of $\delta\underline{x}_D$, the definitions of $\overset{*}{Q}^T$, $\overset{*}{U}$, and $\delta\underline{\tilde{m}}$ must be modified. The new $\overset{*}{Q}^T$ is given by

$$\overset{*}{Q}^T = \begin{Bmatrix} \overset{*}{C}_{ID} \\ \overset{*}{Q}_1^T \\ \vdots \\ \overset{*}{Q}_L^T \end{Bmatrix} \tag{5-42}$$

The new covariance matrix is

$$\overset{*}{U} = \begin{Bmatrix} \overset{*}{U}_I & \overset{*}{O}_{6 \times M} \\ \overset{*}{O}_{M \times 6} & \overset{*}{U}_{M \times M} \end{Bmatrix} \tag{5-43}$$

where $\overset{*}{U}_{M \times M}$ is the original covariance matrix, obtained from the M measurements. It is assumed in (5-43) that uncertainties associated with the injection guidance system are uncorrelated with the later measurements. Finally, the new observed measurement variation vector is

$$\delta \underline{\tilde{m}} = \begin{Bmatrix} \delta \underline{\tilde{x}}_I \\ \delta \underline{\tilde{m}}_1 \\ \vdots \\ \delta \underline{\tilde{m}}_L \end{Bmatrix} = \begin{Bmatrix} \underline{O}_6 \\ \delta \underline{\tilde{m}}_1 \\ \vdots \\ \delta \underline{m}_L \end{Bmatrix} \tag{5-44}$$

With these definitions Equation (5-11) can be solved for an improved estimate of $\delta \underline{\tilde{x}}_D$.

5.9 The Estimate Immediately Following a Midcourse Correction

Whenever a midcourse correction is applied, $\delta \underline{x}_D$ is changed. Subsequent measurements are used to estimate the new $\delta \underline{x}_D$. The concept of the initial estimate, as developed in the proceding section, can be adapted to provide a more accurate estimate of the new $\delta \underline{x}_D$.

On the basis of measurements made prior to the correction time t_C, an estimate is obtained for the uncorrected $\delta \underline{x}_D$, which is designated $\delta \underline{x}_D^-$. The uncorrected state vector at the time of correction is $\delta \underline{x}_C^-$.

$$\delta \underline{x}_C^- = \overset{*}{C}_{CD} \, \delta \underline{x}_D^- \tag{5-45}$$

Immediately after the correction $\underline{c}$ is applied, the new state vector is

$$\delta \underline{x}_C^+ = \delta \underline{x}_C^- + \begin{Bmatrix} \underline{0}_3 \\ \underline{c} \end{Bmatrix} \tag{5-46}$$

$$= \overset{*}{C}_{CD} \; \delta \underline{x}_D^+ \tag{5-47}$$

where $\delta \underline{x}_D^+$ is the new state vector for which an estimate is required.

$\underline{c}$ is the velocity correction actually applied. Because of instrumentation inaccuracy it differs from $\tilde{\underline{c}}$, the "observed" or desired correction. The difference between the two is designated $\underline{\eta}$.

$$\underline{\eta} = \tilde{\underline{c}} - \underline{c} \tag{5-48}$$

The "observed" value of $\delta \underline{x}_C^+$ is

$$\delta \tilde{\underline{x}}_C^+ = \delta \hat{\underline{x}}_C^- + \begin{Bmatrix} \underline{0}_3 \\ \tilde{\underline{c}} \end{Bmatrix} \tag{5-49}$$

The error in the observed value is

$$\begin{aligned} \underline{u}_C^+ &= \delta \tilde{\underline{x}}_C^+ - \delta \underline{x}_C^+ \\ &= (\delta \hat{\underline{x}}_C^- - \delta \underline{x}_C^-) + \begin{Bmatrix} \underline{0}_3 \\ \tilde{\underline{c}} - \underline{c} \end{Bmatrix} \\ &= \underline{\epsilon}_C^- + \begin{Bmatrix} \underline{0}_3 \\ \underline{\eta} \end{Bmatrix} \end{aligned} \tag{5-50}$$

where

$$\delta \hat{\underline{x}}_C = \overset{*}{C}_{CD} \; \delta \hat{\underline{x}}_D \tag{5-51}$$

and

$$\underline{\epsilon}_C^- = \overset{*}{C}_{CD} \; \underline{\epsilon}_D^- \tag{5-52}$$

The covariance matrix of $\underline{\epsilon}_C^-$ is

$$\overset{*}{E}_C^- = \overline{(\underline{\epsilon}_C^-)\ (\underline{\epsilon}_C^-)^T} = \overset{*}{C}_{CD}\ \overset{*}{E}_D^-\ \overset{*}{C}_{CD}^T \tag{5-53}$$

The covariance matrix of $\underline{u}_C^+$ is

$$\overset{*}{U}_C^+ = \overline{(\underline{u}_C^+)\ (\underline{u}_C^+)^T}$$

$$= \overset{*}{E}_C^- + \left\{ \overset{*}{O}_{6 \times 3} \quad \overline{\underline{\epsilon}_C^-\ \underline{\eta}^T} \right\} + \left\{ \begin{matrix} \overset{*}{O}_3 & \overset{*}{O}_3 \\ \overset{*}{O}_3 & \overline{\underline{\eta}\ \underline{\eta}^T} \end{matrix} \right\} \tag{5-54}$$

To evaluate $\overset{*}{U}_C^+$, it is necessary to formulate a model of the control system used to apply the midcourse correction and to analyze the errors in the contemplated system. One such analysis is given in Reference (13).

Equation (5-11) is used to solve for $\delta\hat{\underline{x}}_D^+$ when the following are used for $\overset{*}{Q}^T$, $\overset{*}{U}$, and $\delta\underline{\tilde{m}}$:

$$\overset{*}{Q}^T = \left\{ \begin{matrix} \overset{*}{C}_{CD} \\ \overset{*}{Q}_1^T \\ \vdots \\ \overset{*}{Q}_L^T \end{matrix} \right\} \tag{5-55}$$

$$\overset{*}{U} = \left\{ \begin{matrix} \overset{*}{U}_C^+ & \overset{*}{O}_{6 \times M} \\ \overset{*}{O}_{M \times 6} & \overset{*}{U}_{M \times M} \end{matrix} \right\} \tag{5-56}$$

$$\delta \underline{\tilde{m}} = \begin{Bmatrix} \delta \underline{\tilde{x}}_C^+ \\ \delta \underline{\tilde{m}}_1 \\ \vdots \\ \delta \underline{\tilde{m}}_L \end{Bmatrix} \tag{5-57}$$

The M measurements referred to in these equations are the measurements made subsequent to the correction at $t = t_C$.

The inclusion of the initial observation vector $\delta \underline{\tilde{x}}_C^+$ in the determination of $\delta \underline{\hat{x}}_D^+$ enables all the observations made since injection to be utilized. It therefore has a much more significant effect on the accuracy of estimation than the inclusion of the initial estimate $\delta \underline{x}_I$ has.

5.10 Physical Considerations in the Selection of Optical Sightings

It has been pointed out in Section 5.5 that the designer of a self-contained navigation system has the problem of determining which angles should be measured at each measurement time t_S in order to determine the position variation $\delta \underline{\tilde{r}}_S$. Battin[6] has developed the mathematics for optimizing a set of three angular measurements, from which position is determined uniquely under the assumption that the clock error can be neglected. The analysis in this section is concerned with the optimization of a redundant set of angular measurements; the emphasis is on physical reasoning rather than mathematical rigor.

For the purpose of selecting the sightings, it is justifiable to simplify the problem by neglecting clock error. It is unlikely that the relatively small effect of the clock error on $\delta \underline{\tilde{r}}_S$ can affect the selection, and neglecting this effect simplifies the analysis considerably. With this assumption, Equation (5-18) becomes

$$\delta \underline{m}_S = \begin{Bmatrix} \delta A_{S1} \\ \vdots \\ \delta A_{SK} \end{Bmatrix} = \overset{*}{G}_S^T \, \delta \underline{r}_S \tag{5-58}$$

where

$$ {}^{*}G_S{}^{T} = \left\{ \begin{array}{c} \underline{g}_{S1}{}^{T} \\ \vdots \\ \underline{g}_{SK}{}^{T} \end{array} \right\} \qquad (5\text{-}59) $$

K is greater than 3.

For a sighting of the angle between the line of sight to a near body and the line of sight to a star, a mathematical expression for the vector $\underline{g}_{SR}$ can readily be derived from Figure 5-1. At time t_S the reference position of the planet is X; its actual position is X'. The position of the near body is P; its distance from X is z_P. The line of sight to the star from X is XY; from X' it is X'Y'. Since the star's distance is assumed to be infinite, XY and X'Y' are parallel. The reference value of the angle to be measured is

$$ A_{SR} = \sphericalangle PXY \qquad (5\text{-}60) $$

The actual angle measured is

$$ A_{SR}' = \sphericalangle PX'Y' \qquad (5\text{-}61) $$

The difference between the two is δA_{SR}.

$$ \delta A_{SR} = A_{SR}' - A_{SR} \qquad (5\text{-}62) $$

Unit vectors $\underline{m}_P$ and $\underline{m}_Q$ lie along the lines from X to P and from X to the star, respectively. The unit vector $\underline{n}_P$ is normal to $\underline{m}_P$ and in the plane containing $\underline{m}_P$ and $\underline{m}_Q$.

$$ \underline{n}_P = \frac{1}{\sin A_{SR}} \left(\underline{m}_Q - \underline{m}_P \cos A_{SR} \right) \qquad (5\text{-}63) $$

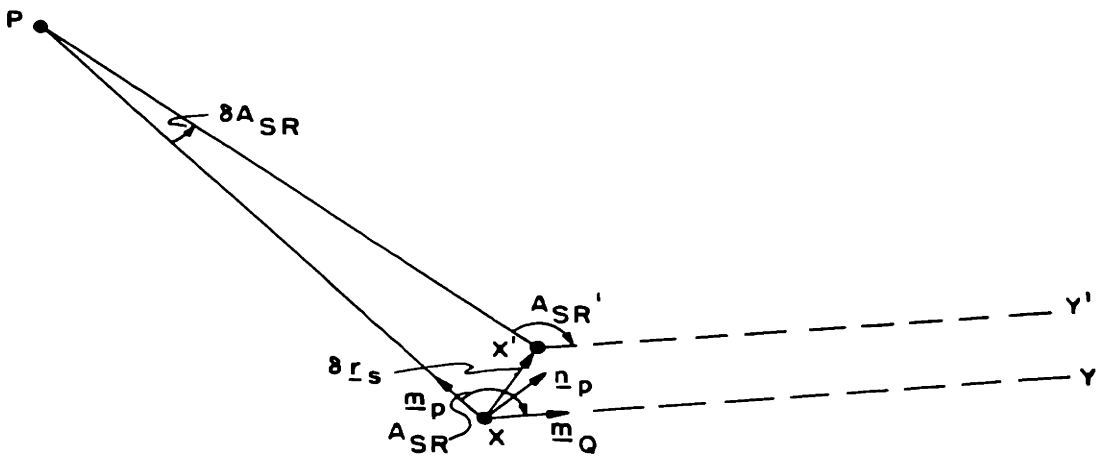

X – vehicle's reference position

X' – vehicle's actual position

P – position of near body

XY, X'Y' – line of sight to star

A_{SR} = ∢ PXY = reference value of angle to be measured

A_{SR}' = ∢ PX'Y' = actual angle to be measured

$\delta A_{SR} = A_{SR}' - A_{SR}$

$\delta \underline{r}_S$ – position variation of vehicle at time t_S

$\underline{m}_P$ – unit vector along nominal line of sight from vehicle to near body

$\underline{m}_Q$ – unit vector along nominal line of sight from vehicle to star

$\underline{n}_P$ – unit vector normal to nominal line of sight from vehicle to near body

Figure 5.1 Geometry of Angular Measurement

From the figure it is apparent that δA_{SR} is related to the component of $\delta \underline{r}_S$ parallel to $\underline{n}_P$.

$$z_P \, \delta A_{SR} = \underline{n}_P{}^T \, \delta \underline{r}_S \tag{5-64}$$

Then

$$\underline{g}_{SR} = \frac{\underline{n}_P}{z_P} \tag{5-65}$$

The error in the computed component of $\delta \underline{r}_S$ caused by an error u_{SR} in the observation of δA_{SR} is directly proportional to z_P. Thus, to minimize the error in the computed value of $\delta \underline{r}_S$, it is desirable to sight on the nearest of the near bodies in several of the measurements.

The plane containing the two lines of sight for a particular angular measurement will be designated the "measurement plane." If two stars are chosen such that the measurement plane of the angle between the nearest body and the first star is perpendicular to the measurement plane of the angle between the nearest body and the second star, two orthogonal components of $\delta \underline{r}_S$ can be determined, both components lying in the plane normal to $\underline{m}_P$.

There still remains the problem of finding the component of $\delta \underline{r}_S$ parallel to $\underline{m}_P$. This component cannot be found by measuring the angle between $\underline{m}_P$ and the line of sight to any star. It is possible to make an estimate of $(\underline{m}_P{}^T \, \delta \underline{r}_S)$ by measuring the angular diameter of the nearest body, but this measurement has little practical value in the midcourse phase of the flight, when the distance of the nearest planet from the vehicle is at least of the order of hundreds of planet diameters. Thus, at least one angular measurement involving another near body is required.

It would be ideal if there were a second near body whose distance from the vehicle is not much greater than that of the nearest body and whose line of sight is perpendicular to the line of sight to the nearest body. Then an angular measurement between the lines of sight to the second body and a star can be made such that the component of $\delta \underline{r}_S$ along the line of sight to the nearest body can be determined. In practice this ideal is seldom, if ever, achieved. As a consequence, the third angular measurement gives the component of $\delta \underline{r}_S$ in a direction different from

$\underline{m}_P$. After three measurements have been made, there is greater uncertainty about the component of $\delta \underline{r}_S$ along $\underline{m}_P$ than there is about the components of $\delta \underline{r}_S$ in the plane perpendicular to $\underline{m}_P$. The first objective of the redundant measurements is to reduce the uncertainty in the component of $\delta \underline{r}_S$ along $\underline{m}_P$.

The near bodies for an interplanetary journey consist of the sun and the inner planets Mercury, Venus, Earth, and Mars. When the vehicle is not too distant from Earth, the moon may also be used. The fact that all the inner planets as well as the moon move in orbits that are inclined by only a few degrees to the ecliptic can be used to advantage in the selection of sightings, for, from considerations of energy required for injection into a heliocentric orbit, the vehicle's orbital plane is also close to the ecliptic.

A measurement of the angle between a near body and a star whose line of sight is inclined only slightly to the ecliptic plane (and hence inclined only slightly to the reference trajectory plane) leads to an estimate of a component of $\delta \underline{r}_S$ which is roughly in the reference trajectory plane. Another measurement, involving a second near body and the same star, yields an estimate of the component of $\delta \underline{r}_S$ in some other direction, also close to the reference trajectory plane. Additional measurements, between additional near bodies and the same star or between pairs of near bodies, refine the accuracy of the estimate of position variation in the reference trajectory plane.

To estimate position variation normal to the reference trajectory plane, a measurement is made of the angle between a near body and a star whose line of sight is normal to the reference trajectory plane, if a star of sufficient brightness for good visibility can be found in this direction. Additional measurements between other near bodies and the same star reduce the uncertainty in the estimate of position variation normal to the reference trajectory plane.

The measurement selection procedure being suggested is in reality another exploitation of the condition that was used to advantage in the guidance analysis of Chapter 3, namely that characteristics associated with the reference trajectory plane are virtually uncoupled from characteristics normal to that plane.

It has been mentioned that angular sightings between two near bodies may be used in addition to near body-star sightings to improve the estimate of position variation in the reference trajectory plane. Equations (5-64) and (5-65) are not applicable to this type of measurement. If the nearest body is P, at distance z_P from the vehicle, and if the other near body is Q, at distance z_Q from the vehicle, Equation (2-5) of Reference (3) indicates that, when clock errors are neglected,

$$\delta A_{SR} = \left(\frac{\underline{n}_P}{z_P} + \frac{\underline{n}_Q}{z_Q} \right) \cdot \delta \underline{r}_S \qquad (5\text{-}66)$$

Thus

$$\underline{g}_{SR} = \frac{\underline{n}_P}{z_P} + \frac{\underline{n}_Q}{z_Q} \qquad (5\text{-}67)$$

where $\underline{n}_P$ is defined by Equation (5-62), and correspondingly,

$$\underline{n}_Q = \frac{1}{\sin A_{SR}} (\underline{m}_P - \underline{m}_Q \cos A_{SR}) \qquad (5\text{-}68)$$

Measuring the angle between two near bodies yields an estimate of the component of $\delta \underline{r}_S$ in a direction which is the weighted average of the normals to the lines of sight to the two bodies, the weighting being inversely proportional to the distance of the body from the vehicle.

The sensitivity factor S will be defined as the error in the relevant component of $\delta \underline{r}_S$ caused by a unit error in the measurement of A_{SR}. S is the reciprocal of the magnitude of $\underline{g}_{SR}$. For a near body-star measurement,

$$S = z_P \qquad (5\text{-}69)$$

For a measurement between two near bodies, the law of cosines is used to show that

$$S = \frac{z_P z_Q}{d} \qquad (5\text{-}70)$$

where d is the distance of Q from P.

It is obviously desirable to keep S as low as possible. Equations (5-69) and (5-70) indicate that the value of S for a measurement between two near bodies is smaller that the value of S for a near body-star measurement only when the distance of Q from the vehicle is less than the distance of Q from P. This sensitivity criterion applies only to the magnitude of the inferred position error. It is occasionally desirable to use a measurement with a higher S in order to obtain an estimate of $\delta \underline{r}_S$ in a direction in which the uncertainty is relatively high.

5.11 Mathematical Criterion for the Selection of Optical Sightings

A useful mathematical criterion for selecting a redundant number of angular measurements for position determination is the minimization of the volume of the equi-probability ellipsoid, subject to the constraint that the three axes of the ellipsoid be kept approximately equal in length.

The concept of the equi-probability ellipsoid is discussed in Appendix P. The equation for the ellipsoid corresponding to measurements made at time t_S is the quadratic form

$$\underline{\beta}_S{}^T \overset{*}{B}_S{}^{-1} \underline{\beta}_S = k^2 \tag{5-71}$$

where k is a constant. The center of the ellipsoid is at the point

$$\underline{\beta}_S = \underline{O}_3 \tag{5-72}$$

The volume of the ellipsoid is

$$V = \frac{4}{3} \pi k^3 \left| \overset{*}{B}_S \right|^{1/2} \tag{5-73}$$

where $\left| \overset{*}{B}_S \right|$ is the determinant of the covariance matrix $\overset{*}{B}_S$.

For any specified value of k, the probability that the error vector $\underline{\beta}_S$ will lie totally within the ellipsoid is a constant. Thus it is desirable to reduce the volume of the ellipsoid for the given k, and this can be accomplished only by reducing $\left| \overset{*}{B}_S \right|$. Maintaining the axes of the ellipsoid roughly equal in length ensures that the reduction in volume is not achieved by means of a reduction in uncertainty in one direction at the expense of a relatively large uncertainty in another direction.

Since clock errors are being neglected,

$$\overset{*}{B}_S = (\overset{*}{G}_S \overset{*}{U}_S^{-1} \overset{*}{G}_S^T)^{-1} \tag{5-74}$$

If it is assumed that the standard deviation of the uncertainty in each of the K angular measurements is σ,

$$\overset{*}{U}_S^{-1} = \frac{1}{\sigma^2} \overset{*}{I}_K \tag{5-75}$$

Then,

$$\overset{*}{B}_S = \sigma^2 (\overset{*}{G}_S \overset{*}{G}_S^T)^{-1} \tag{5-76}$$

Reducing the determinant of $\overset{*}{B}_S$ for a given σ^2 is equivalent to increasing the determinant of $(\overset{*}{G}_S \overset{*}{G}_S^T)$. $\overset{*}{G}_S$ is a 3-by-K matrix.

$$\overset{*}{G}_S = \left\{ \underset{\sim}{g}_{S1} \quad \cdots \quad \underset{\sim}{g}_{SK} \right\} \tag{5-77}$$

$$\overset{*}{G}_S \overset{*}{G}_S^T = \sum_{R=1}^{K} \underset{\sim}{g}_{SR} \underset{\sim}{g}_{SR}^T \tag{5-78}$$

It is convenient to express the components of the $\underset{\sim}{g}_S$ vectors in one of the reference trajectory coordinate systems of Appendix A. In any of these systems the third component of $\underset{\sim}{g}_S$ is zero for an in-plane measurement (a measurement of the angle between two lines of sight, both of which lie in the reference trajectory plane). For an out-of-plane measurement (one in which the angle measured is between the line of sight to a near body in the reference trajectory plane and the line of sight to a star normal to the reference trajectory plane), the first two components of $\underset{\sim}{g}_S$ are zero.

If several measurements of each of the two types are made, the resulting matrix $(\overset{*}{G}_S \overset{*}{G}_S^T)$ has the same uncoupled feature as all of the matrices of Chapter 3; that is, the first two elements of the third row and the first two elements of the third column are all zero. In practice

this condition cannot be achieved precisely, because the lines of sight to the celestial bodies used in the measurements do not lie exactly in or perpendicular to the reference trajectory plane. Moreover, if the lines of sight to two near bodies are roughly perpendicular to each other, the in-plane measurements can be so chosen that $(\overset{*}{G}_S \overset{*}{G}_S{}^T)$ closely resembles a diagonal matrix.

The procedure to be used in selecting measurements is straightforward. If six angles are to be used, four will be in-plane and two out-of-plane. Let P, Q, and R represent three near bodies in order of increasing distance from the vehicle. Let B_1 and B_2 be "in-plane" stars, and let C_1 and C_2 be "out-of-plane" stars, the line of sight to C_1 being closer to the normal to the reference trajectory plane than the line of sight to C_2.

The first two measurements are the obvious ones. P and B_1 are used for an in-plane measurement, and P and C_1 are used for an out-of-plane measurement. These two provide estimates of the components of $\delta \underline{r}_S$ in the plane normal to the line of sight from the vehicle to P. Next, a second out-of-plane measurement can be made; this involves either P and C_2 or Q and C_1, whichever combination gives the larger value of the lower right-hand element of $(\overset{*}{G}_S \overset{*}{G}_S{}^T)$.

The remaining three in-plane measurements depend on the positions of Q and R relative to P and the vehicle. The primary problem is to obtain a reasonably accurate estimate of the component of $\delta \underline{r}_S$ along the line of sight to P. The pairs of bodies used in the measurements are normally chosen from among the following:

1. P and Q
2. Q and B_1
3. Q and R
4. Q and B_2
5. R and B_1
6. P and R

Those three are chosen for which the diagonal elements of the resulting 2-by-2 sub-matrix of $(\overset{*}{G}_S \overset{*}{G}_S{}^T)$ are most nearly equal. A simple graphical method of making the selection is discussed in Section 5.13.

It may be noted that six distinctly different angles are measured even though theoretically greater accuracy can be obtained by repeating some of the original measurements. The reason for using all different angles is to minimize the effect of any unknown non-random errors in the instrumentation system.

5.12 Survey of First Magnitude Stars

The optical system for acquiring and tracking celestial bodies is simplified if only the relatively bright bodies are used for the angular measurements. The apparent brightness of the other planets as seen from Earth varies with time, but all those that are to be used as "near bodies" (except Mars during a short portion of its cycle relative to Earth) are at least as bright as first-magnitude stars. Jupiter and Saturn, although they are not used as near bodies, are also at least as bright as first-magnitude stars. The variations in planet brightness are illustrated in the chart on Pages 34 and 35 of Reference (34). A discussion of the meaning of the "magnitude" of a star may be found in Reference (35), Pages 329 et seq.

There are 22 stars whose brightness as seen from the solar system is greater than that of a star with apparent visual magnitude of 1.5. These stars have been investigated to determine which, if any, are suitable as "in-plane" stars and which are suitable as "out-of-plane" stars. The resulting data are contained in Table 5-1. The stars are listed in order of decreasing brightness. The order and the apparent visual magnitude are taken from Table 11.II of Reference (35).

The computed data for each star consist of celestial longitude, celestial latitude, and the components of the line-of-sight unit vector along the x_E, y_E, z_E axes of the heliocentric ecliptic coordinate system. The computations are based on values of right ascension and declination obtained from the section entitled "Mean Places of Stars, 1962.0" in Reference (36).

If α and δ are, respectively, the right ascension and declination, the components of the line-of-sight unit vector $\underline{m}$ are

$$m_{x_E} = \cos\delta \cos\alpha \qquad (5\text{-}79)$$

TABLE 5-1 Characteristics of First Magnitude Stars

Star Number	Star Name	Apparent Visual Magnitude	m_{x_E}	m_{y_E}	m_{z_E}	Celestial Longitude (degrees)	Celestial Latitude (degrees)
1	Sirius	-1.43	-0.1806	0.7491	-0.6374	103.56	-39.60
2	Canopus	-0.73	-0.0610	0.2371	-0.9696	104.44	-75.83
3	α Centauri	-0.27	-0.3792	-0.6311	-0.6766	239.00	-42.58
4	Arcturus	-0.06	-0.7868	-0.3454	0.5115	203.70	30.76
5	Vega	0.04	0.1208	-0.4579	0.8808	284.78	61.73
6	Capella	0.09	0.1390	0.9109	0.3885	81.33	22.86
7	Rigel	0.15	0.2028	0.8317	-0.5169	76.30	-31.13
8	Procyon	0.37	-0.4102	0.8693	-0.2758	115.26	-16.01
9	Achernar	0.53	0.4915	-0.1338	-0.8605	344.77	-59.38
10	β Centauri	0.66	-0.4293	-0.5752	-0.6963	233.26	-44.13
11	Betelgeuse	0.4 to 1.0	0.0298	0.9606	-0.2762	88.22	-16.03
12	Altair	0.80	0.4522	-0.7456	0.4895	301.24	29.30
13	Aldebaran	0.75 to 0.95	0.3525	0.9309	-0.0953	69.26	- 5.47
14	α Crucis	0.87	-0.4531	-0.3987	-0.7973	221.34	-52.88
15	Antares	0.90 to 1.06	-0.3535	-0.9321	-0.0796	249.23	- 4.57
16	Spica	1.00	-0.9178	-0.3955	-0.0358	203.31	- 2.05
17	Fomalhaut	1.16	0.8335	-0.4187	-0.3605	333.32	-21.13
18	Pollux	1.16	-0.3831	0.9163	0.1163	112.69	6.68
19	Deneb	1.26	0.4537	-0.2134	0.8652	334.81	59.91
20	β Crucis	1.31	-0.4978	-0.4346	-0.7505	221.12	-48.63
21	Regulus	1.36	-0.8598	0.5105	0.0081	149.30	0.46
22	ε Canis Majoris	1.49	-0.2159	0.5858	-0.7811	110.23	-51.36

$$m_{y_E} = \cos\delta \sin\alpha \cos\epsilon + \sin\delta \sin\epsilon \tag{5-80}$$

$$m_{z_E} = -\cos\delta \sin\alpha \sin\epsilon + \sin\delta \cos\epsilon \tag{5-81}$$

ϵ, the obliquity of the ecliptic, is equal to 23.444°. The celestial longitude λ and the celestial latitude β are given by

$$\lambda = \arctan\left[\frac{m_{y_E}}{m_{x_E}}\right] \tag{5-82}$$

$$\beta = \arctan\left[\frac{m_{z_E}}{\left(m_{x_E}^2 + m_{y_E}^2\right)^{1/2}}\right] \tag{5-83}$$

Figure 5.2 is a polar plot of the star locations on the celestial sphere.

The data indicate that five of the stars are at celestial latitudes between −10° and +10° and thus may be used as in-plane stars. In order of increasing magnitude of latitude, they are

21. Regulus
16. Spica
15. Antares
13. Aldebaran
18. Pollux

In addition, either Jupiter or Saturn may be used as far bodies for in-plane measurements.

Canopus, the second brightest star, is the best situated for out-of-plane measurements. Other stars that may be used for out-of-plane measurements, in order of decreasing magnitude of latitude, are

5. Vega
19. Deneb
9. Achernar

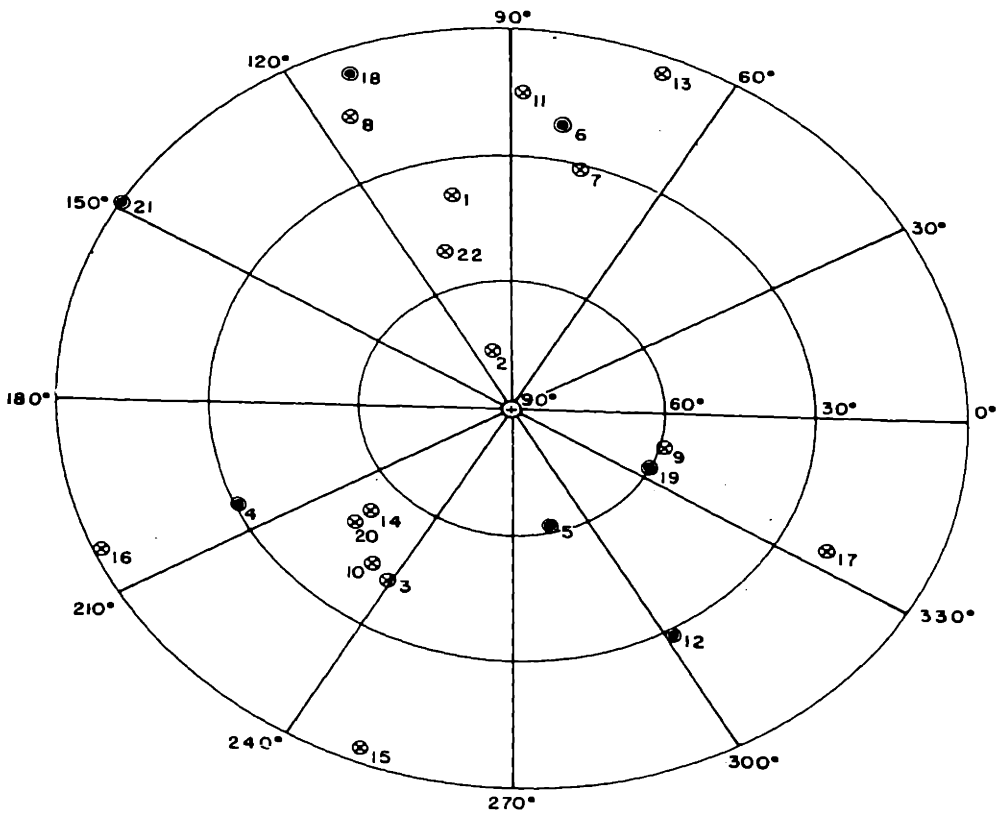

Numbers refer to stars listed in Table 5-1.

⊙ Star in positive celestial latitude.

⊗ Star in negative celestial latitude.

λ = Celestial longitude

β = Celestial latitude

Figure 5.2 Celestial Longitude and Latitude of First Magnitude Stars

5.13 Illustration of Procedure for Selection of Angular Measurements

An illustrative example serves to demonstrate the method of selecting the sightings to be used for position determination. Figure 5.3 shows the nominal position of the space vehicle and the positions of the near bodies one year after launch on Trajectory 1034, which was also used for illustrative purposes in Chapter 4. The lines of sight to the in-plane stars are indicated in the figure. All positions shown are projections of the true positions into the plane of the reference trajectory.

The distances of the near bodies from the vehicle are

for Mars, $z_M = 1.57$ a.u.

for the sun, $z_S = 1.59$ a.u.

for Venus, $z_V = 1.83$ a.u.

for Earth, $z_E = 2.38$ a.u.

Mercury, the other near body, is not used for measurements in this case, because its line of sight is too close to that of the sun. In Reference (5) it is stated that bodies whose lines of sight are within 15° of that of the sun are optically undesirable for measurement purposes.

The configuration shown, which was picked at random, is somewhat unusual in that the vehicle, Mars, and the sun form roughly an equilateral triangle. In manned missions the distance of the vehicle from the launch planet, or from the destination planet, or sometimes from both, is considerably smaller than its distance from the sun.

Six measurements are to be selected, two out-of-plane and four in-plane. The near bodies to be used are Mars, the sun, and Venus.

Since Mars and the sun are virtually equidistant from the vehicle, the two best out-of-plane measurements are the angles that the line of sight to each makes with the line of sight to Canopus, the first-magnitude star situated closest to the celestial polar axis.

The four in-plane measurements are to be selected from the seven shown in Figure 5.3. For simplicity the double-subscript notation of previous sections has been replaced by a set of single numerical

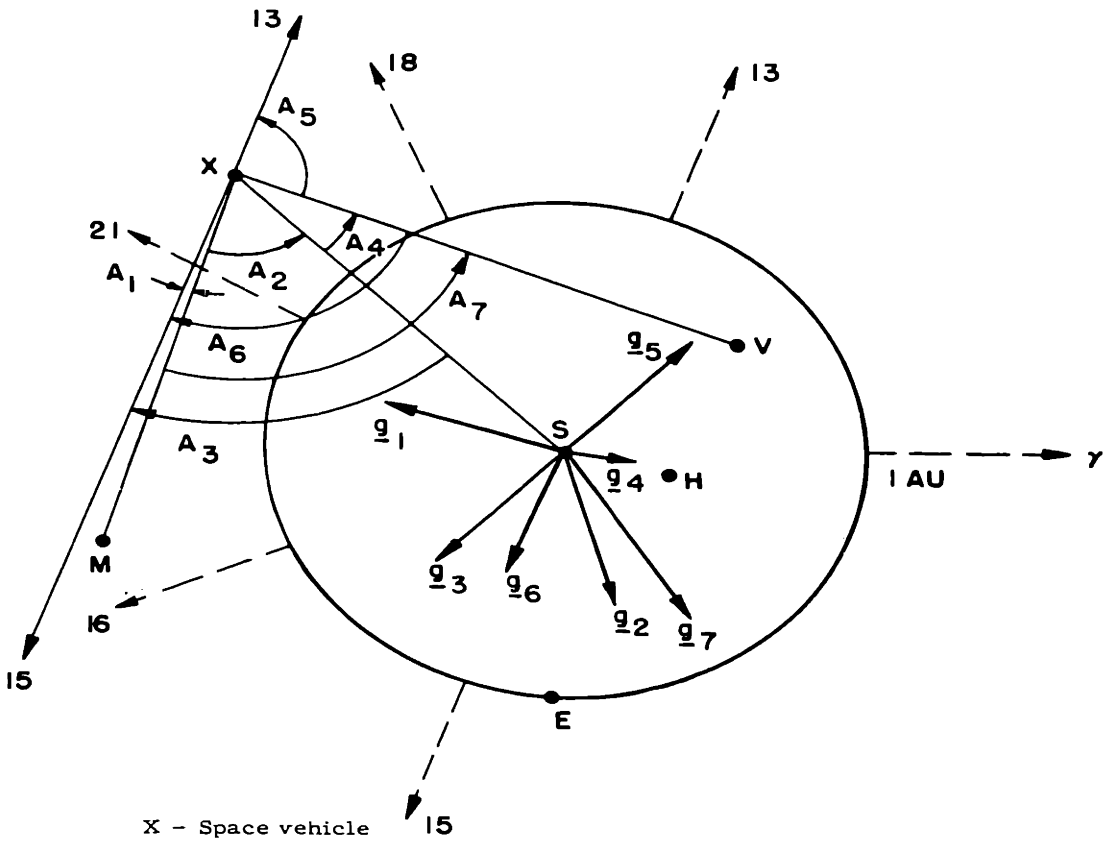

X – Space vehicle
S – Sun
H – Mercury
V – Venus
E – Earth
M – Mars
Dotted lines indicate directions to points on celestial sphere.
γ – First point of Aries
13, 15, 16, 18, 21 – Stars from Table 5-1
$A_1, \cdots, A_7$ – Possible measurement angles
$\underline{g}_1, \cdots, \underline{g}_7$ – Corresponding geometry vectors
Positions and vectors shown are projections of actual quantities into plane of reference trajectory.

Figure 5.3 Selection of Measurement Angles

subscripts. The celestial bodies involved in the seven possible angular measurements are

A_1 : Mars – Antares

A_2 : Mars – Sun

A_3 : Sun – Antares

A_4 : Sun – Venus

A_5 : Sun – Aldebaran

A_6 : Venus – Antares

A_7 : Mars – Venus

Antares is used in all except one of the possible measurements involving stars, because its line of sight forms the smallest angles with the lines of sight to the near bodies. Because there are practical limitations on the maximum angle that the vehicle's tracking system can measure, it is desirable, when other factors are equal, to select the smallest possible angles. All the angles listed above are smaller than 120°.

The geometry vectors g_1 through g_7 are also shown in Figure 5.3. The final selection of four in-plane measurements is based on the magnitude and direction of these vectors. The selection can be made visually if any pair of orthogonal axes can be found in the reference trajectory plane such that the sums of the squares of the components of the selected vectors along each of these axes can be seen to be maximized and roughly equal to each other.

Axes parallel and normal to g_1 are convenient. The first vector selected is g_1. g_4 is immediately ruled out because of its small magnitude. The other three vectors to be chosen should have large components normal to g_1. In this particular example, g_2, g_3, g_5, g_6, and g_7 all have components normal to g_1 that are approximately equal in magnitude, so that the position uncertainty normal to g_1 is not appreciably affected by the selection. In this circumstance, the three vectors of largest magnitude are selected, because they will cause the largest reduction in position uncertainity parallel to g_1. The selected vectors are

$\underline{g}_7$, $\underline{g}_2$, and $\underline{g}_3$. Although $\underline{g}_3$ and $\underline{g}_5$ are equal in magnitude, $\underline{g}_3$ is selected because the measurement angle A_3 is smaller than A_5.

The six angles selected involve the following pairs of celestial bodies:

1. Mars – Canopus
2. Sun – Canopus
3. Mars – Antares
4. Mars – Venus
5. Mars – Sun
6. Sun – Antares

These angles, although selected without need for computation, satisfy the mathematical criterion of producing a large value of the determinant of $(\overset{*}{G}_S \overset{*}{G}_S{}^T)$. Regardless of which of the reference trajectory coordinate systems is used, the diagonal elements of $(\overset{*}{G}_S \overset{*}{G}_S{}^T)$ are large compared to the off-diagonal elements, and the diagonal elements are of the same order of magnitude.

5.14 Physical Considerations

In all of the preceding analysis the navigational problem has been treated from a geometric viewpoint; in this section physical factors that tend to affect the utilization of the measurements are briefly outlined.

In the Earth-based system corrections are applied to the data for the effect of refraction of the radio signals emanating from the vehicle as they pass through the earth's atmosphere, for the difference between the apparent vertical at the tracking station (as measured by a plumb line) and the geocentric vertical, and for the effect of aberration due to the transverse velocity of the vehicle relative to the tracking station. Reference (33) contains an analysis of the first two effects.

Larmore[37] presents a discussion of a number of physical phenomena that affect the angular measurements in the self-contained system. Larmore's analysis is based on the assumption that it is possible to achieve an ultimate accuracy of 0.2 seconds of arc or 1 microradian in the measurement of celestial angles; in the present study the far more conservative

figures of 10 seconds of arc or 50 microradians are regarded as reasonable for the accuracy of on-board angular measurements made with instrumentation systems consistent with the present state of the art. As a consequence, some of the effects that are regarded as significant by Larmore as assumed to be negligible in this study.

One effect that is significant is the aberration of starlight due to the component of vehicle velocity that is normal to the line of sight to the star. This effect may cause an apparent shift of the line of sight to the star of as much as 100 microradians. A related effect is the apparent shift in the line of sight to a planet due to the finite velocity of light. If Mars is being viewed from a distance of 1 a.u., the planet will have moved approximately 7,000 miles in the time that it takes a light ray to travel from it to the vehicle.

The phasing of the planets also presents some difficulty. The optical apparatus is assumed to seek the point of maximum light intensity when the body being tracked is not a point source. When the illuminated portion of a planet is crescent-shaped, the point of maximum light intensity is removed from the center of the planet by an amount which may be significant. The difficulty is compounded by the fact that cloud formations and other variations in planetary atmospheres are not predictable, and their effects on the center of light intensity is not known precisely. For Venus at inferior conjunction the difference between the center of light intensity and the center of the planet could cause an angular measurement error of as much as 100 microradians for a sighting made from the surface of the earth.

Other sources of error mentioned by Larmore which are not considered significant in the present analysis include the small inaccuracies in the planetary position data of Reference (36), the parallax effect due to the fact that the star distances are not truly infinite, the effect of the proper motion of the stars, and the fact that in a double star system the center of light intensity does not coincide with the center of mass of the system.

The inexact knowledge of the size of the astronomical unit in terms of standard lengths used in the laboratory does not directly affect the angular measurements, since the angles are really ratios of lengths rather than lengths themselves. However, this uncertainty does affect the accuracy of

the prediction of vehicle position relative to the destination point. As a result of recent tests in which radar signals have been reflected from Venus, the uncertainty in the ratio of the astronomical unit to a laboratory unit such as the kilometer or the mile has been reduced from one part in 10^4 to three parts in 10^6. The results of the radar investigation are reported in Reference (38). The uncertainty of three parts in 10^6 is equivalent to an uncertainty of 300 miles in the length of the astronomical unit.

The effect of relativity on instrumentation in the space vehicle is discussed in Reference (39). The primary effect is an induced drift rate in the vehicle's clock relative to a standard clock on the surface of the earth. Due to special relativity the vehicle's clock tends to run fast; due to general relativity it tends to run slow. For travel within the solar system both effects are at least two orders of magnitude smaller than the random drift rate of one part in 10^6 which is assumed to be feasible for the clock in the vehicle.

The systematic effects that are significant include the aberration of starlight, the finite velocity of light, and the phasing of the planets. All three can be taken into account in pre-computing the reference value of a space angle that is to be measured at a specified time.

CHAPTER 6

APPLICATIONS OF THE THEORY

6.1 Summary

As an application of the guidance and navigation concepts developed in previous chapters, a midcourse guidance system is proposed for a manned flight from Earth to Mars. Other possible uses of the theory on an interplanetary flight are discussed.

6.2 Introduction

The objective of this chapter is to show how the analytic approach to guidance theory can be effectively utilized in the design of the guidance system for a specific interplanetary mission. The type of mission that is to be discussed is an outbound manned mission from Earth to Mars.

For a practical mission of this type the total transfer angle, $(f_D - f_I)$, is equal to or less than 180°. Both radio-command and self-contained navigation systems are to be used. The nature of the mission is assumed to be such that VTA guidance is permissible.

The system that is to be described is felt to offer the combined advantages of simplicity, reliability, and low cost without any reduction in accuracy relative to previously proposed systems. These advantages are a direct consequence of the analytic solution of the guidance equations.

6.3 Reference Trajectory

The reference trajectory for the interplanetary flight is pre-computed. All known perturbative effects of any significance are included in the formulation of the equations of motion. These equations are integrated numerically on a large-scale digital computer. The method of computation is described in considerable detail in Reference (40).

If several reference trajectories have been computed, all of which are approximately equally advantageous from the standpoint of time of flight and fuel requirements for launch and injection, midcourse guidance characteristics may affect the final choice of a trajectory. Computations such as those embodied in Figures 4.2, 4.13, and 4.16 are use-

ful in comparing trajectories. The latter two indicate the sensitivity of position variation at the destination to error in injection velocity; the first is a composite picture of the effect of the orientation of the relative velocity vector $\underline{v}_R$ on the magnitude of the VTA correction.

6.4 Injection Guidance

Although this study is not directly concerned with the problem of injection guidance, the illustrative example of Chapter 4 indicates clearly where the emphasis should be placed in the design of the injection guidance system. It is of primary importance to control the magnitude of the velocity vector at injection into the heliocentric orbit. In terms of hardware, the emphasis is to be placed on the accuracy of the integrating accelerometer system and on achieving fast, reliable cut-off of the propulsion system.

6.5 Midcourse Guidance

Both the radio-command navigation system and the self-contained navigation system are to be used for midcourse guidance. Each of the two is used as the primary measurement source in the region of its greatest accuracy, and each is used as a stand-by measurement source when the other is the primary source. The vehicle's on-board computer and its control system are designed so that inputs can be accepted from either source at any time.

6.6 Radio-Command Guidance

The Earth-based tracking system is the primary measurement source during the early stages of the heliocentric ballistic trajectory. It remains the primary source at least until the vehicle leaves Earth's sphere of perturbative relevance, at a distance of roughly two million miles from Earth.

The radio measurements, made several times a minute as long as the vehicle is visible to a tracking station, are combined with the initial estimate of the state vector at injection and used to determine the maximum likelihood estimate of the state vector at the nominal time of arrival at the destination.

Within Earth's sphere of perturbative relevance numerical integration is used to compute the elements of the required transition matrices. The computation is most simply accomplished in the non-rotating x y z

coordinate system. The estimate obtained for $\delta \underline{x}_D$ is transformed from x y z coordinates to p q z coordinates and then transmitted to the vehicle's computer by means of radio signals from one of the tracking stations.

The destination point used in the computation is the point at which the reference trajectory intersects the sphere of perturbative relevance of Mars, at a distance of approximately one million miles from the planet.

The first midcourse correction is to be made at the optimum time $t_{C_{opt}}$. As explained in the next section, the determination of this time is accomplished by the computer on board the space vehicle.

Because it corrects for the effects of errors in injection guidance, the first midcourse velocity correction is normally much larger in magnitude than any succeeding corrections. It is therefore quite fortunate that the Earth-based tracking system, with its thousands of individual measurements, can be used to obtain an accurate estimate of $\delta \underline{x}_D^-$, and it is likewise fortunate that the correction can be applied at the time when its magnitude is a minimum.

6.7 Self-Contained Guidance

Although the point at which the self-contained system replaces the radio-command system as the primary source of input data will depend on hardware development in the two types of systems, a reasonable point for the change-over is assumed to be at the surface of the sphere of perturbative relevance. Since the first correction, at $t_{C_{opt}}$, is made at a point considerably beyond this sphere, measurements from both systems are used in the computation of this correction. At the change-over point the final estimate of $\delta \underline{x}_D^-$ made by the Earth-based system serves as an "initial estimate" for the vehicle's computer, to be used in conjunction with subsequent position measurements to compute a more accurate $\delta \hat{\underline{x}}_D^-$, from which $t_{C_{opt}}$ and $\underline{c}_V$ can be determined.

Since all of the computations performed by the vehicle's computer are related to that portion of the flight in which the vehicle is outside the sphere of perturbative relevance of any planet, the analytic forms of the guidance matrices can be used. No numerical integration is required of the computer even though the time $t_{C_{opt}}$ is determined *a posteriori*.

In addition to being used for making the final determination of the first midcourse correction, the self-contained system is used for computing any subsequent corrections that may be required. The accuracy of subsequent corrections is improved by utilizing the concept of the initial estimate immediately after the last correction, as explained in Section 5.9.

Because of the presence of clock errors, the two-step procedure of Chapter 5, involving first determination of both present position and clock error and then determination of the estimated state vector at the destination, is used in all on-board computations.

For a voyage of roughly six months' duration a position determination once a week is deemed reasonable. The nominal time of each position determination and the specific angular measurements to be made at that time are pre-programmed. The graphical procedure illustrated in Section 5.13 is used to select six angles to be observed.

For each sighting at each measurement time the reference value of the angle is stored in the computer. This value includes the effects of the significant physical phenomena mentioned in Section 5.14. In addition, one number per measurement must be stored in the computer to account for the fact that the angular measurement is not made precisely at the time when the space ship clock reads t_S, the nominal time of the measurement; this number is a function of the velocity of the vehicle relative to the two bodies involved in the sighting.

Finally, in order to solve Equation (5-24) for the inferred values of clock error and position variation at time t_S, sufficient information must be stored so that the matrix product $(\overset{*}{G}_S \overset{*}{U}^{-1} \overset{*}{G}_S{}^T)^{-1} \overset{*}{G}_S \overset{*}{U}_S{}^{-1}$ can be determined. All the data required are known a priori with one exception, the variance of the clock error $u_{S0}{}^2$. Normally this variance is small enough to justify an a priori estimate of its value at each t_S. Then the 24 elements of the matrix product may be pre-computed and stored in the memory of the on-board computer.

The intervals between times of position measurement need not be equally spaced. Occasionally improved position accuracy can be achieved by taking advantage of a favorable configuration of the planets at a particular time. For example, it is deemed inadvisable to sight on a planet

whose line of sight makes an angle of less than 15° with the line of sight to the sun. If a planet relatively close to the vehicle lies near the vehicle-sun line at a weekly measurement time, the measurement time is changed so that the planet's proximity can be exploited in improving the accuracy of vehicle position determination.

In the analysis of Chapter 5 only celestial bodies of first magnitude or brighter are considered for the optical sightings. Because the number of such bodies is quite limited, the possibility of ambiguities (i.e., of measuring the angle between an incorrect pair of celestial bodies) is remote. Nevertheless, this possibility should be kept in mind when the angular sightings are being selected.

Another consideration in selecting the sightings is the magnitude of the angle being measured. From practical considerations in the design of the on-board sextants, it is not possible to measure space angles in the vicinity of 180°. A practical limit of 120° in the angle to be measured is felt to be reasonable; this constraint is to be taken into consideration in utilizing the graphical method of selecting the measurements.

After the computation of clock error and position variation is completed at a measurement time, the clock is corrected, and a revised maximum likelihood estimate of $\delta \underline{x}_D$ is determined from Equation (5-37). The determination of the revised $\delta \hat{\underline{x}}_D$ is the most complicated operation required of the on-board computer, because, each time it is performed, a new matrix of the form $(\overset{*}{Q}\ \overset{*}{U}^{-1}\ \overset{*}{Q}^T)$ must be inverted. The inversion cannot be carried out before the flight due to the fact that the uncertainty matrix $\overset{*}{U}$ in (5-37) depends on the actual measured values of the angles.

After the first correction has been applied, there is no further need for determining $t_{C_{opt}}$, because it will have occurred prior to the time of the most recent set of measurements. The time at which any required additional correction is applied is discussed in the next section. Each correction vector $\underline{c}_V$ is computed analytically from the matrix forms of Chapter 3.

6.8 Strategy for Determining Whether to Make a Correction

After the first correction has been made, the necessity for making additional corrections is determined by the predicted miss distance at

the destination. The specification for the mission defines a permissible miss distance. If the predicted miss distance is computed to be well within the permissible value, it is obviously unnecessary to make any additional corrections.

In order to give these statements quantitative significance, the miss distance will be re-defined, and the concept of circular probable error will be introduced. As indicated in Section 2.14, the miss distance vector $\delta\underline{\rho}$ is that component of the position variation $\delta\underline{r}_D$ which lies in the plane normal to the relative velocity vector $\underline{v}_R$. The estimated miss distance vector, $\delta\hat{\underline{\rho}}$, can be computed by transforming the maximum likelihood estimate $\delta\hat{\underline{x}}_D$ into the critical-plane coordinate system. The first two elements of the transformed vector are the components of the two-dimensional vector $\delta\hat{\underline{\rho}}$. The transformation is accomplished mathematically by modifying the equations of Section 5.4 as follows:

$$\delta\underline{m} = \overset{*}{Q}^T \overset{*}{Y}_D^T (\delta\underline{x}_D)_W \tag{6-1}$$

where

$$\overset{*}{Y}_D = \begin{Bmatrix} \overset{*}{X}_D & \overset{*}{O}_3 \\ \overset{*}{O}_3 & \overset{*}{X}_D \end{Bmatrix} \tag{6-2}$$

and $\overset{*}{X}$ is the standard transformation matrix for transforming a three-dimensional vector into the critical-plane coordinate system.

$$(\delta\hat{\underline{x}}_D)_W = (\overset{*}{Y}_D \overset{*}{Q} \overset{*}{U}^{-1} \overset{*}{Q}^T \overset{*}{Y}_D^T)^{-1} \overset{*}{Y}_D \overset{*}{Q} \overset{*}{U}^{-1} \delta\tilde{\underline{m}} \tag{6-3}$$

$$(\overset{*}{E}_D)_W = \overline{(\underline{\epsilon}_D)_W (\underline{\epsilon}_D{}^T)_W} = (\overset{*}{Y}_D \overset{*}{Q} \overset{*}{U}^{-1} \overset{*}{Q}^T \overset{*}{Y}_D^T)^{-1} \tag{6-4}$$

The first two elements of the first two rows of $(\overset{*}{E}_D)_W$ constitute the 2-by-2 covariance matrix of the uncertainty in $\delta\hat{\underline{\rho}}$. This matrix is designated $\overset{*}{E}_\rho$. The equi-probability ellipse associated with the uncertainty in $\delta\hat{\underline{\rho}}$ has the form

$$\left\{ \epsilon_{D_\xi} \quad \epsilon_{D_\eta} \right\} \overset{*}{E}_\rho^{-1} \left\{ \begin{matrix} \epsilon_{D_\xi} \\ \epsilon_{D_\eta} \end{matrix} \right\} = k^2 \qquad (6\text{-}5)$$

where ϵ_{D_ξ} and ϵ_{D_η} are the first two components of the uncertainty vector $(\underline{\epsilon}_D)_W$. If k = 1.1774, the probability that the uncertainty vector of $\delta\hat{\underline{\rho}}$ lies within the boundaries of the ellipse is 0.5. When the measurements are properly chosen, the axes of the ellipse are approximately equal in length, so that the ellipse closely resembles a circle. The radius of the circle whose area is the same as that of the ellipse is known as the "circular probable error" (CPE). The CPE is a convenient measure of the accuracy of the prediction of the miss distance. The equation relating CPE to the determinant of $\overset{*}{E}_\rho$ is

$$\text{CPE} = 1.1774 \left| \overset{*}{E}_\rho \right|^{1/4} \qquad (6\text{-}6)$$

Appendix P contains a more detailed treatment of CPE.

Every time a measurement is made, the CPE is reduced slightly. Every time a velocity correction is applied, the CPE is increased due to the uncertainty $\underline{\eta}$ associated with the correction.

Before a correction is applied, the predicted miss distance is $\delta\hat{\underline{\rho}}^-$, and the circular probable error is $(\text{CPE})^-$. Immediately after application of a VTA correction, the predicted miss distance $\delta\hat{\underline{\rho}}^+$ is zero, and the circular probable error $(\text{CPE})^+$ is greater than $(\text{CPE})^-$.

If the sum of the magnitude of $\delta\hat{\underline{\rho}}^-$ and $(\text{CPE})^-$ is smaller than the required position accuracy at the destination, no further correction is necessary.

If the sum of the magnitude of $\delta\hat{\underline{\rho}}^-$ and $(\text{CPE})^-$ exceeds the required position accuracy, an additional correction should be made. The time of additional correction is determined by the computed value of $(\text{CPE})^+$. As the vehicle gets closer to the destination, the magnitude of $(\text{CPE})^+$ gets smaller, but the magnitude of the required correction gets larger. Therefore, the correction is made at the earliest time at which $(\text{CPE})^+$ falls within the specification for position accuracy at the destination.

With the high accuracy obtained from the Earth-based tracking system for the first correction and with a reasonably accurate midcourse thrust application, it is felt that three midcourse corrections, and possibly only two, are sufficient to meet the requirements of a typical manned interplanetary mission.

6.9 Other Applications

The theory developed in the preceding chapters has several applications in addition to those already illustrated by the proposed guidance system for the manned interplanetary mission. The additional applications include the following:

1. Direct calculation of the midcourse velocity correction by crew members on an interplanetary mission.

2. Calculation of abort guidance requirements by crew members on an interplanetary mission.

3. Systematic study of the effect of parameters associated with the reference trajectory on midcourse guidance requirements for an interplanetary mission.

Equation (3-133), the analytic expression for the elements of the correction matrix $\overset{*}{K}_{CD}$, is sufficiently simple that a hand calculation of the velocity correction is feasible when the correction time t_C is specified and the on-board digital computer has provided an estimate of $\delta \underline{r}_D^-$. Such a calculation serves as a check of the on-board digital computer. On a mission of many months' duration the psychological value of the calculation in providing a useful outlet for the energies of the flight crew may be significant.

Hand calculations for abort guidance are also feasible. If the mission has to be aborted while the vehicle is outbound from Earth and if the on-board computer is incapacitated, it is possible that sufficient tabular data can be supplied to the flight crew so that measurements of angular deviations relative to a special abort reference trajectory can be processed by hand calculation to determine the required velocity corrections.

The use of the analytic forms of the guidance matrices to make a parametric study of reference trajectories is an extension of the type of

analysis presented in Chapter 4, in which only one reference trajectory was studied. There are relatively few parameters involved, and the range of some of these is quite limited for a specified type of mission. Consequently, the amount of computation required falls within reasonable bounds.

6.10 Concluding Remarks

The fundamental difference between the midcourse guidance system proposed in this chapter and those that have been previously suggested is that the correction times in the proposed system are not pre-programmed, but rather are determined as a function of the variations measured during the flight. This degree of flexibility is made practical by the development of the analytic form of the correction matrix $\overset{*}{K}_{CD}$. With this development the velocity correction vector at any correction time t_C can be readily determined by an on-board digital computer of modest capacity.

The flexibility in the selection of time of correction is combined with the empirical method developed for determining the optimum time of correction to ensure that the first midcourse correction, which is much larger than any succeeding correction, is made at the time when its magnitude is minimized. The times of the remaining corrections are adjusted to achieve the best compromise between magnitude of the correction and position accuracy at the destination.

The proposed system also differs from previous systems in that it accounts for clock errors and at the same time utilizes all the measurement data in predicting the vehicle's state at the nominal time of arrival at the destination.

Finally, the uncoupling between in-plane and out-of-plane motion is exploited to provide a method of selecting those optical sightings which provide the most accurate estimate of present position. The method is graphical; no elaborate computer program is required.

CHAPTER 7

CONCLUSIONS AND RECOMMENDATIONS

7.1 Summary

The subject matter of the thesis is briefly reviewed. The features of the analysis that are felt to be original are listed. Those areas in which further study appears desirable are indicated.

7.2 Résumé of Guidance Theory

The problem of midcourse guidance of an interplanetary vehicle has been linearized by assuming that the vehicle's actual trajectory experiences only small departures from a known pre-computed reference trajectory. Matrix forms have been used to obtain a compact set of guidance equations for the vehicle's motion in an n-body gravitational field.

The difference between the actual trajectory and the reference trajectory is expressed mathematically as a six-component vector consisting of the three components of position variation and the three components of velocity variation at some specified time. This vector is known as the state vector. The most useful state vector for guidance analysis is the one for which the specified time is the nominal time of arrival at the destination.

The state vector at one time is related to the state vector at some other time by means of a 6-by-6 matrix known as the transition matrix.

If the time of arrival is fixed, the midcourse velocity correction required at some time t_C is a function of the predicted position variation at the destination. The negative of the 3-by-3 matrix relating the velocity correction vector to the position variation vector is called the correction matrix.

When the time of arrival is not critical and small variations in arrival time are permissible, the velocity correction of minimum magnitude at time t_C is a function of that component of the position variation at the destination which lies in the plane perpendicular to the relative velocity

of the vehicle with respect to the destination planet. This component of position variation is the miss distance. For this type of velocity correction the form of the guidance equations can be simplified by introducing the rotating coordinate system known as the critical-plane coordinate system; in this system both the velocity correction vector and the miss distance vector are two-dimensional vectors.

The magnitude of the velocity correction is a function of the time at which the correction is applied. For the case of variable arrival time, the correction time for which the magnitude of the correction is a minimum is determined empirically as a function of the angular orientation of the miss distance vector in the plane perpendicular to the relative velocity vector.

For the n-body problem the elements of the transition matrix are computed by numerical integration. The correction matrix is the inverse of one of the four 3-by-3 sub-matrices constituting the transition matrix.

For the midcourse phase of an interplanetary journey, when the vehicle is outside the sphere of perturbative relevance of any planet, the n-body problem can be reduced to a two-body problem without any significant loss of accuracy. The reference trajectory is then a conic section. The plane containing the reference trajectory is the reference trajectory plane. The actual trajectory is also a conic section; its plane normally differs slightly from the reference trajectory plane.

The two-body assumption simplifies the equations of motion of the vehicle. The variant motion in the plane of the reference trajectory is uncoupled from the variant motion normal to the reference trajectory plane. By proper choice of a coordinate system the sixth-order system is sub-divided into two independent systems, one of fourth order and the other of second order. These two systems have been integrated analytically for the case when the conic section is an ellipse.

The same analytic solution is also obtained in a different manner, namely by applying the techniques of the calculus of variations to a set of six orbital elements which define the reference trajectory.

The analytic solution is used to obtain analytic expressions for all the elements of the transition matrix, the correction matrix, and several other matrices that are useful in the development of guidance theory.

There are three types of combinations of the correction time t_C and the arrival time t_D in which the matrix that must be inverted in order to evaluate the correction matrix becomes singular. When any of these singularity conditions occurs, the correction matrix is indeterminate, and no finite velocity correction can be computed by means of fixed-time-of-arrival guidance. If variable-time-of-arrival guidance is used, the effects of two of the singularity types are obliterated, and finite velocity corrections can be computed even when the conditions for these singularity types occur.

7.3 Résumé of Navigation Theory

As used in this thesis, the term navigation refers to the obtaining and processing of measurements made during the space voyage in order to compute the predicted state vector at the nominal time of arrival at the destination. This predicted state vector is the one utilized in the guidance theory to determine when and how to make a midcourse velocity correction.

Two types of navigation systems are described, the Earth-based radio-command system and the self-contained optical system. A linear theory is developed to process the measurements made in either system. Since redundant measurements are made, the method of maximum likelihood is used to estimate the predicted state vector at the destination.

The Earth-based system uses radio antennas to track the vehicle. Large amounts of data are processed by a centrally located digital computer facility. The system is most effective when the vehicle is relatively close to Earth.

The self-contained system utilizes two telescopes to measure the angles between lines of sight to pairs of celestial bodies. Relatively few measurements are made and are processed by the computer on board the space craft.

Clock error is a negligible factor in the Earth-based system. However, it can be significant in the self-contained system. To account for clock error and to correct for it, the self-contained system's computation is a two-step process. First, a group of measurements is made at a single

nominal measurement time. From this information estimates are made of the position variation at the nominal measurement time and of the clock error. The clock is corrected immediately. The process is repeated at other measurement times, and from the group of estimates of position variation, an estimate is made of the state vector at the time of arrival at the destination.

A graphical procedure, based on the lack of coupling between in-plane and out-of-plane variant motion, is developed for selecting those optical sightings which give the greatest accuracy of position determination at a given measurement time.

A set of pseudo-measurements, consisting of the components of the state vector at launch or immediately following a midcourse correction, is used to improve the accuracy of the predicted state vector at the time of arrival.

7.4 Novel Features of the Analysis

It is the author's conviction that, in an analytic study of the type that has been presented, he is under some obligation to indicate clearly those results which he considers original. This is a risky undertaking, particularly in a field in which so many investigations are currently being carried on. It is therefore with considerable trepidation that the list appearing below has been prepared. The following features of the analysis are thought to be novel:

1. The relatively simple and straightforward analytic solution of the variant equations of motion by two different methods for the case of an elliptical reference trajectory.

2. The exploitation of the analytic solution to obtain closed-form expressions for the elements of the fundamental guidance matrices.

3. The discovery of the type of singularity called the $X = 0$ singularity in Chapter 3, and the relation between singularities of the $X = 0$ type and the minima of the time-of-flight curves obtained from Lambert's theorem.

analytic approach has not been more actively pursued is closely associated with the present availability of high-speed digital computers. It is difficult for a human being to generate the motivation for obtaining an analytic solution involving weeks, or even months, of algebraic drudgery when the computer offers the tantalizing prospect of providing any desired amount of numerical data with a relatively insignificant amount of human effort. It is felt that in the present case, at least, the drudgery has proved to be justified.

7.6 Recommendations for Further Study

The following topics, related to the subject matter of this thesis, are suggested as possibly fruitful subjects of future investigations:

1. Analytic solution of the variant equations of motion for hyperbolic reference trajectories.

2. Empirical approach to the problem of finding closed-form expressions for the elements of the guidance matrices when the reference trajectory is a three-body trajectory.

3. Further investigation of the critical-plane coordinate system for use in variable-time-of-arrival guidance.

4. Parametric study of reference trajectories for specific types of missions.

The analytic solution for hyperbolic reference trajectories is based on the same approach as that presented in Chapter 3 for elliptical reference trajectories. The solution will be used for obtaining a new set of closed-form expressions for the elements of the guidance matrices.

When a closed-form solution is available for hyperbolic as well as elliptical reference trajectories, there is a distinct possibility that the two solutions can be combined and properly weighted, so that an empirical closed-form solution of the guidance equations can be obtained for an interplanetary vehicle when it is within the sphere of perturbative relevance of the destination planet. If such a solution is achieved, the destination point of the midcourse guidance system can be moved up to the point of closest approach to the planet, and the midcourse and terminal guidance systems can effectively be merged.

It is felt by the author that more can be learned about variable-time-of-arrival guidance by investigation of the variation in orientation of the noncritical vector $\underline{w}$ as a function of the time of correction. A physical explanation should be sought for the fact that one of the four elements relating the velocity correction to the miss distance vector in the critical-plane coordinate system is identically zero.

The analytic solution for elliptical reference trajectories reduces the parameters affecting the guidance equations to a relatively small number. It should be a relatively simple matter to make a systematic numerical study of the effect of variations in these parameters on guidance requirements and thus to determine which reference trajectories are, from a guidance viewpoint, most desirable for a specified mission.

REFERENCES

1. Battin, R.H., "The Determination of Round-Trip Planetary Reconnaissance Trajectories," Journal of the Aero/Space Sciences, Sept. 1959, pp. 545 – 567.
2. Laning, J.H., Jr., Frey, E.J., and Trageser, M.B., "Preliminary Considerations on the Instrumentation of a Photographic Reconnaissance of Mars," Vistas in Astronautics, Vol. II, Pergamon Press, New York, 1959, pp. 63 – 94.
3. Battin, R.H. and Laning, J.H., Jr., "A Navigation Theory for Round-Trip Reconnaissance Missions to Venus and Mars," Planetary and Space Science, Vol. 7, Pergamon Press, Inc., New York, 1961, pp. 40 – 56.
4. Battin, R.H., "A Comparison of Fixed and Variable Time of Arrival Navigation for Interplanetary Flight," Ballistic Missile and Space Technology, Vol. III, Academic Press, New York, 1960, pp. 3 – 31.
5. "A Recoverable Interplanetary Space Probe," M.I.T. Instrumentation Laboratory Report R-235, prepared by M.I.T. Instrumentation Laboratory in collaboration with AVCO Corporation, M.I.T. Lincoln Laboratory, and Reaction Motors Division of Thiokol Chemical Corporation, July 1959.
6. Battin, R.H., "Lecture Notes on Computational Procedures for the Navigational Fix," (unpublished), March 1961.
7. Battin, R.H., "Lecture Notes on Optimum Operations with Celestial Fix Data," (unpublished), March 1961.
8. Battin, R.H., "A Statistical Optimizing Navigation Procedure for Space Flight," ARS Journal, Vol. 32 No. 11, Nov. 1962, pp. 1681 – 1696.
9. Noton, A.R.M., "Interplanetary Post-Injection Guidance," JPL External Publication No. 653, June 1959.
10. Noton, A.R.M., Cutting, E., and Barnes, F.L., "Analysis of Radio-Command Mid-Course Guidance," JPL Technical Report No. 32 – 28, Sept. 1960.

REFERENCES (Cont.)

11. Gates, C.R., Scull, J.R., and Watkins, K.S., "Space Guidance," Astronautics, Vol. 6 No. 11, Nov. 1961, pp. 24 – 27, 64 – 72.

12. Smith, G.L., Schmidt, S.F., and McGee, L.A., "Application of Statistical Filter Theory to the Optimal Estimation of Position and Velocity on board a Circumlunar Vehicle," NASA Tech. Rept. R-135, 1962.

13. McLean, J.D., Schmidt, S.F., and McGee, L.A., "Optimal Filtering and Linear Prediction Applied to a Midcourse Navigation System for the Circumlunar Mission," NASA Tech. Note D-1208, 1962.

14. Porter, J.G., "Navigation without Gravity," Journal of the British Interplanetary Society, Vol. 13 No. 2, March 1954, pp. 68 – 74.

15. Lawden, D.F., "Correction of Interplanetary Orbits," Journal of the British Interplanetary Society, Vol. 13 No. 4, July 1954, pp. 215 – 223.

16. Baker, R.M.L., Jr., "Note on Interplanetary Navigation," Jet Propulsion, Vol. 28, December 1958, pp. 834 – 835.

17. Wheelon, A.D., "Midcourse and Terminal Guidance," Chapter 26 of Space Technology, H.S. Seifert editor, John Wiley and Sons, Inc. N.Y., 1959.

18. Magness, T.A., McGuire, J.B., and Smith, O.K., "Accuracy Requirements for Interplanetary Ballistic Trajectories," Proceedings of Ninth International Astronautical Congress, Amsterdam 1958, Vol. I, Springer-Verlag, Vienna, 1959, pp. 286 – 306.

19. Gunkel, R.J., Lascody, D.N., and Merrilees, D.S., "Impulsive Midcourse Correction of an Interplanetary Transfer," Proceedings of Tenth International Astronautical Congress, London 1959, Vol. II, Springer-Verlag, Vienna, 1960, pp. 650 – 670.

20. Kierstead, F.H., Jr., "Guidance Requirements for Interplanetary Flight," Advances in the Astronautical Sciences, Vol. 5, Plenum Press, Inc., N.Y., 1960, pp. 66 – 81.

REFERENCES (Cont.)

21. Kierstead, F.H., Jr., "Midcourse Guidance Requirements for Mars and Venus Probes," ARS Preprint 914 – 59, Nov. 1959.

22. Breakwell, J.V., "Fuel Requirements for Crude Interplanetary Guidance," Advances in the Astronautical Sciences, Vol. 5, Plenum Press, Inc., N.Y., 1960, pp. 53 – 65.

23. Breakwell, J.V., "The Spacing of Corrective Thrusts in Interplanetary Navigation," Advances in the Astronautical Sciences, Vol. 7, Plenum Press, Inc., N.Y., 1961, pp. 219 – 235.

24. Bock, C.D. and Mundo, C.J., "Guidance Techniques for Interplanetary Travel," ARS Journal, Vol. 29 No. 12, Dec. 1959, pp. 931 – 940.

25. Safren, H.G., "Differential Correction Method of Interplanetary Navigation," Proceedings of the National Specialists Meeting on Guidance of Aerospace Vehicles, published by IAS, N.Y., 1960, pp. 184 - 190.

26. Haake, H.B. and Welch, J.D., "A Self-Contained Interplanetary Navigator," IRE Transactions on Aerospace and Navigational Electronics, Vol. ANE-8 No. 1, March 1961, pp. 28 – 41.

27. Dunn, J.C. and Giannetto, C., "Lunar Trajectory Perturbations Analysis – Some Computational Results via the Adjoint Method," ARS Preprint 2072 – 61, Oct. 1961.

28. Smart, W.M., Celestial Mechanics, Longmans, Green and Co. Inc., New York, 1953.

29. Plummer, H.C., An Introductory Treatise on Dynamical Astronomy, Dover Publications, Inc., New York, 1960. (Originally published by Cambridge University Press, 1918).

30. Ehricke, K.A., Space Flight, Volume I, Environment and Celestial Mechanics, D. Van Nostrand Company, Inc., Princeton, N.J., 1960.

REFERENCES (Cont.)

31. Ehricke, K. A., Space Flight, Volume II, Dynamics, D. Van Nostrand Company, Inc., Princeton, N.J., 1962.

32. Mauldin, M., Jr. and Millard, R. G., "Optimization of Interplanetary Mid-Course Velocity Corrections," M.I.T. Master of Science Thesis T-299, May 1962.

33. Carr, R.E. and Hudson, R.H., "Tracking and Orbit Determination Program of the Jet Propulsion Laboratory," JPL Technical Report No. 32-7, Feb. 1960.

34. Zim, H.S. and Baker, R.H., Stars, Golden Press, Inc., New York, 1956.

35. Baker, R.H., Astronomy, Seventh Edition, D. Van Nostrand Company, Inc., Princeton, N.J., 1959.

36. The American Ephemeris and Nautical Almanac for the Year 1962, U.S. Government Printing Office, Washington, 1960.

37. Larmore, L., "Celestial Observations for Space Navigation," Aero/Space Engineering, Vol. 18 No. 1, Jan. 1959, pp. 37 – 42.

38. Victor, W.K., Stevens, R., and Golomb, S.W., "Radar Exploration of Venus: Goldstone Observatory Report for March – May 1961," JPL Technical Report No. 32 – 132, Aug. 1961.

39. Corben, H.C., "Time Dilatation Effects in Space Travel," Chapter 11 of Space Technology, H.S. Seifert editor, John Wiley and Sons, Inc., N.Y., 1959.

40. Holdridge, D.B., "Space Trajectories Program for the IBM 7090 Computer," JPL Technical Report No. 32 – 223, Revision No. 1, Sept. 1962.

41. Hildebrand, F.B., Advanced Calculus for Engineers, Prentice-Hall, Inc., Englewood Cliffs, N.J., 1949

42. Weyl, H., The Classical Groups, Their Invariants and Representations, Princeton University Press, Princeton, N.J., 1946.

43. Shapiro, I.I., The Prediction of Ballistic Missile Trajectories from Radar Observations, McGraw-Hill Book Company, Inc., N.Y., 1957.

44. Cramér, H., Mathematical Methods of Statistics, Princeton University Press, N.J., 1946.

45. Burington, R.S. and May, D.C., Handbook of Probability and Statistics with Tables, Handbook Publishers, Inc., Sandusky, Ohio, 1953.

46. Locke, A.S. and collaborators from the Naval Research Laboratory, Guidance, D. Van Nostrand Company, Inc., Princeton, N.J., 1955.

In 1956 he left Curtiss-Wright to become a full-time graduate student at M.I.T. For the academic year 1957 – 1958 he held a Sperry Gyroscope Company fellowship at M.I.T. For the academic years since 1958 he has been a research assistant at the M.I.T. Instrumentation Laboratory.

During the summer of 1957 Mr. Stern returned to Curtiss-Wright as a research specialist. He was employed in a similar capacity by the Autonetics Division of North American Aviation, Inc. during the summer of 1959. He has also served briefly as a consultant to Curtiss-Wright in a patent infringement lawsuit involving flight simulator patents.

Mr. Stern is a member of Tau Beta Pi, Sigma Xi, Sigma Gamma Tau, and Phi Eta Sigma. His professional affiliations include the American Association for the Advancement of Science, the American Institute of Aeronautics and Astronautics, and the Institute of Electrical and Electronic Engineers.

VOLUME II – APPENDICES

INTERPLANETARY MIDCOURSE GUIDANCE ANALYSIS

by

ROBERT GOTTLIEB STERN

B.S., Lehigh University, 1941
M.S., Stevens Institute of Technology, 1950

SUBMITTED IN PARTIAL FULFILLMENT
OF THE REQUIREMENTS FOR THE
DEGREE OF DOCTOR OF SCIENCE

at the

MASSACHUSETTS INSTITUTE OF TECHNOLOGY

TABLE OF CONTENTS
VOLUME I

TABLE OF CONTENTS (Cont.)
VOLUME I

TABLE OF CONTENTS (Cont.)
VOLUME I

TABLE OF CONTENTS (Cont.)
VOLUME I

LIST OF ILLUSTRATIONS
VOLUME I

LIST OF ILLUSTRATIONS (Cont.)

VOLUME I

LIST OF TABLES
VOLUME I

TABLE OF CONTENTS
VOLUME II

TABLE OF CONTENTS (Cont.)

VOLUME II

TABLE OF CONTENTS (Cont.
VOLUME II

TABLE OF CONTENTS (Cont.)
VOLUME II

TABLE OF CONTENTS (Cont.)
VOLUME II

Appendix

TABLE OF CONTENTS (Cont.)
VOLUME II

Appendix

LIST OF ILLUSTRATIONS
VOLUME II

LIST OF ILLUSTRATIONS (Cont.)

VOLUME II

LIST OF TABLES
VOLUME II

APPENDIX A
COORDINATE SYSTEMS

A.1 Summary

Judicious choice of a coordinate system is of primary importance in the analysis of two-body motion. Three basic systems, each related to the space vehicle's nominal, or reference, trajectory, are defined in this appendix. The designations of the three basic systems are:

1. Reference trajectory stationary coordinate system
2. Reference trajectory local vertical coordinate system
3. Reference trajectory flight path coordinate system

The orientation of these three systems is specified with respect to the conventional heliocentric ecliptic coordinate system, which is also defined.

A.2 Heliocentric Ecliptic Coordinate System

The heliocentric ecliptic axis system is one of the standard systems in celestial mechanics. Its origin is at the center of the sun. Its axes are designated x_E, y_E, and z_E. The x_E and y_E axes are in the ecliptic plane. The x_E - axis lies along the intersection of the equatorial plane with the ecliptic plane, with the positive direction being the direction of the sun from the earth at the time of the vernal equinox (or the direction of the earth from the sun at the time of the autumnal equinox). The positive y_E - axis is obtained by rotating the positive x_E - axis 90^o in the direction of the earth's rotation about the sun. The z_E - axis is normal to the ecliptic plane and positive in the direction of the angular momentum vector of the earth's motion with respect to the sun.

A.3 Reference Trajectory Stationary Coordinate System

The reference trajectory stationary coordinate system, with axes x, y, and z, is related to the nominal two-body path of the space vehicle in the sun's gravitational field. The origin is at the center of the sun. The x-y plane is the plane containing the vehicle's reference trajectory. The positive x-axis is in the direction of perihelion from the sun. The y-axis lies along the latus rectum; its positive direction is obtained by rotating the positive x-axis 90° in the direction of the motion of the vehicle around the sun. The positive z-axis is in the direction of the angular momentum vector of the vehicle's motion relative to the sun.

The x, y, z axes may be located with respect to the x_E, y_E, z_E axes by means of the three Euler angles Ω_E, i_E, and ω_E. Ω_E is the longitude of the ascending node. It is the angle, measured in the x_E-y_E plane, between the x_E-axis and the positive half of the line of nodes. The line of nodes is the line of intersection between the ecliptic plane and the reference trajectory plane. The ascending node, which lies on the positive half of the line of nodes, is the point at which the vehicle passes through the ecliptic plane in the direction of increasing z_E.

i_E is the inclination angle. It is the angle subtended at the line of nodes between the reference trajectory plane and the ecliptic plane. It is also the angle between the z-axis and the z_E-axis. The range of i_E is 0° to 180°.

ω_E is the latitude of perihelion. It is the angle, measured in the reference trajectory plane, between the positive half of the line of nodes and the positive x-axis.

The sum of Ω_E and ω_E is known as the longitude of perihelion and is designated ϕ_E. ϕ_E is sometimes referred to as a "broken" angle because its two constituent parts lie in different planes. ϕ_E may be substituted for either Ω_E or ω_E in locating the x, y, z axes.

The angles Ω_E, i_E, and ω_E are illustrated in Fig. A.1.

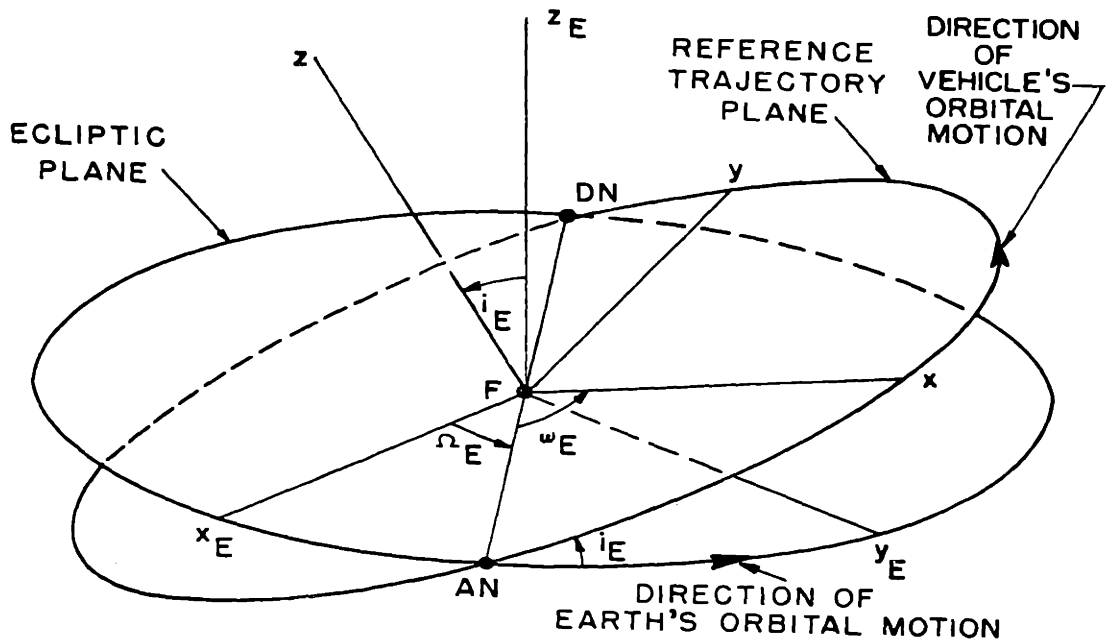

F — origin at center of sun
AN — ascending node
DN — descending node
x_E, y_E, z_E — ecliptic system coordinate axes
x,y,z — reference trajectory stationary system coordinate axes
Ω_E — longitude of ascending node
i_E — inclination of reference trajectory plane
ω_E — latitude of perihelion of reference trajectory

Figure A.1 Euler Angles Ω_E, i_E, ω_E

A.4 Reference Trajectory Local Vertical Coordinate System

The reference trajectory local vertical coordinate system, with axes r, s, and z, has its origin at the center of the sun, and its positive z direction lies along the angular momentum vector of the vehicle's motion with respect to the sun. In these two respects it is the same as the reference trajectory stationary system. Also, the r-s plane coincides with the x-y plane. The two systems differ in that the r and s axes rotate in the reference trajectory plane, with the positive direction of the r-axis at any given time lying in the direction of the nominal position of the vehicle at that time. The positive s-axis is 90^{o} "ahead" (i.e., rotated in the direction of vehicle motion) of the positive r-axis.

The angle between the r-axis and the x-axis at any instant is the true anomaly f. Thus, the local vertical system is rotating about the z-axis with angular velocity $\dot{f}$.

The positive r direction will be referred to as the radial direction; similarly, the positive s direction is the transverse direction, and the positive z direction is the orthogonal direction. The r direction is the direction of the vehicle's local vertical in the sun's gravitational field.

Because of the way in which the axes are defined, the values of s and z on a two-body reference trajectory are identically zero for all values of time.

A.5 Reference Trajectory Flight Path Coordinate System

The axes of the reference trajectory flight path coordinate system are designated p, q, and z. Like the previous two reference trajectory systems, this system has its origin at the center of the sun and its positive z-axis in the direction of the angular momentum vector of the vehicle's motion about the sun. The p-q plane is the reference trajectory plane. The positive q-axis is parallel to the relative velocity vector of the vehicle's nominal motion with respect to the sun. The positive p-axis is 90^{o} "behind" (i.e., rotated in the direction opposite to the vehicle's motion about the sun). the positive q-axis.

The angle between the s-axis and the q-axis is γ, the flight path angle. The angle is positive when the positive q-axis lies between the positive directions of the r and s axes. Since the s-axis represents the "horizontal" direction in the reference trajectory plane, γ is the inclination of the flight path to the horizontal.

The angle between the p-axis and the x-axis is g; it is equal to the difference between f and γ. The angular velocity of the p, q, z coordinate system about the z-axis is $\dot{g}$; which is equal to $(\dot{f} - \dot{\gamma})$.

The orientations of the axes of the three reference trajectory coordinate systems in the reference trajectory plane are shown in Fig. A. 2.

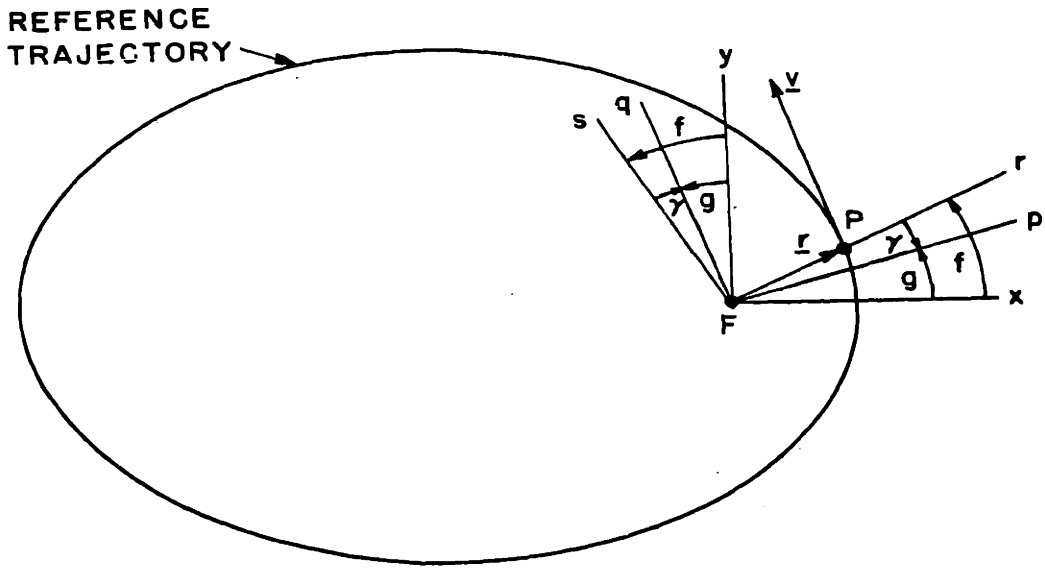

Fq is parallel to $\underline{v}$.
F – attractive focus (center of sun)
P – vehicle position on reference trajectory
$\underline{r}$ – position vector
$\underline{v}$ – velocity vector
x,y – stationary system coordinate axes
r,s – local vertical system coordinate axes
p,q – flight path system coordinate axes
$f = \sphericalangle xFr = \sphericalangle yFs$ = true anomaly
$\gamma = \sphericalangle rFp = \sphericalangle sFq$ = flight path angle
$g = \sphericalangle xFp = \sphericalangle yFq = f - \gamma$

Figure A.2 Orientations of Reference Trajectory Coordinate Systems

APPENDIX B
CELESTIAL MECHANICS

B.1 Summary

Some of the more important relations in celestial mechanics are stated, with particular emphasis on those applicable to elliptical orbits. These relations form the foundation on which much of the subsequent analysis is based. Since all of this material is well known, no attempt is made to supply formal proofs of the equations presented. Such proofs may be found in any standard textbook on this subject, for example, in Chapters 1 and 2 of Smart[28].

B.2 Motion of a Small Mass in a Many-Body Gravitational Field

Figure B.1 shows the relative positions of three bodies, P_0, P, and P_1. The motion of P is to be investigated under the assumption that the only forces acting on P are those due to the gravitational effects of P_0 and P_1.

For a space vehicle on an interplanetary voyage, P_0 represents the sun, P represents the vehicle, and P_1 normally represents one of the planets.

The vector form of the equation of motion of P is

$$\ddot{\underline{r}} + \frac{\mu}{r^3}\,\underline{r} = -G m_1 \left(\frac{1}{d_1^3}\,\underline{d}_1 + \frac{1}{r_1^3}\,\underline{r}_1\right) \qquad \text{(B-1)}$$

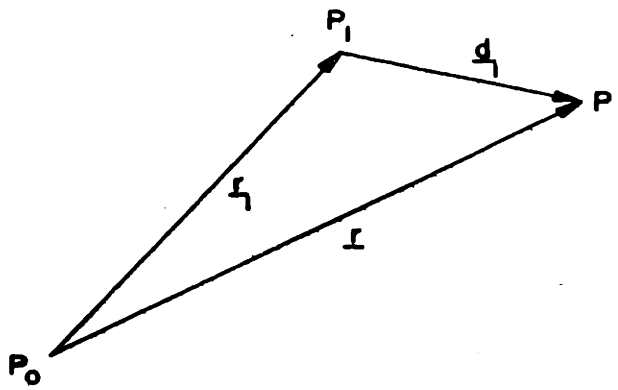

P, P_o, P_1 — three bodies treated as hypothetical point-masses

P — body whose motion is being investigated

P_o, P_1 — bodies whose masses affect the motion of P

$\underline{r}, \underline{r}_1, \underline{d}_1$ — position vectors

Figure B.1 Vector Diagram for the Three-Body Problem

The vectors $\underline{r}$, $\underline{r}_1$, and $\underline{d}_1$ are the position vectors of Fig. B.1, with r, r_1, and d_1 being their respective magnitudes. $\ddot{\underline{r}}$ is the inertial acceleration vector of P with respect to P_0.

The masses of P_0, P, and P_1 are m_0, m, and m_1, respectively. The quantity μ is defined by

$$\mu = G (m_0 + m) \tag{B-2}$$

where G is the constant of gravitation.

Since m_0 is the mass of the sun and m_1 is the mass of a planet, which is very much smaller, the motion of P is due primarily to P_0, with P_1 exerting a relatively minor effect (unless the magnitude of $\underline{r}$ is much greater than that of $\underline{d}_1$). In astronomical parlance, the force exerted by P_1 on P is known as the "disturbing force", and the effect of P_1 on the motion of P is known as a "perturbation".

In general, there may be many disturbing forces, due to planets P_1, P_2, ·····, P_n. The vector equation of motion when there are n disturbing forces is

$$\ddot{\underline{r}} + \frac{\mu}{r^3}\,\underline{r} = -G \sum_{i=1}^{n} m_i \left(\frac{1}{d_i^3}\,\underline{d}_i + \frac{1}{r_i^3}\,\underline{r}_i\right) \tag{B-3}$$

B.3 Equations of Motion in Reference Trajectory Coordinate Systems

The vector Eq. (B-3) is a compact form for three component equations, which can be written in any convenient coordinate system. In this section the component equations will be written in the three reference trajectory coordinate systems described in Appendix A.

In the x y z system,

$$\underline{r} = x\,\underline{u}_x + y\,\underline{u}_y + z\,\underline{u}_z \tag{B-4}$$

$$\underline{v} = \dot{\underline{r}} = \dot{x}\,\underline{u}_x + \dot{y}\,\underline{u}_y + \dot{z}\,\underline{u}_z \tag{B-5}$$

$$\underline{a} = \ddot{\underline{r}} = \ddot{x}\,\underline{u}_x + \ddot{y}\,\underline{u}_y + \ddot{z}\,\underline{u}_z \tag{B-6}$$

The symbol $\underline{u}$ represents a unit vector, with the appended subscript indicating its direction. $\underline{v}$ and $\underline{a}$ are, respectively, the inertial velocity and the inertial acceleration of the body P.

$$r^2 = x^2 + y^2 + z^2 \tag{B-7}$$

$$d_i^2 = (x - x_i)^2 + (y - y_i)^2 + (z - z_i)^2 \tag{B-8}$$

$$r_i^2 = x_i^2 + y_i^2 + z_i^2 \tag{B-9}$$

The three component equations of motion may be written in matrix form as follows:

$$\begin{pmatrix} \ddot{x} \\ \ddot{y} \\ \ddot{z} \end{pmatrix} + \frac{\mu}{r^3} \begin{pmatrix} x \\ y \\ z \end{pmatrix} = -G \sum_{i=1}^{n} m_i \left[\frac{1}{d_i^3} \begin{pmatrix} x - x_i \\ y - y_i \\ z - z_i \end{pmatrix} + \frac{1}{r_i^3} \begin{pmatrix} x_i \\ y_i \\ z_i \end{pmatrix} \right] \tag{B-10}$$

In the r s z coordinate system, the projection of the vector $\underline{r}$ in the r-s plane is designated ρ. The r-axis lies along the projection of $\underline{r}$ in the r-s plane. The coordinate system rotates about the z-axis with angular velocity $\dot{f}$.

$$\underline{r} = \rho\, \underline{u}_r + z\, \underline{u}_z \tag{B-11}$$

$$\underline{v} = \dot{\rho}\, \underline{u}_r + \rho\, \dot{f}\, \underline{u}_s + \dot{z}\, \underline{u}_z \tag{B-12}$$

$$\underline{a} = (\ddot{\rho} - \rho\, \dot{f}^2)\, \underline{u}_r + (\rho\, \ddot{f} + 2\dot{\rho}\, \dot{f})\, \underline{u}_s + \ddot{z}\, \underline{u}_z \tag{B-13}$$

$$r^2 = \rho^2 + z^2 \tag{B-14}$$

$$d_i^2 = (\rho - \rho_i)^2 + s_i^2 + (z - z_i)^2 \tag{B-15}$$

$$r_i^2 = \rho_i^2 + s_i^2 + z_i^2 \tag{B-16}$$

The component equations are

$$\begin{pmatrix} \ddot{\rho} - \rho \dot{f}^2 \\ \rho \ddot{f} + 2\dot{\rho}\, \dot{f} \\ \ddot{z} \end{pmatrix} + \frac{\mu}{r^3} \begin{pmatrix} \rho \\ 0 \\ z \end{pmatrix} = - G \sum_{i=1}^{n} m_i \left[\frac{1}{d_i^3} \begin{pmatrix} \rho - \rho_i \\ - s_i \\ z - z_i \end{pmatrix} + \frac{1}{r_i^3} \begin{pmatrix} \rho_i \\ s_i \\ z_i \end{pmatrix} \right] \tag{B-17}$$

The p q z coordinate system rotates about the z-axis with angular velocity $\dot{g}$. The q-axis is parallel to the projection of $\underline{v}$ in the p-q plane.

$$\underline{r} = p\,\underline{u}_p + q\,\underline{u}_q + z\,\underline{u}_z \tag{B-18}$$

$$\underline{v} = (\dot{p} - q\,\dot{g})\,\underline{u}_p + (\dot{q} + p\,\dot{g})\,\underline{u}_q + \dot{z}\,\underline{u}_z \tag{B-19}$$

$$= v_q\,\underline{u}_q + \dot{z}\,\underline{u}_z \tag{B-20}$$

The angular velocity $\dot{g}$ may be expressed in terms of $\dot{p}$ and q by equating coefficients of $\underline{u}_p$ in (B-19) and (B-20).

$$\dot{p} - q\,\dot{g} = 0 \tag{B-21}$$

$$\dot{g} = \frac{\dot{p}}{q} \tag{B-22}$$

The acceleration $\underline{a}$ is given by

$$\underline{a} = -\,\dot{g}\,v_q\,\underline{u}_p + \dot{v}_q\,\underline{u}_q + \ddot{z}\,\underline{u}_z \tag{B-23}$$

$$= -\,\frac{\dot{p}\,(p\,\dot{p} + q\,\dot{q})}{q^2}\,\underline{u}_p$$

$$+ \left[\,\frac{p\,\ddot{p} + q\,\ddot{q}}{q} + \frac{\dot{p}\,(\dot{p}\,q - \dot{q}\,p)}{q^2}\,\right]\underline{u}_q + \ddot{z}\,\underline{u}_z \tag{B-24}$$

The distance equations are

$$r^2 = p^2 + q^2 + z^2 \tag{B-25}$$

$$d_i^2 = (p - p_i)^2 + (q - q_i)^2 + (z - z_i)^2 \tag{B-26}$$

$$r_i^2 = p_i^2 + q_i^2 + z_i^2 \tag{B-27}$$

The equations of motion in the p q z system are

$$\begin{pmatrix} \dfrac{-\ddot{p}\,(p\,\dot{p} + q\,\dot{q})}{q^2} \\ \dfrac{p\,\ddot{p} + q\,\ddot{q}}{q} + \dfrac{\dot{p}\,(\dot{p}\,q - \dot{q}\,p)}{q^2} \\ \ddot{z} \end{pmatrix} + \frac{\mu}{r^3} \begin{pmatrix} p \\ q \\ z \end{pmatrix}$$

$$= -G \sum_{i=1}^{n} m_i \left[\frac{1}{d_i^3} \begin{pmatrix} p - p_i \\ q - q_i \\ z - z_i \end{pmatrix} + \frac{1}{r_i^3} \begin{pmatrix} p_i \\ q_i \\ z_i \end{pmatrix} \right] \tag{B-28}$$

B.4 Two-Body Motion

When there are no disturbing forces, the motion of P is the classic two-body motion, and the vector equation reduces to

$$\ddot{\underline{r}} + \frac{\mu}{r^3}\ \underline{r} = \underline{0}_3 \qquad \text{(B-29)}$$

The acceleration vector and the position vector are now collinear. Therefore, the motion of P must lie wholly within the plane determined by the position vector and the velocity vector existing at any specified time.

The component equations of motion in the x y z coordinate system are

$$\begin{pmatrix} \ddot{x} \\ \ddot{y} \\ \ddot{z} \end{pmatrix} + \frac{\mu}{r^3} \begin{pmatrix} x \\ y \\ z \end{pmatrix} = \begin{pmatrix} 0 \\ 0 \\ 0 \end{pmatrix} \qquad \text{(B-30)}$$

If the axes are so chosen that z is perpendicular to the plane of the two-body motion, z is always zero, and the motion of P is completely described by the first two equations of (B-30). The distance r is then given by

$$r^2 = x^2 + y^2 \qquad \text{(B-31)}$$

In the r s z coordinate system, ρ becomes equal to r for two-body motion. The equations of motion in the trajectory plane are

$$\begin{pmatrix} \ddot{r} - r\dot{f}^2 \\ r\ddot{f} + 2\dot{r}\dot{f} \end{pmatrix} + \frac{\mu}{r^3} \begin{pmatrix} r \\ 0 \end{pmatrix} = \begin{pmatrix} 0 \\ 0 \end{pmatrix} \qquad \text{(B-32)}$$

When the p q z coordinate system is used to describe the two-body motion,

$$r^2 = p^2 + q^2 \qquad \text{(B-33)}$$

The equations of motion in the trajectory plane are

$$\begin{pmatrix} \frac{-\dot{p}(p\dot{p} + q\dot{q})}{q^2} \\ \frac{p\ddot{p} + q\ddot{q}}{q} + \frac{\dot{p}(\dot{p}q - \dot{q}p)}{q^2} \end{pmatrix} + \frac{\mu}{r^3} \begin{pmatrix} p \\ q \end{pmatrix} = \begin{pmatrix} 0 \\ 0 \end{pmatrix} \qquad \text{(B-34)}$$

B. 5 Integration of Equations of Two-Body Motion

The integration of the equations of two-body motion is most easily accomplished by using (B-32). The lower equation of (B-32) may be integrated directly, with the result

$$r^2 \dot{f} = h \qquad \text{(B-35)}$$

where h, a constant, is the angular momentum of P per unit mass.

To integrate the upper equation of (B-32), f is substituted for t as the independent variable, and the dependent variable r is replaced by u, where

$$u = \frac{1}{r} \tag{B-36}$$

In terms of u and f, the upper equation of (B-32) becomes

$$\frac{d^2 u}{d f^2} + u = \frac{\mu}{h^2} \tag{B-37}$$

The solution for r is

$$r = \frac{\frac{h^2}{\mu}}{1 + e \cos (f - \omega)} \tag{B-38}$$

where e and ω are constants of integration.

Equation (B-38) is the polar-coordinate form of the equation of a general conic section, with the origin at one focus. The constant e is the eccentricity of the conic. ω is the angle between the arbitrarily chosen x-axis in the x-y plane and the major axis of the conic. If new x and y axes are defined such that the new x-axis coincides with the major axis of the conic, then the angle between the new axes and the old axes is ω, and $(f - \omega)$ may be replaced by f in (B-38). The new angle f, measured from the new x-axis, is the true anomaly.

B.6 Orbital Elements

The component equations of (B-30), the general equations of motion of the two-body problem, are three second-order linear differential equations, and consequently their complete solution involves

six arbitrary constants. The six constants may be the three components of position and the three components of velocity occurring at a specified time, or they may be three components of position at each of two specified times. There are many other groupings of six constants that may be used.

A grouping that is widely used in celestial mechanics is one known as the six orbital elements. These elements are:

1. a, The semi-major axis of the conic section
2. e, The eccentricity of the conic section
3. Ω, The longitude of the ascending node
4. i, The inclination of the trajectory plane
5. ω, The latitude of perihelion
6. t_0, The time of perihelion passage

The elements a and e determine the size and shape, respectively, of the conic section.

The angles Ω and i determine the orientation of the trajectory plane, and angle ω locates the axes of the conic section in the trajectory plane. If the standard coordinate system to which the three angles are referred is the heliocentric ecliptic system, the three become Ω_E, i_E, and ω_E, which are defined in Section A. 3 and illustrated in Fig. A. 1.

The element t_0 relates position on the trajectory to some arbitrarily chosen time reference, known as the epoch; t_0 is the time, relative to the epoch, at which the vehicle passes through the perihelion point.

Choices other than these given above may be made for the orbital elements. Obviously, any choice of a new element may be expressed as a combination of those elements already listed.

By convention, the range of e is limited to zero to infinity, while a may take on any value from minus infinity to plus infinity. The basic form of a particular conic section is determined by the values of

e and a associated with it. There are three basic forms, hyperbolas, parabolas, and ellipses. If e is greater than one and a is negative, the trajectory is hyperbolic; if e equals one and a is infinite, the trajectory is parabolic; if e is less than one and a is positive, the trajectory is elliptical.

In the present analysis, which is intended to be applicable primarily to the midcourse phase of interplanetary voyages, only elliptical forms are considered in detail.

B. 7 Geometric Properties of the Ellipse

The polar form of the equation of a conic section, with the origin at one focus, is

$$r = \frac{\ell}{1 + e \cos f} \tag{B-39}$$

where the constant ℓ is the semi-latus rectum. ℓ is the value of r corresponding to

$$f = \pm \frac{\pi}{2}$$

In terms of a and e,

$$\ell = a (1 - e^2) \tag{B-40}$$

When the conic section is an ellipse, its equation in rectangular coordinates, with origin at one focus, is

$$\frac{(x + c)^2}{a^2} + \frac{y^2}{b^2} = 1 \tag{B-41}$$

b is the semi-minor axis of the ellipse.

$$b = a\,(1 - e^2)^{1/2} \tag{B-42}$$

The linear eccentricity c is defined by

$$c = a\,e \tag{B-43}$$

c is the distance along the major axis from the center of the ellipse to either focus. The lengths a, b, and c are related by the equation

$$a^2 = b^2 + c^2 \tag{B-44}$$

The sum of the distances of any point on the ellipse from each of the two foci is equal to 2 a.

The quantities introduced in this section are shown in Fig. B. 2.

B. 8 The Anomalies

The true anomaly has been introduced in Section B. 5. Two other anomalies that are widely used in celestial mechanics are the eccentric anomaly E and the mean anomaly M.

The geometric construction required to obtain the eccentric anomaly is indicated in Fig. B. 3. The eccentric anomaly is related to the circle of radius a circumscribed about the ellipse whose semi-major axis is a.

The mean anomaly varies linearly with elapsed time t.

$$M = n\,(t - t_0) \tag{B-45}$$

where n is a constant known as the mean angular motion. n is the average angular velocity of the space vehicle in its elliptical orbit

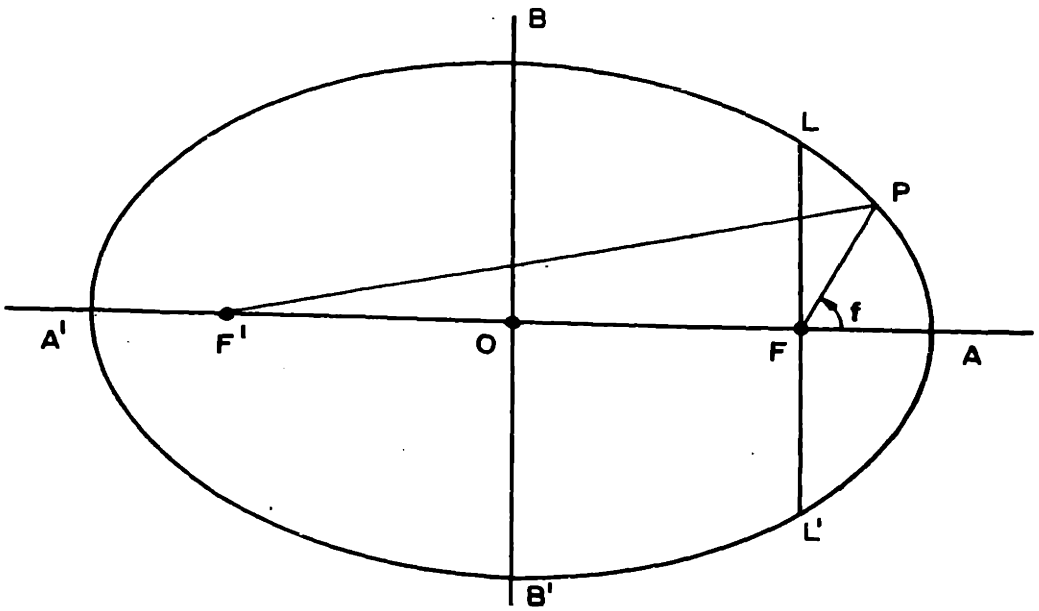

O – center of ellipse

F,F' – foci of ellipse

A'OA – major axis

BOB' – minor axis

LFL' – latus rectum

P – arbitrary point on ellipse

OA = OA' = a = semi-major axis

OB = OB' = b = semi-minor axis

FL = FL' = ℓ = semi-latus rectum

OF = OF' = c = linear eccentricity

$\sphericalangle$ AFP = f = true anomaly

F'P + PF = 2 a

Figure B.2 The Ellipse

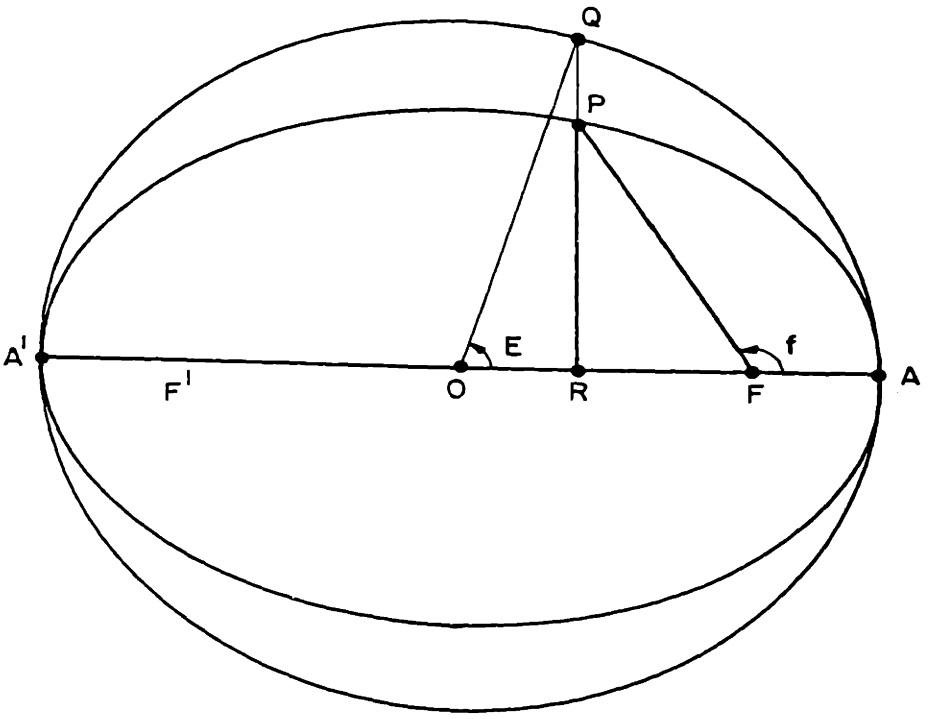

APA' – elliptical arc with semi-major axis a

AQA' – circular arc of radius a

O – center of ellipse and of circle

F,F' – foci of ellipse

P – arbitrary point on ellipse

QPR $\perp$ A'A

$\sphericalangle$AFP = f = true anomaly

$\sphericalangle$AOQ = E = eccentric anomaly

Figure B.3 Graphical Construction of Eccentric Anomaly

about the sun.

$$n = \frac{2\pi}{P} \tag{B-46}$$

where P is the period of the trajectory.

The constant t_0 in Eq. (B-45) is the time of perihelion passage, the sixth orbital element of Section B.5.

An alternate form for Eq. (B-45) is

$$M = n\,t + M_0 \tag{B-47}$$

where $M_0 = -\,n\,t_0$ (B-48)

M_0 is the value of the mean anomaly at time t = 0. M_0 is sometimes used in place of t_0 as one of the orbital elements.

The true anomaly and the eccentric anomaly are related by the following series of equations:

$$r = \frac{a\,(1 - e^2)}{1 + e\cos f} = a\,(1 - e\cos E) \tag{B-49}$$

$$x = r\cos f = a\,(\cos E - e) \tag{B-50}$$

$$y = r\sin f = a\,(1 - e^2)^{1/2}\sin E \tag{B-51}$$

$$(1 + e\cos f)\,(1 - e\cos E) = 1 - e^2 \tag{B-52}$$

$$\sin f = \frac{(1 - e^2)^{1/2}\sin E}{1 - e\cos E} \qquad \sin E = \frac{(1 - e^2)^{1/2}\sin f}{1 + e\cos f} \tag{B-53}$$

$$\cos f = \frac{\cos E - e}{1 - e\cos E} \qquad \cos E = \frac{\cos f + e}{1 + e\cos f} \tag{B-54}$$

The eccentric anomaly and the mean anomaly are related through Kepler's equation.

$$M = E - e \sin E \tag{B-55}$$

The eccentric anomaly serves as a bridge relating the geometric variable f to the dynamic variable M (or t).

B.9 Dynamic Relations for Elliptical Trajectories

The derivatives of the three anomalies are

$$\dot{M} = n \tag{B-56}$$

$$\dot{E} = \frac{n}{1 - e \cos E} = \frac{n (1 + e \cos f)}{1 - e^2} \tag{B-57}$$

$$\dot{f} = \frac{n (1 - e^2)^{1/2}}{(1 - e \cos E)^2} = \frac{n (1 + e \cos f)^2}{(1 - e^2)^{3/2}} \tag{B-58}$$

It is interesting to note that $\dot{M}$ is equal to a constant, $r \dot{E}$ is equal to a constant, and $r^2 \dot{f}$ is equal to a constant.

$$r \dot{E} = n a \tag{B-59}$$

$$r^2 \dot{f} = h = n a^2 (1 - e^2)^{1/2} \tag{B-60}$$

A comparison of Eq. (B-38) with Eq. (B-39) indicates that

$$a\,(1 - e^2) = \frac{h^2}{\mu} \tag{B-61}$$

and therefore,

$$\mu = n^2\, a^3 \tag{B-62}$$

The differentials of E and f may each be expressed in terms of the other.

$$d\,E = \frac{(1 - e^2)^{1/2}\, d\,f}{1 + e \cos f} \tag{B-63}$$

$$d\,f = \frac{(1 - e^2)^{1/2}\, d\,E}{1 - e \cos E} \tag{B-64}$$

The velocity components in the radial and transverse directions may be written in a variety of ways.

$$v_r = \dot{r} = \frac{n\,a\,e \sin E}{1 - e \cos E} = \frac{n\,a\,e \sin f}{(1 - e^2)^{1/2}}$$

$$= \frac{n\,a^2\, e \sin E}{r} = \frac{\mu}{h}\, e \sin f \tag{B-65}$$

$$v_s = r\,\dot{f} = \frac{h}{r} = \frac{n\,a\,(1 - e^2)^{1/2}}{1 - e \cos E} = \frac{n\,a\,(1 + e \cos f)}{(1 - e^2)^{1/2}}$$

$$= \frac{\mu}{h} \cdot \frac{(1 - e^2)}{1 - e \cos E} = \frac{\mu}{h}\,(1 + e \cos f) \tag{B-66}$$

The square of the total orbital velocity is

$$v^2 = \frac{\mu^2}{h^2} (1 + 2 e \cos f + e^2)$$

$$= \mu \left(\frac{2}{r} - \frac{1}{a}\right) \qquad \text{(B-67)}$$

In the literature of celestial mechanics, Eq. (B-67) is known as the "vis viva integral".

The orbital velocity may be expressed in terms of either E or f.

$$v = \frac{\mu}{h} (1 + 2 e \cos f + e^2)^{1/2} \qquad \text{(B-68)}$$

$$= n a \frac{(1 + e \cos E)^{1/2}}{(1 - e \cos E)^{1/2}} \qquad \text{(B-69)}$$

The total energy per unit mass is the sum of the kinetic energy T and the potential energy U.

$$H = T + U = \frac{1}{2} v^2 - \frac{\mu}{r} = - \frac{\mu}{2 a} \qquad \text{(B-70)}$$

The total energy is a function of only one of the six orbital elements, the semi-major axis a.

The velocity components in the x and y directions can also be expressed in many forms.

$$v_x = \dot{x} = - v \sin g$$

$$= - \frac{n\, a \sin E}{1 - e \cos E} = - \frac{n\, a}{(1 - e^2)^{1/2}} \sin f$$

$$= - \frac{n\, a^2 \sin E}{r} = - \frac{\mu}{h} \sin f \qquad \text{(B-71)}$$

$$v_y = \dot{y} = v \cos g$$

$$= \frac{n\, a\, (1 - e^2)^{1/2} \cos E}{1 - e \cos E} = \frac{n\, a}{(1 - e^2)^{1/2}} (\cos f + e)$$

$$= \frac{h}{r} \cos E = \frac{\mu}{h} (\cos f + e) \qquad \text{(B-72)}$$

In the flight path coordinate system the velocity components are simply

$$v_p = 0 \qquad \text{(B-73)}$$

$$v_q = v \qquad \text{(B-74)}$$

The velocity component equations may be used to determine the simple trigonometric functions of γ and g.

$$\sin \gamma = \frac{v_r}{v} = \frac{e \sin E}{(1 - e^2 \cos^2 E)^{1/2}} = \frac{e \sin f}{(1 + 2\, e \cos f + e^2)^{1/2}} \qquad \text{(B-75)}$$

$$\cos \gamma = \frac{v_s}{v} = \frac{(1 - e^2)^{1/2}}{(1 - e^2 \cos^2 E)^{1/2}} = \frac{1 + e \cos f}{(1 + 2 e \cos f + e^2)^{1/2}} \quad \text{(B-76)}$$

$$\sin g = -\frac{v_x}{v} = \frac{\sin E}{(1 - e^2 \cos^2 E)^{1/2}} = \frac{\sin f}{(1 + 2 e \cos f + e^2)^{1/2}} \quad \text{(B-77)}$$

$$\cos g = \frac{v_y}{v} = \frac{(1 - e^2)^{1/2} \cos E}{(1 - e^2 \cos^2 E)^{1/2}} = \frac{\cos f + e}{(1 + 2 e \cos f + e^2)^{1/2}} \quad \text{(B-78)}$$

The angular velocities $\dot{\gamma}$ and $\dot{g}$ are

$$\dot{\gamma} = \frac{n (1 - e^2)^{1/2} e \cos E}{(1 - e \cos E)^2 (1 + e \cos E)} = \frac{n e (1 + e \cos f)^2 (\cos f + e)}{(1 - e^2)^{3/2} (1 + 2 e \cos f + e^2)}$$

(B-79)

$$\dot{g} = \frac{n (1 - e^2)^{1/2}}{(1 - e \cos E)^2 (1 + e \cos E)} = \frac{n (1 + e \cos f)^3}{(1 - e^2)^{3/2} (1 + 2 e \cos f + e^2)}$$

(B-80)

The position components in the flight path system may be expressed in the following ways:

$$p = r \cos \gamma = x \cos g + y \sin g = \frac{h}{v}$$

$$= \frac{a (1 - e^2)^{1/2} (1 - e \cos E)^{1/2}}{(1 + e \cos E)^{1/2}} = \frac{a (1 - e^2)}{(1 + 2 e \cos f + e^2)^{1/2}}$$

(B-81)

$$q = r \sin \gamma = - x \sin g + y \cos g = \frac{h}{v} \tan \gamma$$

$$= \frac{a\, e \sin E\, (1 - e \cos E)^{1/2}}{(1 + e \cos E)^{1/2}} = \frac{a\,(1 - e^2)\, e \sin f}{(1 + e \cos f)\,(1 + 2\, e \cos f + e^2)^{1/2}} \tag{B-82}$$

From (B-66) and (B-81), two alternate forms of the angular momentum equation are

$$h = r\, v_s = p\, v \tag{B-83}$$

The components of acceleration in the three coordinate systems may be obtained from (B-10), (B-17), and (B-28).

$$a_r = \ddot{r} - r\, \dot{f}^2 = - \frac{\mu}{r^2} \tag{B-84}$$

$$a_s = r\, \ddot{f} + 2\, \dot{r}\, \dot{f} = 0 \tag{B-85}$$

$$a_x = \ddot{x} = - \mu \frac{x}{r^3} \tag{B-86}$$

$$a_y = \ddot{y} = - \mu \frac{y}{r^3} \tag{B-87}$$

$$a_p = - \dot{g}\, v = - \frac{\dot{p}\,(p\, \dot{p} + q\, \dot{q})}{q^2} = - \mu \frac{p}{r^3} \tag{B-88}$$

$$a_q = \dot{v} = \frac{p\, \ddot{p} + q\, \ddot{q}}{q} + \frac{\dot{p}\,(\dot{p}\, q - \dot{q}\, p)}{q^2} = - \mu \frac{q}{r^3} \tag{B-89}$$

APPENDIX C
GRAPHICAL CONSTRUCTIONS

C.1 Summary

The review of the equations of celestial mechanics in Appendix B has led to the development of two interesting graphical constructions. The first is an approximate representation for the mean anomaly and when the eccentricity e is less the 0.5. The second is an exact method for determining velocity in an elliptical orbit. These constructions are thought to be novel and are presented here as a by-product of the primary analysis with the thought that they may be of value as class-room demonstrations.

C.2 Graphical Representation of Mean Anomaly

The conventional geometric interpretation of the true anomaly and the eccentric anomaly is given in Section B.8 and Fig. B.3. It would be desirable to get a similar representation of the mean anomaly, M, so that one could see graphically the relation between the angular motion and elapsed time. Unfortunately, no simple, exact geometrical construction is known for the mean anomaly. It is the purpose of this section to show a simple, though inexact, method of obtaining the mean anomaly graphically.

Figure C.1, which illustrates the method, is an extension of Fig. B.3. The construction is as follows:

1. From the focus F lay out FH parallel to OQ and meeting the circumscribed circle at H.
2. Connect the center O with point H by a straight line.

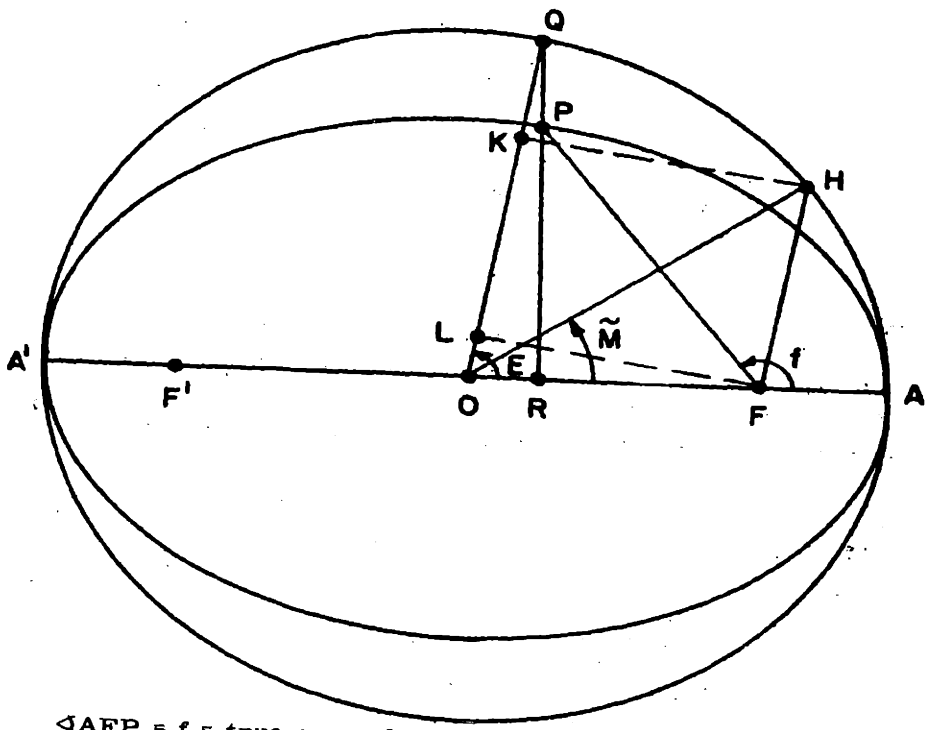

$\sphericalangle AFP = f$ = true anomaly

$\sphericalangle AOQ = E$ = eccentric anomaly

$FH \parallel OQ$

$FL \perp OQ$, $HK \perp OQ$, $FL \parallel HK$

$OF = c = ae$ = linear eccentricity

$HK = FL = ae \sin E$

$OA = OH = OQ = a$

$$\sphericalangle HOQ = \sin^{-1}\left(\frac{HK}{OH}\right) = \sin^{-1}(e \sin E)$$

$$\tilde{M} = \sphericalangle AOH = \sphericalangle AOQ - \sphericalangle HOQ = E - \sin^{-1}(e \sin E)$$

= approximation of mean anomaly

Figure C.1 Graphical Approximation of Mean Anomaly

Then angle AOH is equal to $\tilde{M}$, the approximation to the true anomaly.

In order to prove this statement, two auxiliary lines, FL and HK, are drawn. Both of these are perpendicular to OQ, and therefore, they are parallel to each other. From the figure,

$$HK = FL = OF \sin E = ae \sin E \tag{C-1}$$

$$\sphericalangle HOQ = \sin^{-1}\left(\frac{HK}{OH}\right) = \sin^{-1}\left(\frac{a e \sin E}{a}\right)$$

$$= \sin^{-1}(e \sin E) \tag{C-2}$$

$$\tilde{M} = \sphericalangle AOH = \sphericalangle AOQ - \sphericalangle HOQ$$

$$= E - \sin^{-1}(e \sin E) \tag{C-3}$$

The exact equation for the mean anaomaly is

$$M = E - e \sin E \tag{C-4}$$

The error in the approximation is

$$\Delta M = \tilde{M} - M = e \sin E - \sin^{-1}(e \sin E) \tag{C-5}$$

The maximum magnitude of the error for a given e occurs when

$$E = \pm \frac{\pi}{2}.$$

$$|\Delta M|_{max} = e - \sin^{-1} e \tag{C-6}$$

For eccentricities up to 0.4, $|\Delta M|_{max}$ is less than 1°. For $e = 0.5$, it is $1\frac{1}{3}°$.

It may be seen from Fig. C.1 that for

$$0 < f < \pi, \qquad M < E < f \tag{C-7}$$

for

$$\pi < f < 2\pi, \qquad f < E < M \tag{C-8}$$

for

$$f = 0, \qquad E = 0 = M \tag{C-9}$$

for

$$f = \pi, \qquad E = \pi = M \tag{C-10}$$

C.3 Graphical Solution for Crbital Velocity and Its Components

The objective in this section is to determine graphically the velocity at point P on an elliptical trajectory for which a, e, and n are known.

In Fig. C.2, the known trajectory is APBA'B'A. The steps in the graphical construction are the following:

1. With focus F as center and with radius a, describe a circle.
2. Extend the radius vector FP through P until it intersects the circle at R.
3. Draw a straight line connecting the center of the ellipse at O to R.

The length OR is proportional to the orbital velocity at P. The constant of proportionality is

$$\frac{(1 - e^2)^{1/2}}{n}.$$

To prove these statements, several additional lines are drawn. FR is extended through F until it meets the perpendicular dropped from O to the extension of FP. The two lines intersect at S. Then,

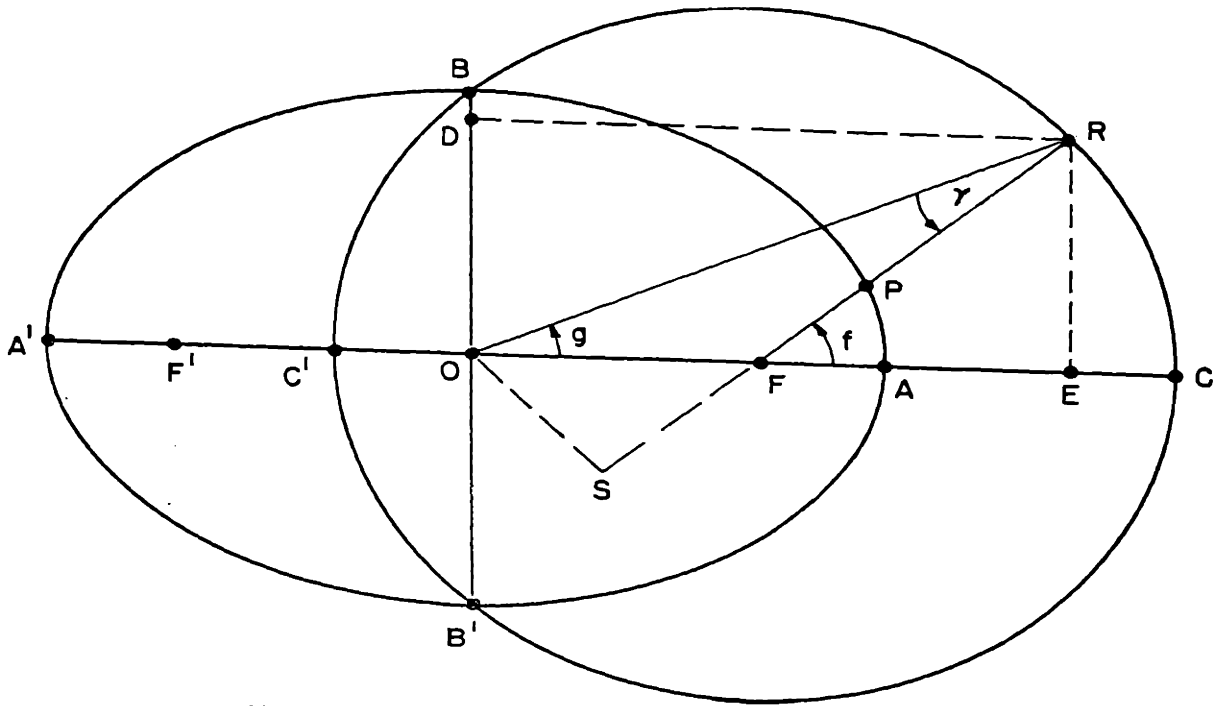

APBA'B'A – ellipse with center at O, foci at F and F', and semi-major axis a = OA

CRBC'B'C – circle with center at F and radius a

P – arbitrary point on ellipse

OS ⊥ SR

$$OR = \frac{(1 - e^2)^{1/2}}{n} v$$

$$OS = \frac{(1 - e^2)^{1/2}}{n} v_r \qquad SR = \frac{(1 - e^2)^{1/2}}{n} v_s$$

$$OD = -\frac{(1 - e^2)^{1/2}}{n} v_x \qquad OE = \frac{(1 - e^2)^{1/2}}{n} v_y$$

$\sphericalangle AFR = f$ = true anomaly

$\sphericalangle ORS = \gamma$ = flight path angle

$\sphericalangle ROA = f - \gamma = g$

Figure C.2 Graphical Determination of Orbital Velocity and Its Components

$$FR = a \tag{C-11}$$

$$OF = a\,e \tag{C-12}$$

$$\sphericalangle AFR = \sphericalangle OFS = f \tag{C-13}$$

In the triangle ORS,

$$SR = a\,(1 + e\cos f) \tag{C-14}$$

$$OS = a\,e\sin f \tag{C-15}$$

$$OR = a\,(1 + 2e\cos f + e^2)^{1/2} \tag{C-16}$$

When the last three equations are compared with Eqs. (B-66), (B-65), and (B-68), it is apparent that

$$SR = \frac{h\,a}{\mu}\,v_s = \frac{(1 - e^2)^{1/2}}{n}\,v_s \tag{C-17}$$

$$OS = \frac{(1 - e^2)^{1/2}}{n}\,v_r \tag{C-18}$$

$$OR = \frac{(1 - e^2)^{1/2}}{n}\,v \tag{C-19}$$

Also,

$$\sphericalangle ORS = \tan^{-1}\left(\frac{OS}{SR}\right) = \tan^{-1}\left(\frac{v_r}{v_s}\right) = \gamma \tag{C-20}$$

$$\sphericalangle AOR = f - \gamma = g \tag{C-21}$$

By constructing the lines RD and RE parallel, respectively, to the major and minor axes of the ellipse, it is easily seen that

$$OD = OR \sin g = \frac{(1 - e^2)^{1/2}}{n} v \sin g = -\frac{(1 - e^2)^{1/2}}{n} v_x \qquad (C\text{-}22)$$

$$OE = OR \cos g = \frac{(1 - e^2)^{1/2}}{n} v \cos g = \frac{(1 - e^2)^{1/2}}{n} v_y \qquad (C\text{-}23)$$

The angle between the positive p-axis of the flight path coordinate system and the positive x-axis is g. Therefore, OR in Fig. C. 2 has the direction of the p-axis associated with point P on the trajectory. Since the direction of the orbital velocity vector is along the positive q-axis, the direction of $\underline{v}$ may be obtained by rotating OR counter-clockwise through 90 degrees. Similarly, the directions of the velocity components may be found by rotating the corresponding lengths in the figure 90 degrees counter-clockwise.

The circle CRBC'B'C provides a simple means of visualizing the variation of the magnitude of the orbital velocity in an elliptical trajectory. As point P progresses on the ellipse, point R progresses on the circle, and OR is a continuous measure of v.

APPENDIX D
ELLIPTICAL CYLINDRICAL COORDINATES

D.1 Summary

Elliptical cylindrical coordinates are known to be particularly well suited to certain problems involving either ellipses or hyperbolas. Consequently, the applicability of this curvilinear coordinate system to the problem of guiding a vehicle traversing an elliptical trajectory has been investigated.

It is shown that there is an interesting relationship between the elliptical system and the flight path system described in Appendix A. The tangents to the three coordinate curves of the elliptical system are parallel, respectively, to the p, q, and z axes of the flight path system.

A comparison of the elliptical system with the reference trajectory rectilinear systems of Appendix A indicates that the curvilinear system has definite advantages for studying motion along a known, fixed elliptical trajectory. On the other hand, the curvilinear system offers no advantage in the study of the variation of an actual trajectory from a known elliptical reference trajectory. Since the guidance problem is primarily a problem of the latter type, the elliptical cylindrical system has not been used in the ensuing analysis.

D.2 Basic Coordinates in the Elliptical System

The analysis presented below is based on Sections 6.16 and 6.17 of Hildebrand[41]; with associated problems 6.25 and 6.26.

Elliptical cylindrical coordinates α, β, z are defined by the equations

$$x_0 = k \cosh \alpha \cos \beta \tag{D-1}$$

$$y = k \sinh \alpha \cos \beta \tag{D-2}$$

$$z = z \tag{D-3}$$

where k is a constant and x_0, y, z are conventional Cartesian coordinates. The reason for the use of x_0 instead of x is explained later in this section.

From (D-1) and (D-2),

$$\frac{x_0^2}{k^2 \cosh^2 \alpha} + \frac{y^2}{k^2 \sinh^2 \alpha} = \cos^2 \beta + \sin^2 \beta = 1 \tag{D-4}$$

If α is a constant, Eq. (D-4) is the equation of an ellipse with the origin at the center of the ellipse. The axes of the ellipse are given by

$$a^2 = k^2 \cosh^2 \alpha \tag{D-5}$$

$$b^2 = a^2 (1 - e^2) = k^2 \sinh^2 \alpha \tag{D-6}$$

k^2 may be determined by subtracting (D-6) from (D-5).

$$k^2 (\cosh^2 \alpha - \sinh^2 \alpha) = k^2 = a^2 e^2 \tag{D-7}$$

With the positive sign being chosen for the square root, k becomes equal to the linear eccentricity

$$k = ae \tag{D-8}$$

By substituting (D-8) into (D-5) and (D-6) and again taking the positive sign for each of the roots, cosh α and sinh α can be expressed in terms of e.

$$\cosh \alpha = \frac{1}{e} \tag{D-9}$$

$$\sinh \alpha = \frac{(1 - e^2)^{\frac{1}{2}}}{e} \tag{D-10}$$

Since the origin of the elliptical coordinate system is at the center of the ellipse rather than at one focus, the quantity x_0 in Eq. (D-1) is not the same as x in the Cartesian system of Appendix A. The equation relating x to x_0 is

$$x = x_0 - a e \tag{D-11}$$

The coordinates y and z in Eqs. (D-2) and (D-3) are the same as y and z in the Cartesian system of Appendix A.

Equations (D-8), (D-9), (D-10), and (D-11) may be incorporated into (D-1) and (D-2).

$$x = a (\cos \beta - e) \tag{D-12}$$

$$y = a (1 - e^2)^{\frac{1}{2}} \sin \beta \tag{D-13}$$

When Eqs. (D-12) and (D-13) are compared with Eqs. (B-50) and (B-51), it is apparent that the coordinate β is equal to the eccentric anomaly E.

Thus, the elliptical cylindrical coordinates α and β for an elliptical path are given by

$$\alpha = \tanh^{-1} (1 - e^2)^{\frac{1}{2}} \tag{D-14}$$

$$\beta = E \tag{D-15}$$

The advantage of this coordinate system lies in the fact that, of the three coordinates α, β, and z, only β is a variable when the path is an ellipse with axes in the directions of x and y.

D.3 Coordinate Curves and Tangent Vectors

The curve obtained by holding two of the three coordinates in a curvilinear system fixed and varying the third is called the coordinate curve of the third coordinate. A tangent vector is defined as a vector tangent to a coordinate curve at a given point and positive in the direction in which the value of the varying coordinate is increasing.

In this section, it will be shown that the tangent vectors of the elliptical cylindrical coordinate system are parallel to the axes of the flight path coordinate system.

The tangent vectors in the α, β, z system are designated $\underline{w}_\alpha$, $\underline{w}_\beta$, $\underline{w}_z$, respectively. The corresponding unit vectors are $\underline{u}_\alpha$, $\underline{u}_\beta$, and $\underline{u}_z$. Similarly, $\underline{u}_x$ and $\underline{u}_y$ are unit vectors in the x and y directions.

The radius vector $\underline{r}$ may be written as

$$\underline{r} = x\,\underline{u}_x + y\,\underline{u}_y + z\,\underline{u}_z \tag{D-16}$$

$$= ae\,(\cosh\alpha\cos\beta - 1)\,\underline{u}_x$$

$$+ ae \sinh\alpha \sin\beta\,\underline{u}_y + z\,\underline{u}_z \tag{D-17}$$

The three tangent vectors are

$$\underline{w}_\alpha = \frac{\partial \underline{r}}{\partial \alpha} = a e \sinh \alpha \cos \beta \, \underline{u}_x + a e \cosh \alpha \sin \beta \, \underline{u}_y$$

$$= a (1 - e^2)^{\frac{1}{2}} \cos E \, \underline{u}_x + a \sin E \, \underline{u}_y \qquad \text{(D-18)}$$

$$\underline{w}_\beta = \frac{\partial \underline{r}}{\partial \beta} = - a e \cosh \alpha \sin \beta \, \underline{u}_x + a e \sinh \alpha \cos \beta \, \underline{u}_y$$

$$= - a \sin E \, \underline{u}_x + a (1 - e^2)^{\frac{1}{2}} \cos E \, \underline{u}_y \qquad \text{(D-19)}$$

$$\underline{w}_z = \frac{\partial \underline{r}}{\partial z} = \underline{u}_z \qquad \text{(D-20)}$$

The magnitudes of the tangent vectors are

$$| \underline{w}_\alpha | = | \underline{w}_\beta | = [a^2 \sin^2 E + a^2 (1 - e^2) \cos^2 E]^{\frac{1}{2}}$$

$$= a (1 - e^2 \cos^2 E)^{\frac{1}{2}} \qquad \text{(D-21)}$$

$$| \underline{w}_z | = 1 \qquad \text{(D-22)}$$

The unit vectors are

$$\underline{u}_\alpha = \frac{(1 - e^2)^{\frac{1}{2}} \cos E}{(1 - e^2 \cos^2 E)^{\frac{1}{2}}} \underline{u}_x + \frac{\sin E}{(1 - e^2 \cos^2 E)^{\frac{1}{2}}} \underline{u}_y \qquad \text{(D-23)}$$

$$\underline{u}_\beta = -\frac{\sin E}{(1 - e^2\cos^2 E)^{\frac{1}{2}}}\,\underline{u}_x + \frac{(1 - e^2)^{\frac{1}{2}}\cos E}{(1 - e^2\cos^2 E)^{\frac{1}{2}}}\,\underline{u}_y \qquad \text{(D-24)}$$

$$\underline{u}_z = \underline{u}_z \qquad \text{(D-25)}$$

It may easily be verified that

$$\underline{u}_\alpha \cdot \underline{u}_\beta = \underline{u}_\alpha \cdot \underline{u}_z = \underline{u}_\beta \cdot \underline{u}_z = 0 \qquad \text{(D-26)}$$

and therefore the elliptical cylindrical coordinate system is an orthogonal system.

The orientation of the $\underline{u}_\alpha$ and $\underline{u}_\beta$ vectors with respect to the Cartesian axes x and y may be obtained by forming the dot products of $\underline{u}_\alpha$ with $\underline{u}_x$ and $\underline{u}_y$.

$$\cos(\alpha, x) = \underline{u}_\alpha \cdot \underline{u}_x = \frac{(1 - e^2)^{\frac{1}{2}}\cos E}{(1 - e^2\cos^2 E)^{\frac{1}{2}}} \qquad \text{(D-27)}$$

$$\cos(\alpha, y) = \sin(\alpha, x) = \underline{u}_\alpha \cdot \underline{u}_y = \frac{\sin E}{(1 - e^2\cos^2 E)^{\frac{1}{2}}} \qquad \text{(D-28)}$$

where (α, x) is the angle between $\underline{u}_\alpha$ and $\underline{u}_x$, and (α, y) is the angle between $\underline{u}_\alpha$ and $\underline{u}_y$.

Comparison of (D-27) and (D-28) with (B-78) and (B-77), respectively, indicates that the angle between $\underline{u}_\alpha$ and the x-axis is equal to g, the angle between the p-axis of the flight path system and the x-axis. Therefore, $\underline{u}_\alpha$ is parallel to the p-axis. Similarly, $\underline{u}_\beta$ is parallel to the q-axis, and $\underline{u}_z$ is parallel to the z-axis. Thus, it has been proved that the tangent vectors of the α, β, z system are parallel to the axes of the p, q, z system.

This result may be verified by the following deductive process. The β coordinate curve for an elliptical path is obtained by varying E with e and z held constant. This curve is the ellipse itself, and its tangent vector at any point is tangent to the ellipse at that point. The q-axis of the flight path system was chosen to be parallel to the instantaneous orbital velocity vector, and this vector is also tangent to the ellipse at any given point. Therefore, $\underline{u}_\beta$ must be parallel to the q-axis. Moreover, $\underline{u}_z$ is obviously parallel to the z-axis. Since $\underline{u}_\beta$ is parallel to the q-axis, and $\underline{u}_z$ is parallel to the z-axis, and both the elliptical cylindrical coordinate system and the flight path coordinate system are orthogonal systems, it follows that $\underline{u}_\alpha$ must be parallel to the p-axis.

These results may be summarized mathematically in the following two equations:

$$\underline{u}_\alpha = \underline{u}_p \tag{D-29}$$

$$\underline{u}_\beta = \underline{u}_q \tag{D-30}$$

where $\underline{u}_p$ and $\underline{u}_q$ are unit vectors along the p and q axes, respectively.

D. 4 Evaluation of the Elliptical Cylindrical Coordinate System

In the elliptical cylindrical coordinate system, the differential change in the radius vector along a known trajectory is

$$d\,\underline{r} = \underline{w}_{\alpha}\, d\,\alpha + \underline{w}_{\beta}\, d\,\beta + \underline{w}_{z}\, d\,z \tag{D-31}$$

When the trajectory is an ellipse,

$$d\,\alpha = 0 = d\,z \tag{D-32}$$

Then,

$$d\,\underline{r} = \underline{w}_{\beta}\, d\,\beta = a\,(1 - e^2 \cos^2 E)^{\frac{1}{2}}\, d\,E\, \underline{u}_{\beta} \tag{D-33}$$

The deviative of $\underline{r}$ with respect to t is

$$\frac{d\,\underline{r}}{dt} = a\,(1 - e^2 \cos^2 E)^{\frac{1}{2}}\, \dot{E}\, \underline{u}_{\beta}$$

$$= \frac{n\,a\,(1 + e \cos E)^{\frac{1}{2}}}{(1 - e \cos E)^{\frac{1}{2}}}\, \underline{u}_{\beta} = \underline{v} \tag{D-34}$$

Equation (D-34) represents a simpler, more elegant method of deriving the velocity along an elliptical trajectory than any obtainable by the use of rectilinear coordinate systems. It is in studies of this nature, involving the dynamic or geometric characteristics associated with a known ellipse, that the elliptical cylindrical coordinate system shows to good advantage.

The guidance problem is primarily concerned not with the differential d $\underline{r}$, but rather with the variation $\delta \underline{r}$. It is important to distinguish between these two quantities. The differential d $\underline{r}$ is the infinitesimal change in the position vector $\underline{r}$ due to an infinitesimal displacement along a known reference trajectory. The variation $\delta \underline{r}$ is the small difference between the radius vector for an actual trajectory at a given time and the radius vector for a known reference trajectory at the same time.

When an elliptical cylindrical coordinate system is used in conjunction with an elliptical reference trajectory, the differentials of a, e, α, and z are all zero. However, the variations of a, e, α, and z need not be zero, and in general they are not. Thus, the main advantage of the elliptical system, the fact that d $\alpha = 0$, is of no consequence when the problem being studied is a variational problem.

The first variation of $\underline{r}$ is

$$\begin{aligned}\delta \underline{r} &= \delta x \, \underline{u}_x + \delta y \, \underline{u}_y + \delta z \, \underline{u}_z \\ &= \delta \, (a e \cosh \alpha \cos \beta - 1) \, \underline{u}_x \\ &\quad + \delta \, (a e \sinh \alpha \sin \beta) \, \underline{u}_y + \delta z \, \underline{u}_z \end{aligned} \tag{D-35}$$

$$\begin{aligned}&= \frac{\partial \underline{r}}{\partial a} \delta a + \frac{\partial \underline{r}}{\partial e} \delta e + \frac{\partial \underline{r}}{\partial \alpha} \delta \alpha \\ &\quad + \frac{\partial \underline{r}}{\partial \beta} \delta \beta + \frac{\partial \underline{r}}{\partial z} \delta z \end{aligned} \tag{D-36}$$

This formulation for $\delta \underline{r}$ offers no advantage over that which can be obtained from any of the three reference trajectory rectilinear coordinate systems of Appendix A. Since the coordinate variables in the rectilinear systems are more familiar than those of the elliptical system, no further use will be made of the elliptical system in this analysis.

APPENDIX E
VARIANT EQUATIONS OF MOTION

E.1 Summary

The variant equations of motion of a vehicle in an n-body gravitational field are developed first in vector form and then in component form for the three different reference trajectory coordinate systems. A simplified matrix notation is introduced which indicates that the variation in acceleration is related to the variation in position by means of a symmetric 3-by-3 matrix.

E.2 The Variant Equation in Vector Form

The vector form of the variant equation of motion is obtained from Eq. (B-3) by taking the first variation with respect to $\underline{r}$ at a fixed time. On the left side of (B-3),

$$\delta \left(\frac{\mu}{r^3}\ \underline{r}\right) = \frac{\mu}{r^4}\ (-3\ \underline{r}\ \delta r + r\ \delta \underline{r}) \tag{E-1}$$

where the symbol δ signifies the first variation.

On the right side of (B-3),

$$\delta \left(-\frac{G\ m_i}{d_i^3}\ \underline{d}_i\right) = -\frac{G\ m_i}{d_i^4}\ (-3\ \underline{d}_i\ \delta\ d_i + d_i\ \delta \underline{d}_i) \tag{E-2}$$

From Fig. B.1,

$$\underline{d}_i = \underline{r} - \underline{r}_i \tag{E-3}$$

Since $\underline{r}_i$ is unaffected by a variation in $\underline{r}$,

$$\delta \underline{d}_i = \delta \underline{r} \tag{E-4}$$

Then,

$$\delta\left(-\frac{G m_i}{d_i^3}\,\underline{d}_i\right) = \frac{G m_i}{d_i^4}\left(3\,\underline{d}_i\,\delta d_i - d_i\,\delta\underline{r}\right) \qquad \text{(E-5)}$$

The variation in the last term of (B-3) due to $\delta\underline{r}$ is zero.

The variant equation in vector form is

$$\delta\ddot{\underline{r}} = \frac{\mu}{r^4}\left(3\,\underline{r}\,\delta r - r\,\delta\underline{r}\right) + G\sum_{i=1}^{n}\frac{m_i}{d_i^4}\left(3\,\underline{d}_i\,\delta d_i - d_i\,\delta\underline{r}\right) \qquad \text{(E-6)}$$

E. 3 Variant Equations in the Reference Trajectory Coordinate Systems

Since the x, y, z coordinate system is non-rotating, $\delta\underline{r}$ and $\delta\ddot{\underline{r}}$ are obtained directly from (B-4) and (B-6).

$$\delta\underline{r} = \delta x\,\underline{u}_x + \delta y\,\underline{u}_y + \delta z\,\underline{u}_z \qquad \text{(E-7)}$$

$$\delta\ddot{\underline{r}} = \delta\ddot{x}\,\underline{u}_x + \delta\ddot{y}\,\underline{u}_y + \delta\ddot{z}\,\underline{u}_z \qquad \text{(E-8)}$$

δr and δd_i are derived from (B-7) and (B-8).

$$\delta r = \frac{x}{r}\,\delta x + \frac{y}{r}\,\delta y + \frac{z}{r}\,\delta z \qquad \text{(E-9)}$$

$$\delta d_i = \frac{(x - x_i)}{d_i}\,\delta x + \frac{(y - y_i)}{d_i}\,\delta y + \frac{(z - z_i)}{d_i}\,\delta z \qquad \text{(E-10)}$$

Equations (E-7) through (E-10) are substituted into (E-6), and the resulting equation is written in matrix form.

$$\begin{pmatrix} \delta\ddot{x} \\ \delta\ddot{y} \\ \delta\ddot{z} \end{pmatrix} = \left\{ \frac{\mu}{r^5} \left[3 \begin{pmatrix} x^2 & xy & xz \\ yx & y^2 & yz \\ zx & zy & z^2 \end{pmatrix} - r^2 \overset{*}{I}_3 \right] \right.$$

$$\left. + G \sum_{i=1}^{n} \frac{m_i}{d_i^5} \left[3 \begin{pmatrix} (x-x_i)^2 & (x-x_i)(y-y_i) & (x-x_i)(z-z_i) \\ (y-y_i)(x-x_i) & (y-y_i)^2 & (y-y_i)(z-z_i) \\ (z-z_i)(x-x_i) & (z-z_i)(y-y_i) & (z-z_i)^2 \end{pmatrix} - d_i^2 \overset{*}{I}_3 \right] \right\} \begin{pmatrix} \delta x \\ \delta y \\ \delta z \end{pmatrix}$$

(E-11)

where $\overset{*}{I}_3$ is the 3-by-3 identity matrix. An asterisk above a capital letter indicates that the letter represents a matrix.

Equation (E-11) may be written more compactly as follows:

$$\delta\ddot{\underline{r}} = \left[\frac{\mu}{r^5} \left(3\, \underline{r}\, \underline{r}^T - \underline{r}^T\, \underline{r}\, \overset{*}{I}_3 \right) + G \sum_{i=1}^{n} \frac{m_i}{d_i^5} \left(3\, \underline{d}_i\, \underline{d}_i^T - \underline{d}_i^T\, \underline{d}_i\, \overset{*}{I}_3 \right) \right] \delta\underline{r} \qquad \text{(E-12)}$$

where $\underline{r}$, $\underline{d}_i$, and $\delta\underline{r}$ are three-dimensional column vectors and the superscript T indicates the transpose.

The expression inside the square brackets in (E-12) is a symmetrical 3-by-3 matrix which is designated $\overset{*}{G}$.

$$\delta\ddot{\underline{r}} = \overset{*}{G}\ \delta\underline{r} \qquad \text{(E-13)}$$

In the r, s, z coordinate system, rotating with angular velocity $\dot{f}$,

$$\underline{r} + \delta\underline{r} = (\rho + \delta\rho)\,\underline{u}_r + \delta s\,\underline{u}_s + (z + \delta z)\,\underline{u}_z \qquad \text{(E-14)}$$

$$\underline{v} + \delta\underline{v} = (\dot{\rho} + \dot{\delta\rho} - \dot{f}\,\delta s)\,\underline{u}_r + (\dot{\delta s} + \rho\,\dot{f} + \dot{f}\,\delta\rho)\,\underline{u}_s + (\dot{z} + \dot{\delta z})\,\underline{u}_z \qquad \text{(E-15)}$$

$$\underline{a} + \delta\underline{a} = (\ddot{\rho} - \rho\,\dot{f}^2 + \delta\ddot{\rho} - \dot{f}^2\,\delta\rho - 2\dot{f}\,\dot{\delta s} - \ddot{f}\,\delta s)\,\underline{u}_r + (\rho\,\ddot{f} + 2\,\dot{\rho}\,\dot{f} + 2\dot{f}\,\dot{\delta\rho} + \ddot{f}\,\delta\rho + \ddot{\delta s} - \dot{f}^2\,\delta s)\,\underline{u}_s + (\ddot{z} + \ddot{\delta z})\,\underline{u}_z \qquad \text{(E-16)}$$

$\delta\underline{a}$ is obtained by subtracting (B-13) from (E-16).

$$\delta\underline{a} = \ddot{\delta\underline{r}} = (\ddot{\delta\rho} - \dot{f}^2\,\delta\rho - 2\dot{f}\,\dot{\delta s} - \ddot{f}\,\delta s)\,\underline{u}_r + (2\dot{f}\,\dot{\delta\rho} + \ddot{f}\,\delta\rho + \ddot{\delta s} - \dot{f}^2\,\delta s)\,\underline{u}_s + \ddot{\delta z}\,\underline{u}_z \qquad \text{(E-17)}$$

Then Eq. (E-12) may be written as

$$\begin{pmatrix} \ddot{\delta\rho} - \dot{f}^2\,\delta\rho - 2\dot{f}\,\dot{\delta s} - \ddot{f}\,\delta s \\ 2\dot{f}\,\dot{\delta\rho} + \ddot{f}\,\delta\rho + \ddot{\delta s} - \dot{f}^2\,\delta s \\ \ddot{\delta z} \end{pmatrix} = \left\{ \frac{\mu}{r^5} \left[3 \begin{pmatrix} \rho^2 & 0 & \rho z \\ 0 & 0 & 0 \\ z\rho & 0 & z^2 \end{pmatrix} - r^2\, \overset{*}{I}_3 \right] \right.$$

$$\left. + G \sum_{i=1}^{n} \frac{m_i}{d_i^5} \left[3 \begin{pmatrix} (\rho - \rho_i)^2 & -(\rho - \rho_i)\,s_i & (\rho - \rho_i)(z - z_i) \\ -s_i(\rho - \rho_i) & s_i^2 & -s_i(z - z_i) \\ (z - z_i)(\rho - \rho_i) & -(z - z_i)\,s_i & (z - z_i)^2 \end{pmatrix} - d_i^2\, \overset{*}{I}_3 \right] \right\} \begin{pmatrix} \delta\rho \\ \delta s \\ \delta z \end{pmatrix}$$

(E-18)

A similar development can be carried out in the p, q, z coordinate system, which rotates with angular velocity $\dot{\underline{g}}$. The resulting equation is

$$\begin{pmatrix} \delta\ddot{p} - \dot{g}^2\,\delta p - 2\dot{g}\,\delta\dot{q} - \ddot{g}\,\delta q \\ 2\dot{g}\,\delta\dot{p} + \ddot{g}\,\delta p + \delta\ddot{q} - \dot{g}^2\,\delta q \\ \delta\ddot{z} \end{pmatrix} = \left\{ \frac{\mu}{r^5} \left[3 \begin{pmatrix} p^2 & pq & pz \\ qp & q^2 & qz \\ zp & zq & z^2 \end{pmatrix} - r^2\, \overset{*}{I}_3 \right] \right.$$

$$\left. + G \sum_{i=1}^{n} \frac{m_i}{d_i^5} \left[3 \begin{pmatrix} (p-p_i)^2 & (p-p_i)(q-q_i) & (p-p_i)(z-z_i) \\ (q-q_i)(p-p_i) & (q-q_i)^2 & (q-q_i)(z-z_i) \\ (z-z_i)(p-p_i) & (z-z_i)(q-q_i) & (z-z_i)^2 \end{pmatrix} - d_i^2\, \overset{*}{I}_3 \right] \right\} \begin{pmatrix} \delta p \\ \delta q \\ \delta z \end{pmatrix} \qquad \text{(E-19)}$$

E.4 Symmetry of Matrix $\overset{*}{G}$

An interesting physical explanation of the symmetry of the matrix $\overset{*}{G}$ in Eq. (E-13) has been given by McLean, Schmidt, and McGee.*

Since all the forces being considered are gravitational, a scalar potential V may be defined such that

$$\ddot{\underline{r}} = \nabla V \qquad \text{(E-20)}$$

where ∇ signifies the gradient of a scalar quantity. In matrix form in the x y z coordinate system,

$$\begin{pmatrix} \ddot{x} \\ \ddot{y} \\ \ddot{z} \end{pmatrix} = \begin{pmatrix} \frac{\partial V}{\partial x} \\ \frac{\partial V}{\partial y} \\ \frac{\partial V}{\partial z} \end{pmatrix} \qquad \text{(E-21)}$$

---

* Page 34 of Reference (13).

The variation in $\ddot{x}$ is

$$\delta\ddot{x} = \frac{\partial \ddot{x}}{\partial x}\,\delta x + \frac{\partial \ddot{x}}{\partial y}\,\delta y + \frac{\partial \ddot{x}}{\partial z}\,\delta z$$

$$= \frac{\partial^2 V}{\partial x^2}\,\delta x + \frac{\partial^2 V}{\partial y\,\partial x}\,\delta y + \frac{\partial^2 V}{\partial z\,\partial x}\,\delta z \qquad \text{(E-22)}$$

Analogous equations may be written for $\delta\ddot{y}$ and $\delta\ddot{z}$. Then the vector $\delta\ddot{\underline{r}}$ is given by

$$\delta\ddot{\underline{r}} = \begin{pmatrix} \delta\ddot{x} \\ \delta\ddot{y} \\ \delta\ddot{z} \end{pmatrix} = \begin{pmatrix} \frac{\partial^2 V}{\partial x^2} & \frac{\partial^2 V}{\partial y\,\partial x} & \frac{\partial^2 V}{\partial z\,\partial x} \\ \frac{\partial^2 V}{\partial x\,\partial y} & \frac{\partial^2 V}{\partial y^2} & \frac{\partial^2 V}{\partial z\,\partial y} \\ \frac{\partial^2 V}{\partial x\,\partial z} & \frac{\partial^2 V}{\partial y\,\partial z} & \frac{\partial^2 V}{\partial z^2} \end{pmatrix} \begin{pmatrix} \delta x \\ \delta y \\ \delta z \end{pmatrix} \qquad \text{(E-23)}$$

A comparison of (E-23) with (E-13) indicates that the 3-by-3 matrix in (E-23) is G^* and that its symmetry is due to the fact that

$$\frac{\partial^2 V}{\partial r_i\,\partial r_j} = \frac{\partial^2 V}{\partial r_j\,\partial r_i}; \quad i, j, = 1, 2, 3 \qquad \text{(E-24)}$$

where r_i and r_j are components of $\underline{r}$.

Thus, as long as the force field is conservative, the matrix G^* relating $\delta\ddot{\underline{r}}$ to $\delta\underline{r}$ is symmetric. The inclusion of the effects of earth oblateness in the analysis does not affect the symmetry of G^*.

APPENDIX F
GENERAL MATRIX FORMULATIONS

F.1 Summary

Several different types of matrix formulations are introduced to represent the solution of the variant equations of motion. The interrelationships among the various matrices are developed. A method is indicated for evaluating the terms in the matrices by the use of numerical integration. Some interesting symmetry properties of the matrices are proved. The symmetry properties are used to find the inverse of the basic 6-by-6 matrix by inspection.

F.2 Path Deviation

Just as the solution of the general equations of motion involves six constants, so does the solution of the variant equations of motion. The analogy may be carried further. It was pointed out in Section B.6 that the six constants in the general solution may be the three components of position and the three components of velocity occurring at a specified time; in the variant solution the constants may be the variations in the three components of position and the three components of velocity occurring at a specified time. The constants in the variant solution may also be the variations in the components of position at two different specified times. If the motion is two-body motion, variations in the six orbital elements may be used. Any one of these groupings of six constants may be regarded as a six-component vector. This type of vector will be referred to as the path deviation vector.

The mathematical representations for the three classes of path deviation vectors mentioned above are

(1) $$\begin{Bmatrix} \delta \underline{r}_k \\ \delta \underline{v}_k \end{Bmatrix}$$

(2) $$\begin{Bmatrix} \delta \underline{r}_i \\ \delta \underline{r}_j \end{Bmatrix}$$

(3) $$\delta \underline{e}$$

$\delta \underline{r}_k$ and $\delta \underline{v}_k$ are, respectively, the position variation and the velocity variation at time t_k. They may be grouped together into a single vector, which will be designated $\delta \underline{x}_k$. $\delta \underline{r}_i$ and $\delta \underline{r}_j$ are the position variations at times t_i and t_j. $\delta \underline{e}$ consists of the variations in some grouping of six orbital elements.

The three different path deviation vectors may be related to each other as follows:

$$\delta \underline{e} = \{ \overset{*}{R}_k \quad \overset{*}{V}_k \} \begin{Bmatrix} \delta \underline{r}_k \\ \\ \delta \underline{v}_k \end{Bmatrix} = \{ \overset{*}{R}_k \quad \overset{*}{V}_k \} \, \delta \underline{x}_k \qquad \text{(F-1)}$$

$$= \overset{*}{H}_{ij} \, \delta \underline{r}_i + \overset{*}{H}_{ji} \, \delta \underline{r}_j \qquad \text{(F-2)}$$

where

$$\overset{*}{R}_k = \left\{ \frac{\partial \underline{e}}{\partial \underline{r}_k} \Big|_{\delta \underline{v}_k = \text{constant}} \right\} \tag{F-3}$$

$$\overset{*}{V}_k = \left\{ \frac{\partial \underline{e}}{\partial \underline{v}_k} \Big|_{\delta \underline{r}_k = \text{constant}} \right\} \tag{F-4}$$

$$\overset{*}{H}_{ij} = \left\{ \frac{\partial \underline{e}}{\partial \underline{r}_i} \Big|_{\delta \underline{r}_j = \text{constant}} \right\} \tag{F-5}$$

$\overset{*}{R}_k$, $\overset{*}{V}_k$, $\overset{*}{H}_{ij}$ and $\overset{*}{H}_{ji}$ are all 6-by-3 matrices. The subscript k in $\overset{*}{R}_k$ and $\overset{*}{V}_k$ indicates that the elements of the two matrices are functions of t_k. Similarly, the elements of $\overset{*}{H}_{ij}$ and $\overset{*}{H}_{ji}$ are functions of t_i and t_j.

F.3 Variation in Position

The variation in position at any arbitrary time t_m may be expressed in terms of the path deviation vector.

$$\delta \underline{r}_m = \overset{*}{F}_m \, \delta \underline{e} \tag{F-6}$$

$$= \overset{*}{F}_m \{ \overset{*}{R}_k \quad \overset{*}{V}_k \} \, \delta \underline{x}_k \tag{F-7}$$

$$= \overset{*}{F}_m \{ \overset{*}{H}_{ij} \, \delta \underline{r}_i + \overset{*}{H}_{ji} \, \delta \underline{r}_j \} \tag{F-8}$$

$$= \{ \overset{*}{M}_{mk} \quad \overset{*}{N}_{mk} \} \, \delta \underline{x}_k \tag{F-9}$$

where

$$\overset{*}{F}_m = \left\{ \frac{\partial \underline{r}_m}{\partial \underline{e}} \right\} \tag{F-10}$$

$$\overset{*}{M}_{mk} = \left\{ \frac{\partial \underline{r}_m}{\partial \underline{r}_k} \bigg|_{\delta \underline{r}_k = \text{ constant}} \right\} \tag{F-11}$$

$$\overset{*}{N}_{mk} = \left\{ \frac{\partial \underline{r}_m}{\partial \underline{r}_k} \bigg|_{\delta \underline{v}_k = \text{ constant}} \right\} \tag{F-12}$$

$\overset{*}{F}_m$ is a 3-by-6 matrix. $\overset{*}{M}_{mk}$ and $\overset{*}{N}_{mk}$ are 3-by-3 matrices.

Since the elements of the path deviation vector are independent of each other, it is apparent from (F-7), (F-8), and (F-9) that

$$\overset{*}{F}_k \overset{*}{R}_k = \overset{*}{F}_i \overset{*}{H}_{ij} = \overset{*}{M}_{kk} = \overset{*}{I}_3 \tag{F-13}$$

$$\overset{*}{F}_k \overset{*}{V}_k = \overset{*}{F}_i \overset{*}{H}_{ji} = \overset{*}{N}_{kk} = \overset{*}{O}_3 \tag{F-14}$$

where $\overset{*}{O}_3$ is the 3-by-3 zero matrix.

In general,

$$\overset{*}{M}_{mk} = \overset{*}{F}_m \overset{*}{R}_k \tag{F-15}$$

$$\overset{*}{N}_{mk} = \overset{*}{F}_m \overset{*}{V}_k \tag{F-16}$$

Equation (F-15) indicates that $\overset{*}{M}_{mk}$, whose elements are functions of both t_m and t_k, can be written as the product of two matrices, the elements of one being functions solely of t_m and the elements of the second being functions solely of t_k. A similar statement may be made with respect to $\overset{*}{N}_{mk}$.

F.4 Variation in Velocity

The variation in velocity at time t_m is

$$\delta \underline{v}_m = \overset{*}{L}_m \, \delta \underline{e} \tag{F-17}$$

$$= \overset{*}{L}_m \left\{ \overset{*}{R}_k \quad \overset{*}{V}_k \right\} \delta \underline{x}_k \tag{F-18}$$

$$= \overset{*}{L}_m \left\{ \overset{*}{H}_{ij} \, \delta \underline{r}_i + \overset{*}{H}_{ji} \, \delta \underline{r}_j \right\} \tag{F-19}$$

$$= \left\{ \overset{*}{S}_{mk} \quad \overset{*}{T}_{mk} \right\} \delta \underline{x}_k \tag{F-20}$$

where

$$\overset{*}{L}_m = \left\{ \frac{\partial \underline{v}_m}{\partial \underline{e}} \right\} \tag{F-21}$$

$$\overset{*}{S}_{mk} = \left\{ \frac{\partial \underline{v}_m}{\partial \underline{r}_k} \,\middle|\, \delta \underline{v}_k = \text{constant} \right\} \tag{F-22}$$

$$\overset{*}{T}_{mk} = \left\{ \frac{\partial \underline{v}_m}{\partial \underline{v}_k} \,\middle|\, \delta \underline{r}_k = \text{constant} \right\} \tag{F-23}$$

From (F-18) and (F-20),

$$\overset{*}{S}_{mk} = \overset{*}{L}_m \overset{*}{R}_k \qquad \text{(F-24)}$$

$$\overset{*}{T}_{mk} = \overset{*}{L}_m \overset{*}{V}_k \qquad \text{(F-25)}$$

The equations corresponding to (F-13) and (F-14) are

$$\overset{*}{T}_{kk} = \overset{*}{L}_k \overset{*}{V}_k = \overset{*}{I}_3 \qquad \text{(F-26)}$$

$$\overset{*}{S}_{kk} = \overset{*}{L}_k \overset{*}{R}_k = \overset{*}{O}_3 \qquad \text{(F-27)}$$

When $t_m = t_i$, Eq. (F-19) becomes

$$\delta \underline{v}_i = \overset{*}{L}_i \left\{ \overset{*}{H}_{ij} \, \delta \underline{r}_i + \overset{*}{H}_{ji} \, \delta \underline{r}_j \right\} \qquad \text{(F-28)}$$

$$= \overset{*}{J}_{ij} \, \delta \underline{r}_i + \overset{*}{K}_{ij} \, \delta \underline{r}_j \qquad \text{(F-29)}$$

where

$$\overset{*}{J}_{ij} = \overset{*}{L}_i \overset{*}{H}_{ij} = \left\{ \frac{\partial \underline{v}_i}{\partial \underline{r}_i} \bigg|_{\delta \underline{r}_j = \text{constant}} \right\} \qquad \text{(F-30)}$$

$$\overset{*}{K}_{ij} = \overset{*}{L}_i \overset{*}{H}_{ji} = \left\{ \frac{\partial \underline{v}_i}{\partial \underline{r}_j} \bigg|_{\delta \underline{r}_i = \text{constant}} \right\} \qquad \text{(F-31)}$$

$\overset{*}{J}_{ij}$ and $\overset{*}{K}_{ij}$ are 3-by-3 matrices.

(F-29) may be solved for $\delta \underline{r}_j$ by pre-multiplying the terms of the equation by $\overset{*}{K}_{ij}^{-1}$, where the superscript -1 indicates the inverse of a square matrix.

$$\delta \underline{r}_j = - \overset{*}{K}_{ij}^{-1} \overset{*}{J}_{ij} \delta \underline{r}_i + \overset{*}{K}_{ij}^{-1} \delta \underline{v}_i$$

$$= \overset{*}{K}_{ij}^{-1} \{ - \overset{*}{J}_{ij} \quad \overset{*}{I}_3 \} \delta \underline{x}_i \qquad \text{(F-32)}$$

Comparison of (F-32) with (F-9) indicates that

$$\overset{*}{M}_{ji} = - \overset{*}{K}_{ij}^{-1} \overset{*}{J}_{ij} \qquad \text{(F-33)}$$

$$\overset{*}{N}_{ji} = \overset{*}{K}_{ij}^{-1} \qquad \text{(F-34)}$$

The path deviation vector at time t_j may be expressed in terms of the path deviation vector at time t_i as follows:

$$\delta \underline{x}_j = \begin{Bmatrix} \delta \underline{r}_j \\ \delta \underline{v}_j \end{Bmatrix} = \begin{Bmatrix} \overset{*}{M}_{ji} & \overset{*}{N}_{ji} \\ \overset{*}{S}_{ji} & \overset{*}{T}_{ji} \end{Bmatrix} \delta \underline{x}_i = \overset{*}{C}_{ji} \delta \underline{x}_i \qquad \text{(F-35)}$$

where

$$\overset{*}{C}_{ji} = \begin{Bmatrix} \overset{*}{M}_{ji} & \overset{*}{N}_{ji} \\ \overset{*}{S}_{ji} & \overset{*}{T}_{ji} \end{Bmatrix} = \left\{ \frac{\partial \underline{x}_j}{\partial \underline{x}_i} \right\} \qquad \text{(F-36)}$$

The 6-by-6 matrix $\overset{*}{C}_{ji}$ is known as the transition matrix. It follows from (F-35) that

$$\delta \underline{x}_j = \overset{*}{C}_{ji} \overset{*}{C}_{ij} \delta \underline{x}_j \tag{F-37}$$

$$\therefore \quad \overset{*}{C}_{ji} \overset{*}{C}_{ij} = \overset{*}{I}_6 \tag{F-38}$$

where $\overset{*}{I}_6$ is the 6-by-6 identity matrix. Then,

$$\overset{*}{M}_{ji} \overset{*}{M}_{ij} + \overset{*}{N}_{ji} \overset{*}{S}_{ij} = \overset{*}{I}_3 = \overset{*}{S}_{ji} \overset{*}{N}_{ij} + \overset{*}{T}_{ji} \overset{*}{T}_{ij} \tag{F-39}$$

$$\overset{*}{M}_{ji} \overset{*}{N}_{ij} + \overset{*}{N}_{ji} \overset{*}{T}_{ij} = \overset{*}{O}_3 = \overset{*}{S}_{ji} \overset{*}{M}_{ij} + \overset{*}{T}_{ji} \overset{*}{S}_{ij} \tag{F-40}$$

F.5 Matrix Differential Equations

The position of a point P with respect to the origin of a rotating coordinate system may be represented by the vector $\underline{r}$, the components of $\underline{r}$ in the rotating system being r_1, r_2, and r_3. The angular velocity of the system with respect to inertial space is $\underline{\omega}$, with components ω_1, ω_2, and ω_3.

The velocity of P in a non-rotating coordinate system is related to its velocity in the rotating system by the equation

$$\underline{v} = \left(\frac{d\underline{r}}{dt}\right)_{NR} = \left(\frac{d\underline{r}}{dt}\right)_{R} + \underline{\omega} \times \underline{r} \tag{F-41}$$

where the subscripts NR and R refer, respectively, to the non-rotating and rotating coordinate systems. The matrix form of Eq. (F-41) is

$$\begin{Bmatrix} v_1 \\ v_2 \\ v_3 \end{Bmatrix} = \begin{Bmatrix} \dot{r}_1 + \omega_2 r_3 - \omega_3 r_2 \\ \dot{r}_2 + \omega_3 r_1 - \omega_1 r_3 \\ \dot{r}_3 + \omega_1 r_2 - \omega_2 r_1 \end{Bmatrix} \tag{F-42}$$

$$= \begin{Bmatrix} \dot{r}_1 \\ \dot{r}_2 \\ \dot{r}_3 \end{Bmatrix} + \overset{*}{W}\, \underline{r} \tag{F-43}$$

where $\overset{*}{W}$ is given by

$$\overset{*}{W} = \begin{Bmatrix} 0 & -\omega_3 & \omega_2 \\ \omega_3 & 0 & -\omega_1 \\ -\omega_2 & \omega_1 & 0 \end{Bmatrix} \tag{F-44}$$

$\overset{*}{W}$ is a skew-symmetric matrix, i.e.,

$$\overset{*}{W}^T = -\overset{*}{W} \tag{F-45}$$

The variation of $\underline{v}$ is

$$\delta \underline{v} = \delta \left(\frac{d\,\underline{r}}{dt} \right)_{NR} = \delta \left(\frac{d\,\underline{r}}{dt} \right)_{R} + \left(\delta\, \overset{*}{W} \right) \underline{r} + \overset{*}{W}\, \delta \underline{r} \tag{F-46}$$

Since the angular velocity of the coordinate system is not affected by variations in $\underline{r}$,

$$\delta \overset{*}{\underline{W}} = \overset{*}{\underline{O}}_3 \qquad \text{(F-47)}$$

From Eq. (F-9), the variation of the velocity of P in the rotating system is

$$\left[\frac{d(\delta \underline{r}_i)}{d t_i}\right]_R = \begin{Bmatrix} \delta \dot{r}_{i1} \\ \delta \dot{r}_{i2} \\ \delta \dot{r}_{i3} \end{Bmatrix} = \begin{Bmatrix} \frac{\partial \overset{*}{M}_{ij}}{\partial t_i} & \frac{\partial \overset{*}{N}_{ij}}{\partial t_i} \end{Bmatrix} \delta \underline{x}_j \qquad \text{(F-48)}$$

Equations (F-47) and (F-48) are substituted into (F-46), and the resulting expression is equated to (F-20).

$$\delta \underline{v}_i = \begin{Bmatrix} \frac{\partial \overset{*}{M}_{ij}}{\partial t_i} + \overset{*}{W}_i \overset{*}{M}_{ij} & \frac{\partial \overset{*}{N}_{ij}}{\partial t_i} + \overset{*}{W}_i \overset{*}{N}_{ij} \end{Bmatrix} \delta \underline{x}_j$$

$$= \begin{Bmatrix} \overset{*}{S}_{ij} & \overset{*}{T}_{ij} \end{Bmatrix} \delta \underline{x}_j \qquad \text{(F-49)}$$

In similar fashion $\delta \underline{a}_i$ may be written in terms of $\overset{*}{S}_{ij}$, $\overset{*}{T}_{ij}$, and their derivatives, and then equated to the right-hand side of (E-13).

$$\delta \underline{a}_i = \begin{Bmatrix} \frac{\partial \overset{*}{S}_{ij}}{\partial t_i} + \overset{*}{W}_i \overset{*}{S}_{ij} & \frac{\partial \overset{*}{T}_{ij}}{\partial t_i} + \overset{*}{W}_i \overset{*}{T}_{ij} \end{Bmatrix} \delta \underline{x}_j$$

$$= \overset{*}{G}_i \delta \underline{r}_i = \overset{*}{G}_i \begin{Bmatrix} \overset{*}{M}_{ij} & \overset{*}{N}_{ij} \end{Bmatrix} \delta \underline{x}_j \qquad \text{(F-50)}$$

By equating coefficients of $\delta \underline{r}_j$ and also of $\delta \underline{v}_j$ in (F-49) and (F-50), the following matrix differential equations are obtained:

$$\frac{\partial \overset{*}{M}_{ij}}{\partial t_i} + \overset{*}{W}_i \overset{*}{M}_{ij} = \overset{*}{S}_{ij} \tag{F-51}$$

$$\frac{\partial \overset{*}{S}_{ij}}{\partial t_i} + \overset{*}{W}_i \overset{*}{S}_{ij} = \overset{*}{G}_i \overset{*}{M}_{ij} \tag{F-52}$$

$$\frac{\partial \overset{*}{N}_{ij}}{\partial t_i} + \overset{*}{W}_i \overset{*}{N}_{ij} = \overset{*}{T}_{ij} \tag{F-53}$$

$$\frac{\partial \overset{*}{T}_{ij}}{\partial t_i} + \overset{*}{W}_i \overset{*}{T}_{ij} = \overset{*}{G}_i \overset{*}{N}_{ij} \tag{F-54}$$

Matrix differential equations may also be obtained for the 3-by-6 matrices $\overset{*}{F}_i$ and $\overset{*}{L}_i$. These are derived from Eqs. (F-6), (F-17), and (E-13).

$$\delta \underline{v}_i = \left\{ \frac{d \overset{*}{F}_i}{dt_i} + \overset{*}{W}_i \overset{*}{F}_i \right\} \delta \underline{e} = \overset{*}{L}_i \, \delta \underline{e} \tag{F-55}$$

$$\delta \underline{a}_i = \left\{ \frac{d \overset{*}{L}_i}{dt_i} + \overset{*}{W}_i \overset{*}{L}_i \right\} \delta \underline{e} = \overset{*}{G}_i \overset{*}{F}_i \, \delta \underline{e} \tag{F-56}$$

The differential equations corresponding to (F-51) through (F-54) are

$$\frac{d \overset{*}{F}_i}{dt_i} + \overset{*}{W}_i \overset{*}{F}_i = \overset{*}{L}_i \tag{F-57}$$

$$\frac{d \overset{*}{L}_i}{dt_i} + \overset{*}{W}_i \overset{*}{L}_i = \overset{*}{G}_i \overset{*}{F}_i \tag{F-58}$$

Finally, it is of interest to relate the 6-by-3 matrices $\overset{*}{R}_i$ and $\overset{*}{V}_i$ to each other. This may be done by taking the time derivative of Eq. (F-1) with respect to the rotating coordinate system and equating the result to $\underline{O}_6$, the six-component zero vector.

$$\frac{d}{dt_i}(\delta \underline{e}) = \frac{d\,\overset{*}{R}_i}{dt_i}\,\delta \underline{r}_i + \frac{d\,\overset{*}{V}_i}{dt_i}\,\delta \underline{v}_i$$

$$+ \overset{*}{R}_i \frac{d}{dt_i}(\delta \underline{r}_i) + \overset{*}{V}_i \frac{d}{dt_i}(\delta \underline{v}_i) = \underline{O}_6 \qquad \text{(F-59)}$$

The derivatives of the variation vectors with respect to the rotating system are

$$\frac{d}{dt_i}(\delta \underline{r}_i) = \delta \underline{v}_i - \overset{*}{W}_i\,\delta \underline{r}_i \qquad \text{(F-60)}$$

$$\frac{d}{dt_i}(\delta \underline{v}_i) = \delta \underline{a}_i - \overset{*}{W}_i\,\delta \underline{v}_i$$

$$= \overset{*}{G}_i\,\delta \underline{r}_i - \overset{*}{W}_i\,\delta \underline{v}_i \qquad \text{(F-61)}$$

(F-60) and (F-61) are substituted into (F-59).

$$\left\{\frac{d\,\overset{*}{R}_i}{dt_i} - \overset{*}{R}_i\,\overset{*}{W}_i + \overset{*}{V}_i\,\overset{*}{G}_i\right\}\delta \underline{r}_i$$

$$+ \left\{\frac{d\,\overset{*}{V}_i}{dt_i} - \overset{*}{V}_i\,\overset{*}{W}_i + \overset{*}{R}_i\right\}\delta \underline{v}_i = \underline{O}_6 \qquad \text{(F-62)}$$

The coupled matrix differential equations are obtained from the coefficients of $\delta \underline{r}_i$ and $\delta \underline{v}_i$ in (F-62).

$$\frac{d \overset{*}{R}_i}{dt_i} - \overset{*}{R}_i \overset{*}{W}_i = - \overset{*}{V}_i \overset{*}{G}_i \qquad \text{(F-63)}$$

$$\frac{d \overset{*}{V}_i}{dt_i} - \overset{*}{V}_i \overset{*}{W}_i = - \overset{*}{R}_i \qquad \text{(F-64)}$$

Equations (F-63) and (F-64) may be used to get relations involving the first partial derivatives of $\overset{*}{M}_{ij}$, $\overset{*}{N}_{ij}$, $\overset{*}{S}_{ij}$, and $\overset{*}{T}_{ij}$ with respect to t_j.

$$\frac{\partial \overset{*}{M}_{ij}}{\partial t_j} = \overset{*}{F}_i \quad \frac{d \overset{*}{R}_j}{dt_j} = \overset{*}{F}_i \left\{ \overset{*}{R}_j \overset{*}{W}_j - \overset{*}{V}_j \overset{*}{G}_j \right\} \qquad \text{(F-65)}$$

$$\frac{\partial \overset{*}{N}_{ij}}{\partial t_j} = \overset{*}{F}_i \quad \frac{d \overset{*}{V}_j}{dt_j} = \overset{*}{F}_i \left\{ \overset{*}{V}_j \overset{*}{W}_j - \overset{*}{R}_j \right\} \qquad \text{(F-66)}$$

$$\frac{\partial \overset{*}{S}_{ij}}{\partial t_j} = \overset{*}{L}_i \quad \frac{d \overset{*}{R}_j}{dt_j} = \overset{*}{L}_i \left\{ \overset{*}{R}_j \overset{*}{W}_j - \overset{*}{V}_j \overset{*}{G}_j \right\} \qquad \text{(F-67)}$$

$$\frac{\partial \overset{*}{T}_{ij}}{dt_j} = \overset{*}{L}_i \quad \frac{d \overset{*}{V}_j}{dt_j} = \overset{*}{L}_i \left\{ \overset{*}{V}_j \overset{*}{W}_j - \overset{*}{R}_j \right\} \qquad \text{(F-68)}$$

These four equations may be written as matrix differential equations in $\overset{*}{M}_{ij}$, $\overset{*}{N}_{ij}$, $\overset{*}{S}_{ij}$, and $\overset{*}{T}_{ij}$.

$$\frac{\partial \overset{*}{M}_{ij}}{\partial t_j} - \overset{*}{M}_{ij}\,\overset{*}{W}_j = -\overset{*}{N}_{ij}\,\overset{*}{G}_j \qquad \text{(F-69)}$$

$$\frac{\partial \overset{*}{N}_{ij}}{\partial t_j} - \overset{*}{N}_{ij}\,\overset{*}{W}_j = -\overset{*}{M}_{ij} \qquad \text{(F-70)}$$

$$\frac{\partial \overset{*}{S}_{ij}}{\partial t_j} - \overset{*}{S}_{ij}\,\overset{*}{W}_j = -\overset{*}{T}_{ij}\,\overset{*}{G}_j \qquad \text{(F-71)}$$

$$\frac{\partial \overset{*}{T}_{ij}}{\partial t_j} - \overset{*}{T}_{ij}\,\overset{*}{W}_j = -\overset{*}{S}_{ij} \qquad \text{(F-72)}$$

F. 6 Numerical Integration

The variant equations of motion are represented by (E-13). The solution of these equations for $\delta \underline{r}$ as a function of time is represented by (F-9). The problem now is to evaluate the elements of $\overset{*}{M}_{ij}$ and $\overset{*}{N}_{ij}$.

No direct analytical solution of (E-13) has yet been devised for the case when there are disturbing forces which affect the motion of the vehicle. However, the elements of $\overset{*}{M}_{ij}$ and $\overset{*}{N}_{ij}$ may be found by numerical integration of the coupled equations (F-51) through (F-54).

Since $\overset{*}{M}_{ij}$, $\overset{*}{N}_{ij}$, $\overset{*}{S}_{ij}$, $\overset{*}{T}_{ij}$ are all 3-by-3 matrices, each of the four matrix differential equations represents nine first-order linear differential equations. The elements of the 3-by-3 matrices $\overset{*}{W}_i$ and $\overset{*}{G}_i$ are

known functions of the characteristics of the reference trajectory.

Equations (F-51) and (F-52) are coupled equations in the elements of $\overset{*}{M}_{ij}$ and $\overset{*}{S}_{ij}$. They can be integrated numerically if initial values are known for the elements of $\overset{*}{M}_{ij}$ and $\overset{*}{S}_{ij}$. Fortunately, such initial values are available from (F-13) and (F-27).

$$\overset{*}{M}_{jj} = \overset{*}{I}_3 \qquad \overset{*}{S}_{jj} = \overset{*}{O}_3 \tag{F-73}$$

Similarly, (F-53) and (F-54) are coupled equations in $\overset{*}{N}_{ij}$ and $\overset{*}{T}_{ij}$ which can be integrated numerically since the initial values are given by

$$\overset{*}{N}_{jj} = \overset{*}{O}_3 \qquad \overset{*}{T}_{jj} = \overset{*}{I}_3 \tag{F-74}$$

The integrations are carried out at a fixed value of t_j. The independent variable is t_i.

The computation can be simplified if a non-rotating coordinate system is used, for in that case the matrix $\overset{*}{W}_i$ vanishes. The accuracy of the computation is improved if the z-axis of the coordinate system is perpendicular to the plane of the motion that would occur if there were no disturbing forces; i.e., if the coordinate system is one of the reference trajectory systems described in Appendix A. With this choice of coordinates, the motion in the z direction is relatively loosely coupled (through the disturbing forces) to the motion in the plane perpendicular to the z-axis, and consequently four of the nine elements in each of the 3-by-3 matrices are close to zero. This fact causes a considerable reduction in the magnitude of the round-off errors.

As a result of the numerical integration, the matrices $\overset{*}{M}_{ij}$, $\overset{*}{N}_{ij}$, $\overset{*}{S}_{ij}$, and $\overset{*}{T}_{ij}$ are found as a function of t_i for a fixed value of t_j and a known reference trajectory. Then, $\delta\underline{r}_i$ and $\delta\underline{v}_i$ are known in terms of

the six constants that constitute $\delta \underline{x}_j$.

Matrices $\overset{*}{K}_{ji}$ and $\overset{*}{J}_{ji}$ may be evaluated by the use of Eqs. (F-34) and (F-33), respectively.

The eighteen-element matrices $\overset{*}{R}_j$, $\overset{*}{V}_j$, $\overset{*}{F}_i$, and $\overset{*}{L}_i$ cannot be evaluated, but they are not needed to solve the guidance problem. These matrices have been introduced because they illustrate the fact that each of the nine-element matrices may be regarded as the product of two matrices, one of which is a function of t_i only and the second of which is a function of only t_j. Moreover, it will be shown in Appendix K that the eighteen-element matrices are useful in deriving an analytic solution of the guidance problem when the reference trajectory is an ellipse.

F.7 Matrix Symmetry

In this section the following relations among the matrices are proved:

$$\overset{*}{T}_{ji} = \overset{*}{M}_{ij}{}^T \tag{F-75}$$

$$\overset{*}{N}_{ji} = -\overset{*}{N}_{ij}{}^T \tag{F-76}$$

$$\overset{*}{S}_{ji} = -\overset{*}{S}_{ij}{}^T \tag{F-77}$$

$$\overset{*}{J}_{ij} = \overset{*}{J}_{ij}{}^T \tag{F-78}$$

$$\overset{*}{K}_{ji} = -\overset{*}{K}_{ij}{}^T \tag{F-79}$$

The superscript T signifies the transpose of a matrix. The proofs utilize the face that $\overset{*}{G}$ is known to be a symmetric matrix and $\overset{*}{W}$ is known to be skew-symmetric.

The first proof will be that of (F-78), which states that the $\overset{*}{J}_{ij}$ matrix is symmetric. This fact was first noted by Battin*. From Eqs. (F-33) and (F-34),

$$\overset{*}{M}_{ji}\,\overset{*}{J}_{ij}^{-1} = -\,\overset{*}{K}_{ij}^{-1} = -\,\overset{*}{N}_{ji} \tag{F-80}$$

Equation (F-80) is differentiated with respect to t_i, with substitutions for the derivatives of $\overset{*}{M}_{ji}$ and $\overset{*}{N}_{ji}$ being made from (F-69) and (F-70).

$$\overset{*}{M}_{ji}\,\frac{\partial \overset{*}{J}_{ij}^{-1}}{\partial t_i} + (\overset{*}{M}_{ji}\,\overset{*}{W}_i - \overset{*}{N}_{ji}\,\overset{*}{G}_i)\overset{*}{J}_{ij}^{-1} = -\,\overset{*}{N}_{ji}\,\overset{*}{W}_i + \overset{*}{M}_{ji} \tag{F-81}$$

(F-81) is pre-multiplied by $\overset{*}{M}_{ji}^{-1}$.

$$\frac{\partial \overset{*}{J}_{ij}^{-1}}{\partial t_i} + \overset{*}{J}_{ij}^{-1}\,\overset{*}{G}_i\,\overset{*}{J}_{ij}^{-1} + \overset{*}{W}_i\,\overset{*}{J}_{ij}^{-1} - \overset{*}{J}_{ij}^{-1}\,\overset{*}{W}_i = \overset{*}{I}_3 \tag{F-82}$$

Since the left-hand side of (F-82) is equal to the identity matrix, which is symmetric, it must be equal to its own transpose. When (F-82) is equated to its transpose and $\overset{*}{G}_i^{\,T}$ and $\overset{*}{W}_i^{\,T}$ are replaced by $\overset{*}{G}_i$ and $-\overset{*}{W}_i$, respectively, the result is

$$\frac{\partial \overset{*}{J}_{ij}^{-1}}{\partial t_i} + \overset{*}{J}_{ij}^{-1}\,\overset{*}{G}_i\,\overset{*}{J}_{ij}^{-1} + \overset{*}{W}_i\,\overset{*}{J}_{ij}^{-1} - \overset{*}{J}_{ij}^{-1}\,\overset{*}{W}_i = \frac{\partial \overset{*}{J}_{ij}^{-1^T}}{\partial t_i} + \overset{*}{J}_{ij}^{-1^T}\,\overset{*}{G}_i\,\overset{*}{J}_{ij}^{-1^T} + \overset{*}{W}_i\,\overset{*}{J}_{ij}^{-1^T} - \overset{*}{J}_{ij}^{-1^T}\,\overset{*}{W}_i \tag{F-83}$$

---

* Page 697 of Reference (5)

It is apparent that this equation can be satisfied if $\overset{*}{J}_{ij}^{-1}$ is a symmetric matrix. It must now be proved that $\overset{*}{J}_{ij}^{-1}$ is necessarily symmetric.

Equation (F-82) consists of nine first-order differential equations, each of which has one constant of integration. If it can be shown that these constants are such that $\overset{*}{J}_{ij}^{-1}$ is symmetric at some particular time, then the matrix must be symmetric for all values of time.

When $t_i = t_j$,

$$\overset{*}{J}_{jj}^{-1} = - \overset{*}{M}_{jj}^{-1} \overset{*}{N}_{jj} = - \overset{*}{I}_3 \overset{*}{O}_3 = \overset{*}{O}_3 \qquad \text{(F-84)}$$

The zero matrix is symmetric. Consequently, $\overset{*}{J}_{ij}^{-1}$ is symmetric when $t_i = t_j$ and hence for all values of time. The inverse of a non-singular symmetric matrix is itself symmetric. Therefore, the matrix $\overset{*}{J}_{ij}$ is symmetric for all combinations of t_i and t_j for which $\overset{*}{J}_{ij}^{-1}$ is non-singular, and Eq. (F-78) has been proved.

The second relation that will be derived is (F-76). Again the proof is a consequence of the symmetry of a matrix differential equation. Equation (F-53) is pre-multiplied by $- \overset{*}{N}_{ji}$. Subscripts i and j are interchanged in (F-70), and the resulting equation is post-multiplied by $\overset{*}{N}_{ij}$. These two equations are then added.

$$- \overset{*}{N}_{ji} \frac{\partial \overset{*}{N}_{ij}}{\partial t_i} + \frac{\partial \overset{*}{N}_{ji}}{\partial t_i} \overset{*}{N}_{ij} - 2 \overset{*}{N}_{ji} \overset{*}{W}_i \overset{*}{N}_{ij} = - \overset{*}{N}_{ji} \overset{*}{T}_{ij} - \overset{*}{M}_{ji} \overset{*}{N}_{ij} \qquad \text{(F-85)}$$

From Eq. (F-40) it is seen that the right-hand side of (F-85) is equal to the zero matrix.

$$\frac{\partial \overset{*}{N}_{ji}}{\partial t_i} \overset{*}{N}_{ij} - \overset{*}{N}_{ji} \frac{\partial \overset{*}{N}_{ij}}{\partial t_i} = 2 \overset{*}{N}_{ji} \overset{*}{W}_i \overset{*}{N}_{ij} \qquad \text{(F-86)}$$

Since W_i is skew-symmetric, the transpose of Eq. (F-86) is

$$-\frac{\partial \overset{*}{N}_{ij}^{T}}{\partial t_i}\ \overset{*}{N}_{ji}^{T} + \overset{*}{N}_{ij}^{T}\ \frac{\partial \overset{*}{N}_{ji}^{T}}{\partial t_i} = -\,2\,\overset{*}{N}_{ij}^{T}\ \overset{*}{W}_i\ \overset{*}{N}_{ji}^{T} \qquad \text{(F-87)}$$

It is clear that both (F-86) and (F-87) can be satisfied if $\overset{*}{N}_{ji} = \pm\,\overset{*}{N}_{ij}^{T}$. The argument to be presented here is essentially the same as the one used in proving the symmetry of $\overset{*}{J}_{ij}$. Both (F-86) and (F-87) consist of first-order differential equations; therefore, if $\overset{*}{N}_{ji} = -\,\overset{*}{N}_{ij}^{T}$ at some particular time, the equality will be maintained for all values of time.

When $t_i = t_j$,

$$\overset{*}{M}_{jj} = \overset{*}{I}_3 \qquad \overset{*}{N}_{jj} = \overset{*}{O}_3 \qquad \overset{*}{T}_{jj} = \overset{*}{I}_3 \qquad \text{(F-88)}$$

From (F-53),

$$\left.\frac{\partial \overset{*}{N}_{ij}}{\partial t_i}\right|_{t_i = t_j} = -\,\overset{*}{W}_j\ \overset{*}{N}_{jj} + \overset{*}{T}_{jj} = \overset{*}{I}_3 \qquad \text{(F-89)}$$

From (F-70),

$$\left.\frac{\partial \overset{*}{N}_{ji}}{\partial t_i}\right|_{t_i = t_j} = \overset{*}{N}_{jj}\ \overset{*}{W}_j - \overset{*}{M}_{jj} = -\,\overset{*}{I}_3 \qquad \text{(F-90)}$$

Equation (F-88) shows that when $t_i = t_j$, $\overset{*}{N}_{ji} = \pm \overset{*}{N}_{ij}^T$, since both are equal to $\overset{*}{O}_3$. Equations (F-89) and (F-90) are used to pick the proper sign; because the diagonal elements of $\overset{*}{N}_{ij}$, and hence of $\overset{*}{N}_{ij}^T$, are increasing with t_i, while the diagonal elements of $\overset{*}{N}_{ji}$ are decreasing with t_i, the negative sign is required.

$$\overset{*}{N}_{ji} = - \overset{*}{N}_{ij}^T \tag{F-91}$$

and (F-76) has been proved.

The proof of (F-79) follows directly from substituting (F-34) into (F-91) and then inverting and transposing both sides of the equation.

$$\overset{*}{N}_{ji} = - \overset{*}{N}_{ij}^T = \overset{*}{K}_{ij}^{-1} = - \overset{*}{K}_{ji}^{T^{-1}} \tag{F-92}$$

$$\overset{*}{K}_{ji} = - \overset{*}{K}_{ij}^T \tag{F-93}$$

(F-78) and (F-79) are used to establish (F-75). The left-hand part of Eq. (F-40) is solved for $\overset{*}{T}_{ji}$, and substitutions are made for $\overset{*}{M}_{ij}$, $\overset{*}{N}_{ji}$, and $\overset{*}{N}_{ij}$ from (F-33) and (F-34).

$$\begin{aligned}
\overset{*}{T}_{ji} &= - \overset{*}{N}_{ij}^{-1} \overset{*}{M}_{ij} \overset{*}{N}_{ji} \\
&= - \overset{*}{K}_{ji} (- \overset{*}{K}_{ji}^{-1} \overset{*}{J}_{ji}) \overset{*}{K}_{ij}^{-1} \\
&= \overset{*}{J}_{ji} \overset{*}{K}_{ij}^{-1} = (- \overset{*}{K}_{ji}^{-1} \overset{*}{J}_{ji})^T \\
&= \overset{*}{M}_{ij}^T
\end{aligned} \tag{F-94}$$

The proof that $\overset{*}{S}_{ji} = - \overset{*}{S}_{ij}^{T}$ involves the same sequence of steps as that used in deriving (F-76). Equation (F-52) is pre-multiplied by $- \overset{*}{S}_{ji} \overset{*}{G}_i^{-1}$. The subscripts in (F-71) are interchanged, and the equation is then post-multiplied by $\overset{*}{G}_i^{-1} \overset{*}{S}_{ij}$. The two resulting equations are added.

$$
\begin{aligned}
& - \overset{*}{S}_{ji} \overset{*}{G}_i^{-1} \frac{\partial \overset{*}{S}_{ij}}{\partial t_i} - \overset{*}{S}_{ji} \overset{*}{G}_i^{-1} \overset{*}{W}_i \overset{*}{S}_{ij} \\
& + \frac{\partial \overset{*}{S}_{ji}}{\partial t_i} \overset{*}{G}_i^{-1} \overset{*}{S}_{ij} - \overset{*}{S}_{ji} \overset{*}{W}_i \overset{*}{G}_i^{-1} \overset{*}{S}_{ij} \\
& = - \overset{*}{S}_{ji} \overset{*}{M}_{ij} - \overset{*}{T}_{ji} \overset{*}{S}_{ij} \qquad \text{(F-95)}
\end{aligned}
$$

The right-hand side of (F-95) is the negative of the right-hand side of (F-40) and is therefore, equal to the zero matrix. (F-95) may then be simplified as follows:

$$
\begin{aligned}
& \frac{\partial \overset{*}{S}_{ji}}{\partial t_i} \overset{*}{G}_i^{-1} \overset{*}{S}_{ij} - \overset{*}{S}_{ji} \overset{*}{G}_i^{-1} \frac{\partial \overset{*}{S}_{ij}}{\partial t_i} \\
& = \overset{*}{S}_{ji} (\overset{*}{G}_i^{-1} \overset{*}{W}_i + \overset{*}{W}_i \overset{*}{G}_i^{-1}) \overset{*}{S}_{ij} \qquad \text{(F-96)}
\end{aligned}
$$

The transpose of (F-96) is

$$
\begin{aligned}
& - \frac{\partial \overset{*}{S}_{ij}^{T}}{\partial t_i} \overset{*}{G}_i^{-1} \overset{*}{S}_{ji}^{T} + \overset{*}{S}_{ij}^{T} \overset{*}{G}_i^{-1} \frac{\partial \overset{*}{S}_{ji}^{T}}{\partial t_i} \\
& = - \overset{*}{S}_{ij}^{T} (\overset{*}{G}_i^{-1} \overset{*}{W}_i + \overset{*}{W}_i \overset{*}{G}_i^{-1}) \overset{*}{S}_{ji}^{T} \qquad \text{(F-97)}
\end{aligned}
$$

Equations (F-96) and (F-97) can both be satisfied if

$$\overset{*}{S}_{ji} = \pm \overset{*}{S}_{ij}{}^{T}. \tag{F-98}$$

When $t_i = t_j$,

$$\overset{*}{S}_{jj} = \overset{*}{O}_3 = \pm \overset{*}{S}_{jj}{}^{T} \tag{F-99}$$

To determine the proper sign in (F-98) it is necessary to examine the derivatives of $\overset{*}{S}_{ij}$ and $\overset{*}{S}_{ji}$ with respect to t_i when $t_i = t_j$. From (F-52),

$$\left.\frac{\partial \overset{*}{S}_{ij}}{\partial t_i}\right|_{t_i = t_j} = - \overset{*}{W}_j \overset{*}{S}_{jj} + \overset{*}{G}_j \overset{*}{M}_{jj} = \overset{*}{G}_j \tag{F-100}$$

From (F-71)

$$\left.\frac{\partial \overset{*}{S}_{ji}}{\partial t_i}\right|_{t_i = t_j} = \overset{*}{S}_{jj} \overset{*}{W}_j - \overset{*}{T}_{jj} \overset{*}{G}_j = - \overset{*}{G}_j \tag{F-101}$$

Since $\overset{*}{G}$ is symmetric,

$$\left.\frac{\partial \overset{*}{S}_{ji}}{\partial t_i}\right|_{t_i = t_j} = - \left.\frac{\partial \overset{*}{S}_{ij}{}^{T}}{\partial t_i}\right|_{t_i = t_j} \tag{F-102}$$

It follows from (F-96), (F-97), (F-99), and (F-102) that

$$\overset{*}{S}_{ji} = - \overset{*}{S}_{ij}^{T} \tag{F-103}$$

All five of the relations stated at the beginning of this section have now been proved.

By the use of the first three relations, the 6-by-6 matrix $\overset{*}{C}_{ij}$ may be inverted by inspection.

$$\overset{*}{C}_{ij}^{-1} = \overset{*}{C}_{ji} = \begin{Bmatrix} \overset{*}{M}_{ji} & \overset{*}{N}_{ji} \\ \overset{*}{S}_{ji} & \overset{*}{T}_{ji} \end{Bmatrix} = \begin{Bmatrix} \overset{*}{T}_{ij}^{T} & -\overset{*}{N}_{ij}^{T} \\ -\overset{*}{S}_{ij}^{T} & \overset{*}{M}_{ij}^{T} \end{Bmatrix} \tag{F-104}$$

F. 8 Method of Adjoints

Since the completion of the work reported in the last section, the author has been apprised of two additional methods of proving the inverse relationship of Eq. (F-104). These are included here to round out the discussion of matrix formulations. The first method employs adjoint functions, and the second involves the properties of symplectic matrices.

The adjoint method is suggested in the work of McLean, Schmidt, and McGee[13]. The technique requires that Eq. (E-13), which consists of three second-order equations, be re-cast as a set of six first-order equations. This is accomplished as follows:

$$\delta \dot{\underline{x}} = \begin{Bmatrix} \delta \dot{\underline{r}} \\ \delta \dot{\underline{v}} \end{Bmatrix} = \begin{Bmatrix} \overset{*}{O}_3 & \overset{*}{I}_3 \\ \overset{*}{G} & \overset{*}{O}_3 \end{Bmatrix} \begin{Bmatrix} \delta \underline{r} \\ \delta \underline{v} \end{Bmatrix} = \overset{*}{Z}\, \delta \underline{x} \tag{F-105}$$

where

$$\overset{*}{Z} = \begin{Bmatrix} \overset{*}{O}_3 & \overset{*}{I}_3 \\ \overset{*}{G} & \overset{*}{O}_3 \end{Bmatrix} \tag{F-106}$$

The vector $\underline{\lambda}$, which is adjoint to $\delta\underline{x}$, is defined by the matrix equation

$$\dot{\underline{\lambda}} = -\overset{*}{Z}^T \underline{\lambda} \tag{F-107}$$

The six-component vector $\underline{\lambda}$ may be partitioned into two three-component vectors $\underline{\mu}$ and $\underline{\nu}$.

$$\dot{\underline{\lambda}} = \begin{Bmatrix} \dot{\underline{\mu}} \\ \dot{\underline{\nu}} \end{Bmatrix} = \begin{Bmatrix} \overset{*}{O}_3 & -\overset{*}{G}^T \\ -\overset{*}{I}_3 & \overset{*}{O}_3 \end{Bmatrix} \begin{Bmatrix} \underline{\mu} \\ \underline{\nu} \end{Bmatrix} \tag{F-108}$$

Since $\overset{*}{G}$ is a symmetric matrix,

$$\dot{\underline{\mu}} = -\overset{*}{G}\,\underline{\nu} \tag{F-109}$$

Also,

$$\dot{\underline{\nu}} = -\underline{\mu} \tag{F-110}$$

(F-109) and (F-110) can be combined into a single second-order vector equation.

$$\ddot{\underline{\nu}} = \overset{*}{G}\,\underline{\nu} \tag{F-111}$$

This equation has the same form as (E-13).

As a consequence of (F-110), $\underline{\lambda}$ may be written as

$$\underline{\lambda} = \begin{Bmatrix} \underline{\mu} \\ \underline{\nu} \end{Bmatrix} = \begin{Bmatrix} -\dot{\underline{\nu}} \\ \underline{\nu} \end{Bmatrix} \tag{F-112}$$

To show the relation between $\delta\underline{x}$ and $\underline{\lambda}$, pre-multiply (F-105) by $\underline{\lambda}^T$, post-multiply the transpose of (F-107) by $\delta\underline{x}$, and add.

$$\underline{\lambda}^T \delta\dot{\underline{x}} + \dot{\underline{\lambda}}^T \delta\underline{x} = \underline{\lambda}^T \overset{*}{Z} \delta\underline{x} - \underline{\lambda}^T \overset{*}{Z} \delta\underline{x} = 0 \tag{F-113}$$

$$\frac{d}{dt} (\underline{\lambda}^T \delta\underline{x}) = 0 \tag{F-114}$$

$$\underline{\lambda}^T \delta\underline{x} = \text{constant} \tag{F-115}$$

Like $\delta\underline{x}$, $\underline{\lambda}$ must be a time-varying vector. By analogy with (F-35) $\underline{\lambda}_j$, the value of $\underline{\lambda}$ at t_j, may be related to $\underline{\lambda}_i$.

$$\underline{\lambda}_j = \overset{*}{D}_{ji} \underline{\lambda}_i \tag{F-116}$$

From (F-115),

$$\underline{\lambda}_j^T \delta\underline{x}_j = \underline{\lambda}_i^T \delta\underline{x}_i \tag{F-117}$$

(F-35) and (F-116) are substituted into (F-117).

$$\underline{\lambda}_i^T \overset{*}{D}_{ji}^T \overset{*}{C}_{ji} \delta\underline{x}_i = \underline{\lambda}_i^T \delta\underline{x}_i \tag{F-118}$$

Since $\delta \underline{x}_i$ is arbitrary and $\underline{\lambda}_i$ is assumed not to be a zero vector,

$$\overset{*}{D}_{ji}{}^{T} \overset{*}{C}_{ji} = \overset{*}{I}_6 \tag{F-119}$$

$$\overset{*}{C}_{ji}{}^{-1} = \overset{*}{D}_{ji}{}^{T} \tag{F-120}$$

Equation (F-120) relates the 6-by-6 solution matrix of (F-35) to the 6-by-6 solution matrix of (F-116).

A new six-component vector $\underline{\lambda}'$ is defined as follows:

$$\underline{\lambda}' = \begin{Bmatrix} \underline{\nu} \\ \dot{\underline{\nu}} \end{Bmatrix} \tag{F-121}$$

$\underline{\lambda}'$ is related to $\underline{\lambda}$ by the skew-symmetric matrix $\overset{*}{P}$.

$$\underline{\lambda}' = \overset{*}{P}\ \underline{\lambda} \tag{F-122}$$

where

$$\overset{*}{P} = \begin{bmatrix} \overset{*}{O}_3 & \overset{*}{I}_3 \\ -\overset{*}{I}_3 & \overset{*}{O}_3 \end{bmatrix} \tag{F-123}$$

$\overset{*}{P}$ has some interesting properties.

$$\overset{*}{P}{}^2 = -\overset{*}{I}_3 \tag{F-124}$$

$$\overset{*}{P}{}^{-1} = \overset{*}{P}{}^{T} = -\overset{*}{P} \tag{F-125}$$

Equation (F-107) can now be written in terms of $\underline{\lambda}'$.

$$\dot{\underline{\lambda}} = \overset{*}{P}^{-1} \dot{\underline{\lambda}}' = - \overset{*}{Z}^{T} \overset{*}{P}^{-1} \underline{\lambda}' \tag{F-126}$$

This equation is pre-multiplied by $\overset{*}{P}$.

$$\dot{\underline{\lambda}}' = \overset{*}{P}\, \overset{*}{Z}^{T}\, \overset{*}{P}\, \underline{\lambda}' \tag{F-127}$$

When the matrix multiplication in (F-127) is carried out, it is found that

$$\overset{*}{P}\, \overset{*}{Z}^{T}\, \overset{*}{P} = \overset{*}{Z} \tag{F-128}$$

$$\therefore \dot{\underline{\lambda}}' = Z \underline{\lambda}' \tag{F-129}$$

The form of (F-129) is identical with that of (F-105). Therefore, the solution for $\underline{\lambda}'$ must be the same as that for $\delta\underline{x}$ except for a difference in the six arbitrary constants. The constants for $\underline{\lambda}'$ are the components of $\underline{\lambda}_i'$. Then, by analogy with (F-35),

$$\underline{\lambda}_j' = \overset{*}{C}_{ji}\, \underline{\lambda}_i' \tag{F-130}$$

From (F-116), (F-122), and (F-130),

$$\underline{\lambda}_j' = \overset{*}{P}\, \underline{\lambda}_j = \overset{*}{C}_{ji}\, \overset{*}{P}\, \underline{\lambda}_i = \overset{*}{P}\, \overset{*}{D}_{ji}\, \underline{\lambda}_i \tag{F-131}$$

For an arbitrary $\underline{\lambda}_i$,

$$\overset{*}{C}_{ji}\, \overset{*}{P} = \overset{*}{P}\, \overset{*}{D}_{ji} \tag{F-132}$$

$$\overset{*}{D}_{ji} = \overset{*}{P}^{-1}\, \overset{*}{C}_{ji}\, \overset{*}{P} = - \overset{*}{P}\, \overset{*}{C}_{ji}\, \overset{*}{P} \tag{F-133}$$

From (F-120), the inverse of $\overset{*}{C}_{ji}$ is

$$\overset{*}{C}_{ji}^{-1} = \overset{*}{D}_{ji}^{T} = - \overset{*}{P}\, \overset{*}{C}_{ji}^{T}\, \overset{*}{P} \qquad \text{(F-134)}$$

The matrix multiplication is carried out by use of the definitions given in (F-36) and (F-123).

$$\overset{*}{C}_{ji}^{-1} = \begin{Bmatrix} \overset{*}{T}_{ji}^{T} & -\overset{*}{N}_{ji}^{T} \\ -\overset{*}{S}_{ji}^{T} & \overset{*}{M}_{ji}^{T} \end{Bmatrix} \qquad \text{(F-135)}$$

This equation is the equivalent of (F-104).

F.9 Symplectic Matrices

The author is indebted to Dr. James E. Potter, of the staff of the M.I.T. Instrumentation Laboratory, who first pointed out to him that the transition matrix is symplectic and that this fact can be exploited in studying the properties of the transition matrix. A mathematically rigorous discussion of symplectic groups is presented in Chapter VI of Weyl.[42]

A symplectic matrix can be defined by analogy with an orthogonal matrix. The matrix $\overset{*}{A}$ is orthogonal if

$$\overset{*}{A}^{T}\, \overset{*}{I}\, \overset{*}{A} = \overset{*}{I} \qquad \text{(F-136)}$$

$\overset{*}{I}$ being the familiar identity matrix. The matrix $\overset{*}{Y}$ is symplectic if

$$\overset{*}{A}^{T}\, \overset{*}{P}\, \overset{*}{A} = \overset{*}{P} \qquad \text{(F-137)}$$

where $\overset{*}{P}$ is given by (F-123).

It will now be shown that $\overset{*}{C}_{ji}$ is symplectic. The time derivative of the scalar quantity $\delta\underline{x}^T \overset{*}{P} \delta\underline{x}$ is

$$\frac{d}{dt}(\delta\underline{x}^T \overset{*}{P} \delta\underline{x}) = \delta\dot{\underline{x}}^T P \delta\underline{x} + \delta\underline{x}^T P \delta\dot{\underline{x}}$$

$$= \delta\underline{x}^T \overset{*}{Z}^T \overset{*}{P} \delta\underline{x} + \delta\underline{x}^T \overset{*}{P} \overset{*}{Z} \delta\underline{x}$$

$$= \delta\underline{x}^T (\overset{*}{Z}^T \overset{*}{P} + \overset{*}{P} \overset{*}{Z}) \delta\underline{x} \qquad \text{(F-138)}$$

From the definitions of $\overset{*}{Z}$ and $\overset{*}{P}$ and the fact that $\overset{*}{G}$ is symmetric, it can be shown that $(\overset{*}{Z}^T \overset{*}{P} + \overset{*}{P} \overset{*}{Z})$ is equal to the 6-by-6 zero matrix. Then,

$$\frac{d}{dt}(\delta\underline{x}^T \overset{*}{P} \delta\underline{x}) = 0 \qquad \text{(F-139)}$$

$$\delta\underline{x}_j^T \overset{*}{P} \delta\underline{x}_j = \delta\underline{x}_i^T \overset{*}{P} \delta\underline{x}_i = \text{constant} \qquad \text{(F-140)}$$

(F-35) is substituted into (F-140).

$$\delta\underline{x}_i^T \overset{*}{C}_{ji}^T \overset{*}{P} \overset{*}{C}_{ji} \delta\underline{x}_i = \delta\underline{x}_i^T \overset{*}{P} \delta\underline{x}_i \qquad \text{(F-141)}$$

Since $\delta\underline{x}_i$ is arbitrary,

$$\overset{*}{C}_{ji}^T \overset{*}{P} \overset{*}{C}_{ji} = \overset{*}{P} \qquad \text{(F-142)}$$

and hence $\overset{*}{C}_{ji}$ is a symplectic matrix.

To find $\overset{*}{C}_{ji}^{-1}$, (F-142) is pre-multiplied by $-\overset{*}{P}$ and post-multiplied by $\overset{*}{C}_{ji}^{-1}$.

$$\overset{*}{C}_{ji}^{-1} = -\overset{*}{P} \overset{*}{C}_{ji}^T \overset{*}{P} \qquad \text{(F-143)}$$

Equation (F-143) is the same as (F-134). Thus, the triple matrix product of (F-143) leads to the expression for $\overset{*}{C}_{ji}^{-1}$ given by (F-135).

Equation (F-142) may be used to evaluate the determinant of $\overset{*}{C}_{ji}$. Since the determinant of a matrix is equal to the determinant of its transpose,

$$(\det \overset{*}{C}_{ji})\,(\det \overset{*}{P})\,(\det \overset{*}{C}_{ji}) = \det \overset{*}{P} \qquad \text{(F-144)}$$

From the definition of $\overset{*}{P}$ in (F-123),

$$\det \overset{*}{P} = +1 \qquad \text{(F-145)}$$

Then,

$$(\det \overset{*}{C}_{ji})^2 = 1 \qquad \text{(F-146)}$$

$$\det \overset{*}{C}_{ji} = \pm 1 \qquad \text{(F-147)}$$

Since $\overset{*}{C}_{ii} = \overset{*}{I}_6$ and the elements of $\overset{*}{C}_{ji}$ are continuous functions of time, the plus sign is required in (F-147).

$$\det \overset{*}{C}_{ji} = +1 \qquad \text{(F-148)}$$

This equation is useful in checking the numerical evaluation of the elements of $\overset{*}{C}_{ji}$.

APPENDIX G

INTEGRATION OF THE VARIANT EQUATIONS OF MOTION FOR ELLIPTICAL REFERENCE TRAJECTORIES

G.1 Summary

The variant equations of motion are developed for the two-body problem. The system consists of three second-order linear differential equations with variable coefficients. By choosing as a set of coordinate axes one of the reference trajectory sets of Appendix A, the sixth-order system is sub-divided into two uncoupled systems, one of fourth order and the other of second order. The two uncoupled systems are integrated directly to yield position variation relative to the reference trajectory.

G.2 Variant Equations for Two-Body Motion

The variant equations for many-body motion are developed in Appendix E. The matrix equations in the three reference trajectory coordinate systems are (E-11), (E-18), and (E-19). For two-body motion the equations are considerably simplified by the removal of all effects of disturbing forces.

Just as the r s z coordinate system was used to integrate the general equations of two-body motion in Appendix B, so it has been found that the same coordinate system is most effective in integrating the variant equations of two-body motion. When the disturbing forces are neglected in Eq. (E-18), z is equal to zero, and ρ may be replaced

by r. Then the variant equations become

$$\begin{pmatrix} \ddot{\delta r} - \dot{f}^2\,\delta r - 2\dot{f}\,\dot{\delta s} - \ddot{f}\,\delta s \\ 2\dot{f}\,\dot{\delta r} + \ddot{f}\,\delta r + \ddot{\delta s} - \dot{f}^2\,\delta s \\ \ddot{\delta z} \end{pmatrix} = \frac{\mu}{r^3}\begin{pmatrix} 2 & 0 & 0 \\ 0 & -1 & 0 \\ 0 & 0 & -1 \end{pmatrix}\begin{pmatrix} \delta r \\ \delta s \\ \delta z \end{pmatrix} \qquad \text{(G-1)}$$

This equation can be simplified by expressing δs and its derivatives in terms of δf and its derivatives.

$$\delta s = r\,\delta f \qquad \text{(G-2)}$$

$$\dot{\delta s} = r\,\dot{\delta f} + \dot{r}\,\delta f \qquad \text{(G-3)}$$

$$\ddot{\delta s} = r\,\ddot{\delta f} + 2\,\dot{r}\,\dot{\delta f} + \ddot{r}\,\delta f \qquad \text{(G-4)}$$

These three equations are substituted into the left-hand side of (G-1).

$$\begin{pmatrix} \ddot{\delta r} - \dot{f}^2\,\delta r - 2\,r\,\dot{f}\,\dot{\delta f} - (2\,\dot{r}\,\dot{f} + r\,\ddot{f})\,\delta f \\ 2\,\dot{f}\,\dot{\delta r} + \ddot{f}\,\delta r + r\,\ddot{\delta f} + 2\,\dot{r}\,\dot{\delta f} + (\ddot{r} - r\,\dot{f}^2)\,\delta f \\ \ddot{\delta z} \end{pmatrix}$$

$$= \frac{\mu}{r^3}\begin{pmatrix} 2 & 0 & 0 \\ 0 & -1 & 0 \\ 0 & 0 & -1 \end{pmatrix}\begin{pmatrix} \delta r \\ \delta s \\ \delta z \end{pmatrix} \qquad \text{(G-5)}$$

The equations of (B-32) are substituted into (G-5).

$$\begin{pmatrix} \delta\ddot{r} - \dot{f}^2\,\delta r - 2\,r\,\dot{f}\,\delta\dot{f} \\ 2\,\dot{f}\,\delta\dot{r} + \ddot{f}\,\delta r + r\,\delta\ddot{f} + 2\,\dot{r}\,\delta\dot{f} \\ \delta\ddot{z} \end{pmatrix} = \frac{\mu}{r^3}\begin{pmatrix} 2\,\delta r \\ 0 \\ -\,\delta z \end{pmatrix} \qquad \text{(G-6)}$$

It is immediately apparent from (G-6) that the variant motion in the reference trajectory plane and the variant motion perpendicular to that plane are completely independent of each other. Therefore, the two types of motion will be studied separately.

G.3 Three Solutions for Motion in Reference Trajectory Plane

The motion in the reference trajectory plane will be investigated first. This motion involves the first two equations of (G-6). The two equations are coupled equations in the variables δr and δf. They may be re-written as follows:

$$(D^2 - \dot{f}^2 - \frac{2\mu}{r^3})\,\delta r - 2\,r\,\dot{f}\,D\,\delta f = 0 \qquad \text{(G-7)}$$

$$(2\,\dot{f}\,D + \ddot{f})\,\delta r + (r\,D + 2\,\dot{r})\,D\,\delta f = 0 \qquad \text{(G-8)}$$

where the operator D is equal to $\frac{d}{dt}$.

These two equations constitute a fourth-order system in the variables δr and δf. Since δf itself does not appear in either equation, the system may be regarded as third-order in the variables δr and $D\,\delta f$.

The fact that δf does not appear in either equation indicates that δr is dependent on only the derivatives of δf, not on δf itself. One solution of the coupled equations is then

$$\delta r = 0 \qquad \delta f = k_1 \tag{G-9}$$

where k_1 is an arbitrary constant.

The solution of the third-order system of (G-7) and (G-8) is expedited if the independent variable is changed from t to f. The symbol F is used to represent $\frac{d}{df}$. The following substitutions may be made:

$$D = \dot{f}\, F \tag{G-10}$$

$$D^2 = \dot{f}\, F\, (\dot{f}\, F) \tag{G-11}$$

From (B-58),

$$F\, \dot{f} = \frac{-\, 2\, n\, e \sin f\, (1 + e \cos f)}{(1 - e^2)^{3/2}}$$

$$= -\, \frac{2\, e \sin f}{1 + e \cos f}\, \dot{f} \tag{G-12}$$

(G-12) is substituted into (G-11).

$$D^2 = \dot{f}^2 \left(F^2 - \frac{2\, e \sin f}{1 + e \cos f}\, F\right) \qquad \text{(G-13)}$$

From (B-39), (B-60), and (B-61),

$$-\frac{2\mu}{r^3} = -\frac{2\,\mu\, r\, \dot{f}^2}{h^2} = -\frac{2\,\dot{f}^2}{1 + e \cos f} \qquad \text{(G-14)}$$

The coefficient of δf in (G-7) is

$$-2\, r\, \dot{f}\, D = -\frac{2\, a\,(1 - e^2)\, \dot{f}^2}{1 + e \cos f}\, F \qquad \text{(G-15)}$$

Equations (G-13), (G-14), and (G-15) are incorporated into (G-7), and the resulting equation is multiplied by

$$\frac{(1 + e \cos f)}{\dot{f}^2}$$

$$\left[(1 + e \cos f)\, F^2 - (2\, e \sin f)\, F - (3 + e \cos f)\right] \delta r$$

$$- 2\, a\,(1 - e^2)\, F\, \delta f = 0 \qquad \text{(G-16)}$$

The coefficient of δr in (G-8) is

$$(2\dot{f} D + \ddot{f}) = 2\dot{f}^2 \left(F - \frac{e \sin f}{1 + e \cos f}\right) \qquad \text{(G-17)}$$

With the aid of (B-65) and (B-66), the coefficient of δf in (G-8) may be written as follows:

$$r D^2 + 2\dot{r} D = r\dot{f}^2 \left(F^2 - \frac{2e \sin f}{1 + e \cos f} F\right) + 2\dot{r}\dot{f} F$$

$$= r\dot{f}^2 F^2 + 2\dot{f}\left(\dot{r} - \frac{e \sin f}{1 + e \cos f} r\dot{f}\right) F$$

$$= r\dot{f}^2 F^2 \qquad \text{(G-18)}$$

(G-17) and (G-18) are substituted into (G-8), and this equation, like (G-2) is multiplied by

$$\frac{(1 + e \cos f)}{\dot{f}^2}.$$

$$2\left[(1 + e \cos f) F - e \sin f\right] \delta r + a(1 - e^2) F^2 \delta f = 0 \qquad \text{(G-19)}$$

The variable δf may be eliminated from the coupled equations (G-16) and (G-19) by pre-multiplying the former by the operator F,

multiplying the latter by 2, and then adding.

$$[(1 + e \cos f) F^3 - (3 e \sin f) F^2$$

$$+ (1 + e \cos f) F - (3 e \sin f)] \delta r = 0 \qquad \text{(G-20)}$$

The terms of (G-20) may be re-grouped as follows:

$$[(1 + e \cos f) F - (3 e \sin f)] (F^2 + 1) \delta r = 0 \qquad \text{(G-21)}$$

Two solutions of (G-16) are obtained from

$$(F^2 + 1) \delta r = 0 \qquad \text{(G-22)}$$

These solutions are obviously

$$\delta r = k_2 \cos f \qquad \text{(G-23)}$$

$$\delta r = k_3 \sin f \qquad \text{(G-24)}$$

The solution of (G-23) is substituted into (G-16) in order to solve for $F\ \delta f$.

$$F\ \delta f = - \frac{k_2}{a (1 - e^2)} [2 \cos f + e (\cos^2 f - \sin^2 f)] \qquad \text{(G-25)}$$

Then δf is obtained by integration.

$$\delta f = - \frac{k_2}{a (1 - e^2)} (2 + e \cos f) \sin f \qquad \text{(G-26)}$$

The solution of (G-24) is handled in similar fashion.

$$F\ \delta f = -\frac{2\,k_3}{a\,(1 - e^2)}\,(1 + e\cos f)\sin f \qquad \text{(G-27)}$$

$$\delta f = \frac{k_3}{a\,(1 - e^2)}\,(2 + e\cos f)\cos f \qquad \text{(G-28)}$$

G.4 Fourth Solution for Motion in Reference Trajectory Plane

The first three solutions of Eqs. (G-7) and (G-8) were obtained relatively easily. The fourth solution requires considerably more mathematical manipulation.

One technique for obtaining the fourth solution is to substitute the two known solutions, (G-23) and (G-24), successively into (G-20) and by so doing to reduce (G-20) from a third-order equation to a first-order equation, which can be solved directly by the use of an integrating factor. A method which might be considered mathematically more elegant is the method of variation of parameters. Both methods are described in detail in the first chapter of Hildebrand[41] The second method is used in the following analysis.

In Eq. (G-21), let

$$x = (F^2 + 1)\,\delta r \qquad \text{(G-29)}$$

Then (G-21) may be written as follows:

$$\frac{dx}{df} - \frac{3\,e\sin f}{1 + e\cos f}\,x = 0 \qquad \text{(G-30)}$$

The variables x and f are now separable.

$$\frac{dx}{x} - \frac{3\,e \sin f}{1 + e \cos f}\,df = 0 \qquad \text{(G-31)}$$

This equation may be integrated directly. The result of the integration is

$$\log x + 3 \log (1 + e \cos f) = \log C \qquad \text{(G-32)}$$

where C is an arbitrary constant. Then,

$$x = (F^2 + 1)\,\delta r = \frac{C}{(1 + e \cos f)^3} \qquad \text{(G-33)}$$

Since the two homogeneous solutions of (G-33) are known to be cos f and sin f, the method of variation of parameters may be used to get the particular solution of (G-33). In this method, the solution is assumed to be of the form.

$$\delta r = u \cos f + v \sin f \qquad \text{(G-34)}$$

where u and v are functions of f. The variables u and v must satisfy the following two criteria:

$$\frac{du}{df} \cos f + \frac{dv}{df} \sin f = 0 \qquad \text{(G-35)}$$

$$\frac{du}{df}\,\frac{d\,(\cos f)}{df} + \frac{dv}{df}\,\frac{d\,(\sin f)}{df}$$

$$= -\frac{du}{df} \sin f + \frac{dv}{df} \cos f = \frac{C}{(1 + e \cos f)^3} \qquad \text{(G-36)}$$

The two simultaneous equations (G-35) and (G-36) are solved for $\frac{du}{df}$ and $\frac{dv}{df}$.

$$\frac{du}{df} = - \frac{C \sin f}{(1 + e \cos f)^3} \qquad \text{(G-37)}$$

$$\frac{dv}{df} = \frac{C \cos f}{(1 + e \cos f)^3} \qquad \text{(G-38)}$$

Equation (G-37) may be integrated directly.

$$u = - C \int \frac{\sin f \, df}{(1 + e \cos f)^3} = \frac{C}{e} \frac{d(1 + e \cos f)}{(1 + e \cos f)^3}$$

$$= - \frac{C}{2 e (1 + e \cos f)^2} \qquad \text{(G-39)}$$

The integration of (G-38) is less obvious. It is desirable to remove the polynomial in the denominator by making a change of variable from the true anomaly f to the eccentric anomaly E. Equations (B-52), (B-54), and (B-64) are used in making the change.

$$v = C\int \frac{\cos f \; df}{(1 + e \cos f)^3}$$

$$= C\int \frac{\cos E - e}{1 - e \cos E} \cdot \frac{(1 - e \cos E)^3}{(1 - e^2)^3} \cdot \frac{(1 - e^2)^{1/2}}{1 - e \cos E} \; dE$$

$$= \frac{C}{(1 - e^2)^{5/2}} \int (1 - e \cos E)(\cos E - e) \, dE$$

$$= \frac{C}{(1 - e^2)^{5/2}} \int [-e + (1 + e^2) \cos E - e \cos^2 E] \, dE \qquad \text{(G-40)}$$

The individual terms of (G-40) can now be integrated.

$$v = \frac{C}{(1 - e^2)^{5/2}} \left[-e E + (1 + e^2) \sin E - \frac{e}{2} (E + \sin E \cos E)\right]$$

$$= \frac{C}{2 (1 - e^2)^{5/2}} \{ -3 e E + [2 (1 + e^2) - e \cos E] \sin E \} \qquad \text{(G-41)}$$

No constants of integration have been added in (G-39) and (G-41) because such constants, which would simply be multiplied by cos f and sin f respectively, may be incorporated into the constants k_2 and k_3 of Eqs. (G-23) and (G-24).

In (G-41), the eccentric anomaly E may be written in terms of the mean anomaly M and sin E by the use of Kepler's equation (B-55). Then the terms in E may be converted back to functions of f by using (B-53) and (B-54).

$$v = \frac{C}{2\,(1-e^2)^{5/2}} \left\{ -3e\left[M + \frac{e\,(1-e^2)^{1/2}\sin f}{1+e\cos f}\right] + \left[2\,(1+e^2) - \frac{e\,(\cos f + e)}{1+e\cos f}\right] \frac{(1-e^2)^{1/2}\sin f}{1+e\cos f} \right\}$$

$$= \frac{C}{2\,(1-e^2)}\left[-\frac{3\,e\,M}{(1-e^2)^{3/2}} + \frac{(2+e\cos f)\sin f}{(1+e\cos f)^2}\right] \qquad \text{(G-42)}$$

Equations (G-39) and (G-42) are substituted into (G-34) to yield the fourth solution for δr.

$$\delta r = C\left[-\frac{\cos f}{2e\,(1+e\cos f)^2} - \frac{3\,e\,M\sin f}{2\,(1-e^2)^{5/2}} + \frac{(2+e\cos f)\sin^2 f}{2(1-e^2)(1+e\cos f)^2}\right]$$

$$= \frac{C}{1-e^2}\left[-\frac{3\,e\,M\sin f}{2\,(1-e^2)^{3/2}} + \frac{1}{1+e\cos f} - \frac{\cos f}{2e}\right] \qquad \text{(G-34)}$$

The term

$$-\frac{C}{2e\,(1-e^2)}\cos f$$

in Eq. (G-43) may be incorporated into the constant k_2 of Eq. (G-23),

so that the fourth solution becomes, finally,

$$\delta r = k_4 \left[- \frac{3\, e\, M \sin f}{2\,(1 - e^2)^{3/2}} + \frac{1}{1 + e \cos f} \right] \qquad \text{(G-44)}$$

where

$$k_4 = \frac{C}{1 - e^2} \qquad \text{(G-45)}$$

To determine the fourth solution for δf from (G-16), the first and second derivatives of (G-44) with respect to f must be found. The derivative of M with respect to f is obtained from (B-56) and (B-58).

$$F(M) = \frac{\dot{M}}{f} = \frac{(1 - e^2)^{3/2}}{(1 + e \cos f)^2} \qquad \text{(G-46)}$$

The derivatives of (G-44) are

$$F(\delta r) = k_4 \left\{ - \frac{3\, e}{2\,(1 - e^2)^{3/2}} \left[M \cos f + \frac{(1 - e^2)^{3/2} \sin f}{(1 + e \cos f)^2} \right] + \frac{e \sin f}{(1 + e \cos f)^2} \right\}$$

$$= - k_4 \left[\frac{3\, e\, M \cos f}{2\,(1 - e^2)^{3/2}} + \frac{e \sin f}{2\,(1 + e \cos f)^2} \right] \qquad \text{(G-47)}$$

$$F^2(\delta r) = -k_4 \left\{ \frac{3e}{2(1-e^2)^{3/2}} \left[-M \sin f + \frac{(1-e^2)^{3/2} \cos f}{(1+e\cos f)^2} \right] + \frac{e\cos f}{2(1+e\cos f)^2} + \frac{e^2 \sin^2 f}{(1+e\cos f)^3} \right\}$$

$$= k_4 \left[\frac{3e\,M \sin f}{2(1-e^2)^{3/2}} - \frac{1}{1+e\cos f} + \frac{1-e^2}{(1+e\cos f)^3} \right] \qquad \text{(G-48)}$$

When (G-47) and (G-48) are substituted into (G-16), the resulting expression for $F(\delta f)$ is

$$F(\delta f) = \frac{3k_4}{2a(1-e^2)} \left[\frac{2e\,M(1+e\cos f)\sin f}{(1-e^2)^{3/2}} - 1 \right] \qquad \text{(G-49)}$$

Integration by parts is used to solve for δf from (G-49). Note that

$$dM = (1-e\cos E)\,dE = \frac{(1-e^2)^{3/2}\,df}{(1+e\cos f)^2} \qquad \text{(G-50)}$$

Therefore,

$$e\,M(1+e\cos f)\sin f\,df = -M(1+e\cos f)\,d(1+e\cos f)$$

$$= -d\left[\tfrac{1}{2} M(1+e\cos f)^2\right] + \tfrac{1}{2}(1+e\cos f)^2\,dM$$

$$= -d\left[\tfrac{1}{2} M(1+e\cos f)^2\right] + \tfrac{1}{2}(1-e^2)^{3/2}\,df \qquad \text{(G-51)}$$

The integral of (G-49) is simply

$$\delta f = - \frac{3\, k_4}{2a\,(1-e^2)^{5/2}}\, M\,(1+e\cos f)^2 \qquad \text{(G-52)}$$

No constant of integration is needed in deriving δf from $F(\delta f)$ because of the presence of the constant k_1, which is the first solution of δf.

G. 5 Solutions for Motion Normal to Reference Trajectory Plane

The differential equation for the motion normal to the reference trajectory plane is the third equation of (G-6).

$$\left(D^2 + \frac{\mu}{r^3}\right)\, \delta z = 0 \qquad \text{(G-53)}$$

To solve for δz, the independent variable is changed from t to the eccentric anomaly E. The symbol J is used for the operator $\frac{d}{dE}$. The operator D^2 in (G-53) can be expressed in terms of J and J^2.

$$D = \dot{E}\, J \qquad \text{(G-54)}$$

$$D^2 = \dot{E}\, J\,(\dot{E}\, J) = \dot{E}\left[\, \dot{E}\, J^2 + \frac{d\dot{E}}{dE}\, J \,\right] \qquad \text{(G-55)}$$

From (B-57),

$$\frac{d\dot{E}}{dE} = - \frac{n\, e \sin E}{(1 - e\cos E)^2} = - \frac{e \sin E}{1 - e\cos E}\, \dot{E} \qquad \text{(G-56)}$$

Then,

$$D^2 = \frac{\dot{E}^2}{(1 - e \cos E)} \left[(1 - e \cos E) J^2 - (e \sin E) J \right] \qquad \text{(G-57)}$$

From (B-49), (B-57), and (B-62),

$$\frac{\mu}{r^3} = \frac{n^2 a^3}{a^3 (1 - e \cos E)^3} = \frac{\dot{E}^2}{(1 - e \cos E)} \qquad \text{(G-58)}$$

(G-57) and (G-58) are substituted into (G-53), and the equation is multiplied by

$$\frac{1 - e \cos E}{\dot{E}^2}.$$

$$\left[(1 - e \cos E) J^2 - (e \sin E) J + 1 \right] \delta z = 0 \qquad \text{(G-59)}$$

The terms in (G-59) may be re-arranged as follows:

$$\left[(J^2 + 1) - e (\cos E J + \sin E) J \right] \delta z = 0 \qquad \text{(G-60)}$$

From the appearance of (G-60), two possible trial solutions for δz are immediately suggested, namely, sin E and cos E. It is found that sin E is indeed a solution. However, when δz = cos E is tried, the result is

$$\left[(J^2 + 1) - e (\cos E J + \sin E) J \right] (\cos E) = e \qquad \text{(G-61)}$$

Since e is a constant and since the coefficient of the undifferentiated term in (G-59) is unity, the second solution is (cos E - e).

The two solutions may be expressed in terms of the true anomaly f by making use of (B-52), (B-53), and (B-54).

$$\delta z = \frac{k_5}{(1 - e^2)^{1/2}} \sin E = k_5 \frac{\sin f}{1 + e \cos f} \qquad \text{(G-62)}$$

$$\delta z = \frac{k_6}{(1 - e^2)} (\cos E - e) = k_6 \frac{\cos f}{1 + e \cos f} \qquad \text{(G-63)}$$

G. 6 Complete Solution for Position Variation

The results of this appendix may be summarized by tabulating the complete solution for the position variation vector $\delta \underline{r}$ in the r s z coordinate system. The component δs, in the transverse direction, is related to δf by the equation

$$\delta s = r \, \delta f = \frac{a (1 - e^2)}{1 + e \cos f} \delta f \qquad \text{(G-64)}$$

From Sections (G. 3), (G. 4), and (G. 5), the complete solution in terms of the variables f and M is

$$\delta r = k_2 \cos f + k_3 \sin f + k_4 \left[- \frac{3 e M \sin f}{2 (1 - e^2)^{3/2}} + \frac{1}{1 + e \cos f} \right] \qquad \text{(G-65)}$$

$$\delta s = \frac{k_1 a (1 - e^2)}{1 + e \cos f} - \frac{k_2 (2 + e \cos f) \sin f}{1 + e \cos f}$$

$$+ \frac{k_3 (2 + e \cos f) \cos f}{1 + e \cos f} - \frac{3 k_4 M (1 + e \cos f)}{2 (1 - e^2)^{3/2}} \qquad \text{(G-66)}$$

$$\delta z = \frac{k_5 \sin f}{1 + e \cos f} + \frac{k_6 \cos f}{1 + e \cos f} \qquad \text{(G-67)}$$

The variant motion in the z direction is an undamped oscillation whose period is equal to the period of the reference trajectory.

The variant motion in the reference trajectory plane is more easily analyzed if the equation for δs is re-arranged as follows:

$$\delta s = \frac{k_1 a (1 - e^2)}{1 + e \cos f} - k_2 \left(1 + \frac{1}{1 + e \cos f}\right) \sin f$$

$$+ k_3 \left(1 + \frac{1}{1 + e \cos f}\right) \cos f - \frac{3 k_4 M (1 + e \cos f)}{2 (1 - e^2)^{3/2}} \qquad \text{(G-68)}$$

In addition to an undamped oscillation whose period is equal to that of the reference trajectory, the variant motion in the reference trajectory plane contains an oscillation that is modulated by a ramp function. Thus, the motion in the reference plane is dynamically unstable; the amplitude of the variation in position increases steadily as the number of periods is increased.

It should be pointed out that this analysis is based on linear perturbation theory; the conclusions drawn are applicable only as long as the position variations from the reference trajectory are small.

APPENDIX H

DETERMINATION OF VARIANT MOTION FROM FIRST VARIATIONS OF ORBITAL ELEMENTS

H. 1 Summary

First variations are taken of the six orbital elements that define the motion along an elliptical reference trajectory. The motion along the actual trajectory is a function of these six variations and the known characteristics of the reference trajectory. The basic analysis is applicable to ellipses of low eccentricity (approximately circular) as well as ellipses of moderate eccentricity; it is not applicable when e is equal to unity.

The general equations are applied to the particular case when e is not very close to either zero or unity. It is shown that the resulting equations for position variation are analogous to those developed in Appendix G.

H. 2 Introduction

In the variant two-body problem, if the reference trajectory is known to be an ellipse of moderate eccentricity, and if there are no disturbing forces, then the actual trajectory, which is assumed to differ only slightly from the reference trajectory, must also be an ellipse of moderate eccentricity. One method of attacking the variant problem is to assume small variations in each of the six known orbital elements of the reference trajectory and to determine the effect of these variations on position as a function of time. It is convenient to use, instead of position on the actual trajectory, the difference between position on the actual trajectory at time t and position on the reference trajectory at the same time. This difference, in vector form, is $\delta \underline{r}$.

This approach to the problem is primarily geometric; it depends on the a priori assumption that the variant trajectory is an ellipse.

In contrast, the approach of Appendix G is analytic; it requires no such assumption. Indeed, the solution of Appendix G, with its secular term, hardly resembles any of the more familiar forms of the equations of elliptical motion.

H. 3 Effect of Variation in Euler Angles

The x y z coordinate system, as defined in Appendix A, is related to the vehicle's reference trajectory plane. A new coordinate system, designated x' y' z', will now be introduced, with the axes of the new system bearing the same relationship to the actual trajectory that the axes of x y z bear to the reference trajectory. The origin of the new system is at the center of the sun. The x' - y' plane is the plane of the actual two-body trajectory. The positive x'-axis lies in the direction of perihelion from the sun. The positive y'-axis is 90° ahead of the positive x'-axis in the direction of vehicle motion. The positive z'-axis is parallel to the angular momentum vector of the actual trajectory. The x' y' z' coordinate system, like the x y z system, is a non-rotating coordinate system.

The Euler angles defining the orientation of the x' y' z' system relative to the x y z system are $\delta\Omega$, δi, and $\delta\omega$, as shown in Fig. H. 1. Each of the three angles is regarded as a variation from its reference value, which is zero in each case. If the launch guidance were perfect, the x' y' z' and x y z systems would coincide.

The prime notation is used to designate characteristics of the actual trajectory. Thus, $\underline{r}'$ is the position vector on the actual trajectory, and f' is the true anomaly on the actual trajectory.

The vector $\underline{r}'$ can be resolved into its components along the r, s, and z axes of the reference trajectory local vertical coordinate system. The symbols used for the components are r'_r, r'_s, and r'_z. From Fig. H. 1,

$$r'_r = r' [\cos (f' + \delta\omega) \cos (f - \delta\Omega) + \sin (f' + \delta\omega) \cos \delta i \sin (f - \delta\Omega)] \qquad \text{(H-1)}$$

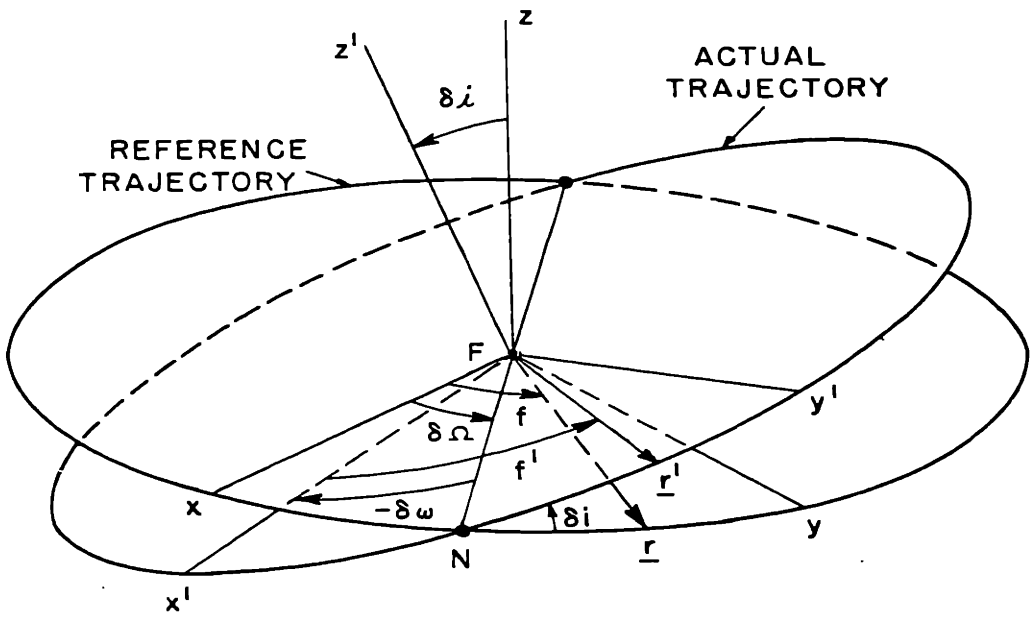

F – focus at center of sun

FN – line of nodes

Fx,Fy,Fz – axes of reference trajectory stationary coordinate system

Fx',Fy',Fz' – axes of actual trajectory stationary coordinate system

$\delta\Omega, \delta i, \delta\omega$ – orientation angles between two coordinate systems

$\underline{r}$ – position vector on reference trajectory at time t

$\underline{r}'$ – position vector on actual trajectory at time t

f – true anomaly on reference trajectory at time t

f' – true anomaly on actual trajectory at time t

Figure H.1 Orientation of Actual Trajectory Relative to Reference Trajectory

$$r'_s = r' [-\cos (f' + \delta\omega) \sin (f - \delta\Omega)$$

$$+ \sin (f' + \delta\omega) \cos \delta i \cos (f - \delta\Omega)] \qquad \text{(H-2)}$$

$$r'_z = r' \sin (f' + \delta\omega) \sin \delta i \qquad \text{(H-3)}$$

The components of position variation vector $\delta \underline{r}$ along the r, s, and z axes are

$$\delta r = r'_r - r \qquad \text{(H-4)}$$

$$\delta s = r'_s \qquad \text{(H-5)}$$

$$\delta z = r'_z \qquad \text{(H-6)}$$

The fundamental assumption of linear perturbation theory is that all variations from reference values be small. Thus, in Fig. H. 1, the separation of P' from P must be small, and, as a consequence, angle δi must be small. It is also necessary that the difference between $(f' + \delta\omega)$ and $(f - \delta\Omega)$ be small. This difference may be written as

$$(f' + \delta\omega) - (f - \delta\Omega) = \delta f + \delta\phi \qquad \text{(H-7)}$$

where

$$\delta f = f' - f \qquad \text{(H-8)}$$

$$\delta\phi = \delta(\omega + \Omega) \qquad \text{(H-9)}$$

When the reference trajectory has appreciable eccentricity, it is necessary that the major axis of the actual trajectory be situated close to the major axis of the reference trajectory if P' is to be close to P for all values of f. Then, $\delta\phi$ must be small, and, since $(\delta f + \delta\phi)$ is always small, δf must likewise be small. It should be noted that the individual angles $\delta\phi$ and δf need not be small if the reference trajectory is circular or nearly circular, because for such trajectories a large displacement of the x'-axis from the x-axis has no appreciable effect, <u>per se</u>, on the distance of P' from P.

When the usual small-angle assumptions are applied to δi and $(\delta f + \delta\phi)$, the components of $\delta \underline{r}$ become

$$\delta r = r' \cos(\delta f + \delta\phi) - r = r' - r \tag{H-10}$$

$$\delta s = r' \sin(\delta f + \delta\phi) = r'(\delta f + \delta\phi) \tag{H-11}$$

$$\delta z = r' \, \delta i \sin(f' + \delta\omega) \tag{H-12}$$

In the last equation, $(f' + \delta\omega)$ may be written as

$$\begin{aligned} f' + \delta\omega &= (f + \delta f) + (\delta\phi - \delta\Omega) \\ &= (f - \delta\Omega) + (\delta f + \delta\phi) \end{aligned} \tag{H-13}$$

Since δr is a small quantity, linear theory permits the following additional simplification of Eqs. (H-11) and (H-12).

$$\delta s = (r + \delta r)(\delta f + \delta\phi) = r(\delta f + \delta\phi) \tag{H-14}$$

$$\begin{aligned} \delta z &= (r + \delta r)\, \delta i \sin[(f - \delta\Omega) + (\delta f + \delta\phi)] \\ &= r \, \delta i \sin(f - \delta\Omega) \end{aligned} \tag{H-15}$$

Equations (H-10), (H-14), and (H-15) show the effects of variations in the Euler angles on the components of $\delta \underline{r}$. The radial component δr is unaffected. The transverse component δs varies linearly with $\delta\phi$. The orthogonal component δz depends upon both δi and $\delta\Omega$.

H.4 Variation in Eccentric Anomaly

As an intermediate step in the determination of δr and δs, it is useful to derive an expression for δE, the variation in the eccentric anomaly, in terms of variations in the orbital elements.

The discussion in the last section concerning the angle $(\delta f + \delta\phi)$ is applicable to both $(\delta E + \delta\phi)$ and $(\delta M + \delta\phi)$; i.e., $(\delta E + \delta\phi)$ and $(\delta M + \delta\phi)$ are small angles regardless of the eccentricity of the reference ellipse; if the eccentricity of the reference ellipse is not near zero, δE and δM are individually small, but they need not be if

the eccentricity is near zero. These considerations also apply to δM_0, the variation in the mean anomaly at epoch. To preserve generality, the angles δE, δM, and δM_0 will not be assumed to be small in the initial development. Then

$$E' = E + \delta E = (E - \delta\phi) + (\delta E + \delta\phi) \tag{H-16}$$

$$M' = (M - \delta\phi) + (\delta M + \delta\phi) \tag{H-17}$$

$$M_o' = (M_0 - \delta\phi) + (\delta M_0 + \delta\phi) \tag{H-18}$$

From Eqs. (B-47) and (B-55),

$$M = n\,t + M_0 = E - e \sin E \tag{H-19}$$

For the actual orbit, at time t,

$$M' = (n + \delta n)\,t + M_o' = E' - (e + \delta e) \sin E' \tag{H-20}$$

(H-19) is subtracted from (H-20).

$$\begin{aligned}(\delta M + \delta\phi) &= t\,\delta n + (\delta M_0 + \delta\phi) \\ &= (\delta E + \delta\phi) - (e + \delta e) \sin E' + e \sin E\end{aligned} \tag{H-21}$$

The variation δn may be expressed in terms of δa by the use of (B-62).

$$\delta\mu = 0 = \delta(n^2 a^3) = 2\,n\,a^3\,\delta n + 3\,n^2\,a^2\,\delta a \tag{H-22}$$

$$\delta n = -\frac{3\,n}{2\,a}\,\delta a \tag{H-23}$$

Also,

$$\sin E' = \sin(E - \delta\phi) + (\delta E + \delta\phi)\cos(E - \delta\phi) \tag{H-24}$$

(H-23) and (H-24) are substituted into (H-21), second-order terms are neglected, and the resulting equation is solved for $(\delta E + \delta\phi)$.

$$\delta E + \delta\phi = \frac{-\frac{3}{2} n t \frac{\delta a}{a} + (\delta M_0 + \delta\phi) + (e + \delta e) \sin(E - \delta\phi) - e \sin E}{1 - e \cos(E - \delta\phi)} \tag{H-25}$$

H.5 General Equations for Components of Position Variation

Equation (B-49) is used to determine δr.

$$r = a(1 - e \cos E) \tag{H-26}$$

On the actual trajectory,

$$\begin{aligned} r' &= (a + \delta a)[1 - (e + \delta e) \cos E'] \\ &= (a + \delta a)\left\{1 - (e + \delta e)[\cos(E - \delta\phi) - (\delta E + \delta\phi) \sin(E - \delta\phi)]\right\} \\ &= a[1 - (e + \delta e) \cos(E - \delta\phi) + e(\delta E + \delta\phi) \sin(E - \delta\phi)] \\ &\quad + [1 - e \cos(E - \delta\phi)]\, \delta a \end{aligned} \tag{H-27}$$

$$\begin{aligned} \delta r = r' - r = a[&e \cos E - (e + \delta e) \cos(E - \delta\phi) \\ &+ e(\delta E + \delta\phi) \sin(E - \delta\phi)] + [1 - e \cos(E - \delta\phi)]\, \delta a \end{aligned} \tag{H-28}$$

From (H-14), the deviation in the transverse direction is

$$\begin{aligned} \delta s &= r(\delta f + \delta\phi) = r'(\delta f + \delta\phi) \\ &= r' \sin(\delta f + \delta\phi) = r' \sin[f' - (f - \delta\phi)] \\ &= r'[\sin f' \cos(f - \delta\phi) - \cos f' \sin(f - \delta\phi)] \end{aligned} \tag{H-29}$$

From (B-53),

$$\sin f' = \frac{[1 - (e + \delta e)^2]^{1/2} \sin E'}{1 - (e + \delta e) \cos E'}$$

$$= \frac{(a + \delta a)}{r'} [1 - (e + \delta e)^2]^{1/2} [\sin (E - \delta\phi) + (\delta E + \delta\phi) \cos (E - \delta\phi)] \qquad \text{(H-30)}$$

From (B-54),

$$\cos f' = \frac{\cos E' - (e + \delta e)}{1 - (e + \delta e) \cos E'}$$

$$= \frac{(a + \delta a)}{r'} [\cos (E - \delta\phi) - (\delta E + \delta\phi) \sin (E - \delta\phi) - (e + \delta e)] \qquad \text{(H-31)}$$

(H-30) and (H-31) are substituted into (H-29). When higher-order terms are neglected, the expression for δs is

$$\delta s = a\Big\{(1 - e^2 - 2 e \delta e)^{1/2} \sin (E - \delta\phi) \cos (f - \delta\phi)$$
$$- [\cos (E - \delta\phi) - (e + \delta e)] \sin (f - \delta\phi)$$
$$+ [(1 - e^2)^{1/2} \cos (E - \delta\phi) \cos (f - \delta\phi)$$
$$+ \sin (E - \delta\phi) \sin (f - \delta\phi)] (\delta E + \delta\phi)\Big\} \qquad \text{(H-32)}$$

Equations (H-28) and (H-32) are the general equations for δr and δs, applicable over a wide range of eccentricities for ellipses, from $e = 0$ to e approaching unity as a limit. The equations are not applicable when the reference ellipse is rectilinear (that is, when e is equal to one), for in that case a positive variation in e causes the actual trajectory to become hyperbolic.

(H-28) and (H-32) are used in conjunction with (H-25) to express δr and δs in terms of variations in the elements a, e, M_0, and ϕ. δz is independent of variations in these elements.

H.6 Position Deviation for Trajectories of Moderate Eccentricity

Elliptical reference trajectories for which e is not very small (close to zero) or very large (close to unity) may be referred to as trajectories of "moderate" eccentricity. Practical trajectories for voyages to neighboring planets fall into this category. The general equations of Sections H. 4 and H. 5 will be used to obtain simplified expressions for δr and δs when the eccentricity is moderate.

Whenever the eccentricity is appreciably greater than zero, if the position variations are to remain small, δf, δE, δM, δM_0, and $\delta\phi$ must be small angles. Then Eq. (H-25) becomes

$$(\delta E + \delta\phi)(1 - e\cos E - e\,\delta\phi\,\sin E) \simeq -\frac{3}{2} n t \frac{\delta a}{a} + \delta M_0 + \delta\phi - e\,\delta\phi\cos E + \sin E\,\delta e \tag{H-33}$$

$$\delta E = \frac{-\frac{3}{2} n t \frac{\delta a}{a} + \delta M_0 + \sin E\,\delta e}{1 - e\cos E} \tag{H-34}$$

From (H-28), the equation for δr is

$$\delta r = a[-e\sin E\,\delta\phi - \cos E\,\delta e + e\sin E(\delta E + \delta\phi)] + (1 - e\cos E)\,\delta a \tag{H-35}$$

(H-34) is substituted into (H-35)

$$\delta r = \left[a(1 - e\cos E) - \frac{\frac{3}{2} n a e \sin E}{1 - e\cos E} t\right]\frac{\delta a}{a} + \frac{a e \sin E}{1 - e\cos E}\delta M_0 - \frac{a(\cos E - e)}{1 - e\cos E}\delta e \tag{H-36}$$

With the use of the relations of Appendix B, (H-36) reduces to

$$\delta r = \left(r - \frac{3}{2} v_r t\right) \frac{\delta a}{a} + \frac{v_r}{n} \delta M_0 - a \cos f \, \delta e \qquad \text{(H-37)}$$

The derivation for δs proceeds in a similar fashion from Eqs. (H-32) and (H-34) and the standard forms of Appendix B. Note that

$$(1 - e^2 - 2e\,\delta e)^{1/2} = \left[(1 - e^2)\left(1 - \frac{2e\,\delta e}{1 - e^2}\right)\right]^{1/2}$$

$$= (1 - e^2)^{1/2} - \frac{e}{(1 - e^2)^{1/2}} \delta e \qquad \text{(H-38)}$$

Then δs is obtained as follows:

$$\delta s = a\left\{\left[(1 - e^2)^{1/2} - \frac{e}{(1 - e^2)^{1/2}} \delta e\right](\sin E - \cos E\,\delta\phi)(\cos f + \sin f\,\delta\phi)\right.$$

$$- (\cos E - e + \sin E\,\delta\phi - \delta e)(\sin f - \cos f\,\delta\phi)$$

$$\left. + [(1 - e^2)^{1/2} \cos E \cos f + \sin E \sin f](\delta E + \delta\phi)\right\}$$

$$= a\left\{\left[-\frac{e}{(1 - e^2)^{1/2}} \sin E \cos f + \sin f\right] \delta e\right.$$

$$+ [(1 - e^2)^{1/2}(\sin E \sin f - \cos E \cos f) + (\cos E - e)\cos f$$

$$\left. - \sin E \sin f]\,\delta\phi + (1 - e^2)^{1/2}(\delta E + \delta\phi)\right\}$$

$$= a\left[\frac{\sin f}{1 + e \cos f} \delta e + (1 - e \cos E)\,\delta\phi + (1 - e^2)^{1/2}\,\delta E\right]$$

$$= \frac{-\frac{3}{2} n a (1 - e^2)^{1/2}}{1 - e \cos E} t \frac{\delta a}{a} + \frac{a(1 - e^2)^{1/2}}{1 - e \cos E} \delta M_0$$

$$+ a\left(\frac{2 + e \cos f}{1 + e \cos f}\right) \sin f\,\delta e + a(1 - e \cos E)\,\delta\phi$$

$$= -\frac{3}{2} v_s t \frac{\delta a}{a} + \frac{v_s}{n} \delta M_0 + \left(a + \frac{r}{1 - e^2}\right) \sin f\,\delta e + r\,\delta\phi \qquad \text{(H-39)}$$

H. 7 Relation between Solution of Appendix G and Solution of Appendix H

Since the component equations of Appendix G, specifically (G-65), (G-66), and (G-67), are written in terms of the variables f and M, Eqs. (H-37), (H-39), and (H-15) of this appendix will be written in terms of the same variables so that the two solutions can be compared.

From (H-37),

$$\delta r = \left[\frac{a(1-e^2)}{1+e\cos f} - \frac{\frac{3}{2} n a e \sin f}{(1-e^2)^{1/2}} t \right] \frac{\delta a}{a}$$

$$+ \frac{a e \sin f}{(1-e^2)^{1/2}} \delta M_0 - a \cos f \, \delta e$$

$$= a(1-e^2) \left[-\frac{3 M e \sin f}{2(1-e^2)^{3/2}} + \frac{1}{1+e\cos f} \right] \frac{\delta a}{a}$$

$$+ \frac{a e}{(1-e^2)^{1/2}} \sin f \left[\delta M_0 + \frac{3}{2} M_0 \frac{\delta a}{a} \right] - a \cos f \, \delta e \qquad \text{(H-40)}$$

The expression $[\delta M_0 + 3/2\, M_0\, \delta a/a]$ may be simplified.

$$\delta M_0 = \delta(-n t_o) = -n \delta t_0 - t_0 \delta n$$

$$= -n \delta t_0 - \frac{3}{2} M_0 \frac{\delta a}{a} \qquad \text{(H-41)}$$

$$\delta M_0 + \frac{3}{2} M_0 \frac{\delta a}{a} = -n \delta t_0 \qquad \text{(H-42)}$$

Finally,

$$\delta r = a(1-e^2) \left[-\frac{3 M e \sin f}{2(1-e^2)^{3/2}} + \frac{1}{1+e\cos f} \right] \frac{\delta a}{a}$$

$$- \frac{n a e}{(1-e^2)^{1/2}} \sin f \, \delta t_0 - a \cos f \, \delta e \qquad \text{(H-43)}$$

From (H-39),

$$\delta s = -\frac{3\,n\,a\,(1 + e\cos f)}{2\,(1 - e^2)^{1/2}}\,t\,\frac{\delta a}{a} + \frac{a\,(1 + e\cos f)}{(1 - e^2)^{1/2}}\,\delta M_0$$

$$+ a\left(\frac{2 + e\cos f}{1 + e\cos f}\right)\sin f\,\delta e + \frac{a\,(1 - e^2)}{1 + e\cos f}\,\delta\phi$$

$$= a\,(1 - e^2)\left[-\frac{3\,M\,(1 + e\cos f)}{2\,(1 - e^2)^{3/2}}\right]\frac{\delta a}{a}$$

$$-\frac{n\,a\,e}{(1 - e^2)^{1/2}}\left(\frac{2 + e\cos f}{1 + e\cos f}\right)\cos f\,\delta t_0$$

$$+ a\left(\frac{2 + e\cos f}{1 + e\cos f}\right)\sin f\,\delta e$$

$$+ \frac{a\,(1 - e^2)}{1 + e\cos f}\left[\delta\phi - \frac{n\,\delta t_0}{(1 - e^2)^{3/2}}\right] \qquad \text{(H-44)}$$

From (H-15),

$$\delta z = \frac{a\,(1 - e^2)}{1 + e\cos f}\,\delta i\,(\sin f\cos\delta\Omega - \cos f\sin\delta\Omega) \qquad \text{(H-45)}$$

When (H-43), (H-44), and (H-45) are compared with (G-65), (G-66), and (G-67), respectively, it is evident that the two sets of equations are identical if

$$k_1 = \delta\phi - \frac{n\,\delta t_0}{(1 - e^2)^{3/2}} \qquad \text{(H-46)}$$

$$k_2 = -\,a\,\delta e \qquad \text{(H-47)}$$

$$k_3 = -\frac{n\,a\,e}{(1 - e^2)^{1/2}}\,\delta t_0 \qquad \text{(H-48)}$$

$$k_4 = a(1 - e^2) \frac{\delta a}{a} \tag{H-49}$$

$$k_5 = a(1 - e^2)\, \delta i \cos \delta\Omega \tag{H-50}$$

$$k_6 = -a(1 - e^2)\, \delta i \sin \delta\Omega \tag{H-51}$$

Thus, despite the presence of the secular term, the motion described by Eqs. (G-65), (G-66), and (G-67) is elliptical motion. The secular term is simply a manifestation of the fact that the period of the actual elliptical trajectory differs slightly from the period of the reference trajectory.

APPENDIX I

VARIATION IN POSITION, VELOCITY, AND ACCELERATION

I.1 Summary

The equations for position variation and velocity variation are expressed in vector form and also in matrix form in the three reference trajectory coordinate systems. An expression developed for variation in acceleration serves as a check of the basic solution of the variant equations of motion.

I.2 Vector Forms

It is evident from Fig. A.2 that components along the x, y axes and p, q axes may be derived from the r, s components by means of the following coordinate transformations:

$$\begin{pmatrix} \delta x \\ \delta y \end{pmatrix} = \begin{pmatrix} \cos f & -\sin f \\ \sin f & \cos f \end{pmatrix} \begin{pmatrix} \delta r \\ \delta s \end{pmatrix} \tag{I-1}$$

$$\begin{pmatrix} \delta p \\ \delta q \end{pmatrix} = \begin{pmatrix} \cos \gamma & -\sin \gamma \\ \sin \gamma & \cos \gamma \end{pmatrix} \begin{pmatrix} \delta r \\ \delta s \end{pmatrix} \tag{I-2}$$

With the aid of these transformations and the relations of Sections B.8 and B.9, Eqs. (H-15), (H-37), and (H-39) may be combined into a

single vector equation.

$$\delta \underline{r} = v\left(\frac{\delta M_0}{n} - \frac{3}{2} t \frac{\delta a}{a}\right) \underline{u}_q + r \frac{\delta a}{a} \underline{u}_r$$

$$+\left(\frac{y}{1-e^2} \delta e + r \delta \phi\right) \underline{u}_s - a \delta e \underline{u}_x$$

$$+ r \sin (f - \delta\Omega) \delta i \underline{u}_z \qquad \text{(I-3)}$$

The velocity deviation vector $\delta \underline{v}$ is obtained by vector differentiation of $\delta \underline{r}$. The angular velocity of the p, q axes is $\dot{g}$, the angular velocity of the r, s axes is $\dot{f}$, and the x, y, z axes are non-rotating.

$$\delta \underline{v} = - v \dot{g} \left(\frac{\delta M_0}{n} - \frac{3}{2} t \frac{\delta a}{a}\right) \underline{u}_p$$

$$+ \left[\dot{v} \frac{\delta M_0}{n} - \frac{3}{2} (\dot{v} t + v) \frac{\delta a}{a}\right] \underline{u}_q$$

$$+ \left[\dot{r} \frac{\delta a}{a} - \dot{f} \left(\frac{y}{1-e^2} \delta e + r \delta \phi\right)\right] \underline{u}_r$$

$$+\left(r \dot{f} \frac{\delta a}{a} + \frac{\dot{y}}{1-e^2} \delta e + \dot{r} \delta \phi\right) \underline{u}_s$$

$$+ \left[\dot{r} \sin (f - \delta\Omega) + r \dot{f} \cos (f - \delta\Omega)\right] \delta i \underline{u}_z \qquad \text{(I-4)}$$

The terms in (I-4) may be simplified when the proper substitutions are made for $\dot{f}$, $\dot{\gamma}$, $\dot{r}$, and $\dot{y}$ from the relations of Appendix B.

The coefficient of $\left(\frac{\delta M_0}{n} - \frac{3}{2} t \frac{\delta a}{a} \right)$ in (I-4) is

$$- v \dot{g} \underline{u}_p + \dot{v} \underline{u}_q = (a_p \underline{u}_p + a_q \underline{u}_q) = a_r \underline{u}_r \qquad \text{(I-5)}$$

The additional terms involving $\frac{\delta a}{a}$ are

$$- \frac{3}{2} v \underline{u}_q + \dot{r} \underline{u}_r + r \dot{f} \underline{u}_s = - \frac{v}{2} \underline{u}_q \qquad \text{(I-6)}$$

The coefficient of $\frac{\delta e}{1 - e^2}$ is

$$- y \dot{f} \underline{u}_r + \dot{y} \underline{u}_s = - r \dot{f} \sin f \, \underline{u}_r + (\dot{r} \sin f + r \dot{f} \cos f) \underline{u}_s$$

$$= - v \sin f \, \underline{u}_p + v_s \cos f \, \underline{u}_s \qquad \text{(I-7)}$$

The coefficient of $\delta \phi$ is

$$- r \dot{f} \underline{u}_r + \dot{r} \underline{u}_s = - v \underline{u}_p \qquad \text{(I-8)}$$

The coefficient of $\delta i\, \underline{u}_z$ is

$$\dot{r} \sin (f - \delta\Omega) + r \dot{f} \cos (f - \delta\Omega)$$

$$= v [\sin \gamma \sin (f - \delta\Omega) + \cos \gamma \cos (f - \delta\Omega)]$$

$$= v \cos (g - \delta\Omega) \qquad \text{(I-9)}$$

With these substituions, Eq. (I-4) becomes

$$\delta \underline{v} = - v\left(\frac{\sin f}{1 - e^2}\ \delta e + \delta\phi\right) \underline{u}_p$$

$$- \frac{v}{2}\ \frac{\delta a}{a}\ \underline{u}_q + a_r \left(\frac{\delta M_0}{n} - \frac{3}{2}\ t\ \frac{\delta a}{a}\right) \underline{u}_r$$

$$+ \frac{v_s \cos f}{1 - e^2}\ \delta e\, \underline{u}_s + v \cos (g - \delta\Omega)\ \delta i\, \underline{u}_z \qquad \text{(I-10)}$$

I. 3 Component Equations in Matrix Form

The component equations for $\delta \underline{r}$ and $\delta \underline{v}$ in the three reference trajectory coordinate systems are obtained from (I-3) and (I-10). Equations (I-11), (I-12), and (I-13) relate position variation and velocity variation in the reference trajectory plane to variations in the elements a, M_0, e, and ϕ. Equation (I-14) relates δz and δv_z to variations in i and Ω.

$$\begin{pmatrix} \delta x \\ \delta y \\ \delta v_x \\ \delta v_y \end{pmatrix} = \begin{pmatrix} x - \frac{3}{2} v_x t & \frac{v_x}{n} & -a - \frac{y \sin f}{1-e^2} & -y \\ y - \frac{3}{2} v_y t & \frac{v_y}{n} & \frac{y \cos f}{1-e^2} & x \\ -\frac{v_x}{2} - \frac{3}{2} a_x t & \frac{a_x}{n} & -\frac{(v_y + v_s \cos f) \sin f}{1-e^2} & -v_y \\ -\frac{v_y}{2} - \frac{3}{2} a_y t & \frac{a_y}{n} & \frac{v_x \sin f + v_s \cos^2 f}{1-e^2} & v_x \end{pmatrix} \begin{pmatrix} \frac{\delta a}{a} \\ \delta M_0 \\ \delta e \\ \delta \phi \end{pmatrix} \qquad \text{(I-11)}$$

$$\begin{pmatrix} \delta r \\ \delta s \\ \delta v_r \\ \delta v_s \end{pmatrix} = \begin{pmatrix} r - \frac{3}{2} v_r t & \frac{v_r}{n} & -a \cos f & 0 \\ -\frac{3}{2} v_s t & \frac{v_s}{n} & a \sin f + \frac{y}{1-e^2} & r \\ -\frac{v_r}{2} - \frac{3}{2} a_r t & \frac{a_r}{n} & -\frac{v_s \sin f}{1-e^2} & -v_s \\ -\frac{v_s}{2} & 0 & \frac{v_y}{1-e^2} & v_r \end{pmatrix} \begin{pmatrix} \frac{\delta a}{a} \\ \delta M_0 \\ \delta e \\ \delta \phi \end{pmatrix} \qquad \text{(I-12)}$$

$$\begin{pmatrix} \delta p \\ \delta q \\ \delta v_p \\ \delta v_q \end{pmatrix} = \begin{pmatrix} p & 0 & -a\cos g - \dfrac{y \sin \gamma}{1-e^2} & -q \\ q - \dfrac{3}{2} v t & \dfrac{v}{n} & 2a \sin g & p \\ -\dfrac{3}{2} a_p t & \dfrac{a_p}{n} & -\dfrac{v \sin f + v_s \cos f \sin \gamma}{1-e^2} & -v \\ -\dfrac{v}{2} - \dfrac{3}{2} a_q t & \dfrac{a_q}{n} & \dfrac{v_s \cos f \cos \gamma}{1-e^2} & 0 \end{pmatrix} \begin{pmatrix} \dfrac{\delta a}{a} \\ \delta M_0 \\ \delta e \\ \delta \phi \end{pmatrix} \tag{I-13}$$

$$\begin{pmatrix} \delta z \\ \delta v_z \end{pmatrix} = \begin{pmatrix} y & -x \\ v_y & -v_x \end{pmatrix} \begin{pmatrix} \delta i \cos \delta\Omega \\ \delta i \sin \delta\Omega \end{pmatrix} \qquad \text{(I-14)}$$

I.4 Variation in Acceleration

The variation in acceleration may be obtained by vector differentiation of (I-10), and the result can be used to check the solution obtained for the matrix differential equation

$$\delta \underline{a} = \overset{*}{G}\, \delta \underline{r} \qquad \text{(I-15)}$$

The result of differentiating (I-10) is

$$\delta \underline{a} = \left[-\dot{v}\left(\frac{\sin f}{1-e^2}\,\delta e + \delta\phi\right) - \frac{v\dot{f}\cos f}{1-e^2}\,\delta e + \frac{v\dot{g}}{2}\,\frac{\delta a}{a} \right] \underline{u}_p$$

$$+ \left[-v\dot{g}\left(\frac{\sin f}{1-e^2}\,\delta e + \delta\phi\right) - \frac{\dot{v}}{2}\,\frac{\delta a}{a} \right] \underline{u}_q$$

$$+ \left[\dot{a}_r\left(\frac{\delta M_0}{n} - \frac{3}{2}\,t\,\frac{\delta a}{a}\right) - \frac{3}{2}\,a_r\,\frac{\delta a}{a} - \frac{v_s\dot{f}\cos f}{1-e^2}\,\delta e \right] \underline{u}_r$$

$$+ \left[a_r\dot{f}\left(\frac{\delta M_0}{n} - \frac{3}{2}\,t\,\frac{\delta a}{a}\right) + \frac{\dot{v}_s\cos f - v_s\dot{f}\sin f}{1-e^2}\,\delta e \right] \underline{u}_s$$

$$+ \left[\dot{v}\cos(g - \delta\Omega) - v\dot{g}\sin(g - \delta\Omega)\right] \delta i\, \underline{u}_z \qquad \text{(I-16)}$$

The coefficient of $\delta\phi$ in (I-16) is

$$- (\dot{v}\,\underline{u}_p + v\,\dot{g}\,\underline{u}_q) = - (a_q \underline{u}_p - a_p\,\underline{u}_q)$$

$$= - a_r\,(\sin\gamma\,\underline{u}_p - \cos\gamma\,\underline{u}_q) = a_r\,\underline{u}_s \qquad \text{(I-17)}$$

The coefficient of $\frac{1}{2}\,\frac{\delta a}{a}$ is

$$v\,\dot{g}\,\underline{u}_p - \dot{v}\,\underline{u}_q = - a_p\,\underline{u}_p - a_q\,\underline{u}_q = - a_r\,\underline{u}_r \qquad \text{(I-18)}$$

The coefficient of $\left(\frac{\delta M_0}{n} - \frac{3}{2}\,t\,\frac{\delta a}{a}\right)$ is

$$\dot{a}_r\,\underline{u}_r + a_r\,\dot{f}\,\underline{u}_s = \frac{\mu}{r^3}\,(2\,\dot{r}\,\underline{u}_r - r\,\dot{f}\,\underline{u}_s)$$

$$= \frac{\mu}{r^3}\,(2\,v_r\,\underline{u}_r - v_s\,\underline{u}_s) \qquad \text{(I-19)}$$

The complete coefficient of $\frac{\delta a}{a}$ is

$$\frac{\dot{v}\,g}{2}\,\underline{u}_p - \frac{v}{2}\,\underline{u}_q - \frac{3}{2}\,(\dot{a}_r\,t + a_r)\,\underline{u}_r - \frac{3}{2}\,a_r\,\dot{f}\,t\,\underline{u}_s$$

$$= - \frac{1}{2}\,a_r\,\underline{u}_r - \frac{3}{2}\,t\,\frac{\mu}{r^3}\,(2\,v_r\,\underline{u}_r - v_s\,\underline{u}_s) - \frac{3}{2}\,a_r\,\underline{u}_r$$

$$= \frac{\mu}{r^3}\,\left[\,(2\,r - 3\,v_r\,t)\,\underline{u}_r + \frac{3}{2}\,v_s\,t\,\underline{u}_s\,\right] \qquad \text{(I-20)}$$

One of the terms in the coefficient of δe contains the derivative $\dot{v}_s$. A substitution may be made for $\dot{v}_s$ by utilizing the fact that the angular momentum of the reference trajectory is constant.

$$h = r^2 \dot{f} = r v_s \tag{I-21}$$

$$\dot{h} = \dot{r} v_s + r \dot{v}_s = 0 \tag{I-22}$$

$$\dot{v}_s = - \frac{\dot{r} v_s}{r} = - v_r \dot{f} \tag{I-23}$$

The complete coefficient of $\frac{\delta e}{1 - e^2}$ is

$$\begin{aligned} &(-\dot{v} \sin f - v \dot{f} \cos f) \underline{u}_p - v \dot{g} \sin f \underline{u}_q - v_s \dot{f} \cos f \underline{u}_r \\ &+ (\dot{v}_s \cos f - v_s \dot{f} \sin f) \underline{u}_s \\ &= a_r \sin f \underline{u}_s - v \dot{f} \cos f \underline{u}_p - v_s \dot{f} \cos f \underline{u}_r \\ &- \dot{f} (v_r \cos f + v_s \sin f) \underline{u}_s \end{aligned} \tag{I-24}$$

The product $v_s \dot{f}$ may be expanded as follows:

$$v_s \dot{f} = r \dot{f}^2 = \frac{h^2}{r^3} = \frac{h^2}{\mu} \frac{\mu}{r^3} = \frac{\mu a (1 - e^2)}{r^3} \tag{I-25}$$

With the aid of (I-25), the coefficient of $\frac{\delta e}{1 - e^2}$ becomes

$$- 2 v_s \dot{f} \cos f \, \underline{u}_r + (a_r - v_s \dot{f}) \sin f \, \underline{u}_s$$

$$= \frac{\mu}{r^3} \left\{ - 2 a (1 - e^2) \cos f \, \underline{u}_r + [- y - a (1 - e^2) \sin f \,] \, \underline{u}_s \right\} \qquad \text{(I-26)}$$

The coefficient of $\delta i \, \underline{u}_z$ in (I-16) is

$$\dot{v} \cos (g - \delta\Omega) - v \dot{g} \sin (g - \delta\Omega)$$

$$= a_r \, [\sin \gamma \cos (g - \delta\Omega) + \cos \gamma \sin (g - \delta\Omega) \,]$$

$$= a_r \sin (f - \delta\Omega) \qquad \text{(I-27)}$$

The relations for the terms comprising $\delta \underline{a}$, as expressed in Equations (I-17) through (I-27), contain components only in the r, s, and z directions. On the basis of these relations a matrix equation can now be written for $\delta \underline{a}$ in terms of the variations in the orbital elements.

$$\begin{pmatrix} \delta a_r \\ \delta a_s \\ \delta a_z \end{pmatrix} = \frac{\mu}{r^3} \begin{pmatrix} 2r - 3v_r t & \frac{2v_r}{n} & -2a\cos f & 0 & 0 & 0 \\ \frac{3}{2} v_s t & -\frac{v_s}{n} & -a\sin f - \frac{y}{1-e^2} & -r & 0 & 0 \\ 0 & 0 & 0 & 0 & -y & x \end{pmatrix} \begin{pmatrix} \frac{\delta a}{a} \\ \delta M_0 \\ \delta e \\ \delta \phi \\ \delta i \cos \delta\Omega \\ \delta i \sin \delta\Omega \end{pmatrix}$$

(I-28)

When Eq. (I-28) is compared with Eqs. (I-12) and (I-14), it may be seen that

$$\begin{pmatrix} \delta a_r \\ \delta a_s \\ \delta a_z \end{pmatrix} = \frac{\mu}{r^3} \begin{pmatrix} 2 & 0 & 0 \\ 0 & -1 & 0 \\ 0 & 0 & -1 \end{pmatrix} \begin{pmatrix} \delta r \\ \delta s \\ \delta z \end{pmatrix} \qquad \text{(I-29)}$$

The 3-by-3 diagonal matrix on the right-hand side of (I-29) is identical with the matrix on the right-hand side of (G-1). This is the $\overset{*}{G}$ matrix in the r s z coordinate system. Thus the solution for $\delta \underline{r}$ given by (I-3) has been checked.

APPENDIX J
LOW-ECCENTRICITY REFERENCE TRAJECTORIES

J.1 Summary

Equations are developed for position variation and velocity variation in low-eccentricity reference orbits. The differential equation solution of Appendix G is shown to be applicable to low-eccentricity orbits as well as orbits of moderate eccentricity.

J.2 Introduction

Although low-eccentricity trajectories cannot be used as transfer orbits on interplanetary voyages, the variant equations for such trajectories are derived in this appendix in order to illustrate the applicability of the general equations developed in Sections H.4 and H.5. The results obtained are of value in preliminary qualitative studies of the motion of satellites in circular or near-circular orbits.

J.3 Position Variation and Velocity Variation

In order to distinguish the results of this appendix from those of previous appendices, the subscript o will be added to all designations for orbital elements.

The distinctive feature of the reference orbits now being considered is that the eccentricity e is of the same order of magnitude as the orbital element variations. This characteristic is used in deriving expressions for δr and δs from Eqs. (H-25), (H-28), and (H-32.)

For low-eccentricity orbits,

$$1 - e_o \cos (E - \delta\phi_o) = 1 \tag{J-1}$$

$$r = a_o \tag{J-2}$$

$$\sin E = \frac{(1 - e_o^2)^{1/2} \sin f}{1 + e_o \cos f} = \sin f \tag{J-3}$$

$$\cos E = \frac{\cos f + e_o}{1 + e_o \cos f} = \cos f + e_o \tag{J-4}$$

$$v = \frac{n_o a_o (1 + e_o \cos E)^{1/2}}{(1 - e_o \cos E)^{1/2}} = n_o a_o \tag{J-5}$$

$$v_r = \frac{n_o a_o e_o \sin f}{(1 - e_o^2)^{1/2}} = n_o a_o e_o \sin f \tag{J-6}$$

$$v_s = \frac{n_o a_o (1 + e_o \cos f)}{(1 - e_o^2)^{1/2}} = n_o a_o = v \tag{J-7}$$

In Eq. (H-25) the term $(e_o + \delta e_o) \sin (E - \delta\phi_o)$ may be expanded as

$$(e_o + \delta e_o) \sin (E - \delta\phi_o) = (e_o + \delta e_o)(\sin f \cos \delta\phi_o - \cos f \sin \delta\phi_o) \tag{J-8}$$

The angle $(\delta E + \delta\phi_o)$, which must be small, is

$$\delta E + \delta\phi_o = -\frac{3}{2} n_o t \frac{\delta a_o}{a_o} + (\delta M_{oo} + \delta\phi_o)$$

$$- \sin f \left[e_o - (e_o + \delta e_o) \cos \delta\phi_o\right] - \cos f (e_o + \delta e_o) \sin \delta\phi_o$$

(J-9)

In Eq. (H-28), the term $e_o (\delta E + \delta\phi_o)$ is of second order in the small quantities. Therefore, the expression for δr is simply,

$$\delta r = a_o \left\{\frac{\delta a_o}{a_o} + \cos f \left[e_o - (e_o + \delta e_o) \cos \delta\phi_o\right]\right.$$

$$\left. - \sin f (e_o + \delta e_o) \sin \delta\phi_o\right\} \qquad \text{(J-10)}$$

From Eq. (H-32),

$$\delta s = a_o \left[\sin (E - f) + (e_o + \delta e_o) \sin (f - \delta\phi_o)\right.$$

$$\left. + (\delta E + \delta\phi_o) \cos (E - f)\right] \qquad \text{(J-11)}$$

$$\sin (E - f) = \sin E \cos f - \sin f \cos E = - e_o \sin f \qquad \text{(J-12)}$$

$$\cos (E - f) = \cos E \cos f + \sin E \sin f = 1 + e_o \cos f = 1 \qquad \text{(J-13)}$$

Equations (J-9), (J-12), and (J-13) are substituted into (J-11).

$$\delta s = a_o \left\{ -\frac{3}{2} n_o t \frac{\delta a_o}{a_o} + (\delta M_{oo} + \delta \phi_o) \right.$$
$$- 2 \sin f \left[e_o - (e_o + \delta e_o) \cos \delta \phi_o \right]$$
$$\left. - 2 \cos f (e_o + \delta e_o) \sin \delta \phi_o \right\} \qquad \text{(J-14)}$$

From Eq. (H-15),

$$\delta z = a_o \, \delta i_o \sin (f - \delta \Omega_o) \qquad \text{(J-15)}$$

The velocity deviation components are obtained by differentiating the components of $\delta \underline{r}$, with consideration being given to the fact that the coordinate system is rotating with angular velocity $\dot{f}$.

$$\dot{f} = \frac{v_s}{r} = n_o \qquad \text{(J-16)}$$

$$\delta v_r = v \left\{ \frac{3}{2} n_o t \frac{\delta a_o}{a_o} - (\delta M_{oo} + \delta \phi_o) \right.$$
$$+ \sin f \left[e_o - (e_o + \delta e_o) \cos \delta \phi_o \right]$$
$$\left. + \cos f (e_o + \delta e_o) \sin \delta \phi_o \right\} \qquad \text{(J-17)}$$

$$\delta v_s = v \left\{ -\frac{1}{2} \frac{\delta a_o}{a_o} - \cos f \left[e_o - (e_o + \delta e_o) \cos \delta \phi_o \right] \right.$$
$$\left. + \sin f (e_o + \delta e_o) \sin \delta \phi_o \right\} \qquad \text{(J-18)}$$

$$\delta v_z = v\ \delta i_o \cos (f - \delta\Omega_o) \qquad \text{(J-19)}$$

The position and velocity deviations may be written in matrix form as shown in Eq. (J-20).

J.4 Variation in Acceleration

As in Appendix I, the variation in acceleration may be used to check the solution of the variant problem. The matrix for $\delta\underline{a}$ is obtained by differentiating the lower half of (J-20). Equations (J-21) and (J-22) indicate that the solution checks satisfactorily.

J.5 Comparison with Differential Equation Solution of Appendix G

When the eccentricity is small, the differential equation solution given by Eqs. (G-65), (G-66), and (G-67) reduces to the following:

$$\delta r = k_2 \cos f + k_3 \sin f + k_4 \qquad \text{(J-23)}$$

$$\delta s = k_1 a_o - 2 k_2 \sin f + 2 k_3 \cos f - \frac{3}{2} k_4 M \qquad \text{(J-24)}$$

$$\delta z = k_5 \sin f + k_6 \cos f \qquad \text{(J-25)}$$

A comparison of Eqs. (J-23), (J-24), and (J-25) with the first three equations of (J-20) indicates that the two sets are identical if

$$k_1 = \delta\phi_o - n_o\ \delta t_{oo} \qquad \text{(J-26)}$$

$$k_2 = a_o \left[e_o - (e_o + \delta e_o) \cos\ \delta\phi_o \right] \qquad \text{(J-27)}$$

$$k_3 = - a_o (e_o + \delta e_o) \sin \delta\phi_o \qquad \text{(J-28)}$$

$$k_4 = \delta a_o \qquad \text{(J-29)}$$

$$k_5 = a_o\ \delta i_o \cos \delta\Omega_o \qquad \text{(J-30)}$$

$$
\begin{pmatrix} \frac{\delta r}{a_o} \\ \frac{\delta s}{a_o} \\ \frac{\delta z}{a_o} \\ \frac{\delta v_r}{v} \\ \frac{\delta v_s}{v} \\ \frac{\delta v_z}{v} \end{pmatrix} = \begin{pmatrix} 1 & 0 & \cos f & -\sin f & 0 & 0 \\ -\frac{3}{2} n_o t & 1 & -2 \sin f & -2 \cos f & 0 & 0 \\ 0 & 0 & 0 & 0 & \sin f & -\cos f \\ \frac{3}{2} n_o t & -1 & \sin f & \cos f & 0 & 0 \\ -\frac{1}{2} & 0 & -\cos f & \sin f & 0 & 0 \\ 0 & 0 & 0 & 0 & \cos f & \sin f \end{pmatrix} \begin{pmatrix} \frac{\delta a_o}{a_o} \\ \delta M_{oo} + \delta \phi_o \\ e_o - (e_o + \delta e_o) \cos \delta \phi_o \\ (e_o + \delta e_o) \sin \delta \phi_o \\ \delta i_o \cos \delta \Omega_o \\ \delta i_o \sin \delta \Omega_o \end{pmatrix}
$$

(J-20)

$$\begin{pmatrix} \delta a_r \\ \delta a_s \\ \delta a_z \end{pmatrix} = n_o^2 a_o \begin{pmatrix} 2 & 0 & 2\cos f & -2\sin f & 0 & 0 \\ \frac{3}{2} n_o t & -1 & 2\sin f & 2\cos f & 0 & 0 \\ 0 & 0 & 0 & 0 & -\sin f & \cos f \end{pmatrix} \begin{pmatrix} \frac{\delta a_o}{a_o} \\ \delta M_{oo} + \delta\phi_o \\ e_o - (e_o + \delta e_o)\cos\delta\phi_o \\ (e_o + \delta e_o)\sin\delta\phi_o \\ \delta i_o \cos\delta\Omega_o \\ \delta i_o \sin\delta\Omega_o \end{pmatrix} \tag{J-21}$$

$$= \frac{\mu}{a_o^3} \begin{pmatrix} 2 & 0 & 0 \\ 0 & -1 & 0 \\ 0 & 0 & -1 \end{pmatrix} \begin{pmatrix} \delta r \\ \delta s \\ \delta z \end{pmatrix} \tag{J-22}$$

$$k_6 = - a_o \quad \delta i_o \sin \delta\Omega_o \tag{J-31}$$

Thus, the differential equation solution is applicable to low-eccentricity reference orbits as well as reference orbits of moderate eccentricity. The distinction between the two types of reference orbits reduces simply to a difference in the physical interpretation of the six constants of integration.

APPENDIX K
MATRICES FOR ELLIPTICAL TRAJECTORIES

K.1 Summary

For the case when the reference trajectory is an ellipse, analytic expressions are developed for the elements of the matrices defined in Appendix F. The eccentric anomaly E is the independent variable. The reference trajectory flight path coordinate system is used.

K.2 Selection of a Coordinate System

The matrices associated with the problem of small departures from a known reference trajectory are defined in Appendix F. In Appendices G, H, and I, the variational problem is solved analytically for the case when the reference trajectory is an ellipse of moderate eccentricity. The solution is an expression for position variation and velocity variation in terms of the variations in the orbital elements and the characteristics of the reference trajectory. From this basic solution analytic expressions can be derived for all the matrices of Appendix F.

The algebraic and trigonometric manipulations required are straightforward but quite formidable in length and in number. Therefore, the choice of coordinate system, of independent variable, and of a group of six orbital elements should be carefully considered from the standpoint of reducing as much as possible the amount of mathematical drudgery.

The reference trajectory coordinate systems have the obvious advantage of uncoupling the z-axis variant motion from the variant motion in the reference trajectory plane. The consequence of this uncoupling is that in each 3-by-3 matrix or sub-matrix of the group of matrices in Appendix F, at least four of the nine elements are zero.

The problem now is to select one of the three reference trajectory systems. Each of the three has an advantage not possessed by the other two. The x y z system is non-rotating, and hence the matrix $\overset{*}{W}$ in Appendix F is the zero matrix. In the r s z system, both the nominal position vector and the nominal acceleration vector lie in the r direction, so that there is no component of either vector in the s direction. The p q z system has the advantage that the nominal velocity vector is in the q direction; hence, there is no component of $\underline{v}$ in the p direction.

The matrix formulations (I-11), (I-12), and (I-13) may be used to compare the three systems. The 4-by-4 matrix of the x y z system has no zeros; the 4-by-4 matrix of the r s z system has two zeros, one due to the fact that s = 0 and the other due to the fact that $a_s = 0$; the p q z system's 4-by-4 matrix has two zeros, both due to the fact that $v_p = 0$. It is apparent that both the r s z and p q z systems are preferable to the x y z system.

The final choice between the r s z system and the p q z system is a difficult one. Actually, a considerable amount of analysis was done in each of the two systems before it became apparent that the matrix formulations are simpler in the p q z system. The relative simplicity of the p q z system is associated with the fact that in this system the secular term in position variation is wholly along the q-axis.

It might be argued that the r s z system has a similar property, in that the secular term in velocity variation is wholly along the r-axis, and therefore, analysis in the r s z system ought to be just as simple as analysis in the p q z system. This argument is not valid because one of the useful formulations in guidance theory involves expressing the variant path in terms of the three components of position variation at two different times, as illustrated by Eqs. (F-2), (F-8), and (F-19), and no such formulation in terms of the three components of velocity variation at two different times is required.

K. 3 Selection of an Independent Variable

The analysis is facilitated if all time-varying quantities are expressed in terms of one independent variable. Variables that might be used include time itself and the three anomalies f, E, and M.

Inasmuch as t and M are linearly related, the choice of one or the other of the two would appear to be equally desirable. Both have the decided disadvantage that trigonometric functions of E and f can be expressed in terms of M (or t) only through Kepler's equation, (B-55), which cannot be solved explicitly for E in terms of M.

On the other hand, the use of the true anomaly f as the independent variable causes difficulty when the secular term in the solution of the variant equations is expressed in terms of f.

By process of elimination, then, the eccentric anomaly is chosen as the independent variable. Both trigonometric and secular terms can be expressed directly in terms of E.

K. 4 Selection of a Grouping of Orbital Elements

The final selection problem is that of selecting a group of six independent constants which characterize the variant path. As in the case of choosing a coordinate system and an independent variable, the criterion in making the selection is to reduce the amount of algebra to manageable proportions.

The six constants serve as a bridge linking position and velocity variation at one time to position and velocity variation at another time. First, a 6-by-6 matrix is obtained which relates position and velocity variation at time t_j to the six constants; then the 6-by-6 matrix is inverted so that the six constants can be expressed in terms of the position and velocity variations at time t_i. Finally, the two 6-by-6 matrices, one in terms of t_j and the other in terms of t_i, are multiplied together to yield a single 6-by-6 matrix by means of which position and velocity variations at t_j may be expressed in terms of position and velocity variations at t_i. The final matrix is the transition matrix $\overset{*}{C}_{ji}$ of Appendix F.

The six constants may be conveniently expressed in terms of variations of some combination of the six orbital elements. The grouping that has finally been chosen, written in vector form, is the following:

$$\delta\underline{e} = \begin{Bmatrix} (1 - e^2)^{1/2} \ \delta\phi - n \ \delta t_o \\ \dfrac{\delta e}{(1 - e^2)^{1/2}} \\ \dfrac{1}{2} \ \dfrac{\delta a}{a} \\ e \ \delta\phi \\ (1 - e^2)^{1/2} \ \delta i \cos \delta\Omega \\ \delta i \sin \delta\Omega \end{Bmatrix} \qquad \text{(K-1)}$$

K. 5 The Use of Position Variation and Velocity Variation to Describe the Motion in the Reference Trajectory Plane

The first four elements of $\delta\underline{e}$ are related to the motion in the reference trajectory plane; the last two are related to the motion normal to the reference trajectory plane. Since the two types of motion are uncoupled, they can be studied independently. This section and the one immediately following will be devoted to a study of the motion in the reference trajectory plane.

If the elements in the vector on the right-hand side of (I-13) are replaced by the first four elements of (K-1), the equation may be rewritten in the form shown in (K-2). When the factor $1/(1 - e^2 \cos^2 E)^{1/2}$ is considered as part of the 4-by-4 matrix of (K-2), the determinant of the matrix is unity. Equation (K-3) is obtained by inverting (K-2). The dashed lines in (K-2) and (K-3) indicate matrix partitioning.

$$\begin{Bmatrix} \frac{\delta p}{a} \\ \frac{\delta \ell}{a} \\ \frac{\delta \nu_p}{na} \\ \frac{\delta \nu_q}{na} \end{Bmatrix} = \frac{1}{(1-e^2\cos^2 E)^{1/2}} \begin{Bmatrix} (1-e\cos E) & \begin{pmatrix} 0 & -(\cos E+e) & 2(1-e^2)^{1/2} & -\sin E \end{pmatrix} \\ & \begin{pmatrix} 1+e\cos E & 2(1-e^2)^{1/2}\sin E & -3(E-e\sin E)(1+e\cos E) & -2(1-e^2)^{1/2}\cos E \\ & & +2e\sin E(1-e\cos E) & \end{pmatrix} \\ \frac{1}{(1-e\cos E)^2} & \begin{pmatrix} -(1-e^2)^{1/2} & -\left[(1-e\cos E)e\cos E + (1-e^2)\right]\sin E & 3(E-e\sin E)(1-e^2)^{1/2} & (1-e\cos E)e\cos^2 E + (\cos E-e) \\ -e\sin E & (1-e^2)^{1/2}(\cos E-e) & 3(E-e\sin E)e\sin E - (1+e\cos E)(1-e\cos E)^2 & (1-e^2)^{1/2}\sin E \end{pmatrix} \end{Bmatrix} \begin{Bmatrix} (1-e^2)^{1/2}\,\delta\phi \\ -n\,\delta t_o \\ \frac{\delta e}{(1-e^2)^{1/2}} \\ \frac{1}{2}\frac{\delta a}{a} \\ e\,\delta\phi \end{Bmatrix} \qquad (K\text{-}2)$$

$$\begin{Bmatrix} (1-e^2)^{1/2}\,\delta\phi \\ -n\,\delta t_o \\ \frac{\delta e}{(1-e^2)^{1/2}} \\ \frac{1}{2}\frac{\delta a}{a} \\ e\,\delta\ell \end{Bmatrix} + \frac{1}{(1-e^2\cos^2 E)^{1/2}} \frac{1}{(1-e\cos E)^2} \left(\begin{array}{cccc} 3(E-e\sin E)(1-e^2)^{1/2} & 3(E-e\sin E)e\sin E - (1+e\cos E)(1-e\cos E)^2 & & -2(1-e^2)^{1/2} \\ (1-e\cos E)e\cos^2 E + (\cos E-e) & (1-e^2)^{1/2}\sin E & & \sin E \\ (1-e^2)^{1/2} & e\sin E & (1-e\cos E) & 0 \\ \left[(1-e\cos E)e\cos E + (1-e^2)\right]\sin E & -(1-e^2)^{1/2}(\cos E-e) & & -(\cos E+e) \end{array}\right) \left(\begin{array}{c} 3(E-e\sin E)(1+e\cos E) - 2e\sin E(1-e\cos E) \\ 2(1-e^2)^{1/2}\cos E \\ 1+e\cos E \\ 2(1-e^2)^{1/2}\sin E \end{array}\right) \begin{Bmatrix} \frac{\delta p}{a} \\ \frac{\delta \ell}{a} \\ \frac{\delta \nu_p}{na} \\ \frac{\delta \nu_q}{na} \end{Bmatrix}$$

(K-3)

There is a striking similarity between the elements of the 4-by-4 matrix of (K-2) and the elements of the 4-by-4 matrix of (K-3). The similarity is made more apparent by partitioning the matrix of (K-2) into four 2-by-2 matrices as follows:

$$\begin{Bmatrix} \frac{\delta p}{a} \\ \frac{\delta q}{a} \\ \frac{\delta v_p}{n\,a} \\ \frac{\delta v_q}{n\,a} \end{Bmatrix} = \begin{Bmatrix} \overset{*}{A}_1 & \overset{*}{A}_2 \\ \overset{*}{A}_3 & \overset{*}{A}_4 \end{Bmatrix} \begin{Bmatrix} (1 - e^2)^{1/2}\ \delta\phi - n\ \delta t_o \\ \frac{\delta e}{(1 - e^2)^{1/2}} \\ \frac{1}{2}\ \frac{\delta a}{a} \\ e\ \delta\phi \end{Bmatrix} \tag{K-4}$$

In terms of the four $\overset{*}{A}$ matrices, Eq. (K-3) becomes

$$\begin{Bmatrix} (1 - e^2)^{1/2}\ \delta\phi - n\ \delta t_o \\ \frac{\delta e}{(1 - e^2)^{1/2}} \\ \frac{1}{2}\ \frac{\delta a}{a} \\ e\ \delta\phi \end{Bmatrix} = \begin{Bmatrix} \overset{*}{A}_4{}^T & -\overset{*}{A}_2{}^T \\ -\overset{*}{A}_3{}^T & \overset{*}{A}_1{}^T \end{Bmatrix} \begin{Bmatrix} \frac{\delta p}{a} \\ \frac{\delta q}{a} \\ \frac{\delta v_p}{n\,a} \\ \frac{\delta v_q}{n\,a} \end{Bmatrix} \tag{K-5}$$

The terms of the 4-by-4 matrix of (K-5), which is the inverse of the 4-by-4 matrix of (K-4), can obviously be obtained from the matrix of (K-4) by inspection. This relationship between (K-4) and (K-5) is not true in general for any arbitrary selection of orbital element variations; in fact, the grouping of the elements that is being used has been chosen primarily because it validates the simple relation between (K-4) and (K-5).

When the subscript j is added to each of the $\overset{*}{A}$ matrices in (K-4) in order to indicate that the matrices are evaluated at time t_j, the equation gives the position and velocity variations corresponding to $t = t_j$. Similarly, adding the subscript i to the $\overset{*}{A}^T$ matrices of (K-5) signifies that the variations in the orbital elements are being expressed in terms of position and velocity variations at $t = t_i$. If the two resulting equations are combined, the variations in the elements may be eliminated and the position and velocity variations at $t = t_j$ are related to the position and velocity variations at $t = t_i$.

$$\begin{Bmatrix} \delta p_j \\ \delta q_j \\ \delta v_{p_j} \\ \delta v_{p_j} \end{Bmatrix} = \begin{Bmatrix} \overset{*}{A}_{1j} & \overset{*}{A}_{2j} \\ n\overset{*}{A}_{3j} & n\overset{*}{A}_{4j} \end{Bmatrix} \begin{Bmatrix} \overset{*}{A}_{4i}{}^T & -\frac{1}{n}\overset{*}{A}_{2i}{}^T \\ -\overset{*}{A}_{3i}{}^T & \frac{1}{n}\overset{*}{A}_{1i}{}^T \end{Bmatrix} \begin{Bmatrix} \delta p_i \\ \delta q_i \\ \delta v_{p_i} \\ \delta v_{p_i} \end{Bmatrix} \qquad \text{(K-6)}$$

$$\begin{Bmatrix} \delta p_j \\ \delta q_j \\ \delta v_{p_j} \\ \delta v_{q_j} \end{Bmatrix} = \begin{matrix} \overset{*}{A}_{1j}\overset{*}{A}_{4i}^T - \overset{*}{A}_{2j}\overset{*}{A}_{3i}^T & \frac{1}{n}(-\overset{*}{A}_{1j}\overset{*}{A}_{2i}^T + \overset{*}{A}_{2j}\overset{*}{A}_{1i}^T) \\ n(\overset{*}{A}_{3j}\overset{*}{A}_{4i}^T - \overset{*}{A}_{4j}\overset{*}{A}_{3i}^T) & -\overset{*}{A}_{3j}\overset{*}{A}_{2i}^T + \overset{*}{A}_{4j}\overset{*}{A}_{1i}^T \end{matrix} \begin{matrix} \delta p_i \\ \delta q_i \\ \delta v_{p_i} \\ \delta v_{q_i} \end{matrix} \qquad \text{(K-7)}$$

$$= \begin{matrix} \overset{*}{M}_{ji}' & \overset{*}{N}_{ji}' \\ \overset{*}{S}_{ji}' & \overset{*}{T}_{ji}' \end{matrix} \begin{matrix} \delta p_i \\ \delta q_i \\ \delta v_{p_i} \\ \delta v_{q_i} \end{matrix} \qquad \text{(K-8)}$$

The primed matrices of (K-8) are the two-dimensional versions of the corresponding matrices defined in Appendix F. It is apparent from (K-7) and (K-8) that

$$\overset{*}{M}_{ji}' = (\overset{*}{T}_{ij}')^T \qquad \text{(K-9)}$$

$$\overset{*}{N}_{ji}' = (-\overset{*}{N}_{ij}')^T \qquad \text{(K-10)}$$

$$\overset{*}{S}_{ji}' = (-\overset{*}{S}_{ij}')^T \qquad \text{(K-11)}$$

$$\overset{*}{T}_{ji}' = (\overset{*}{M}_{ij}')^T \qquad \text{(K-12)}$$

$$
\begin{Bmatrix} \frac{\delta p_i}{a} \\ \frac{\delta q_i}{a} \\ \frac{\delta p_j}{a} \\ \frac{\delta q_j}{a} \end{Bmatrix} =
\begin{Bmatrix}
\frac{1 - e\cos E_i}{(1 - e^2\cos^2 E_i)^{1/2}} & \left(0 \quad -(\cos E_i + e) \quad 2(1-e^2)^{1/2} \quad -\sin E_i \right) \\
\frac{1}{(1 - e^2\cos^2 E_i)^{1/2}} & \left(1 + e\cos E_i \quad 2(1-e^2)^{1/2}\sin E_i \quad -(3E_i - e\sin E_i)(1 + e\cos E_i) + 4e\sin E_i \quad -2(1-e^2)^{1/2}\cos E_i \right) \\
\frac{1 - e\cos E_j}{(1 - e^2\cos^2 E_j)^{1/2}} & \left(0 \quad -(\cos E_j + e) \quad 2(1-e^2)^{1/2} \quad -\sin E_j \right) \\
\frac{1}{(1 - e^2\cos^2 E_j)^{1/2}} & \left(1 + e\cos E_j \quad 2(1-e^2)^{1/2}\sin E_j \quad -(3E_j - e\sin E_j)(1 + e\cos E_j) + 4e\sin E_j \quad -2(1-e^2)^{1/2}\cos E_j \right)
\end{Bmatrix}
\begin{Bmatrix} (1-e^2)^{1/2}\,\delta\phi - n\,\delta t_o \\ \frac{\delta e}{(1-e^2)^{1/2}} \\ \frac{1}{2}\frac{\delta a}{a} \\ e\,\delta\phi \end{Bmatrix}
$$

(K-13)

These two-dimensional matrix equations are in agreement with the corresponding three-dimensional matrix equations of Section F. 7.

K. 6 The Use of Two Position Variations to Describe the Motion in the Reference Trajectory Plane

Another way of expressing the variations in the orbital elements is in terms of the position variations at two different times, t_i and t_j. This is accomplished by inverting Eq. (K-13). The expression for the inverse is simplified to some extent by the introduction of two new angles, E_P ("E plus") and E_M ("E minus").

$$E_P = \frac{1}{2} (E_j + E_i) \tag{K-14}$$

$$E_M = \frac{1}{2} (E_j - E_i) \tag{K-15}$$

The determinant of the 4-by-4 matrix of (K-13) is

$$(\det)_{pq} = - 4 X \sin E_M \tag{K-16}$$

where $X = (3 E_M - e \sin E_M \cos E_P)(\cos E_M + e \cos E_P) - 4 \sin E_M$ (K-17)

The inverse equation is (K-18).

(K-13) and (K-18) illustrate the reason previously mentioned for selecting the p q z coordinate system. Only two of the sixteen elements in the matrix of (K-13) contain the secular term; if the r s z system were used, there would be four elements with secular terms. Eight elements in the (K-18) matrix have secular terms; with the r s z system there would be twelve elements with secular terms.

Note that the element $\frac{1}{2} \frac{\delta a}{a}$ is unaffected by the secular term.

The factor 1/2 X is common to all the elements in the (K-18) matrix. Since X is a time-varying quantity that goes through zero, there are combinations of E_i and E_j for which the matrix of (K-13) become singular; for these combinations (K-18) cannot be evaluated.

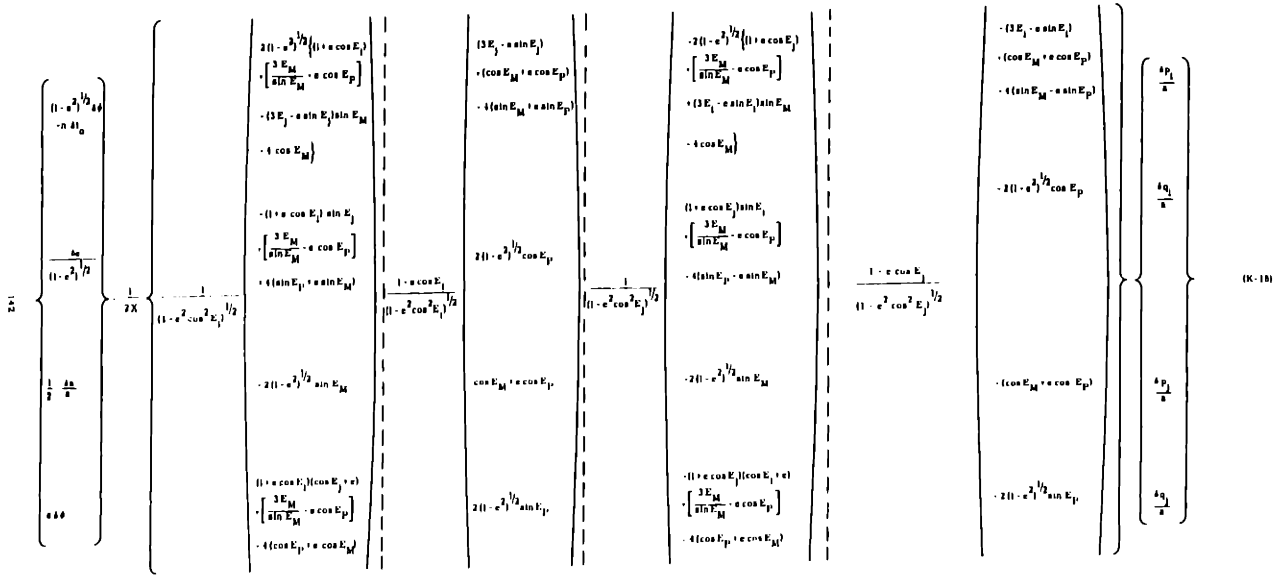

(K-18)

The remarks about X are also applicable to sin E_M. Whenever sin E_M equals zero, the (K-13) matrix is singular. The significance of the singularities is discussed in Appendix O.

K. 7 Motion Normal to the Reference Trajectory Plane

The position and velocity variations along the z-axis are

$$\begin{Bmatrix} \delta z \\ \delta v_z \end{Bmatrix} = \begin{Bmatrix} y & -x \\ v_y & -v_x \end{Bmatrix} \begin{Bmatrix} \delta i \cos & \delta\Omega \\ \delta i \sin & \delta\Omega \end{Bmatrix} \tag{K-19}$$

$$\begin{Bmatrix} \frac{\delta z}{a} \\ \frac{\delta v_z}{na} \end{Bmatrix} = \begin{Bmatrix} \sin E & -(\cos E - e) \\ \frac{\cos E}{1 - e \cos E} & \frac{\sin E}{1 - e \cos E} \end{Bmatrix} \begin{Bmatrix} (1 - e^2)^{1/2} \ \delta i \cos & \delta\Omega \\ \delta i \sin & \delta\Omega \end{Bmatrix} \tag{K-20}$$

The determinant of the 2-by-2 matrix of (K-20) is equal to one. The inverse of (K-20) is

$$\begin{Bmatrix} (1 - e^2)^{1/2} \ \delta i \cos & \delta\Omega \\ \delta i \sin & \delta\Omega \end{Bmatrix} = \begin{Bmatrix} \frac{\sin E}{1 - e \cos E} & \cos E - e \\ \frac{-\cos E}{1 - e \cos E} & \sin E \end{Bmatrix} \begin{Bmatrix} \frac{\delta z}{a} \\ \frac{\delta v_z}{na} \end{Bmatrix} \tag{K-21}$$

By combining (K-20) and (K-21), δz_j and δv_{z_j} are expressed in terms of δz_i and δv_{z_i}.

$$\begin{Bmatrix} \delta z_j \\ \delta v_{z_j} \end{Bmatrix} = \begin{bmatrix} \sin E_j & -(\cos E_j - e) \\ \dfrac{n \cos E_j}{1 - e \cos E_j} & \dfrac{n \sin E_j}{1 - e \cos E_j} \end{bmatrix} \begin{bmatrix} \dfrac{\sin E_i}{1 - e \cos E_i} & \dfrac{1}{n}(\cos E_i - e) \\ -\dfrac{\cos E_i}{1 - e \cos E_i} & \dfrac{1}{n} \sin E_i \end{bmatrix} \begin{Bmatrix} \delta z_i \\ \delta v_{z_i} \end{Bmatrix} \tag{K-22}$$

$$= \begin{bmatrix} 1 - \dfrac{2 \sin^2 E_M}{1 - e \cos E_i} & \dfrac{2 \sin E_M (\cos E_M - e \cos E_P)}{n} \\ \dfrac{-2n \sin E_M \cos E_M}{(1 - e \cos E_i)(1 - e \cos E_j)} & 1 - \dfrac{2 \sin^2 E_M}{1 - e \cos E_j} \end{bmatrix} \begin{Bmatrix} \delta z_i \\ \delta v_{z_i} \end{Bmatrix} \tag{K-23}$$

Note that when $\sin E_M = 0$, i.e., when $(E_j - E_i)$ is an integer multiple of 360°, $\delta z_j = \delta z_i$ and $\delta v_{z_j} = \delta v_{z_i}$, irrespective of the nature of the variations in the orbital elements.

The variations in the elements may be expressed in terms of δz_i and δz_j by inverting Eq. (K-24).

$$\begin{Bmatrix} \dfrac{\delta z_i}{a} \\ \dfrac{\delta z_j}{a} \end{Bmatrix} = \begin{bmatrix} \sin E_i & -(\cos E_i - e) \\ \sin E_j & -(\cos E_j - e) \end{bmatrix} \begin{Bmatrix} (1 - e^2)^{1/2} \ \delta i \cos \ \delta\Omega \\ \delta i \sin \ \delta\Omega \end{Bmatrix} \tag{K-24}$$

The determinant of the 2-by-2 matrix is

$$(\det)_z = \sin (E_j - E_i) - e (\sin E_j - \sin E_i) \qquad \text{(K-25)}$$

$$= 2 \sin E_M (\cos E_M - e \cos E_P) \qquad \text{(K-26)}$$

The inverted equation is

$$\begin{matrix} (1 - e^2)^{1/2} \ \delta i \cos \delta\Omega \\ \delta i \sin \delta\Omega \end{matrix} = \frac{1}{(\det)_z} \begin{matrix} -(\cos E_j - e) & \cos E_i - e \\ -\sin E_j & \sin E_i \end{matrix} \begin{matrix} \frac{\delta z_i}{a} \\ \frac{\delta z_j}{a} \end{matrix} \qquad \text{(K-27)}$$

The condition for singularity of the matrix of (K-24) is most easily interpreted when $(\det)_z$ is expressed in terms of the difference in true anomalies, $(f_j - f_i)$.

$$(\det)_z = \frac{r_i \ r_j}{a^2 (1 - e^2)^{1/2}} \sin (f_j - f_i) \qquad \text{(K-28)}$$

The matrix becomes singular when

$$f_j - f_i = N \pi \qquad \text{(K-29)}$$

where N is any integer.

K. 8 The Transition Matrix $\overset{*}{C}_{ji}$

The results of Section K. 5 and K. 7 can be combined to give analytic expressions for the matrices defined in Appendix F. In this section, such expressions are developed for the elements of the transition matrix $\overset{*}{C}_{ji}$.

The 3-by-6 matrices $\overset{*}{F}_j$ and $\overset{*}{L}_j$ satisfy the equation

$$\delta\underline{x}_j = \begin{Bmatrix} \delta p_j \\ \delta q_j \\ \delta z_j \\ \delta v_{p_j} \\ \delta v_{q_j} \\ \delta v_{z_j} \end{Bmatrix} = \begin{Bmatrix} \overset{*}{F}_j \\ \overset{*}{L}_j \end{Bmatrix} \begin{Bmatrix} (1-e^2)^{1/2}\ \delta\phi - n\ \delta t_o \\ \dfrac{\delta e}{(1-e^2)^{1/2}} \\ \dfrac{1}{2}\ \dfrac{\delta a}{a} \\ e\ \delta\phi \\ (1-e^2)^{1/2}\ \delta i \cos\ \delta\Omega \\ \delta i \sin\ \delta\Omega \end{Bmatrix} \qquad \text{(K-30)}$$

The elements of $\overset{*}{F}_j$ and $\overset{*}{L}_j$ are given in Eqs. (K-31) and (K-32).

$$\ddot{F}_j = a \left\{ \begin{array}{l} \dfrac{1 - e\cos E_j}{(1 - e^2\cos^2 E_j)^{1/2}} \\ \dfrac{1}{(1 - e^2\cos^2 E_j)^{1/2}} \\ \\ \end{array} \right. \left(\begin{array}{cccccc} 0 & -(\cos E_j + e) & 2(1-e^2)^{1/2} & -\sin E_j & 0 & 0 \\ 1 + e\cos E_j & 2(1-e^2)^{1/2}\sin E_j & -3(1+e\cos E_j)(E_j - e\sin E_j) & -2(1-e^2)^{1/2}\cos E_j & 0 & 0 \\ & & +2e\sin E_j(1-e\cos E_j) & & & \\ 0 & 0 & 0 & 0 & \sin E_j & -(\cos E_j - e) \end{array} \right) \left. \begin{array}{l} \\ \\ \\ \end{array} \right\}$$

(K-31)

$$\ddot{I}_j = na \left\{ \begin{array}{l} \dfrac{1}{(1 - e\cos E_j)^2(1 - e^2\cos^2 E_j)^{1/2}} \\ \\ \dfrac{1}{1 - e\cos E_j} \end{array} \right. \left(\begin{array}{cccccc} -(1-e^2)^{1/2} & -\left[(1-e\cos E_j)e\cos E_j + (1-e^2)\right]\sin E_j & 3(1-e^2)^{1/2}(E_j - e\sin E_j) & (1-e\cos E_j)e\cos^2 E_j + (\cos E_j - e) & 0 & 0 \\ -e\sin E_j & (1-e^2)^{1/2}(\cos E_j - e) & 3e\sin E_j(E_j - e\sin E_j) - (1+e\cos E_j)(1-e\cos E_j)^2 & (1-e^2)^{1/2}\sin E_j & 0 & 0 \\ 0 & 0 & 0 & 0 & \cos E_j & \sin E_j \end{array} \right) \left. \begin{array}{l} \\ \\ \\ \end{array} \right\}$$

(K-32)

$$
\overset{*}{R}_1 = \frac{1}{a}
\left\{
\begin{array}{c|ccc}
\dfrac{1}{(1 - e\cos E_1)^2 (1 - e^2\cos^2 E_1)^{1/2}}
\begin{pmatrix}
3(1-e^2)^{1/2}(E_1 - e\sin E_1) & 3e\sin E_1 (E_1 - e\sin E_1) & 0 \\
 & - (1 + e\cos E_1)(1 - e\cos E_1)^2 & \\
(1 - e\cos E_1)e\cos^2 E_1 & (1-e^2)^{1/2}\sin E_1 & 0 \\
+ (\cos E_1 - e) & & \\
(1-e^2)^{1/2} & e\sin E_1 & 0 \\
\left[(1 - e\cos E_1)e\cos E_1\right. & - (1-e^2)^{1/2}(\cos E_1 - e) & 0 \\
\left. + (1-e^2)\right]\sin E_1 & &
\end{pmatrix} \\
\hline
\dfrac{1}{(1 - e\cos E_1)}
\begin{pmatrix}
0 & 0 & \sin E_1 \\
0 & 0 & -\cos E_1
\end{pmatrix}
\end{array}
\right\}
\qquad \text{(K-34)}
$$

$$V_i = \frac{1}{na} \left\{ \frac{1 - e\cos E_i}{(1 - e^2\cos^2 E_i)^{1/2}} \begin{pmatrix} 2(1-e^2)^{1/2} \\ \sin E_i \\ 0 \\ -(\cos E_i + e) \\ 0 \\ 0 \end{pmatrix} \middle| \frac{1}{(1 - e^2\cos^2 E_i)^{1/2}} \begin{pmatrix} 3(1 + e\cos E_i)(E_i - e\sin E_i) \\ -2e\sin E_i(1 - e\cos E_i) \\ 2(1-e^2)^{1/2}\cos E_i \\ 1 + e\cos E_i \\ 2(1-e^2)^{1/2}\sin E_i \\ 0 \\ 0 \end{pmatrix} \middle| \begin{pmatrix} 0 \\ 0 \\ 0 \\ 0 \\ \cos E_i - e \\ \sin E_i \end{pmatrix} \right\} \qquad \text{(K-35)}$$

The inverse of Eq. (K-30) establishes the 6-by-3 matrices $\overset{*}{R}_i$ and $\overset{*}{V}_i$.

$$\delta\underline{e} = \begin{Bmatrix} (1-e^2)^{1/2}\ \delta\phi - n\ \delta t_o \\ \dfrac{\delta e}{(1-e^2)^{1/2}} \\ \dfrac{1}{2}\ \dfrac{\delta a}{a} \\ e\ \delta\phi \\ (1-e^2)^{1/2}\ \delta i \cos\ \delta\Omega \\ \delta i \sin\ \delta\Omega \end{Bmatrix} = \begin{Bmatrix} \overset{*}{R}_i & \overset{*}{V}_i \end{Bmatrix} \begin{Bmatrix} \delta p_i \\ \delta q_i \\ \delta z_i \\ \delta v_{p_i} \\ \delta v_{q_i} \\ \delta v_{z_i} \end{Bmatrix} \qquad \text{(K-33)}$$

The elements of $\overset{*}{R}_i$ and $\overset{*}{V}_i$ are given in Eqs. (K-34) and (K-35).

The transition matrix $\overset{*}{C}_{ji}$ is obtained from $\overset{*}{F}_j$, $\overset{*}{L}_j$, $\overset{*}{R}_i$, and $\overset{*}{V}_i$.

$$\overset{*}{C}_{ji} = \begin{Bmatrix} \overset{*}{M}_{ji} & \overset{*}{N}_{ji} \\ \overset{*}{S}_{ji} & \overset{*}{T}_{ji} \end{Bmatrix} \qquad \text{(K-36)}$$

$$= \begin{Bmatrix} \overset{*}{F}_j \\ \overset{*}{L}_j \end{Bmatrix} \begin{Bmatrix} \overset{*}{R}_i & \overset{*}{V}_i \end{Bmatrix} \qquad \text{(K-37)}$$

$$= \begin{Bmatrix} \overset{*}{F}_j\overset{*}{R}_i & \overset{*}{F}_j\overset{*}{V}_i \\ \overset{*}{L}_j\overset{*}{R}_i & \overset{*}{L}_j\overset{*}{V}_i \end{Bmatrix} \qquad \text{(K-38)}$$

$$
M_{ji} = \left\{ \frac{1}{(1 - e^2\cos^2 E_i)^{1/2}(1 - e^2\cos^2 E_j)^{1/2}} \right.
$$

$$
\left(\begin{array}{ccc}
(1 + e\cos E_i)(1 - e\cos E_j) & \dfrac{2(1-e^2)^{1/2}(1 - e\cos E_i)}{(1 - e\cos E_i)^2} & \\
+ \dfrac{2\sin E_M (1 - e\cos E_j)}{(1 - e\cos E_i)^2} \cdot \Big[(1 - e^2)\sin E_M & \cdot \sin E_M(\cos E_M - e\cos E_P) & 0 \\
- (1 - e\cos E_i) e \sin E_i \cos E_M \Big] & & \\
\dfrac{2(1-e^2)^{1/2}}{(1 - e\cos E_i)^2} & (1 - e\cos E_j)(1 + e\cos E_j) & \\
\cdot \Big\{ -(1 + e\cos E_j) & + \dfrac{2}{(1 - e\cos E_i)^2} \Big\{ -(1 + e\cos E_j) & 0 \\
\cdot (3E_M - e\sin E_M \cos E_P) & \cdot e\sin E_i (3E_M - e\sin E_M \cos E_P) & \\
+ 2\sin E_M \Big[e\cos E_P & + 2\sin E_M \Big[2e\sin E_P & \\
+ (1 + e\cos E_i - e^2\cos^2 E_i)\cos E_M \Big] \Big\} & -(1 + e^2)\sin E_M \Big] \Big\} &
\end{array} \right)
$$

$$
\left(\begin{array}{ccc}
0 & 0 & 1 - \dfrac{2\sin^2 E_M}{1 - e\cos E_i}
\end{array} \right) \Bigg\}
$$

(K-39)

$$\dot{N}_{jl} = \frac{2}{n} \left\{ \begin{array}{c|ccc} \multirow{2}{*}{$\dfrac{1}{(1 - e^2\cos^2 E_l)^{1/2}(1 - e^2\cos E_j)^{1/2}}$} & (1 - e\cos E_l)(1 - e\cos E_j) & 2(1 - e^2)^{1/2}(1 - e\cos E_j)\sin^2 E_M & 0 \\ & \cdot \sin E_M (\cos E_M + e\cos E_P) & & \\ & - 2(1 - e^2)^{1/2}(1 - e\cos E_l)\sin^2 E_M & -(1 + e\cos E_l)(1 + e\cos E_j) & 0 \\ & & \cdot (3 E_M - e\sin E_M \cos E_P) & \\ & & + 4\sin E_M (\cos E_M + e\cos E_P) & \\ \hline & 0 & 0 & \sin E_M (\cos E_M - e\cos E_P) \end{array} \right\} \qquad \text{(K-40)}$$

$$
S_{II} = \left\{ \frac{1}{(1-e\cos E_i)^2 (1-e\cos E_j)^2 (1-e^2\cos^2 E_i)^{1/2} (1-e^2\cos^2 E_j)^{1/2}} \right.
$$

$$
\begin{vmatrix}
(1-e^2)(3E_M - 2e\sin E_M \cos E_P) & (1-e)^{1/2}\left\{3e\sin E_i (E_M - e\sin E_M \cos F_P)\right. & 0 \\
-\left\{(1-e\cos E_i)(1-e\cos E_j)e^2 \sin E_i \sin E_j\right. & +\left[(1-e^2)+(1-e\cos E_j)e\cos E_j\right]\sin^2 E_M & \\
+(1-e^2)\left[1+(1-e\cos E_i)e\cos E_i\right. & -e^2\left[2(1-e\cos E_i)\cos E_M \cos E_P\right. & \\
\left.\left.+(1-e\cos E_j)e\cos E_j\right]\right\}\sin E_M \cos E_M & \left.+(1-e\cos E_j)\cos E_j\right]\sin E_M \sin E_P\Big\} & \\
(1-e^2)^{1/2}\left\{3e\sin E_j (E_M - e\sin E_M \cos F_P)\right. & e^2 \sin E_i \sin E_j \left[3E_M - 4e\sin E_M \cos E_P\right. & 0 \\
-\left[(1-e^2)+(1-e\cos E_i)e\cos E_i\right]\sin^2 E_M & \left.+e^2 \sin E_M \cos E_M(\cos^2 E_P - \sin^2 E_P)\right] & \\
+e^2\left[2(1-e\cos E_j)\cos E_M \cos E_P\right. & -(1-e^2)\sin E_M\left[(1+e^2)\cos E_M - 2e\cos E_P\right] & \\
\left.+(1-e\cos E_i)\cos E_i\right]\sin E_M \sin E_P\Big\} & &
\end{vmatrix}
$$

$$
\left.
\begin{vmatrix}
0 & 0 & -\dfrac{\sin E_M \cos E_M}{(1-e\cos E_i)(1-e\cos E_j)}
\end{vmatrix}
\right\}
$$

(K-41)

$$
\overset{+}{T}_{jI} = \left\{ \frac{1}{(1-e^2\cos^2 E_I)^{1/2}\,(1-e^2\cos^2 E_j)^{1/2}} \right.
\left(\begin{array}{ccc}
\begin{array}{l}(1+e\cos E_j)(1-e\cos E_I) \\ + \dfrac{2\sin E_M (1-e\cos E_I)}{(1-e\cos E_j)^2}\Big[(1-e^2)\sin E_M \\ + (1-e\cos E_j)\, e\sin E_j \cos E_M\Big]\end{array} &
\begin{array}{l}\dfrac{2(1-e^2)^{1/2}}{(1-e\cos E_j)^2} \\ \cdot\Big\{(1+e\cos E_I) \\ \cdot (3E_M - e\sin E_M\cos E_P) \\ - 2\sin E_M\Big[e\cos F_P \\ + (1+e\cos F_j - e^2\cos^2 F_j)\cos F_M\Big]\Big\}\end{array} & 0 \\
\begin{array}{l} - \dfrac{2(1-e^2)^{1/2}(1-e\cos E_i)}{(1-e\cos E_j)^2} \\ \cdot \sin E_M(\cos E_M - e\cos F_P)\end{array} &
\begin{array}{l}(1-e\cos E_j)(1+e\cos E_I) \\ + \dfrac{2}{(1-e\cos E_j)^2}\Big\{(1+e\cos E_I) \\ \cdot e\sin E_j\,(3E_M - e\sin E_M\cos E_P) \\ - 2\sin F_M\Big[2e\sin E_P \\ + (1+e^2)\sin E_M\Big]\Big\}\end{array} & 0 \\
0 & 0 & 1 - \dfrac{2\sin^2 E_M}{1-e\cos E_j}
\end{array} \right)
\left. \right\}
$$

(K-42)

The matrix multiplications indicated in (K-38) have been performed. The four resulting 3-by-3 sub-matrices, $\overset{*}{M}_{ji}$, $\overset{*}{N}_{ji}$, $\overset{*}{S}_{ji}$ and $\overset{*}{T}_{ji}$, are presented in Eqs. (K-39), (K-40), (K-41), and (K-42). Taken together, these four sub-matrices constitute the desired solution for $\overset{*}{C}_{ji}$.

It is interesting to note that only nine of the sixteen non-zero in-plane elements of $\overset{*}{C}_{ji}$ have secular terms. There is no secular term in the expression for δp_j. The coefficient of δv_{p_i} contains no secular term.

K.9 Matrices Associated with Position Variations at Two Different Times

The matrices of Appendix F that are used in conjunction with a path deviation vector composed of two position variation vectors are $\overset{*}{H}_{ij}$, $\overset{*}{H}_{ji}$, $\overset{*}{J}_{ij}$, and $\overset{*}{K}_{ij}$. The first two are defined by the following equation:

$$\begin{Bmatrix} (1-e^2)^{1/2}\ \delta\phi - n\ \delta t_o \\ \dfrac{\delta e}{(1-e^2)^{1/2}} \\ \dfrac{1}{2}\dfrac{\delta a}{a} \\ e\ \delta\phi \\ (1-e^2)^{1/2}\ \delta i \cos\ \delta\Omega \\ \delta i \sin\ \delta\Omega \end{Bmatrix} = \begin{Bmatrix} \overset{*}{H}_{ij} & \overset{*}{H}_{ji} \end{Bmatrix} \begin{Bmatrix} \delta p_i \\ \delta q_i \\ \delta z_i \\ \delta p_j \\ \delta q_j \\ \delta z_j \end{Bmatrix} \qquad \text{(K-43)}$$

$$
\overset{*}{H}_{ij} = \frac{1}{2a}
\begin{Bmatrix}
\dfrac{1}{(1-e^2\cos^2 E_j)^{1/2}} X
\begin{vmatrix}
2(1-e^2)^{1/2}\left\{(1+e\cos E_i)\left(\dfrac{3E_M}{\sin E_M} - e\cos E_P\right)\right. \\
\quad -(3E_j - e\sin E_j)\sin E_M \\
\quad \left. -4\cos E_M\right\} \\
-(1+e\cos E_i)\sin E_j\left(\dfrac{3E_M}{\sin E_M} - e\cos E_P\right) \\
+4(\sin E_P + e\sin E_M) \\
-2(1-e^2)^{1/2}\sin E_M \\
(1+e\cos E_i)(\cos E_j + e)\left(\dfrac{3E_M}{\sin E_M} - e\cos E_P\right) \\
-4(\cos E_P + e\cos E_M) \\
0 \\
0
\end{vmatrix}
&
\dfrac{1-e\cos E_i}{(1-e^2\cos^2 E_i)^{1/2}} X
\begin{vmatrix}
(3E_j - e\sin E_j) \\
\cdot(\cos E_M + e\cos E_P) \\
-4(\sin E_M + e\sin E_P) \\
2(1-e^2)^{1/2}\cos E_P \\
\cos E_M + e\cos E_P \\
2(1-e^2)^{1/2}\sin E_P \\
0 \\
0
\end{vmatrix}
&
\dfrac{1}{\sin E_M(\cos E_M - e\cos E_P)}
\begin{vmatrix}
0 \\
0 \\
0 \\
0 \\
-(\cos E_j - e) \\
-\sin E_j
\end{vmatrix}
\end{Bmatrix}
$$

(K-44)

$$
\dot{J}_{ij} = n \left\{ \begin{array}{c|ccc}
\dfrac{1}{1+e\cos E_i} \left(\begin{array}{ccc}
\dfrac{e\sin E_i}{(1-e\cos E_i)^2} & & \\
+\dfrac{1}{2(1-e\cos E_i)} X \left\{ (1+e\cos F_i) & & \\
\cdot\left[2\sin^2 E_M - (1+e\cos E_i) \right] & -(1-e^2)^{1/2}\left[\dfrac{1}{(1-e\cos E_i)^2} + \dfrac{\sin E_M}{X} \right] & 0 \\
\cdot\left[\dfrac{3E_M}{\sin E_M} - e\cos E_P \right] & & \\
+4\left[(1+e\cos E_i)\cos E_M & & \\
+e\sin E_i \sin E_M \right] \right\} & & \\
-(1-e^2)^{1/2}\left[\dfrac{1}{(1-e\cos E_i)^2} + \dfrac{\sin E_M}{X} \right] & -\dfrac{e\sin E_i}{(1-e\cos E_i)^2} & \\
 & +\dfrac{1}{2X}(1-e\cos E_i)(\cos E_M + e\cos E_P) & 0
\end{array} \right) \\
\hline
\left(\begin{array}{ccc} 0 & 0 & \dfrac{2\sin^2 E_M - (1-e\cos E_i)}{2\sin E_M (\cos E_M - e\cos E_P)(1-e\cos E_i)} \end{array} \right)
\end{array} \right\}
$$

(K-47)

$$
{}^{\circ}K_{ij} = \frac{n}{2}
\left\{
\begin{array}{c}
\dfrac{1}{(1-e^2\cos^2 E_i)^{1/2}(1-e^2\cos^2 E_j)^{1/2}\,X}
\begin{pmatrix}
(1+e\cos E_i)(1+e\cos E_j) & & \\
\cdot\left(\dfrac{3E_M}{\sin E_M} - e\cos E_P\right) & 2(1-e^2)^{1/2}(1-e\cos E_j)\sin E_M & 0 \\
-4(\cos E_M + e\cos E_P) & & \\
-2(1-e^2)^{1/2}(1-e\cos E_i)\sin E_M & -(1-e\cos E_i)(1-e\cos E_j) & 0 \\
 & \cdot(\cos E_M + e\cos E_P) &
\end{pmatrix} \\
\hline
\begin{pmatrix} 0 & 0 & \dfrac{1}{\sin E_M(\cos E_M - e\cos E_P)} \end{pmatrix}
\end{array}
\right\}
\qquad \text{(K-48)}
$$

Both $\overset{*}{H}_{ij}$ and $\overset{*}{H}_{ji}$ are 6-by-3 matrices. The elements of $\overset{*}{H}_{ij}$ are shown in Eq. (K-44). $\overset{*}{H}_{ji}$ may be obtained from $\overset{*}{H}_{ij}$ by a simple interchange of all subscripts i and j.

Matrices $\overset{*}{J}_{ij}$ and $\overset{*}{K}_{ij}$ relate $\delta\underline{v}_i$ to $\delta\underline{r}_i$ and $\delta\underline{r}_j$.

$$\delta\underline{v}_i = \overset{*}{L}_i \left(\overset{*}{H}_{ij} \quad \delta\underline{r}_i + \overset{*}{H}_{ji} \quad \delta\underline{r}_j\right) \tag{K-45}$$

$$= \overset{*}{J}_{ij} \quad \delta\underline{r}_i + \overset{*}{K}_{ij} \quad \delta\underline{r}_j \tag{K-46}$$

The matrix products indicated by (K-45) and (K-46) have been obtained and are recorded as Eqs. (K-47) and (K-48).

The factor X appears in the denominator of each of the in-plane elements of all four matrices, $\overset{*}{H}_{ij}$, $\overset{*}{H}_{ji}$, $\overset{*}{J}_{ij}$, and $\overset{*}{K}_{ij}$. The factor $(\det)_z$ appears in the denominator of all out-of-plane elements. Also, there are elements containing the term $3\,E_M/\sin E_M$. Therefore, the matrices are not applicable when X or $(\det)_z$ or $\sin E_M$ is equal to zero.

The elements of $\overset{*}{K}_{ij}$ in Eq. (K-48) may be compared with those of $\overset{*}{N}_{ji}$ in Eq. (K-40). Let k_{rs} be the element in the r-th row and the s-th column of $\overset{*}{K}_{ij}$.

$$\overset{*}{K}_{ij} = \begin{Bmatrix} k_{11} & k_{12} & 0 \\ k_{21} & k_{22} & 0 \\ 0 & 0 & k_{33} \end{Bmatrix} \tag{K-49}$$

Matrix $\overset{*}{N}_{ji}$ can be expressed in terms of the elements of $\overset{*}{K}_{ij}$.

$$\overset{*}{N}_{ji} = \left\{ \begin{array}{ccc} \frac{4 X \sin E_M}{n^2} & -k_{22} & k_{12} & 0 \\ & k_{21} & -k_{11} & 0 \\ \hline & 0 & 0 & \frac{1}{k_{33}} \end{array} \right\} \qquad \text{(K-50)}$$

Equation (F-34) indicates that $\overset{*}{K}_{ij}$ is the inverse of $\overset{*}{N}_{ji}$. Therefore,

$$\overset{*}{K}_{ij} \; \overset{*}{N}_{ji} = \overset{*}{I}_3 \qquad \text{(K-51)}$$

The off-diagonal elements of $\overset{*}{K}_{ij} \; \overset{*}{N}_{ji}$ are easily verified as being zero from (K-49) and (K-50). It is also obvious that the element in the third row and the third column is unity. The equation for either of the other two diagonal elements yields a simple relationship between the k's and the factor X.

$$\frac{4 X \sin E_M}{n^2} \; (-k_{11} k_{22} + k_{12} k_{21}) = 1 \qquad \text{(K-52)}$$

$$k_{11} k_{22} - k_{12} k_{21} = - \frac{n^2}{4 X \sin E_M} \qquad \text{(K-53)}$$

The combination $(k_{11}\, k_{22} - k_{12}\, k_{21})$ is the determinant of the 2-by-2 sub-matrix of $\overset{*}{K}_{ij}$ which relates to motion in the plane of the reference trajectory. The determinant of the sub-matrix is equal to

$$- \frac{n^2}{4\, X \sin E_M} \, .$$

Then the determinant of the 2-by-2 sub-matrix of $\overset{*}{N}_{ji}$ is

$$- \frac{4\, X \sin E_M}{n^2} \, .$$

The quantity $- 4\, X \sin E_M$ has been encountered once before, in Eq. (K-16), where it was indicated as the determinant of the 4-by-4 matrix of Eq. (K-13).

K.10. Checks of the Matrix Elements

Some of the equations developed in Appendix F for the n-body problem may be used as a check of the validity of the matrix formulations of Sections K.8 and K.9. In particular, Eqs. (F-75) through (F-79) may be checked by inspection.

A simple cross-check of $\overset{*}{N}_{ji}$ and $\overset{*}{K}_{ij}$ was made in the last section. The author has verified Eq. (K-53) by actually performing the indicated multiplication of matrix elements. Equation (F-33) has been used to check the elements of $\overset{*}{M}_{ji}$, $\overset{*}{K}_{ij}$, and $\overset{*}{J}_{ij}$.

Additional checks are obtainable from the matrix differential equations of Section F.5. These include Eqs. (F-51) through (F-54), (F-57) and (F-58), (F-63) and (F-64), and (F-69) through (F-72). The matrices $\overset{*}{G}$ and $\overset{*}{W}$ are needed for these checks.

From Eqs. (E-19), (B-81), and (B-82),

$$\overset{*}{G} = \frac{n^2}{(1 - e\cos E)^3} \left\{ \frac{3}{1 - e^2\cos^2 E} \begin{pmatrix} 1 - e^2 & (1 - e^2)^{1/2} e \sin E & 0 \\ (1 - e^2)^{1/2} e \sin E & e^2 \sin^2 E & 0 \\ 0 & 0 & 0 \end{pmatrix} - \overset{*}{I}_3 \right\}$$

(K-54)

The angular velocity of the p q z coordinate system is $\dot{g}\underline{u}_z$. From Eqs. (B-80) and (F-44), the W matrix is given by

$$\overset{*}{W} = \frac{n (1 - e^2)^{1/2}}{(1 + e\cos E)(1 - e\cos E)^2} \begin{pmatrix} 0 & -1 & 0 \\ 1 & 0 & 0 \\ 0 & 0 & 0 \end{pmatrix} \qquad \text{(K-55)}$$

The differential equation checks have not actually been carried out analytically, although spot checks have been made for some of the elements in Eqs. (F-63) and (F-64). In general, the equations serve as a "back-up" in case any element of any matrix is open to question.

APPENDIX L
FIXED-TIME-OF-ARRIVAL GUIDANCE

L.1 Summary

When the destination point is fixed in space and time, the required velocity correction may be expressed in terms of the predicted position variation at the destination by means of the simple matrix equation

$$\underline{c}_F = - \overset{*}{K}_{CD} \delta \underline{r}_D^- \qquad \text{(L-1)}$$

where $\underline{c}_F$ is the velocity correction vector for fixed-time-of-arrival guidance. $\delta \underline{r}_D^-$ is the position variation vector at the destination which would exist if no correction were applied. $\overset{*}{K}_{CD}$ is a 3-by-3 matrix which can be evaluated numerically for the many-body problem and can be determined analytically for the two-body problem.

L.2 The Velocity Correction

The basic assumption in the guidance theory to be developed is that all variations from the known reference trajectory are small. This assumption holds both before and after the application of a velocity correction. Consequently, the correction itself must be a small quantity.

The velocity correction is assumed to be the result of a thrust impulse. At the time of the correction, the thrust impulse causes an impulse in vehicle acceleration, which in turn produces a step change in vehicle velocity. The correction causes no instantaneous change in vehicle position.

The subscript C appended to a time-varying quantity signifies the value of the quantity corresponding to the time of application of the correction. The superscripts - and + are used, respectively, to indicate conditions existing before and after the correction.

The position and velocity variations at the instant after the correction $\underline{c}$ are related to the variations immediately before the correction as follows:

$$\delta \underline{r}_C^{+} = \delta \underline{r}_C^{-} \tag{L-2}$$

$$\delta \underline{v}_C^{+} = \delta \underline{v}_C^{-} + \underline{c} \tag{L-3}$$

These two relations may be combined into a single equation by use of the six-dimensional vector $\delta \underline{x}$.

$$\delta \underline{x}_C^{+} = \begin{Bmatrix} \delta \underline{r}_C^{+} \\ \delta \underline{v}_C^{+} \end{Bmatrix} = \delta \underline{x}_C^{-} + \begin{Bmatrix} \underline{0}_3 \\ \underline{c} \end{Bmatrix} \tag{L-4}$$

From Eq. (L-3) the velocity correction is given by

$$\underline{c} = \delta \underline{v}_C^{+} - \delta \underline{v}_C^{-} \tag{L-5}$$

The six quantities constituting $\delta \underline{x}_C$ completely define the variant path of the vehicle in the gravitational field. From Eq. (L-4) it is apparent that only three of the six can be altered by the correction $\underline{c}$; hence, only three mathematical conditions can be satisfied by the correction. Many different guidance schemes may be formulated by the simple expedient of varying the conditions to be satisfied by $\underline{c}$.

L. 3 The Velocity Correction for FTA Guidance

For some types of missions, the goal is to have the vehicle arrive at a fixed point (the destination) in heliocentric space at a fixed time. This type is known as a fixed-time-of-arrival (FTA) mission.

The three mathematical conditions to be met in an FTA mission are obviously those involved in reducing to zero the three components of position variation at the destination. In mathematical language, it is desired that

$$\delta \underline{r}_D^+ = \underline{0}_3 \tag{L-6}$$

where the subscript D refers to conditions at the time of arrival at the destination.

The problem now is to determine $\underline{c}_F$ such that Eq. (L-6) is satisfied. Equation (F-29) is used to get expressions for $\delta \underline{v}_C^-$ and $\delta \underline{v}_C^+$, from which $\underline{c}_F$ may be obtained by use of (L-5).

$$\delta \underline{v}_C^- = \overset{*}{J}_{CD}\, \delta \underline{r}_C^- + \overset{*}{K}_{CD}\, \delta \underline{r}_D^- \tag{L-7}$$

$$\delta \underline{v}_C^+ = \overset{*}{J}_{CD}\, \delta \underline{r}_C^+ + \overset{*}{K}_{CD}\, \delta \underline{r}_D^+ \tag{L-8}$$

$$= \overset{*}{J}_{CD}\, \delta \underline{r}_C^- \tag{L-9}$$

$$\underline{c}_F = \delta \underline{v}_C^+ - \delta \underline{v}_C^- = -\overset{*}{K}_{CD}\, \delta \underline{r}_D^- \tag{L-10}$$

It is interesting to note that, although six quantities are needed to specify completely the vehicle's variant path, only three quantities are required to determine the velocity correction vector in FTA guidance. This fact can effect an appreciable saving in computation.

A simple logical argument can be made for the validity of Eq. (L-10) without recourse to mathematics. Since the objective of the guidance system is to reduce $\delta \underline{r}_D$ to zero, it is obvious that $\underline{c}_F$ must be zero if $\delta \underline{r}_D^-$ is zero, and $\underline{c}_F$ must be non-zero if $\delta \underline{r}_D^-$ is non-zero. Therefore, the correction depends on $\delta \underline{r}_D^-$ and is not affected by any characteristics of the variant path that are independent of $\delta \underline{r}_D^-$.

The velocity correction does not, and indeed it cannot, cause the vehicle to return instantaneously to the reference trajectory, inasmuch as such a procedure would require that six, rather than three, conditions be met (i.e., $\delta \underline{r}_C^+ = 0$, $\delta \underline{v}_C^+ = 0$). What the correction does accomplish is to set the vehicle on a new variant path which intersects the original variant path at $t = t_C$ and intersects the reference path at $t = t_D$. This concept is illustrated in Fig. L.1.

L.4 Velocity Variation at the Destination

The impulsive thrust correction which nullifies the position variation at the destination does not have the same effect on the velocity variation. From Eq. (F-29), after the correction is applied, the residual velocity variation at the destination is

$$\delta \underline{v}_D^+ = \overset{*}{J}_{DC} \delta \underline{r}_D^+ + \overset{*}{K}_{DC} \delta \underline{r}_C^+ \qquad \text{(L-11)}$$

Equations (L-2) and (L-6) are substituted into (L-11).

$$\delta \underline{v}_D^+ = \overset{*}{K}_{DC} \delta \underline{r}_C^- \qquad \text{(L-12)}$$

Thus, for a path deviation vector composed of $\delta \underline{r}_C^-$ and $\delta \underline{r}_D^-$, $\delta \underline{v}_D^+$ depends only on that part of the path deviation vector contained in $\delta \underline{r}_C^-$, while $\underline{c}_F$ depends only on that part contained in $\delta \underline{r}_D^-$.

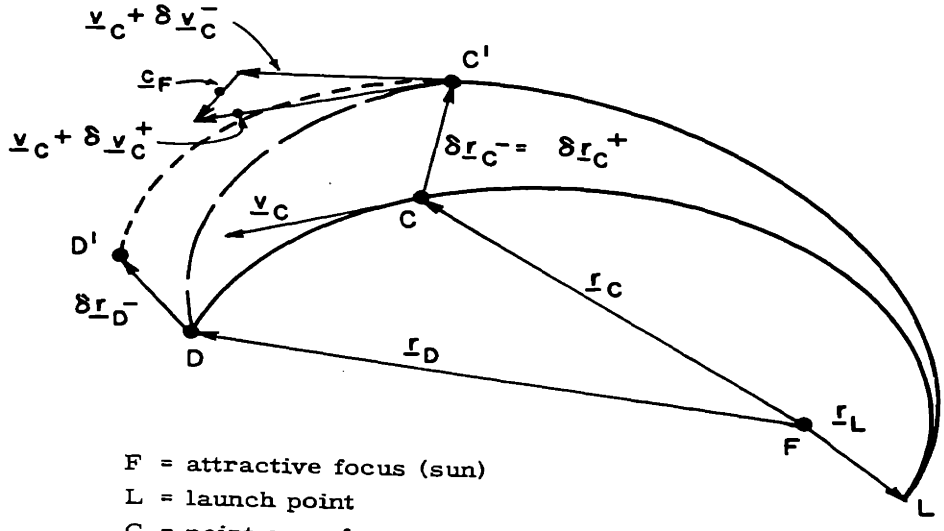

F = attractive focus (sun)

L = launch point

C = point on reference path corresponding to time of correction t_C

C' = point on actual path corresponding to time of correction t_C

D = destination point

D' = predicted position of vehicle at nominal time of arrival at destination if no correction is applied

LCD = reference path

LC' = actual path from launch to time of correction

C'D' = predicted actual path if no correction is applied

C'D = corrected path

$\delta\underline{r}_C^- = \delta\underline{r}_C^+$ = position variation at time of correction

$\delta\underline{r}_D^-$ = predicted position variation at target if no correction is applied

$\underline{c}_F$ = velocity correction vector

$$= (\underline{v}_C + \delta\underline{v}_C^+) - (\underline{v}_C + \delta\underline{v}_C^-) = \delta\underline{v}_C^+ - \delta\underline{v}_C^-$$

Figure L.1 Fixed-Time-of-Arrival Guidance

Since the most practical method of expressing the characteristics of the original variant path is in terms of the components of $\delta\underline{x}_D^-$, it is desirable to express $\delta\underline{v}_D^+$ in terms of $\delta\underline{r}_D^-$ and $\delta\underline{v}_D^-$, rather than $\delta\underline{r}_C^-$. Such an expression is readily obtained from the difference $(\delta\underline{v}_D^+ - \delta\underline{v}_D^-)$.

$$\delta\underline{v}_D^+ - \delta\underline{v}_D^- = \overset{*}{J}_{DC}(\delta\underline{r}_D^+ - \delta\underline{r}_D^-) + \overset{*}{K}_{DC}(\delta\underline{r}_C^+ - \delta\underline{r}_C^-)$$

$$= -\overset{*}{J}_{DC}\,\delta\underline{r}_D^- \qquad \text{(L-13)}$$

$$\delta\underline{v}_D^+ = -\overset{*}{J}_{DC}\,\delta\underline{r}_D^- + \delta\underline{v}_D^- = \{-\overset{*}{J}_{DC} \quad \overset{*}{I}_3\}\,\delta\underline{x}_D^- \qquad \text{(L-14)}$$

Equations (L-6) and (L-14) may be combined into a single equation relating $\delta\underline{x}_D^+$ to $\delta\underline{x}_D^-$.

$$\delta\underline{x}_D^+ = \begin{Bmatrix} \overset{*}{O}_3 & \overset{*}{O}_3 \\ -\overset{*}{J}_{DC} & \overset{*}{I}_3 \end{Bmatrix} \delta\underline{x}_D^- \qquad \text{(L-15)}$$

L.5 Change in the Orbital Elements

When the reference trajectory is an ellipse, it may be of interest to determine the change in the orbital elements caused by the correction $\underline{c}_F$. From Eqs. (F-1) and (F-2), the original path deviation vector $\delta\underline{e}^-$ may be written as

$$\delta\underline{e}^- = \{\overset{*}{R}_D \quad \overset{*}{V}_D\}\,\delta\underline{x}_D^- \qquad \text{(L-16)}$$

$$= \{\overset{*}{H}_{CD} \quad \overset{*}{H}_{DC}\}\begin{Bmatrix} \delta\underline{r}_C^- \\ \delta\underline{r}_D^- \end{Bmatrix} \qquad \text{(L-17)}$$

After the corrective thrust is applied, the path deviation vector becomes

$$\delta \underline{e}^{+} = \{ \overset{*}{H}_{CD} \qquad \overset{*}{H}_{DC} \} \begin{Bmatrix} \delta \underline{r}_C^{+} \\ \delta \underline{r}_D^{+} \end{Bmatrix}$$

$$= \overset{*}{H}_{CD} \; \delta \underline{r}_C^{-} \tag{L-18}$$

The change in the variations of the orbital elements is

$$\delta \underline{e}^{+} - \delta \underline{e}^{-} = - \overset{*}{H}_{DC} \, \delta \underline{r}_D^{-} \tag{L-19}$$

Like $\underline{c}_F$, $(\delta \underline{e}^{+} - \delta \underline{e}^{-})$ depends on $\delta \underline{r}_D^{-}$ and no other parameters of the original variant trajectory. The close relationship between $\underline{c}_F$ and $(\delta \underline{e}^{+} - \delta \underline{e}^{-})$ is clearly shown by means of Eq. (F-17).

$$\underline{c}_F = \delta \underline{v}_C^{+} - \delta \underline{v}_C^{-} = \overset{*}{L}_C \, (\delta \underline{e}^{+} - \delta \underline{e}^{-}) \tag{L-20}$$

Equations (L-10) and (L-19) can be combined to obtain a relationship that is the inverse of (L-20). Equation (F-34) is used to simplify the result.

$$\delta \underline{e}^{+} - \delta \underline{e}^{-} = \overset{*}{H}_{DC} \, \overset{*}{K}_{CD}^{-1} \, \underline{c}_F = \overset{*}{H}_{DC} \, \overset{*}{N}_{DC} \, \underline{c}_F \tag{L-21}$$

L. 6 Method of Numerical Evaluation

Once $\delta \underline{r}_D^-$ has been determined, the correction $\underline{c}_F$ corresponding to any given t_C can be computed as soon as the elements of $\overset{*}{K}_{CD}$ have been evaluated.

For the many-body problem the elements of $\overset{*}{K}_{CD}$ are computed by numerical integration, as shown in Section F. 6. In accordance with the suggestion made in that section, the equations to be integrated are simplified by using a non-rotating coordinate system, and the round-off error is reduced by choosing the z-axis to be perpendicular to the plane of the basic motion (i. e., the motion that would exist in the absence of disturbing forces).

From (F-53) and (F-54), the matrix differential equations are

$$\frac{\partial \overset{*}{N}_{CD}}{\partial t_C} = \overset{*}{T}_{CD} \tag{L-22}$$

$$\frac{\partial \overset{*}{T}_{CD}}{\partial t_C} = \overset{*}{G}_C \overset{*}{N}_{CD} \tag{L-23}$$

These equations are integrated in the negative time direction, starting from $t_C = t_D$. For a given reference trajectory, t_D is a fixed quantity, and the selected time for applying the correction lies in the range t_I to t_D, where t_I is the time of injection. The initial conditions are

$$\overset{*}{N}_{DD} = \overset{*}{O}_3 \qquad \overset{*}{T}_{DD} = \overset{*}{I}_3 \tag{L-24}$$

For the non-rotating coordinate system, the elements of $\overset{*}{G}_C$ are known as a function of t_C from Eq. (E-11). The matrix combination inside the braces on the right side of (E-11), when evaluated at $t = t_C$, constitutes $\overset{*}{G}_C$.

The two matrix equations (L-22) and (L-23) consist of eighteen coupled first-order differential equations in the eighteen variables composed of the elements of $\overset{*}{N}_{CD}$ and $\overset{*}{T}_{CD}$. The numerical integration yields these elements as a function of t_C.

$\overset{*}{K}_{DC}$ and $\overset{*}{K}_{CD}$ are obtained from $\overset{*}{N}_{CD}$ by simple matrix manipulation.

From (F-34),

$$\overset{*}{K}_{DC} = \overset{*}{N}_{CD}^{-1} \tag{L-25}$$

From (F-79),

$$\overset{*}{K}_{CD} = - \overset{*}{K}_{DC}^{T} = - (\overset{*}{N}_{CD}^{T})^{-1} \tag{L-26}$$

If the reference trajectory is an ellipse, there is no need for the numerical integration. An analytic solution for the elements of $\overset{*}{K}_{CD}$, in the flight path coordinate system, may be obtained by the proper substitution of subscripts in Eqs. (K-14), (K-15), and (K-48).

The mechanization of the guidance system does not require a knowledge of $\delta \underline{v}_D^{+}$. However, such knowledge is of value if more than one midcourse correction is to be applied.

The additional information needed to compute $\delta \underline{v}_D^{+}$ includes the components of $\delta \underline{v}_D^{-}$ and the elements of $\overset{*}{J}_{DC}$. $\delta \underline{v}_D^{-}$, like $\delta \underline{r}_D^{-}$, is based on the observations made during the course of the flight. The determination of $\overset{*}{J}_{DC}$ involves a procedure similar to the one described for evaluating $\overset{*}{K}_{CD}$.

For the many-body solution, eighteen additional coupled first-order differential equations are integrated numerically in the negative time direction, starting from $t = t_D$. The eighteen are contained in two

matrix differential equations derived from (F-51) and (F-52).

$$\frac{\partial \overset{*}{M}_{CD}}{\partial t_C} = \overset{*}{S}_{CD} \tag{L-27}$$

$$\frac{\partial \overset{*}{S}_{CD}}{\partial t_C} = \overset{*}{G}_C \overset{*}{M}_{CD} \tag{L-28}$$

The initial conditions are

$$\overset{*}{M}_{DD} = \overset{*}{I}_3 \qquad \overset{*}{S}_{DD} = \overset{*}{O}_3 \tag{L-29}$$

The solution contains the elements of $\overset{*}{M}_{CD}$ and $\overset{*}{S}_{CD}$ as a function of t_C. $\overset{*}{J}_{DC}$ is obtained from $\overset{*}{K}_{CD}$ and $\overset{*}{M}_{CD}$ by the use of Eq. (F-33).

$$\overset{*}{J}_{DC} = - \overset{*}{K}_{DC} \overset{*}{M}_{CD} = \overset{*}{K}_{CD}{}^T \overset{*}{M}_{CD} \tag{L-30}$$

A check on the compuations is afforded by the fact that $\overset{*}{J}_{DC}$ is a symmetric matrix.

For an elliptical reference trajectory, the analytic form of $\overset{*}{J}_{DC}$, in the flight path coordinate system, comes directly from Eqs. (K-14), (K-15), and (K-47).

Numerical evaluation of the elements of $\delta \underline{e}$, either before or after the correction, is not necessary for the mechanization of the guidance system. If for some reason the numerical values are desired, the matrices $\overset{*}{R}_D$ and $\overset{*}{V}_D$ are required to determine $\delta \underline{e}^-$ from Eq. (L-17), and $\overset{*}{H}_{CD}$ is needed to determine $\delta \underline{e}^+$ from Eq. (L-18). Analytical expressions for $\overset{*}{R}_D$, $\overset{*}{V}_D$, and $\overset{*}{H}_{CD}$ may be obtained from Eqs. (K-34), (K-35), and (K-44), respectively.

APPENDIX M
VARIABLE-TIME-OF-ARRIVAL GUIDANCE

M.1 Summary

When the nature of the space mission is such that the time of arrival at the destination need not be rigidly constrained, the velocity correction may be expressed in terms of only two components of the predicted position variation at the nominal time of arrival. The correction can be computed in such a way that, for the particular time of correction selected, the magnitude of the correction is minimized. This method of computation is known as variable-time-of-arrival (VTA) guidance.

Equations are developed for the velocity correction in VTA guidance and also for the change in the time of arrival.

M.2 Design Philosophy of VTA Guidance

The concept of VTA guidance is clarified by the introduction of two new vectors, the relative velocity vector $\underline{v}_R$ and the miss distance vector $\delta\underline{\rho}$.

$\underline{v}_R$ is the relative velocity of the space vehicle, on its reference trajectory, with respect to the destination planet at the nominal time of arrival at the destination. In mathematical terms,

$$\underline{v}_R = \underline{v}_S - \underline{v}_P \tag{M-1}$$

where $\underline{v}_S$ is the velocity of the space vehicle on its reference trajectory at the nominal time of arrival and $\underline{v}_P$ is the velocity of the

destination planet at that time. Fig. M.1 gives a schematic representation of $\underline{v}_R$.

$\delta\underline{\rho}$ is defined as the component of $\delta\underline{r}_D$, the position variation vector at the destination, that is perpendicular to $\underline{v}_R$. It represents the minimum distance between vehicle and destination point.

The objective of VTA guidance is to reduce $\delta\underline{\rho}$ to zero. Since $\delta\underline{\rho}$ lies in the plane perpendicular to $\underline{v}_R$, accomplishing this objective accounts for only two of the three conditions that can be satisfied by the velocity correction. A third condition must be specified before the correction can be determined uniquely.

Although there are several practical possibilities for the third condition, as indicated in References (9) and (10), the only one considered in this analysis is the minimization of the magnitude of the midcourse velocity correction.

M.3 Basic Guidance Equations for VTA Guidance

The change in the time of arrival due to VTA guidance is designated Δt_D. The variation Δt_D, unlike the variational quantities previously discussed, is deliberately inserted into the system; the use of the symbol Δ rather than δ is intended to emphasize this distinction. The actual time of arrival at the destination in VTA guidance is $t_D + \Delta t_D$.

Prior to the application of the correction, the predicted velocity of the vehicle relative to the destination planet at $t = t_D$ is $\underline{v}_R + \delta\underline{v}_D^-$. After the correction is applied, the relative velocity at $t = t_D$ is $\underline{v}_R + \delta\underline{v}_D^+$.

With both Δt_D and $\delta\underline{v}_D^+$ recognized as small variational quantities, linear theory gives the following relationship for $\delta\underline{r}_D^+$ in VTA guidance:

$$\delta\underline{r}_D^+ = -(\underline{v}_R + \delta\underline{v}_D^+)\,\Delta t_D$$

$$= -\underline{v}_R\,\Delta t_D \qquad \text{(M-2)}$$

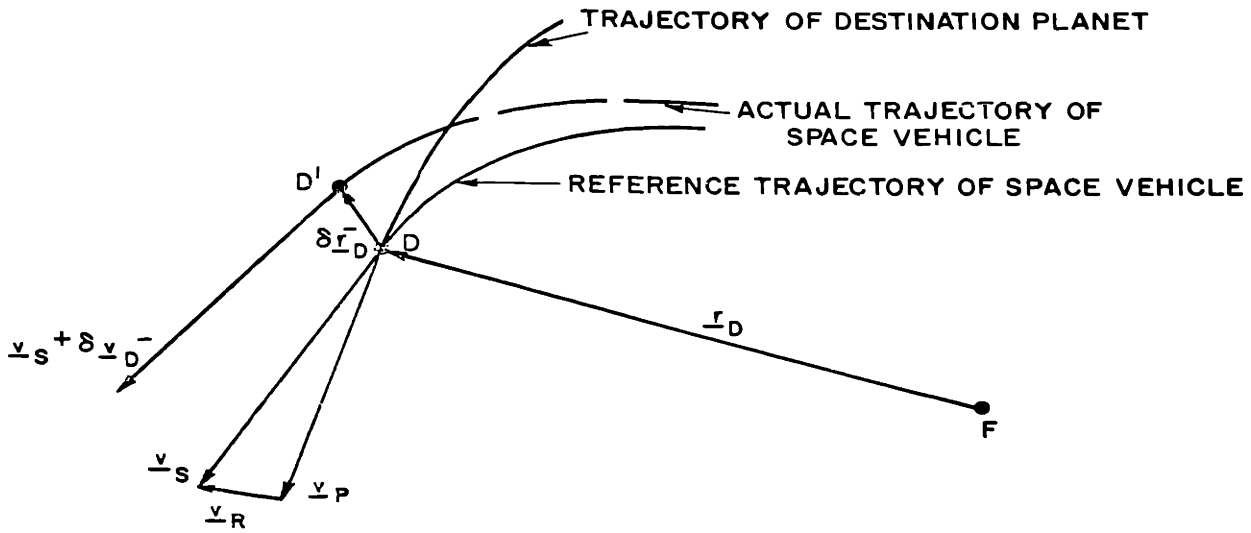

F = attractive focus (sun)

D = destination point on reference trajectory

D' = predicted position of vehicle at nominal time of arrival at destination ($t = t_D$)

$\delta \underline{r}_D^-$ = predicted position variation at $t = t_D$

$\delta \underline{v}_D^-$ = predicted velocity variation at $t = t_D$

$\underline{v}_S$ = velocity of space vehicle on reference trajectory at $t = t_D$

$\underline{v}_P$ = velocity of destination planet at $t = t_D$

$\underline{v}_R$ = relative velocity of space vehicle with respect to destination planet at $t = t_D$

$= \underline{v}_S - \underline{v}_P$

Figure M.1 Relative Velocity Vector

In Fig. M. 2, the VTA correction moves the predicted vehicle position at $t = t_D$ from D' to H. The distance of H from D, the position of the destination planet at $t = t_D$, is the magnitude of $\delta \underline{r}_D^{+}$. Note that $\delta \underline{r}_D^{+}$ is not, in general, equal in magnitude to the component of $\delta \underline{r}_D^{-}$ in the $\underline{v}_R$ direction.

Figure M. 2 illustrates the basic difference between the FTA and VTA systems. The correction in FTA guidance is made such that the vehicle passes through the specific point D at $t = t_D$, while the correction in the general concept of VTA guidance requires only that at $t = t_D$ the vehicle be situated on the line through D parallel to $\underline{v}_R$.

Let $\underline{c}_V$ denote the velocity correction in VTA guidance.

$$\underline{c}_V = \delta \underline{v}_C^{+} - \delta \underline{v}_C^{-}$$

$$= (\overset{*}{J}_{CD}\, \delta \underline{r}_C^{+} + \overset{*}{K}_{CD}\, \delta \underline{r}_D^{+}) - (\overset{*}{J}_{CD}\, \delta \underline{r}_C^{-} + \overset{*}{K}_{CD}\, \delta \underline{r}_D^{-})$$

$$= \overset{*}{K}_{CD}\, (\delta \underline{r}_D^{+} - \delta \underline{r}_D^{-}) \qquad \text{(M-3)}$$

$$= \underline{c}_F - \underline{w}\, \Delta t_D \qquad \text{(M-4)}$$

where

$$\underline{w} = \overset{*}{K}_{CD}\, \underline{v}_R \qquad \text{(M-5)}$$

Equations (M-3), (M-4), and (M-5) are the basic equations of VTA guidance, independent of the third condition to be satisfied by the correction vector $\underline{c}_V$. Specifying a third condition is analogous to specifying Δt_D; when this is done, $\underline{c}_V$ is determined uniquely.

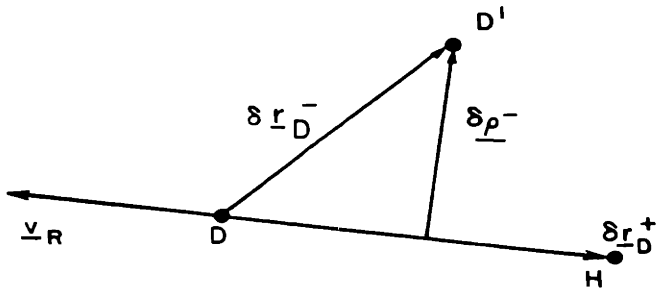

D = nominal destination point

D' = predicted position of vehicle at $t = t_D$ if no correction is applied

H = predicted position of vehicle at $t = t_D$ if VTA correction is applied at $t = t_C$

$\delta \underline{r}_D^-$ = predicted position variation vector at $t = t_D$ if no correction is applied

$\delta \underline{\rho}^-$ = miss distance vector

= component of $\delta \underline{r}_D^-$ perpendicular to $\underline{v}_R$

$\underline{v}_R$ = nominal velocity vector of vehicle relative to destination point at $t = t_D$

$\delta \underline{r}_D^+$ = predicted position variation vector at $t = t_D$ if VTA correction is applied at $t = t_C$

Figure M.2 Miss Distance Vector and VTA Guidance

M. 4 Variation in Time of Arrival

The variation in time of arrival is to be determined such that it satisfies the condition that the magnitude of $\underline{c}_V$ be a minimum.

From Eq. (M-4),

$$c_V^2 = \underline{c}_V^T \underline{c}_V = \underline{c}_F^T \underline{c}_F - 2 \underline{w}^T \underline{c}_F \Delta t_D + \underline{w}^T \underline{w} (\Delta t_D)^2 \qquad \text{(M-6)}$$

The partial derivative of c_V^2 with respect to Δt_D is equated to zero. The vectors $\underline{c}_F$ and $\underline{w}$ are both independent of Δt_D.

$$\frac{\partial (c_V^2)}{\partial (\Delta t_D)} = 0 = - 2 \underline{w}^T \underline{c}_F + 2 \underline{w}^T \underline{w} \Delta t_D \qquad \text{(M-7)}$$

The solution of this equation for Δt_D is

$$\Delta t_D = \frac{\underline{w}^T \underline{c}_F}{\underline{w}^T \underline{w}} \qquad \text{(M-8)}$$

M. 5 Velocity Correction in VTA Guidance

Equation (M-8) may be substituted into Equation (M-4).

$$\underline{c}_V = \underline{c}_F - \frac{\underline{w} \underline{w}^T}{\underline{w}^T \underline{w}} \underline{c}_F = \left(\overset{*}{I}_3 - \frac{\underline{w} \underline{w}^T}{\underline{w}^T \underline{w}} \right) \underline{c}_F \qquad \text{(M-9)}$$

$$= - \left(\overset{*}{I}_3 - \frac{\underline{w} \underline{w}^T}{\underline{w}^T \underline{w}} \right) \overset{*}{K}_{CD} \delta \underline{r}_D \qquad \text{(M-10)}$$

Equation (M-9) shows the mathematical relationship between VTA and FTA velocity corrections. It was developed in this form by Battin [4].

An interesting result is obtained from the scalar product of $\underline{c}_V$ with $\underline{w}$.

$$\underline{w} \cdot \underline{c}_V = \underline{w}^T \underline{c}_V = \left(\underline{w}^T - \frac{\underline{w}^T \underline{w}}{\underline{w}^T \underline{w}} \underline{w}^T \right) \underline{c}_F = 0 \qquad \text{(M-11)}$$

Since neither the vector $\underline{c}_V$ nor the vector $\underline{w}$ is in general a zero vector, it is apparent that $\underline{c}_V$ is always perpendicular to $\underline{w}$. Thus, $\underline{c}_V$ is constrained to lie in the plane perpendicular to $\underline{w}$. Noton[9] refers to the direction of $\underline{w}$ as the "noncritical direction" and the plane normal to $\underline{w}$ as the "critical plane".

The vector $\underline{w}$ depends on $\overset{*}{K}_{CD}$, which is a function of both t_C and t_D. For a specified reference trajectory, t_D is fixed, but t_C can vary. Consequently, the noncritical direction and the orientation of the critical plane both depend on the time at which the correction is to be made.

From (M-4), $\underline{c}_F$ is the vector sum of $\underline{c}_V$ and $\underline{w}\,\Delta t_D$. Since Δt_D is a scalar, the vector $\underline{w}\,\Delta t_D$ is parallel to $\underline{w}$. The other term in the vector sum, namely $\underline{c}_V$, is perpendicular to $\underline{w}$. Thus, the vector triangle, shown in Fig. M.3, is a right triangle whose hypotenuse is $\underline{c}_F$, and $\underline{c}_V$ is simply the component of $\underline{c}_F$ in the critical plane.

M.6 Position Variation and Velocity Variation at the Destination

The position variation $\delta \underline{r}_D{}^+$ can be expressed as a function of $\delta \underline{r}_D{}^-$ by combining Eqs. (M-2), (M-8), and (L-1).

$$\delta \underline{r}_D{}^+ = -\underline{v}_R \,\Delta t_D$$

$$= -\frac{\underline{v}_R \underline{w}^T}{\underline{w}^T \underline{w}} \underline{c}_F \qquad \text{(M-12)}$$

$$= \frac{\underline{v}_R \underline{w}^T}{\underline{w}^T \underline{w}} \overset{*}{K}_{CD} \delta \underline{r}_D{}^- \qquad \text{(M-13)}$$

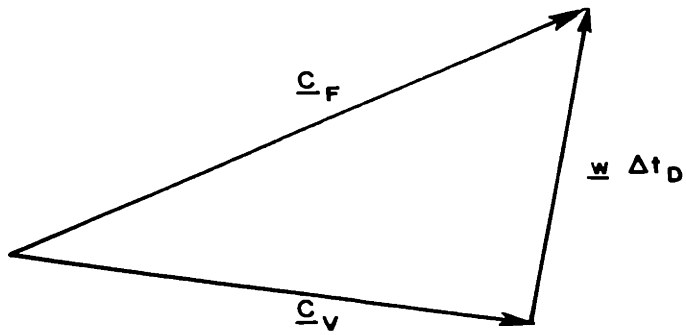

$\underline{c}_F$ = FTA velocity correction vector

$\underline{c}_V$ = VTA velocity correction vector

$\underline{w} = \overset{*}{K}_{CD}\,\underline{v}_R$ = vector in noncritical direction

$\overset{*}{K}_{CD}$ = 3-by-3 matrix depending on t_C and t_D

$\underline{v}_R$ = relative velocity vector

Δt_D = change in time of arrival at destination

Figure M.3 Vector Relation between Velocity Corrections in FTA and VTA Guidance

The velocity deviation $\delta \underline{v}_D^+$ is

$$\delta \underline{v}_D^+ = \overset{*}{J}_{DC}\, \delta \underline{r}_D^+ + \overset{*}{K}_{DC}\, \delta \underline{r}_C^+ \qquad \text{(M-14)}$$

From Eqs. (L-2), (L-12), and (L-14),

$$\overset{*}{K}_{DC}\, \delta \underline{r}_C^+ = \overset{*}{K}_{DC}\, \delta \underline{r}_C^- = \{-\overset{*}{J}_{DC} \qquad \overset{*}{I}_3\}\ \delta \underline{x}_D^- \qquad \text{(M-15)}$$

The final expression for $\delta \underline{v}_D^+$ is the result of combining (M-13), (M-14), and (M-15).

$$\delta \underline{v}_D^+ = -\overset{*}{J}_{DC} \left(\overset{*}{I}_3 - \frac{\underline{v}_R\, \underline{w}^T}{\underline{w}^T\, \underline{w}}\, \overset{*}{K}_{CD} \right) \delta \underline{r}_D^- + \delta \underline{v}_D^- \qquad \text{(M-16)}$$

A composite equation can now be written in which $\delta \underline{x}_D^+$ is expressed in terms of $\delta \underline{x}_D^-$.

$$\delta \underline{x}_D^+ = \begin{Bmatrix} \dfrac{\underline{v}_R\, \underline{w}^T}{\underline{w}^T\, \underline{w}}\, \overset{*}{K}_{CD} & \overset{*}{O}_3 \\ -\overset{*}{J}_{DC} \left(\overset{*}{I}_3 - \dfrac{\underline{v}_R\, \underline{w}^T}{\underline{w}^T\, \underline{w}}\, \overset{*}{K}_{CD} \right) & \overset{*}{I}_3 \end{Bmatrix} \delta \underline{x}_D^- \qquad \text{(M-17)}$$

This equation can be compared with Eq. (L-15), the corresponding expression for FTA guidance.

M. 7 Change in the Orbital Elements

The six-component vector $\delta \underline{e}^-$, expressing the variations in the orbital elements before application of corrective thrust, is obviously unaffected by the type of correction that is contemplated. It can be expressed in terms of $\delta \underline{x}_D^-$ or in terms of $\delta \underline{r}_C^-$ and $\delta \underline{r}_D^-$, as indicated in Eqs. (L-16) and (L-17).

After the correction, the new vector $\delta \underline{e}^+$ for VTA must differ from the $\delta \underline{e}^+$ for FTA, since different corrections are applied. For VTA,

$$\delta \underline{e}^+ = \{ \overset{*}{H}_{CD} \quad \overset{*}{H}_{DC} \} \begin{Bmatrix} \delta \underline{r}_C^+ \\ \delta \underline{r}_D^+ \end{Bmatrix}$$

$$= \left\{ \overset{*}{H}_{CD} \quad \overset{*}{H}_{DC} \; \frac{\underline{v}_R \, \underline{w}^T}{\underline{w}^T \, \underline{w}} \; \overset{*}{K}_{CD} \right\} \begin{Bmatrix} \delta \underline{r}_C^- \\ \delta \underline{r}_D^- \end{Bmatrix} \qquad \text{(M-18)}$$

The change in $\delta \underline{e}$ due to the VTA correction is obtained by subtracting (L-17) from (M-18).

$$\delta \underline{e}^+ - \delta \underline{e}^- = - \overset{*}{H}_{DC} \left(\overset{*}{I}_3 - \frac{\underline{v}_R \, \underline{w}^T}{\underline{w}^T \, \underline{w}} \overset{*}{K}_{CD} \right) \delta \underline{r}_D^- \qquad \text{(M-19)}$$

The analogous equations to (L-20) and (L-21) are valid for VTA.

$$\underline{c}_V = \overset{*}{L}_C \left(\delta \underline{e}^+ - \delta \underline{e}^-\right) \tag{M-20}$$

$$\delta \underline{e}^+ - \delta \underline{e}^- = \overset{*}{H}_{DC} K_{CD}^{-1} \underline{c}_V = \overset{*}{H}_{DC} \overset{*}{N}_{DC} \underline{c}_V \tag{M-21}$$

M. 8 Numerical Evaluation

The number of quantities to be evaluated for VTA guidance is obviously greater than the number in FTA guidance. Foremost is the correction $\underline{c}_V$. Second in importance is $\delta \underline{x}_D^+$, which now includes a non-zero $\delta \underline{r}_D^+$. Third is the change in arrival time, Δt_D. Finally, for elliptical trajectories, there is the capability, though not the necessity, of computing $\delta \underline{e}^-$ and $\delta \underline{e}^+$.

The matrices required for the first three are $\overset{*}{K}_{CD}$ and $\overset{*}{J}_{DC}$, the evaluation of which has been described in Section L. 6. The new quantities involved are the vectors $\underline{v}_R$ and $\underline{w}$. The former is obtained directly from the reference trajectory, and the latter comes from the matrix product of Eq. (M-5). The matrices $\overset{*}{R}_D$, $\overset{*}{V}_D$, and $\overset{*}{H}_{CD}$, needed to evaluate $\delta \underline{e}^-$ and $(\delta \underline{e}^+ - \delta \underline{e}^-)$ are obtained from Appendix K.

It is quite obvious that VTA guidance entails somewhat more computation than FTA guidance. The added steps, however, are simple ones; they consist primarily of multiplications and additions of 3-by-3 matrices; there are no new matrix inversions, and the additional divisions all involve the same scalar quantity, $\underline{w}^T \underline{w}$.

APPENDIX N

OPTIMIZATION OF TIME OF CORRECTION

N.1 Summary

A new rotating coordinate system, called the critical-plane coordinate system, is introduced, in which the VTA velocity correction is expressed as a two-dimensional vector and the miss distance is also expressed as a two-dimensional vector. Then the matrix relating the correction vector to the miss distance vector is reduced to a 2-by-2 matrix. For elliptical reference trajectories, one of the four elements of this matrix is equal to zero.

If the two-dimensional miss distance vector is represented by a magnitude and a phase angle, the magnitude of the correction vector is a linear function of the magnitude of the miss distance vector but varies in a non-linear fashion with the phase angle of the miss distance vector. A technique is developed for determining the time of correction as a function of the phase angle such that the magnitude of the VTA correction is minimized.

N.2 Introduction

Appendix M develops the method of computing the VTA velocity correction corresponding to a given time t_C, but no consideration has yet been given to the means of specifying t_C. Since the magnitude of the correction $\underline{c}_V$ varies with t_C, it is desirable to specify that particular t_C for which the magnitude of $\underline{c}_V$ is minimized. The minimization procedure is facilitated by the introduction of the critical-plane coordinate system.

N.3 Critical-Plane Coordinate System

The axes of the critical-plane coordinate system are designated ξ_C, η_C, and ζ_C. The $\xi_C - \eta_C$ plane is the critical plane corresponding to the given t_C. The ζ_C-axis is in the noncritical direction; i.e., it is parallel to $\underline{w}$. From Eq. (M-5),

$$\underline{w} = \overset{*}{K}_{CD}\, \underline{v}_R \qquad \text{(N-1)}$$

Since $\overset{*}{K}_{CD}$ varies with t_C, the critical-plane coordinate system is a rotating system. Its origin, like that of the three reference trajectory systems of Appendix A, is at the center of the sun. The ξ_C-axis lies along the line of nodes between the critical plane and the reference trajectory plane.

In the analysis of Appendix M, it may be assumed that one of the three reference trajectory coordinate systems described in Appendix A is used. Let r_1, r_2, r_3 indicate the three axes of the particular system being used. Then Euler angles Ω_C and i_C serve to orient the critical-plane coordinate system with respect to the r_1, r_2, r_3 system. Ω_C is the angle measured in the reference trajectory plane from the positive r_1-axis to the positive ξ_C-axis. i_C is the angle between the positive r_3-axis (i.e., the z-axis) and the positive ζ_C-axis.

The positive ζ_C-axis is in the direction of $\underline{w}$. The positive ξ_C-axis is chosen as that half of the line of nodes for which Ω_C lies between 0° and 180°. (Ω_C is positive in the direction of vehicle motion.) The positive η_C-axis is such that ξ_C, η_C, ζ_C form a right-handed orthogonal triad. It may be noted that i_C, as well as Ω_C, lies in the range 0° to 180°.

N.4 Critical-Plane System Coordinate Axes at Nominal Time of Arrival

The orientation of the critical-plane system coordinate axes depends on $\underline{w}$, which depends on $\overset{*}{K}_{CD}$. For all values of t_C for which the elements of $\overset{*}{K}_{CD}$ can be determined, the axes are defined uniquely. However, if the elements of $\overset{*}{K}_{CD}$ cannot be determined, some other means must be used for specifying the axis directions. Such a problem arises when $t_C = t_D$.

$\overset{*}{K}_{CD}$ is computed from the equation

$$\overset{*}{K}_{CD} = -\left(\overset{*}{N}_{CD}{}^{T}\right)^{-1} \qquad \text{(N-2)}$$

and $\overset{*}{N}_{CD}$ is obtained by integration of eighteen coupled first-order differential equations. At $t_C = t_D$ the matrix $\overset{*}{N}_{DD}$ is the zero matrix; hence it has no finite inverse, and $\overset{*}{K}_{DD}$ cannot be determined.

A physical, rather than purely mathematical, approach can be used effectively to attack this problem. If the vehicle's position at t_D is along the line through the nominal destination point and parallel to $\underline{v}_R$, the objective of the VTA guidance system has been attained, and no further correction is desired. Thus, the non-critical ζ_D-axis is in the direction of $\underline{v}_R$, and the critical plane (i.e., the $\xi_D - \eta_D$ plane) is perpendicular to $\underline{v}_R$.

For the case of elliptical reference trajectories, a mathematical explanation is possible. Let t_C be very close to t_D, so that E_M, which is equal to half the difference between E_D and E_C, is a small angle. For small values of E_M,

$$\sin E_M = E_M \tag{N-3}$$

$$\cos E_M = 1 \tag{N-4}$$

$$\cos E_C = \cos (E_D - 2E_M) = \cos E_D + 2E_M \sin E_D \tag{N-5}$$

$$\cos E_P = \cos (E_D - E_M) = \cos E_D + E_M \sin E_D \tag{N-6}$$

When these relations are substituted into the negative transpose of Eq. (K-40), $\overset{*}{N}_{CD}$ for small E_M becomes

$$\overset{*}{N}_{CD} = -\frac{2(1 - e\cos E_D) E_M}{n} \begin{Bmatrix} 1 & -\dfrac{2(1-e^2)^{1/2} E_M}{1 - e^2\cos^2 E_D} & 0 \\ \dfrac{2(1-e^2)^{1/2} E_M}{1 - e^2\cos^2 E_D} & 1 & 0 \\ 0 & 0 & 1 \end{Bmatrix} \tag{N-7}$$

In the limit as t_C approaches t_D,

$$\overset{*}{N}_{CD} \longrightarrow - \frac{2(1 - e \cos E_D) E_M}{n} \overset{*}{I}_3 \qquad \text{(N-8)}$$

From Eq. (N-2), when t_C approaches t_D,

$$\overset{*}{K}_{CD} \longrightarrow \frac{n}{2(1 - e \cos E_D) E_M} \overset{*}{I}_3 \qquad \text{(N-9)}$$

When $t_C = t_D$, $E_M = 0$, so that $\overset{*}{K}_{DD}$ is given by

$$\overset{*}{K}_{DD} = \infty \overset{*}{I}_3 \qquad \text{(N-10)}$$

Substitution of (N-10) into (N-1) indicates that the $\underline{w}$ vector corresponding to $t_C = t_D$ is infinite in magnitude and parallel to $\underline{v}_R$. Therefore, the ζ_D-axis is parallel to $\underline{v}_R$, in agreement with the result obtained by physical reasoning.

N.5 Transformation Relations

The 3-by-3 matrix for transforming from r_1, r_2, r_3 coordinates to ξ, η, ζ coordinates at any specified time will be designated $\overset{*}{X}$.

$$\overset{*}{X} = \begin{Bmatrix} \cos \Omega & \sin \Omega & 0 \\ - \sin \Omega \cos i & \cos \Omega \cos i & \sin i \\ \sin \Omega \sin i & - \cos \Omega \sin i & \cos i \end{Bmatrix} \qquad \text{(N-11)}$$

$\overset{*}{X}$ is an orthogonal matrix; therefore,

$$\overset{*}{X}^{-1} = \overset{*}{X}^{T} \qquad \text{(N-12)}$$

Subscript W will be used to indicate that a vector is expressed in terms of its components in the critical-plane coordinate system.

The vector $\underline{w}$ for a given t_C transforms as follows:

$$(\underline{w})_W = \overset{*}{X}_C \, \underline{w} = w \begin{Bmatrix} 0 \\ 0 \\ 1 \end{Bmatrix} \qquad \text{(N-13)}$$

where $\overset{*}{X}_C$ is the transformation matrix evaluated at $t = t_C$. The transformation for $\underline{v}_R$ is

$$(\underline{v}_R)_W = \overset{*}{X}_D \, \underline{v}_R = v_R \begin{Bmatrix} 0 \\ 0 \\ 1 \end{Bmatrix} \qquad \text{(N-14)}$$

$\overset{*}{X}_D$ is evaluated at $t = t_D$. (N-13) may be combined with (N-1).

$$(\underline{w})_W = \overset{*}{X}_C \, \overset{*}{K}_{CD} \, \overset{*}{X}_D{}^{-1} \, (\underline{v}_R)_W \qquad \text{(N-15)}$$

$$w \begin{Bmatrix} 0 \\ 0 \\ 1 \end{Bmatrix} = v_R \, \overset{*}{X}_C \, \overset{*}{K}_{CD} \, \overset{*}{X}_D{}^T \begin{Bmatrix} 0 \\ 0 \\ 1 \end{Bmatrix} \qquad \text{(N-16)}$$

The matrix product $\overset{*}{X}_C \, \overset{*}{K}_{CD} \, \overset{*}{X}_D{}^T$, itself a 3-by-3 matrix, appears in the equation for $(\underline{c}_V)_W$ which will be derived in the next section. Analytic expressions for the elements of $\overset{*}{X}_C \, \overset{*}{K}_{CD} \, \overset{*}{X}_D{}^T$ can be found in terms of the fixed angles Ω_D and i_D and the time-varying elements of $\overset{*}{K}_{CD}$.

From (N-16) it can be deduced that the elements in the third column of $\overset{*}{X}_C \overset{*}{K}_{CD} \overset{*}{X}_D{}^T$ are 0, 0, and $\frac{w}{v_R}$. In order to find the elements in the first two columns of the matrix product, the following notation is introduced:

$$\overset{*}{K}_{CD} = \begin{Bmatrix} k_{11} & k_{12} & k_{13} \\ k_{21} & k_{22} & k_{23} \\ k_{31} & k_{32} & k_{33} \end{Bmatrix} = \begin{Bmatrix} \underline{k}_1{}^T \\ \underline{k}_2{}^T \\ \underline{k}_3{}^T \end{Bmatrix} \qquad \text{(N-17)}$$

For i = 1, 2, or 3, $\underline{k}_i$ is a vector with components k_{i1}, k_{i2}, and k_{i3} along the r_1, r_2, and r_3 axes corresponding to time t_D.

$$\overset{*}{K}_{CD}\,\overset{*}{X}_D{}^T = (\overset{*}{X}_D\,\overset{*}{K}_{CD}{}^T)^T = \left\{ \overset{*}{X}_D \begin{pmatrix} \underline{k}_1 & \underline{k}_2 & \underline{k}_3 \end{pmatrix} \right\}^T$$

$$= \left\{ \begin{pmatrix} (\underline{k}_1)_W & (\underline{k}_2)_W & (\underline{k}_3)_W \end{pmatrix} \right\}^T$$

$$= \begin{Bmatrix} (\underline{k}_1{}^T)_W \\ (\underline{k}_2{}^T)_W \\ (\underline{k}_3{}^T)_W \end{Bmatrix} = \begin{Bmatrix} k_{1\xi} & k_{1\eta} & k_{1\zeta} \\ k_{2\xi} & k_{2\eta} & k_{2\zeta} \\ k_{3\xi} & k_{3\eta} & k_{3\zeta} \end{Bmatrix} \qquad \text{(N-18)}$$

$k_{i\xi}$, $k_{i\eta}$, and $k_{i\zeta}$ are the components of $\underline{k}_i$ along the ξ_D, η_D, and ζ_D axes, respectively.

$$(\underline{k}_i)_W = \begin{Bmatrix} k_{i\xi} \\ k_{i\eta} \\ k_{i\zeta} \end{Bmatrix} = \begin{Bmatrix} k_{i1} \cos \Omega_D + k_{i2} \sin \Omega_D \\ -(k_{i1} \sin \Omega_D - k_{i2} \cos \Omega_D) \cos i_D + k_{i3} \sin i_D \\ (k_{i1} \sin \Omega_D - k_{i2} \cos \Omega_D) \sin i_D + k_{i3} \cos i_D \end{Bmatrix} \qquad \text{(N-19)}$$

With $\overset{*}{K}_{CD}\ \overset{*}{X}_D{}^T$ expressed in terms of the k-components by Equation (N-18), the next step is to obtain similar expressions for the elements of $\overset{*}{X}_C$. The elements of the third row of $\overset{*}{X}_C$ are readily derived.

$$\begin{aligned}
\underline{w}^T &= \left\{ \overset{*}{X}_C{}^T \, (\underline{w})_W \right\}^T = (\underline{w}^T)_W \, \overset{*}{X}_C \\
&= w \left\{ 0 \quad 0 \quad 1 \right\} \overset{*}{X}_C \\
&= \left\{ \overset{*}{K}_{CD} \, \overset{*}{X}_D{}^T \, (\underline{v}_R)_W \right\}^T \\
&= v_R \left\{ 0 \quad 0 \quad 1 \right\} (\overset{*}{K}_{CD} \, \overset{*}{X}_D{}^T)^T
\end{aligned} \tag{N-20}$$

The third row of $\overset{*}{X}_C$ is

$$\begin{aligned}
\left\{ 0 \quad 0 \quad 1 \right\} \overset{*}{X}_C &= \left\{ \sin \Omega_C \sin i_C \quad -\cos \Omega_C \sin i_C \quad \cos i_C \right\} \\
&= \frac{v_R}{w} \left\{ 0 \quad 0 \quad 1 \right\} (\overset{*}{K}_{CD} \, \overset{*}{X}_D{}^T)^T \\
&= \frac{v_R}{w} \left\{ k_{1\zeta} \quad k_{2\zeta} \quad k_{3\zeta} \right\}
\end{aligned} \tag{N-21}$$

From (N-20),

$$w^2 = \underline{w}^T \, \underline{w} = v_R{}^2 \, (k_{1\zeta}{}^2 + k_{2\zeta}{}^2 + k_{3\zeta}{}^2) \tag{N-22}$$

$$\frac{w}{v_R} = (k_{1\zeta}{}^2 + k_{2\zeta}{}^2 + k_{3\zeta}{}^2)^{1/2} \tag{N-23}$$

With the aid of (N-21) and (N-23), the entire $\overset{*}{X}_C$ matrix can be written as shown in (N-24). Only the ζ-components of the three $\underline{k}$ vectors are involved in X_C. Finally, (N-18) and (N-24) can be combined to yield the expression for $\overset{*}{X}_C \overset{*}{K}_{CD} \overset{*}{X}_D{}^T$ given by (N-25).

$$\overset{*}{X}_C = \begin{Bmatrix} \dfrac{1}{(k_{1\zeta}^2 + k_{2\zeta}^2)^{1/2}} & \begin{pmatrix} -k_{2\zeta} & k_{1\zeta} & 0 \end{pmatrix} \\ \dfrac{1}{(k_{1\zeta}^2 + k_{2\zeta}^2)^{1/2}\,(k_{1\zeta}^2 + k_{2\zeta}^2 + k_{3\zeta}^2)^{1/2}} & \begin{pmatrix} -k_{1\zeta}k_{3\zeta} & -k_{2\zeta}k_{3\zeta} & k_{1\zeta}^2 + k_{2\zeta}^2 \end{pmatrix} \\ \dfrac{1}{(k_{1\zeta}^2 + k_{2\zeta}^2 + k_{3\zeta}^2)^{1/2}} & \begin{pmatrix} k_{1\zeta} & k_{2\zeta} & k_{3\zeta} \end{pmatrix} \end{Bmatrix} \qquad \text{(N-24)}$$

$$\overset{*}{X}_C \overset{*}{K}_{CD} \overset{*}{X}_D{}^T = \begin{Bmatrix} \dfrac{1}{(k_{1\zeta}^2 + k_{2\zeta}^2)^{1/2}} & \begin{pmatrix} -k_{2\zeta}k_{1\xi} + k_{1\zeta}k_{2\xi} & -k_{2\zeta}k_{1\eta} + k_{1\zeta}k_{2\eta} & 0 \end{pmatrix} \\ \dfrac{1}{(k_{1\zeta}^2 + k_{2\zeta}^2)^{1/2}\,(k_{1\zeta}^2 + k_{2\zeta}^2 + k_{3\zeta}^2)^{1/2}} & \begin{pmatrix} -k_{3\zeta}(k_{1\zeta}k_{1\xi} + k_{2\zeta}k_{2\xi}) + k_{3\xi}(k_{1\zeta}^2 + k_{2\zeta}^2) & -k_{3\zeta}(k_{1\zeta}k_{1\eta} + k_{2\zeta}k_{2\eta}) + k_{3\eta}(k_{1\zeta}^2 + k_{2\zeta}^2) & 0 \end{pmatrix} \\ \dfrac{1}{(k_{1\zeta}^2 + k_{2\zeta}^2 + k_{3\zeta}^2)^{1/2}} & \begin{pmatrix} k_{1\zeta}k_{1\xi} + k_{2\zeta}k_{2\xi} + k_{3\zeta}k_{3\xi} & k_{1\zeta}k_{1\eta} + k_{2\zeta}k_{2\eta} + k_{3\zeta}k_{3\eta} & k_{1\zeta}^2 + k_{2\zeta}^2 + k_{3\nu}^2 \end{pmatrix} \end{Bmatrix} \qquad \text{(N-25)}$$

N.6 Velocity Correction

In the critical-plane coordinate system both the VTA velocity correction vector and the miss distance vector become two-dimensional vectors. Therefore, the matrix relating the two must reduce to a 2-by-2 matrix. The characteristics of this 2-by-2 matrix are investigated in this section.

From Equation (M-10),

$$(\underline{c}_V)_W = \overset{*}{X}_C \underline{c}_V = - \overset{*}{X}_C \left(\overset{*}{I}_3 - \frac{\underline{w}\,\underline{w}^T}{\underline{w}^T\,\underline{w}} \right) \overset{*}{K}_{CD}\, \delta\underline{r}_D^-$$

$$= - \overset{*}{X}_C \left(\overset{*}{I}_3 - \frac{\overset{*}{X}_C{}^T (\underline{w})_W (\underline{w}^T)_W \overset{*}{X}_C}{w^2} \right) \overset{*}{K}_{CD}\, \overset{*}{X}_D{}^T (\delta\underline{r}_D^-)_W$$

$$= - \left(\overset{*}{I}_3 - \frac{(\underline{w})_W (\underline{w}^T)_W}{w^2} \right) \overset{*}{X}_C \overset{*}{K}_{CD}\, \overset{*}{X}_D{}^T (\delta\underline{r}_D^-)_W$$

$$= - \begin{pmatrix} 1 & 0 & 0 \\ 0 & 1 & 0 \\ 0 & 0 & 0 \end{pmatrix} \overset{*}{X}_C \overset{*}{K}_{CD}\, \overset{*}{X}_D{}^T (\delta\underline{r}_D^-)_W \qquad \text{(N-26)}$$

When (N-25) is substituted into (N-26), the equation for the VTA correction may be written as

$$\underline{c}_W = \overset{*}{Y} (\delta\underline{\rho}^-)_W \qquad \text{(N-27)}$$

The two-dimensional correction vector $\underline{c}_W$ consists of the components of $\underline{c}_V$ in the ξ_C and η_C directions.

$$\underline{c}_W = \begin{Bmatrix} c_\xi \\ c_\eta \end{Bmatrix} \qquad \text{(N-28)}$$

Then $\overset{*}{Y}$ becomes

$$\overset{*}{Y} = \begin{Bmatrix} k_{1\xi} \sin\alpha - k_{2\xi} \cos\alpha & k_{1\eta} \sin\alpha - k_{2\eta} \cos\alpha \\ (k_{1\xi} \cos\alpha + k_{2\xi} \sin\alpha) \sin\beta - k_{3\xi} \cos\beta & (k_{1\eta} \cos\alpha + k_{2\eta} \sin\alpha) \sin\beta - k_{3\eta} \cos\beta \end{Bmatrix} \qquad \text{(N-33)}$$

The ζ-components of the $\underline{k}$-vectors no longer appear explicitly. Only the ξ-components appear in the first column of $\overset{*}{Y}$; only the η-components appear in the second column. These observations may be related to the velocity correction equation, (N-27), by stating that the coefficients of $\delta\xi_D^-$ contain only the ξ-components of the $\underline{k}$-vectors, while the coefficients of $\delta\eta_D^-$ contain only the η-components.

N.7 Selection of Time of Correction

For a known miss distance vector, the optimum time of correction is defined as that time for which the magnitude of the required correction is a minimum.

Let the two-dimensional miss distance vector $(\delta\underline{\rho}^-)_W$ be represented by a magnitude $\delta\rho^-$ and a phase angle ψ. ψ is the angle in the $\xi_D - \eta_D$ plane between the ξ_D-axis and $\delta\underline{\rho}^-$. From (N-29),

$$(\delta\underline{\rho}^-)_W = \begin{Bmatrix} \delta\xi_D^- \\ \delta\eta_D^- \end{Bmatrix} = (\delta\rho^-) \begin{Bmatrix} \cos\psi \\ \sin\psi \end{Bmatrix} \qquad \text{(N-34)}$$

The square of the magnitude of the VTA correction is

$$c_V^2 = \underline{c}_W^T \underline{c}_W = (\delta\underline{\rho}^-)_W^T \overset{*}{Y}^T \overset{*}{Y} (\delta\underline{\rho}^-)_W$$

$$= (\delta\rho^-)^2 \begin{Bmatrix} \cos\psi & \sin\psi \end{Bmatrix} \overset{*}{Y}^T \overset{*}{Y} \begin{Bmatrix} \cos\psi \\ \sin\psi \end{Bmatrix} \qquad \text{(N-35)}$$

It is apparent that c_V varies linearly with $\delta\rho^-$, but its variation with ψ is non-linear. Its variation with t_C is also non-linear due to the dependence of $\overset{*}{Y}$ on t_C.

The procedure to be followed in determining the optimum correction time is to use Equation (N-35) to plot $c_V/\delta\rho^-$ as a function of t_C for a number of fixed values of ψ. The minimum value of $c_V/\delta\rho^-$ for a given ψ occurs at the optimum correction time for that ψ. Finally, cross-plots are made of $(c_V/\delta\rho^-)_{min}$ and $t_{C\ opt}$ versus ψ. The latter curve defines the optimum correction time as a function of the single parameter ψ of the space vehicle's variant path.

Although ψ can have any value between 0° and 360°, only values between 0° and 180° need be used in the plots, since an increment of 180° in ψ reverses the direction of $\underline{c}_V$ but has no effect on its magnitude.

N.8 Application to Two-Body Reference Trajectories

For two-body reference trajectories the elements k_{13}, k_{23}, k_{31}, and k_{32} of $\overset{*}{K}_{CD}$ are all zero. From Equation (N-19), the three $(\underline{k}_i)_W$ vectors are given by

$$(\underline{k}_1)_W = \begin{Bmatrix} k_{1\xi} \\ k_{1\eta} \\ k_{1\zeta} \end{Bmatrix} = \begin{Bmatrix} k_{11}\cos\Omega_D + k_{12}\sin\Omega_D \\ -(k_{11}\sin\Omega_D - k_{12}\cos\Omega_D)\cos i_D \\ (k_{11}\sin\Omega_D - k_{12}\cos\Omega_D)\sin i_D \end{Bmatrix} \tag{N-36}$$

$$(\underline{k}_2)_W = \begin{Bmatrix} k_{2\xi} \\ k_{2\eta} \\ k_{2\zeta} \end{Bmatrix} = \begin{Bmatrix} k_{21}\cos\Omega_D + k_{22}\sin\Omega_D \\ -(k_{21}\sin\Omega_D - k_{22}\cos\Omega_D)\cos i_D \\ (k_{21}\sin\Omega_D - k_{22}\cos\Omega_D)\sin i_D \end{Bmatrix} \tag{N-37}$$

$$(\underline{k}_3)_W = \begin{Bmatrix} k_{3\xi} \\ k_{3\eta} \\ k_{3\zeta} \end{Bmatrix} = \begin{Bmatrix} 0 \\ k_{33} \sin i_D \\ k_{33} \cos i_D \end{Bmatrix} \qquad \text{(N-38)}$$

Then,

$$\tan i_D = -\frac{k_{1\zeta}}{k_{1\eta}} = -\frac{k_{2\zeta}}{k_{2\eta}} = \frac{k_{3\eta}}{k_{3\zeta}} \qquad \text{(N-39)}$$

The upper right-hand element of $\overset{*}{Y}$ in Equation (N-30) becomes zero, and the matrix may be written

$$\overset{*}{Y} = \begin{Bmatrix} k_{1\xi} \sin\alpha - k_{2\xi} \cos\alpha & 0 \\ (k_{1\xi} \cos\alpha + k_{2\xi} \sin\alpha) \sin\beta & (k_{1\eta} \cos\alpha + k_{2\eta} \sin\alpha) \sin\beta - k_{3\eta} \cos\beta \end{Bmatrix} \qquad \text{(N-40)}$$

The triangular form taken by $\overset{*}{Y}$ for two-body reference trajectories indicates that for such trajectories the component of the correction in the direction of the line of nodes at t_C depends on only that component of the miss distance which lies in the direction of the line of nodes at t_D. This partial uncoupling effect is somewhat surprising; it was not anticipated when the critical-plane coordinate system was originally introduced.

It is of some interest to express the elements of $\overset{*}{Y}$ in (N-40) in terms of the fundamental parameters, namely, the elements of $\overset{*}{K}_{CD}$ and angles Ω_D and i_D. Let y_{ij} be the element in the i-the row and j-th column of $\overset{*}{Y}$.

$$y_{11} = k_{1\xi} \sin \alpha - k_{2\xi} \cos \alpha$$

$$= \frac{k_{1\xi} k_{2\zeta} - k_{2\xi} k_{1\zeta}}{(k_{1\zeta}^2 + k_{2\zeta}^2)^{1/2}}$$

$$= \frac{1}{A} [(k_{11} \cos \Omega_D + k_{12} \sin \Omega_D)(k_{21} \sin \Omega_D - k_{22} \cos \Omega_D)$$

$$- (k_{21} \cos \Omega_D + k_{22} \sin \Omega_D)(k_{11} \sin \Omega_D - k_{12} \cos \Omega_D)]$$

$$= \frac{1}{A} (k_{12} k_{21} - k_{11} k_{22}) \qquad \text{(N-41)}$$

where

$$A = \frac{(k_{1\zeta}^2 + k_{2\zeta}^2)^{1/2}}{\sin i_D}$$

$$= [(k_{11} \sin \Omega_D - k_{12} \cos \Omega_D)^2 + (k_{21} \sin \Omega_D - k_{22} \cos \Omega_D)^2]^{1/2}$$

(N-42)

$$y_{21} = (k_{1\xi} \cos \alpha + k_{2\xi} \sin \alpha) \sin \beta$$

$$= \frac{k_{3\zeta} (k_{1\xi} k_{1\zeta} + k_{2\xi} k_{2\zeta})}{(k_{1\zeta}^2 + k_{2\zeta}^2)^{1/2} (k_{1\zeta}^2 + k_{2\zeta}^2 + k_{3\zeta}^2)^{1/2}}$$

$$= \frac{k_{33} v_R \cos i_D}{Aw} [(k_{11} \cos \Omega_D + k_{12} \sin \Omega_D)(k_{11} \sin \Omega_D - k_{12} \cos \Omega_D)$$

$$+ (k_{21} \cos \Omega_D + k_{22} \sin \Omega_D)(k_{21} \sin \Omega_D - k_{22} \cos \Omega_D)]$$

$$= \frac{k_{33} v_R \cos i_D}{Aw} [(k_{11}^2 - k_{12}^2 + k_{21}^2 - k_{22}^2) \sin \Omega_D \cos \Omega_D$$

$$+ (k_{11} k_{12} + k_{21} k_{22})(\sin^2 \Omega_D - \cos^2 \Omega_D)] \qquad \text{(N-43)}$$

From (N-23),

$$\frac{v_R}{w} = (k_{1\zeta}^2 + k_{2\zeta}^2 + k_{3\zeta}^2)^{-1/2}$$

$$= \left\{ [(k_{11} \sin \Omega_D - k_{12} \cos \Omega_D)^2 + (k_{21} \sin \Omega_D - k_{22} \cos \Omega_D)^2] \sin^2 i_D \right.$$
$$\left. + k_{33}^2 \cos^2 i_D \right\}^{-1/2}$$

$$= (A^2 \sin^2 i_D + k_{33}^2 \cos^2 i_D)^{-1/2} \qquad \text{(N-44)}$$

$$y_{22} = (k_{1\eta} \cos \alpha + k_{2\eta} \sin \alpha) \sin\beta - k_{3\eta} \cos \beta$$

$$= k_{1\eta} \left(\cos \alpha + \frac{k_{2\zeta}}{k_{1\zeta}} \sin \alpha \right) \sin \beta - k_{3\eta} \cos \beta$$

$$= \frac{k_{1\eta}}{(k_{1\zeta}^2 + k_{2\zeta}^2)^{1/2}} \left(k_{1\zeta} + \frac{k_{2\zeta}^2}{k_{1\zeta}} \right) \sin \beta - k_{3\eta} \cos \beta$$

$$= \frac{k_{1\eta}}{k_{1\zeta}} (k_{1\zeta}^2 + k_{2\zeta}^2)^{1/2} \sin \beta - k_{3\eta} \cos \beta$$

$$= \frac{v_R}{w} (k_{1\zeta}^2 + k_{2\zeta}^2)^{1/2} \left(\frac{k_{1\eta} k_{3\zeta}}{k_{1\zeta}} - k_{3\eta} \right)$$

$$= - \frac{v_R}{w} k_{33} A \qquad \text{(N-45)}$$

$\overset{*}{Y}$ for two-body reference trajectories is then

$$\overset{*}{Y} = \begin{Bmatrix} \frac{1}{A}\,(k_{12}\,k_{21} - k_{11}\,k_{22}) & 0 \\ \frac{1}{A}\,\frac{v_R}{w}\,k_{33}\cos i_D\,[(k_{11}{}^2 - k_{12}{}^2 + k_{21}{}^2 - k_{22}{}^2)\sin\Omega_D\cos\Omega_D + (k_{11}\,k_{12} + k_{21}\,k_{22})(\sin^2\Omega_D - \cos^2\Omega_D)] & -A\,\frac{v_R}{w}\,k_{33} \end{Bmatrix} \tag{N-46}$$

N.9 Evaluation of Parameters

The two fundamental parameters used in the analysis contained in this appendix are the orientation angles Ω_D and i_D. They can be evaluated by means of Equations (N-11), (N-12), and (N-14).

$$\underline{v}_R = \begin{Bmatrix} v_{R_1} \\ v_{R_2} \\ v_{R_3} \end{Bmatrix} = \overset{*}{X}_D{}^T\,(\underline{v}_R)_W = v_R \begin{Bmatrix} \sin\Omega_D \sin i_D \\ -\cos\Omega_D \sin i_D \\ \cos i_D \end{Bmatrix} \tag{N-47}$$

The components of $\underline{v}_R$ along the r_1, r_2, and r_3 axes are known for the specified reference trajectory. The desired angles are computed from these components.

$$\Omega_D = -\arctan\left(\frac{v_{R_1}}{v_{R_2}}\right) \tag{N-48}$$

$$i_D = \arccos\left(\frac{v_{R_3}}{v_R}\right) \tag{N-49}$$

The quadrant location of each of the two angles is determined by stipulating that each lies in the range between 0 and π radians.

When Ω_D and i_D have been evaluated, the transformation matrix $\overset{*}{X}_D$ is computed from (N-11). This matrix and matrix $\overset{*}{K}_{CD}$, the evaluation of which has been discussed in Section L.6, are used to calculate the components of the three $\underline{k}$ vectors in the critical-plane coordinate system.

From (N-18),

$$\begin{Bmatrix} k_{1\xi} & k_{1\eta} & k_{1\zeta} \\ k_{2\xi} & k_{2\eta} & k_{2\zeta} \\ k_{3\xi} & k_{3\eta} & k_{3\zeta} \end{Bmatrix} = \overset{*}{K}_{CD}\, \overset{*}{X}_D{}^T \qquad \text{(N-50)}$$

The elements of $\overset{*}{Y}$ can then be determined from (N-30) or from (N-33) used in conjunction with (N-31) and (N-32).

An estimate of the components of $\delta\underline{r}_D^-$ along the r_1, r_2, and r_3 axes is assumed to be available. Matrix $\overset{*}{X}_D$ transforms $\delta\underline{r}_D^-$ into its components along ξ_D, η_D, and ζ_D axes.

$$\overset{*}{X}_D\, \delta\underline{r}_D^- = (\delta\underline{r}_D^-)_W = \begin{Bmatrix} \delta\xi_D^- \\ \delta\eta_D^- \\ \delta\zeta_D^- \end{Bmatrix} = \begin{Bmatrix} (\delta\underline{\rho}^-)_W \\ \delta\zeta_D^- \end{Bmatrix} \qquad \text{(N-51)}$$

$\overset{*}{Y}$ and $(\delta\underline{\rho}^-)_W$ are used to compute the components of the VTA velocity correction along critical-plane coordinate axes by means of Equation (N-27). The components of the correction along the r_1, r_2, and r_3 axes are obtained from the equation

$$\underline{c}_V = \overset{*}{X}_C{}^T\, \underline{c}_W \qquad \text{(N-52)}$$

Equation (N-24) can be used to compute the elements of $\overset{*}{X}_C$ from the ζ-components of the three $\underline{k}$ vectors, which have already been computed.

An alternative method of computing the elements of $\overset{*}{X}_C$, which serves as a partial check of the computing procedure, is by means of Equation (N-13).

$$\underline{w} = \begin{Bmatrix} w_1 \\ w_2 \\ w_3 \end{Bmatrix} = \overset{*}{K}_{CD}\, \underline{v}_R = \overset{*}{X}_C{}^T (\underline{w})_W = w \begin{Bmatrix} \sin \Omega_C \sin i_C \\ -\cos \Omega_C \sin i_C \\ \cos i_C \end{Bmatrix} \qquad \text{(N-53)}$$

The components w_1, w_2, and w_3 are determined, and the angles Ω_C and i_C are expressed in terms of these components.

$$\Omega_C = -\arctan\left(\frac{w_1}{w_2}\right) \qquad \text{(N-54)}$$

$$i_C = \arccos\left(\frac{w_3}{w}\right) \qquad \text{(N-55)}$$

Both angles are restricted to the range 0 to π radians. The elements of $\overset{*}{X}_C$ can be found from the angles by the use of (N-11).

The angle ψ, used in determining the optimum correction time, can be computed from Equation (N-34).

$$\psi = \arctan\left(\frac{\delta\eta_D}{\delta\xi_D}\right) \qquad \text{(N-56)}$$

It has already been pointed out in Section N.7 that only values of ψ in the range 0 to π radians need be considered in the procedure for optimizing the time of correction; consequently, the angles computed by means of (N-56) can be restricted to that range.

The computational procedure is simplified in the case of two-body reference trajectories. The matrix $\overset{*}{Y}$ can be found from Ω_D, i_D, and the elements of $\overset{*}{K}_{CD}$ by the use of Equations (N-42), (N-44), and (N-46). If the alternate form is used to compute Ω_C and i_C, there is no need to transform the $\underline{k}$ vectors into the critical-plane coordinate system.

APPENDIX O

SINGULARITIES IN THE MATRIX SOLUTION FOR ELLIPTICAL TRAJECTORIES

O.1 Summary

In the analytical development for elliptical trajectories presented in Appendix K, it has been shown that the variations in the orbital elements, represented by the vector $\delta \underline{e}$, can be expressed in terms of two position variations $\delta \underline{r}_i$ and $\delta \underline{r}_j$. The 6-by-6 matrix relating $\delta \underline{e}$ to $\delta \underline{r}_i$ and $\delta \underline{r}_j$ is obtained by inverting the 6-by-6 matrix through which $\delta \underline{r}_i$ and $\delta \underline{r}_j$ are expressed in terms of $\delta \underline{e}$. However, the latter matrix becomes singular and hence cannot be inverted, for three different types of combinations of t_i and t_j. These three types are

$$(1) \quad t_j - t_i = N P$$

$$(2) \quad f_j - f_i = (2 N - 1) \pi$$

$$(3) \quad X = 0$$

where N is a positive integer, P is the period of the reference trajectory, and the factor X is defined by Eqs. (K-14), (K-15), and (K-17).

This appendix examines the mathematical consequences of the singularities and interprets them physically. Explanation of the first two types of singularities is relatively simple. The third type is more subtle; Lambert's theorem, in classical celestial mechanics theory, is used in its interpretation.

If the time of midcourse correction is related to the nominal time of arrival in such a manner that any one of the singularity conditions is satisfied, no finite FTA velocity correction can be computed.

The use of VTA guidance tends to mitigate the effect of the singularities. For a correction time corresponding to either the second or the third type of singularity, a VTA correction of finite magnitude can be determined. However, if the correction time meets the condition for the first type of singularity, the magnitude of the computed correction is infinite even in VTA guidance.

O.2 Preliminary Remarks

When the analytic solution of the guidance problem for elliptical trajectories was first obtained, it became a matter of considerable interest to find a physical explanation for the various singularities. Singularities of the first two types had already been recognized by Laning and Battin from their numerical studies. (See Pages 201 and 202 of Reference (5)). There is no indication of the singularity at $X = 0$ in any of the technical literature that has been reviewed.

The verbal disclosure of the $X = 0$ singularity was initially greeted with a degree of skepticism, because, unlike the other types, it did not have a physical interpretation that was immediately apparent. Much of the skepticism was allayed when evidence of the existence of this singularity was found in the computer data used in Reference (5). It was not until some time later that the mathematical connection between the singularity at $X = 0$ and the minimum point on the time-of-flight curve was proved and a physical explanation of the singularity was presented.

O.3 The Singular Matrix

The position variations $\delta \underline{r}_i$ and $\delta \underline{r}_j$ are related to $\delta \underline{e}$ by the equation

$$\begin{Bmatrix} \delta \underline{r}_i \\ \\ \delta \underline{r}_j \end{Bmatrix} = \begin{Bmatrix} \overset{*}{F}_i \\ \\ \overset{*}{F}_j \end{Bmatrix} \delta \underline{e} = \overset{*}{A}_{ij} \, \delta \underline{e} \qquad \text{(O-1)}$$

An analytic expression for the 3-by-6 matrix $\overset{*}{F}_j$ is given by Eq. (K-31). $\delta \underline{e}$ is defined by Eq. (K-1).

It is the 6-by-6 matrix $\overset{*}{A}_{ij}$, comprised of $\overset{*}{F}_i$ and $\overset{*}{F}_j$, that becomes singular under the conditions specified in Section O. 1. When this matrix is singular, the six components comprising $\delta \underline{r}_i$ and $\delta \underline{r}_j$ are not linearly independent, and consequently all the elements of $\delta \underline{e}$ cannot be determined uniquely.

The non-zero elements of $\overset{*}{A}_{ij}$ may be grouped into two sub-matrices, the first of which is the 4-by-4 matrix pertaining to motion in the plane of the reference trajectory and the second of which is the 2-by-2 matrix pertaining to motion parallel to the z-axis. A singularity may occur in either or both sub-matrices. The first four components of $\delta \underline{e}$ are used in conjunction with the 4-by-4 sub-matrix; the last two components of $\delta \underline{e}$ are used in conjunction with the 2-by-2 sub-matrix.

Because the two types of motion are uncoupled, if a singularity occurs only in the 4-by-4 sub-matrix, the last two components of $\delta \underline{e}$ can still be evaluated; conversely, if a singularity occurs only in the 2-by-2 sub-matrix, the first four elements of the $\delta \underline{e}$ can still be evaluated.

O. 4 Mathematical Study of Singularities at $(t_j - t_i) = N P$

The singularities for which $(t_j - t_i) = N P$ will be examined first. Even without mathematical analysis, it is intuitively reasonable to expect that two position variations obtained at times that are an exact number of reference periods apart will bear some relation to each other and hence will not be independent.

In one circuit about the attractive focus, the change in each of the three anomalies – real, eccentric, and mean – is exactly 2π radians. Thus, when $(t_j - t_i) = N P$, the eccentric anomaly difference is $2N\pi$ radians. It may be deduced from Eq. (K-31) that the rank of matrix $\overset{*}{A}_{ij}$ is reduced to four when $(t_j - t_i) = N P$. The rank of the 4-by-4 sub-matrix is reduced to three, and the rank of the 2-by-2 sub-matrix is reduced to one.

Eq. (K-31) may also be used to show the relation between $\delta \underline{r}_j$ and $\delta \underline{r}_i$ for the singularity condition.

$$\begin{Bmatrix} \delta p_j \\ \delta q_j \\ \delta z_j \end{Bmatrix} = \begin{Bmatrix} \delta p_i \\ \delta q_i \\ \delta z_i \end{Bmatrix} - \begin{Bmatrix} 0 \\ \frac{3}{2} \quad \frac{(1 + e \cos E_i)^{1/2}}{(1 - e \cos E_i)^{1/2}} \quad 2 N\pi \quad \delta a \\ 0 \end{Bmatrix} \tag{O-2}$$

With the aid of Eq. (B-69), (O-2) may be expressed in terms of the nominal orbital velocity v_i and the nominal period P.

$$\begin{Bmatrix} \delta p_j \\ \delta q_j \\ \delta z_j \end{Bmatrix} = \begin{Bmatrix} \delta p_i \\ \delta q_i \\ \delta z_i \end{Bmatrix} - \begin{Bmatrix} 0 \\ \frac{3}{2} N P v_i \frac{\delta a}{a} \\ 0 \end{Bmatrix} \tag{O-3}$$

Eq. (O-3) can be solved for the third component of $\delta \underline{e}$.

$$\frac{1}{2} \frac{\delta a}{a} = - \frac{\delta q_j - \delta q_i}{3 N P v_i} \tag{O-4}$$

It is interesting that this unique solution for $\frac{1}{2} \frac{\delta a}{a}$ exists despite the fact that $\overset{*}{A}_{ij}$ contains singularities in both of its non-zero sub-matrices.

If t_i is associated with t_C, the time at which the correction is to be applied, and if t_j is associated with t_D, the nominal time of arrival, Eq. (O-3) becomes

$$\begin{Bmatrix} \delta p_D \\ \delta q_D \\ \delta z_D \end{Bmatrix} = \begin{Bmatrix} \delta p_C \\ \delta q_C \\ \delta z_C \end{Bmatrix} - \begin{Bmatrix} 0 \\ \frac{3}{2} N P v_C \frac{\delta a}{a} \\ 0 \end{Bmatrix} \tag{O-5}$$

If a position variation exists in either the p_C or the z_C direction at time t_C, that same position variation will exist at time t_D irrespective of the nature of the path traversed by the vehicle in the N circuits between t_C and t_D. Linear theory does not permit the computation of a velocity correction which, if applied at $t = t_C$, will cause the position variations δp and δz to be reduced to zero when $t = t_D$.

In the special case when $\delta p_C = 0 = \delta z_C$ and $\delta q_C \neq 0$, it is possible to compute a velocity correction $\underline{c}_F$ which will enable the vehicle to arrive at the desired destination at the proper time. The correction required to reduce the predicted value of δq_D to zero is such that

$$\left(\frac{\delta a}{a}\right)^+ = \frac{2\,\delta q_C^-}{3\,N\,P\,v_C} = \frac{2\,\delta q_C^-}{3\,N\,P\,v_D} \qquad (O\text{-}6)$$

The + and - superscripts have been added to distinguish characteristics of the corrected path from characteristics of the original path. From Eqs.(O-5) and (O-6),

$$\left(\frac{\delta a}{a}\right)^+ = \frac{2\,\delta q_D^-}{3\,N\,P\,v_D} + \left(\frac{\delta a}{a}\right)^- \qquad (O\text{-}7)$$

so that the change in $\frac{\delta a}{a}$ to be provided by the correction is

$$\left(\frac{\delta a}{a}\right)^+ - \left(\frac{\delta a}{a}\right)^- = \frac{2\,\delta q_D^-}{3\,N\,P\,v_D} \qquad (O\text{-}8)$$

The velocity correction itself for this special case may be found from Eq. (K-48) and (L-1).

$$\underline{c}_F = -\overset{*}{K}_{CD}\,\delta \underline{r}_D^- = \frac{n\,(1 - e\cos E_C)\,(\cos E_M + e\cos E_P)}{2\,(1 + e\cos E_C)\,X}\,(\delta q_D^-)\,\underline{u}_{q_C} \qquad (O\text{-}9)$$

From Eqs. (K-14), (K-15), and (K-17), with $E_D - E_C = 2N\pi$,

$$E_P = \frac{1}{2}(E_D + E_C) = E_C + N\pi = E_D - N\pi \qquad \text{(O-10)}$$

$$E_M = \frac{1}{2}(E_D - E_C) = N\pi \qquad \text{(O-11)}$$

$$X = (3E_M - e \sin E_M \cos E_P)(\cos E_M + e \cos E_P) - 4 \sin E_M$$
$$= 3N\pi(\cos E_M + e \cos E_P) \qquad \text{(O-12)}$$

Eq. (B-62), (B-69), and (O-12) are used to simplify the expression for $\underline{c}_F$ given by Eq. (O-9).

$$\underline{c}_F = \frac{\mu}{3NPa\,v_C^2}(\delta q_D^-)\,\underline{u}_{q_C} = \frac{\mu}{3NPa\,v_D^2}(\delta q_D^-)\,\underline{u}_{q_D} \qquad \text{(O-13)}$$

For this special case the correction is in the direction of the nominal orbital velocity, and its magnitude is inversely proportional to the square of the nominal orbital velocity.

O.5 Physical Interpretation of Singularities at $(t_j - t_i) = NP$

The physical interpretation of the singularities at $(t_j - t_i) = NP$ will be treated in two distinct phases. In the first phase a reference trajectory is assumed, and the interpretation is based on linear perturbation theory. The second phase is more general; there is no reference trajectory and no requirement for linearization.

For the first phase, consider a vehicle traveling in an elliptical orbit which differs only slightly from a known reference ellipse. At time t_i the vehicle's position variation with respect to the reference ellipse is determined from measurements, and at time t_j, which is exactly N reference periods later than t_i, the position variation is again determined.

Let P be the period of the reference orbit and P' the period of the actual orbit. If P' = P, it is obvious that $\delta \underline{r}_j$ must be identical with $\delta \underline{r}_i$. Any difference between $\delta \underline{r}_j$ and $\delta \underline{r}_i$ must be proportional to $\delta P = (P' - P)$ and to N. $\delta \underline{r}_j$ may be expressed as follows:

$$\delta \underline{r}_j = \delta \underline{r}_i - (\underline{v}_j + \delta \underline{v}_j) \, N \, \delta P \qquad \text{(O-14)}$$

The minus sign is due to the fact that an increase in the period causes a lag in the vehicle's position.

Since $\delta \underline{v}_j$ and δP are both small quantities, linear theory reduces Eq. (O-14) to

$$\begin{aligned} \delta \underline{r}_j &= \delta \underline{r}_i - N \, \underline{v}_j \, \delta P \\ &= \delta \underline{r}_i - N \, v_j \, \delta P \, \underline{u}_{q_j} \\ &= \delta \underline{r}_i - N \, v_i \, \delta P \, \underline{u}_{q_i} \end{aligned} \qquad \text{(O-15)}$$

Kepler's third law states that P^2 is proportional to a^3. From this law it follows that

$$\frac{\delta P}{P} = \frac{3}{2} \, \frac{\delta a}{a} \qquad \text{(O-16)}$$

Therefore,

$$\delta \underline{r}_j = \delta \underline{r}_i - \frac{3}{2} \, N \, P \, v_i \, \frac{\delta a}{a} \, \underline{u}_{q_i} \qquad \text{(O-17)}$$

Eq. (O-17) is exactly the same relationship that was previously obtained as Eq. (O-3).

The foregoing discussion pertains to the problem of the determination of orbital elements from two position fixes. It can be directly related to the problem of applying a velocity correction at t_C which nulls

the position variation at t_D. The analysis is the same as that presented in Section O. 4. Only if the predicted position variation at t_D is in the q_D-direction can a finite velocity correction be computed by linear theory. The computed correction for that case is given by Eq. (O-13).

For the second phase of the physical interpretation, a body is assumed to be moving in an elliptical path about an attractive focus. There is no a priori knowledge of the body's trajectory except for the fact that it is an ellipse. At time t_i the body's position relative to the focus is measured. At time t_j a second set of measurements indicates that the body's relative position is exactly the same as it was at t_i. In the interval between t_i and t_j the body has completed N circuits about the focus.

In this example the observed data consist of the times t_i and t_j, the integer N, and the three components of position.

From t_i, t_j, and N, it is possible to compute the period P, the mean angular motion n, and the semi-major axis a.

$$P = \frac{t_j - t_j}{N} \tag{O-18}$$

$$n = \frac{2\pi}{P} \tag{O-19}$$

$$a = \left(\frac{\mu}{n^2}\right)^{1/3} \tag{O-20}$$

The semi-major axis is the only one of the six orbital elements that can be obtained from the available data; all the others are indeterminate. Eq. (O-20) corresponds to Eq. (O-4) in the development based on linear theory.

Now suppose that a space vehicle is in an elliptical orbit around the sun. At time t_C, when the vehicle is at point C, a velocity correction is to be applied such that the new orbit will enable the vehicle to reach the desired destination point D at time t_D. The points C and D are relatively close to each other compared to the distance of either from the sun. The time interval $(t_D - t_C)$ is approximately N times the period of the vehicle's original orbit.

Regardless of the orientation of the line C D, it is always possible to find a new elliptical orbit which will enable the vehicle to reach D at the proper time. The plane of the new orbit must contain vectors $\underline{r}_C$ and $\underline{r}_D$, and its semi-major axis is determined by the required time interval and the number of circuits to be made between C and D.

If C D is parallel to $\underline{v}_C^-$, the velocity vector at t_C before the correction, the new orbit will closely resemble the old. All that is required is a small change in the period, which in turn causes a small change in the semi-major axis. Thus, the velocity correction itself is small in magnitude and can be computed from the linear theory. This situation is represented by the points C_1 and D in Fig. O. 1.

On the other hand, if point C has any arbitrary position in the vicinity of D, the required new orbit will in general differ drastically from the original orbit, and the velocity correction will be so large in magnitude that it cannot be determined from the linear theory.

Two special cases serve to illustrate this point. In the first, the vehicle is situated at C_2 in Fig. O. 1. C_2 lies along the radial line connecting the focus (sun) with D. In this case, the new path is a rectilinear ellipse; i. e., a straight line of finite length. Obviously, the velocity correction required to change from an orbit such as the one indicated in the sketch to a rectilinear ellipse is sizable.

In the second special case C D is parallel to the z-axis; i. e., C is directly above or below D (out of the plane of the paper) in Fig. O. 1. The new path is then an ellipse in the r_D-z plane. If the distance C D is small, the velocity vector immediately after the correction, $\underline{v}_C^+$, is perpendicular to position vector $\underline{r}_C$; therefore, F C lies along the line of apsides of the new trajectory, and C is either at perihelion or at aphelion. It is clear that the magnitude of the correction required to rotate the trajectory plane through 90° is beyond the scope of the linear theory.

O. 6 Mathematical Study of Singularities at $(f_j - f_i) = (2\,N - 1)\,\pi$

When $(f_j - f_i) = (2\,N - 1)\,\pi$, the rank of matrix $\overset{*}{A}_{ij}$ is reduced to five. The rank of the 4-by-4 sub-matrix is unchanged; the rank of the 2-by-2 sub-matrix becomes one.

Since the 4-by-4 sub-matrix is not singular under these conditions, the four components of $\delta\underline{e}$ relating to motion in the reference

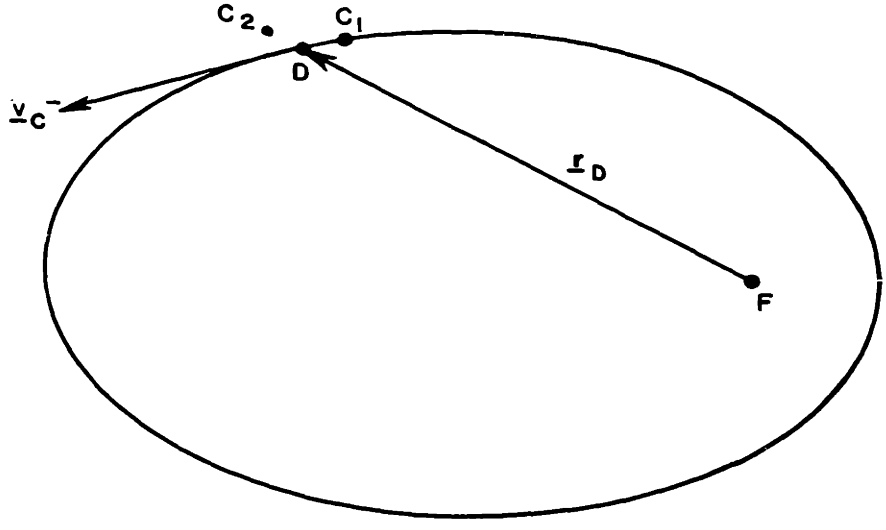

F – attractive focus (sun)
D – destination point
C_1, C_2 – possible vehicle positions at time of correction
$\underline{v}_C^-$ – vehicle velocity vector just prior to application of correction
$\underline{r}_D$ – vehicle position vector at destination
t_C – time of correction
t_D – time of arrival at destination
P – nominal period

Figure O.1 Special Cases of Vehicle Position at Time of Correction for Singularities at $t_D - t_C = NP$

trajectory plane can be determined from $\delta \underline{r}_i$ and $\delta \underline{r}_j$ even though $\overset{*}{A}_{ij}$ is singular.

The dependence of δz_j and δz_i is made apparent by use of Eq. (H-15).

$$\frac{\delta z_i}{r_i} = \delta i \sin (f_i - \delta \Omega) \qquad \text{(O-21)}$$

With $f_j = f_i + (2\,N - 1)\,\pi$,

$$\frac{\delta z_j}{r_j} = - \delta i \sin (f_i - \delta \Omega) \qquad \text{(O-22)}$$

Then,

$$\delta z_j = - \frac{r_j}{r_i} \delta z_i \qquad \text{(O-23)}$$

Obviously, δz_i and δz_j cannot be used to obtain the two elements of $\delta \underline{e}$ which describe the variant motion normal to the reference trajectory plane.

If the correction time and the arrival time are such that $(f_D - f_C) = (2\,N - 1)\,\pi$, Eqs. (K-48) and (L-1) indicate that a finite FTA correction can be computed only if $\delta z_D = 0$. In that special case, the velocity correction vector $\underline{c}_F$ lies in the reference trajectory plane.

O.7 Physical Interpretation of Singularities at $(f_j - f_i) = (2\,N - 1)\,\pi$

Consider a body in an elliptical orbit about an attractive focus F, as shown in Fig. O. 2. The orbit must lie in one plane; therefore, if the body passes through point C, it must eventually pass through some point such as D, which lies on the extension of CF through F. This statement has general validity, irrespective of the nature of the elliptical trajectory and of the inclination of the trajectory plane. Thus, the position of the body at D is not completely independent of the position at C.

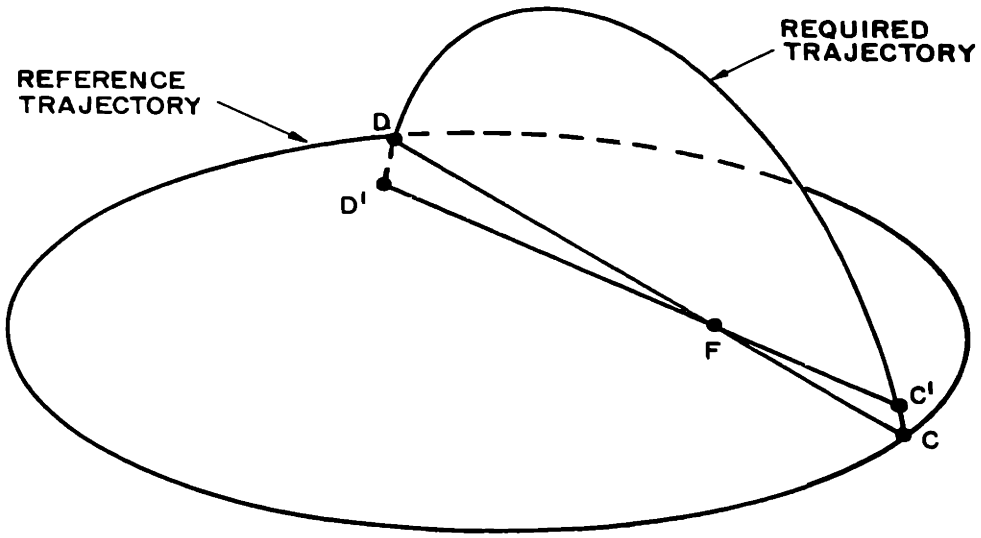

F – attractive focus (sun)

D – destination point

C – position on reference trajectory corresponding to $t = t_C$

C' – position on actual trajectory corresponding to $t = t_C$

D' – predicted position at $t = t_D$ if no correction is applied

t_C – time of correction

t_D – time of arrival at destination

Figure O.2 Effect of z-Component of Position Variation when $f_D - f_C = (2N-1)\pi$

Suppose that at time t_C a vehicle is at point C' and the corresponding point on the reference trajectory is C. The distance CC is parallel to the z-axis and small. A correction is to be applied at C' such that the vehicle will arrive at the prescribed destination point D at time t_D. If no correction is made, the vehicle's position at t_D will be D'. This example is similar to the second special case cited at the end of Section O. 5.

The corrected trajectory must contain the line segments F C' and F D. The plane containing these two segments is the r_C - z plane, which is perpendicular to the reference trajectory plane. As stated in Section O. 5, the magnitude of the velocity correction required to rotate the trajectory plane through approximately 90° is beyond the scope of linear theory and hence cannot be computed by the use of that theory.

Any small velocity correction applied in the z-direction when the vehicle is at C' has the effect of rotating the trajectory plane about the axis D' F C'. The size and shape of the orbit are not affected, so that the vehicle must pass through D' at time t_D.

O. 8 Numerical Example of Singularities at X = 0

The singularity factor X is defined by Eqs. (K-14), (K-15), and (K-17), which are repeated here for convenience.

$$X = (3 E_M - e \sin E_M \cos E_P)(\cos E_M + e \cos E_P) - 4 \sin E_M \tag{O-24}$$

where

$$E_P = \frac{1}{2}(E_j + E_i) \tag{O-25}$$

$$E_M = \frac{1}{2}(E_j - E_i) \tag{O-26}$$

Unlike the first two types of singularities, those for which X = 0 depend on the reference trajectory, as indicated by the presence of the eccentricity e in Eq. (O-24).

Because the formulation for X in Eq. (O-24) may be considered somewhat formidable, a graph of X versus $(E_j - E_i)$ is presented in Fig. O. 3. The plot is made for a varying E_i, with e and E_j held constant. The value of e is 0. 25, a typical value for journeys to Venus or Mars. The angle E_j is 210°, which is representative of an inbound journey from Venus to Earth or an outbound journey from Earth to Mars. The plot covers the range 0° to 1800° in $(E_j - E_i)$.

Although Fig. O. 3 is drawn for specific values of e and E_j, it is characteristic of the relationship between X and $(E_j - E_i)$ for any value of e in the elliptical range and any angle E_j.

There are several interesting characteristics of the curve. It has the general appearance of a sinusoid whose amplitude is steadily increasing as $(E_j - E_i)$ gets larger. At $(E_j - E_i) = 0$, both X and its partial derivative with respect to $(E_j - E_i)$ are equal to zero.

The zero crossings of the curve are of particular interest, since those are the points at which the matrix $\overset{*}{A}_{ij}$ becomes singular. There is no zero crossing for $0° < (E_j - E_i) < 360°$. For each succeeding interval of 360° there is one zero crossing.

As $(E_j - E_i)$ gets large, the curve is dominated by the term $3 E_M (\cos E_M + e \cos E_P)$. In the limit as the anomaly difference approaches infinity,

$$\lim_{E_M \to \infty} \left(\frac{X}{E_M}\right) = 3 (\cos E_M + e \cos E_P)$$

$$= \frac{3}{2 \sin E_M} [\sin (E_j - E_i) + e (\sin E_j - \sin E_i)] \qquad (O-27)$$

The special case of $\sin E_M = 0$ constitutes a singularity of the first type, which has already been discussed, and hence will be ignored in this analysis.

For large values of $(E_j - E_i)$, the singularity occurs when the limit expression of Eq. (O-27) is equal to zero.

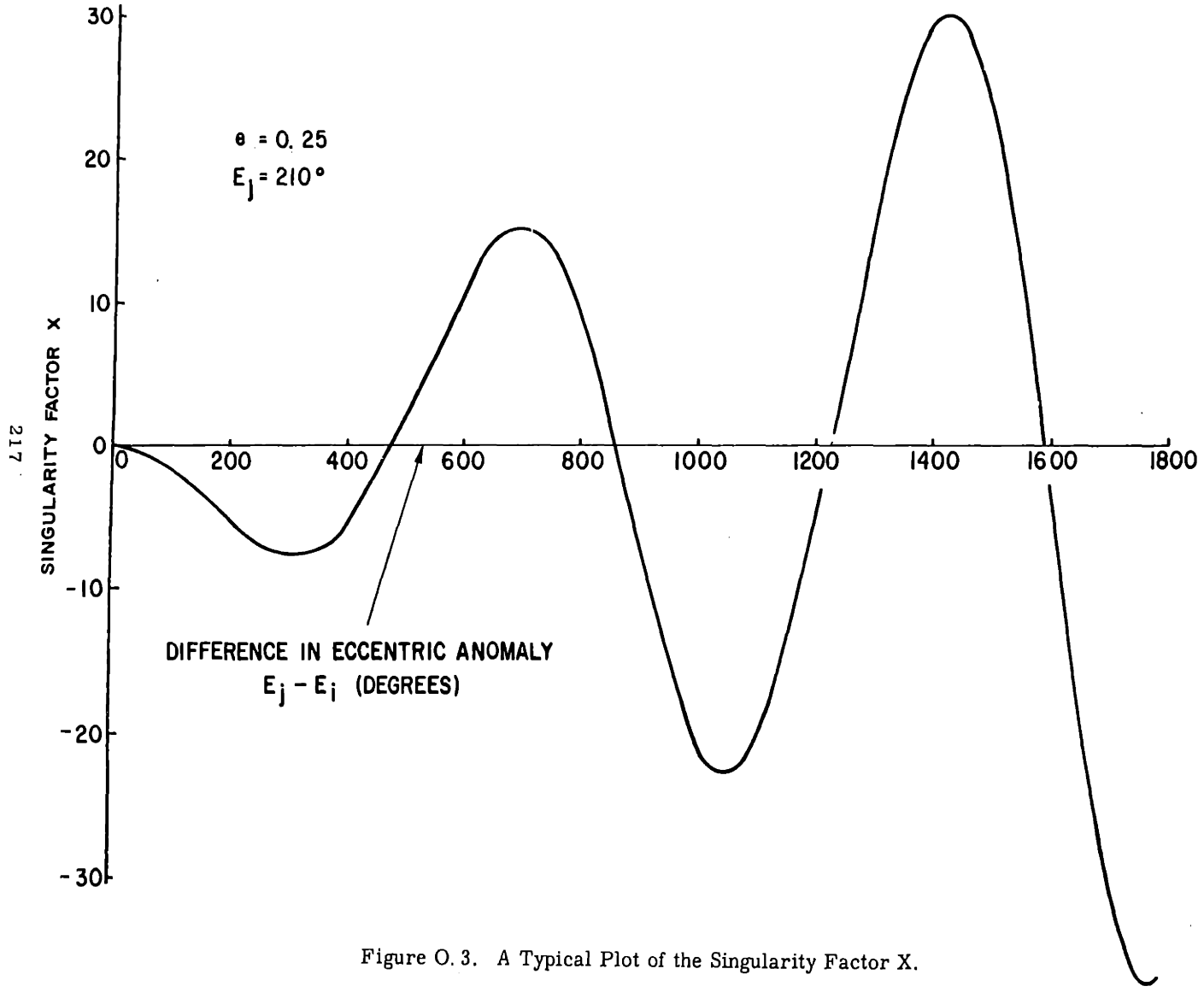

Figure O. 3. A Typical Plot of the Singularity Factor X.

$$0 = \sin (E_j - E_i) + e (\sin E_j - \sin E_i)$$

$$= \sin E_j (\cos E_i + e) - \sin E_i (\cos E_j + e)$$

$$= \frac{1}{a^2 (1 - e^2)^{1/2}} [(x_i + 2 a e) y_j - (x_j + 2 a e) y_i] \qquad (O-28)$$

Then the condition for the existence of the singularity at large values of $(E_j - E_i)$ is

$$\frac{y_j}{x_j + 2 a e} = \frac{y_i}{x_i + 2 a e} \qquad (O-29)$$

The distances $(x_i + 2 a e)$ and y_i are, respectively, the x and y components of the distance of the point P_i on the ellipse from the vacant focus. Thus, when $(E_j - E_i)$ is very large, the singularity condition occurs when the straight line through the points P_i and P_j on the ellipse passes through the vacant focus.

Table O-1 lists the points at which the first few singularities occur, as well as the singular point for $(E_j - E_i) \to \infty$. The symbol N in the table denotes the number of complete circuits between E_i and E_j.

For a fixed point P_j, the effect of increasing N is to move the corresponding singular point P_i along the ellipse from P_j toward the point at which the straight line through P_j and the vacant focus intersects the ellipse. The singular point approaches the latter point asymptotically as N tends toward infinity. The progression of P_i is illustrated in Fig. O. 4.

$e = 0.25$

$E_2 = 210°$

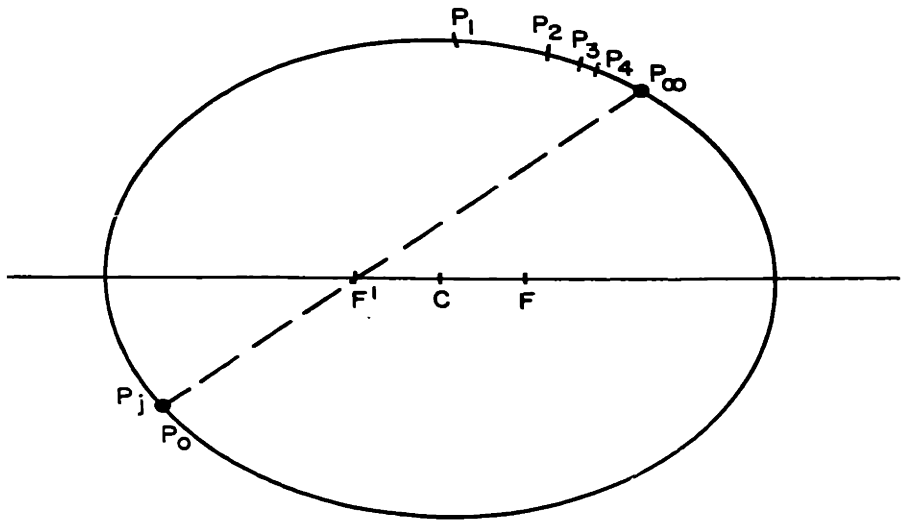

C — center of ellipse

F — attractive focus

F' — vacant focus

P_j — fixed destination point on ellipse

$P_o, P_1, \ldots P_N \ldots P_\infty$ — singularity points for each value of N

N — number of complete circuits between P_N and P_j

Figure O.4 Positions of the Singularities at X = 0

TABLE O-1

The Singularity Points X = 0 for e = 0.25 and E_j = 210°

N	$E_j - E_i$	$E_j - E_i - N360°$	$E_i + N360°$	$f_i + N360°$
0	0°	0°	210°	204°
1	482°	122°	88°	102°
2	860°	140°	70°	84°
3	1227°	147°	63°	77°
4	1589°	149°	61°	74°
∞	∞	162°	48°	60°

O.9 Mathematical Study of Singularities at X = 0

The singularities at X = 0 reduce the rank of the 4-by-4 sub-matrix of $\overset{*}{A}_{ij}$ to three and have no effect on the rank of the 2-by-2 sub-matrix; the rank of $\overset{*}{A}_{ij}$ is reduced from six to five. (This discussion of the singularities for which X = 0 does not apply to the trivial case, $E_j - E_i = 0$.)

When X = 0, there must be a linear relationship between δp_i, δq_i, δp_j, and δq_j. After some algebraic manipulation of Eq. (K-13) and the use of several of the celestial mechanics relations of Appendix B, this linear relationship may be written as

$$p_j \, \delta q_j - p_i \, \delta q_i = -\frac{b}{2} (3 E_M - e \sin E_M \cos E_P) (\cos \gamma_j \, \delta p_j + \cos \gamma_i \, \delta p_i) \tag{O-30}$$

where $b = a (1 - e^2)^{1/2}$ is the semi-minor axis of the reference ellipse.

When correction time t_C and arrival time t_D are such that X = 0, it is possible to compute a finite FTA velocity correction only if δp_C and δq_C are related to each other in the manner defined by setting δp_j and δq_j equal to zero in Eq. (O-30) and substituting δp_C for δp_i, δq_C for δq_i. The relation between δp_C and δq_C is then given by

$$\frac{\delta p_C}{\delta q_C} = \frac{2\, r_C}{b\,(3\, E_M - e \sin E_M \cos E_P)} \qquad \text{(O-31)}$$

Eq. (O-31) specifies the ratio of the two components of position variation at $t = t_C$ but does not stipulate any particular value for either. Thus, when $X = 0$, a finite FTA correction can be applied only if the position variation component in the reference trajectory plane at time t_C lies along the line defined by Eq. (O-31). In Fig. O.5 this line is indicated as ACB.

Let μ_C be the angle between line ACB and the q_C-axis. Then,

$$\tan \mu_C = \frac{\delta p_C}{\delta q_C} \qquad \text{(O-32)}$$

Because r_C and b are normally of the same order of magnitude and E_M is large at the singularity points, the angle μ_C is small. As N gets larger, μ_C gets smaller, until finally ACB is parallel to the q_C-axis when N approaches infinity. Table O-2 lists μ_C as a function of N for the conditions used in the plot of Fig. O.3.

By substituting Eq. (O-31) into (O-30), a relation is obtained for the ratio of the predicted position variation components δp_D^- and δq_D^- for the special case when a finite correction can be computed at $X = 0$.

$$\frac{\delta p_D^-}{\delta q_D^-} = -\frac{2\, r_D}{b\,(3\, E_M - e \sin E_M \cos E_P)} \qquad \text{(O-33)}$$

The line defined by Eq. (O-33) is HDK in Fig. O.5. The angle between HDK and the q_D-axis is designated μ_D.

$$\tan \mu_D = \frac{\delta p_D^-}{\delta q_D^-} \qquad \text{(O-34)}$$

Table O-2 lists values of μ_D as well as μ_C.

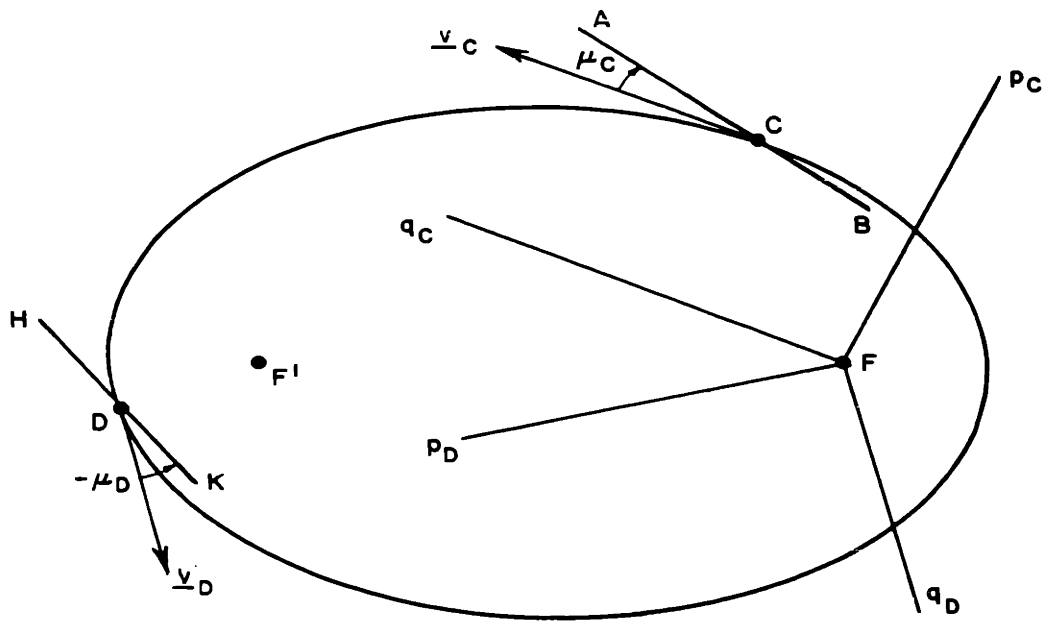

D – nominal destination point

C – singularity point corresponding to D

$\underline{v}_C$ – nominal velocity vector at C

Fp_C, Fq_C – instantaneous position of flight path system coordinate axes at $t = t_C$

ACB – straight-line locus of points at which a finite velocity correction can be computed

μ_C – angle between ACB and q_C-axis

$\underline{v}_D$ – nominal velocity vector at D

Fp_D, Fq_D – instantaneous position of flight path system coordinate axes at $t = t_D$

HDK – straight-line locus of predicted destination points if no correction is applied at $t = t_C$

μ_D – angle between HDK and q_D-axis

Figure O.5 Special Case for which Velocity Correction Can Be Computed at X = 0

$$\zeta_F = -\frac{\pi}{2} \left\{ \begin{array}{cc} \dfrac{1}{(1 - e^2\cos^2 E_C)^{1/2}(1 - e^2\cos^2 E_D)^{1/2}} \begin{pmatrix} \dfrac{\cos E_M + e\cos E_P}{\sin E_M} & 0 \\ \dfrac{1}{2}(1 - e^2)^{1/2}(1 - e\cos E_C) & 0 \end{pmatrix} \\ \begin{pmatrix} 0 & \dfrac{1}{(\cos E_M - e\cos E_P)\sin E_M} \end{pmatrix} \end{array} \right\} \begin{Bmatrix} \delta p_D \\ \delta z_D \end{Bmatrix} \tag{O-36}$$

The Lambert problem may be stated as follows: A body is moving about an attractive focus at F in an elliptical trajectory whose semi-major axis is a. It is desired to find an expression for the time required by the body to travel from an arbitrary point P to an arbitrary point Q on the trajectory. This expression is to be independent of the eccentricity of the trajectory.

The given data consist of the space triangle FPQ in Fig. O.6 and the semi-major axis length a. The position of F', the vacant focus, is not known; neither is the eccentricity e. The known distances FP, FQ, and PQ are designated r_1, r_2, and d, respectively.

The subscript 1 is used for conditions at point P; the subscript 2 is used for conditions at point Q. The time of flight t_F is

$$t_F = t_2 - t_1 \tag{O-37}$$

In this section, E_P and E_M are given by

$$E_P = \frac{1}{2}(E_2 + E_1) \tag{O-38}$$

$$E_M = \frac{1}{2}(E_2 - E_1) \tag{O-39}$$

Three additional angles are used in the derivation. They are defined by the following equations:

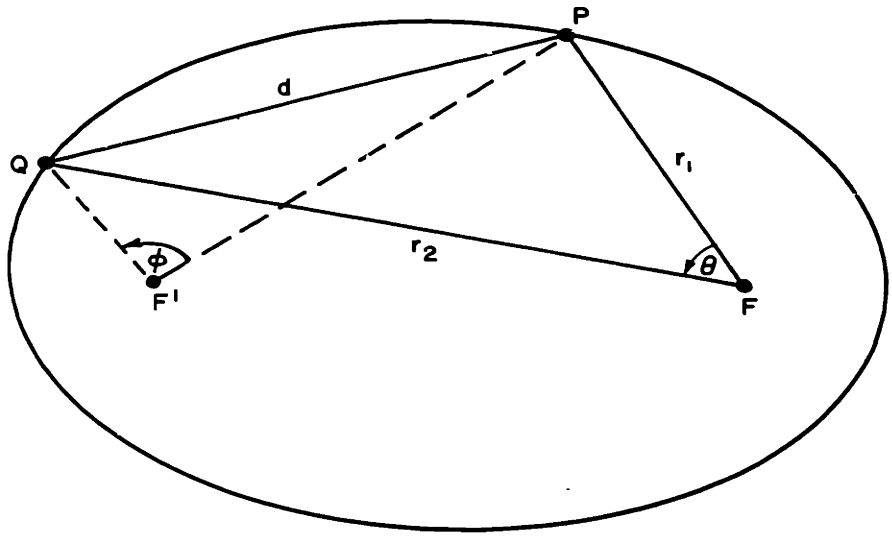

F — attractive focus
F' — vacant focus
P — initial position
Q — final position

Figure O.6 Illustration for Lambert's Theorem

$$\cos \eta = e \cos E_P \tag{O-40}$$

$$\alpha = \eta + E_M \tag{O-41}$$

$$\beta = \eta - E_M \tag{O-42}$$

With the aid of Eqs. (B-45), (B-55), and (B-62), the time-of-flight equation may be written as

$$\begin{aligned} t_F &= \frac{1}{n} (M_2 - M_1) \\ &= \frac{1}{n} [(E_2 - E_1) - e (\sin E_2 - \sin E_1)] \\ &= \frac{2}{n} (E_M - \cos \eta \sin E_M) \\ &= \left(\frac{a^3}{\mu}\right)^{1/2} [(\alpha - \beta) - (\sin \alpha - \sin \beta)] \end{aligned} \tag{O-43}$$

Eq. (O-43) in itself does not solve the Lambert problem, since α and β are known only in terms of e. The task now is to express α and β in terms of the known quantities r_1, r_2, d, and a. As a start, $(r_1 + r_2)$ and d are found in terms of a, η, and E_M.

$$\begin{aligned} r_1 + r_2 &= a (1 - e \cos E_1) + a (1 - e \cos E_2) \\ &= 2 a (1 - \cos \eta \cos E_M) \end{aligned} \tag{O-44}$$

$$\begin{aligned} d^2 &= (x_2 - x_1)^2 + (y_2 - y_1)^2 \\ &= a^2 (\cos E_2 - \cos E_1)^2 + a^2 (1 - e^2) (\sin E_2 - \sin E_1)^2 \\ &= 4 a^2 \sin^2 \eta \sin^2 E_M \end{aligned} \tag{O-45}$$

$$d = 2 a \sin \eta \sin E_M \tag{O-46}$$

By first adding Eq. (O. 46) to (O-44) and then subtracting Eq. (O-46) from (O-44), it may be shown that

$$\sin^2 \frac{\alpha}{2} = \frac{r_1 + r_2 + d}{4a} \qquad \text{(O-47)}$$

$$\sin^2 \frac{\beta}{2} = \frac{r_1 + r_2 - d}{4a} \qquad \text{(O-48)}$$

The combination of Eqs. (O-43), (O-47), and (O-48) constitutes the solution of the Lambert problem. By means of the three equations, t_F is determined as a function of $(r_1 + r_2)$, d, and a.

There are two possible sources of ambiguity when Eqs. (O-47) and (O-48) are used to compute α and β. The first arises from the sign of the square root; the second involves the determination of the quadrant of an angle whose sine is known. The ambiguities may be resolved by arbitrary definitions in Eqs. (O-47) and (O-48), and modification of Eq. (O-43) to accommodate these definitions.

The positive sign is chosen for $\sin(\alpha/2)$ and $\sin(\beta/2)$. It is further stipulated that both $\alpha/2$ and $\beta/2$ lie in the first quadrant. Then the following inequality defines the ranges of α and β:

$$0 \leq \beta \leq \alpha \leq \pi \qquad \text{(O-49)}$$

Eq. (O-43) must be revised not only because of the arbitrary definitions of α and β but also due to the fact that there may be N complete circuits of the focus between t_1 and t_2. The revised equation is

$$t_F = \left(\frac{a^3}{\mu}\right)^{1/2} [(2N + 1)\pi + \operatorname{sgn}(\sin\phi)(\alpha - \sin\alpha - \pi) - \operatorname{sgn}(\sin\theta)(\beta - \sin\beta)] \qquad \text{(O-50)}$$

The angles θ and ϕ are shown in Fig. O. 6. θ is the angle subtended at F by the initial position P and the final position Q; ϕ is the angle subtended

at F' by P and Q. Both θ and ϕ are positive in the direction of the orbital motion. The symbol "sgn", or signum, is defined by the relations

$$\begin{aligned} \text{sgn}(x) &= +1 \quad \text{if} \quad x > 0 \\ \text{sgn}(x) &= 0 \quad \text{if} \quad x = 0 \\ \text{sgn}(x) &= -1 \quad \text{if} \quad x < 0 \end{aligned} \tag{O-51}$$

Eq. (O-50) can be solved for the proper time of flight for any combination of P, Q, and F except for the case when points P and Q coincide. In this special case, the signum notation causes an incorrect result; the correct time of flight is simply N times the period.

There is also a restriction on the semi-major axis; it must be large enough so that the values of $\sin^2(\alpha/2)$ and $\sin^2(\beta/2)$, obtained from Eqs. (O-47) and (O-48), are never larger than unity. Thus, the minimum value of a is

$$a_{min} = \frac{r_1 + r_2 + d}{4} \tag{O-52}$$

Battin[1] has shown that for a given space triangle FPQ and a given value of a which is greater than a_{min}, there are two possible elliptical paths from P to Q. These are shown in Fig. O.7. The two vacant focus positions are F' and $\tilde{F}'$. The line PQ is the perpendicular bisector of the line joining F' and $\tilde{F}'$.

Since the value of a is the same for the two ellipses, they both have the same period. Kepler's second law states that the radius vector (from F) sweeps through equal areas in equal times. Then, for each of the two ellipses the time of flight from P to Q is equal to the period times the ratio, for that ellipse, of the area of the sector FPQF to the total area of the ellipse. If all motion is assumed to be counter-clockwise in Fig. O.7, it is apparent that the area ratio for the ellipse whose vacant focus is F' is less than the area ratio for the ellipse with vacant focus at $\tilde{F}'$, and therefore, t_F, the time of flight for the former ellipse, is less than $\tilde{t}_F$, the time of flight for the latter.

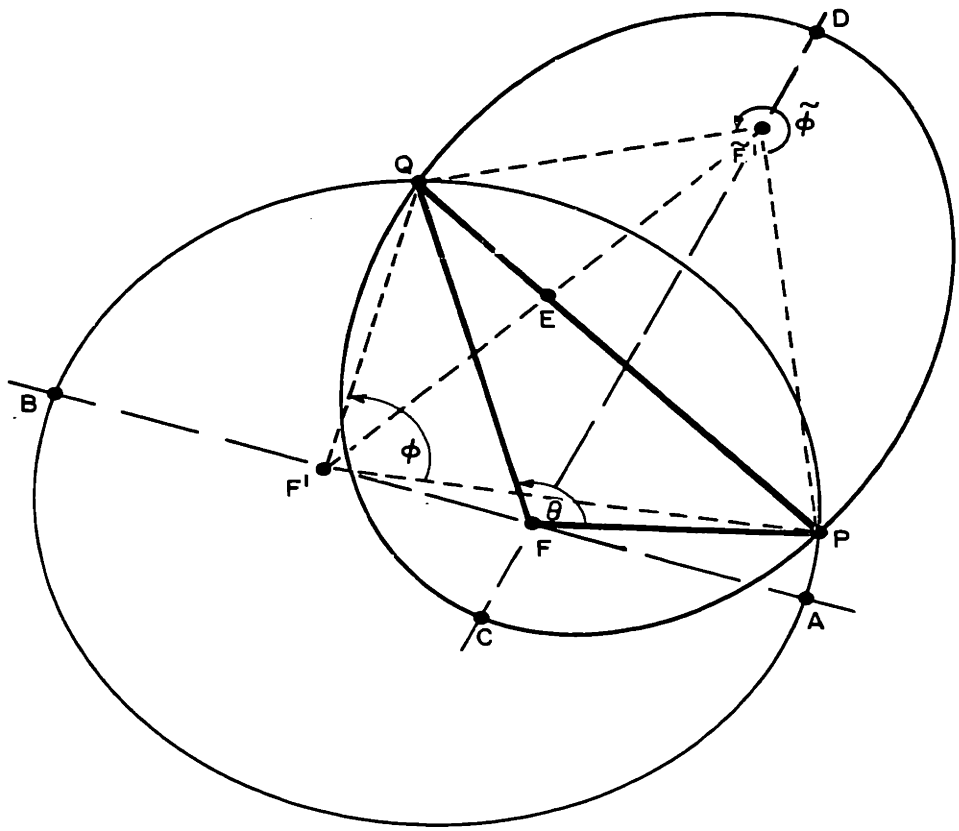

F — attractive focus
P — initial position
Q — final position
$F', \tilde{F}'$ — two permissible vacant foci for same value of a
AB = CD = 2a = length of major axis of each ellipse
$F'\tilde{F}' \perp PQ$; $F'E = E\tilde{F}'$
$\phi + \tilde{\phi} = 2\pi$

Figure O.7 The Two Ellipses for a Given Space Triangle and a Given Length of the Major Axis

The relation between t_F and $\tilde{t}_F$ can be developed mathematically from Eq. (O-50). With the exception of the angle ϕ, all the quantities on the right-hand side of that equation are the same for both ellipses of Fig. O.7. The coefficient of sgn (sin ϕ) in the equation is (α - sin α - π) which, for $a > a_{min}$, is always negative. Therefore, the time of flight for a value of ϕ less than π radians is smaller than the time of flight corresponding to ϕ greater than π radians. Because the triangles PF'Q and P $\tilde{F}$' Q are congruent, the sum of angles ϕ and $\tilde{\phi}$, shown in the figure, is 2 π radians. Since the angles are not equal except in the special case $a = a_{min}$, one must be less than π radians and the other greater than π radians. If the tilde notation is associated with the value of ϕ greater than π, $\tilde{t}_F$ is always greater than t_F. The difference between $\tilde{t}_F$ and t_F is

$$\tilde{t}_F - t_F = 2 \left(\frac{a^3}{\mu}\right)^{1/2} (\pi - \alpha + \sin \alpha) \qquad \text{(O-53)}$$

O.11 Minimum Time of Flight

In this section it will be shown that, for a given space triangle FPQ, the rate of change of the time of flight with change in semi-major axis is proportional to the factor X, and consequently a singularity of the X = 0 type occurs when the time of flight is a minimum.

Figure O.8 is a plot of t_F vs. a for a journey from Earth to Mars. For such a journey r_1 = 1 astronomical unit (a.u.), and r_2 = 1.524 a.u. Curves are presented for three values of θ at N = 0 and for the same three values of θ at N = 1. Figure O.8 duplicates the curves of Fig. 3-3 of Reference (1).

It may be noted that the curves corresponding to N = 0 have no minimum values of t_F for any finite value of a. As a is increased beyond a_{min}, the two possible values of t_F get farther and farther apart, one continuously increasing and the other continuously decreasing.

Each of the curves for N = 1 has a definite minimum value of t_F; the minimum t_F for each curve occurs at a value of a that is slightly larger than a_{min} for that curve.

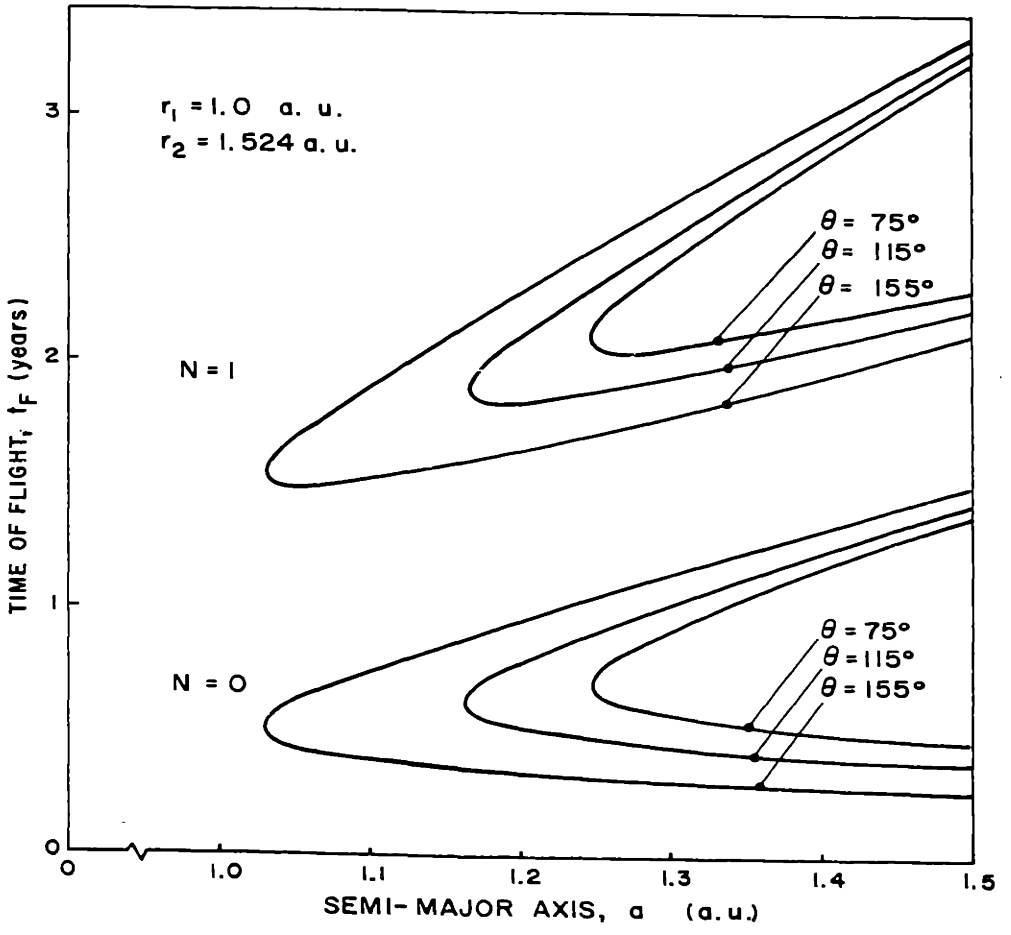

Figure O.8 Time of Flight for One-Way Trip from Earth to Mars

If curves were drawn for values of N greater than one, they would also exhibit the characteristic of a minimum t_F. As N gets larger, for a given θ, the distance between a_{min} and the a corresponding to $t_{F_{min}}$ gets smaller.

In order to gain further insight into the time-of-flight curves and their minima, an analytic expression for the slope will be derived. In this section the notation $\partial(\ )/\partial a$ signifies the partial derivative of the argument with respect to a, with r_1, r_2, d, and N all constant. Inasmuch as there are no ambiguities involved in the differentiation, the expression for t_F given by Eq. (O-43) will be used rather than the more complicated Eq. (O-50).

$$\frac{\partial t_F}{\partial a} = \frac{1}{2}\left(\frac{a}{\mu}\right)^{1/2}\left[3(\alpha - \beta) - 3(\sin\alpha - \sin\beta) + 2a(1 - \cos\alpha)\frac{\partial\alpha}{\partial a} - 2a(1 - \cos\beta)\frac{\partial\beta}{\partial a}\right] \qquad \text{(O-54)}$$

$\partial\alpha/\partial a$ is obtained by differentiating Eq. (O-47).

$$\sin\frac{\alpha}{2}\cos\frac{\alpha}{2}\frac{\partial\alpha}{\partial a} = -\frac{r_1 + r_2 + d}{4a^2} \qquad \text{(O-55)}$$

$$\frac{\partial\alpha}{\partial a} = -\frac{1 - \cos\alpha}{a\sin\alpha} = -\frac{1}{a}\tan\frac{\alpha}{2} \qquad \text{(O-56)}$$

$\partial\beta/\partial a$ is obtained in similar fashion from Eq. (O-48)

$$\frac{\partial\beta}{\partial a} = -\frac{1 - \cos\beta}{a\sin\beta} = -\frac{1}{a}\tan\frac{\beta}{2} \qquad \text{(O-57)}$$

Eqs. (O-56) and (O-57) are substituted into (O-54). After some trigonometric manipulation, the result is

From Eqs. (O-40), (O-41), and (O-42),

$$\alpha - \beta = 2 E_M \tag{O-61}$$

$$\alpha + \beta = 2 \eta \tag{O-62}$$

$$\sin \alpha - \sin \beta = 2 \cos \frac{\alpha + \beta}{2} \sin \frac{\alpha - \beta}{2}$$

$$= 2 \cos \eta \sin E_M$$

$$= 2 e \cos E_P \sin E_M \tag{O-63}$$

Eqs. (O-61) and (O-63) are substituted into (O-60), and both numerator and denominator are divided by 2 sin E_M.

$$\frac{\partial t_F}{\partial a} = \frac{\left(\frac{a}{\mu} \right)^{1/2}}{\cos E_M + e \cos E_P}$$

$$\cdot \left[(3 E_M - e \sin E_M \cos E_P)(\cos E_M + e \cos E_P) - 4 \sin E_M \right] \tag{O-64}$$

The quantity inside the brackets is identical with the expression for X in Eq. (O-24). Finally,

$$\frac{\partial t_F}{\partial a} = \frac{\left(\frac{a}{\mu} \right)^{1/2} X}{\cos E_M + e \cos E_P} \tag{O-65}$$

Thus, it has been proved that the slope of each time-of-flight curve is proportional to X, and the minimum time of flight, if it exists

for a particular curve, occurs at the X = 0 singularity point for that curve.

O.12 Physical Interpretation of Singularities at X = 0

In the preceding section it was shown that the time of flight, as depicted in the curves of Fig. O.8, is insensitive to small changes in the semi-major axis when X = 0. In this section, it will be proved that, for a given vector $\underline{r}_1$ and given values of t_F and N, the vector $\underline{r}_2$ is insensitive to small changes in the semi-major axis when X = 0, and consequently it is not possible to apply a small velocity correction at t_1 which will alter $\underline{r}_2$.

Consider a case in which r_1, t_F, d, and N are specified, and r_2 is regarded as a function of a. The partial derivative of the time-of-flight equation, (O-43), is taken with respect to a.

$$0 = \frac{3}{2}\left(\frac{a}{\mu}\right)^{1/2}\left[(\alpha - \beta) - (\sin\alpha - \sin\beta)\right] + \left(\frac{a^3}{\mu}\right)^{1/2}\left[(1 - \cos\alpha)\left(\frac{\partial\alpha}{\partial a}\right)_{r_1,\, t_F,\, d,\, N} - (1 - \cos\beta)\left(\frac{\partial\beta}{\partial a}\right)_{r_1,\, t_F,\, d,\, N}\right] \qquad \text{(O-66)}$$

The subscript symbols following the partial derivative indicate the quantities that are being held constant.

From Eqs. (O-47) and (O-48), the partial derivatives in Eq. (O-66) may be expressed as

$$\left(\frac{\partial\alpha}{\partial a}\right)_{r_1,\, t_F,\, d,\, N} = \frac{1}{2a\sin\alpha}\left[\left(\frac{\partial r_2}{\partial a}\right)_{r_1,\, t_F,\, d,\, N} - 4\sin^2\frac{\alpha}{2}\right] \qquad \text{(O-67)}$$

$$\left(\frac{\partial \beta}{\partial a}\right)_{r_1,\ t_F,\ d,\ N} = \frac{1}{2\,a\,\sin\beta}\left[\left(\frac{\partial r_2}{\partial a}\right)_{r_1,\ t_F,\ d,\ N} - 4\sin^2\frac{\beta}{2}\right] \tag{O-68}$$

Eqs. (O-66), (O-67), and (O-68) are combined and solved for $(\partial r_2/\partial a)_{r_1,\ t_F,\ d,\ N}$.

$$\left(\frac{\partial r_2}{\partial a}\right)_{r_1,\ t_F,\ d,\ N} = -\frac{X}{\sin E_M} \tag{O-69}$$

The derivation of Eq. (O-69) involves a division of numerator and denominator by $\sin E_M$; therefore, the equation is not valid for the special case when $\sin E_M = 0$; i.e., when $(E_2 - E_1) = 2N\pi = (f_2 - f_1)$. In general, for $\sin E_M \neq 0$, the rate of change of r_2 with a is proportional to X.

As a second case, consider r_1, t_F, r_2, and N to be specified, and d to be a function of a. The same procedure as that of the first example is followed. The equations analogous to Eqs. (O-66) through (O-69) are

$$0 = \frac{3}{2}\left(\frac{a}{\mu}\right)^{1/2}[(\alpha - \beta) - (\sin\alpha - \sin\beta)] + \left(\frac{a^3}{\mu}\right)^{1/2}\left[(1 - \cos\alpha)\left(\frac{\partial \alpha}{\partial a}\right)_{r_1,\ t_F,\ r_2,\ N} - (1 - \cos\beta)\left(\frac{\partial \beta}{\partial a}\right)_{r_1,\ t_F,\ r_2,\ N}\right] \tag{O-70}$$

$$\left(\frac{\partial \alpha}{\partial a}\right)_{r_1,\ t_F,\ r_2,\ N} = \frac{1}{2\,a\sin\alpha}\left[\left(\frac{\partial d}{\partial a}\right)_{r_1,\ t_F,\ r_2,\ N} - 4\sin^2\frac{\alpha}{2}\right] \tag{O-71}$$

$$\left(\frac{\partial \beta}{\partial a}\right)_{r_1,\ t_F,\ r_2,\ N} = \frac{1}{2\ a\ \sin\beta}\left[\left(\frac{\partial d}{\partial a}\right)_{r_1,\ t_F,\ r_2,\ N} - 4\ \sin^2\frac{\beta}{2}\right] \tag{O-72}$$

$$\left(\frac{\partial d}{\partial a}\right)_{r_1,\ t_F,\ r_2,\ N} = -\frac{X}{\sin\eta} \tag{O-73}$$

From Eq. (O-40),

$$\sin\eta = (1 - e^2\cos^2 E_P)^{1/2} \tag{O-74}$$

Because the denominator term in Eq. (O-73) is obtained by dividing $+\sin^2\eta$ by $+\sin\eta$, the positive sign must be used for the root in Eq. (O-74). For values of e less than one, $\sin\eta$ cannot be zero, and hence Eq. (O-73) always produces a finite value of the partial derivative.

Eqs. (O-69) and (O-73) indicate that $(\partial r_2/\partial a)_{r_1,\ t_F,\ d,\ N}$ and $(\partial d/\partial a)_{r_1,\ t_F,\ r_2,\ N}$ are proportional to X. For given values of r_1, t_F, and N, if X = 0, the distances r_2 and d are unaffected by a small change in the length of the semi-major axis. From Figure O.6 it is apparent that, if F and P are fixed points and r_2 and d are unaffected by small changes in a, then the point Q is unaffected by small changes in a. Therefore, under the given conditions, the vector $\underline{r}_2$ is insensitive to small changes in a when X = 0. Vectors $\underline{r}_1$ and $\underline{r}_2$ are not independent when X = 0.

When small changes in the semi-major axis a are mentioned, it should not be inferred that the other three orbital elements defining motion in the trajectory plane are unaffected. The changes in all four elements must be related in such a manner that the given vector $\underline{r}_1$ is conserved. Then the conclusion reached in the preceding paragraph may be generalized to indicate that, with $\underline{r}_1$, t_F, and N specified such that X = 0, the position vector $\underline{r}_2$ is not affected by small changes in the orbital elements defining motion in the trajectory plane.

Therefore, it is not possible to compute a small step change in velocity which, if applied at t_1, will alter (i.e., "correct") the position of the vehicle at t_2.

In recapitulation, the developments in the last three sections establish a connection between the X = 0 singularities, which evolve from linear perturbation theory, and Lambert's theorem in celestial mechanics. Whenever there is a minimum in the curve of time of flight versus semi-major axis length for fixed values of r_1, r_2, d, and N, that minimum occurs under conditions for which X = 0. By the use of partial differentiation on the time-of-flight equation of Lambert, it has been shown that, for a given $\underline{r}_1$, the position vector $\underline{r}_2$ is unaffected by small changes in the orbital elements when X = 0, and consequently it is not possible to compute a small velocity correction which, if applied at t_1, changes the vehicle's predicted position at t_2.

The special case discussed in Section O.9, for which it is possible to compute a velocity correction even though X = 0, is not explained by the analysis that has been presented in this section.

O.13 Analytic Formulation of the VTA Velocity Correction

It has already been shown that, in general, it is not possible to compute a finite FTA velocity correction when t_C and t_D are related in such a manner that any one of the three types of singularities exists. In the following sections, the feasibility of applying a finite VTA correction under these conditions will be investigated.

In the critical-plane coordinate system the relations defining the VTA correction are Eqs. (N-27) and (N-46), which are repeated here for convenience.

$$\underline{c}_W = \overset{*}{Y} \left(\delta \underline{\rho}^- \right)_W \tag{O-75}$$

where

$$\overset{*}{Y} = \begin{Bmatrix} \frac{1}{A}\left(k_{12}\,k_{21} - k_{11}\,k_{22}\right) & 0 \\ \frac{1}{A}\frac{v_R}{w}\,k_{33}\cos i_D\left[\left(k_{11}^{\,2} - k_{12}^{\,2}\right.\right. & \\ \left. + k_{21}^{\,2} - k_{22}^{\,2}\right)\sin\Omega_D\cos\Omega_D & -A\frac{v_R}{w}\,k_{33} \\ + \left(k_{11}\,k_{12} + k_{21}\,k_{22}\right)\left(\sin^2\Omega_D\right. & \\ \left.\left. - \cos^2\Omega_D\right)\right] & \end{Bmatrix} \qquad \text{(O-76)}$$

In order to emphasize the effect of the singularities, the elements k_{11}, k_{12}, k_{21}, k_{22}, and k_{33} will be replaced by K_{11}, K_{12}, K_{21}, K_{22}, and K_{33}, respectively. The new terms are defined in such a manner that they remain finite even under the singularity conditions. With the aid of Eq. (K-48), they are expressed as follows:

$$K_{11} = \frac{1}{n}\,X\sin E_M\,k_{11}$$

$$= \frac{\left(1 + e\cos E_C\right)\left(1 + e\cos E_D\right)\left(3E_M - e\sin E_M\cos E_P\right) - 4\sin E_M\left(\cos E_M + e\cos E_P\right)}{2\left(1 - e^2\cos^2 E_C\right)^{1/2}\left(1 - e^2\cos^2 E_D\right)^{1/2}} \qquad \text{(O-77)}$$

$$K_{12} = \frac{1}{n}\,X\sin E_M\,k_{12}$$

$$= \frac{\left(1 - e^2\right)^{1/2}\left(1 - e\cos E_D\right)\sin^2 E_M}{\left(1 - e^2\cos^2 E_C\right)^{1/2}\left(1 - e^2\cos^2 E_D\right)^{1/2}} \qquad \text{(O-78)}$$

$$K_{21} = \frac{1}{n} X \sin E_M \, k_{21}$$

$$= - \frac{(1 - e^2)^{1/2} (1 - e \cos E_C) \sin^2 E_M}{(1 - e^2 \cos E_C)^{1/2} (1 - e^2 \cos^2 E_D)^{1/2}} \qquad \text{(O-79)}$$

$$K_{22} = \frac{1}{n} X \sin E_M \, k_{22}$$

$$= - \frac{(1 - e \cos E_C) (1 - e \cos E_D) (\cos E_M + e \cos E_P) \sin E_M}{2 (1 - e^2 \cos^2 E_C)^{1/2} (1 - e^2 \cos^2 E_D)^{1/2}} \qquad \text{(O-80)}$$

$$K_{33} = \frac{1}{n} \sin (f_D - f_C) \, k_{33}$$

$$= \frac{\sin (f_D - f_C)}{2 \sin E_M (\cos E_M - e \cos E_P)}$$

$$= \frac{(1 - e^2)^{1/2}}{(1 - e \cos E_C) (1 - e \cos E_D)} \qquad \text{(O-81)}$$

The terms A and v_R/w in Eq. (O-76) can be expressed as functions of the K's. From Eq. (N-42),

$$A = [(k_{11} \sin \Omega_D - k_{12} \cos \Omega_D)^2 + (k_{21} \sin \Omega_D - k_{22} \cos \Omega_D)^2]^{1/2}$$

$$= \frac{n B}{X \sin E_M} \qquad \text{(O-82)}$$

where

$$B = [(K_{11} \sin \Omega_D - K_{12} \cos \Omega_D)^2 + (K_{21} \sin \Omega_D - K_{22} \cos \Omega_D)^2]^{1/2} \tag{O-83}$$

From Eq. (N-44),

$$\frac{v_R}{w} = (A^2 \sin^2 i_D + k_{33}^2 \cos^2 i_D)^{-1/2}$$

$$= \frac{1}{n}\left[\frac{B^2 \sin^2 i_D}{X^2 \sin^2 E_M} + \frac{K_{33}^2 \cos^2 i_D}{\sin^2 (f_D - f_C)}\right]^{-1/2} \tag{O-84}$$

The parameter B, like the K factors, remains finite at the singularity points.

The elements of $\overset{*}{Y}$ can now be written in terms of the K's. A simple form for the upper left-hand term, y_{11}, is obtained by the use of Eq. (K-53).

$$y_{11} = \frac{1}{A}(k_{12} k_{21} - k_{11} k_{22})$$

$$= \frac{\dfrac{n^2}{4 X \sin E_M}}{\dfrac{n B}{X \sin E_M}} = \frac{n}{4 B} \tag{O-85}$$

The expression evolved for $\overset{*}{Y}$ is

$$\overset{*}{Y} = n \left\{ \begin{array}{c|c} \left(\dfrac{1}{4 B} \right. & \left. 0 \right) \\ \hline \dfrac{K_{33}}{C} \left(\dfrac{D \cos i_D}{B} \right. & \left. - B \right) \end{array} \right\} \tag{O-86}$$

where

$$C = [B^2 \sin^2 (f_D - f_C) \sin^2 i_D + K_{33}{}^2 X^2 \sin^2 E_M \cos^2 i_D]^{1/2} \quad \text{(O-87)}$$

$$D = (K_{11}{}^2 - K_{12}{}^2 + K_{21}{}^2 - K_{22}{}^2) \sin \Omega_D \cos \Omega_D + (K_{11} K_{12} + K_{21} K_{22}) (\sin^2 \Omega_D - \cos^2 \Omega_D) \quad \text{(O-88)}$$

The effect of each of the three types of singularities on the elements of $\overset{*}{Y}$ in Eq. (O-86) will now be investigated.

O. 14 Effect on VTA Guidance of Singularities at $(t_D - t_C) = NP$

When $(t_D - t_C)$ is very close to NP, both $\sin E_M$ and $\sin (f_D - f_C)$ may be equated to ϵ, a small quantity which reduces to zero when $(t_D - t_C)$ equals NP. From Eqs. (O-10), (O-11), and (O-12),

$$\cos E_M + e \cos E_P = (-1)^N (1 + e \cos E_D) \quad \text{(O-89)}$$

$$X = (-1)^N 3 N \pi (1 + e \cos E_D) \quad \text{(O-90)}$$

When ϵ is small, the K factors are given by

$$K_{11} = \frac{3 N \pi (1 + e \cos E_D)}{2 (1 - e \cos E_D)} \quad \text{(O-91)}$$

$$K_{12} = \frac{(1 - e^2)^{1/2} \epsilon^2}{1 + e \cos E_D} \quad \text{(O-92)}$$

$$K_{21} = -\frac{(1 - e^2)^{1/2} \epsilon^2}{1 + e \cos E_D} \quad \text{(O-93)}$$

$$K_{22} = \frac{1}{2} (-1)^{N+1} (1 - e \cos E_D) \epsilon \quad \text{(O-94)}$$

$$K_{33} = \frac{(1 - e^2)^{1/2}}{(1 - e \cos E_D)^2} \tag{O-95}$$

The expressions for parameters B, C, and D are

$$B = K_{11} \sin \Omega_D = \frac{3 N \pi (1 + e \cos E_D) \sin \Omega_D}{2 (1 - e \cos E_D)} \tag{O-96}$$

$$C = (B^2 \sin^2 i_D + K_{33}{}^2 X^2 \cos^2 i_D)^{1/2} \epsilon$$

$$= \left[\frac{3 N \pi (1 + e \cos E_D)}{2 (1 - e \cos E_D)^2}\right] [(1 - e \cos E_D)^2 \sin^2 \Omega_D \sin^2 i_D$$

$$+ 4 (1 - e^2) \cos^2 i_D]^{1/2} \epsilon \tag{O-97}$$

$$D = K_{11}{}^2 \sin \Omega_D \cos \Omega_D = \left[\frac{3 N \pi (1 + e \cos E_D)}{2 (1 - e \cos E_D)}\right]^2 \sin \Omega_D \cos \Omega_D \tag{O-98}$$

Because C approaches zero as $(t_D - t_C)$ approaches N P, the elements of the second row of $\overset{*}{Y}$ in Eq. (O-86) becomes infinite at the singularity points. Consequently, it is not possible in the general case to compute a finite VTA velocity correction when $(t_D - t_C)$ is equal to N P.

There are three special cases in which the vehicle can be made to reach the proper destination by means of VTA guidance even though a correction is contemplated at a time such that $(t_D - t_C) = NP$. The first special case is the trivial one which occurs when $\delta \underline{r}_D$ is parallel to $\underline{v}_R$. Then no correction is required, and the change in the time of arrival is proportional to the magnitude of $\delta \underline{r}_D$.

The second special case occurs when $\delta \underline{r}_D^-$ is parallel to the orbital velocity vector $\underline{v}_D$. Then

$$(\delta\rho^-)_W = \begin{Bmatrix} \sin \Omega_D \\ \cos \Omega_D \cos i_D \end{Bmatrix} \delta q_D^- \qquad \text{(O-99)}$$

$$\underline{c}_W = \begin{Bmatrix} c_\xi \\ c_\eta \end{Bmatrix} = n \left\{ \begin{array}{c|c} & \frac{1}{4B} \quad 0 \\ \hline \frac{K_{33}}{C} & \frac{D \cos i_D}{B} \quad -B \end{array} \right\} \begin{Bmatrix} \sin \Omega_D \\ \cos \Omega_D \cos i_D \end{Bmatrix} \delta q_D^- \qquad \text{(O-100)}$$

For $(t_D - t_C)$ very close to N P, the expression for c_η obtained from Eq. (O-100) is

$$c_\eta = \frac{n K_{33} \cos i_D}{B C} (D \sin \Omega_D - B^2 \cos \Omega_D) \delta q_D^- \qquad \text{(O-101)}$$

It will now be shown that c_η, which ordinarily goes to infinity at a singularity point because the demoninator factor C reduces to zero, is equal to zero in this special case. c_η can be regarded as consisting of three factors, $n K_{33} \cos i_D/B$, $1/C$, and $(D \sin \Omega_D - B^2 \cos \Omega_D)$. From Eqs. (O-95) and (O-96) it is apparent that, as long as neither $\sin \Omega_D$ nor $\cos i_D$ is zero, the first factor is non-zero and finite. Eq. (O-97) indicates that C is an infinitesimal of order ϵ. When terms of higher order than ϵ^2 are neglected, the third factor may be treated as follows:

$$(D \sin \Omega_D - B^2 \cos \Omega_D) = (K_{11}{}^2 - K_{22}{}^2) \sin^2 \Omega_D \cos \Omega_D$$

$$+ K_{11} K_{12} (\sin^2 \Omega_D - \cos^2 \Omega_D) \sin \Omega_D$$

$$- (K_{11}{}^2 \sin^2 \Omega_D - 2 K_{11} K_{12} \sin \Omega_D \cos \Omega_D$$

$$+ K_{22}{}^2 \cos^2 \Omega_D) \cos \Omega_D$$

$$= K_{11} K_{12} \sin \Omega_D - K_{22}{}^2 \cos \Omega_D \qquad \text{(O-102)}$$

Since K_{12} is of order ϵ^2 and K_{22} is of order ϵ, the third factor is of order ϵ^2. Therefore, c_η, being proportional to the ratio of $(D \sin \Omega_D - B^2 \cos \Omega_D)$ to C, is of order ϵ, and hence for the special case

$$c_\eta = 0 \qquad \text{(O-103)}$$

The component c_ξ in Eq. (O-100) is

$$c_\xi = \frac{n \sin \Omega_D}{4 B} \delta q_D^-$$

$$= \frac{n (1 - e \cos E_D)}{6 N \pi (1 + e \cos E_D)} \delta q_D^-$$

$$= \frac{\mu}{3 N P a v_D{}^2} \delta q_D^- \qquad \text{(O-104)}$$

The VTA velocity correction vector is

$$\underline{c}_v = \frac{\mu}{3 N P a v_D{}^2} (\delta q_D^-) \underline{u}_{\xi_D} \qquad \text{(O-105)}$$

where $\underline{u}_{\xi_D}$ is a unit vector in the ξ_D direction.

Eq. (O-105) can be compared with Eq. (O-13), which is an expression for the FTA velocity correction for the same special case (i.e., $\delta \underline{r}_D$ is in the q_D direction). The magnitude of the correction is the same for both FTA and VTA guidance; hence there is no propellant saving when VTA guidance is used. A more interesting result is that the FTA correction is applied in the q_D direction, while the VTA correction is applied in the ξ_D direction. It is surprising, to say the least, that two corrections of the same magnitude but seemingly in different directions achieve the objectives of the two guidance schemes. This confusing state of affairs can be clarified by an investigation of the orientation of the vector $\underline{w}$.

$$\underline{w} = \overset{*}{K}_{CD}\, \underline{v}_R = \begin{Bmatrix} k_{11}\, v_{R_p} + k_{12}\, v_{R_q} \\ k_{21}\, v_{R_p} + k_{22}\, v_{R_q} \\ k_{33}\, v_{R_z} \end{Bmatrix}$$

$$= n \begin{Bmatrix} \dfrac{1}{X \sin E_M} & \begin{pmatrix} K_{11}\, v_{R_p} + K_{12}\, v_{R_q} \\ K_{21}\, v_{R_p} + K_{22}\, v_{R_q} \end{pmatrix} \\ \dfrac{1}{\sin (f_D - f_C)} & \begin{pmatrix} K_{33}\, v_{R_z} \end{pmatrix} \end{Bmatrix} \qquad \text{(O-106)}$$

When $(t_D - t_C)$ is very nearly equal to NP,

$$\underline{w} = \frac{n}{\epsilon} \left\{ \begin{array}{c} \dfrac{(-1)^N v_{R_p}}{2(1 - e \cos E_D)} \\ -\dfrac{(1 - e \cos E_D)\, \epsilon\, v_{R_q}}{6 N \pi (1 + e \cos E_D)} \\ \dfrac{(1 - e^2)^{1/2} v_{R_z}}{(1 - e \cos E_D)^2} \end{array} \right\} \qquad \text{(O-107)}$$

The only term inside the braces in Eq. (O-107) that contains the infinitesimal ϵ is the term representing the component of $\underline{w}$ in the q_C direction. Thus, when $(t_D - t_C)$ is equal to N P, the $\underline{w}$ vector, although infinite in magnitude, must lie in the plane normal to the q_C-axis. But the q_C-axis and the q_D-axis coincide when $(t_D - t_C)$ equals N P. Therefore, regardless of the orientation of the relative velocity vector the noncritical vector $\underline{w}$ is perpendicular to the q_D-axis when $(t_D - t_C)$ equals N P. The ξ_D-axis has been defined as the axis normal to $\underline{w}$ and lying in the reference trajectory plane. Since both the q_D-axis and the ξ_D-axis are in the reference trajectory plane and perpendicular to $\underline{w}$, they must coincide, and consequently Eqs. (O-13) and (O-105) give the identical velocity correction for this special case.

Eq. (O-107) indicates that the p_C component of $\underline{w}$ changes sign on each successive circuit of the focus. This would appear to indicate that $\underline{w}$ rotates with a period that is twice the period P of the orbital motion. The rotation of $\underline{w}$ has not been investigated further in this study, but it is suggested as a possibly fruitful topic for future work in the field.

The third special case is the two-dimensional case, in which both δz_D and v_{R_z} are equal to zero. Under these conditions, the $\underline{v}_R$ vector lies in the reference trajectory plane. In the critical-plane coordinate system the ζ_D-axis lies along $\underline{v}_R$ in the reference trajectory

plane, the ξ_D-axis is perpendicular to $\underline{v}_R$ and in the reference trajectory plane, and the η_D-axis coincides with the z-axis. Since δz_D^- is taken as zero, it follows that

$$\delta \eta_D^- = 0 \tag{O-108}$$

For a correction at $(t_D - t_C)$ equal to N P, it has been shown that the ξ_C-axis is the same as the q_D-axis. Thus, the miss distance vector $\delta \underline{\rho}^-$ must be parallel to the orbital velocity vector $\underline{v}_D$.

$$\delta \underline{\rho}^- = (\delta q_D^-)\ \underline{u}_{\xi_D} \tag{O-109}$$

Eq. (O-109) is the defining characteristic of the second special case. Therefore, both cases have the same solution for $\underline{c}_v$, which is given by Eq. (O-105).

It is of interest to note the difference in initial hypotheses between the second and the third special cases. In the second, the predicted position variation vector $\delta \underline{r}_D^-$ is assumed to be parallel to $\underline{v}_D$, and the orientation of the relative velocity vector $\underline{v}_R$ is arbitrary. In the third case, both $\delta \underline{r}_D^-$ and $\underline{v}_R$ lie in the reference trajectory plane, but each may have any arbitrary orientation in that plane.

The third case illustrates the pitfalls that may be encountered if the mathematical model is over-simplified. If a preliminary guidance study of a journey involving more than one circuit of the focus is based on a two-dimensional model, that is, a model in which both $\underline{v}_R$ and $\delta \underline{r}_D^-$ are assumed to lie in the reference trajectory plane, the analysis will indicate that a finite VTA correction can be computed when $(t_D - t_C) = N P$, whereas a three-dimensional model shows that, in general, such a computation is not possible.

O.15 Effect on VTA Guidance of Singularities at $(f_D - f_C) = (2N-1)\pi$

When $(f_D - f_C) = (2N-1)\pi$, k_{33} is the only element of $\overset{*}{K}_{CD}$ that becomes infinite. The factors B and D in Eq. (O-86) are determined in routine fashion, and factor C reduces to

$$C = K_{33} X \sin E_M \cos i_D \tag{O-110}$$

The matrix $\overset{*}{Y}$ becomes

$$\overset{*}{Y} = \left\{ \begin{array}{cc} & \left(\frac{1}{4B} \quad 0 \right) \\ \hline \frac{1}{X \sin E_M} & \left(\frac{D}{B} \quad -\frac{B}{\cos i_D} \right) \end{array} \right\} \tag{O-111}$$

A finite VTA velocity correction can be computed when $(f_D - f_C) = (2N - 1)\pi$ except for the special case when the relative velocity vector lies in the reference trajectory plane (that is, $\cos i_D = 0$).

The vector $\underline{w}$ corresponding to $(f_D - f_C) = (2N - 1)\pi$ may be expressed as

$$\underline{w} = \left\{ \begin{array}{l} k_{11} v_{R_p} + k_{12} v_{R_q} \\ \\ k_{2i} v_{R_p} + k_{22} v_{R_q} \\ \\ \dfrac{n K_{33}}{\sin (f_D - f_C)} \quad v_{R_z} \end{array} \right\} \tag{O-112}$$

Only the z-component of $\underline{w}$ goes to infinity in the singularity condition. Therefore, $\underline{w}$ is parallel to the z-axis, and, depending on the sign of v_{R_z},

$$i_C = 0° \text{ or } 180° \tag{O-113}$$

The ζ_C-axis is the z-axis, and the $\xi_C - \eta_C$ plane is the reference trajectory plane. Thus, the VTA correction vector must lie in the reference trajectory plane, regardless of the orientation of $\underline{v}_R$ (as long as $\cos i_D \neq 0$).

The equation for the VTA correction in the p q z coordinate system is obtained by substituting Eq. (O-112) into Eq. (M-10).

$$\underline{c}_V = -\begin{bmatrix} k_{11} & k_{12} & -\dfrac{k_{11}\, v_{R_p} + k_{12}\, v_{R_q}}{v_{R_z}} \\ k_{21} & k_{22} & -\dfrac{k_{21}\, v_{R_p} + k_{22}\, v_{R_q}}{v_{R_z}} \\ 0 & 0 & 0 \end{bmatrix} \delta \underline{r}_D \qquad \text{(O-114)}$$

The z-component of the correction is zero, as required by the fact that the z-axis is the noncritical axis. The elements in the first two columns of the matrix in Eq. (O-114) are the same as the corresponding elements in the matrix of the equation for the FTA correction.

O.16 Effect on VTA Guidance of Singularities at X = 0

For the singularities at X equal to zero,

$$C = B \sin (f_D - f_C) \sin i_D \qquad \text{(O-115)}$$

The $\overset{*}{Y}$ matrix is

$$\overset{*}{Y} = n \begin{bmatrix} \dfrac{K_{33}}{\sin (f_D - f_C) \sin i_D} & \begin{pmatrix} \dfrac{1}{4B} & 0 \end{pmatrix} \\ \begin{pmatrix} \dfrac{D \cos i_D}{B^2} & -1 \end{pmatrix} & \end{bmatrix} \qquad \text{(O-116)}$$

Parameters B and D are computed from Eq. (O-83) and (O-88), respectively.

A finite VTA correction can be determined when this type of singularity occurs except for the special case when the relative velocity vector is parallel to the z-axis (that is, $\sin i_D = 0$).

When $X = 0$, the vector $\underline{w}$ can be written as

$$\underline{w} = \begin{Bmatrix} \dfrac{n}{X \sin E_M} \begin{pmatrix} K_{11} v_{R_p} + K_{12} v_{R_q} \\ K_{21} v_{R_p} + K_{22} v_{R_q} \end{pmatrix} \\ \hline \begin{pmatrix} k_{33} v_{R_z} \end{pmatrix} \end{Bmatrix} \qquad \text{(O-117)}$$

Both w_p and w_q go to infinity, but w_z remains finite. Therefore, the $\underline{w}$ vector lies in the reference trajectory plane. The $\xi_C - \zeta_C$ plane is the reference trajectory plane, the η_C-axis is the z-axis, and

$$i_C = 90° \qquad \text{(O-118)}$$

The direction of $\underline{w}$ in the reference trajectory plane varies with N, the number of circuits between t_C and t_D.

In the general case the correction component along the line of nodes at t_C (i.e., the ξ_C-component of $\underline{c}_W$) is affected by only that component of the miss distance lying along the line of nodes at t_D. Under conditions of the $X = 0$ singularity the ξ_C-component of the correction is the only correction component in the reference trajectory plane. Therefore, when $X = 0$, the entire correction component in the reference trajectory plane is due to only that component of the miss distance vector which lies along the line of nodes at t_D. The component of the miss distance that is in the reference trajectory plane but normal to the line of nodes must be compensated completely by the component of the correction that is parallel to the z-axis.

The X = 0 singularity does not affect the out-of-plane motion of the vehicle. The nature of the VTA correction will now be investigated for the case when position variation $\delta \underline{r}_D^-$ is parallel to the z-axis. The miss distance vector for this case is

$$(\delta \underline{\rho}^-)_W = \begin{Bmatrix} \delta \xi_D^- \\ \delta \eta_D^- \end{Bmatrix} = \begin{Bmatrix} 0 \\ \sin i_D \end{Bmatrix} \delta z_D^- \qquad \text{(O-119)}$$

From Eqs. (O-75) and (O-116), the correction is

$$\underline{c}_W = \begin{Bmatrix} c_\xi \\ c_\eta \end{Bmatrix} = \begin{Bmatrix} 0 \\ -k_{33} \end{Bmatrix} \delta z_D^- \qquad \text{(O-120)}$$

In vector form,

$$\underline{c}_v = - k_{33} (\delta z_D^-) \underline{u}_{\eta_C} = - k_{33} (\delta z_D^-) \underline{u}_z \qquad \text{(O-121)}$$

Thus, when X = 0, a position variation in the z direction calls for a VTA correction in the z direction, and the motion in the reference trajectory plane is not affected.

O.17 Physical Interpretation of the Effect of the Singularities on VTA Guidance

In the past three sections, it has been shown that, in general, it is not possible to compute a finite VTA velocity correction when a singularity of the first type occurs, i.e., when $(t_D - t_C) = N P$, and it is possible to compute a finite correction when either of the other two types of singularities occurs, i.e., when $(f_D - f_C) = (2 N - 1) \pi$ or when X = 0. This capability is in contrast with the FTA method of guidance, in which no finite correction can generally be computed when any one of the three types of singularities occurs.

The key to a physical understanding of the difference between the two guidance concepts lies in the fact that FTA requires that the

vehicle be at the specific point D at time t_D, while VTA has the less stringent requirement that the vehicle's position at $t = t_D$ be at any point near D on a specified straight line which passes through D.

In Fig. O.9, the relative velocity vector $\underline{v}_R$ is not in the reference trajectory plane. If at time $t_C = (t_D - NP)$ the vehicle is at some arbitrary point C_1 near D, the required VTA correction is such that the new trajectory contains the point C_1 and intersects the line of action of vector $\underline{v}_R$ at $t = t_D$. In the general three-dimensional case, it is not possible to find a trajectory which meets these requirements and at the same time differs only slightly from the reference trajectory. Therefore, the linear theory does not allow for the computation of a finite VTA velocity correction when $(t_D - t_C) = NP$.

In Section O.14, three special cases are considered. In the first, the vehicle's predicted position at $t = t_D$ is D', which lies along the line of action of $\underline{v}_R$. In this case the time at which a correction is contemplated is immaterial, since no correction is needed.

In the second special case, the vehicle's position at $t = t_C$ is C_2, which lies along the line of action of the orbital velocity vector $\underline{v}_D$. This case has already been taken up in Section O.5 in connection with FTA guidance. Irrespective of the nature of $\underline{v}_R$, the vehicle can be made to arrive at D at time t_D by applying a correction in the direction of $\underline{v}_D$ which causes the proper change in the period of the orbital motion.

The third special case occurs when the correction point C_1 and the vector $\underline{v}_R$ both lie in the reference trajectory plane. Then if $\underline{v}_R$ and $\underline{v}_D$ are not collinear, the trajectory passing through C_1 must cross the line of action of $\underline{v}_R$, and a small correction can be applied in the direction of $\underline{v}_D$ to ensure that such a crossing will take place at $t = t_D$. If $\underline{v}_R$ and $\underline{v}_D$ are collinear, the trajectory through C_1 does not cross the line of action of $\underline{v}_R$, and it is not possible to compute a small VTA velocity correction.

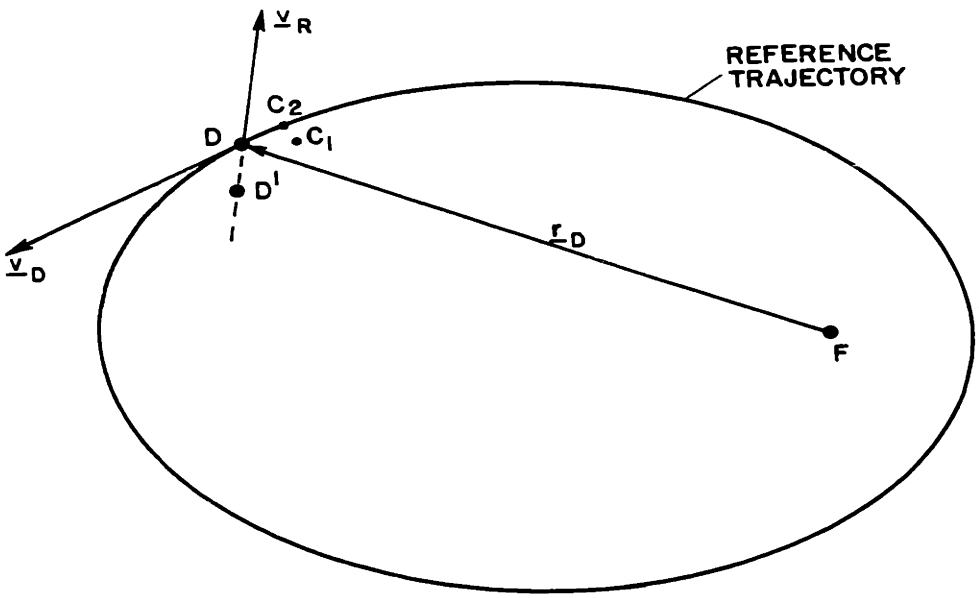

F – attractive focus

D – nominal destination point

D' – possible predicted position at nominal time of arrival at destination

C_1, C_2 – possible vehicle positions at time of correction

$\underline{v}_D$ – vehicle's nominal orbital velocity vector at time of arrival at destination

$\underline{v}_R$ – vehicle's nominal relative velocity with respect to destination planet at time of arrival

Figure O.9 VTA Guidance for Singularities at $t_D - t_C = NP$

The second type of singularity, for which $(f_D - f_C) = (2N - 1)\pi$, is due to the vehicle's component of motion normal to the reference trajectory plane. If the z-component of $\delta \underline{r}_D^-$ can be effectively eliminated, a finite velocity correction can be computed. The VTA guidance concept provides a method of accomplishing this elimination as long as the relative velocity vector has a non-zero component in the z-direction.

In Fig. O.10, the vehicle's actual trajectory prior to any correction will cause it to be at point D' at $t = t_D$. The nominal destination point is D. The requirement of VTA guidance is that the vehicle's position at t_D lie along the line through D parallel to $\underline{v}_R$. Since $\underline{v}_R$ is assumed to have a non-zero z-component, a line through D parallel to $\underline{v}_R$ must intersect the plane of the actual trajectory; the point of intersection is D'' in the figure. The VTA guidance scheme computes the velocity correction required to get the vehicle to D'' at $t = t_D$. Thus, the correction is determined in such a way that the plane of the actual trajectory is not altered; the correction vector lies in the plane of the actual trajectory.

If $\delta z_D^- = 0$, the VTA correction computed by Eq. (O-114) is the same as the FTA correction which would be computed under the same circumstances. This is consistent with the argument that has just been presented since, when $\delta z_D^- = 0$, the points D and D'' coincide, and hence VTA and FTA corrections are identical.

The third type of singularity, for which $X = 0$, involves a fairly complex relationship between the eccentricity e and the eccentric anomalies E_C and E_D. When the delicate balance among these three quantities which must exist at $X = 0$ is upset by permitting some leeway in the choice of a time and place of arrival, it is reasonable to expect that the singularity will vanish and a finite VTA correction can be computed.

The $X = 0$ singularity is a characteristic of the motion in the plane of the reference trajectory. It is possible to use FTA guidance to compute a z-axis correction to a z-axis position variation even when $X = 0$. Comparison of Eq. (O-121) with Eq. (K-48) indicates that VTA and FTA systems yield the same z-axis correction to a z-axis position

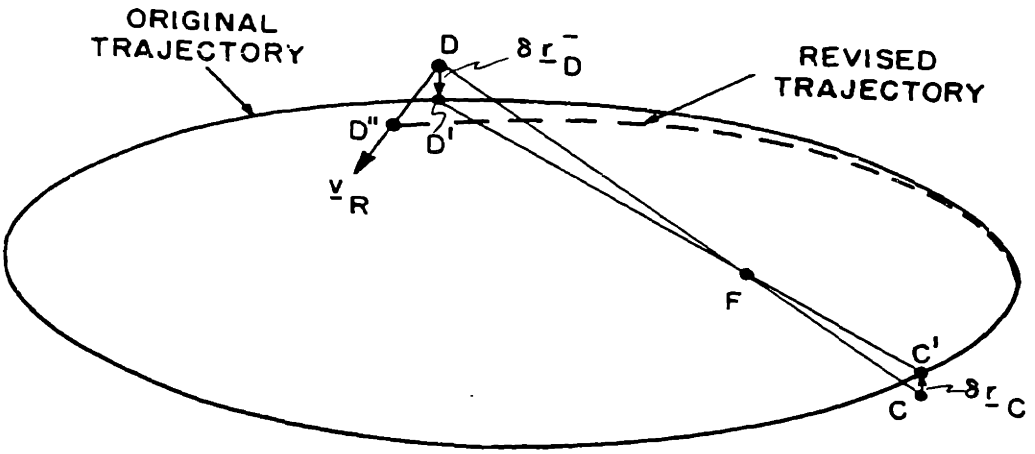

F – attractive focus

C – position on reference trajectory at $t = t_C$

C' – position on actual original trajectory at $t = t_C$

D – position on reference trajectory at $t = t_D$

D' – position on actual original trajectory at $t = t_D$

D'' – position on revised trajectory at $t = t_D$

$\delta \underline{r}_C$ – position variation at $t = t_C$

$\delta \underline{r}_D$ – predicted position variation at $t = t_D$ before correction is applied

$\underline{v}_R$ – relative velocity vector of vehicle with respect to destination planet at $t = t_D$

Figure O.10 VTA Guidance for Singularities at $f_D - f_C = (2N-1)\pi$

variation when $X = 0$. Thus, if the predicted position variation at the destination is entirely in the z direction, the correction of smallest magnitude that can be made at a time for which $X = 0$ is the FTA correction corresponding to that time, and there is no change in the time of arrival. In this special case the component of position variation in the reference trajectory plane is zero, hence there is no need for the computation of the correction to become involved with the troublesome aspects of the $X = 0$ condition. The VTA system automatically takes this fact into consideration and provides a velocity correction which is parallel to the z-axis.

APPENDIX P

STATISTICAL THEORY

P.1 Summary

The components of a multi-dimensional random variable are to be estimated from a redundant set of measurements, associated with each of which there is some uncertainty. The estimation technique known as the method of maximum likelihood is used to make the estimate. The equations of the maximum likelihood method are developed in matrix form.

The concept of the equi-probability ellipsoid is introduced and is used as a quantitative indication of the accuracy of the estimate.

P.2 Introduction

The mathematical development of the method of maximum likelihood presented in the following sections is patterned after the work of Shapiro,[43] the primary difference being that in the case treated by Shapiro the likelihood equations are nonlinear, while in the present application they are linear. As a consequence, a closed-form solution is obtained in this appendix, whereas such a solution is not possible in the nonlinear case.

The method of maximum likelihood was originally developed by the British statistician R.A. Fisher. A rigorous mathematical treatment of the method is presented by Cramér.[44]

P.3 Mathematical Preliminaries

The number of measurements to be processed in the estimation procedure is designated as M. These measurements are collected in a single M-dimensional column vector $\underline{m}$. In the linear analysis the vector used in the computations is $\delta\underline{m}$, which consists of the variations of the components of $\underline{m}$ from their reference values. The reference values are computed *a priori*.

The parameters to be estimated are collected in the column vector $\underline{x}$. The linear analysis leads to an estimate of the variation of each of the components of $\underline{x}$ from its reference value. The variation in $\underline{x}$ is $\delta\underline{x}$. In the general case, $\delta\underline{x}$ is an N-dimensional vector, where N is any positive integer. For the problem of orbit determination N is equal to six.

For the i-th measurement the linear relationship between δm_i and $\delta \underline{x}$ can be expressed as the scalar product of the vector $\underline{q}_i$ and the vector $\delta \underline{x}$.

$$\delta m_i = \underline{q}_i^T \, \delta \underline{x} \qquad \text{(P-1)}$$

$\underline{q}_i$ is a six-dimensional column vector whose components are the partial derivatives of m_i with respect to the components of $\underline{x}$. The partial derivatives are known functions of the parameter vector $\underline{x}$ and the time t_i. In the orbit determination problem, they can be expressed as functions of $\underline{r}_i$ and $\underline{v}_i$, the space vehicle's position and velocity vectors on the reference trajectory at time t_i.

The composite vector $\delta \underline{m}$ is obtained by extension of (P-1).

$$\delta \underline{m} = \left\{ \begin{array}{c} \delta m_1 \\ \vdots \\ \delta m_M \end{array} \right\} = \left\{ \begin{array}{c} \underline{q}_1^T \\ \vdots \\ \underline{q}_M^T \end{array} \right\} \delta \underline{x} = \overset{*}{Q}^T \, \delta \underline{x} \qquad \text{(P-2)}$$

where the M-by-6 matrix $\overset{*}{Q}^T$ is defined by

$$\overset{*}{Q}^T = \left\{ \begin{array}{c} \underline{q}_1^T \\ \vdots \\ \underline{q}_M^T \end{array} \right\} \qquad \text{(P-3)}$$

The transpose of $\overset{*}{Q}^T$ is the 6-by-M matrix $\overset{*}{Q}$.

$$\overset{*}{Q} = \left\{ \underline{q}_1 \cdots \cdots \underline{q}_M \right\} \qquad \text{(P-4)}$$

The observed values of the measurements differ from the true values due to inaccuracies in instrumentation. If $\delta \tilde{\underline{m}}$ is the observed measurement variation vector, the measurement uncertainty vector $\underline{u}$ is defined by

$$\underline{u} = \delta \tilde{\underline{m}} - \delta \underline{m} \qquad \text{(P-5)}$$

The covariance matrix of measurement uncertainties is

$$\overset{*}{U} = \overline{\underline{u}\ \underline{u}^T} \qquad \text{(P-6)}$$

Each component of $\underline{u}$ is assumed to have a Gaussian probability distribution with zero mean. The elements of $\overset{*}{U}$ are determined a priori.

P.4 Conditional Probability Density

After a set of measurements has been made, the vector $\delta\underline{\tilde{m}}$ is known. The problem then is to estimate $\delta\underline{x}$ on the basis of the known $\delta\underline{\tilde{m}}$. The most probable value of $\delta\underline{x}$ is that value for which the conditional probability density $p(\delta\underline{x} \mid \delta\underline{\tilde{m}})$ is a maximum. $p(\delta\underline{x} \mid \delta\underline{\tilde{m}})$ is the probability density of the vector $\delta\underline{x}$ for the given measurement variation vector $\delta\underline{\tilde{m}}$.

Maximizing $p(\delta\underline{x} \mid \delta\underline{\tilde{m}})$ is not analytically feasible. However, the conditional probability density $p(\delta\underline{\tilde{m}} \mid \delta\underline{x})$ can be maximized; this probability density is known as the likelihood function $L(\delta\underline{x})$. The two conditional probabilities are related by the following equation:

$$L(\delta\underline{x}) = p(\delta\underline{\tilde{m}} \mid \delta\underline{x}) = \frac{p(\delta\underline{x} \mid \delta\underline{\tilde{m}}) \cdot p(\delta\underline{\tilde{m}})}{p(\delta\underline{x})} \qquad \text{(P-7)}$$

$p(\delta\underline{\tilde{m}} \mid \delta\underline{x})$ is the conditional probability of obtaining the $\delta\underline{\tilde{m}}$ vector actually observed when the vector $\delta\underline{x}$ is specified. $p(\delta\underline{\tilde{m}})$ and $p(\delta\underline{x})$ are a priori probability densities.

The maximum likelihood estimate of $\delta\underline{x}$ is obtained by setting to zero the partial derivative of $L(\delta\underline{x})$ with respect to each component of $\underline{x}$ and then solving the resulting likelihood equations for the vector $\delta\underline{x}$. The maximum likelihood estimate of $\delta\underline{x}$ is designated $\delta\underline{\hat{x}}$.

From Equation (P-7) it is apparent that the maximum likelihood estimate and the most probable value of $\delta\underline{x}$ coincide if both $p(\delta\underline{\tilde{m}})$ and $p(\delta\underline{x})$ are independent of $\delta\underline{x}$.

P.5 The Maximum Likelihood Estimate

The observed measurement vector $\delta\underline{\tilde{m}}$ is the sum of a deterministic function of $\delta\underline{x}$ and the M-dimensional random variable $\underline{u}$.

$$\delta\underline{\tilde{m}} = \overset{*}{Q}^T\ \delta\underline{x} + \underline{u} \qquad \text{(P-8)}$$

Therefore, the likelihood function becomes

$$L(\delta \underline{x}) = p(\delta \underline{\tilde{m}} \mid \delta \underline{x}) = p(\underline{u} \mid \delta \underline{x}) \tag{P-9}$$

The probability density of $\underline{u}$ is independent of $\delta \underline{x}$. Then,

$$L(\delta \underline{x}) = p(\underline{u}) \tag{P-10}$$

$p(\underline{u})$ represents the joint probability density of $u_1, u_2, \ldots\ldots, u_M$. The equation for the M-dimensional joint probability density is

$$p(\underline{u}) = p(u_1, \ldots\ldots, u_M)$$

$$= \frac{1}{\left[(2\pi)^M \left| \overset{*}{U} \right| \right]^{1/2}} \exp\left(-\frac{1}{2} \underline{u}^T \overset{*}{U}^{-1} \underline{u}\right) \tag{P-11}$$

where $\left| \overset{*}{U} \right|$ is the determinant of $\overset{*}{U}$.

Since $\log [p(\underline{u})]$ is a monotonically increasing function of $p(\underline{u})$, maximizing the logarithm yields the same value of $\delta \underline{x}$ as maximizing $p(\underline{u})$ itself. The mathematics is simplified slightly if $\log [p(\underline{u})]$ is the function that is maximized.

$$\log [p(\underline{u})] = -\frac{1}{2} \log \left[(2\pi)^M \left| \overset{*}{U} \right| \right] - \frac{1}{2} \underline{u}^T \overset{*}{U}^{-1} \underline{u} \tag{P-12}$$

The first term on the right-hand side of (P-12) is a constant.

The partial derivative of $\log [p(\underline{u})]$ with respect to x_i, one of the components of $\underline{x}$, is

$$\frac{\partial \log [p(\underline{u})]}{\partial x_i} = -\frac{1}{2} \left(\frac{\partial \underline{u}^T}{\partial x_i} \overset{*}{U}^{-1} \underline{u} + \underline{u}^T \overset{*}{U}^{-1} \frac{\partial \underline{u}}{\partial x_i} \right) \tag{P-13}$$

The matrix product $\underline{u}^T \overset{*}{U}^{-1} \frac{\partial \underline{u}}{\partial x_i}$ is a scalar quantity, which is equal to its transpose. Since $\overset{*}{U}$ is a symmetric matrix, $\overset{*}{U}^{-1}$ is also symmetric. Then

$$\underline{u}^T \overset{*}{U}^{-1} \frac{\partial \underline{u}}{\partial x_i} = \left(\underline{u}^T \overset{*}{U}^{-1} \frac{\partial \underline{u}}{\partial x_i} \right)^T = \frac{\partial \underline{u}^T}{\partial x_i} \overset{*}{U}^{-1} \underline{u} \qquad \text{(P-14)}$$

When (P-14) is substituted into (P-13) and (P-13) is equated to zero, the result is

$$\frac{\partial \underline{u}^T}{\partial x_i} \overset{*}{U}^{-1} \underline{u} = 0 \qquad \text{(P-15)}$$

Since the observed measurement variation vector $\delta \underline{\tilde{m}}$ is independent of the components of $\delta \underline{x}$,

$$\frac{\partial \underline{u}^T}{\partial x_i} = \frac{\partial (\delta \underline{\tilde{m}} - \delta \underline{m})^T}{\partial x_i} = - \frac{\partial (\delta \underline{m})^T}{\partial x_i} \qquad \text{(P-16)}$$

The expression on the right side of (P-16) is the negative of the elements composing the i-th row of the matrix $\overset{*}{Q}$, which is defined by Equation (P-4). The six equations corresponding to i = 1, ..., 6 in (P-15) can be combined into a single matrix equation

$$\overset{*}{Q} \overset{*}{U}^{-1} \underline{u} = \underline{0}_6 \qquad \text{(P-17)}$$

In order to solve the set of simultaneous equations represented by (P-17) for the maximum likelihood estimate $\delta \underline{\hat{x}}$, it is necessary to relate $\underline{u}$ to $\delta \underline{\hat{x}}$. Although (P-5) defines $\underline{u}$ as being the difference between $\delta \underline{\tilde{m}}$ and $\delta \underline{m}$, a new vector $\delta \underline{\hat{m}}$ will now be defined, and $\underline{u}$ will be taken as the difference between $\delta \underline{\tilde{m}}$ and $\delta \underline{\hat{m}}$. $\delta \underline{\hat{m}}$ is the maximum likelihood estimate of the true measurement variation vector $\delta \underline{m}$.

$$\delta \underline{\hat{m}} = \overset{*}{Q}^T \delta \underline{\hat{x}} \qquad \text{(P-18)}$$

$$\underline{u} = \delta \underline{\tilde{m}} - \delta \underline{\hat{m}} = \delta \underline{\tilde{m}} - \overset{*}{Q}^T \delta \underline{\hat{x}} \qquad \text{(P-19)}$$

(P-17) and (P-19) are combined and solved for $\delta \underline{\hat{x}}$.

$$\delta \underline{\hat{x}} = (\overset{*}{Q} \overset{*}{U}^{-1} \overset{*}{Q}^T)^{-1} \overset{*}{Q} \overset{*}{U}^{-1} \delta \underline{\tilde{m}} \qquad \text{(P-20)}$$

This is the matrix form of the equation for the maximum likelihood estimate of $\delta \underline{x}$ based on the observed measurements represented by $\delta \underline{\tilde{m}}$.

P.6 Uncertainty in the Maximum Likelihood Estimate

Let $\underline{\epsilon}$ be the difference between the estimate $\delta \underline{\hat{x}}$ and the true parameter variation vector $\delta \underline{x}$. $\underline{\epsilon}$ represents the uncertainty in the maximum likelihood estimate.

$$\underline{\epsilon} = \delta \underline{\hat{x}} - \delta \underline{x} \tag{P-21}$$

$\underline{\epsilon}$ can be written as a function of the measurement uncertainty vector $\underline{u}$ by performing a few simple matrix manipulations of (P-20).

$$\overset{*}{Q}\, \overset{*}{U}^{-1}\, \overset{*}{Q}^{T}\, \delta \underline{\hat{x}} = \overset{*}{Q}\, \overset{*}{U}^{-1}\, \delta \underline{\tilde{m}}$$

$$= \overset{*}{Q}\, \overset{*}{U}^{-1}\, (\delta \underline{m} + \underline{u}) \tag{P-22}$$

$$\overset{*}{Q}\, \overset{*}{U}^{-1}\, \overset{*}{Q}^{T}\, (\delta \underline{\hat{x}} - \delta \underline{x}) = \overset{*}{Q}\, \overset{*}{U}^{-1}\, \underline{u} \tag{P-23}$$

$$\underline{\epsilon} = (\overset{*}{Q}\, \overset{*}{U}^{-1}\, \overset{*}{Q}^{T})^{-1}\, \overset{*}{Q}\, \overset{*}{U}^{-1}\, \underline{u} \tag{P-24}$$

The covariance matrix $\overset{*}{E}$ of the vector $\underline{\epsilon}$ is

$$\overset{*}{E} = \overline{\underline{\epsilon}\ \underline{\epsilon}^{T}} = (\overset{*}{Q}\, \overset{*}{U}^{-1}\, \overset{*}{Q}^{T})^{-1}\, \overset{*}{Q}\, \overset{*}{U}^{-1}\, \overline{\underline{u}\ \underline{u}^{T}}\ \overset{*}{U}^{-1}\, \overset{*}{Q}^{T}\, (\overset{*}{Q}\, \overset{*}{U}^{-1}\, \overset{*}{Q}^{T})^{-1}$$

$$= (\overset{*}{Q}\, \overset{*}{U}^{-1}\, \overset{*}{Q}^{T})^{-1} \tag{P-25}$$

P.7 The Equi-Probability Ellipsoid

For an N-dimensional parameter estimate, the joint probability density of the components of the associated uncertainty vector $\underline{\epsilon}$ is

$$p(\underline{\epsilon}) = \frac{1}{\left[(2\pi)^{N}\, \left|\, \overset{*}{E}\, \right|\right]^{1/2}}\ \exp\left(-\ \frac{1}{2}\ \underline{\epsilon}^{T}\, \overset{*}{E}^{-1}\, \underline{\epsilon}\right) \tag{P-26}$$

Some useful results are obtained by setting the quadratic form in the argument of the exponential equal to a constant.

$$\underline{\epsilon}^T \overset{*}{E}^{-1} \underline{\epsilon} = k^2 \qquad \text{(P-27)}$$

(P-27) is the equation of an N-dimensional ellipsoid centered at $\underline{\epsilon} = \underline{0}_N$. For a specified value of k, the joint probability density of any point on the ellipsoidal surface is

$$p_k(\underline{\epsilon}) = \frac{1}{\left[(2\pi)^N \left|\overset{*}{E}\right|\right]^{1/2}} \exp\left(-\frac{k^2}{2}\right) \qquad \text{(P-28)}$$

Because the joint probability density is constant for all points on the surface, the ellipsoid of (P-27) is known as the equi-probability ellipsoid.

The equi-probability ellipsoid is a convenient means of comparing the accuracies obtained from various estimation methods. If for a given k the ellipsoid obtained by one estimation technique lies wholly inside the ellipsoid obtained by a second technique, the first technique obviously is more accurate than the second. If the ellipsoids derived from the two estimation methods intersect, the issue is not so clear-cut; depending on the distribution of the uncertainties in the measurements, either method may lead to a more accurate estimate of the parameter vector in a specific case.

If k^2 in Equation (P-27) is set equal to (N + 2), the resulting ellipsoid is known as the ellipsoid of concentration. This particular ellipsoid has the characteristic that, if the joint probability density is constant throughout the volume of the ellipsoid and zero everywhere outside the surface of the ellipsoid, the covariance matrix of the resulting distribution is the same as the covariance matrix $\overset{*}{E}$ of the original distribution.

Cramér has shown that there is a certain minimum size of the ellipsoid of concentration. Estimation techniques are compared on the basis of the ratios of the volumes of their ellipsoids of concentration to the volume of the minimum ellipsoid. For a linear process with Gaussian distribution of measurement uncertainties, the ellipsoid of concentration

obtained by the method of maximum likelihood is equal to the minimum ellipsoid; therefore, the maximum likelihood estimate is an optimal estimate for such a case.

Another type of equi-probability ellipsoid that is frequently used in error analysis is that for which $k^2 = 1$. This type is known as the error ellipsoid. All equi-probability ellipsoids are geometrically similar. The ratio of the axis lengths of the ellipsoid of concentration to the corresponding axis lengths of the error ellipsoid is $(N + 2)^{1/2}$.

For a specified value of N, the probability that the uncertainty vector $\underline{\epsilon}$ falls completely within the error ellipsoid is a constant. For N = 2, the probability is 0.393; for N = 3, the probability is 0.199.

P.8 Circular Probable Error and Spherical Probable Error

Another type of equi-probability ellipsoid that is used in error analyses is the 50% probability ellipsoid, which is defined as the ellipsoid for which the probability is 0.5 that the vector $\underline{\epsilon}$ will lie totally within its boundaries. This concept is particularly useful when N is equal to 2 or 3, for in these cases it has a simple physical interpretation.

The volume of the N-dimensional equi-probability ellipsoid is

$$V = \frac{\pi^{\frac{N}{2}} k^N \left| \overset{*}{\underline{E}} \right|^{1/2}}{\Gamma\left(\frac{N}{2} + 1\right)} \qquad \text{(P-29)}$$

where $\Gamma(\ )$ represents the gamma function of the argument.

For N = 2 the ellipsoid reduces to an ellipse, and its area is

$$A = \pi k^2 \left| \overset{*}{\underline{E}} \right|^{1/2} \qquad \text{(P-30)}$$

The value of k for the 50% probability ellipse is 1.1774. The area of the 50% probability ellipse is

$$A_{0.5} = \pi (1.1774)^2 \left| \overset{*}{\underline{E}} \right|^{1/2} \qquad \text{(P-31)}$$

When the measurements are carefully chosen, it is usually possible to obtain an ellipse whose two major axes are nearly equal in length. Then

the ellipse closely resembles a circle. The radius of the circle with the same area as that given by (P-31) is known as the circular probable error (CPE). The CPE is frequently used as an accuracy criterion for two-dimensional parameter vectors. From (P-31),

$$CPE = 1.1774 \left| \overset{*}{E} \right|^{1/4} \tag{P-32}$$

A similar criterion can be derived for N = 3. The volume of the three-dimensional equi-probability ellipsoid is

$$V = \frac{4}{3} \pi k^3 \left| \overset{*}{E} \right|^{1/2} \tag{P-33}$$

For the 50% probability ellipsoid, k = 1.5382.

$$V_{0.5} = \frac{4}{3} \pi (1.5382)^3 \left| \overset{*}{E} \right|^{1/2} \tag{P-34}$$

where $V_{0.5}$ is the volume of the 50% probability ellipsoid. When the axes of the ellipsoid are roughly equal in length, the spherical probable error (SPE) is defined as the radius of the sphere whose volume is equal to $V_{0.5}$.

$$SPE = 1.5382 \left| \overset{*}{E} \right|^{1/6} \tag{P-35}$$

The numerical values used in the last two sections have been obtained from Burington and May[45] and from Locke.[46]